The role of thymosin beta 4 in renal podocyte function

William John Mason

A thesis submitted in partial fulfilment of the requirements of the University of Kent and the University of Greenwich for the Degree of Doctor of Philosophy

May 2021

ABSTRACT

Ten percent of the world have chronic kidney disease (CKD). In some patients, CKD can be catastrophic, leading to end stage kidney disease (ESKD), requiring lifelong dialysis or kidney transplant. Identification and analysis of molecules that can halt the progression of CKD to ESKD has the potential to save lives. The glomerulus is the site of the kidney, where the blood is filtered to produce urine. The glomerular filtration barrier consists of endothelial cells, a basement membrane and podocytes, epithelial cells with a unique shape maintained by the actin cytoskeleton. Damage to the structure of podocytes, is a significant contributing factor to CKD progression, and disorganisation of the podocyte cytoskeleton is a key factor associated with podocyte damage. Thymosin β4 (TB4) is the major G-actin sequestering molecule in mammalian cells and it regulates cell morphology, inflammation, and fibrosis. TB4 has beneficial effects in rodent models of kidney injury, including protection of the glomerulus, but the effect of exogenous TB4 on podocytes is currently unknown. The aim of this thesis was to examine the effect of exogenous TB4 in cytotoxic and immune mediated podocyte injury models. Podocyte injury induced by the toxin Adriamycin (ADR) resulted in downregulation of the mRNA transcript for TB4 in podocytes. Examination of the F-actin cytoskeleton in mouse immortalised podocytes by phalloidin staining demonstrated that exogenous TB4 completely prevented ADR-induced F-actin disorganisation *in vitro*, a key factor in glomerular filtration barrier damage *in vivo*. The effect of exogenous TB4 was then examined in ADR nephropathy and nephrotoxic serum (NTS) nephritis in mice. Systemic upregulation of TB4 was achieved by recombinant adeno associated virus (AAV) mediated gene delivery prior to disease induction. Exogenous TB4 prevented damage to the glomerular filtration barrier, shown by reduced urine levels of albumin, in ADR nephropathy and early NTS nephritis. This was most likely due to prevention of podocyte loss, protection of glomerular F-actin in ADR nephropathy, and suppression of inflammation in NTS nephritis, as determined by light and fluorescent microscopy. In summary, this thesis has provided strong evidence that exogenous TB4 is a beneficial molecule in the context of glomerular and podocyte injury. In the future, it is hoped that use of exogenous TB4 can translate to human physiology and be developed as a therapeutic strategy to alleviate the progression of CKD to ESKD.

Declaration

I certify that this work has not been accepted in substance for any degree and is not concurrently being submitted for any degree other than that of Doctor of Philosophy being studied at Universities of Greenwich and Kent. I also declare that this work is the result of my own investigations except where otherwise identified by references and that I have not plagiarised the work of others.

I would also like to declare that this project occurred during the COVID-19 pandemic. The laboratory that I was working in closed for an extended period, meaning that I was unable to complete some of the experiments originally planned for this project.

Signed:

William John Mason

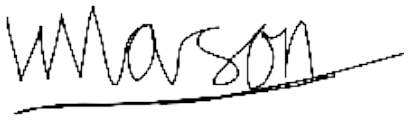

1st May 2021

Word Count: 66,943

ACKNOWLEDGEMENTS

I would first like to say thank you to my family members and friends for supporting me throughout my Ph.D. In particular, my mother and father, Susan and Stephen, my sister, Jessica, and my maternal grandparents, David and Isabel and Lucy. Although not with us for some, or all, of the process, I would also like to thank my paternal grandparents, Kenneth and Denise, for all the love they gave me while they were alive. I hope I have made each and every one of them proud with my academic achievements.

I would also like to say thank you to my Ph.D. supervisors who have provided me with the training and guidance required to complete this demanding degree and become the scientist that I am. In particular, I am eternally grateful to Dr Elisavet Vasilopoulou and Professor David Andrew Long. I would not be able to call myself a scientist without the world class training to undertake laboratory experiments, data analysis and scientific writing that they spent their time providing me with.

I would not have been able to complete my Ph.D. without the help of the friends I made at the Medway School of Pharmacy. Whether that be assistance with laboratory experiments, emotional support during the stresses of Ph.D. life or socialising during our free time in order to relax. I made some amazing friends there who I will always keep in touch with. During my Ph.D. I also spent a year with the Kidney Development and Disease group at the University College London Great Ormond Street Institute of Child Health (GOSHICH). I would like to thank all members, past and present, of the GOSHICH team for making me feel so welcome when I joined, and for assistance with laboratory experiments and data analysis. I will not forget the time I spent there, which accelerated my development as a researcher and gave me some friends for life.

Finally, I would like to acknowledge all of the animals used in this study and throughout the history of scientific research. They have paid the ultimate sacrifice in order to advance scientific knowledge, and ultimately save lives, which we, as the human race, will be forever in their debt.

CONTENTS

FIGURES

TABLES

List of abbreviations

AAV – Adeno associated virus

AAVR – Adeno associated virus receptor

Abs – Absorbance

ACE – Angiotensin converting enzyme

ACR – Albumin to creatinine ratio

AcSDKP - N-acetyl-seryl-aspartyl-lysyl-proline

ADF – Actin depolymerising factor

ADP – Adenosine diphosphate

ADR – Adriamycin

AGE – Advanced glycosylation end products

α-SMA - α-smooth muscle actin

ANCA – Anti-neutrophil cytoplasm antibodies

Arp2/3 – Actin related protein subunits 2/3

ATP – Adenosine triphosphate

A549 – Human adenocarcinomic alveolar basal epithelial cells

BSA – Bovine serum albumin

BUN – Blood urea nitrogen

cAMP - Adenosine-3′,5′-cyclic monophosphate

CCL2 – (C-C motif) ligand 2

CCN1 – Cysteine rich angiogenic protein 1

CCN2 – Cellular communication network factor 2

cDNA – Complementary deoxyribonucleic acid

CD3 – Cluster of differentiation 3

Cd2ap – CD2 associated protein

CD68 – Cluster of differentiation 68

CKD – Chronic kidney disease

CPT1A - Carnitine Palmitoyltransferase 1A

CRISPR/CAS-9 – Clustered regularly interspaced short palindromic repeats/CRISPR-associated protein 9

Ct – Threshold cycle

CTCF – Corrected total cell fluorescence

DAB - 3,3'-Diaminobenzidine

DMSO – Dimethyl sulfoxide

DOCA – Deoxycorticosterone acetate

DMEM – Dulbecco's modified eagle medium

D-PBS – Dulbecco's phosphate buffered saline

EDTA - Ethylenediaminetetraacetic acid

eGFR – Estimated glomerular filtration rate

ELISA – Enzyme linked immunosorbent assay

Ena/VASP – Enabled/vasodilator-stimulated phosphoprotein

ERM – Ezrin, radixin and moesin

ESKD – End stage kidney disease

F-actin – Filamentous actin

FAK – Focal adhesion kinase

FCS – Foetal calf serum

FFPE – Formalin fixed paraffin embedded

FH2 – Formin homology domain 2

Fn1 – Fibronectin 1

FSGS – Focal segmental glomerulosclerosis

G-actin – Globular actin

GAPDH - Glyceraldehyde 3-phosphate dehydrogenase

GBM – Glomerular basement membrane

GCW – Glomerular capillary wall

GDP – Gross domestic product

GDP – Guanosine diphosphate

Glp1r – Glucagon-like peptide-1 receptor

GLUT1 – Glucose transporter 1

GMP – Good manufacturing practice

GN - Glomerulonephritis

GPA – Granulomatosis with polyangiitis

GTP – Guanosine triphosphate

HB-EGF – Heparin-binding epidermal growth factor

HCEC – Human corneal epithelial cells

HEK – Human embryonic kidney

HeLa – Henrietta Lacks

Hprt - Hypoxanthine-guanine phosphoribosyl transferase

HRP – Horse radish peroxidase

HPLC – High performance liquid chromatography

Huh7 – Human hepatocyte cell line 7

HUVEC – Human umbilical vein endothelial cells

ICAM-1 – Intercellular adhesion molecule-1

IF – Immunofluorescence

IFN-γ - Interferon-γ

IgA – Immunoglobulin A

IGF-1 – Insulin-like growth factor 1

IgG – Immunoglobulin G

IHC – Immunohistochemistry

IL-1 – Interleukin 1

IL-2 – Interleukin 2

ILK – Integrin linked kinase

ITR – Inverted terminal repeat

kDa – Kilodaltons

LacZ - β-galactosidase

LN – Lupus nephritis

LPS – Lipopolysaccharide

LRP1 – Low density lipoprotein receptor related protein 1

MafB - V-maf musculoaponeurotic fibrosarcoma oncogene homolog B

MAGI-2 – Membrane associated guanylate kinase, WW and PDZ domain containing 2

MCP-1 – Monocyte chemoattractant protein 1

MDM-2 – Murine double minute - 2

MIP1&2 – Macrophage inflammatory protein 1&2

MRI – Magnetic resonance imaging

mRNA – messenger ribonucleic acid

MTT – 3-(4,5-dimethylthiazol-2-yl)-2,5-diphenyltetrazolium bromide

$NADP^+$ - Nicotinamide adenine dinucleotide phosphate

NEFH/*Nefh* – Neurofilament heavy polypeptide

NFκB – Nuclear factor kappa-light-chain-enhancer of activated B cells

Nherf2 - Sodium-hydrogen exchange regulatory cofactor NHE-RF2

NSAID – Non-steroidal anti-inflammatory drugs

NTS – Nephrotoxic serum nephritis

OCT – Optimal cutting temperature

OMP – Osmotic mini pump

ORF – Open reading frame

PAI-1 – Plasminogen activator inhibitor-1

PAN – Puromycin aminonucleoside nephrosis

PBS – Phosphate buffered saline

PCA – Principal component analysis

PCR – Polymerase chain reaction

PDGF-BB – Platelet derived growth factor (2β subunits)

PDK4 – Pyruvate dehydrogenase kinase 4

PEC – Parietal epithelial cell

PFA – Paraformaldehyde

PGC1α - Peroxisome proliferator-activated receptor γ coactivator 1 α

PKD – Polycystic kidney disease

PKM-2 – Pyruvate kinase isozyme 2

PRKDC/*Prkdc* – Protein kinase, DNA activated, catalytic subunit

P/S - Penicillin/streptomycin

RAAS – Renin-angiotensin-aldosterone system

rAAV – Recombinant adeno-associated virus

RAGE – Receptor for advanced glycosylation end products

ROCK – Rho-associated protein kinase

ROCK2 – Rho-associated protein kinase 2

RPGN – Rapidly progressing glomerulonephritis

RPM – Revolutions per minute

RPMI 1640 – Roswell Park Memorial Institute 1640 medium

qPCR – Quantitative polymerase chain reaction

SCAR/WAVE – WASP-family verprolin homologous protein 1

SD – Slit diaphragm

SGLT-2 – Sodium-glucose cotransporter-2

siRNA – Small interfering ribonucleic acid

SIRt3 – Sirtuin 3

SLE – Systemic lupus erythematosus

STORM – Stochastic optical reconstruction microscopy

Sulf1 – Sulphatase 1

suPAR – Soluble urokinase receptor

SV40 – Simian virus 40

TB4 – Thymosin β-4

TB4-SO – Thymosin β-4 sulfoxide

TGF-β - Transforming growth factor β

Tmsb4x/TMSB4x – Thymosin β-4, x-linked

TUNEL - Terminal deoxynucleotidyl transferase dUTP nick end labeling

TNF-α - Tumour necrosis factor alpha

U.K. – United Kingdom

UMAP – Uniform manifold approximation and projection

UUO – Unilateral ureteral obstruction

VASP - Vasodilator stimulated phosphoprotein

VEGF – Vascular endothelial growth factor

VP1/2/3 – Virion protein 1/2/3

WASP – Wiskott-Aldrich syndrome protein

ZEN – Zeiss efficient navigation

ZO-1 – Zonula occludens 1

Chapter 1: General introduction

1.1 Structure and function of the kidney

1.1.1 What do the kidneys do?

The kidneys are two bean shaped organs located in the upper abdomen of most vertebrates (**Figure 1.1a**) (Ditrich 2007). Each adult human kidney measures between 12.4 – 13.7 cm in length and weighs between 81 – 176 g (Moëll 1956; Molina and DiMaio 2012). The kidneys are vital for homeostasis, excreting unwanted substances from the blood by filtering up to 180 litres of blood per day, whilst conserving those substances that are required for healthy physiology (Shoskes and McMahon 2012). The ultrafiltration of the blood is considered their main responsibility, however the kidneys also produce erythropoietin to stimulate red blood cell production (Zhou and Sacks 2001), renin which maintains sodium balance and blood pressure (Castrop et al. 2010), calcitriol to modulate bone homeostasis (Gallagher, Rapuri, and Smith 2007) and gluconeogenesis during fasting (Stumvoll et al. 1998). The kidneys contain nerves from both the autonomic and somatic nervous system to tailor their function to the body's current requirements (Shoskes and McMahon 2012).

1.1.2 Blood filtration and reabsorption by the nephron

Uninterrupted and regulated blood flow is critical for proper kidney function. The kidneys regulate the composition of the blood plasma by filtration, secretion and reabsorption of molecules (Pocock and Richards 2009). Blood enters the kidney via the renal artery at the hilus, which branches into arcuate arteries distributed in the outer medulla. The arcuate arteries branch into cortical radial arteries, then afferent arterioles that enter the glomerulus, which supply nephrons (Shoskes and McMahon 2012). Nephrons are the functional unit of the kidney and are responsible for the filtration of blood and production of urine (**Figure 1.1b**) (Bertram et al. 2011). The nephron is composed of 5 main components: renal corpuscle; proximal convoluted tubule; loop of Henle; distal convoluted tubule and the collecting duct (Shoskes and McMahon 2012).

The renal corpuscle is where blood enters the nephron and is the site of ultrafiltration (Deen et al. 1972). The renal corpuscle is composed of the Bowman's capsule (lined by parietal epithelial cells), afferent and efferent arterioles and the glomerular tuft. The glomerular tuft contains a complex network of capillaries, mesangial cells, the glomerular basement membrane (GBM) and glomerular epithelial cells called podocytes (Mueller, Mason, and Stout 1955). Ultrafiltration of the blood occurs across the glomerular filtration barrier, which is comprised of the capillary endothelial cells, the GBM and podocyte foot processes (**Figure 1.2a**). Small (<40 nm), positively charged molecules are forced through the glomerular filtration barrier into the urinary space to form the ultrafiltrate (Pocock and Richards 2009; Shoskes and McMahon 2012). Examples of such molecules are, glucose, amino acids, water, sodium and calcium ions (Wartiovaara et al. 2004). Molecules that are larger than 40 nm and negatively charged, such as albumin, are not filtered in healthy glomeruli (G. W. Liu et al. 2018; Rodewald and Karnovsky 1974). Neutrally charged molecules smaller than 40 nm are also freely filtered through the glomerular filtration barrier (Miner 2008). The ultrafiltrate exits the renal corpuscle via the proximal convoluted tubule (Pocock and Richards 2009; Shoskes and McMahon 2012).

The glomerular capillaries re-join to form the efferent arteriole through which the filtered blood exits the renal corpuscle. The efferent arteriole branches into

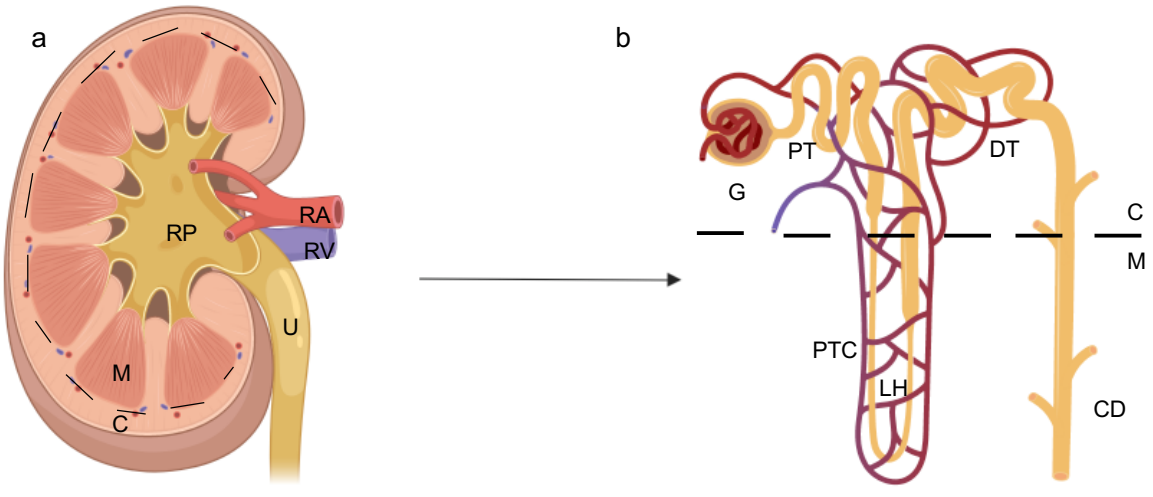

Figure 1.1 – Macro and microstructure of the kidney. *Diagram to illustrate the different parts of the kidney responsible for the ultrafiltration of the blood. The diagram shows* ***(a)*** *the whole kidney and* ***(b)*** *a single nephron. Black dashed line indicates cortex-medullary boundaries. C, Cortex; M, Medulla; RP, Renal Pelvis; U, Ureter; RA, Renal Artery; RV, Renal Vein; G, Glomerulus; PT, Proximal tubule; PTC, Peritubular Capillaries; LH, Loop of Henle; DT, Distal tubule; CD, Collecting duct. Original figure.*

peritubular capillaries that wrap around the tubules throughout the whole nephron (Seldin and Giebisch 2008). The proximal convoluted tubule is one of the sites of reabsorption of molecules back into the blood stream and is lined by thick cuboidal cells (Curthoys and Moe 2014). Reabsorption occurs via membrane transporters or points of passive transport on the proximal tubular cells, and molecules such as amino acids, small positively charged proteins and peptides, glucose and salts are reabsorbed into the blood (Shoskes and McMahon 2012). Secretion from the peritubular capillaries allows molecules that were not filtered by the glomerulus to be added to the ultrafiltrate. Such molecules include urea, uric acid, some forms of drugs, and hydrogen ions (Braam et al. 1993). The ultrafiltrate is forced through the proximal convoluted tubule lumen by hydrostatic pressure to the descending limb of the loop of Henle in the medulla (Vallon et al. 2011).

Secretion and reabsorption also occur in the loop of Henle, which is located in the renal medulla and split into two components, the thin descending limb followed by the thick ascending limb (Seldin and Giebisch 2008; Shoskes and McMahon 2012). The squamous epithelial cells of the thin descending limb allow water to be reabsorbed to concentrate the ultrafiltrate, and urea to be secreted from the peritubular capillaries (Kokko 1970). When the ultrafiltrate reaches the thick ascending limb, ions, such as sodium, potassium and chlorine are reabsorbed into the blood stream while the ultrafiltrate travels to the distal convoluted tubule. The thick ascending limb is impermeable to water, therefore the ultrafiltrate becomes more dilute the further it travels (Mount 2014).

The thick ascending loop of Henle travels back to the renal cortex before becoming the distal convoluted tubule. The distal convoluted tubular epithelial cells are cuboidal and the lumen loops back on itself several times in the cortex (Pocock and Richards 2009). Once again, the ultrafiltrate undergoes reabsorption and secretion, where sodium and chlorine ions and water leave the ultrafiltrate to re-join the blood stream, and hydrogen and potassium ions leave the blood stream (Elalouf, Roinel, and de Rouffignac 1984). The distal convoluted tubule then becomes the collecting duct. The peritubular capillaries drain into stellate veins, cortical radial veins and arcuate veins before leaving the kidney via the renal vein (Pocock and Richards 2009). The collecting duct lumen is much wider than the tubular lumen in diameter

and travels deep into the kidney medulla (Shoskes and McMahon 2012). When the ultrafiltrate travels through the medulla, water is reabsorbed into the blood stream through aquaporin II channels to concentrate the urine (Deen, Van Balkom, and Kamsteeg 2000). The collecting duct joins the minor and major calyces in the renal pelvis, where it pools the urine produced by all nephrons. The kidneys are connected to the bladder by a duct called the ureter, which transports freshly produced urine to the bladder, ready for excretion (Shoskes and McMahon 2012).

1.2 **Podocytes**

1.2.1 What are podocytes?

The glomerular filtration barrier is comprised of 3 components, the capillary endothelial cells, the GBM and podocytes (Jarad and Miner 2009). Podocytes are terminally differentiated epithelial cells that form a key component of the glomerular filtration barrier (Reiser and Altintas 2016). They are located in the renal corpuscle on the glomerular tuft, wrapping around the glomerular capillaries and are highly specialised with a unique structure that facilitates their crucial role in homeostasis. Podocytes have a cell body, that projects cellular extensions called processes, that vastly increase their surface area, allowing individual podocytes to reach distant areas of the glomerular tuft (Faul et al. 2007).

There are three types of podocyte processes: primary processes, secondary processes and foot processes (Garg 2018). The primary processes are the largest of the three types and extend from the cell body. They are crucial for podocyte structure as they protrude many secondary processes, which can reach a large surface area of the capillary walls (**Figure 1.2b**) (Pavenstädt, Kriz, and Kretzler 2003). The secondary processes are affixed to the GBM and extend along the GBM to portions that are relatively far from the cell body. The secondary processes then project fine foot processes, which are ultimately responsible for ultrafiltration (Faul et al. 2007).

Podocytes are constantly subjected to a strong hydrostatic pressure of the ultrafiltrate, so tightly regulated adherence to the GBM is crucial for glomerular health. A recent study in rat glomeruli *in vivo* characterised a “ridge like process” that

runs longitudinal to the GBM, and serves to anchor the podocyte cell body and primary processes to the GBM (Ichimura et al. 2019). The discovery and characterisation of the sub-podocyte space (Arkill et al. 2014; Neal et al. 2005) suggests that the cell body is “floating” in the urinary space and that podocytes adhere to the GBM through their processes. The foot processes adhere to the GBM via expression of a3β1 integrin and a & β dystroglycan molecules that bind to laminin or agrin in the GBM (Korhonen et al. 1990; Pozzi et al. 2008; Raats et al. 2000; Regele et al. 2000).

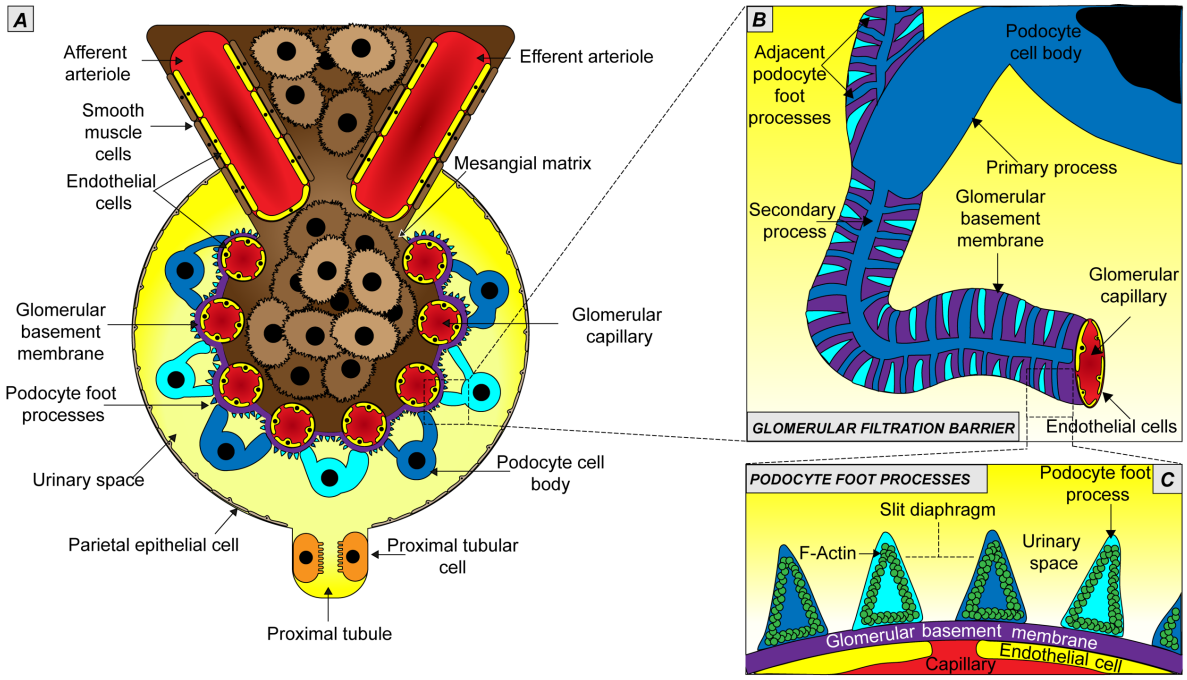

Figure 1.2 - Structure and components of the renal corpuscle. ***(a)*** *Diagram depicting the key components of the renal corpuscle.* ***(b)*** *Enhanced view of adjacent podocyte foot processes wrapping around GBM.* ***(c)*** *Lateral view of the glomerular filtration barrier. Podocyte foot processes of differing colours represent two different podocytes.*

1.2.2 Podocyte development in mice

Most experiments undertaken in this thesis were based on mouse podocytes, therefore this section will focus on mouse podocyte development. Kidney development initiates at embryonic day 11 in mice from 2 distinct components, the ureteric bud and metanephric mesenchyme (Costantini and Kopan 2010). Mature podocytes, along with epithelial cells from other nephron components, are derived

from metanephric mesenchymal nephron progenitor cells (Kobayashi et al. 2008). Wnt signalling from the ureteric bud causes the formation of the pretubular aggregate, which is a cluster of nephron progenitor cells (Stark et al. 1994). The pretubular aggregate undergoes mesenchymal to epithelial transition to form a spherical arrangement of cells called the renal vesicle (Carroll et al. 2005; Stark et al. 1994). The renal vesicle then elongates, and the nephron progenitor cells begin to differentiate into their respective cell types. The proximal pole starts to express podocyte related genes, such as *Wt1, MafB* and *Sulf1* (Brunskill et al. 2014; Moriguchi et al. 2006; Mundlos et al. 1993). A Wnt/β-catenin activity gradient is formed along the nephron, with the lowest β-catenin levels at the proximal pole (Lindström et al. 2014; Yoshimura and Nishinakamura 2019). The nephron epithelia undergo segmentation, stimulated by different strengths and durations of ureteric bud Wnt9b signalling, to form the S shaped body which contains the precursors to podocytes. Fully formed glomeruli can be detected at embryonic day 14.5 in mice and it is suggested that they start to filter urine at embryonic day 16.5 – 17.5 (McMahon 2016). New-born mice have a fully formed and functioning glomerulus (Farber et al. 2018).

1.2.3 How do podocytes filter the blood?

Podocyte foot processes are approximately 500 - 600 nm in width in humans and 200 – 300 nm in mice (Deegens et al. 2008; Wharram et al. 2000) and adjacent podocyte foot processes interdigitate to form a slit diaphragm (SD) (Karnovsky and Ainsworth 1972). The foot process shape is dictated by the F-actin cytoskeleton and is critical for glomerular function (Welsh and Saleem 2012), and will be described in detail in later sections of this introduction (1.3.3). The SD is regarded as a modified adherens junction that allows molecules smaller than 40 nm to be filtered into the urinary space from the blood stream, while preserving larger molecules (**Figure 1.2c**) (Reiser et al. 2000; Wartiovaara et al. 2004).

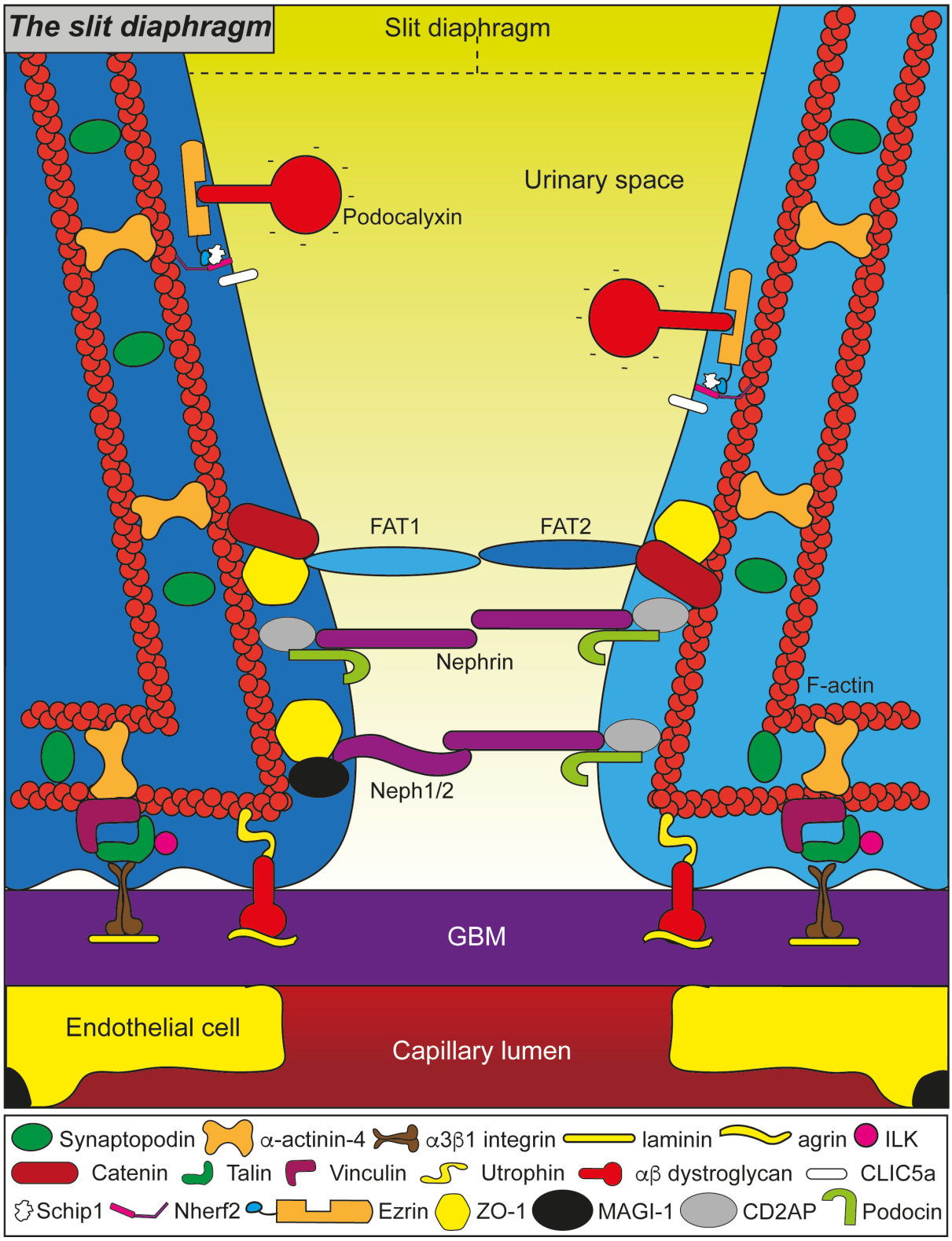

Figure 1.3 – Molecular view of the SD. *A diagram of some of the proteins that compose the SD, which is approximately 40 nm wide in mice. The large blue structures are adjacent podocyte foot processes that form the SD. The red structures are F-actin filaments that dictate the shape of the foot processes and anchor the cell to the GBM via integrin and dystroglycan. Original diagram.*

The foot processes contain a rich network of extracellular and intracellular SD proteins that form homophilic and heterophilic bonds, produce signalling cascades and maintain the size and charge selectivity of the glomerular filtration barrier (Barletta et al. 2003; Grahammer, Schell, and Huber 2013; Khoshnoodi et al. 2003). Nephrin was one of the first SD proteins to be discovered in the late 1990s, when it was identified that some cases of the congenital nephrotic syndrome of the Finnish type were due to *NPHS1* mutations (Kestilä et al. 1998). This study prompted more investigation, and a year later it was shown that nephrin belongs to the immunoglobulin G (IgG) superfamily of cell surface receptors and plays a crucial role in cell-cell adhesion and intracellular signalling (Lenkkeri et al. 1999).

Since then, research on nephrin, and other SD proteins, has grown exponentially. Nephrin is linked to the actin cytoskeleton by the CD2 associated protein (CD2AP)/Nck complex (Jones et al. 2006; Yuan, Takeuchi, and Salant 2002) and its phosphorylation sets off intracellular signalling cascades that affect podocyte polarity, survival, calcium mechano-signalling, membrane trafficking and actin organisation (Martin and Jones 2018). The extracellular SD protein podocin is also linked to the cytoskeleton via CD2AP and Nck and interacts with nephrin (Roselli et al. 2002; Schwarz et al. 2001; Tryggvason, Pikkarainen, and Patrakka 2006). Podocin recruits nephrin to the SD and mutations to the podocin gene *NPHS2*/*Nphs2* have been linked with the development of nephrotic syndrome and decline in kidney function (Amr et al. 2020; Tabatabaeifar et al. 2017) demonstrating the crucial role of podocin in podocyte health. There are also two proteins, known as NEPH1 and NEPH2 which are structurally similar and are ligands to nephrin in the SD (Gerke et al. 2003, 2005). NEPH1 and NEPH2 link to the cytoskeleton via zonula occludens-1 (ZO-1) and membrane associated guanylate kinase, WW and PDZ domain containing 2 (MAGI-2) (Wagner et al. 2008; Yamada et al. 2020) and disruption of their genes results in heavy proteinuria, foot process effacement and perinatal death in mice (Donoviel et al. 2001).

The main SD protein that is responsible for charge exclusion of the ultrafiltrate is podocalyxin (Nielsen and Mcnagny 2009). Podocalyxin is coated in sialic acid residues (Kerjaschki, Sharkey, and Farquhar 1984), rendering the protein negatively charged and repelling negatively charged molecules to remain in the blood stream.

Podocalyxin is linked to the cytoskeleton in foot processes via the ezrin/sodium-hydrogen exchange regulatory cofactor NHE-RF2 (Nherf2) complex (Orlando et al. 2001; Takeda 2003) and it has recently been shown that schwannomin interacting protein 1 (Schip1), a novel foot process protein first characterised in the brain, is also a member of this complex (Perisic et al. 2015). Breakdown of this complex and mutations in the *PODXL*/*Podxl* gene has been linked with foot process effacement, albuminuria and development of CKD in mice and humans (Lin et al. 2019; Takeda et al. 2001).

FAT1 and FAT 2 are intracellular protocadherin SD proteins that are essential for the maintenance of the SD (Yaoita et al. 2005). FAT1/2 are linked to the cytoskeleton via ZO-1 and β-catenin molecules, and it has been shown that mice lacking *Fat1* experience perinatal mortality through lack of SD formation and impaired renal function (Ciani et al. 2003). In contrast, the intercellular protein P-cadherin is not essential for SD development and maintenance, as P-cadherin null mice showed no renal phenotype (Radice et al. 1997). Collectively, it is clear that the SD protein network is complex and finely tuned. There are many different molecules that form the SD and maintain its function; however, the one common feature is the majority of SD molecules are all linked to the actin cytoskeleton (**Figure 1.3**).

1.3 **The actin cytoskeleton**

1.3.1 What is the cytoskeleton?

There are three main types of cytoskeletal structures: microtubules, intermediate filaments and microfilaments (Gavin 1997; Goldman et al. 1996; Hollenbeck 2001). Their names derive from their sizes, as microtubules are thought to be 24 nm in diameter, intermediate filaments 10 nm and microfilaments 7 nm in diameter in mice (Franke, Grund, and Fink 1978; Kandel et al. 2017; Steinert, Jones, and Goldman 1984). Microtubules are composed of heterodimers of α and β-tubulin that form hollow, unstable, tubular polymers from less than 1 μm to more than 100 μm in length (Goodson and Jonasson 2018). They are highly dynamic structures that originate in the perinuclear region of podocytes and extend to the primary processes (Andrews 1977). Microtubules undertake roles in maintaining cell shape and can facilitate mitosis, actuation of cilia and intracellular trafficking (Hueschen et al. 2017;

Vladar et al. 2012; Welte 2004). Podocyte microtubules are essential for process formation and their role in the maintenance of cell shape is crucial, as impairment of microtubule formation results in altered podocyte morphology *in vitro* (Kim et al. 2010; Kobayashi et al. 1998, 2001; Mon La et al. 2020; Welsh and Saleem 2012).

Intermediate filaments are located in the nucleus and the cytoplasm of cells and form by self-assembly (Kim and Coulombe 2007; Pinto et al. 2014). Intermediate filaments are extremely stable and less dynamic than microtubules and microfilaments, and intermediate filaments mainly serve to preserve cellular structure, cell signalling and cell adhesion (Etienne-Manneville 2018). In podocytes, intermediate filaments are localised to the primary processes and cell bodies (Drenckhahn and Franke 1988). Intermediate filaments are heterogenous, and podocytes express three types of intermediate filament proteins: vimentin, desmin and nestin (Zou et al. 2006). Intermediate filaments in podocytes are thought not to be essential to process formation, however their role in signalling and transport of intracellular cargo is hypothesised to be important for podocyte function (Schell and Huber 2017).

Microfilaments, also known as the actin cytoskeleton, are structural cellular formations found in most eukaryotic cell types and can mediate a variety of functions, such as motility, polarity, adhesion and mitosis (Faul et al. 2007; Heng and Koh 2010; Mitchison and Cramer 1996; Parsons, Horwitz, and Schwartz 2010). The actin cytoskeleton is comprised of globular actin (G-actin) monomers which polymerise to form filamentous actin (F-actin) (Oosawa et al. 1959). F-actin microfilaments are polarised, as the barbed end (positive) polymerises faster than the pointed end (negative) (Woodrum, Rich, and Pollard 1975). F-actin polymerisation is reversible at both ends and F-actin filaments are highly dynamic structures that undergo “treadmilling” as a form of regulation. Treadmilling is defined as the turnover of actin filaments, where “newer” G-actin monomers join at the barbed end and “travel” down the filament as the “older” G-actin monomers dissociate at the pointed end. Treadmilling is mediated by a number of cellular proteins, such as the Rho family of small GTPases, Cofilins, Profilins, and TB4 (Hall 1998; Hotulainen et al. 2005; Neuhaus et al. 1983; Sanders, Goldstein, and Wang 1992).

1.3.2 F-actin dynamics

There are three distinct stages of actin polymerisation: activation, nucleation and elongation (Steinmetz, Goldie, and Aebi 1997). A visualisation of actin dynamics, including all the following proteins, is provided (**Figure 1.4**).

1.3.2.1 *Activation*

G-actin exists in the cytosol bound to actin sequestering molecules, such as thymosin β-4 (TB4), thymosin β-10 and profilin (Yu *et al.*, 1993; Xue *et al.*, 2014), and actin dynamics are controlled by ATP hydrolysis (Rould et al. 2006). TB4 is the main G-actin sequestering peptide in the cytosol and serves to preserve a pool of G-actin that does not readily polymerise (Sanders et al. 1992). G-actin bound to ATP, Mg^{2+} and TB4 is the dominant form in the cytosol (Carlier et al. 1993). However, there are small numbers of G-actin monomers that bind to Ca^{2+}, ADP+P_i and AMP, which are far less stable than the dominant form (Carlier et al. 1993; A Weber et al. 1992).

TB4 and profilin maintain the cytoplasmic G-actin concentration between 20 – 100 μM, which is 200 – 1000-fold higher than the critical concentration required for actin polymerisation (0.1 μM) (Carliers, Pantalonis, and Korns 1987; Xue et al. 2014). The TB4-G-actin complex is incapable of polymerisation (Yu *et al.*, 1993), therefore, there must be an exchange of G-actin between TB4 and profilin. The profilin-G-actin complex readily promotes G-actin polymerisation and profilin competes with TB4 for the binding of G-actin (Goldschmidt-Clermont et al. 1992), creating a system which can be tuned by the cell to promote or prevent polymerisation (**Figure 1.4a**). The TB4-G-actin complex can readily support the formation of a ternary complex including profilin (Goldschmidt-Clermont et al. 1992; Xue et al. 2014). This ternary complex formation causes TB4 to undergo allosteric changes and releases the G-actin monomer to profilin (Xue et al. 2014). The profilin-G-actin complex is then ready for polymerisation. This exchange also promotes the conversion of ADP-G-actin to ATP-G-actin, which polymerises much more readily (Goldschmidt-Clermont et al. 1992).

1.3.2.2 *Nucleation*

All actin filaments must originate from somewhere and the process of polymerisation initiation is called nucleation. Nucleation is mediated by several actin binding proteins, such as formins. Formins have been associated with the formation of stress fibres, actin rings and actin cables (Miao et al. 2013; Takeya et al. 2008; Tolliday, VerPlank, and Li 2002). Formins contain the unique FH2 domain that promote *de novo* actin nucleation. Two FH2 domains from a dimer that stabilises G-actin monomers in the cytosol, bringing them to close proximity and catalyse G-actin dimer formation. This is a slow process, as the affinity for FH2-G-actin is low (<5 μM), however, it has been shown that the actin binding protein profilin vastly accelerates the subsequent elongation process (**Figure 1.4a**) (Neidt, Scott, and Kovar 2009; Romero et al. 2004; Yu et al. 2018). At low cellular concentrations, it has also been shown that cofilin promotes the *de novo* nucleation of F-actin filaments (Andrianantoandro and Pollard 2006; Siton and Bernheim-Groswasser 2014).

The second actin nucleation promoting molecule is the Arp2/3 complex which works in conjunction with nucleation promoting factors, such as Wiskott-Aldrich syndrome protein (WASP) and SCAR/WAVE (Pollitt and Insall 2009; Robinson et al. 2001; Rouiller et al. 2008). Arp2/3 complex catalyses polymerisation of an F-actin filament that is branched from an already existing filament (Smith et al. 2013), mimicking the structure of G-actin to recruit 1 to 2 G-actin monomers, therefore stimulating nucleation and polymerisation (**Figure 1.4a**) (Rouiller et al. 2008). The key difference between formins and the Arp2/3 complex is the necessity of a pre-existing F-actin filament, however, both methods of nucleation serve their own respective cellular purposes. This form of F-actin nucleation is most commonly associated with lamellipodia and focal adhesion formation (Suraneni et al. 2012).

1.3.2.3 *Elongation*

Once nucleation is complete, actin filaments readily extend at their barbed end until the reservoir of G-actin is depleted, or capping proteins halt this extension (Atkinson, Hosford, and Molitoris 2004; Edwards et al. 2014). Since these capping proteins are abundant in cells, there are factors present that “shield” the barbed end of the

polymerising filament. The nucleation factors formins use their unique donut shaped FH2 domain homodimers to encapsulate the barbed end of the filament and move along the growing filament to shield the barbed end from capping factors (Vavylonis et al. 2006). The FH1 domains of formins interact with profilin with an affinity of 3.4 – 17.8 μM (Kursula et al. 2008; Neidt et al. 2009) to recruit G-actin monomers to the barbed end of the filament, accelerating F-actin polymerisation up to 5-fold over free barbed ends (Kovar et al. 2006; Paul and Pollard 2009), although the exact mechanism by which this occurs is still unclear. The dissociation constant of profilin to G-actin monomers is much lower (~0.1 μM) than F-actin (~25 μM) (Bubb et al. 2003; Courtemanche and Pollard 2013; Le et al. 2020), meaning that profilin will dissociate from the G-actin monomers once they polymerise (**Figure 1.4b**).

Another polymerising factor is the Ena/vasodilator stimulated phosphoprotein (VASP) protein family (Kwiatkowski, Gertler, and Loureiro 2003). These proteins localise to actin-rich areas of cells, such as focal adhesions, stress fibres, cell-cell contacts, lamellipodia and filopodia and contribute to cell motility and adhesion (Chesarone and Goode 2009). The Ena/VASP proteins have three parts: an N-terminal EVH1 domain, a central proline-rich region and a C-terminal EVH2 domain (Gertler et al. 1996; Kwiatkowski et al. 2003). The EVH1 domain links VASP to key ligands, such as formins and is important for cellular localisation (Ball et al. 2002; Bilancia et al. 2014). The central region contains at least three binding sites for profilin-G-actin and G-actin and the EVH2 region interacts with G-actin and F-actin (Ferron et al. 2007; Hansen and Mullins 2010; Harker et al. 2019). Ena/VASP proteins form tetramers that bind to the profilin-G-actin complex and can protect the growth of the barbed from capping proteins, but this requires much higher concentrations of Ena/VASP compared to formins (Applewhite et al. 2007; Bachmann et al. 1999; Breitsprecher et al. 2011). Formins and Ena/VASP mediated polymerisation are currently the only two known promotors of elongation (**Figure 1.4b**).

1.3.2.4 *Filament capping, severing and depolymerisation*

Actin filaments will polymerise indefinitely if the components are available and therefore need to be negatively regulated. Proteins that cap the barbed end of filaments contribute to this negative regulation. The heterodimeric α and β subunits of CapZ form a capping protein complex that binds to the barbed end of filaments with a high affinity (dissociation constant of ~ 1 nM) (Wegner et al. 1989). The binding of capping protein halts the polymerisation of actin and also prevents loss of monomers, therefore stabilising the filament (**Figure 1.4c**) (Yamashita, Maeda, and Maéda 2003). Gelsolin is another molecule involved in actin capping, which relies on intracellular Ca^{2+} concentration (Silacci et al. 2004). Gelsolin has two G-actin binding domains and one F-actin binding domain and can bind to the barbed end of the filament, breaking non-covalent bonds between actin filaments and ceasing polymerisation (**Figure 1.4c**) (Feldt et al. 2019; Nag et al. 2013).

F-actin is a slow hydrolyser of ATP, therefore the ATP-G-actin monomers that comprise the newly polymerised F-actin will mediate ATP hydrolysis to ADP + P_i the longer they remain in the filament (Carliers et al. 1987; McCullagh, Saunders, and Voth 2014). F-actin bound to ADP is less stable than ATP bound F-actin, so is more likely to disassemble at the pointed end, where polymerisation is slower than the barbed end (Isambert et al. 1995; Kardos et al. 2007; Merino et al. 2018). Actin depolymerisation factor (ADF) and cofilin are a protein family involved in the severing and depolymerisation of F-actin filaments (Andrianantoandro and Pollard 2006; Bernstein and Bamburg 2010). ADF and cofilin bind to F-actin regions that contain ADP bound monomers creating ADF/cofilin domains of the filament (Suarez et al. 2011; Wioland et al. 2017). These saturated domains become more flexible and shorten their helical structure (Fan et al. 2013; Huehn et al. 2018; Prochniewicz et al. 2005). The saturated regions themselves do not sever, but the regions at domain boundaries will sever and in effect, these severed filaments become their own outright filament (**Figure 1.4d**) (De La Cruz 2009; Ngo et al. 2015). It is currently not clear how these severed filaments depolymerise, and it is suggested that the severed filaments undergo slow depolymerisation from the pointed end (**Figure 1.4d**) (Brieher 2013), although cofilin/ADF is potentially involved in this process as it

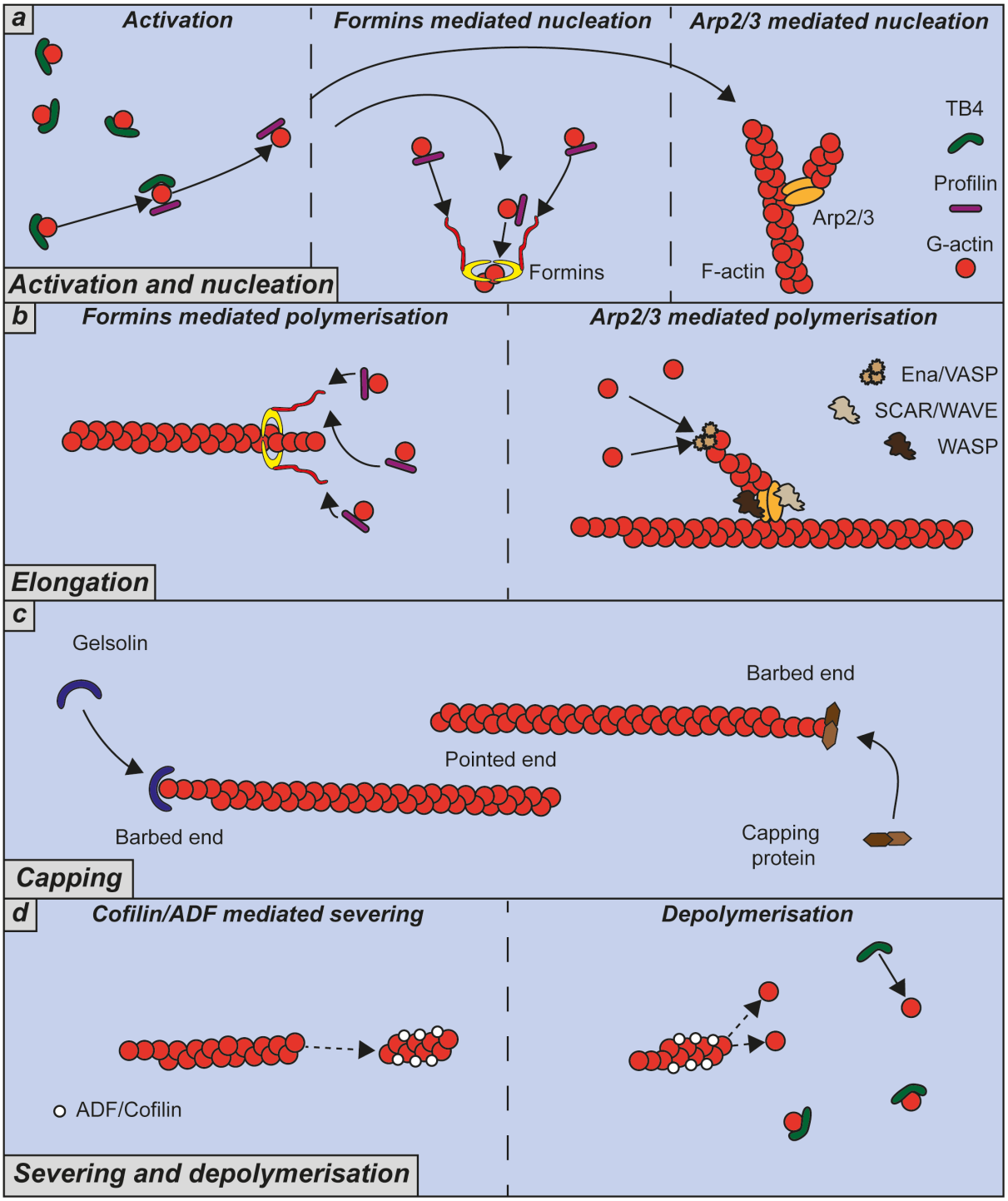

Figure 1.4 – Schematic of actin dynamics in eukaryotic cells. *Diagram depicting the stages of actin treadmilling.* ***(a)*** *Activation and nucleation. G-actin exists in cells sequestered by TB4. Profilin binding initiates activation and nucleation via either Formins or the Arp2/3 complex.* ***(b)*** *Elongation occurs after nucleation. F-actin filaments polymerise de novo from G-actin monomers catalysed by formins or the Arp2/3 complex.* ***(c)*** *F-actin filaments are capped by either gelsolin or capping proteins.* ***(d)*** *Severing of F-actin occurs via cofilin/actin depolymerising factor (ADF) and depolymerisation occurs naturally from severed filaments. Black lines indicate movement of G-actin. Dashed line indicates detachment of F-actin/G-actin. Original diagram.*

has been shown *in vitro* that cofilin/ADF knockout leads to a reduction in the G-actin : F-actin ratio (Hotulainen et al. 2005).

1.3.2.5 *Rho GTPases*

The Rho family of small GTPases includes RhoA, Cdc42 and Rac1 and performs several essential cellular functions, such as cytoskeletal organisation, regulation of cell shape and motility (Etienne-Manneville and Hall 2002; Hanna and El-Sibai 2013; Kim et al. 2018; Sit and Manser 2011). The Rho GTPases cycle between two states; the active state bound to GTP and the inactive state bound to GDP. The active state recognises target proteins, such as Rho-associated protein kinase-1 (ROCK1) and ROCK2 to generate a cellular response until GTP hydrolysis to GDP returns the GTPases to their inactive state (Etienne-Manneville and Hall 2002).

1.3.3 The podocyte cytoskeleton

The podocyte cytoskeleton is extremely complex and critical for glomerular function (Blaine and Dylewski 2020; Schell and Huber 2017; Welsh and Saleem 2012). Phalloidin staining, which is the gold standard to reveal F-actin (Melak, Plessner, and Grosse 2017), of isolated glomeruli from adult rats displayed an intense F-actin signal in podocyte foot processes, with a weaker signal in the cell body (Cortes et al. 2000), demonstrating that the foot processes are the main site of F-actin in podocytes. Electron microscopy immunogold labelling of adult rat podocyte F-actin *in vivo* further characterised this network as a thick F-actin cable that runs longitudinal along the foot processes parallel to the GBM and cortical actin fibres which occupy the cytoplasm around the cable (Ichimura, Kurihara, and Sakai 2003) (**Figure 1.5a**).

It has been suggested that the thick, central actin cable could be involved in generating the tensional forces, whereas the cortical actin purely provides the unique pyramidal structure of the foot processes (Ichimura, Kurihara, and Sakai 2007). Recent studies have supported this hypothesis. Super-resolution microscopy to visualise BALB/c adult mouse glomeruli suggested that the foot process network is non-contractile due to the absence of myosin IIa and that the contractile actin fibres are located in the cell body and major processes (Suleiman et al. 2017). The authors went on to suggest that the contractile fibres in the cell body and primary processes

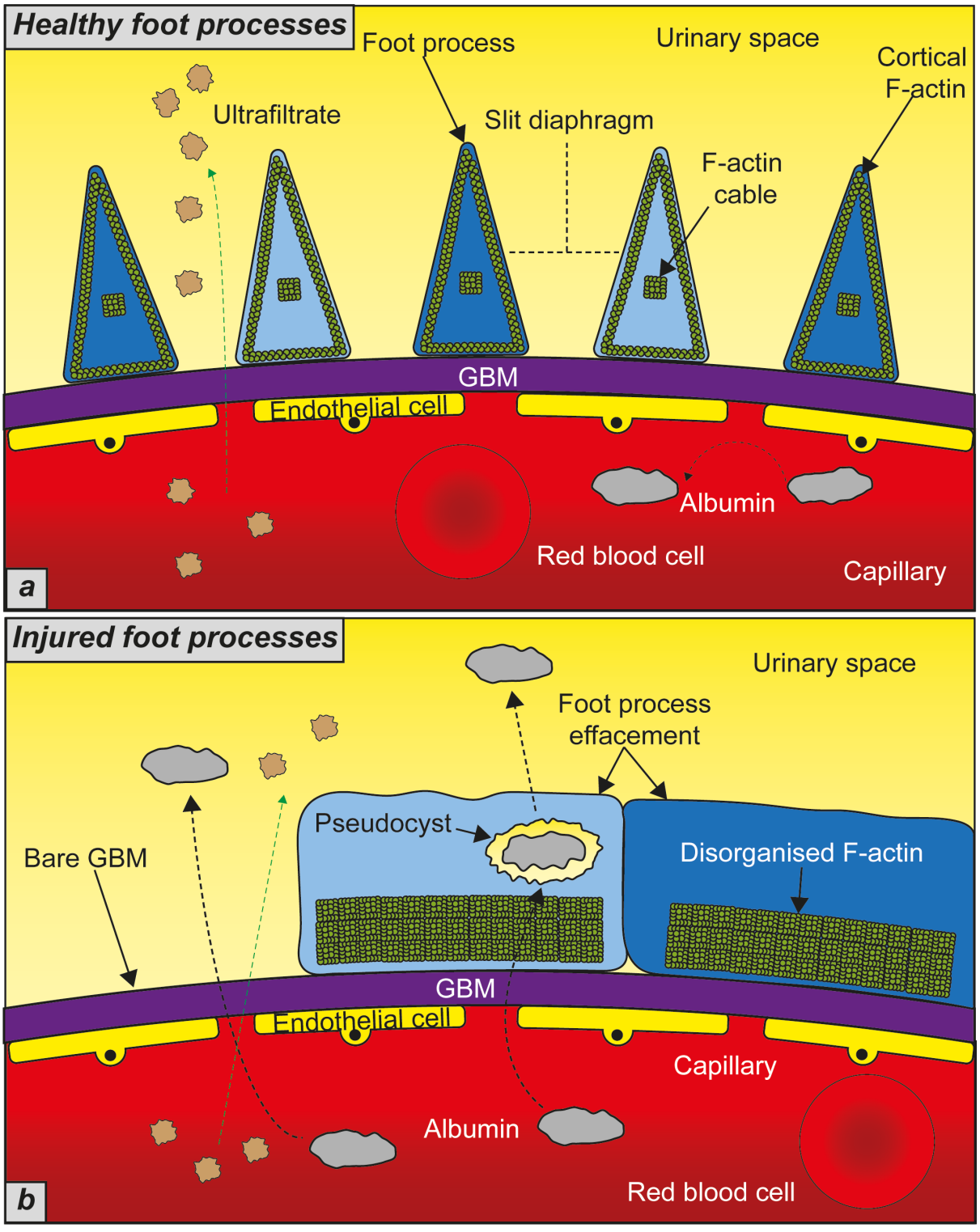

Figure 1.5 – Comparison of podocyte foot processes in health and injury. (a) *Lateral view of the glomerular filtration barrier in healthy podocytes. Ultrafiltrate can freely filter through into the urinary space while albumin is excluded due to charge and size. F-actin is arranged with a thick central cable and cortical F-actin.* ***(b)*** *Example of how F-actin could be disorganised in podocytopathies. Albumin is lost to urinary space through bare areas of GBM and podocyte pseudocyst formation. F-actin is disorganised to a mat adjacent to the GBM. Black dashed arrows indicate direction of albumin and green dashed arrows indicate direction of ultrafiltrate. Original figure.*

generate tension to the foot processes that strengthen the focal adhesion complexes in order to maintain the SD.

There are certain proteins in podocyte foot processes that have a role in F-actin organisation. Synaptopodin is a proline-rich actin binding protein in podocytes that promotes F-actin stress fibres formation and organisation, and cell motility (Asanuma et al. 2006; Mundel, Heid, et al. 1997). Mice lacking synaptopodin have no renal phenotype, but the effect of glomerular injury is exacerbated *in vivo* (Ning, Suleiman, and Miner 2020). The authors also showed by immunofluorescent staining and scratch wound assays that podocytes lacking synaptopodin *in vitro* displayed reorganisation of F-actin, increased adhesion molecules and impaired motility (Ning et al. 2020). Mechanistically, synaptopodin promotes the formation of stress fibres in podocytes by inhibiting ubiquitination and proteasomal degradation of RhoA and the activation of Rac1 (Asanuma et al. 2006; Buvall et al. 2013, 2017; Wong et al. 2012).

Synaptopodin works in conjunction with another important foot process actin binding protein, α-actinin. The most well defined feature of α-actinin is its ability to bundle and cross link F-actin filaments, creating a more resilient structure (Asanuma et al. 2005; Honda et al. 1998) (**Figure 1.3**). It has been demonstrated *in vitro* and *in vivo* that synaptopodin directly interacts with and regulates the activity of α-actinin-4 in the foot processes, leading to elongation of actin filaments and improved plasticity of the actin filaments, meaning a lower chance of the filaments breaking (Asanuma et al. 2005). More recently, it has also been shown that mutations to the gene encoding α-actinin-4, which are present in some forms of focal segmental glomerulosclerosis (FSGS), lead to exacerbated podocyte detachment and irreparable F-actin damage in response to mechanical stress *in vitro* (Feng et al. 2018; Kaplan et al. 2000), demonstrating the importance of α-actinin to podocytes.

The basal membrane of the foot processes adhere to the GBM through focal adhesions. These focal adhesions are mostly composed of a3β1 integrin and aβ dystroglycan molecules, which bind to laminin and agrin in the GBM and are linked to the cytoskeleton through linker proteins (Korhonen et al. 1990; Pozzi et al. 2008; Raats et al. 2000; Regele et al. 2000) (**Figure 1.3**). Integrins link to the cytoskeleton

via a complex of α-actinin-4, talin, vinculin and integrin linked kinase (ILK) (Drenckhahn and Franke 1988; Faul et al. 2007; Otey et al. 1993; Yamaji et al. 2004), whereas dystroglycan links the cytoskeleton to the GBM via utrophin (Raats et al. 2000). The focal adhesion complexes can also initiate intracellular signalling in response to stimuli, such as mechanical stress (K. Endlich, Kliewe, and Endlich 2017; Friedland, Lee, and Boettiger 2009; Vogtländer et al. 2009).

Disorganisation of the foot process actin network *in vivo* has been associated with foot process effacement, SD destruction and albuminuria (Faul et al. 2007; McClatchey and Fehon 2009; Perico et al. 2016; Suleiman et al. 2017; Welsh and Saleem 2012; Yu et al. 2013). When the foot processes efface and retract into the primary processes, the cell body can adhere to the GBM and the F-actin network can disorganise into a mat of F-actin running parallel to the GBM. This is accompanied by widespread myosin IIa expression and an increase in F-actin, α-actinin and synaptopodin expression (**Figure 1.5b**) (Shirato *et al.*, 1996; Shirato, 2002; Suleiman *et al.*, 2017; Ning, Suleiman and Miner, 2020). The exact mechanisms and disorganisation of F-actin in podocyte injury will be discussed later in this introduction.

1.4 **Chronic kidney disease**

1.4.1 Prevalence of chronic kidney disease

The term CKD refers to a group of highly heterogenous diseases affecting the structure and function of the kidney (Levey and Coresh 2012). Some patients with CKD will progress to ESKD, requiring life-long dialysis or a kidney transplant (Eckardt et al. 2013). CKD affects approximately 5.6 million people in the U.K. with many cases remaining undiagnosed, and the mean age of ESKD diagnosis is 72.2, suggesting that progression to ESKD occurs in older patients (Bikbov et al. 2020; Hirst et al. 2020; Nguyen et al. 2018). Sadly, some patients with ESKD can succumb to the condition. It was estimated that in 2017, 6766 people in the U.K. died of CKD (Bikbov et al. 2020). However, the prevalence and death rate of CKD in the U.K. per 100,000 people fell 11.4% and 14.5% respectively from 1990 to 2017 (Bikbov et al. 2020). However, even though the prevalence per 100,000 people has declined, the absolute number of people with CKD in the U.K. has risen, as population has

increased between 1990-2017 (the time frame analysed by Bikbov *et al.*), therefore the pressure on the NHS from CKD is still increasing.

It has been estimated that in 2009-2010 the cost to NHS England of CKD was between £1.44-1.45 billion, equating to ~1.3% of all NHS spending that year. Renal replacement therapy (dialysis or transplant) alone was responsible for over half of this amount, but only 2% of CKD patients required it (Kerr et al. 2012). According to NHS Kidney Care, the cost of CKD is more than breast, colon, lung and skin cancer combined. The same report states that between ages of 65 and 74, 1 in 5 men and 1 in 4 women have CKD and that recipients could wait up to 3 years for a transplant (Kerr et al. 2012).

CKD is not only a significant issue in the U.K. It is estimated that CKD affects up to 750 million people worldwide, which is a global prevalence of 9.1% (Bikbov et al. 2020). The global prevalence per 100,000 people increased 1.2% from 1990 - 2017, demonstrating that CKD diagnosis globally is rising with time. In 2017 it was estimated that globally 1,230,168 people died of CKD, an increase of 2.8% per 100,000 since 1990 (Bikbov et al. 2020). The prevalence and death rate of CKD is much higher in countries with lower GDPs and less developed health care systems (Bikbov et al. 2020) that may not be able to afford as many dialysis machines, drugs or highly trained surgeons. Death by CKD is expected to rise to 4 million globally in a worst-case scenario by 2040 (Foreman et al. 2018) underlying the urgent need for novel, widely accessible therapies.

1.4.2 Risk factors of CKD

The prevalence of CKD increases with age and poor life-style choices. Diets with low nutritional value, high caloric intake, high animal protein, saturated fat, sodium and phosphorous intake are all related to higher CKD incidence (Crews et al. 2014; Gutiérrez 2015). Physical inactivity leads to greater chance of cardiovascular disease, and CKD can develop as a co-morbidity, through endothelial dysfunction and hypertension (Bharakhada et al. 2012; Stengel et al. 2003; Stump 2011). It is a well-established fact that physical activity improves cardiovascular health. The

kidneys and heart have an intimate relationship, with pathogenesis in one organ being linked to pathogenesis in the other (Chrysohoou et al. 2010).

A major risk factor for CKD is diabetes. It is thought that between 20% and 40% of patients with diabetes will develop diabetic nephropathy, and advanced diabetic nephropathy is the leading cause of glomerulosclerosis and ESKD worldwide (Dronavalli, Duka, and Bakris 2008). The interaction between hyperglycaemia-induced metabolic and haemodynamic changes, as well as genetic predispositions, are major mechanisms by which diabetic nephropathy occurs (Ziyadeh 2004).

Tobacco smoking is another factor associated with CKD onset. One study of a population in Wisconsin, America, stated that tobacco smokers had almost a 2-fold higher chance of developing CKD than non-smokers (Shankar, Klein, and Klein 2006). Another study based in America has shown that smokers have on average a 1.63 higher chance of developing CKD, and heavier tobacco use was associated with a higher chance of CKD. The study also made distinctions between CKD groups, and hypertensive nephropathy (2.85 higher chance) and diabetic nephropathy (2.24 higher chance) showed an increased incidence compared to non-smokers, whereas there was no increased risk of developing glomerulonephritis (Yacoub et al. 2010).

Illicit and pharmacological drug use is a risk factor for decline in kidney function. Cocaine and opiate use was associated with a 1.2 and 1.8 higher chance of albuminuria development and estimated glomerular filtration rate (eGFR) decline respectively in a study of a population in Baltimore, Maryland, U.S.A (Novick et al. 2016). Heroin use has also been associated with acute kidney injury, immune-complex membranoproliferative glomerulonephritis, FSGS, amyloidosis and chronic interstitial nephritis (Sethi 2018). Non-steroidal anti-inflammatory drugs (NSAIDs) that inhibit cyclo-oxygenase mediated formation of prostaglandins, such as ibuprofen, are also linked to decline in kidney function via damage to the mesangium, GBM and podocytes (Gooch et al. 2007; Nasrallah et al. 2013).

It has been thought that high alcohol intake is also associated with declining kidney function and CKD development, which was more apparent at younger ages

compared with older people (Pan et al. 2018; Shankar et al. 2006), however, conflicting reports are now emerging. One report showed that alcohol drinkers were actually 30% less likely to develop CKD than non-drinkers in a 10 year follow up study (Bundy et al. 2018) and another report associated heavy alcohol consumption with an inverse risk of developing CKD (Koning et al. 2015). This is an area of research that requires further investigation, especially due to how common alcohol consumption is worldwide.

1.4.3 Current treatment for CKD

Pharmacological intervention aims to slow CKD progression. Angiotensin converting enzyme (ACE) inhibitors are widely used to supress the progression of CKD to ESKD. ACE inhibitors reduce proteinuria, rate of renal function loss, blood pressure and protect against the cardiovascular comorbidities in CKD (Chiurchiu, Remuzzi, and Ruggenenti 2005; Turner et al. 2012). ACE inhibitors interfere with renin angiotensin aldosterone system (RAAS) activity by reducing the production of angiotensin II and aldosterone. This leads to vasodilation of renal vessels, in particular, efferent arterioles, and reduction of systemic, renal and glomerular blood pressure (Sidorenkov and Navis, 2014). ACE inhibitors can however lead to adverse effects, such as reduction in renal function, hypotension, hyperkalaemia, elevated bradykinin levels and hepatotoxicity (Sidorenkov and Navis 2014).

Patients begin dialysis once they are diagnosed with ESKD, because there is a build-up of waste products in the blood, such as urea and creatinine (Aronson, Mittleman, and Burger 2004). Dialysis was first conceptualised by John Jacob Abel in 1912 and the first dialysis performed on humans was in 1943 (Crowther, Reynolds, and Tansey 2010; Eknoyan 2009). Haemodialysis involves an intravenous needle attached to a tube that transports the patient's blood into the dialysis machine. The dialysis machine works in a similar way to the kidney – there is a semipermeable membrane where molecules that are small enough to pass through will, and other larger molecules, e.g. blood cells, will not pass through the membrane. The filtered blood is then transported back into the patient (Mallick and Gokal 1999). There are alternatives to haemodialysis, such as peritoneal dialysis, which involves inserting a tube into the abdominal cavity and using the peritoneal

membrane as the partially permeable membrane (Gokal and Mallick 1999). Since metabolism causes a regular build-up of waste products, dialysis must be performed 3-4 times per week, which can have an impact on the patient's quality of life (Daugirdas, Blake, and Ing 2007).

Current and emerging treatment options are tailored to specific types of CKD. Many forms of CKD are immune mediated, so immunosuppressive drugs such as steroids are used to suppress the immune reaction (Berg and Nilsson-Ehle 1996; Hanamura et al. 2012). Adenosine-3′,5′-cyclic monophosphate (cAMP) inhibitors, such as tolvaptan are sometimes prescribed to PKD patients in attempts to lower total kidney volume (Torres et al. 2012). Finerenone, a non-steroidal mineralocorticoid receptor agonist (Kolkhof et al. 2014), is emerging as a candidate to treat diabetic kidney disease as it has reduced albuminuria in randomised clinical trials (Bakris et al. 2015; Filippatos et al. 2016; Licette, Liu, and Schutte 2015). The novel use of SGLT-2 inhibitors is also growing traction in the clinical field for treatment of CKD patients. SGLT-2 inhibitors block the reabsorption of glucose into the blood during filtration in order to reduce hyperglycaemia in diabetic kidney disease patients (Scheen 2015) and have been shown to decelerate loss in eGFR and reduce proteinuria in patients (Heerspink et al. 2020; Neuen et al. 2019; Sugiyama et al. 2019).

The final option for ESKD patients is a kidney transplant. Humans can live with only one kidney, so it is possible to receive a transplant from a living or deceased donor. If the transplant is successful, the patient would have their life extended by 10-15 years on average in comparison to a patient solely on dialysis (Wolfe et al. 1999). However, there are complications with transplantation, such as organ rejection. The patient's antigens must be the same in order for rejection not to occur, and immunosuppressive drugs used post-operatively that lower the risk of rejection may pose a higher risk of infection (Zou et al. 2007). There may also a long waiting time before a compatible donor becomes available. Kidney transplantation is the option that all CKD patients will desire, as it offers the best clinical outcome. However, this is a highly invasive procedure and requires recovery following the surgery. Also, available organs for transplant are in short supply, highlighting the need for novel, non-invasive interventions.

1.4.4 CKD pathophysiology

CKD in humans and other mammals can be a result of defects in any component of the nephron. Glomerular injury is regarded as damage to one more component of the glomerulus that hinders its ability to perform ultrafiltration of the blood. This can manifest in a diverse range of phenotypes, such as mesangial matrix expansion, podocyte detachment, thickening of the GBM, macrophage infiltration, podocyte foot process effacement, podocyte motility and glomerulosclerosis (Butt et al. 2020; Gross et al. 2004; Reiser et al. 2004; Samnegård et al. 2005; Vasilopoulou et al. 2016; M.-S. Zou et al. 2010). This section will focus on the pathophysiology of glomerular diseases in humans, and particularly FSGS and glomerulonephritis (GN).

1.4.4.1 *Pathophysiology of FSGS*

FSGS, by definition, is sclerosis of a compartment (not the whole glomerulus) of some (but not all) glomeruli in the kidneys. FSGS is characterised as an increase in sclerotic and mesangial matrix in the glomeruli, which causes capillary loop collapse and a dysfunctional glomerular filtration barrier (Reidy and Kaskel 2007). The glomerular compartment the sclerotic region is found in defines the classification of FSGS. Sclerosis at the vascular pole is classified as the perihilar variant. The cellular variant of FSGS is associated with hypercellularity in the capillary lumen. The tip variant is sclerosis near the tubular pole of the glomeruli and the collapsing variant is one or more glomeruli with global or segmental capillary loop collapse (Reidy and Kaskel 2007). There are two types of FSGS based on their origins: primary and secondary FSGS. Primary FSGS involves direct podocyte injury that contributes to capillary loop collapse and sclerosis. Secondary FSGS is mediated by external factors, such as drug toxicity, obesity, hypertension or viral infections (Lim et al. 2016). Both primary and secondary FSGS normally cause an increase in proteinuria and are typically diagnosed by kidney biopsy (Rosenberg and Kopp 2017).

Podocyte injury is one of the earliest observable features in human FSGS. A number of genetic defects in podocytes have been identified to contribute to the pathogenesis of FSGS. *NPHS1*, *NPHS2*, *CD2AP* and *ACTN4* are all transcripts which encode podocyte SD proteins, and mutations in these genes can result in FSGS (Boute et al. 2000; Gigante et al. 2009; Kaplan et al. 2000; Kestilä et al.

1998). Alterations to one or more of these transcripts induces morphological and functional changes to the foot processes and SD, resulting in a defective glomerular filtration barrier. Mutations in *WT1* (Wilms tumour 1) can also cause FSGS. *WT1* is a podocyte transcription factor which regulates *NPHS1* transcription, therefore *WT1* mutations can have detrimental effects to nephrin expression and SD integrity (Wagner et al. 2004).

There is also evidence that circulating factors may contribute to podocyte injury in FSGS patients. Electron microscopy studies have identified that within minutes of blood reperfusion to healthy transplanted kidneys in FSGS patients, podocyte foot process effacement is initiated (Chang et al. 2012). One serum factor possibly involved in the pathogenesis of FSGS is soluble urokinase receptor (suPAR). suPAR is a receptor for urokinase that can act as a signalling orchestrator by associating with other transmembrane receptors, such as integrins (Wei et al. 2011). suPAR was increased by 2-fold in the serum of patients with recurrent FSGS compared to healthy patients (Wei et al. 2011), suggesting that suPAR may be an important circulating factor causing FSGS. However, circulating suPAR increase has also been identified in other glomerular diseases, such as lupus nephritis (Qin et al. 2015). Therefore, more investigation is required into the role of suPAR, and other circulating factors, in FSGS.

Podocyte loss is one mechanism of FSGS pathophysiology. Viable cells have been collected from the urine of patients with FSGS. The cells were then cultured *in vitro* and immunostained for podocalyxin, a SD protein found in podocyte foot processes, strongly suggesting that FSGS causes podocyte detachment (Vogelmann et al. 2003). Cytoskeletal disorganisation has also been implicated in the pathogenesis of FSGS by super resolution microscopy. The authors used synaptopodin as a marker for podocyte foot process F-actin, and myosin IIa as a marker for contractile F-actin. In healthy kidney biopsies, synaptopodin was restricted to the foot processes and myosin IIa was localised to the podocyte cell bodies. In FSGS, myosin IIa was found to co-localise with synaptopodin in the foot processes, which resembled sarcomere like structures (Suleiman et al. 2017). This suggests that in FSGS, there is a shift of contractile F-actin from the cell body to the foot processes, which could result in

conformational changes to the podocytes and glomerular filtration barrier.

1.4.4.2 *Pathophysiology of GN*

GN is a term that describes a group of conditions where an autoimmune response is generated against components of the glomerulus, resulting in nephrotic syndrome. There are five main sub-groups of diseases classed as GN: post-infectious GN; immunoglobulin A (IgA) nephropathy; anti-GBM nephritis; anti-neutrophil cytoplasm antibodies (ANCA)-positive GN and lupus nephritis (Couser 2012). GN typically results in proteinuria, glomerular crescent formation and high levels of glomerular inflammation (Couser 2012).

Post-infectious GN occurs as the result of an infection and is generally not thought of as an autoimmune response. Circulating immune complexes, composed of pathogenic antigens and IgG antibodies to them, can get trapped in the glomeruli (Couser 2012). This complex results in complement activation, resulting in neutrophil activation and recruitment to the glomeruli, where oxidants and proteases are released causing glomerular injury. The classical and alternative complement pathways are important mediators of glomerular injury. Patients with complement deficiencies often have long-term post-infectious glomerulonephritis, compared with childhood patients who normally recover (Sethi et al. 2013).

IgA nephropathy is the most common form of glomerular injury worldwide and is a result of an autoimmune response against the glomeruli (Cattran et al. 2009). Over 100 gene mutations that are associated with IgA nephropathy have been identified in patients (Magistroni et al. 2015). It is likely that IgA nephropathy is triggered by a genetically predisposed autoimmune reaction following exposure to toxins (Couser 2012). *Staphylococcus aureus* antigens have been identified in the mesangium of IgA nephropathy patients, causing deposition of IgA and IgG in the glomerular tuft (Nasr and D'Agati 2011; Worawichawong et al. 2011). Immunoglobulin deposition results in complement activation and sub lytic C5b-9 attack on mesangial cells and endothelial cells (Daha and van Kooten 2016). The mesangial cells then become activated and proliferate, and also release cytokines to recruit neutrophils and macrophages, causing the immune response against the glomeruli (Couser 2012).

The antigen that is mostly targeted in anti-GBM GN is a 14 amino acid fragment of type IV collagen, and some immunoreactivity has also been seen in type III collagen (Pedchenko et al. 2010). These antigens have been shown to have an almost identical structure to some pathogen associated molecular patterns in some bacteria, such as *Clostridia botulinum* (Arends et al. 2006). The antigens in collagen have to undergo confirmational changes in order to become exposed, but it is unclear what the cause of these conformational changes are (Pedchenko et al. 2010). IgG antibodies bind to the exposed antigens activating the classical complement pathway and recruitment of T helper cells. The innate and adaptive immune response then causes damage to the glomeruli, such as what is seen in IgA nephropathy and post-infectious GN (Couser 2016).

ANCA-associated vasculitis is a group of autoimmune diseases that target antigens on the endothelial cells in the glomerular capillaries. *In vitro* studies have shown that cytokines released in response to some infections can prime neutrophils and upregulate adhesion molecules in glomerular endothelial cells and neutrophils, that could result in neutrophil localisation to the glomeruli (Nagao et al. 2007; Radford, Savage, and Nash 2000). Primed neutrophils trapped in the glomeruli express ANCA-specific antigens on their cell surface, which ANCAs bind to causing over activation of neutrophils (Nakazawa et al. 2019). Excessive neutrophil activation induces abnormal cytokine production, release of lytic enzymes and reactive oxygen species that damage the glomerular endothelial cells and can cause endothelial cell death (Nakazawa et al. 2019).

Lupus nephritis is a complication that can occur in patients with systemic lupus erythematosus (SLE) (Almaani, Meara, and Rovin 2017). Viral infections that initiate interferon-α signalling pathways can trigger lupus nephritis (Gatto et al. 2013). Defects in clearing of apoptotic cells can lead to nucleosome, containing DNA, presenting on the surface of cells, and sometimes histones containing DNA can escape into the blood stream (Liu and Anders 2014). It is theorised that the negatively charged components of the glomerulus (podocyte foot processes and endothelium) can bind to the cationic histones in circulation (Couser 2016). Deposits

of IgG are formed inside the glomeruli and the glomerular injury is primarily mediated by activation of the classical complement response (Birmingham and Hebert 2015). Complement C5b-9 induces cell lysis of glomerular cells and recruits leukocytes to the glomeruli which release reactive oxygen species and proteases, causing glomerular tissue damage (Birmingham and Hebert 2015).

Although the triggers and targets differ between forms of GN, some of the basic mechanisms are similar. Glomerular deposits of IgG result in complement activation, neutrophil and macrophage accumulation (Couser 2012). Macrophages trigger the release of pro-inflammatory cytokines and chemokines to promote the inflammatory response (Couser 2016). Neutrophils release proteases, reactive oxygen species and other factors that damage and lyse glomerular cells (Nagao et al. 2007; Radford et al. 2000). The collective result of the autoimmune response is damage to the glomerular filtration barrier and nephrotic syndrome, which can result in CKD progression (Couser 2016).

1.5 **Glomerular and podocyte injury**

Experimental models of rodent diseases have been developed to mimic some of the phenotypes observed in human glomerular disease models. These experimental models of rodent kidney disease allow deeper investigation into the cellular and molecular mechanisms that occur in kidney injury. Podocytopathies are a common mechanism of glomerular injury in humans and mice (Bierzynska, Soderquest, and Koziell 2014), therefore, this section will aim to explain some causes and underlying mechanisms in podocyte injury, with a focus on the cytoskeleton. Some of the features of glomerular and podocyte injury can be found in **Figure 1.6**.

1.5.1 Adriamycin nephropathy

1.5.1.1 *Overview of Adriamycin nephropathy*

Adriamycin (ADR), also known as doxorubicin hydrochloride, is an anthracycline chemotherapeutic drug. It has been historically used in combination with other chemotherapeutic drugs to treat leukaemia, breast cancer, lung cancer, myelomas, bladder cancer and Hodgkin's lymphoma, among other forms of cancer (Lankelma et

al. 1999; Lipshultz et al. 2010; Von Der Maase et al. 2005; Myrehaug et al. 2008; Orlowski et al. 2007; Piscitelli et al. 1993). ADR prevents cancer cell proliferation by DNA intercalation to prevent transcription and translation of RNA and replication of DNA (Cutts et al. 1996; Raje, Pandav, and Barthwal 2020). ADR also inhibits topoisomerase-II activity, an enzyme which cleaves double stranded DNA for repair, therefore promoting apoptosis (Berger et al. 1996; Deffie, Batra, and Goldenberg 1989; Walker et al. 1991). However, it has been documented that some patients receiving ADR chemotherapy experience nephrotoxic side effects, such as decreased creatinine clearance and podocyte foot process effacement (Burke et al. 1977; Klastersky et al. 1985; Wollina, Graefe, and Karte 2000).

ADR can be used to cause podocyte injury *in vitro* and in rodents *in vivo* to replicate some of the characteristics of FSGS in humans (Bertani et al. 1986; Chen et al. 1998; Lee and Harris 2011). While most strains of rat are susceptible to ADR nephropathy, this is not the case with mice (Pippin et al. 2009). The mouse strains FVB/NJ, CAST/EiJ and the widely used C57BL/6 strain are all resistant to ADR nephropathy, whereas BALB/c and 129/SvJ are both susceptible to ADR injury (Pippin et al. 2009). The difference in sensitivity is due to the presence of protein kinase, DNA activated, catalytic subunit (PRKDC), a protein responsible for the protection of the mitochondrial genome (Papeta et al. 2010). Genome-wide analysis of a range of mouse strains localised the ADR susceptibility locus to chromosome 16A1-B1 (Zheng et al. 2005) and identified the *Prkdc* gene. To confirm that *Prkdc* was responsible, the authors obtained a C57BL/6-*Prkdc* global knockout mouse strain (Kurimasa et al. 1999) and found that the level of glomerulosclerosis was comparable to BALB/c mice after 10 mg/kg intravenous ADR administration. It was also found that podocytes express *Prkdc in vitro* by Western blot, and overexpression of *Prkdc* prevented any loss in cell survival after 0.1 μg/ml and 0.2 μg/ml ADR treatment (Papeta et al. 2010). Mitochondrial genome damage is a major mechanism for toxicity in senescent cells (Suliman et al. 2007), such as podocytes, therefore the authors analysed the mitochondrial genome after ADR injury. There was a significant reduction in the mitochondrial DNA to nuclear DNA ratio in BALB/c mice compared to wild-type C57BL/6 mice, demonstrating a potential mechanism for ADR susceptibility in BALB/c mice (Papeta et al. 2010). Therefore,

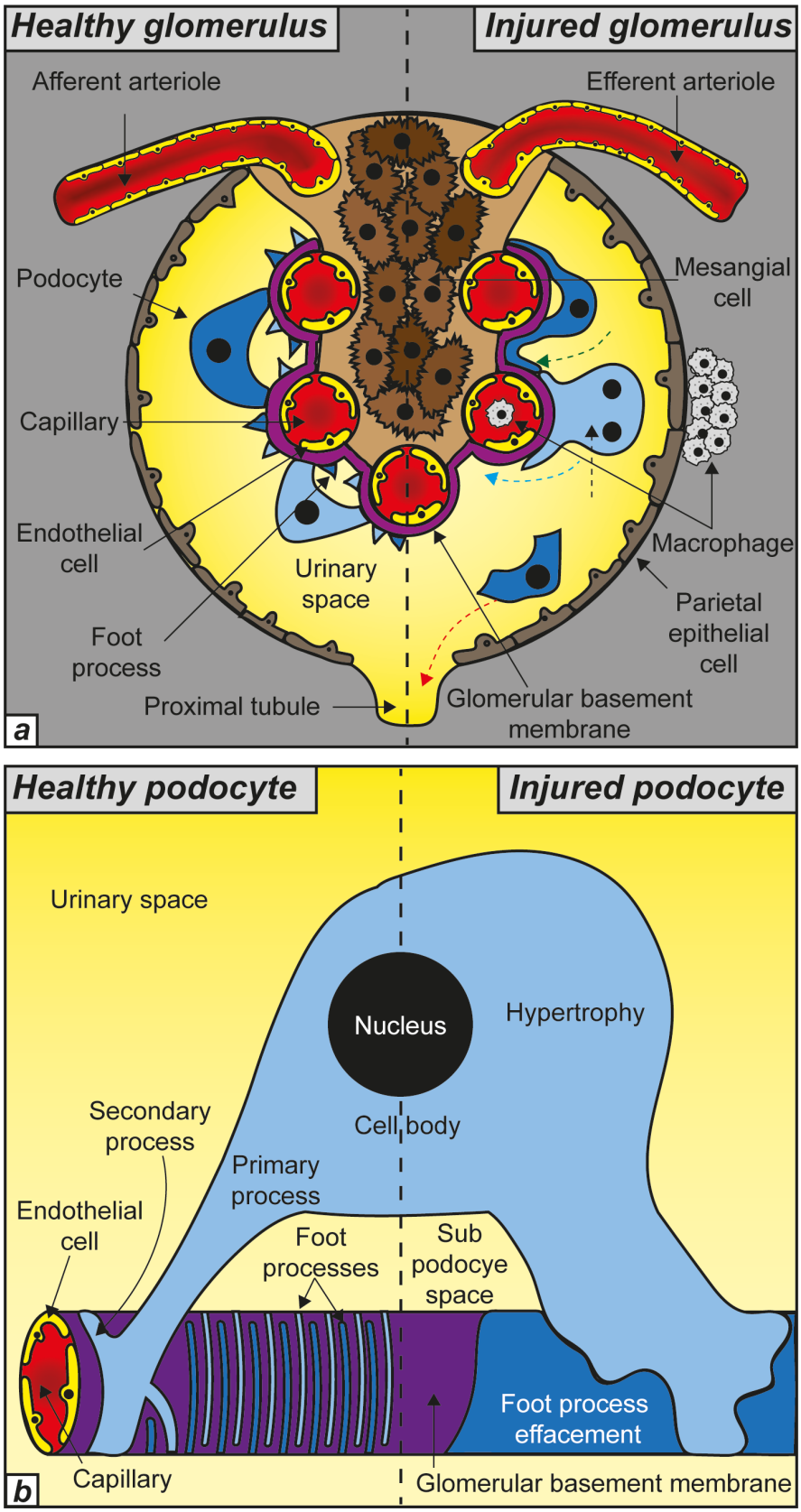

Figure 1.6 – Glomeruli and podocytes in health and disease. ***(a)*** *Comparison of glomeruli in health and disease. Green dashed arrow indicates foot process effacement. Blue dashed arrow indicates podocyte migration. Black dashed arrow indicated podocyte mitotic catastrophe. Red dashed line indicates loss of podocytes to urine.* ***(b)*** *Comparison of podocytes in health and disease. Dashed line indicates barrier between health and disease. Original diagram.*

the majority of *in vivo* studies employing ADR as a glomerular injury model use BALB/c or 129/SvJ mice.

One of the first studies to associate rodent administration of ADR with nephrotoxicity was in the 1980's (Bertani et al. 1982). The authors administered 7.5 mg/kg of ADR to rats and found proteinuria, foot process effacement and loss of sialic acid residues on foot processes at 13 and 28 days after administration (Bertani et al. 1982). Since then, ADR has become a widely used podocyte cytotoxin and the histologic and molecular events have been documented (Lee and Harris 2011; Okuda et al. 1986; Pereira et al. 2015; Wang et al. 2000, 2015; Yang et al. 2018). The standard dosing for ADR in mice is 10 mg/kg, but this can be fine-tuned to increase or reduce disease severity. There are standard biochemical and histological features that scientists employing the ADR injury model can expect. Mice will experience a drop in body weight from which they do not recover (Lee and Harris 2011; Wang et al. 2000). After 5 days, albuminuria will be significantly increased and can peak after 1 week before remaining steadily high up to 6 weeks after induction (Lee and Harris 2011; Wang et al. 2000). Serum albumin concentration and creatinine clearance will drop after 1 week and 4 weeks respectively (Lee and Harris 2011; Wang et al. 2000). Histologically, glomerulosclerosis will begin to occur after 2 weeks and steadily progress (Lee and Harris 2011; Wang et al. 2000). Podocyte foot processes will begin to fuse after 1 week. Podocyte detachment from the GBM and tubular protein casts will be visible after 2 weeks (Lee and Harris 2011; Wang et al. 2000). Some macrophage and immune cell interstitial accumulation may occur in the later stages of injury (Lee and Harris 2011). ADR nephropathy is a model that causes a low degree of mortality, with a high degree of tissue damage, however, mortality may occur after over dosing (Lee and Harris 2011; Wang et al. 2015).

1.5.1.2 *Cytoskeletal reorganisation*

Cytoskeletal disorganisation in podocytes has been associated with foot process effacement and albuminuria *in vivo* (Shirato *et al.*, 1996; Welsh and Saleem, 2012; Yu *et al.*, 2013; Suleiman *et al.*, 2017; Blaine and Dylewski, 2020). In BALB/c mice injured with 14 mg/kg of ADR for 9 days where synaptopodin and myosin IIa were used as surrogates for F-actin staining, there was a shift from non-contractile actin to

contractile actin in podocyte foot processes. There was also an increase in the thickness and distance between synaptopodin clusters in the foot processes, indicative of actin spreading in effaced foot processes (Suleiman et al. 2017). Another recent study administered mice with a C57BL/6 background 12 and 18 mg/kg of ADR and assessed the glomerular F-actin cytoskeleton with FITC-phalloidin after 4 weeks. This study stated that there is a reorganisation of F-actin in the glomeruli from a capillary loop pattern to a collapsing pattern, accompanied by an increase in F-actin fluorescence intensity (Woychyshyn et al. 2020). Podocytes, endothelial cells and mesangial cells all express F-actin (Cortes et al. 2000), so the alterations to F-actin organisation and fluorescence intensity cannot be deemed podocyte specific as there was no double labelling performed. C57BL6/J mice are also inherently less sensitive to ADR nephropathy (Papeta et al. 2010), so the F-actin phenotype in this study may not be representative of human FSGS.

One study using mouse immortalised podocytes exposed them to 0.125 μg/ml ADR and quantified F-actin reorganisation by FITC-phalloidin staining. In this study, the authors found that the predominant form of F-actin in healthy podocytes was cytoplasmic stress fibres, and administration of ADR caused cortical F-actin accumulation and lamellipodia formation (Marshall et al. 2010). Another study treated mouse immortalised podocytes with 0.27 μg/ml of ADR, visualised F-actin with FITC-phalloidin, and quantified stress fibre percentage and mean fluorescence intensity over time. After 12 hours of ADR treatment, the stress fibre prevalence fell from 100% to 75%, which steadily decreased to 20% at 24 hours. From the representative images, the stress fibres formed a “mat” of unorganised F-actin throughout the cell body, with no clear arrangements following ADR treatment, however, this would be clearer if quantification was performed by the authors. The mean fluorescence intensity also fell by over 50% at 12 hours and remained at this level until 24 hours after ADR treatment (Liu et al. 2012). There was also a 3-fold increase in α-actinin-4 mRNA and protein expression, which is responsible for actin bundling (Asanuma et al. 2005). The authors postulated that an increase of α-actinin-4 may be responsible for the uncontrolled F-actin reorganisation that was quantified.

In another study, mouse immortalised podocytes *in vitro* were treated with a higher dose of 0.5 μg/ml of ADR and the cytoskeleton was visualised with FITC-conjugated phalloidin 12 hours later (Ni et al. 2018). The authors did not quantify the F-actin changes, but they could be observed from the representative images displayed. The non-treated podocytes showed a mix of cytoplasmic stress fibres and cortical stress fibres, however, treatment with ADR decreased the F-actin fluorescence shown in representative images. It was not clear if the distribution of F-actin changed following ADR treatment, as this was not quantified. This was accompanied by a reduction in synaptopodin and Wilms tumour 1 (WT-1) expression, as quantified by Western blot (Ni et al. 2018).

One of the most recent papers exploring the effect of ADR on the podocyte cytoskeleton comprehensively quantified F-actin reorganisation in primary podocytes isolated from BALB/c mice injected with 8 mg/kg of ADR via the retro-orbital sinus (Ning et al. 2020). The authors classified F-actin organisation into cytoplasmic or cortical F-actin arrangements and found that there was over 20% reduction in stress fibre prevalence in ADR treated mice compared to saline treated mice. Incidentally, this loss of stress fibres was aggravated by synaptopodin knockout, demonstrating the crucial role of synaptopodin in slowing disease progression (Ning et al. 2020). The deficiency in synaptopodin also decreased RhoA activation, which is responsible for stress fibre formation (Asanuma et al. 2006), and α-actinin-4 did not co-localise with stress fibres, suggesting loss of synaptopodin meant crucial actin regulating signalling cascades did not occur.

WT-1 is a nuclear transcription factor that is specific to podocytes in the glomerular tuft and crucial for proper podocyte development and function (Guo et al. 2002; Morrison et al. 2008). In BALB/c mice treated with 10.5 mg/kg ADR, *Wt1* mRNA was significantly downregulated in kidneys compared to untreated controls. This was accompanied by a 2-fold upregulation of the microRNA miR-206, which was shown to target the 3' untranslated region of WT-1. Furthermore, the characteristics of ADR were mimicked by upregulating miR-206 in podocytes *in vitro*, including a significant reduction in synaptopodin and a reorganisation of podocyte cytoplasmic stress fibres to cortical stress fibres (Guo, Guo, and Su 2016). The wide range of published

literature demonstrate that F-actin reorganisation is a common feature of ADR podocytopathy *in vitro* and *in vivo*.

1.5.1.3 *Podocyte motility*

Two different types of cellular motility have been described – translocative motility and stationary motility (Haemmerli, Arnold, and Sträuli 1983). Translocative motility was described as motility in the X, Y or Z plane, whereas stationary motility was described as cellular motility without any directional migration. An example of stationary motility in podocytes is the theory proposed that the foot processes are slightly motile *in vivo* in order to "clean" the sub-cellular space between the GBM and the foot processes of proteins that have been trapped there during ultrafiltration (Welsh and Saleem 2012). This theory has been supported by the evidence of a sub-podocyte space between podocyte cell bodies, podocyte foot processes and the GBM in healthy rat and human samples as visualised and quantified by electron microscopy (Arkill et al. 2014). Rat and zebrafish glomeruli imaged with high powered, time lapse, multi-photon microscopy revealed that healthy podocytes show very little translocative motility (Endlich et al. 2014; Peti-Peterdi and Sipos 2010). The authors theorised that the low number of podocytes showing translocative motility was due to these podocytes becoming activated and damaged in the healthy kidney by an unknown cause. Therefore, the available evidence and theory currently is that healthy podocytes display high levels of stationary motility and low levels of translocative motility in order to maintain a functioning filtration barrier.

Multiphoton microscopy using fluorescently tagged cells is the main way to assess podocyte motility *in vivo* as it is the only technique that allows serial imaging of intact, living tissue (Larson 2011). One study, using podocin-Cre mice of a C57BL6/J, crossed with R26R-Confetti construct expressing mice, to fluorescently label podocytes different colours, assessed podocyte motility in ADR nephropathy (Hackl et al. 2013). The study revealed that glomerular injury caused podocyte clustering and the podocyte processes seemed to overlap and form bridges with the parietal epithelial cell layer and the glomerular tuft. This effect was also mimicked in the early stages (<6 days) of ADR nephropathy. Critically, the study used confetti mice to label individual podocytes different colours in order to track the fate of individual

podocytes to confirm their findings (Hackl et al. 2013). Since both the C57BL6/J and FvB mice are both resistant to ADR nephropathy, the results shown here may not fully mimic the human FSGS phenotype, nevertheless, this study shows that podocytes that are subjected to ADR injury show increased motility.

1.5.1.4 *Podocyte loss*

Podocyte adhesion to the GBM is critical for a functioning glomerulus and podocytes face strong hydrostatic force from the capillary blood flow, which pushes them away from the capillary wall towards the urinary space (Kriz et al. 1994; Kriz, Gretz, and Lemley 1998). One of the classical features of ADR administration is podocyte loss (Kubo et al. 2020). Sprague-Dawley rats injected with 10 mg/kg of ADR displayed a 1/3 decrease in podocyte number per glomerulus and the protein level of a3β1 integrin and α + β dystroglycan, the major podocyte adhesion molecules, in the glomeruli was also markedly decreased. BALB/c mice injected with a slightly lower dose of ADR (8 mg/kg) showed ~45% decrease in podocyte number at 14 days which increased to ~55% decrease at 28 days (Hosoe-Nagai et al. 2017). (M.-S. Zou et al. 2010). Primary podocytes cultured from 129S5 background mice and treated with 1 μmol/ml of ADR showed a 50% decrease in cell adhesion to the matrix. The cells also showed a 90% decrease in a3 integrin and 50% decrease in β1 protein levels with a ~2 fold increase in ILK (Dai et al. 2019). ILK activation has been shown to be a downstream effector in the onset of proteinuria and blockade of ILK activation in puromycin aminonucleoside (PAN) nephrosis prevented podocyte detachment by protection of cell adhesion molecules (Kretzler et al. 2001; De Paulo Castro Teixeira et al. 2005).

Intermediate filaments are normally found in the podocyte cell bodies and primary processes, with no presence in the podocyte foot processes (Zou et al. 2006). Immortalised mouse podocytes treated with 0.25 μg/ml of ADR showed increase in transcript levels of *Nefh,* a type IV intermediate filament, at 6 and 24 hours (Wang et al. 2018). The authors then explored the role of NEFH in cell detachment. Wild type cells treated with ADR showed ~30% cellular detachment, which was increased to ~40% when in NEFH knockdown cells, whereas NEFH overexpression showed no increase in detachment when compared to the wild type (Wang et al. 2018). This

finding implies that the intermediate filaments of podocytes may play a role in cellular adhesion, however, more investigation is required. There have been direct links shown between intermediate filaments and molecules involved in cellular adhesion, such as α-actinin-4, vinculin and utrophin (Leube, Moch, and Windoffer 2015), which are all expressed in podocytes.

Podocytes are terminally differentiated cells that do not replicate under normal conditions, and mitosis in podocyte injuries can lead to podocyte loss (Liapis, Romagnani, and Anders 2013). ADR has been shown to cause mitosis prior to podocyte loss in BALB/c mice injected with 13 mg/kg of ADR (Mulay et al. 2013). Murine double minute-2 (MDM-2) inhibits p53 dependent cell cycle arrest and apoptosis, therefore promoting mitosis (Haupt et al. 1997) and inhibiting MDM-2 in ADR-treated treated mice suppressed podocyte mitosis and detachment. Podocyte mitosis was confirmed by tubulin immunostaining (to identify mitotic spindle), analysis of nuclei shape (bi-nucleated or mini-nucleated cells) and histone-3 immunostaining (marker for metaphase) (Mulay et al. 2013). Furthermore, presence of the cyclin-dependent kinase inhibitor p21 has been shown to prevent podocyte loss in ADR injury in C57BL/6 mice injected with 12 mg/kg of ADR (Marshall et al. 2010). Overall, ADR administration to rodents is an ideal candidate to inflict damage targeted to podocytes.

1.5.2 Nephrotoxic serum nephritis

1.5.2.1 *Induction of nephrotoxic serum nephritis*

Nephrotoxic serum (NTS) nephritis is an inducible model of rodent glomerular injury that mimics some of the pathological features of human autoimmune glomerulonephritis (Pippin et al. 2009). It is one of the oldest models of rodent glomerular injury and studies can be found as early as the 1930's (Smadel 1937). NTS nephritis has the advantage over ADR injury in that it can be used in C57BL/6 mice, which makes using transgenic mice much more accessible (Pippin et al. 2009). NTS nephritis can be induced in two forms; an acute form and a chronic form, which depends on the addition or omittance of a pre-immunisation step (Chen et al. 2002; Hoppe and Vielhauer 2014). Pre-immunisation of the experimental animal with sheep IgG in complete Freund's adjuvant, which normally occurs 5 days before NTS

administration primes the immune system to recognise the NTS antibodies, therefore accelerating the onset of the autologous phase (Chen et al. 2002; Hoppe and Vielhauer 2014).

To create the nephrotoxic serum, glomerular extracts from the experimental species (normally mouse or rat) are homogenised and injected into a secondary species (normally rabbit or sheep) in incomplete Freund's adjuvant (Hoppe and Vielhauer 2014). The secondary species will then create an immune response and polyclonal antibodies against the glomerular structures, such as the GBM, podocytes and endothelial cells. The serum and said antibodies are then extracted. There are two phases of NTS injury – the heterologous and autologous stages (Hoppe and Vielhauer 2014). The heterologous stage is initiated within minutes of injection of NTS, where the polyclonal antibodies will bind to their respective glomerular structures. The binding of the antibodies can also sometimes interfere with podocyte integrin molecules causing foot process effacement (Shirato *et al.*, 1996). Glomerular injury is mediated by complement activation and neutrophil inflammation in the heterologous stage (Assmann et al. 1985; Hébert et al. 1998). Podocytes and endothelial cell toll like receptor molecules can also be stimulated which activates the production of cytokines and chemokines, accelerating macrophage accumulation and NTS nephritis onset (Hoppe and Vielhauer 2014).

The heterologous phase then develops into the autologous phase within 1 week which is the development of the systemic, adaptive immune response against the anti-glomerular antibodies (Chen et al. 2002; Hoppe and Vielhauer 2014). T-cells are released that promote macrophage accumulation to the glomerulus (Tipping and Holdsworth 2006). Furthermore, the T-cells stimulate B-cell activation to promote the production of autologous antibodies against the sheep anti-glomerular antibodies, which are deposited in the glomerulus (Hoppe and Vielhauer 2014). This glomerular deposition of autologous antibodies exacerbates glomerular injury by forming large immune complexes of IgG (Chen et al. 2002; Hoppe and Vielhauer 2014). This glomerular deposition of IgG is reflective of IgG build up in human vasculitis patients (Jennette and Falk 1997).

1.5.2.2 *Expected renal outcomes of NTS nephritis*

Since NTS nephritis is a widely used glomerular injury model, the renal manifestations are well characterised. One study documented the course of NTS nephritis 7, 14 and 21 days after NTS induction in C57BL/6 mice. Urinary albumin to creatinine ratio rose at 7 days, then then further rose at 14 days and finally rose even more at 21 days, suggesting progressive glomerular filtration barrier degradation (Hoppe and Vielhauer 2014). Serum protein concentration was decreased, but serum cholesterol and urea concentration were sharply increased after 21 days. There was also severe glomerular crescent formation and sclerosis, and monocyte, T cell and macrophage accumulation at 21 days (Hoppe and Vielhauer 2014).

Further studies have confirmed and expanded on these characteristics. One study pre-immunised male wild type C57BL/6 mice with 200 μg of sheep IgG 5 days prior to intravenous injection of 150 μl of NTS per 20 g of body weight (Tham et al. 2020). The urinary albumin to creatinine ratio rose sharply after 7 days, suggesting a high level of damage to the glomerular filtration barrier. Damage to the glomerular filtration barrier was further confirmed where serum creatinine levels doubled after 7 days. Histologically, over 35% of glomeruli assessed showed crescent formation and signs of thrombosis, as analysed by light microscopy. Immunofluorescent experiments also revealed a high level of neutrophils and IgG deposition within the glomerular tuft, confirming the role of the immune system in this model of NTS nephritis (Tham et al. 2020).

In another study, C57BL/6 mice injected with sheep IgG prior to administration of sheep NTS were examined 21 days after disease induction (Vasilopoulou et al. 2016). Both urinary albumin concentration and the albumin to creatinine ratio of NTS injected mice increased significantly. This was accompanied by glomerulosclerosis and increased glomerular *Col4a1* expression. There was also an increase in glomerular IgG1 and IgG2a protein expression, as determined by enzyme linked immunosorbent assay (ELISA), demonstrating that the disease induction was in the autologous phase by 21 days post NTS injection. Interestingly, there was an increase in TUNEL positive (apoptotic) glomerular cells which were not WT-1

positive (podocytes) indicating there was significant apoptosis of either mesangial cells or capillary endothelial cells (Vasilopoulou et al. 2016).

It has been shown in the non-accelerated NTS nephritis model (omitting pre-immunisation) that CD1 mice are more sensitive to intravenous NTS injection than C57BL/6 mice (Ougaard et al. 2018). Albuminuria was exacerbated in CD1 mice 2 and 16 days after NTS injection, but interestingly, albumin excretion returned to basal levels after 42 days (Ougaard et al. 2018). There was also an increase in complement 3 and monocyte chemoattractant protein 1 (MCP-1) gene expression in kidney lysates at 7, 21 and 42 days (Ougaard et al. 2018).

One major mediator of glomerular and kidney injury is the innate immune response, and in particular, macrophages. This has been proven in a study injecting mice of a FVB/N background intravenously with NTS, where macrophages were conditionally ablated using diphtheria toxin (Duffield et al. 2005). The authors found that ablating macrophages protected the glomerular filtration barrier, as serum creatinine concentration and the urinary protein to creatinine ratio were both reduced compared to non-ablated mice after 15 and 20 days of NTS treatment. Furthermore, suppressing macrophages reduced glomerulosclerosis and crescent formation, and there were less apoptotic and proliferative cells within glomerular crescents (Duffield et al. 2005). This key study demonstrated that macrophages significantly contributed to the pathogenesis of NTS nephritis.

Another of the key mediators of kidney injury is the adaptive immune response. C57BL/6 mice were pre-immunised with 200 μg of rabbit IgG and then injected with rabbit anti-mouse GBM antiserum 3 days later and the authors assessed the effect of stimulating glucagon-like peptide-1 receptor (Glp1r), a receptor found in the pre-glomerular vascular smooth muscle cells and juxtaglomerular cells (Moschovaki Filippidou et al. 2020). Glp1r is known to have anti-inflammatory properties, including inhibiting cytotoxic T-cell proliferation and increasing the number and function of regulatory T-cells in mice and humans (Hadjiyanni et al. 2010). Treatment with the Glp1r agonist Liraglutide ameliorated some of the effects of NTS nephritis, including increase in the albumin to creatinine ratio, number of glomerular crescents,

expression of *Col1a1*, and macrophage and T-cell accumulation (Filippidou *et al.*, 2020).

Another feature of NTS nephritis is glomerular cell proliferation. Mice with a mixed 129/Sv and C57BL/6 background were pre-immunised with sheep IgG and then 6 days later injected with NTS. Ki-67 immunostaining revealed a significant increase in glomerular proliferative cells compared with vehicle injected mice, although the exact cell type was not identified. Interestingly, NTS also induced an increase in the parietal epithelial cell marker claudin-1 in the glomerular tuft, suggesting that there may be parietal epithelial migration into the glomerular tuft (Dai et al. 2017). Another study administered Wistar-Kyoto rats with 1 ml/kg body weight of sheep anti-rat NTS and studied glomerular proliferation 14 days after NTS nephritis induction by Ki67 immunohistochemistry (IHC). The authors found there was a 7.1 fold increase in Ki67 positive glomerular nuclei compared to saline treated rats, however, there was no double labelling so it was unclear which glomerular cells were proliferating (Succar et al. 2014).

1.5.2.3 *NTS and the podocyte cytoskeleton*

Studies have also attempted to quantify changes to the F-actin cytoskeleton in NTS nephritis. One study in the 1990's associated F-actin disorganisation in the foot processes *in vivo* with foot process effacement (Shirato *et al.*, 1996). NTS nephritis was induced in Sprague-Dawley rats with rabbit anti-rat-GBM serum and F-actin was visualised in the foot processes by immunogold electron microscopy. The authors described an increase in podocyte foot process F-actin accumulation at day 3, 10 and 28 after NTS injection. Interestingly, the F-actin expression in the mesangium was markedly decreased at days 1 and 3 (Shirato *et al.*, 1996). The cytoskeletal disorganisation in the foot processes correlated with foot process effacement, suggesting this is a key underlying mechanism in the pathogenesis of NTS nephritis.

C57BL/6 mice injected with NTS per g body weight were culled after 9 days, and kidneys cryosections were immunostained to visualise synaptopodin and F-actin (Kvirkvelia et al. 2013). NTS induction decreased the glomerular fluorescence intensity of synaptopodin and F-actin. There was also a reorganisation of the

staining, where the glomeruli of control mice would display a “fine linear” expression of F-actin and synaptopodin which was reorganised to a thicker expression. This thicker expression in disease in the study by Kvirkvelia et al., may be representative of the accumulation of F-actin described by Shirato et al. The authors also attempted an *in vitro* model of NTS injury, where they incubated mouse immortalised podocytes with 6% NTS in media for 5 hours. The synaptopodin in untreated cells was spread throughout the whole podocyte cell, but NTS administration led to peri-nuclear accumulation of synaptopodin. Untreated cells also showed a cortical arrangement of F-actin, which was reorganised to accumulation of cytoplasmic stress fibres in NTS treated cells (Kvirkvelia et al. 2013). This *in vitro* model does not fully represent the *in vivo* effects of NTS to podocytes, as the injury is due to a mix of multi-cellular actions *in vivo*, however, is a reasonable starting point and may provide some insight into the earlier mechanisms of podocyte injury.

A different study attempted to replicate the conditions of NTS nephritis *in vitro* by incubating podocytes with macrophage conditioned media. This media had been generated by incubation of macrophages in Dulbecco’s modified eagle medium (DMEM) with 5 mg/ml of lipopolysaccharide (LPS) to activate the macrophages for 48 hours and is a good *in vitro* model of NTS nephritis. The macrophages and LPS were then extracted by filtration followed by the addition of the DMEM to mouse immortalised podocytes for 6, 24, 48 and 96 hours (Succar et al. 2016). The untreated podocytes showed cortical F-actin stress fibres, which did not change over time. The macrophage conditioned media treated cells showed an increase in stress fibre accumulation and fragmentation of F-actin filaments to form unorganised F-actin structures, with 90% of podocytes displaying disorganised F-actin by 96 hours (Succar et al. 2016). This was accompanied by an increase in ZO-1 disorganisation and mRNA expression, a marker for tight junctions and is present in the SD of podocytes connected to the cytoskeleton (Huber et al. 2003). Perhaps cytoskeletal disorganisation could be prevented by modulating ZO-1 transcript levels. Although these conditions do not fully replicate NTS nephritis *in vivo*, this study does provide interesting insight into the role of macrophages in podocyte health, and the conditions of this experiment could be improved by co-culturing with macrophages. Macrophage-induced podocyte cytoskeletal disorganisation has been attributed to

the secretion of tumour necrosis factor α (TNF-α) (Ikezumi et al. 2008), which may potentially be the active pathway in this study.

Another protein expressed by mesangial cells and podocytes during the inflammatory response in NTS nephritis is heparin-binding epidermal growth factor (HB-EGF) (Feng et al. 2000). HB-EFG is a growth factor that is involved in cellular development and inflammatory processes (Miyata et al. 2012), and is not normally found in healthy glomeruli (Nakagawa et al. 1997). HB-EGF mRNA and protein was upregulated after NTS induction in 129S2 mice, as determined by *in situ* hybridisation and immunofluorescent assays. Therefore, the authors then incubated mouse immortalised podocytes with 30 nM of HB-EGF for 48 hours and then visualised F-actin with phalloidin. HB-EGF led to a 60% increase in the formation of F-actin ring-like structures in the podocytes, with the accumulation of membrane F-actin ruffles, similar to lamellipodia (Feng et al. 2000). Ring-like F-actin structures have been associated with mitosis induction in other cell types (Lu et al. 2014), which is detrimental to podocytes and may be occurring here, however the authors did not assess proliferation.

Overall, the diverse effects to the glomeruli and podocytes make NTS nephritis a prime candidate to explore potential therapeutic agents.

1.6 **Thymosin β4**

1.6.1 Discovery of TB4 and early characterisation

Thymosin β4 (TB4) was first isolated in 1981 from calf thymus through a combination of ion-exchange chromatography and gel filtration, and the authors originally thought it to be a thymic hormone that induces terminal deoxynucleotidyl transferase activity in thymocyte populations (Low, Hu, and Goldstein 1981). After its isolation from the thymus, it was discovered by high performance liquid chromatography (HPLC) that TB4 was ubiquitous in mouse and rat tissues, including the spleen, thymus, brain, lung, liver and heart muscles and that TB4 was composed of 43 amino acids and 4.9 kDa in size (Hannappel et al. 1982; Low and Goldstein 1982). The same study found that in rats, TB4 was most abundant in the spleen, with the brain, kidney, liver and testis contained 10 – 20% of splenic levels, and the heart and muscles containing 5

– 10% (Goodall, Hempstead, and Morgan 1983). This was the first study to identify TB4 in the kidney. The same year, synthetic TB4 was generated for the first time in *Staphylococcus aureus* using isolated rat splenic mRNA and validated using co-immunoprecipitation (Filipowicz and Horecker 1983), paving the way for *in vitro* and *in vivo* studies using synthetic and recombinant TB4. The secretion of TB4 has been confirmed in the thymus of rats (Wise et al. 1992).

Nine years after the isolation of TB4 from calf thymus, an actin sequestering peptide was isolated from human platelets using a combination of nondenaturing polyacrylamide gel electrophoresis and *N*-(iodoacetyl)-*N'*-1-sulfo-5-naphthylethylenediamine actin labelling. The authors described the peptide as "binding to the bulk of the unpolymerized actin in platelets and preventing it from polymerising" and designated the protein "Fx" (Safer, Golla, and Nachmias 1990). They found this peptide bound stoichiometrically to muscle G-actin and the authors investigated the amino acid composition of Fx by HPLC. However, they did not link the Fx amino acid composition and the TB4 amino acid sequence discovered previously until a year later, when the actin binding and sequestering abilities of TB4 and Fx were compared by nondenaturing polyacrylamide gel electrophoresis. The amino acid sequence of Fx was deciphered by HPLC and compared to the amino acid sequence of TB4 as published in 1981. The authors found that Fx and TB4 were identical, and therefore the same peptide (Safer, Elzinga, and Nachmias 1991).

1.6.2 TB4 and the actin cytoskeleton

TB4 is a member of the actin binding β-thymosin family and is the major G-actin sequestering protein in mammalian cells (Cassimeris et al. 1992; Nachmias 1993; Safer et al. 1991). One of the first studies to fully investigate the actin binding properties of TB4 determined that TB4 would not bind to isolated muscle and platelet F-actin, only G-actin, and that TB4 suppressed the rate of actin polymerisation. The authors also determined that the dissociation constant of G-actin : TB4 complexes was between 2 – 3 μM (Weber *et al.*, 1992). Since then, the actin binding properties of TB4 have been investigated in detail. Using muscle actin and TB4 purified from sheep spleen by HPLC, it was shown that TB4 binds to ATP-G-actin with a much higher affinity than ADP-G-actin. The former produced a dissociation constant of 1.7

– 2 μM, whereas the latter gave a dissociation constant of 80 – 85 μM (Carlier et al. 1993). The difference in the affinity is most likely due to alteration of the TB4 binding site on actin due to the nucleotide that is bound to it, as shown by HPLC (Carlier et al. 1993).

Around the same time, TB4 was found to decrease the rate in which the barbed end of F-actin grew (Yu *et al.*, 1993), prolong the nucleation phase of actin and decrease the rate of initial elongation of actin filaments (Sanders et al. 1992). This occurs when the concentration of the intracellular pool of G-actin falls below the critical concentration of actin polymerisation (0.1 μM) so actin polymerisation stalls. The mechanism was proposed that once G-actin disassociates from the ends of the filaments *in vivo*, TB4 binds to the G-actin monomers and blocks these monomers from re-polymerising (Sanders et al. 1992) (**Figure 1.7**). TB4 primarily binds to subdomain 2 on G-actin molecules and the binding of TB4 causes conformational and steric changes to the G-actin molecule, as determined by mass spectrometry (Enrique M. De La Cruz et al. 2000). It was also shown by circular dichroism that TB4 binds preferentially to Mg-G-actin than to Ca-G-actin (De La Cruz *et al.*, 2000), suggesting that actin dynamics can be controlled by the ratio of Mg and Ca in the cell. A recent *in vitro* study that overexpressed fluorescently labelled TB4 and profilin in COS-7 cells (fibroblast-like cells derived from monkey kidney tissue), and observed no effect on the rate of polymerisation or density of actin filaments when either protein was overexpressed (Zhang et al. 2017). The authors suggested that this was due to most of the G-actin being naturally sequestered by each molecule respectively, so overexpression had no effect. TB4 forms 4 cross links with subdomains 1, 2 and 3 of G-actin. It is also proposed that a ternary complex of DNase1 and cross-linked actin-TB4 is formed when DNase 1 binds (De La Cruz *et al.*, 2000). G-actin acts as an inhibitor to the activity of DNase 1 (Lazarides and Lindberg 1974), which degrades DNA in nuclei (Choi et al. 2020), and it has been shown that the dissociation of G-actin from DNase 1 leads to increased chromatin degradation (Eulitz and Mannherz 2007), suggesting that the binding of G-actin to TB4 could also mediate this cellular function.

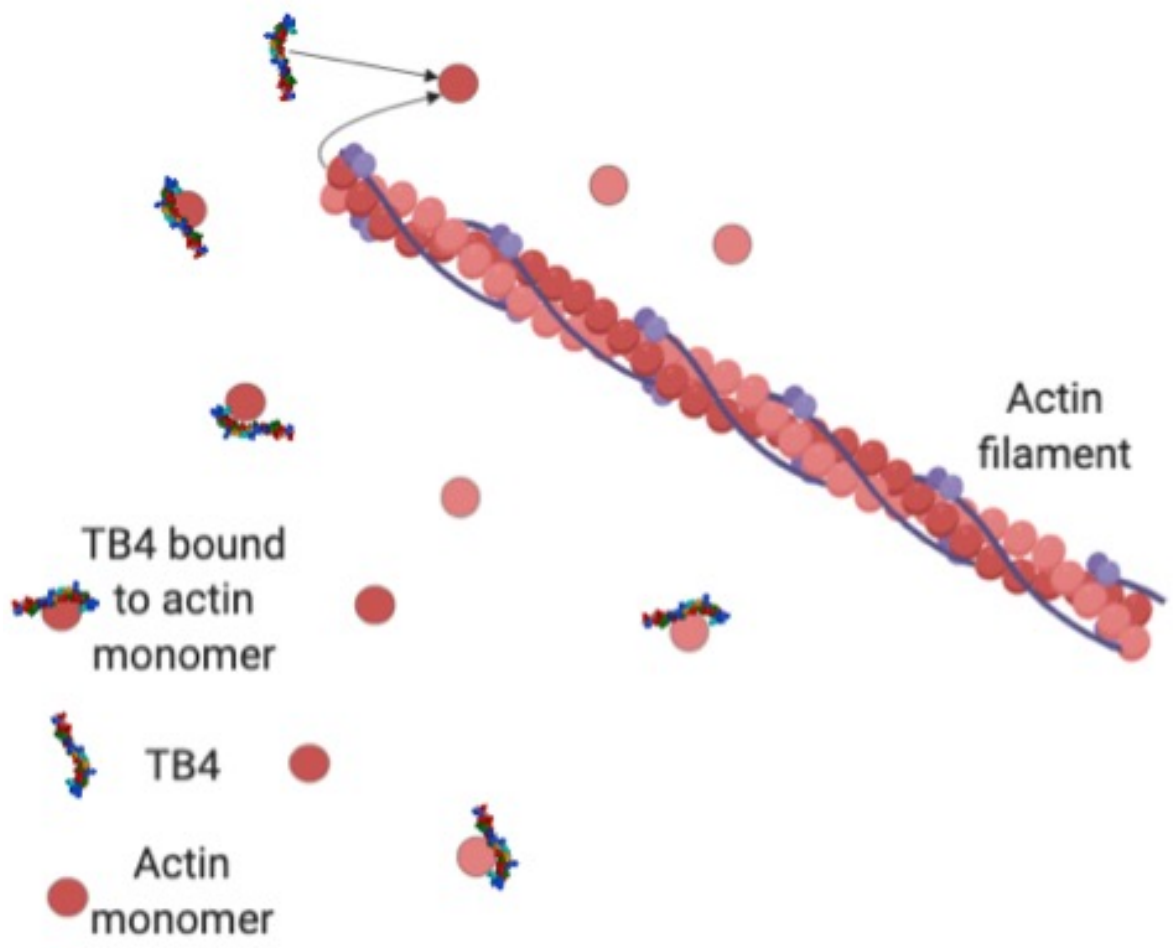

Figure 1.7 – Mechanism of G-actin sequestering. *Simplified diagram depicting how TB4 sequesters G-actin that detaches from F-actin. Original diagram.*

A recent study has explored the role of TB4 in the F-actin cytoskeleton in the developing epidermis and eyes. The study found that embryonic *Tmsb4x* knockdown by lentiviral short hairpin RNA transfection prevented eyelid closure of neonatal mice, which is an essential morphogenetic process (Padmanabhan et al. 2020). Eyelid closure is often hindered by mutated planar cell polarity genes (Curtin et al. 2003; Wang and Nathans 2007), defects in planar cell polarity were seen in *Tmsb4x* knockdown in the form of improper hair follicle alignment and orientation of papillary dermal cells in embryos. Planar cell polarity is required for the correct orientation of cells, embryogenesis and embryonic physiological functions (Papakrivopoulou et al. 2021). The embryos also showed a lower fluorescence intensity of F-actin in the epidermis, which can be directly correlated to defective adherens junction formation and stability, as shown by an increased thickness in E-

cadherin immunostaining. The decrease in F-actin was mirrored by a decrease in G-actin in keratinocytes *in vitro* and the authors suggested that the defect in adherens junction formation was via the loss of the G-actin pool that would normally be available in wild type mice (Padmanabhan et al. 2020).

The actin binding ability of TB4 has been shown to protect the actin cytoskeleton from disorganisation. One study explored the interaction of advanced glycosylation end products (AGE) and their receptors (RAGE) in human umbilical vein epithelial cells (HUVEC) *in vitro,* two molecules which are known to disrupt the cytoskeleton (Kim and Kwon 2015). AGE caused a reduction in cell viability, RAGE expression, increased the F-actin to G-actin ratio. The authors found that increasing concentrations of exogenous TB4 (0.01 – 0.5 μg/ml) protected AGE induced increase in F-actin to G-actin ratio. TB4 siRNA was used to decrease the expression of endogenous TB4, and it was shown that loss of endogenous TB4 exacerbated the effects of AGE on HUVECs, demonstrating the importance of endogenous and exogenous TB4 in cytoskeletal protection (Kim and Kwon 2015). Another *in vitro* study using Henrietta Lacks (HeLa) cells found a reduction in F-actin filaments and lamellipodia when endogenous TB4 was overexpressed by transfection with the opposite effect seen in TB4 downregulation by siRNA. It was also shown in this study that TB4 inhibits the cofilin-stimulated F-actin-ATPase, therefore slowing the progression of F-actin depolymerisation (Al Haj et al. 2014).

Cell migration is modulated by the F-actin cytoskeleton (Svitkina 2018) and endogenous TB4 has been shown to prevent migration in podocytes (Vasilopoulou et al. 2016), but increase migration in other cell types, such as colon cancer cells (Tang et al. 2011). TB4 has been shown to interact with the kinase domain of integrin linked kinase (ILK) in endothelial cells by surface plasmon resonance (Fan et al. 2009) and the increase in migration in colon cancer cells was attributed to TB4 overexpression enhancing the ILK activation. This ILK activation, in turn, caused an upregulation of IQGAP1 (Brown and Sacks 2006), an activator of Rac1, which indeed caused an increase in Rac1 signalling and cell migration, as shown by Transwell assay (Tang et al. 2011). Since an increase in cancer cells is known as

metastasis, which is detrimental to disease progression, this is one potential drawback of using exogenous TB4 as a therapy.

1.6.3 TB4 and inflammation

The suppression of inflammation is vital in preventing disease progression in a wide range of pathologies. TB4 has moonlighting abilities, meaning it can perform multiple cellular functions (Husson et al. 2010; Tompa 2005; Xue and Robinson 2016).

One of the first studies to implicate a therapeutic role of TB4 in inflammation was published in 1999. Through reverse-phase HPLC, it was identified that an alternative form of TB4, called TB4 sulfoxide (TB4-SO), is formed by oxidation of methionine-6 residue. By live cell tracking, it was shown that TB4-SO, but not TB4, caused altered motility of neutrophils, where the neutrophils migrated in a more disperse manner compared with untreated cells. Furthermore, scratch wound assay of neutrophils revealed that TB4-SO improved wound closure compared to both TB4 and untreated cells. The authors then transitioned to an *in vivo* study, and induced footpad swelling by carrageenin-induced inflammation. Daily intraperitoneal injection of 1 μg TB4-SO, but not an equivalent dose of TB4, was found to significantly reduce swelling in the footpads compared to untreated cells (Young et al. 1999).

Thirteen years later, TB4-SO was examined in inflammation using zebrafish larvae (Evans et al. 2013). TB4-SO absorbed into latex beads were injected into the larvae, causing inflammation. Imaging after 3 and 6 hours revealed a significantly lower number of macrophages proximal to the TB4-SO bead compared to vehicle beads, suggesting TB4-SO induced macrophage dispersion. Next, the authors used laser and needle-induced injuries in the cardiac tissue of the zebrafish larvae. At both 3 and 6 hours, administration of TB4-SO resulted in a reduced number of leukocytes in the injury area compared to vehicle treated fish. The authors then examined the effects of exogenous TB4 or TB4-SO (6 mg/kg every 2 days) in a murine model myocardial infarction, while also using TB4 global knockout mice to examine the role of endogenous TB4 in inflammation and observe the effects of exogenous TB4 administration in the absence of endogenous TB4. Exogenous TB4 attenuated neutrophil and macrophage infiltration into injured tissue at 4 and 7 days respectively

compared to vehicle treated mice, but the number of immune cells in TB4 knockout mice, without exogenous TB4, was exacerbated. TB4 administration also resulted in lower levels of TNFα, interleukin (IL)-6 and IL-10 cytokines compared to vehicle treated mice, which TB4 knockout also exacerbated. Flow cytometry determined that TB4-SO reduced the number of macrophages and monocytes 28 days after infarction. Serial magnetic resonance imaging (MRI) determined that TB4 and TB4-SO reduced infarct volume and reduced fibrosis in the heart (Evans et al. 2013). This study showed that when TB4 is oxidised in would sites, immune cells are resolved, which promotes reparative wound healing and anti-inflammation.

The anti-inflammatory effects of exogenous TB4 have been examined extensively in eye injuries. Topical administration of TB4 to treat corneal wounds in rats showed that 1 μg/μl of TB4 induced closure of the corneal wounds 12 and 24 hours after administration. The study then went on to investigate this further *in vitro* using primary human corneal epithelial cells (HCECs), where it was found that 50 – 1000 ng/ml of TB4 induced cell migration in a dose dependent manner (Sosne et al. 2001). A year later, the therapeutic role of TB4 was further characterised in corneal alkali injury in 129 Sv mice, which showed increased corneal re-epithelialisation and suppression of inflammatory genes, such as MCP-1, IL-1, IL-2 and MIP1&2 (Sosne et al. 2002). This was then further expanded in BALB/c mice inflicted with alkali corneal injury. The authors found using quantitative polymerase chain reaction (qPCR) and ELISA that TB4 inhibited neutrophil infiltration, decreased chemokine expression and modulated corneal matrix metalloproteinase (MMP) levels, which are involved in promotion of cell motility (Sosne et al. 2005). Furthermore, using TNF-α injured HCEC culture *in vitro* it was demonstrated with ELISA and immunofluorescence that TB4 administration prevented NFκB phosphorylation and translocation to the nucleus, therefore suppressing the TNF-a induced activation of the NFκB pathway, one of the earliest signalling events in the inflammatory response (Sosne, Qiu, Christopherson, et al. 2007).

The extensive studies of TB4 in the eye prompted investigation into the inflammatory response of other cell/tissue types. LPS administration to rodents, which mimics some phenotypes of septic shock in humans (Amura, Silverstein, and Morrison

1998), led to a sharp decrease in blood TB4 concentration, indicating that TB4 was being metabolised in response to the early inflammatory response (Bongiovanni *et al.*, 2015). Intraperitoneal administration of 100 μg of synthetic TB4 dramatically improved survival rate compared to LPS alone. Use of adeno associated virus (AAV) expressing *Tmsb4x* improved LPS induced systemic inflammation by prevention of pericyte loss and perivascular leakage protection. TB4 also prevented the haemodynamic effects, such as drop in blood pressure, that are normally seen in murine sepsis models (Bongiovanni *et al.*, 2015). A reduction of circulating TB4 concentration was also seen in patients that had been admitted to an intensive care unit with septic shock (Badamchian et al. 2003).

Interestingly, it was also found that TB4 was increased in the sera of inflammatory bowel disease (IBS) patients (Mutchnick et al. 1988). Rodent models of colonic inflammation were suppressed after TB4 overexpression, in the form of reduced inflammatory cell infiltration, suppression of colonic epithelial cell apoptosis, prevention of oxidative damage and modulation of pro-inflammatory cytokines (Zheng et al. 2017). The anti-inflammatory properties of TB4 have also been demonstrated in the lungs of male C57BL/6 mice injected with bleomycin, which mimics some of the characteristics of human pneumonitis (Yoshimi et al. 2008). Intraperitoneal injection of 6 mg/kg of TB4 suppressed polymorphonuclear leucocyte infiltration, lung oedema and collagen deposition (Conte et al. 2013). Mice of a C57BL/6 background with chronic granulomatous disease, which is an autoimmune disorder that targets phagocytes (Holland 2010), were challenged with a fungal infection of *Aspergillus fumigatus* and treated daily intraperitoneally with 5 mg/kg of exogenous TB4. TB4 was shown to suppress the inflammatory response and granuloma formation in these mice (Renga et al. 2019).

1.6.4 TB4 in angiogenesis and cardiac injury

Another well documented property of TB4 is its protection of the heart muscle and vasculature. TB4 has been detected as early as embryonic day 10 in the hearts of murine embryos on a 129 background (Smart et al. 2002) indicating that TB4 may play a role in development of the heart. Mice in which TB4 was knocked down in cardiomyocytes using short hairpin RNA were developmentally hampered and there

was a clear lack of neovascularisation and evidence of ischaemia (Smart et al. 2007). The effect of exogenous TB4 in myocardial infarction in C57BL/6 mice was then explored (Smart et al. 2011). Mice were primed with daily intraperitoneal injection of 12 mg/kg of TB4 for 10 days and myocardial infarction was induced 3 days later. Priming with exogenous TB4 significantly improved cardiac functional parameters after 28 days compared to vehicle treated mice, such as reducing infarct volume and improving diastolic and systolic volumes. Exogenous TB4 also reduced cardiac scar volume, with increased left ventricular mass at 28 days, as determined by MRI (Smart et al. 2011).

In a model of acute myocardial infarction in C57BL/6 mice, treatment with 1.6 mg/kg/day of TB4 via an osmotic mini pump (OMP) reduced death by cardiac rupture by 30% compared with vehicle treated mice. TB4 treated mice also showed less cardiac inflammatory cell infiltration, cardiac $TUNEL^+$ (apoptotic) cells and increased angiogenesis after 1 week (Peng et al. 2014). More recently, it has been shown that endothelial progenitor cells *in vitro* treated with 10 ng/ml of TB4 formed tubules more readily (mimicking angiogenesis) than untreated cells, and increased the expression of angiogenic growth factors, such as platelet derived growth factor (2β subunits) (PDGF-BB), insulin-like growth factor 1 (IGF-1) and vascular endothelial growth factor (VEGF). The authors then transplanted these cells to diabetic fatty rats *in vivo* after myocardial infarction and saw increased angiogenesis, and increased recruitment of endogenous cardiac progenitor cells, therefore an improvement in cardiac function (Poh et al. 2020). A study using the hind limb ischaemia model in mice suggested that TB4 may actually enhance the $NK\kappa B$ pathway to promote angiogenesis (Lv et al. 2020), which is in contrast to the inflammatory studies that stated TB4 suppresses this pathway (Sosne et al. 2001).

TB4 has been shown to be involved in other pathways that affect angiogenesis. TB4 competes with myocardin-related transcription factor A (MRTF-A) for the binding of G-actin. Once MRTF-A is released from G-actin, it translocates to the nucleus, activating serum response factor (SRF) target genes. This was shown by Luciferase activity in HeLa cells (Morita and Hayashi 2013). MRTF-A signalling upregulates the expression of cysteine-rich angiogenic protein 61 (CCN1) and cellular

communication network factor 2 (CCN2), two molecules which drive angiogenesis and vessel stabilisation (Hanna et al. 2009; Hinkel et al. 2014). Using AAV vectors, upregulating TB4 and MRTF-A resulted in a significant upregulation in angiogenesis in a model of ischaemia in the hindlimbs of rabbits, suggesting that the MRTF-A release, modulated by TB4 binding to G-actin, could be responsible for TB4s role in angiogenesis (Ziegler et al. 2018).

It was also shown in rat cardiomyocytes *in vitro* that addition of 10 ng/μl of TB4 promoted cell migration and survival and increased the beating frequency of rat neonatal cardiomyocytes 2 and 4 weeks after explant through ILK and Akt activation. The most physiological significant finding of the paper was that TB4 was able to protect heart function in mice after myocardial infarction, as represented by a higher volume of blood ejection and increased cardiac contraction 4 weeks after infarction (Bock-Marquette et al. 2004; Srivastava et al. 2007).

It is clear from the extensive literature that TB4 plays a major role in protection of the heart, however, it is emerging that it also plays a role in the vasculature in other organs, such as the brain (Morris, Zhang, and Chopp 2018). Stroke refers to a number of conditions that cause haemorrhage or blockage of the blood vessels that supply the brain (Lo, Dalkara, and Moskowitz 2003). In a model of acute stroke in aged Wistar rats, where the middle cerebral artery was occluded, daily treatment with 12 mg/kg of TB4 intraperitoneally reduced vascular lesion volume (Morris et al. 2017). The same model was also undertaken in younger Wistar rats, where exogenous TB4 improved neurological outcome, promoted myelination and oligodendrocyte progenitor cell proliferation (Morris et al. 2014).

1.6.5 TB4 in the kidney

The role of TB4 in the kidney is a relatively new and unexplored area compared to other organs. A study from 2010 analysed the expression of TB4 in human foetal kidneys using IHC. The authors found TB4 expression in the developing and adult kidney was restricted to the tubules and ducts and was absent from the glomeruli (Nemolato et al. 2010). Endogenous *Tmsb4x* transcripts have also been identified in the kidney by qPCR, where *Tmsb4x* was found to be enriched in the glomeruli of

adult mice compared to the rest of the kidney and glomerular *Tmsb4x* transcripts could be detected at embryonic day 16.5. By embryonic day 18, some TB4 expression also co-localised with nephrin, a major SD protein found in the podocyte foot processes, as confirmed by immunocytochemistry (Vasilopoulou et al. 2016). The discrepancies in glomerular TB4 positive immunostaining between these two studies are likely due to different antibodies used, different techniques used (immunofluorescent versus IHC), and different stages of kidney development. Another study used *in situ* hybridisation and immunocytochemistry on C57BL/6 mice kidney sections. *Tmsb4x* was present throughout the kidney, but more extensively in the cortex. The authors stated that TB4 peptide immunoreactive cells had small cell bodies and long branched processes, and were clearly in direct contact with the Bowman's capsule and lined the tubules (Paulussen et al. 2009). However, the exact cell types expressing TB4 were not identified.

A recent study that assessed the amniotic fluid of patients with developmental kidney disease found that TB4 was upregulated and positively correlated with the severity of disease (Klein et al. 2020). The study used ELISA to quantify the amniotic fluid concentration of TB4 where it was shown that TB4 was upregulated 2-fold in compromised renal outcome patients compared to healthy patients. The authors performed IHC on human foetal kidney formalin fixed, paraffin embedded (FFPE) sections, and showed that in healthy foetuses, TB4 was expressed mainly in the tubules, with no glomerular staining, which did not change with disease. The absence of glomerular staining is likely due to the developmental stage (foetal), as other studies have reported a lack of TB4 expression in developing glomeruli (Nemolato et al. 2010). Finally, they generated mutant zebrafish larvae using CRISPR/CAS-9 to form a truncated TB4 protein. TB4 knockout lead to defective development of the tubular components of the developing zebrafish kidney, but no change to the glomeruli (Klein et al. 2020). This is the first study to implicate TB4 in the progression of developmental defects to the human kidney. Another recent study in human adult CKD patients showed by mass spectrometry that urinary TB4 was upregulated 44.3-fold in ESKD patients compared to healthy patients (Kim et al. 2021). These studies combined suggest that TB4 may have a role in the progression of CKD in humans.

The expression and function of TB4 in kidney disease has been further investigated in rodent models (Vasilopoulou, Riley, and Long 2018). One study quantified the expression of TB4 in CKD using the 5/6 nephrectomy model of FSGS in rats, which involves removing 1 kidney and 2/3 of the other kidney. In this model, the authors performed mass spectrometry and showed that TB4 expression was increased 3-fold in non-sclerotic glomeruli and 4-fold in sclerotic glomeruli of 5/6 nephrectomy rats compared with sham operated rats, with the expression predominantly in the endothelial cells (Xu et al. 2005). A later study employing mass spectrometry in the same 5/6 nephrectomy model of kidney injury in rats also reported a 4-fold upregulation of TB4 peptide in whole kidney tissues compared to sham operated rats (Kim et al. 2021).

The first study to explore the role of endogenous *Tmsb4x* was published by Vasilopoulou et al. Global knockout of TB4 was achieved by deleting exon 2 of the *Tmsb4x* locus in mice of a C57BL/6 background. Interestingly, global knockout of *Tmsb4x* in these mice had no renal phenotype – the albuminuria and blood urea nitrogen (BUN) concentrations were equivocal to their wild type littermates. There was also no glomerulosclerosis or foot process effacement, exhibiting that endogenous *Tmsb4x* is expendable for healthy glomeruli and kidneys. However, this was not the case in the context of glomerular injury. The authors employed NTS nephritis in order to create an immune mediated glomerular injury, which mimics some of the features seen in human glomerulonephritis (Pippin et al. 2009). Loss of endogenous *Tmsb4x* exacerbated the effects of NTS nephritis at 21 days after disease induction, including a further 5-fold enhancement of albuminuria in *Tmsb4x* knockout mice with NTS nephritis compared to wild type mice with NTS nephritis, indicating glomerular filtration barrier leakage. Loss of *Tmsb4x* caused a significant decrease in creatinine clearance and an increase in BUN when compared with wild-type mice with NTS injury. *Tmsb4x* knockout also led to exacerbated glomerular histological damage, in the form of enhanced crescent formation and hyaline deposits. The distribution of podocytes was further analysed by WT-1 immunofluorescence. NTS did not cause changes to the number of WT-1 positive cells inside the glomerular tuft or in the parietal epithelium in wild type mice, however, *Tmsb4x* knockout caused a reduction of glomerular tuft WT-1 positive cells and increase in parietal WT-1 expression. The total number of renal corpuscle WT-1

positive cells did not change (Vasilopoulou et al. 2016), suggesting that the podocytes may be migrating from the glomerular tuft towards the parietal epithelium, which has previously been seen in podocyte injury *in vivo* (Brähler et al. 2016; Burford et al. 2014; Hackl et al. 2013).

Next, the authors looked at glomerular inflammation at 21 days after disease induction by IHC. There were no statistical changes to the number of CD3 cells (T cell marker (Call et al. 2002)) or F4/80 positive cells (macrophage marker (Austyn and Gordon 1981)) inside or outside the glomerular tuft in wild type NTS nephritis compared with vehicle treated mice. Lack of *Tmsb4x,* however, caused a significant increase in the number of glomerular CD3 positive cells, glomerular F4/80 positive cells and F4/80 positive peri-glomerular cells compared to wild type littermates treated with NTS. The final *in vivo* component analysed was fibrosis, which was assessed by IHC and qPCR. NTS nephritis led to significant fibrosis in wild type mice, which was presented as collagen IV deposition inside and around the glomerular tuft and increased whole kidney *Col4a* gene expression compared with vehicle treated mice. NTS nephritis in *Tmsb4x* knockout mice caused an exacerbated increase in whole kidney *Col4a* and *Acta2* (a-SMA) gene expression compared with wild-type mice with NTS nephritis. The *in vivo* data taken as a whole demonstrates a potential role of endogenous *Tmsb4x* in limiting onset of glomerular disease.

To further explore the role of endogenous TB4 specifically in podocytes, the authors transfected mouse immortalised podocytes (Mundel, Reiser, et al. 1997) with siRNA that targeted *Tmsb4x*. A greater than 95% reduction in *Tmsb4x* mRNA levels following siRNA transfection was confirmed by qPCR. Three aspects were analysed: cell viability (MTT assay); cell migration (scratch wound) and F-actin (phalloidin staining and Rho GTPase activity). There was no change to podocyte viability 24, 48 or 72 hours after *Tmsb4x* siRNA transfection. Knock-down of endogenous *Tmsb4x* led to a 50% increase in podocyte migration *in vitro*. This may be a potential mechanism to explain the effects of NTS nephritis *in vivo*, podocyte migration has been associated with foot process effacement and proteinuria *in vivo* (George et al. 2012; Harris et al. 2013; Kriz et al. 2013). Finally, the analysis of the cytoskeleton showed an increase in cytoplasmic stress fibres in *Tmsb4x* knock-down podocytes,

with an upregulation of RhoA activity. RhoA activation has been shown to increase the formation of stress fibres in podocytes (Asanuma et al. 2006), so is likely to contribute to the mechanism by which this reorganisation of the actin cytoskeleton occurred.

Two of the major properties of TB4 are G-actin regulation and suppression of inflammation. The disorganisation of podocyte F-actin *in vitro* provides evidence that this could be the mechanism of exacerbated albuminuria *in vivo*. The podocyte cytoskeleton is critical for the unique shape of the foot processes and its disorganisation leads to albuminuria (Shirato *et al.*, 1996; Blaine and Dylewski, 2020). It is possible that the absence of the actin binding properties of endogenous TB4 from podocytes caused exacerbated damage to the glomerular filtration barrier leading to an increase in albuminuria in NTS nephritis. The anti-inflammatory properties of TB4 also clearly played a role in the enhanced progression of injury in this model of immune mediated glomerular disease as shown by the increased macrophage accumulation in *Tmsb4x* knockout with NTS nephritis. It would be interesting to explore if the anti-inflammatory effect of TB4 was mediated by changes in the expression and activity of TNF-a and NFκB, as shown in the eye (Sosne, Qiu, Christopherson, et al. 2007).

Angiotensin II administration to rodents is a model of renal injury that mimics some of the effects of hypertension in humans (Johnson et al. 1992). A study explored the effects of globally knocking out *Tmsb4x* and inducing hypertension in mice of a C57BL/6 background (Kumar *et al.*, 2018). *Tmsb4x* knockout exacerbated albuminuria ~26-fold and reduced *Nphs1* mRNA levels compared with wild type hypertensive mice, suggesting significant damage to the SD and glomerular filtration barrier. Macrophage infiltration and expression of ICAM-1, a pro-inflammatory protein, were also exacerbated in *Tmsb4x* knockout along with interstitial fibrosis (Kumar *et al.*, 2018). Interestingly, loss of *Tmsb4x* did not exacerbate the increase in blood pressure, suggesting that the protective effects of endogenous TB4 were not involved in blood pressure regulation.

Further studies investigated the use of TB4 as a therapeutic agent in renal injury. One of the first studies used the unilateral ureteral obstruction (UUO) model in C57BL/6 mouse kidneys to induce interstitial fibrosis, tubular dilation, tubular atrophy and interstitial collagen deposition. Endogenous expression of TB4 in interstitial and tubular cells increased as disease progressed in UUO mice compared with control mice. Administration of 150 μg/day of TB4 intraperitoneally reduced interstitial fibrosis by 33% 14 days after obstruction as determined by Sirius red staining (Zuo et al. 2013). Another study employed the UUO model in Sprague Dawley rats to induce tubular interstitial fibrosis and a low dose (1 mg/kg/day) and high dose (5 mg/kg/day) of TB4 were administered via intragastric lavage (Yuan et al. 2017). The low dose suppressed the onset of UUO-induced proteinuria, and the effect was more pronounced when the high dose was used. UUO also increased the relative area of fibrotic interstitial tissue, as determined by Sirius red staining, which both the low and high dose of TB4 prevented. TB4 also prevented UUO induced glomerulosclerosis, tubular lumen dilation and apoptosis of tubular epithelial cells. Transforming growth factor β (TGF-β) is a cytokine that promotes fibrosis and can induce tubular epithelial cells and mesangial cells to transform into fibroblast cells (Qiao et al. 2013; Yang and Liu 2001) and TB4 suppressed whole kidney expression of TGF-β and a-SMA in UUO mice, suggesting a potential mechanistic pathway. Interestingly, TB4 administration in UUO also preserved E-cadherin expression in tubulointerstitial tissue, providing more evidence of its role in adherens junction preservation (Padmanabhan et al. 2020). The authors expanded on their *in vivo* findings by challenging tubular epithelial cells *in vitro* with TGF-β and treating with exogenous TB4. Exogenous TB4 prevented alterations to the gene transcripts and protein levels of E-cadherin and α-SMA. TB4 also prevented the TGF-β-induced increase in tubular apoptotic cells and markers, such as cleaved caspase-3, Bax and Bcl2 in tubular cells *in vitro* (Yuan et al. 2017). Combined, these two studies of the UUO model of kidney injury demonstrate that TB4 has a potential therapeutic role in this model of fibrosis.

KK Cg-Ay mice of a C57BL/6 background are commonly used as a model of glomerular injury that reflects some of the features of human type 2 diabetic nephropathy (O'Brien et al. 2013). A study in these mice has explored the role of

exogenous TB4 via intraperitoneal administration of 100 ng/10 g body weight daily. TB4 decreased blood glucose levels and suppressed the urinary albumin concentration by 33%. TB4 also suppressed glomerular hypertrophy and mesangial matrix expansion seen in the KK Cg-Ay mice, suggesting that TB4 decelerates the onset of early-stage diabetic nephropathy (Zhu et al. 2015). There were no mechanistic assays undertaken in this study so the improvement of renal function could be associated with the reduction in blood glucose seen following TB4 administration. The injury model induced in KK Cg-Ay mice is less severe than in the more widely used *db/db* mouse strain (Kitada, Ogura, and Koya 2016), and perhaps it would have been a more informative study to explore the role of exogenous TB4 in a more severe form of diabetic nephropathy.

Exogenous TB4 has also been explored in the ischaemia reperfusion injury (IRI) model of kidney injury. Sprague-Dawley rats injected intravenously with 10 mg/kg of exogenous TB4 showed decreased inflammatory and apoptotic markers than sham control rats (Aksu et al. 2019). TB4 also suppressed the increase in BUN and blood creatinine concentration seen in IRI, indicating TB4 was protective of kidney function (Aksu et al. 2019). This work could have been taken further by showing the localisation of the inflammatory and apoptotic markers by IHC experiments, to identify if these markers were located in the medulla or cortex.

All together, the *in vitro* and *in vivo* data strongly demonstrate that endogenous TB4 is crucial in the progression of glomerular disease in mice, providing further rationale to explore the role of exogenous TB4 in glomerular disease models.

1.6.6 Clinical applications of TB4

The World Health Organisation has recently declared that the international non-proprietary name for use of TB4 in clinical settings is Timbetasin (World Health Organisation 2018) and the company RegenRx is heavily involved in the clinical application of TB4. A number of clinical trials have investigated the safety and efficacy of administering exogenous TB4 to humans in 3 main forms; RGN-137, RGN-259 and RGN-352, all manufactured by RegeneRx. RGN-137 is a topical gel containing TB4 that was designed to be applied to external skin wounds, RGN-259

comes in the form of sterile TB4 containing eye drops and RGN-352 is a solution containing TB4 that was designed to be administered intravenously (Anon 2021)

The earliest clinical trials of TB4 were in skin conditions. Venous stasis ulcers can develop on the ankle or lower leg of patients with chronic vascular diseases (Olin et al. 1999). A phase 2 clinical trial applied 0.01%, 0.03% and 0.1% of TB4 in the form of RGN-137 to patients experiencing these ulcers. There were no major adverse events when using any doses, showing that TB4 was safe to use and 0.03% of RGN-137 led to a 45% decrease in wound closure time compared to placebos ((Guarnera, DeRosa, and Camerini 2010; RegeneRx - NCT00832091 2010) all references containing NCTXXXXXXXX refer to the clinical trial identification number on www.clinicaltrials.gov). Epidermolysis bullosa is a genetic group of skin conditions that can cause blistering of the skin in response to mechanical trauma (Pai and Marinkovich 2002) which can be due to the absence or functional loss of laminin-332, type XVII collagen or integrin a6β4 (Keith et al. 2020). TB4 has been shown to synthesise laminin-332 (Sosne et al. 2004), making it an attractive therapy for epidermolysis bullosa. A previous phase 2 clinical trial using RGN-137 in epidermolysis bullosa was established between 2006 – 2012, however this was terminated due to lack of patient enrolment (RegeneRx - NCT00311766 2012). In mid-2019 patient recruitment re-started to study the efficacy and safety of RGN-137 in patients with junctional and dystrophic epidermolysis bullosa, with the aim to apply RGN-137 topically to wounds once a day for up to 84 days. The primary outcome is to achieve a 50% reduction in the area of the wounds in less than 84 days (RegeneRx - NCT03578029 2019).

Exogenous TB4 to treat disorders of the eye has almost fully completed the journey from lab bench to bedside in the form of RGN-259 (Sosne 2018). The stage two clinical trials for dry eye syndrome were successful. There was a statistical difference in mean ocular discomfort, tear film break up time and corneal fluorescein scores (marker for inflammation) (Nichols, Evans, and Karpecki 2020) in patients treated with RGN-259 groups compared to the vehicle groups, with a very low percentage of adverse events (RegeneRx - NCT01393132 2015; Sosne et al. 2013; Sosne and Ousler 2015). Stage three trials are currently ongoing. According to the RegenRx

website, as of August 2020 there had been 600 patients recruited to the current stage 3 clinical trials of RGN-259 in dry eye syndrome (Anon 2021; RegeneRx - NCT03937882 2020). RGN-259 is also currently in the third stage of phase 3 trials to treat neurotrophic keratopathy, which is a disease of the eye that causes corneal epithelial breakdown, impairment of healing and development of corneal ulceration, melting and perforation (Sacchetti and Lambiase 2014). The phase 2 trials performed in neurotrophic keratopathy were in four patients that all showed a reduction in epithelial defects with no discomfort when administered RGN-259 (Dunn et al. 2010). There was also an early clinical trial to examine the effect of RGN-259 in corneal wounds of diabetic patients following vitrectomy surgery, however this trial was terminated due to slow recruitment (RegeneRx - NCT00598871 2010).

Doses of 42 mg, 120 mg, 420 mg and 1260 mg of RGN-352 have been tested in phase 1 clinical trials for their safety and efficacy when administered intravenously. There were no toxic or adverse events to patients given RGN-352 as a single dose or daily for 14 days (Ruff et al. 2010). RGN-352 was designed to be an interventional treatment for patients with myocardial infarction and other vascular and neurological disorders, such as multiple sclerosis and stroke (Anon 2021). Phase 2 trials hoped to improve cardiac function in a 28-day time frame by a single injection of 1200 mg or daily injection of 450 mg (for 3 three days) and then weekly injections of 450 mg. Unfortunately, the recruitment of patients was suspended in 2015 due to RegeneRx not being good manufacturing practice (GMP) compliant (exact reason unknown) (RegeneRx - NCT01311518 2015).

It is also worth noting that TB4 has recently begun clinical trials sponsored by a Chinese company called Beijing Northland Biotech. Co., Ltd under the name of NL005 (Beijing Northland Biotech. Co. Ltd. 2021). These trials are similar to RGN-352, where they have completed phase 1 clinical trials of recombinant human TB4 in an injectable form to study the safety at doses of 0.5 μg/kg, 2.0 μg/kg, 2.5 μg/kg, 5.0 μg/kg, 12.5 μg/kg and 25 μg/kg of TB4 in healthy patients. The phase 1a and 1b trials were completed In late 2020 (Beijing Northland Biotech. Co. Ltd. - NCT04555850 2020; Beijing Northland Biotech. Co. Ltd - NCT04555824 2020) but no results have been posted to the clinical trial data base (www.clinicaltrials.gov).

However, the company website states that the phase 1 trials were successful and that they are currently in phase 2a clinical trials to study NL005 in patients with ischaemia-reperfusion injury caused by myocardial infarction (Beijing Northland Biotech. Co. Ltd. 2021).

Overall, the safety data from the clinical trials is promising, and paves the way for TB4 to be explored in other tissue pathologies, such as CKD.

1.6.7 AcSDKP

In vivo, TB4 is metabolised relatively quickly as demonstrated by a time course study injecting synthetic TB4 into Swiss-Webster mice (Mora et al. 1997). Synthetic TB4 (400 μg) was injected intraperitoneally and serum was collected via cardiac puncture at 2 minutes, 2 hours, 6 hours and 24 hours after administration and TB4 concentration assessed by ELISA. Serum TB4 concentration peaked after 2 hours and returned to baseline after 6 hours, indicating that TB4 is metabolised during this time (Mora et al. 1997). One of the peptides that TB4 is metabolised to is a tetrapeptide termed N-acetyl-seryl-aspartyl-lysyl-proline (AcSDKP), which is ubiquitous throughout mammalian cell types and also present in the plasma and urine (Junot et al. 1999; Le Meur et al. 2001; Pradelles et al. 1991). AcSDKP is located at the N terminus of TB4 and is generated through stepwise hydrolysis, involving meprin-a and prolyl oligopeptidase (POP) (Kumar et al. 2016). AcSDKP has anti-inflammatory and anti-fibrotic benefits in animal models of hypertension, stroke, myocardial infarction, autoimmune diseases and CKD, by reducing organ macrophage infiltration, cytokine and chemokine expression, NFκB activation, TGF-β expression and collagen deposition (Cavasin et al. 2007; Ding et al. 2014; Kumar and Yin 2018; C. Li et al. 2019; Yang et al. 2004). This section will focus on the role of AcSDKP in CKD models.

The plasma concentration of AcSDKP in patients with CKD increases proportionally with disease severity and ACE inhibitors further enhance AcSDKP plasma concentration (Azizi et al. 1999; Le Meur et al. 2001). ACE is known to degrade AcSDKP, therefore the exacerbated increase in plasma concentration is likely due to ACE inhibition (Nagai et al. 2015). Diminished AcSDKP in Sprague-Dawley rats, as

achieved by inhibiting prolyl oligopeptidase via OMP secretion of buprenorphine, causes increased collagen formation around the glomeruli and vasculature, and glomerulosclerosis, as determined by IHC (Cavasin et al. 2007). This occurred without any disease induction, suggesting that endogenous AcSDKP is essential for regulation of renal collagen.

The role of exogenous AcSDKP in the UUO model of renal fibrosis and inflammation has been explored in detail. Administration of 0.4 mg/kg/day of AcSDKP by OMP to Wistar rats was initiated on the day of UUO induction, which led to decreased fibrosis and inflammation in the obstructed kidney after 14 days. AcSDKP suppressed macrophage infiltration, lowered activation of NFκB and suppressed expression of TGF-β, aSMA and MCP-1 (Wang et al. 2010). In mice of a C57BL/6 background, 1.6 mg/kg/day of AcSDKP was administered via OMP and the effects were assessed 5 and 14 days after UUO induction. AcSDKP decreased fibrosis at both time points, which was determined by a reduction in Sirius red IHC. There was also a decrease in fibronectin, plasminogen activator inhibitor-1 (PAI-1) and TGF-β signalling compared to UUO mice without AcSDKP (Zuo et al. 2013). Finally, in BALB/c mice, 1 mg/kg/day of AcSDKP via OMP suppressed tubulointerstitial fibrosis and collagen deposition in the cortex in UUO mice. Surprisingly, there was no reduction of macrophage accumulation after AcSDKP administration, which could be due to different doses and strains of mice (Chan et al. 2015).

Exogenous AcSDKP has also shown therapeutic benefits in glomerulonephritis models. Wistar-Kyoto rats were administered with 1 mg/kg/day AcSDKP by subcutaneous OMP 2 weeks after the induction of anti-GBM glomerulonephritis (Omata et al. 2006). Exogenous AcSDKP suppressed the onset of glomerulosclerosis, interstitial collagen deposition and fibrosis 42 days after disease induction, as determined by IHC. Albuminuria increase and BUN development were prevented and levels of fibronectin, collagen I and collagen III were all suppressed with AcSDKP administration. TGF-β, a signalling protein that induces fibrosis, was also suppressed 42 days after disease induction (Omata et al. 2006).

Systemic lupus erythematosus (SLE) is another autoimmune disorder in which the body generates autoantibodies that target the glomerulus (Almaani et al. 2017). A study used transgenic *MRL/MpJ-Fas^{lpr}/2J* mice, which develop renal phenotypes that simulate SLE (Wu et al. 2016), that were treated with 800 ug/day of AcSDKP via OMP (Liao et al. 2015). Protein array analysis, Western blot and IHC revealed that AcSDKP suppressed glomerular complement levels and ICAM-1 expression as well as attenuated macrophage and T cell infiltration to the kidney. The suppression of these inflammatory compounds proved beneficial to kidney function, as AcSDKP significantly improved eGFR, albuminuria, and glomerulosclerosis. Furthermore, AcSDKP suppressed interstitial collagen formation, demonstrating its anti-inflammatory and anti-fibrotic effects (Liao et al. 2015).

AcSDKP is detectable in the urine of diabetic patients and urinary concentration increases as eGFR declines (Nitta et al. 2019). The role of exogenous AcSDKP has been explored in rodent models of type 1 and type 2 diabetic nephropathy, which were achieved by injection of streptozotocin and using *db/db* transgenic mice respectively (Wu and Yan 2015). Sprague-Dawley rats, 8 weeks after streptozotocin injection, were treated with 1 mg/kg/day of AcSDKP by OMP. While there was no improvement in renal function, AcSDKP improved fibrosis and diabetes-induced loss of glomerular nephrin (Castoldi et al. 2013). Further studies explored AcSDKP co-administration with the ACE inhibitor Imidapril in type 1 diabetic nephropathy. AcSDKP (0.5 mg/kg/day via OMP) and Imidapril co-treatment of CD1 mice 16 weeks after streptozotocin injection was maintained for 8 weeks. Mesangial expansion, fibrosis and αSMA positive cells were all reduced with commination treatment compared to ACE inhibitor treatment alone (Nagai et al. 2014). AcSDKP was also found to restore the expression of the anti-fibrotic microRNAs miR-29 and miR-let-7 in diabetic kidneys. To further elucidate potential mechanisms, the authors cultured human dermal microvascular endothelial cells and found that AcSDKP blocked endothelial to mesenchymal transition, which has been shown to contribute to glomerulosclerosis in diabetic nephropathy (Li, Qu, and Bertram 2009; Nagai et al. 2014). More recently, type 1 diabetic CD1 mice were also treated with 0.5 mg/kg/day of AcSDKP via OMP, in co-treatment with Imidapril 16 weeks after disease induction. It was shown that co-treatment of Imidapril and AcSDKP prevent endothelial to

mesenchymal transition, collagen 1 and fibronectin deposition in the kidney. AcSDKP and ACE inhibition disrupted the metabolic reprograming in diabetic nephropathy by restoring the protein levels of SIRt3, CPT1a and PGC1a, while suppressing the diabetic-induced increased protein levels of GLUT1, PKM2 and PDK4 (Srivastava et al. 2020). AcSDKP has also been administered (1 mg/kg/day via OMP) in a model of type 2 diabetes in *db/db* mice of a C57BL/6 background. Although AcSDKP was not able to prevent the increase in albuminuria, it was able to supress the increase in glomerular mesangial matrix expansion and plasma creatinine concentration. AcSDKP also alleviated the upregulation of fibronectin in *db/db* mice, and collagen IV, through suppression of TGF-β expression (Shibuya et al. 2005).

Finally, AcSDKP has been shown to be therapeutic in hypertension related CKD rodent models. C57BL/6 mice treated with DOCA-salt, which reproduces some of the effects of hypertension in humans, saw a reversal of detrimental effects when treated with 800/kg/day AcSDKP by OMP. AcSDKP suppressed kidney monocyte and macrophage infiltration, reduced glomerulosclerosis and mesangial matrix expansion and furthermore, prevented albuminuria and glomerular nephrin loss. The protective effects of AcSDKP were independent of blood pressure regulation, as the systolic blood pressure of treated mice remained high (Rhaleb et al. 2011). More recently, exogenous 1.6 mg/kg/day of AcSDKP has been administered to Zucker Obese rats via OMP that develop hypertension upon consuming a high salt diet. The rats also developed diabetes-like symptoms, as glucose intolerance and urine volume rose. IHC revealed that the Zucker obese rat kidneys had more Cd68 positive macrophages on the high salt diet compared to the normal salt diet, which AcSDKP prevented. AcSDKP also prevented the high salt induced development of cortical and medullary fibrosis, as quantified by Sirius red staining. Zucker obese rats developed glomerulosclerosis compared to the Zucker lean rats, which was exacerbated by the high salt, but AcSDKP prevented this exacerbation (Maheshwari et al. 2018). Overall, the protective effects of AcSDKP are well documented in rodent models of kidney injury, in particularly demonstrating anti-inflammatory and anti-fibrotic effects.

1.7 **Gene therapy using AAVs**

1.7.1 What is AAV?

TB4 is metabolised rapidly when administered to mice. Therefore, some previous studies have used AAV encoding *Tmsb4x* as a therapeutic strategy in experimental models of animal injury to induce a persistent, systemic upregulation of TB4. AAV.*Tmsb4x* has been shown to induce neovascularisation and vessel maturation in a model of ischaemia in rabbit hind limbs (Hinkel et al. 2014). AAV.*Tmsb4x* also improved the cardiac output of pigs 56 days after myocardial infarction when used as a preventative strategy, as determined by increased ejection fraction, reduced blood pressure and improved myocardial contractile capability (Ziegler et al. 2018). These studies have shown that AAV.*Tmsb4x* can provide a beneficial effect in experimental models.

AAV is a non-pathogenic single stranded DNA parvovirus with potential as a therapeutic tool (Schultz and Chamberlain 2008). AAV normally require a helper virus, such as an adenovirus, for replication and assembly *in vitro* (Muzyczka 1992), hence the name AAV. The first documented production of genetically modified AAV particles that could infect and transduce mammalian cells *in vitro* was in the mid-1980's (Hermonat and Muzyczka 1984; Tratschin et al. 1984). Since then, AAV gene vectors are emerging as serious candidates to induce long term gene expression in scientific and clinical settings. The viral genome is ~4.7 kilobases that contains two open reading frames (ORFs) – the *rep* (replication proteins) and *cap* (capping proteins) regions (Vincent, Piraino, and Wadsworth 1997). The capsule is composed of 3 types of proteins; Virion protein 1 (VP1), VP2 and VP3, which assemble to form a spherical shell composed of ~60 subunits in a 1:1:10 ratio (Li and Samulski 2020; Xie et al. 2002).

The viral genome is flanked by inverted terminal repeats (ITRs) which can be manipulated to package recombinant DNA into the viral particles (Zhou et al. 2017). Since the viral particles are so small in size, the recombinant transgene must be smaller than ~5 kilobases in length (Muzyczka 1992). The transgene is inserted into the ITR between a promotor and a poly (A) tail (Gao et al. 2002). One common method to engineer the transgene into the cassette is by triple transfection of host

cells *in vitro* (Nass et al. 2018). Commonly used host cells are human embryonic kidney (HEK) cells, due to the human-like post translational modifications and high transfection efficiency (Feng et al. 2007; Hu et al. 2018; Senís et al. 2014). The recombinant transgene, equipped with the ITR of choice and a promotor (commonly cytomegalovirus (Gorman et al. 1989)), are transfected into the host cells *in vitro* with *cis*-plasmid adenovirus helper plasmids along with a second plasmid in *trans* containing the viral *cap* and *rep* genes (Gao et al. 2002). The third plasmid contains the adenoviral helper plasmid, which assists the formation of the viral particles in the host cells. The host cellular machinery then generates the viral proteins and, along with the helper plasmid, assembles them into the viral particles (Sonntag et al. 2011). Once the viral assembly has occurred, cells are harvested and the virus is purified (Gao et al. 2002).

Although there are hundreds of serotypes and pseudo-serotypes of AAVs, 12 main primate isolated serotypes have been described (AAV 1-12) (Chiorini et al. 1997, 1999; Gao et al. 2004; Mori et al. 2004; Muramatsu et al. 1996; Rutledge, Halbert, and Russell 1998; Schultz and Chamberlain 2008; Srivastava, Lusby, and Berns 1983; Xiao et al. 1993). The capsid subunits each contain 9 variable regions that determine tissue tropism and intracellular trafficking (Li and Samulski 2020; Xie et al. 2002). Researchers can also generate hybrids of two different serotypes to tailor the viral characteristics to their needs. For example, AAV 2/7 can be generated by the triple transfection method on the *trans* plasmid to produce a hybrid virus that contains the reproduction genome of serotype 2 and the capsid of serotype 7 (Hildinger et al. 2001). Therefore, the tissue tropism of this hybrid virus would be the same as serotype 7.

AAVs are commonly used in rodents as a vector to upregulate genes of interest (Li and Samulski 2020; Schultz and Chamberlain 2008), but the appropriate serotype must be used depending on the target organ. Tissue tropism means that the virus will bind to a receptor on a cell type located in said tissue, be internalised and take effect. An excellent study assessed the tissue tropism of AAV serotypes 1-9 in BALB/c mice by loading each serotype with luciferase (Zincarelli et al. 2008). The AAVs were injected via the tail vain ($1x10^{11}$ viral particles). D-Luciferin substrate was then injected intraperitoneally before the whole mouse was imaged in a light-tight

chamber that detected photons emitted by luciferase binding to its substrate. The injection of D-luciferin took place 7, 14, 29, 59 and 100 days after AAV administration (Zincarelli et al. 2008). AAV serotypes 1, 6, 7, 8 and 9 luciferase activity could be detected at day 7, serotypes 4 and 5 at day 14 and serotypes 2 and 3 at day 29. Serotypes 2, 3, 4 and 5 were deemed low expression due to the number of photons emitted. AAV1, 6 and 8 were deemed medium expression and AAV7 and 9 were deemed to cause high expression (Zincarelli et al. 2008). The authors then isolated the heart, liver, lung, hamstring, gastrocnemius muscle, quadricep, brain, testes and kidney to measure luciferase activity. The heart contained high luciferase levels from serotypes 1-4 and 6-9, but AAV5 luciferase was not present. The liver was also transduced by a wide range of serotypes and only AAV3 luciferase expression was not present. Luciferase from AAV4, 6, 7, 8 and 9 were present in the lung and luciferase from all serotypes (AAV1-9) were present in the hamstring. The gastrocnemius muscle was transduced by AAV1, 3, 6, 7 8 and 9 and the quadricep was transduced by AAV 3, 6, 7, 8 and 9. The brain showed transduction of only AAV 8 and 9 and the testes only AAV9. There was no signal from the kidneys, suggesting AAV transduction had not occurred. However, all serotypes were detected in all tissue types analysed by qPCR (Zincarelli et al. 2008). The serotypes could have infected the cells but not have been packaged and transported to the nucleus so that transcription and translation of the transgene could occur. Another more recent study has confirmed this theory and found that while most AAV serotypes can infect cells in most organ systems, some were unable to express their respective transgenes at the RNA level (Westhaus et al. 2020). The mechanism is not fully understood; however, a working theory is that although AAV serotypes can enter the cells, they require helper viruses to express their transgene.

The ability of AAV for effective gene transduction to the kidney is currently unclear, as researchers face challenges targeting the kidney in animal studies. Studies are beginning to emerge that altered AAV capsids and administration methods may have improved tropism to the kidney in experimental models (Kevany et al. 2019; C. Yang et al. 2020), A synthetic AAV has recently been generated, serotype Anc80, that has shown high efficiency to transduce adult kidney mesenchymal cells and myofibroblast progenitors (Ikeda et al. 2018). Furthermore, engineering of AAV serotypes with alternative promotors to target the kidney has also shown effective

transduction of kidney cells (Schievenbusch et al. 2010). Alternatively, transduction with AAVs that encode secreted peptides presents another way to deliver viral peptides to the kidney.

1.7.2 Mechanisms of cellular entry and transgene expression

For the transgene to be upregulated, the AAV needs to gain entry to the host cell and translocate to the nucleus (**Figure 1.8**). A glycosylated cell surface AAV receptor (AAVR) was identified in host cells through genome-wide screening for genes essential for signal transduction (Pillay et al. 2016). The authors then used CRISPR/Cas9 to genetically alter AAVR to block the binding to AAV1, 2, 3, 5, 8, and 9 in HeLa cells and showed no serotype could enter the cells. Furthermore, they then created AAVR knockout mice with an FVB background and demonstrated by luciferase assay that AAVR knockout mice were resistant to AAV infection (Pillay et al. 2016). Finally, they also demonstrated through immunofluorescence *in vitro* in HeLa cells that binding of AAV to AAVR causes endocytosis of AAVR which then traffics AAV to the Golgi-apparatus (Pillay et al. 2016). However, another study emerged that showed some AAV serotypes are able to enter cells independently of AAVR (Dudek et al. 2018). The authors demonstrated in AAVR knockout cells of different cell lines (HeLa, Huh7 and A549) that AAV4 was able to gain entry to the cells in a comparable manner to wild type cells. Furthermore, they proved that AAV4 was unable to bind to AAVR, even in the presence of adenovirus helpers, demonstrating multiple entry mechanisms for different virus serotypes (Dudek et al. 2018).

It is thought that the AAV particles are delivered to the nucleus via endosomes and lysosome trafficking, in which the cytoskeleton is implicated (Li and Samulski 2020; Wang, Tai, and Gao 2019). The theory is that after internalisation the virus is encapsulated in an early endosome that is coated in clathrin. The clathrin coated endosome is then tracked to the peri-nuclear area, carried by the microtubule cytoskeleton, as demonstrated by disruption of microtubules in HeLa cells where AAV2 was unable to translocate to nuclei (Xiao and Samulski 2012). The intact virus inside the endosome will be exposed to an increasingly acidic environment, as the early endosome (pH 6) transitions to the late endosome (pH 5) and then the

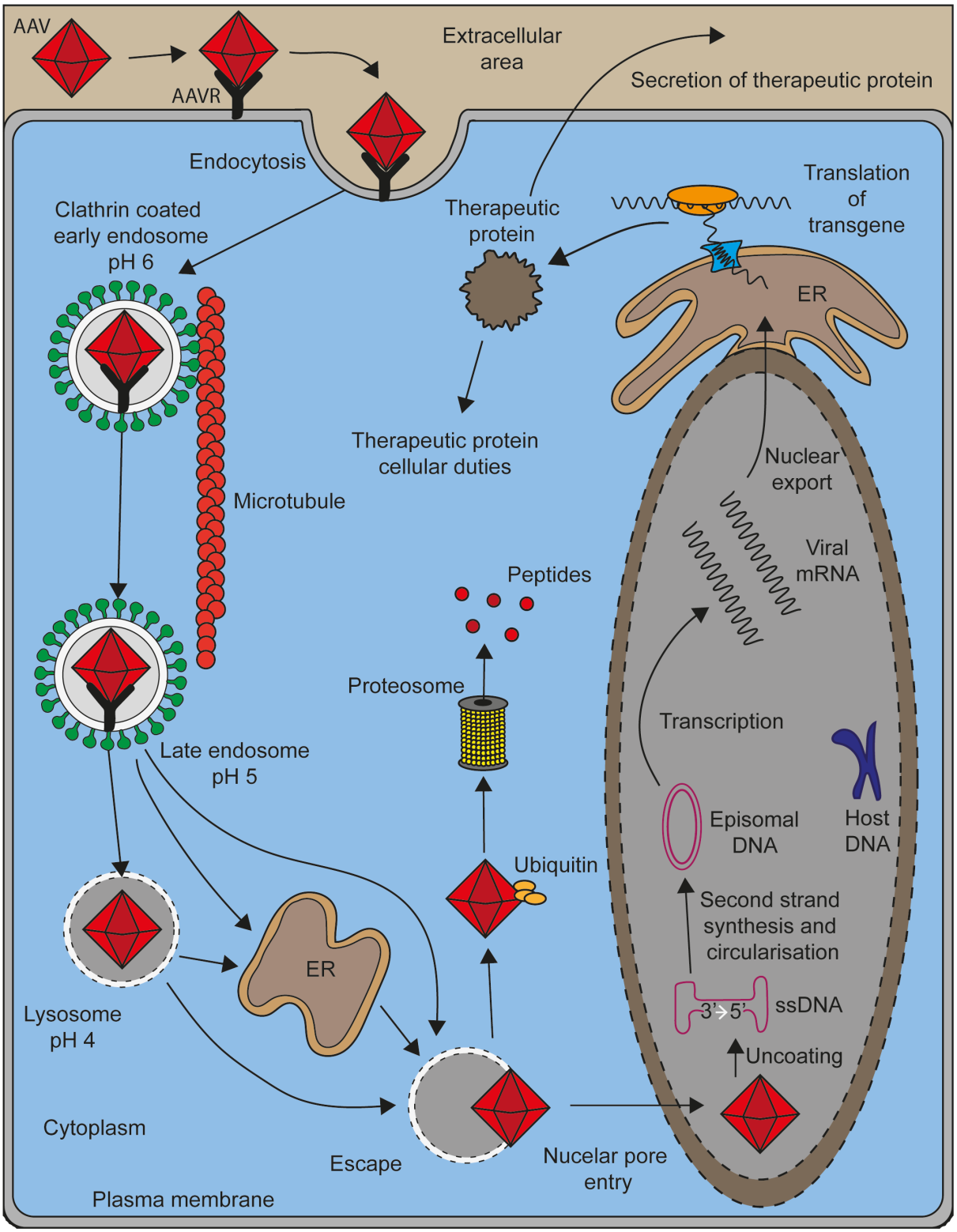

Figure 1.8 – Mechanism of AAV entry and transgene expression. *Diagram depicting AAV transduction. Viral particles can enter cell via AAVR and endocytosis. AAVs are translocated to nucleus in an endosome/lysosome before escape. AAVs are either degraded by proteosome or enter the nucleus. The capsid is uncoated, and the transgene undergoes second strand synthesis and circularisation. The episomal DNA is then converted to mRNA, exits the nucleus and the viral protein is synthesised by the cell. The viral protein is then either secreted by the cell or it undertakes its cellular duties. ssDNA, single stranded deoxyribonucleic acid; ER, endoplasmic reticulum; AAV, adeno associated virus; AAVR, adeno associated virus receptor. Original diagram.*

lysosome (pH4) (Sonntag et al. 2006). The AAV then escapes from the lysosome (or late endosome) as the membrane is degraded (Sonntag et al. 2006).

The virus can then follow 1 of 2 paths – it can either enter the nuclear pores (successful gene delivery) (Kelich et al. 2015; Xiao et al. 2002), or it can be ubiquitinated and degraded by proteasomes into peptides (unsuccessful gene delivery) (Zhong, Li, et al. 2008). If the gene delivery is successful, the AAV capsid is uncoated in the nucleus and the viral single stranded DNA is exposed (Thomas et al. 2004). However, this single stranded DNA molecule must undergo second strand synthesis to form double stranded DNA, a rate limiting step in gene transduction (Ferrari et al. 1996; Fisher et al. 1996). Second strand synthesis is initiated at the self-primed 3' end of the ITR (Zhong, Zhou, et al. 2008; Zhou et al. 2008). The transduction window can be shortened by utilising a mutated ITR to form self-complementary genome configurations. This can also be achieved by strand annealing, where 5' and 3' genomes are packaged into separate viral particles and when the capsid degradation occurs, the two strands pair inside the nuclear envelope (McCarty et al. 2003; Nakai, Storm, and Kay 2000). The genome is then circularised to increase the stability (Duan et al. 1998). It is important to note that in most AAV transduction, the viral gene is not integrated into the host genome (Li and Samulski 2020). The AAV genome is classed as episomal DNA, as it is located in the nucleus, but not in the hosts chromatin (Wang et al. 2019). This is particularly important, as it means that the expression of the trans gene persists even after mitosis (Wang et al. 2019).

The transgene then undergoes transcription, translation and post-translational modifications like any other protein innately synthesised by the host cell. The viral protein will then undertake its natural cellular tasks, or it can be secreted into the blood stream to reach off site targets (Streck et al. 2005; Subbarayan et al. 2020; Yoshioka et al. 2004). The persistence of AAV transgenes can be months or years depending on the host or virus serotype. One study injected rhesus monkeys with AAV9 and AAV2/8 that carried a firefly luciferase cassette and measured the transgene expression monthly and found stable expression up to 2 years after first injection (Tarantal et al. 2017). This was taken further and the levels of AAV1 and its transgene erythropoietin were assessed 5 years after administration to *Macaca*

fascicularis (Guilbaud et al. 2019). The authors found that there was a peak in erythropoietin levels throughout the first year but the level remained steadily higher than control animals after 5 years (Guilbaud et al. 2019).

Transgene persistence studies in mice take place over considerably less time than non-human primates due to differences in life span. One early study injected Swiss Webster mice with $3x10^6$ viral particles of AAV-LacZ (study does not state serotype) and immunostained various muscles with anti-β-galactosidase antiserum 8 months after injection. The study found stable expression of β-galactosidase at 8 months post injection and the level of positive immunostaining was comparable to mice analysed after 7 days (Xiao, Li, and Samulski 1996). Luciferase encoding AAV 1-9 administration in BALB/c mice demonstrated luciferase activity 9 months after the injections of each respective AAV and found that only AAV2 transgene expression was not sustained (Zincarelli et al. 2008).

Gene therapy strategies have been trialled in clinical settings since the first clinical trial in 2012 that restored lipoprotein lipase deficiency in order to prevent pancreatitis attacks (Ylä-Herttuala 2012). Since the success of this trial, more clinical trials have been approved. AAV therapy has been successfully trialled in haemophilia A and B by restoring Factor VII and Factor IX (George et al. 2017; Nathwani et al. 2011, 2014). Clinical trials have also been undertaken and well tolerated in a range of eye disorders with some success, however a large amount of variability between patients (Jacobson et al. 2015; Li and Samulski 2020; Moore et al. 2018). AAV therapy has also been explored in heart disease, however, with limited success. AAV therapy was well tolerated with no adverse effects, but failed induce a therapeutic benefit (Li and Samulski 2020). Currently, there are no clinical trials listed to treat any kind of kidney disease with AAVs.

1.8 **Aims and hypothesis**

Ten percent of the world have CKD. In some patients, CKD can be catastrophic, leading to ESKD, requiring lifelong dialysis or kidney transplant. Identification and analysis of molecules that can slow the progression of CKD to ESKD has the potential to save lives. Prevention of podocyte cytoskeletal disorganisation is thought to be a mechanism that can slow the development of ESKD by protection of the glomerular filtration barrier. Therefore, manipulation of actin regulating molecules is an attractive target to alleviate glomerular disease. To investigate this, this thesis examined the role of TB4, a molecule which sequesters G-actin (Sanders et al. 1992), in animal and cell culture models of glomerular a podocyte injuries.

The hypothesis of this thesis was that administration of exogenous TB4 would prevent the onset of podocyte and glomerular damage via its actin modulating and anti-inflammatory properties.

The aims of this thesis were to:

- Develop an *in vitro* model to assess the therapeutic effect of exogenous TB4 on healthy and ADR-injured mouse immortalised podocytes.
- Explore the protective role of exogenous TB4 in cytotoxic ADR injury *in vivo.*
- Examine the effects of exogenous TB4 in immune-mediated NTS nephritis *in vivo*.

Chapter 2: Exogenous thymosin β4 prevents Adriamycin induced cytoskeletal disorganisation *in vitro*

2.1 Introduction

CKD is a devastating condition that affects around 5.6 million people in the U.K. (Bikbov et al. 2020). Screening studies revealed many cases of CKD remain undiagnosed (Hirst et al. 2020) causing a number of CKD patients to progress to ESKD. The current therapies for CKD patients include lifestyle changes, lifelong dialysis, pharmacological intervention (such as ACE inhibitors) or kidney transplantation (Chen, Knicely, and Grams 2019). However, these therapies are not sufficient to stop the progression of CKD to ESKD. One of the main causes of ESKD is the breakdown of the glomerular filtration barrier (Gorriz and Martinez-Castelao 2012), which consists of capillary endothelial cells, the GBM and epithelial cells named podocytes (Patrakka and Tryggvason 2010). Podocytes project finger like extensions called foot processes, which wrap around the glomerular capillaries. The unique shape of healthy podocytes is maintained by the actin cytoskeleton (Faul et al. 2007; Welsh and Saleem 2012), a dynamic structure found in most eukaryotic cells (Gunning et al. 2015). The responsibilities of F-actin include maintenance of cellular architecture (Clarke and Spudich 1977), cell motility (Mitchison and Cramer 1996), focal adhesion (Parsons et al. 2010) and vesicular transport (Schuh 2011). Regulation of F-actin architecture in podocytes is essential for a functioning filtration barrier and is maintained by a number of actin regulating proteins, including TB4 (Paavilainen et al. 2004). During podocyte injury, the foot process network of F-actin can become disorganised, leading to foot process effacement and proteinuria (Faul et al. 2007; Welsh and Saleem 2012).

The cellular role of TB4 is to sequester G-actin monomers in the cytosol (Sanders et al. 1992) to maintain a cellular reservoir of G-actin that is readily available for polymerisation. Expression of TB4 peptide, and its mRNA precursor *Tmsb4x,* have been found in embryonic mouse and human kidneys as well as mature mouse, rat and human podocytes (Guinobert et al. 2005; Vasilopoulou et al. 2016, 2018; Xu et al. 2005). Loss of podocyte *Tmsb4x* mRNA leads to reorganisation of cortical actin stress fibres to cytoplasmic stress fibres and an increase in podocyte migration *in vitro* (Vasilopoulou et al. 2016). As it is thought that F-actin reorganisation and

podocyte migration *in vitro* represents foot process effacement *in vivo* (N. Endlich, Siegerist, and Endlich 2017; Suleiman et al. 2017). This data demonstrates the critical role of endogenous TB4 in maintaining the cytoskeletal structure and function in podocytes. The same study showed that while a loss of global *Tmsb4x* transcripts in C57BL/6 mice had no effect on healthy glomeruli, it exacerbated nephrotoxic serum nephritis, with an increase in albuminuria, glomerulosclerosis accompanied by podocyte loss (Vasilopoulou et al. 2016). These *in vivo* findings indicate that endogenous TB4 may play an important role in the progression of CKD, however, the effects of exogenous TB4 on podocytes are not known.

Due to the critical role that the presence of TB4 plays in maintaining the function of the podocyte cytoskeleton, it was postulated that treatment with exogenous TB4 may have a therapeutic role in a podocyte injury model that directly targets the cytoskeleton. ADR, an anti-cancer drug (Kim and Kim, 1972; Momparler *et al.*, 1976; Mirski, Gerlach and Cole, 1987) that has been associated with nephrotoxic side effects in some patients (Burke et al. 1977; Klastersky et al. 1985; Wollina et al. 2000), was used to induce podocyte injury in this chapter. ADR mimics some of the characteristics of human FSGS (Wang et al. 2000) when administered to rodents, and has previously been shown to lead to podocyte damage *in vitro* and *in vivo* (Huang et al. 2016; Marshall et al. 2010; Xie et al. 2019). The specific characteristics of ADR-injury *in vitro* include F-actin rearrangements, a loss of cytoplasmic and cortical actin stress fibres (Chen et al. 2017; Liu et al. 2012; X. Liu et al. 2018), and a decrease in podocyte viability, either by apoptosis (Karger et al. 2016; Xu et al. 2018) or detachment from the matrix (Dai et al. 2019; Wang et al. 2018). These detrimental effects to podocytes make ADR an ideal injury model to employ in this study.

2.2 **Aims and Hypothesis**

The hypothesis of this section of the thesis is that exogenous TB4 prevents ADR-induced podocyte cytoskeletal reorganisation, changes to motility and loss of cell viability *in vitro*. The first aim of this section is to assess the effects of TB4 on healthy podocytes by analysis of the F-actin cytoskeleton, motility and viability. Secondly, this section aims to determine the optimal concentration of ADR to induce podocyte

injury. The final aim of this chapter is to assess the effect of exogenous TB4 on ADR-injured podocyte F-actin organisation, cellular motility, and cell viability.

2.3 **Materials and methods**

Unless stated otherwise, all materials were obtained from ThermoFisher Scientific, MA, U.S.A.

2.3.1 Immortalised mouse podocyte cell culture

The flasks used for mouse podocyte cell culture were coated in 0.1 mg/ml of collagen I (Merck U.K., Dorset, U.K.) for 1 hour in a 37 °C incubator. The collagen I solution was extracted from the flasks, which were then washed twice with Dulbecco's phosphate buffered saline (D-PBS) before adding the cells. The media used to culture mouse podocytes was Roswell Park Memorial Institute – 1640 (RPMI-1640) cell culture media with 10% foetal calf serum (FCS) and 1% penicillin/streptomycin (P/S). All reagents were prewarmed to 37 °C prior to use unless stated otherwise.

To study the therapeutic effect of exogenous TB4 on podocytes, an immortalised cell line was used, kindly provided by Dr Peter Mundel, Harvard Medical School (Mundel, Reiser, et al. 1997). The cell line was generated from isolated glomeruli of kidneys from adult H-2K^{b}-tsA58 mice. The mice harbour the gene transcript for simian virus 40 (*SV40)* under the control of the mouse major histocompatibility complex H-2K^{b} promoter. SV40 is a large T antigen on the surface of the cell which, when exposed to interferon gamma (IFN-γ) at 33 °C, allows cells to freely proliferate (Jat et al. 1991). When cells are then deprived of IFN-γ and thermo-switched to 37 °C, the SV40 large T antigen is inactivated, inducing cell growth arrest and cellular senescence leading to podocyte differentiation (Mundel, Reiser, et al. 1997).

Undifferentiated mouse podocyte cells were thawed rapidly from -80 °C in a 37 °C water bath, added to 9 ml of media and centrifuged at 1200 rpm for 5 minutes. The cell pellet was resuspended in 5 ml of media and the cell suspension added to a collagen I-coated T25 flask along with 50 U/ml of IFN-γ. The flask was then placed in a 33 °C incubator with 5% CO_2. Once the cells reached 90% confluence, the media

was extracted, and the cell layer washed with D-PBS. Next, the cell layer was disrupted with 1 ml of 0.25% Trypsin-EDTA at 33 °C for no more than 5 minutes. Trypsinisation was halted by diluting in 9 ml of media before centrifuging for 5 minutes at 1200 revolutions per minute (rpm). Fresh collagen-1 T75 flasks were washed with D-PBS prior to addition of cells. After centrifugation, the cell pellet was resuspended in 10 ml of RPMI-1640 media. To achieve 1:10 dilution, 1 ml of the cell suspension was added to the flask and the remaining 9 ml was discarded. Finally, 9 ml of RPMI-1640 was added to the new flask containing the cells, with 50 units per ml (U/ml) of IFN-γ. The cells were then returned to 33 °C for maintenance of the undifferentiated cell line. Fresh media/IFN-γ changes occurred every 2 days.

The protocol for induction of podocyte differentiation was similar to the maintenance of the undifferentiated cell line. After trypsinisation and centrifugation, the cells were once again diluted 1:10 before addition to a collagen coated T75 flask. Differentiated podocytes were cultured in the absence of IFN-γ and were thermoswitched to 37 °C for 14 days. Media changes occurred every 2 days. For experimental studies, all cells were used between passage 15 and 30.

2.3.2 Counting and plating of differentiated mouse podocytes

All plates were coated with 1% of Matrigel basement matrix membrane (Corning, NY, USA) in RPMI-1640 for 40 minutes at 37 °C. Matrigel contains a high concentration of cell matrix proteins, such as laminin and collagen IV, to facilitate cell adhesion. The Matrigel solution was then removed, and the plates were washed twice with D-PBS before adding the differentiated cells. The cells were harvested by trypsinisation, media was added to the disrupted cells and the suspension was centrifuged at 1200 rpm for 5 minutes. The supernatant was then discarded, and the pellet resuspended in 2 ml of media. To determine cell number, 10 μl of the cell suspension was mixed with 10 μl of 0.4% Trypan Blue and transferred to a haemocytometer. The average cell number of 4 fields of view was calculated and it was ensured there were no more than 10% of dead cells present in the suspension. For 6 well plate assays, 50,000 cells were plated, for 4 well chamber slides, 5,000 cells were plated and for 96 well plates, 2,000 cells were plated per well. The cells were then placed back in 37 °C for a further 24 hours before each assay.

2.3.3 Administration of TB4 or ADR to mouse podocytes

Synthetic TB4 was obtained in a stock solution of 1.5 mg/ml dissolved in D-PBS (ReGeneRx Biopharmaceuticals Inc, USA). Working doses were achieved by serial dilution; 66.67 μl of the 1.5 mg/ml TB4 stock was diluted in 9.93 ml of RPMI-1640 media for a concentration of 10,000 ng/ml TB4. The 10,000 ng/ml TB4 solution was then further diluted 1:100 to achieve the working concentration of 1000 ng/ml TB4. Further 1:10 serial dilutions achieved the three doses of 10 and 100 ng/ml TB4. The final doses of 10, 100 and 1000 ng/ml were chosen due to their occurrence in previous studies using exogenous TB4 *in vitro* (Sosne et al. 2004; Sosne, Qiu, Christopherson, et al. 2007; Zhang et al. 2008). RPMI-1640 media alone was used as the control for all cell culture experiments. A wide range of ADR concentrations have previously been used to induce podocyte injury (Cormack-Aboud et al. 2008; Dai et al. 2010; Nijenhuis et al. 2011; Schneider et al. 2017). Therefore, dose response assays were undertaken to determine the appropriate concentration to induce podocyte injury. Concentrations of 0, 0.0125, 0.125, 0.25, 0.5, 1.0 or 2.5 μg/ml of ADR (Merck U.K.) were achieved by serial dilutions before addition to the cell culture media. Finally, to determine the effect of exogenous TB4 on ADR injured podocytes, concentrations of 0.0125 μg/ml and 0.125 μg/ml ADR were chosen with or without all three doses of 10 ng/ml, 100 ng/ml and 1,000 ng/ml TB4 used previously. A summary of the experimental set up can be found below (**Figure 2.1**).

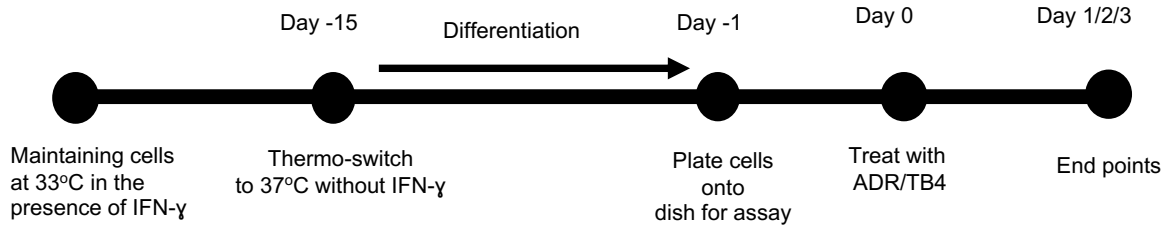

Figure 2.1 - Experimental design for in vitro assays. *Schematic of the in vitro experimental design. Immortalised, undifferentiated mouse podocytes were grown at 33 °C before thermoswitching to 37 °C for 14 days. The differentiated podocyte cells were then plated onto the appropriate dish for 24 hours before assays were undertaken.*

2.3.4 Cell viability

Cell viability was determined by methyltetrazolium (MTT) assay 24, 48 and 72 hours after RPMI-1640/TB4/ADR treatment to 2,000 mouse immortalised podocytes in a 96 well plate (Greiner Bio-One, Kremsmünster, Austria). At the desired end point, 10% (v/v) MTT reagent (3-(4,5-Dimethylthiazole-2-yl)-2,5-diphenyltetrazolium Bromide) (Merck U.K.) (dissolved in 5 mg/ml in PBS) was added to the media of each well for 3 hours at 37 °C. After 3 hours, the media was aspirated and 100 μl of dimethyl sulfoxide (DMSO) (Merck U.K.) was added to each well for 15 minutes in the dark. Absorbance of 4 replicates was read at 565 nm on a plate reader (Tecan Infinite M200 Pro, Männedorf, Switzerland). Due to variability of the assay, the results were normalised to the 24-hour RPMI-1640 only values of their respective independent experiments. Experiments were repeated independently at least 3 times.

2.3.5 Scratch wound assay

To assess podocyte migration, a scratch wound assay was used. Mouse podocytes were plated onto 6 well plates and treated with RPMI-1640 alone or containing TB4 and/or ADR as described in 2.3.2 and 2.3.3. After 24 hours, the scratch wound was generated by dragging a 200 μL pipette tip along the cell surface so that the cells detached from the plate, creating a wound. The wells were washed with 2 ml of warmed media, so that there were not detached cells left in the well. Cells were treated with 2 ml of media alone or the media containing ADR/TB4 were added to each well. Four fields of view of the cells were imaged at 0, 6 and 24 hours at 10x magnification. The images were taken on the brightfield mode of an Olympus IX71 inverted Tissue Culture scope (Olympus, Tokyo, Japan). The number of cells that migrated into the wound area were counted at 6 and 24 hours after wound induction. The average of 4 fields of view were calculated and the experiments were repeated independently at least 3 times.

2.3.6 Phalloidin staining of mouse podocytes

F-actin organisation and amount was analysed after staining and visualisation with Acti-stain™ 488 Phalloidin (Cytoskeleton Inc., USA). Cells were plated onto 4 well chamber slides and administered with RPMI-1640 alone or TB4 and/or ADR as described in 2.3.2 and 2.3.3. After 24 hours, media was aspirated, and the cells were

treated with the desired dose of TB4/ADR for 24 hours at 37 ^{O}C. The cells were then washed with D-PBS and fixed with 5% PFA and 5% sucrose in PBS for 20 minutes. After fixation, cells were washed in PBS and permeabilised in 0.5% Triton X-100 in PBS for 10 minutes. The cells were then washed in 0.1% Triton X-100 in PBS and incubated in block solution (10% FCS, 1% BSA and 0.1% Triton X-100 in PBS) for 60 minutes. Directly after blocking, the cells were incubated with 100 nM of Acti-stain™ 488 Phalloidin for 30 minutes in the dark to stain for F-actin. After another washing stage in PBS, the cells were incubated in 10 μg/ml Hoechst 33342 to stain nuclear chromatin for 10 minutes in the dark. The slide was then mounted on a coverslip with SlowFade fluorescent mounting media prior to imaging with an air 40x objective on an Eclipse 50i upright fluorescent microscope (Nikon Instruments, Melville, USA). Hoechst 33342 was excited with a DAPI filter cube and imaged at 405 nm. Acti-stain™ 488 Phalloidin was excited with a Nikon filter B-2A and imaged at 520 nm. Fifty cells were imaged per dose in each experiment.

The composite images of nuclei and F-actin were opened in Fiji ImageJ software (Schindelin et al. 2012) and the channels were split. Only the F-actin channel was used for analysis. The doses were made blind to the scorer to eliminate any form of bias. The circumference of the cell was traced and measured, obtaining the area of the podocyte cells, mean grey value and integrated density of podocyte F-actin. An area of the background adjacent to the cell was also measured. Corrected total cell fluorescence (CTCF), which is proportional to the fluorescence of F-actin in the cell was calculated by the following formula: CTCF = Integrated density – (cell area x mean grey area of background). The F-actin arrangements were then classed according to their arrangements. Cortical F-actin stress fibres were defined as the majority of the F-actin accumulated around the cortex of the cell. Cytoplasmic stress fibres were defined as F-actin filaments that traversed the cell body in parallel organisation. Unorganised F-actin filaments showed no recognisable organisation and resembled a “mat” of unorganised F-actin across the whole cell. Cell area and CTCF were normalised by dividing each dose by 0 ng/ml TB4 and 0 μg/ml of ADR of the same experiment due to variability between experiments. Experiments were repeated independently at least 3 times.

2.3.7 mRNA extraction

To determine mRNA levels of gene in different conditions, mRNA was extracted from podocytes. Mouse podocytes were plated onto 6 well plates and exposed to either RPMI-1640 alone or containing TB4 and/or ADR as described in in 2.3.2 and 2.3.3. After 24 hours mRNA was extracted using an RNeasy mini kit (Qiagen, Düsseldorf, Germany). The media was aspirated and 350 μL of buffer RLT with 1% β-mercaptoethanol was used to disrupt and lyse the cell layer. The cell suspension was then vortexed for 1 minute before mechanical homogenisation with a blunt 20-guage RNAse-free syringe and needle. An equal homogenous mixture with 70% ethanol was then created with the cell lysate by pipetting. The homogenous cell lysate-ethanol mixture was then transferred to a spin column attached to a collection tube and centrifuged at 8000 x g for 15 seconds. Genomic deoxyribonucleic acid (gDNA) was digested by incubation for 15 minutes at room temperature in RNase free DNase 1 (Qiagen). Buffer RW1 (350 μl) was added to the column which was then centrifuged at 8000 x g for 15 seconds. The flow through was discarded in each of the following steps after centrifugation. The collection tube was reused and 700 μl of buffer RW1 was added to the spin column and centrifuged for a further 15 seconds at 8000 x g. Next, 500 μL of buffer RPE (diluted to 20% buffer RPE in 100% ethanol) was added twice to the spin column and centrifuged at 8000 x g for 15 seconds and 2 minutes for the first and second addition respectively. The collection tube was then discarded, and the spin column placed in an RNAse free Eppendorf tube before 50 μl of RNAse free water was added to the column membrane and centrifuged at 8000 x g for 1 minute. The resulting flow through contained purified mRNA which was stored at -80 °C until ready for further use.

2.3.8 cDNA synthesis

mRNA was converted to cDNA prior to qPCR. The following protocol used the iScript cDNA synthesis kid (Biorad, CA, USA). Prior to cDNA synthesis, the purity and concentration of mRNA was determined using a Nanodrop machine. To assess purity, the absorbance at 260 nm and 280 nm was read. An A_{260}/A_{280} ratio between 1.8 – 2.1 is indicative of highly purified mRNA. mRNA concentration was calculated by the Nanodrop automatically using the Beer-Lambert law ($A = \in Cl$), which predicts a linear change in absorbance with concentration, where A is absorbance at 260 nm,

ϵ = extinction coefficient of mRNA (0.025 mg/ml)$^{-1}$cm^{-1}, C = concentration of mRNA and l = path length of the chamber.

The amount needed for 0.1 μg mRNA was added to a PCR tube (Greiner Bio-One) and made up to 15 μl with RNase free water. A master-mix was prepared with 4 μl of 5x iScript reaction mix and 1 μl of iScript reverse transcriptase per sample. Negative controls were also prepared, one without reverse transcriptase and one without mRNA. The PCR tubes containing the mRNA were then mixed with 5 μl of the master-mix (excluding reverse transcriptase negative control, which contained mRNA plus 5 μl of reaction mix alone). The PCR tubes were then placed into a PCR Thermocycler (Eppendorf, Stevenage, U.K.) and the following program was started:

25 °C – 5 minutes (primer annealing)

42 °C – 30 minutes (reverse transcription)

85 °C – 5 minutes (removal of mRNA template)

4 °C – hold

The samples were then stored at -20 °C until further analysis undertaken.

2.3.9 Primer design

Primers for qPCR experiments were designed using Primer-BLAST (https://www.ncbi.nlm.nih.gov/tools/primer-blast/) and Primer3 (https://primer3.ut.ee/). The details of the primers used are listed (**Table 2.1**). The β-thymosin family of peptides was examined to determine if ADR leads to a loss of actin sequestering molecules. TB4 is predicted to bind to Schip1 (Miyamoto-Sato et al. 2010), a protein in the ezrin complex that preserves cortical F-actin arrangements in podocytes *in vitro* (Perisic et al. 2015). Other members of the ezrin complex were examined to see if they were altered by potential interactions. Other actin regulating proteins, such as synaptopodin, destrin, cofilin and profilin were examined to determine changes following ADR injury.

Table 2.1 – Primer details

Target gene/translated protein (annealing temp, °C)	**Primer sequence (5' to 3')**	**Location on mRNA (amplicon size, base pairs)**
Tmsb4x/TB4 (60)	Fwd: ATGTCTGACAAACCCGATATGGC	Bp 76 - 200. Exon 1 – 2 (125)
	Rvs: CCAGCTTGCTTCTCTTGTTCA	
Tmsb10/Thymosin β10 (60)	Fwd: CAGCTTCGATAAGGCCAAGC	Bp 264 - 337. Exon 3 – 4 (74).
	Rvs: CAATGGTCTCTTTGGTCGGC	
Tmsb15a/Thymosin β15a (64)	Fwd: CCAGACTTGTCGGAAGTGGAG	Bp 153 - 260. Exon 2 – 3 (108).
	Rvs: CTCCTTCTCTTGCTCGATGGT	
Tmsb15b/Thymosin β15b (64)	Fwd: AGCGATAAACCAGACTTGTCAGA	Bp 125 - 231. Exon 2 – 3 (107).
	Rvs: TGCTGGATAGTTTCATTCGACG	
Tmsb15l/Thymosin β15-like (60)	Fwd: TGAGCGATAAACCAGACTTGTCA	Bp 88 - 196. Exon 1 – 2 (109).
	Rvs: TGCTGGATAGTTTCCTTCGAC	
Schip1/Schip1 (60)	Fwd: GCACACAGAACAAGATGCCA	Bp 1337 - 1557. Exon 7 – 8 (221).
	Rvs: GCTCGGACGTTACCAATGAC	
Slc9a3r2/Nherf2 (58)	Fwd: TGCTGGTAGTCGATCCTGAG	Bp 829 - 967. Exon 4 – 6 (139).
	Rvs: CACACAGAGCCACCATTGAG	
Podxl/Podocalyxin (58)	Fwd: GCCTGTGGATTCTTCACCGA	Bp 808 - 959. Exon 2 – 3 (152).
	Rvs: CTTCAGAGGTGCCCAATGGT	
Ezr/Ezrin (64)	Fwd: AAGTGTGGTACTTCGGCCTG	Bp 259 - 936. Exon 3 – 8 (678).
	Rvs: AGTCAGGTGCCTTCTTGTCG	
Clic5/CLIC5a (58)	Fwd: TCTACACAACCTGGCTCCTG	Bp 998 - 1123. Exon 6 (126).
	Rvs: AGTTTGGGGTACTTCTCGGG	
Nf2/Neurofibromin 2 (60)	Fwd: AAAAGGTCTACTGCCCTCCC	Bp 945 - 1033. Exon 4 – 5 (89).
	Rvs: GTGCACAGAGGGGTCATAGT	
Dstn/Destrin (60)	Fwd: TCTCCTGCTTTTGCTACCCG	Bp 227 - 329. Exon 1 – 2 (103).
	Rvs: AACTCCTGAGGCCATGTTCG	
Synpo/Synaptopodin (62)	Fwd: ACCCAATCAGAACCTCTCGG	Bp 1735 - 1879. Exon 2 (145).
	Rvs: TGAAGGCAGGGACATGGTAG	
Cfl1/Cofilin 1 (58)	Fwd: AGACAAGGACTGCCGCTATG	Bp 373 - 460. Exon 2 (88).
	Rvs: GGCCCAGAAGATGAACACCA	
Pfn1/Profilin 1 (60)	Fwd: GTGGAACGCCTACATCGACA	Bp 623 - 786. Exon 3 (164).
	Rvs: TTGACCGGTCTTTGCCTACC	
Pfn2/Profilin 2 (60)	Fwd: GCTACTGCGACGCCAAATAC	Bp 346 - 537. Exon 1 – 2 (192).
	Rvs: TGTCCATTGTGCAGTCACCA	
Gapdh/Glyceraldehyde-3-phosphate dehydrogenase (same as gene of interest)	Fwd: TGCCCCCATGTTTGTGATG	Bp 801 - 951. Exon 5 – 6 (151).
	Rvs: TGTGGTCATGAGCCCTTCC	

Table 2.1 – Primer details. *Details of all primers used for in vitro experiments, including target gene and its translated protein; the nucleotide sequences; the size of the amplicons; the location of the amplicon on the target gene and the annealing temperature used in quantitative PCR experiments. Tmsb4x, Thymosin β4, TB4; Schip1, Schip1, Schwannomin interacting protein 1; Slc9a3r2, Nherf 2, Sodium-hydrogen exchange regulatory cofactor 2; fwd, forward; rvs, Reverse; temp, temperature. Bp, base pairs.*

2.3.10 qPCR

qPCR experiments used cDNA that was prepared as in 2.3.8. A master-mix was prepared containing the necessary components for the reaction and included per sample:

10 μl of 2x SYBR Green supermix (PCR Biosystems, London, U.K.)
0.5 μl of forward primer (10 μM) (Fisher Scientific, NH, USA)
0.5 μl of reverse primer (10 μM) (Fisher Scientific)
8 μl nuclease-free water (Qiagen).

Following this, 1 μl of cDNA samples was added to each well of a 96 well plate (Roche, Basel, Switzerland) in duplicate for the gene of interest and also glyceraldehyde-3-phosphate deydrogenase (*Gapdh*) (housekeeping gene) along with 19 μl of the master-mix. The plate was then sealed with transparent film (Roche), and vortexed and then added to the real-time PCR Light Cycler 480 (Roche), the experiment was started using a previously determined protocol (below), where X refers to annealing temperature of primers (**Table 2.1**).

95 °C	-	3 mins	
95 °C	-	30 secs	x45 cycles
X °C	-	30secs	
72 °C	-	30secs	
65 °C	-	15secs	
95 °C	-	15secs	

The average Ct value for each duplicate was calculated for the target gene and the housekeeping gene. The difference in the Ct values (ΔCt) of the target gene and

housekeeping gene was calculated. The average ΔCt value for RPMI-1640 alone was calculated and then subtracted from the ΔCt value of the treated cells giving the ΔΔCt.

The formula $2^{-\Delta\Delta Ct}$ was used to determine fold changes in mRNA levels. Negative controls omitting cDNA or reverse transcriptase were included on each plate to identify potential contamination. Melt curves with a single peak were generated to confirm primer specificity. Experiments were repeated independently at least 4 times. Expression of *Gapdh* was unaltered by ADR/TB4 treatment, confirming the validity of *Gapdh* as the housekeeping gene (**Figure 2.2**).

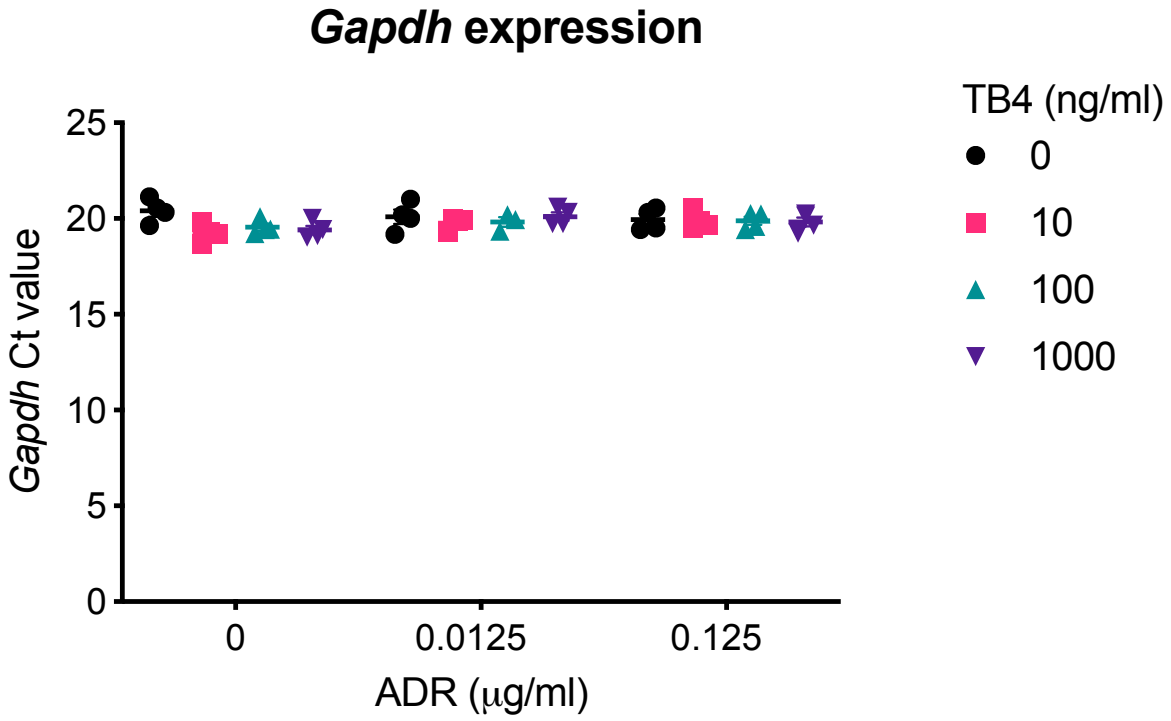

Figure 2.2 – Effect of ADR/TB4 on Gapdh expression. *The threshold values of Gapdh were unaffected by ADR/TB4 treatment compared to media alone. Each data-point represents 1 experiment showing the mean ±SEM of 2 replicate wells. Experiments were repeated independently at least 4 times.*

2.3.11 Statistical analysis

All statistical analysis was performed using GraphPad Prism 9.00 for Mac, GraphPad Software, La Jolla California USA, www.graphpad.com. All data were plotted as the mean value ±SEM. Normal distribution was assessed by Shapiro-Wilk test. If data were not normally distributed, they were either log_{10} or square root transformed or normalised to RPMI-1640 only treated values to achieve normality before statistical tests were used.

For experiments with just 1 variable, for example TB4 dose response cytoskeleton analysis, one-way analysis of variance tests (ANOVA) with Dunnett's multiple comparison tests were used to compare experimental doses with RPMI-1640. For experiments with two variables, such as TB4 and ADR co-treatment experiments, two-way ANOVA with Tukey's multiple comparison test was used to compare statistical difference between all values.

2.4 **Results**

2.4.1 Exogenous TB4 has no effect on podocyte viability, migration or cytoskeleton

It has been previously shown that loss of endogenous *Tmsb4x* mRNA and TB4 peptide leads to increased podocyte motility and cytoskeletal disorganisation *in vitro* (Vasilopoulou et al. 2016). It is not known if exogenous TB4 has any effect to podocytes, therefore the first section of the chapter aims to identify any effects of TB4 to podocyte viability, migration, and the cytoskeleton.

2.4.1.1 *Exogenous TB4 has no effect on podocyte viability*

Podocyte viability was assessed by MTT assay as per 2.3.4. There was no statistical significance between any value, indicating exogenous TB4 did not affect podocyte viability at 24, 48 or 72 hours after treatment (**Figure 2.3**).

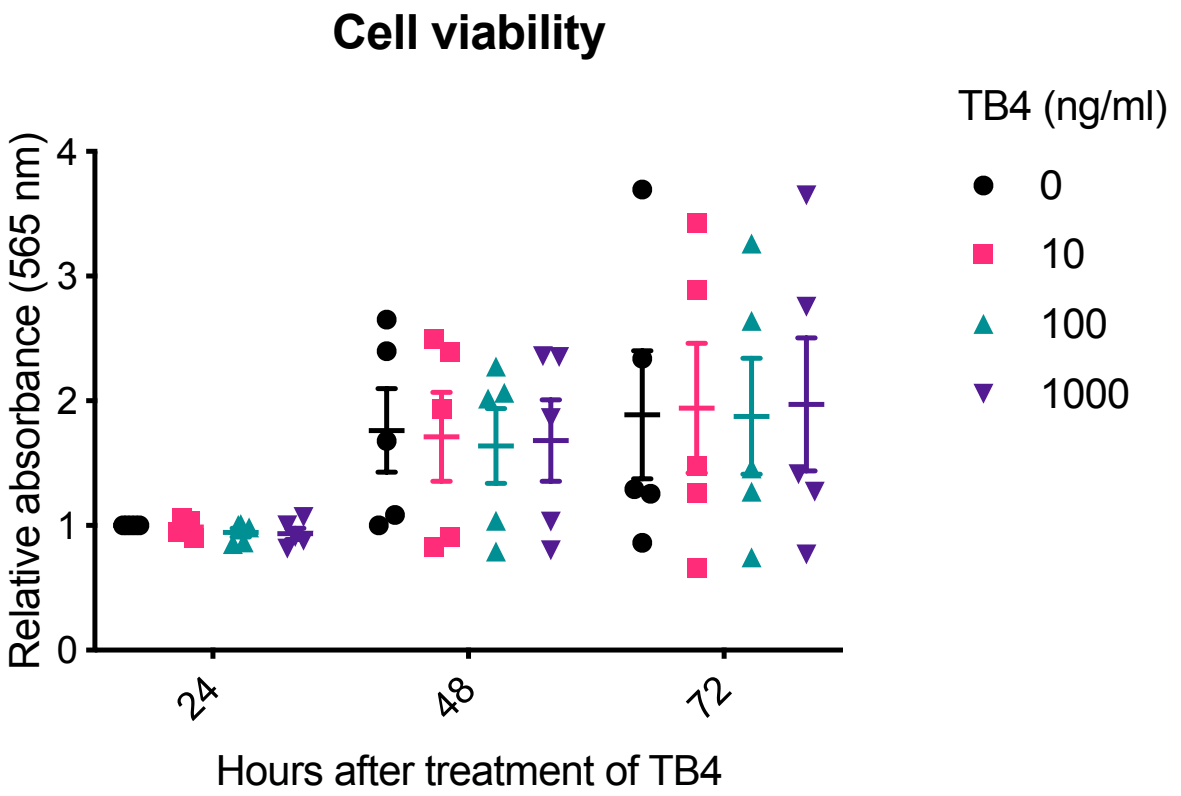

Figure 2.3 – TB4 has no effect on podocyte viability. *Differentiated immortalised mouse podocytes were treated with 0 - 1000 ng/ml of TB4 and cell viability was assessed by MTT assay 24, 48 and 72 hours after TB4 treatment. Each data point represents the average of 4 replicates. Individual experiments were repeated at least 5 times. Data has been normalised to 0 ng/ml of TB4 to reduce variability and achieve normal distribution. Data shown as the mean ±SEM.*

2.4.1.2 *Exogenous TB4 does not alter podocyte migration*

Podocyte migration was assessed by scratch wound assay as described in 2.3.5. Images were taken at 0, 6 and 24 hours after wound formation, with representative images of each time point provided in **Figure 2.4a, b, c**. All doses of TB4 and media only treated cells showed increase in cell migration between 6 and 24 hours ($P<0.01$ for 0 ng/ml, 100 ng/ml, 1000 ng/ml; $P<0.001$ for 10 ng/ml), however, there was no statistical difference between cells treated with TB4 compared to media treated cells alone at 6 or 24 hours (**Figure 2.4d**). Therefore, exogenous TB4 does not alter migration of healthy podocytes.

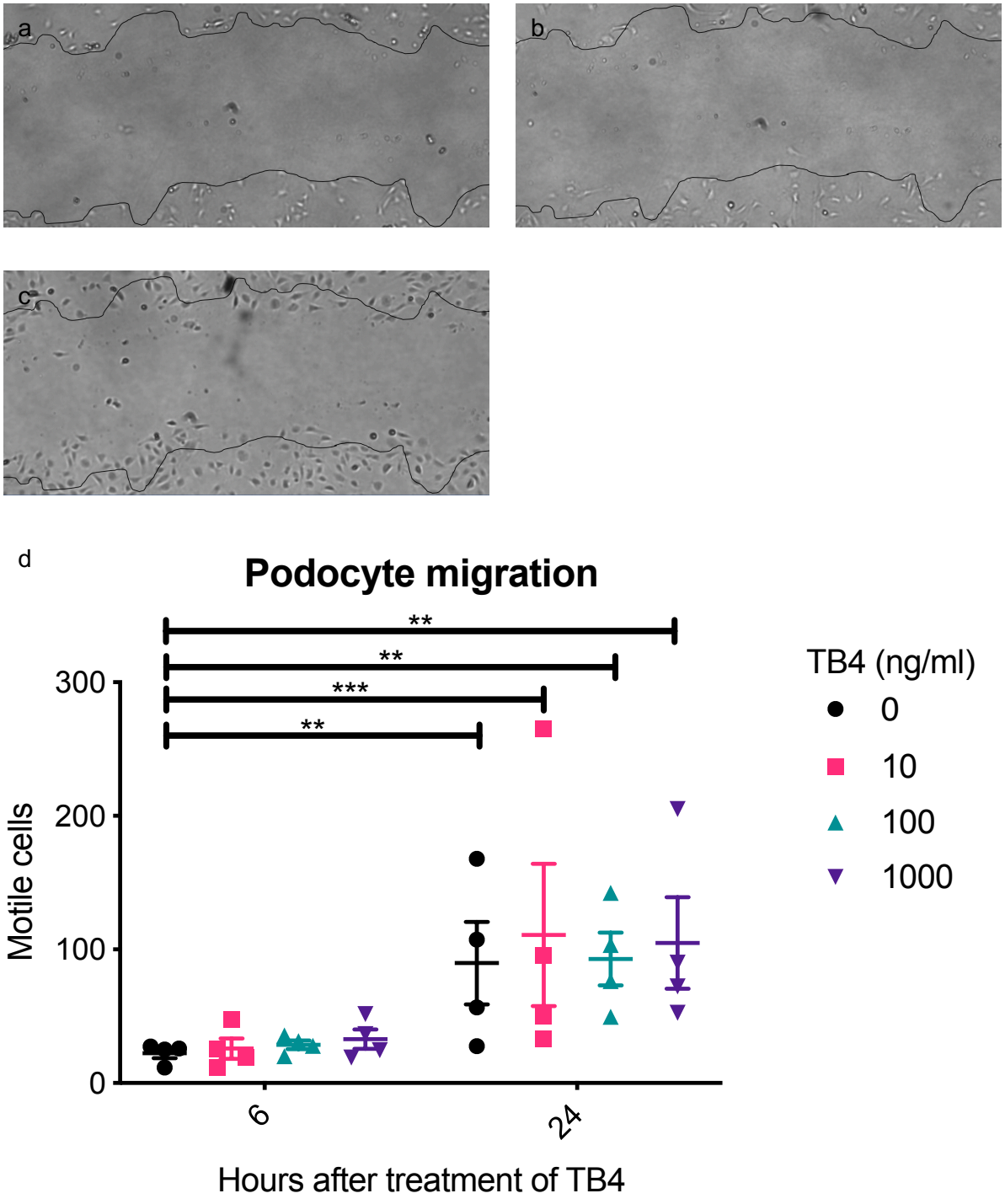

Figure 2.4 – Exogenous TB4 does not alter podocyte migration. *Differentiated immortalised mouse podocytes were treated with 0 - 1000 ng/ml of TB4 and cell migration assessed by scratch wound assay. Representative images of podocytes treated with 0 ng/ml of TB4 at* ***(a)*** *0 hours,* ***(b)*** *6 hours and* ***(c)*** *24 hours imaged with x10 magnification. The black line indicates the boundaries of the wound which was transferred from 0h to images of subsequent time points. Each data point represents the average of 4 fields of view of 1 experiment. Data are shown as mean ±SEM of 4 independent experiments. **P≤0.01, ***P≤0.001.*

2.4.1.3 *Exogenous TB4 does not alter the podocyte cytoskeleton*

To analyse the podocyte cytoskeleton cells were fixed and stained with Acti-Stain™ 488 Phalloidin and analysed as described in 2.3.6. Podocyte F-actin arrangements were sorted into three sub-types: cortical actin stress fibres (**Figure 2.5a**); cytoplasmic stress fibres (**Figure 2.5b**) or unorganised actin fibres (**Figure 2.5c**). Cortical actin stress fibres displayed as an F-actin network around the periphery of the cell. Unorganised actin fibres did not show any specific actin arrangement. Cytoplasmic stress fibres displayed as organised F-actin filaments traversing the cell body perpendicular to adjacent fibres.

The results show that the predominant F-actin organisation in podocytes is cortical actin stress fibres, with a prevalence of 53.5 ± 2.2% (**Figure 2.5d**), whereas the prevalence of cytoplasmic stress fibres was 26.4 ± 2.5 (**Figure 2.5e**) and unorganised actin was 12.4 ± 2.0% (**Figure 2.5f**). Exogenous TB4 had no effect on the proportion of cells displaying each type of F-actin organisation, total F-actin fluorescence in podocytes (**Figure 2.5g**) or the cell area (**Figure 2.5h**).

Collectively, the results presented in this subsection provide evidence that exogenous TB4 had no effects on healthy podocyte cells *in vitro*. Next, the effect of ADR on podocyte cells *in vitro* was examined to determine appropriate doses to explore if TB4 modulates podocyte injury induced by ADR.

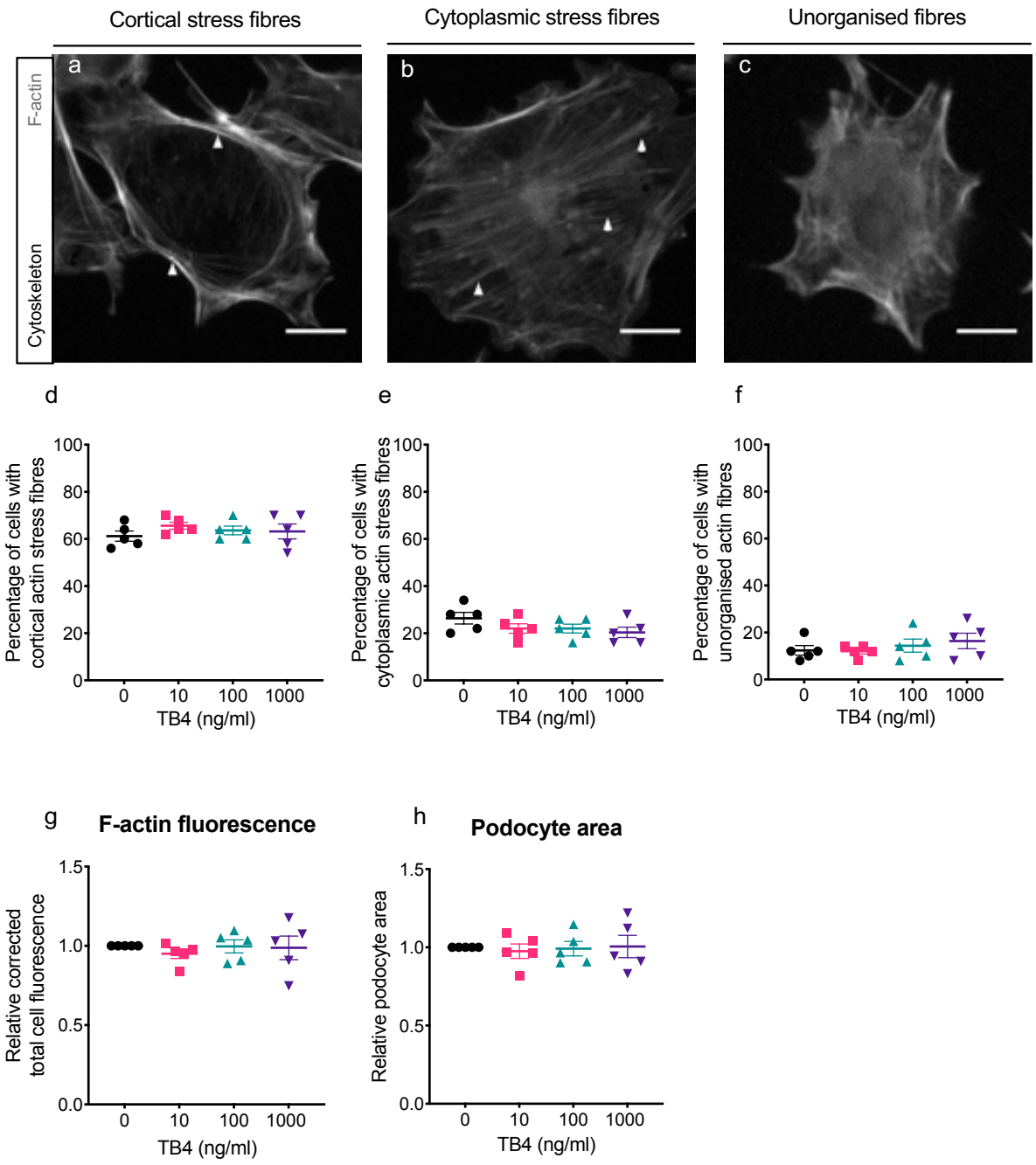

Figure 2.5 – Exogenous TB4 does not alter podocyte F-actin organisation.
Differentiated immortalised mouse podocytes were treated with 0 - 1000 ng/ml of TB4, fixed after 24 hours and stained with phalloidin conjugated to Actin-stain 488 to examine F-actin. Nuclei were stained using Hoechst 33342. Representative images of cells with ***(a)*** *cortical actin stress fibres,* ***(b)*** *unorganised actin fibres and* ***(c)*** *cytoplasmic actin stress fibres at 40x magnification. White arrowheads indicate stress fibres. Scale bar = 10 µm. Quantification of the effect of exogenous TB4 on the percentage of cells with* ***(d)*** *cortical actin stress fibres,* ***(e)*** *unorganised actin fibres,* ***(f)*** *cytoplasmic stress fibres,* ***(g)*** *the normalised F-actin fluorescence and* ***(h)*** *total area of the cell.* ***(g)*** *and* ***(f)*** *have been normalised to media only treated cells to reduce variability. Each data point represents the average of 50 cells. Data are shown as mean ±SEM of 5 independent experiments.*

2.4.2 Characterisation of ADR-induced podocyte injury *in vitro*

ADR was identified as a candidate to induce podocyte damage, however, a range of 0.125 μg/ml – 2.5 μg/ml have been used previously (Cormack-Aboud et al. 2008; Dai et al. 2010; Nijenhuis et al. 2011; Schneider et al. 2017). Therefore, dose response experiments were conducted in order to determine appropriate concentrations to use in co-treatment experiments with TB4.

2.4.2.1 *ADR reduces podocyte viability*

Firstly, a dose response experiment was carried out to determine the effect of ADR on podocyte viability by MTT assay as described in 2.3.4. Treatment of podocytes with doses equivalent to or higher than 0.125 μg/ml of ADR caused between 60-70% decrease in podocyte viability after 24 hours (**Figure 2.6a**). At 48 and 72 hours,

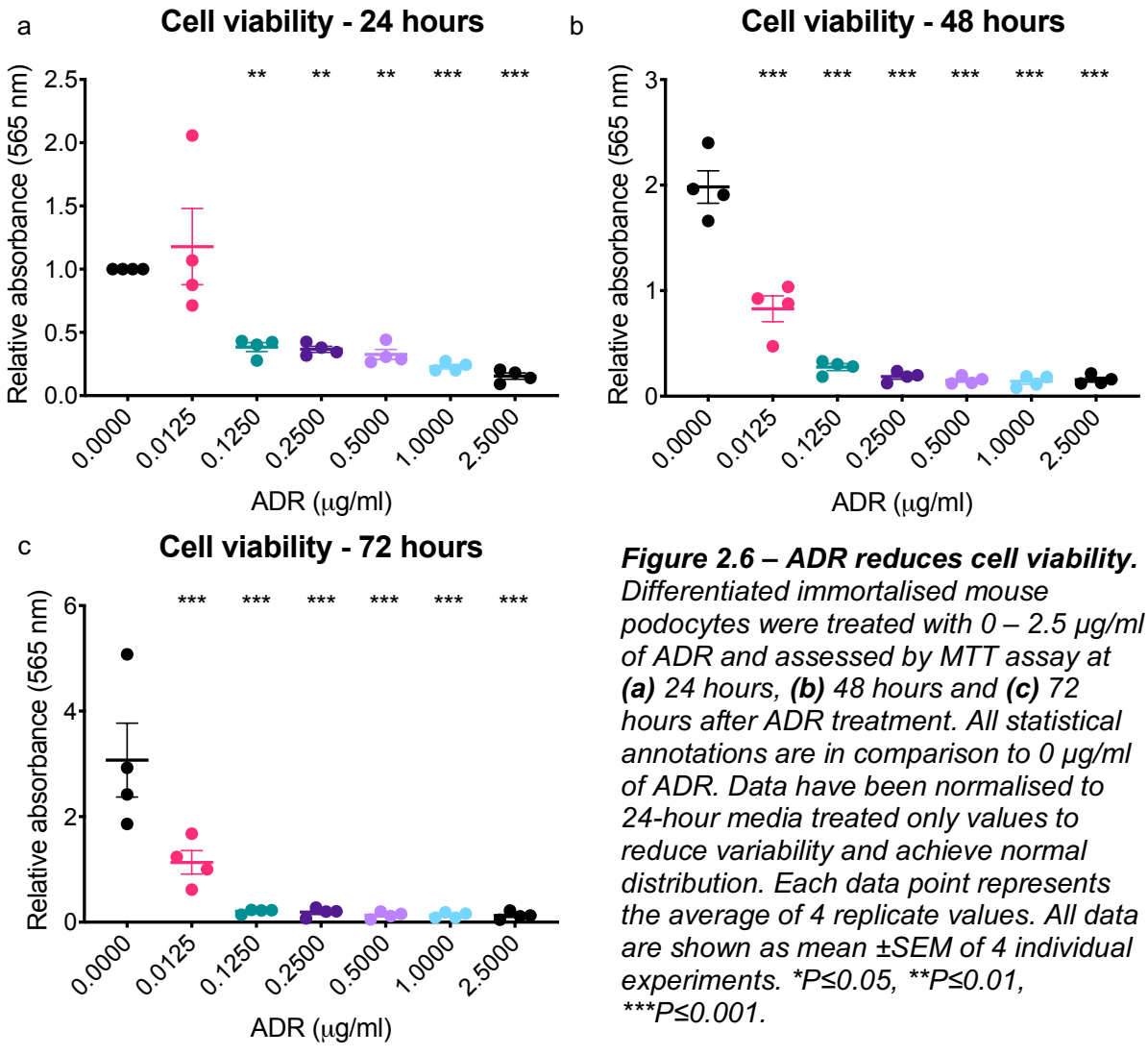

Figure 2.6 – ADR reduces cell viability. *Differentiated immortalised mouse podocytes were treated with 0 – 2.5 μg/ml of ADR and assessed by MTT assay at* ***(a)*** *24 hours,* ***(b)*** *48 hours and* ***(c)*** *72 hours after ADR treatment. All statistical annotations are in comparison to 0 μg/ml of ADR. Data have been normalised to 24-hour media treated only values to reduce variability and achieve normal distribution. Each data point represents the average of 4 replicate values. All data are shown as mean ±SEM of 4 individual experiments. *P≤0.05, **P≤0.01, ***P≤0.001.*

0.0125 μg/ml of ADR reduced podocyte viability by 60% (P<0.01 versus media treated cells) and 0.125 – 2.5 μg/ml of ADR decreased cell viability by 90% (P<0.001 vs media treated cells for both time points) (**Figure 2.6b c**).

2.4.2.2 *Effect of ADR on podocyte migration*

Next, the effect of ADR on podocyte migration was assessed by a scratch wound assay as described in 2.3.5 at 0, 6 and 24 hours after ADR treatment (**Figure 2.7a, b, c**). ADR did not cause changes to podocyte migration after 6 hours (**Figure 2.7d**). As expected, the cells treated with media only showed a significant increase in wound closure between 6 and 24 hours (P<0.01).

The representative images display cells treated with 1 μg/ml of ADR, where there is a significant loss of cells at 24 hours (**Figure 2.7a, b, c**). Comparing this data with the representative image of untreated cells 24 hours after scratch wound (**Figure 2.6d**), where 0.125 μg/ml and above caused a loss in podocyte viability after 24 hours, the conclusion can be drawn that doses above this concentration are inappropriate for scratch wound analysis due to significant loss of viability.

The number of cells migrating into the wound was reduced when podocytes were treated with ADR compared to cells treated with media alone; this was significant at doses of 0.25 μg/ml ADR and above (**Figure 2.7e**). Between 6 and 24 hours, 0.0125 – 0.5 μg/ml ADR showed no difference in cell number compared with and 1 – 2.5 μg/ml ADR showed a decrease in cell number (P<0.05 vs respective 6-hour values).

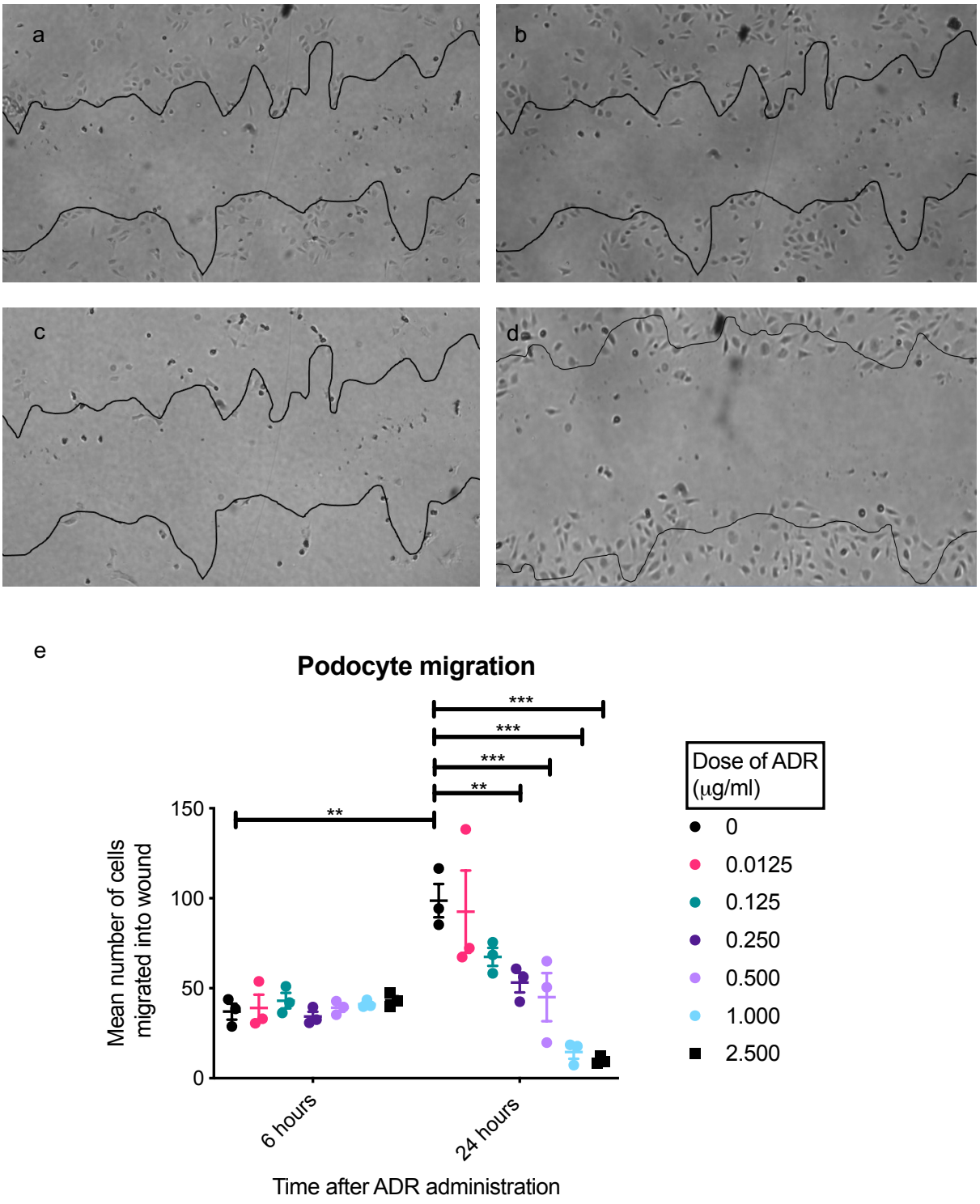

Figure 2.7 – Assessment of cell motility after ADR treatment. *Differentiated immortalised mouse podocytes were treated with 0 – 2.5 μg/ml ADR and cell migration was assessed by scratch wound assay at* ***(a)*** *0,* ***(b)*** *6 and* ***(c)*** *24 hours after wound induction.* ***(d)*** *Representative image of untreated cells 24 hours after scratch wound. Black line indicates borders of wound area. Images taken at 10x magnification.* ***(e)*** *Quantification of cells that migrated into wound at 6- and 24-hour time points. Each data point represents the average of 4 fields of view. Data are shown as the mean ±SEM of 3 independent experiments. **P≤0.01, ***P≤0.001.*

2.4.2.3 *ADR causes podocyte cytoskeletal disorganisation*

To determine which concentrations lead to significant cytoskeletal changes in these laboratory conditions, a comprehensive analysis of a wide range of doses was undertaken. Cells were treated with 0 – 2.5 μg/ml ADR and stained with Acti-Stain™ 488 Phalloidin as described in 2.3.6. Podocyte cytoskeletal organisation was sorted into the same three sub-groups as the TB4 dose response experiment (**Figure 2.5a, b, c**) after 24 hours of ADR treatment.

The lowest dose of 0.0125 μg/ml of ADR caused a 21 ± 0.7% reduction in cortical stress fibres ($P<0.01$ versus untreated cells), 0.125 μg/ml caused a 50 ± 2.9% decrease in cortical stress fibres ($P<0.001$ versus untreated cells). Treating cells with 2.5 μg/ml ADR caused a 42 ± 1.1 % reduction in cortical stress fibres compared with untreated cells ($P<0.001$). Both doses of 0.5 μg/ml and 1 μg/ml ADR caused a 41 ± 2.9 % reduction in cortical stress fibre prevalence compared with untreated cells ($P<0.001$ for both doses). The highest dose of 2.5 μg/ml caused a 44 ± 1.2% reduction in cortical stress fibres compared with untreated cells ($P<0.001$) (**Figure 2.8a**). No dose of ADR altered cytoplasmic stress fibre prevalence compared with untreated cells (**Figure 2.8b**). The low dose of 0.0125 μg/ml of ADR lead to 3.5 ± 0.4-fold increase in unorganised actin filaments ($P<0.001$ versus untreated cells). Cells treated with 0.125 μg/ml ADR showed 5.3 ± 0.1-fold increase in unorganised actin prevalence ($P<0.001$ versus untreated cells). Podocytes treated with 0.25 μg/ml ADR showed a 5.7 ± 0.1-fold increase in unorganised actin prevalence ($P<0.001$ versus untreated cells). In cells treated with 0.5 μg/ml ADR, there was a 6 ± 0.1-fold increase in unorganised actin compared with untreated cells ($P<0.001$). In cells treated with 1 μg/ml and 2.5 μg/ml ADR, there was a 5.4 ± 0.1 and 6.3 ± 0.1-fold increase in unorganised F-actin respectively ($P<0.001$ in both doses versus untreated cells) (**Figure 2.8c**).

Next, the podocyte cell area and total F-actin fluorescence were also analysed. Doses of 0.0125 μg/ml 0.125, 0.25 and 0.5 μg/ml of ADR did not significantly alter F-actin fluorescence. Doses of 1 ($P<0.05$) and 2.5 ($P<0.001$) μg/ml of ADR lead to a 55 ± 0.23% and 82 ± 0.06% decrease in podocyte F-actin fluorescence respectively compared with untreated cells (**Figure 2.8d**).

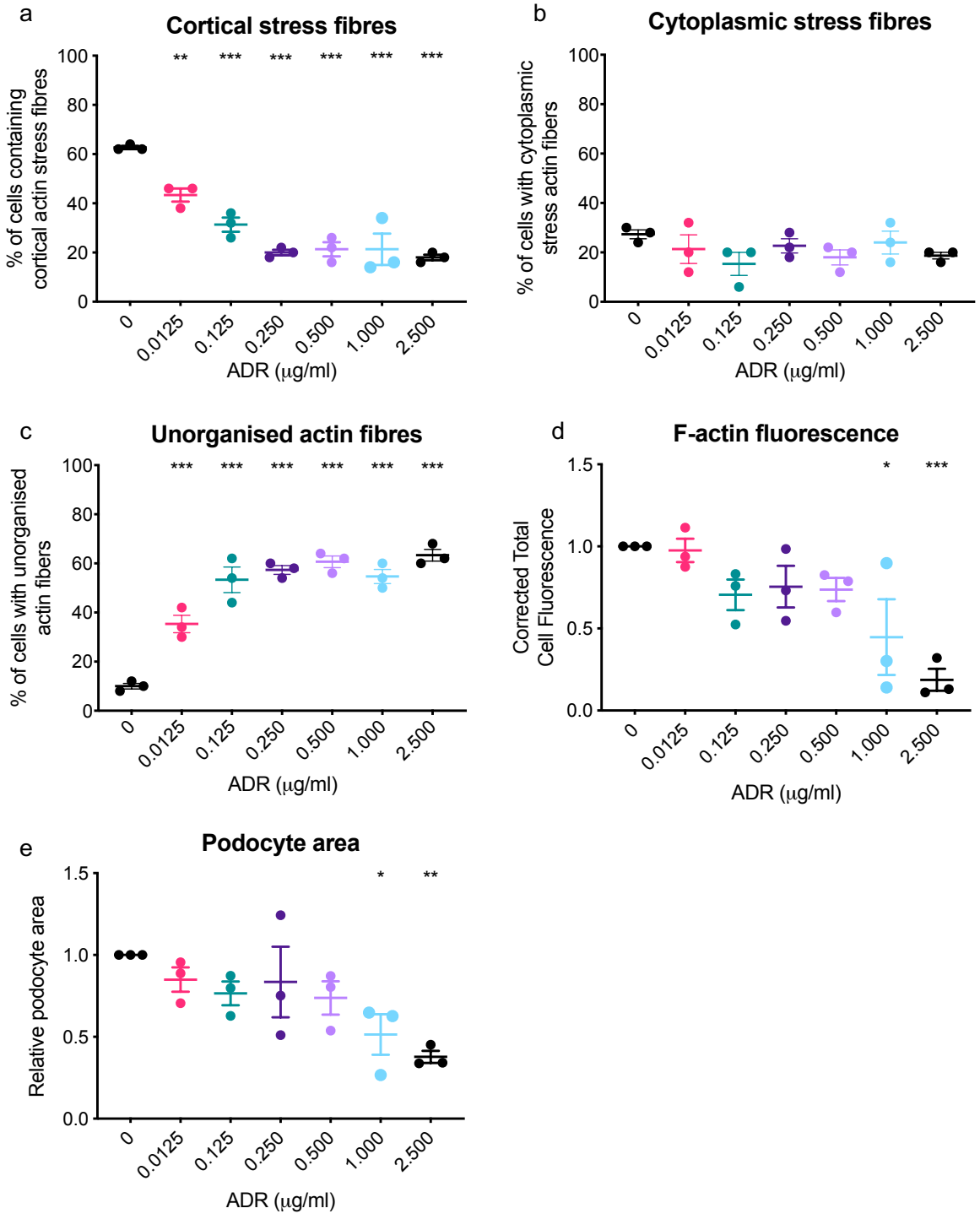

Figure 2.8 - ADR induces podocyte cytoskeletal disorganisation. *Differentiated immortalised mouse podocytes were treated with 0 – 2.5 µg/ml of ADR, fixed after 24 hours and stained with phalloidin conjugated to Actin-stain 488 to assess F-actin. Nuclei were stain with Hoechst 33342. Quantification of the effect of ADR on the percentage of cells with **(a)** cortical actin stress fibres, **(b)** unorganised actin fibres, **(c)** cytoplasmic stress fibres, **(d)** the normalised podocyte F-actin fluorescence and **(e)** total area of the cell. All statistical annotations are in comparison to 0 µg/ml of ADR. Data points represent the average of 50 podocytes. Data are shown as the mean ±SEM of 3 independent experiments. *P≤0.05, **P≤0.01, ***P≤0.001.*

Finally, the podocyte cell area was examined. Cells treated with 0.0125 μg/ml, 0.125 μg/ml, 0.25 μg/ml or 0.5 μg/ml ADR did not show significantly altered cell size compared with untreated cells. Cells treated with 1 μg/ml ADR showed a 49 ± 0.1% reduction in F-actin fluorescence compared with untreated cells ($P<0.05$). Cells treated with 2.5 μg/ml ADR showed a 63 ± 0.1% reduction in F-actin fluorescence compared with untreated cells ($P<0.01$) (**Figure 2.8e**).

2.4.2.4 *ADR alters actin associated gene levels*

After 24 hours, the lower dose of 0.0125 μg/ml ADR did not cause a loss of viability (but loss of viability was seen at 48 and 72 hours), podocyte cell area or F-actin fluorescence but did cause cytoskeletal disorganisation. Since foot process F-actin disorganisation leads to foot process effacement *in vivo* (Suleiman et al. 2017) and which can precede podocyte loss *in vivo* (Ichimura et al. 2019), it was concluded that 0.0125 μg/ml ADR *in vitro* mimics the early stages of ADR injury *in vivo*. In contrast, the higher dose of 0.125 μg/ml ADR led to a decrease in viability at 24, 48 and 72 hours, decrease of podocyte cell area and F-actin fluorescence, while also causing a higher degree of cytoskeletal disorganisation. Therefore, it was decided that these two doses would be used to study the effect of treating the cells with exogenous TB4 in ADR-induced podocyte injury; one dose where there is minor damage to the cytoskeleton but initially not effect on cell viability, and another dose where there was significant podocyte damage associated with a reduction in cell number after 24 hours of ADR exposure.

After the working doses of ADR had been determined, the mRNA expression of *Tmsb4x*, *Cfl1* and *Schip1* were examined by qPCR after ADR injury. The translated proteins (TB4, cofilin-1 and Schip1) of these transcripts have been shown to modulate podocyte actin (Garg et al. 2010; Perisic et al. 2015; Vasilopoulou et al. 2016), therefore a small number of actin regulating protein transcript expression were screened to determine if ADR induces changes.

The low dose of 0.0125 μg/ml ADR slightly reduced podocyte *Tmsb4x* expression by 15 ±0.1%, however this was not significant compared to media only treated cells. The higher dose of 0.125 μg/ml led to an exacerbated loss of 65 ± 0.1% *Tmsb4x*

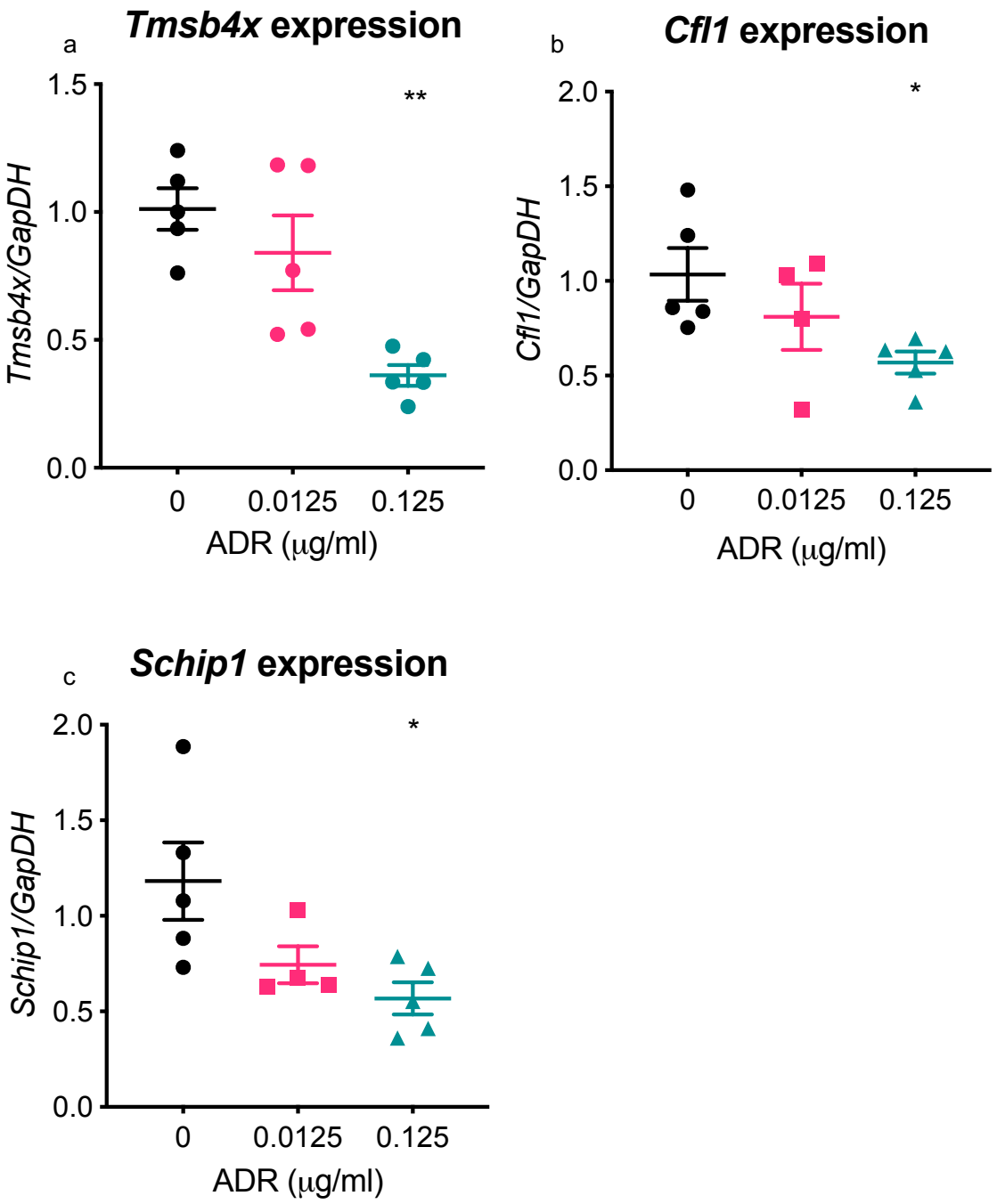

Figure 2.9 – ADR reduced actin associated mRNA expression. *Differentiated immortalised mouse podocytes were treated with 0, 0.0125 and 0.125 μg/ml of ADR and mRNA was extracted after 24 hours. Expression of* ***(a)*** *Tmsbx4,* ***(b)*** *Cfl1 and* ***(c)*** *Schip1 was quantified by qPCR and Gapdh was used as a housekeeping gene. Statistical annotations are in comparison to 0 μg/ml of ADR. Each data point represents the average of duplicate assays from the same independent experiment. Data are shown as the mean ±SEM of at least 4 individual experiments. *P≤0.05, **P≤0.01.*

expression compared to the control (P<0.01) (**Figure 2.9a**). This observation alongside the finding of cytoskeletal disorganisation provides a strong rationale for replenishing ADR-injured podocyte TB4 levels with exogenous TB4.

Cofilin-1 is a major actin regulating protein in eukaryotic cells (Bernstein and Bamburg 2010) that contributes to actin severing and treadmilling (Al Haj et al. 2014; De La Cruz 2009). Endogenous TB4 suppresses the expression of *Cfl1* (Vasilopoulou et al. 2016) therefore the effect of ADR on *Cfl1* was examined. The low dose of 0.0125 μg/ml ADR caused a 19 ± 0.2% reduction in *Cfl1* compared to media only treated cells, but this was not statistically significant. The higher dose of 0.125 μg/ml ADR reduced *Cfl1* expression by 44 ± 0.1% (P<0.05) compared to media only treated cells (**Figure 2.9b**).

Schip1 is expressed in podocytes and associates with the membrane-ezrin-cytoskeleton complex playing a role in actin dynamics by promoting cortical F-actin accumulation (Perisic *et al.*, 2015). The human homologue, which shares 98.77% sequence similarity with the mouse homologue, is predicted to interact with TB4 (Miyamoto-Sato et al. 2010). There was no statistical difference between media treated cells and cells treated with 0.0125 μg/ml ADR. Podocyte *Schip1* expression was decreased by 45 ± 0.8% in cells treated with 0.125 μg/ml of ADR (P<0.05) compared with media only treated cells (**Figure 2.9c**).

These results suggest that there is a loss of actin regulating protein gene expression in podocytes in ADR-injury. This may provide insight into why cytoskeletal disorganisation in podocytes is occurring (2.4.2.3). The next subsection of this thesis chapter will explore the effect of ADR and TB4 on podocyte actin regulating gene expression in more detail.

2.4.3 The effect of exogenous TB4 on ADR-injured podocytes

The data so far in this chapter has shown that exogenous TB4 does not induce changes to healthy podocyte viability, migration or cytoskeletal organisation. Subsequently, ADR-induced podocyte injury has been characterised at a wide range of doses and 0.0125 μg/ml ADR and 0.125 μg/ml ADR were selected to study the

effect of exogenous TB4 on injured podocytes. These two doses allowed the effect of exogenous TB4 to be studied in: (i) cells that have a constant expression of *Tmsb4x* with only damage to the cytoskeleton at 24 hours and (ii) cells with depleted expression of *Tmsb4x*, loss of viability at all time points and higher damage to the cytoskeleton. This part of the thesis therefore proceeded to investigate the effect of exogenous TB4 on ADR-injured podocytes.

2.4.3.1 *Exogenous TB4 does not prevent ADR-induced loss of podocyte viability*
While exogenous TB4 did not alter podocyte viability, 0.0125 μg/ml reduced podocyte viability at 48 and 72 hours and 0.125 μg/ml reduced cell viability at all 3 time points (2.4.2.1). It was hypothesised that TB4 would prevent ADR-induced podocyte viability loss, therefore, cell viability was assessed by MTT assay as described in 2.3.4.

The lower dose of 0.0125 μg/ml ADR did not alter cell viability after 24 hours compared with untreated cells, but reduced cell viability by 45 ± 6.4% at 48 hours ($P<0.001$ versus untreated cells) and 51 ± 10% at 72 hours ($P<0.001$ versus untreated cells) respectively. The higher dose of 0.125 μg/ml ADR caused a 49 ±7.8% reduction of cell viability at 24 hours compared to media only treated cells ($P<0.01$). Furthermore, 0.125 μg/ml ADR caused a 87 ± 3.5% reduction at 48 hours ($P<0.001$ versus untreated cells) and 93 ± 1.5% decrease at 72 hours ($P<0.001$ versus untreated cells). Exogenous TB4 was unable to prevent this loss of viability at either dose or time point (**Figure 2.10a**, **b, c**).

These results indicate that while ADR causes a decrease in podocyte viability at all 3-time points studied, this could not be prevented by doses of 10, 100 and 1000 ng/ml of exogenous TB4.

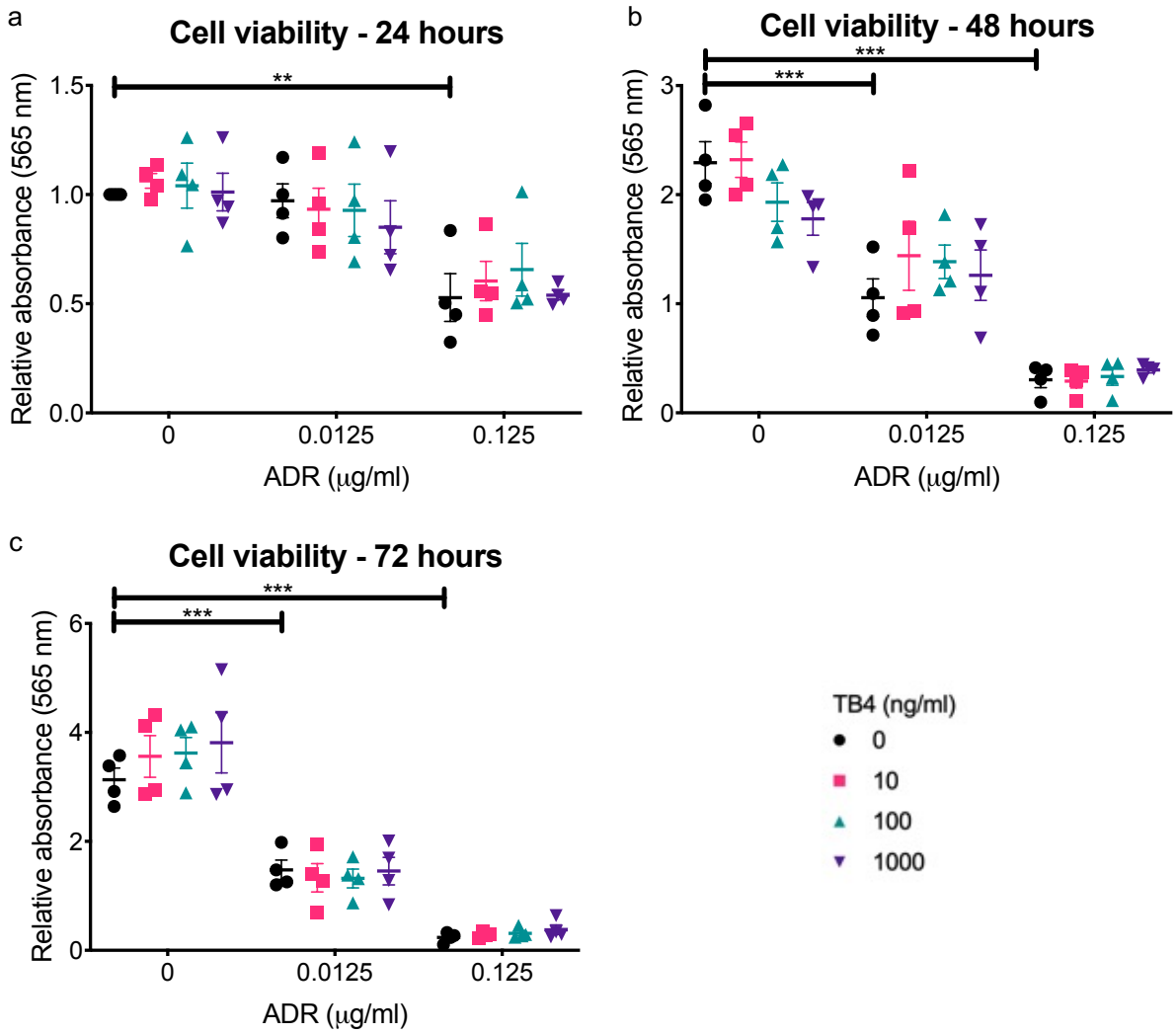

Figure 2.10 – Exogenous TB4 does not protect ADR-induced loss of podocyte viability. *Differentiated immortalised podocytes were treated with 0 – 0.125 μg/ml ADR and 0 – 1000 ng/ml exogenous TB4 and viability was assessed by MTT assay at* ***(a)*** *24,* ***(b)*** *48 and* ***(c)*** *72 hours after treatment. Data have been normalised to media only treated cells of respective experiments to achieve normal distribution and reduce variability. Each data point represents the average of 4 replicates of 1 individual experiment. Data are shown as the mean ±SEM of 4 individual experiments. *P≤0.05, **P≤0.01, ***P≤0.001 between treatment groups.*

2.4.3.2 *Exogenous TB4 prevents ADR-induced F-actin disorganisation*

Both doses of ADR caused cytoskeletal rearrangements in podocytes, namely a reduction in cortical actin stress fibre frequency and an increase in the prevalence of unorganised actin filaments. Due to its actin sequestering and regulating properties (Safer et al. 1991; Sanders et al. 1992) it was hypothesised that exogenous TB4 treatment would be able to prevent these cytoskeletal rearrangements.

Podocytes were treated with TB4 and/or ADR and stained with Acti-Stain™ 488 Phalloidin as described in 2.3.6. Podocytes injured with 0.0125 μg/ml ADR reduced their cortical actin stress fibre prevalence from 61 ± 2.2% to 33 ± 2.3% (P<0.001), while increasing the prevalence of unorganised actin from 12 ± 2% to 31 ± 3.2% (P<0.001) compared with media only treated cells. The higher dose of 0.125 μg/ml ADR exacerbated this effect, decreasing cortical actin stress fibre prevalence to 25 ± 2.1% (P<0.001) and increasing the prevalence of unorganised fibres to 50 ± 4.2% (P<0.001) compared with media treated cells (**Figure 2.11a, c**).

Cells exposed to 10 ng/ml of exogenous TB4 suppressed reduction of cortical actin stress fibre prevalence at 0.0125 μg/ml ADR (47 ± 3.7%, P<0.001 compared with 0.0125 μg/ml ADR only) and 0.125 μg/ml ADR (40 ± 2.4%, P<0.01 compared with 0.125 μg/ml ADR only) while supressing the unorganised fibre formation at 0.125 μg/ml (35 ± 3.7%, P<0.01 compared with 0.125 μg/ml ADR only) (**Figure 2.11a, c**).

Treatment of podocytes with 100 ng/ml of exogenous TB4 fully prevented the reduction of cortical actin stress fibres at both doses of 0.0125 μg/ml (63 ± 1.3%, P<0.001 compared to 0.0125 μg/ml ADR alone) and 0.125 μg/ml (57 ± 2.6%, P<0.001 compared to 0.125 μg/ml ADR). This was accompanied by the suppression of unorganised actin prevalence at 0.0125 μg/ml ADR (20 ± 2.6%, P<0.05 compared with 0.0125 μg/ml ADR) and 0.125 μg/ml ADR (24 ± 4.2%, P<0.001 compared with 0.125 μg/ml ADR) (**Figure 2.11a, c**). ADR injured cells exposed to 1000 ng/ml of TB4 also displayed cytoskeletal stability. Cortical stress fibre prevalence was preserved at both 0.0125 μg/ml (63 ± 1.8%, P<0.001 compared to 0.0125 μg/ml ADR) and 0.125 μg/ml ADR (51 ± 2.2%, P<0.001 compared to 0.125 μg/ml ADR). Unorganised actin fibre prevalence was suppressed at 0.0125 μg/ml (12 ± 2.5%, P<0.001 compared with 0.0125 μg/ml ADR) and 0.125 μg/ml ADR (24 ± 2.8%, P<0.001 compared with 0.125 μg/ml ADR) (**Figure 2.11a, c**).

Neither dose of ADR altered cytoplasmic stress fibre prevalence compared to media treated cells. At the lower dose of 0.0125 μg/ml ADR, 100 ng/ml and 1000 ng/ml of exogenous TB4 reduced the prevalence of cytoplasmic stress fibres (P<0.01

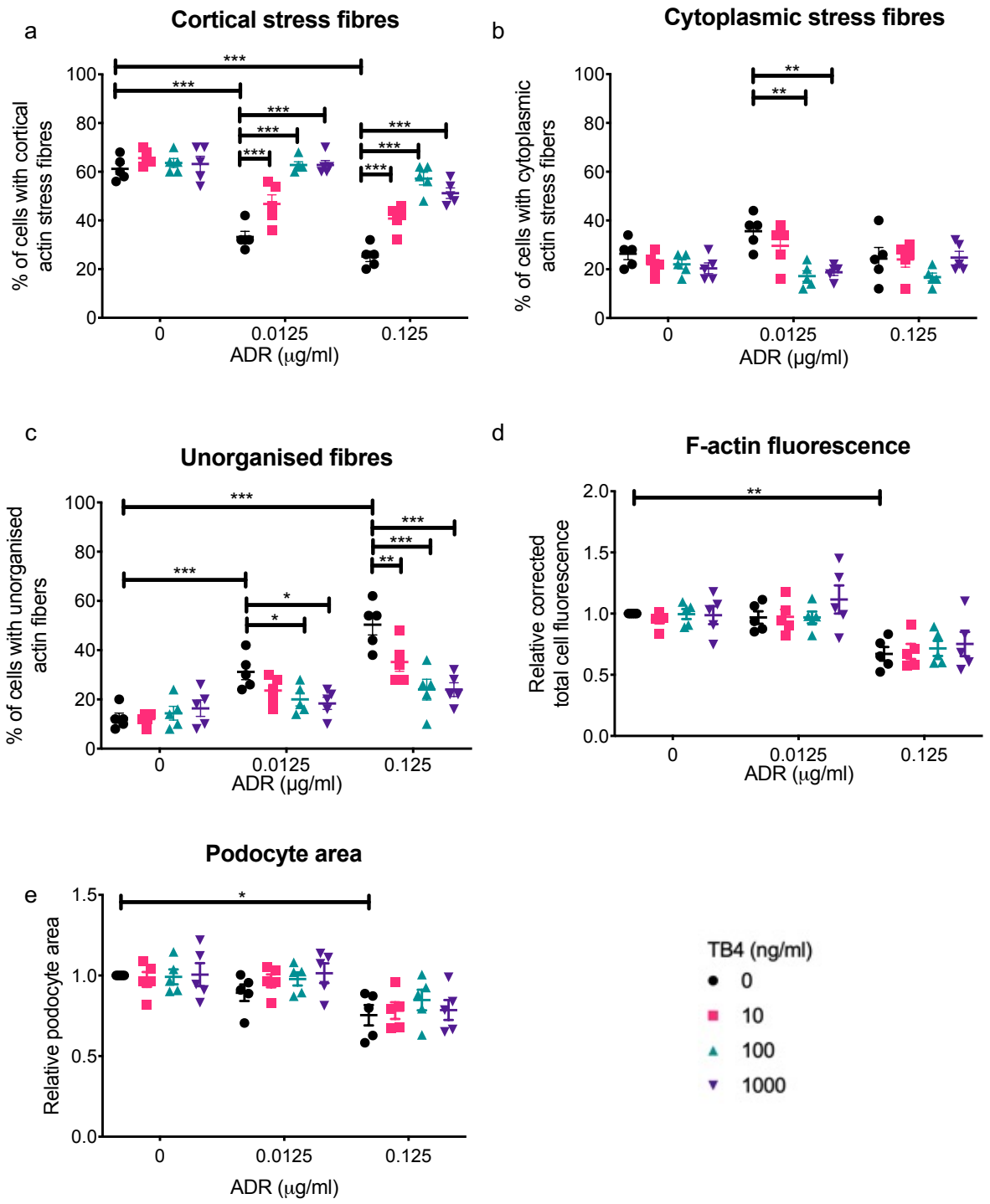

Figure 2.11 – Exogenous TB4 prevents ADR-induced cytoskeletal disorganisation. *Differentiated immortalised mouse podocytes were treated with 0, 0.0125 or 0.125 µg/ml of ADR and 0, 10, 100 or 1000 ng/ml of TB4, fixed after 24 hours and stained with phalloidin conjugated to Actin-stain 488 to examine F-actin. Nuclei were stained with Hoechst 33342. Quantification of the effect of exogenous TB4 on the percentage of cells with **(a)** cortical actin stress fibres, **(b)** unorganised actin fibres, **(c)** cytoplasmic stress fibres, **(d)** the normalised corrected total cell fluorescence and **(e)** total area of the cells that have been injured with ADR. **(d)** and **(e)** have been normalised to achieve normal distribution and reduce variability. Each data point represents the average of 50 cells from an individual experiment. All data are shown as the mean ±SEM of 5 individual experiments. *P≤0.05, **P≤0.01, ***P≤0.001.*

compared with 0.0125 μg/ml ADR alone) (**Figure 2.11b**). The low dose of 0.0125 μg/ml ADR did not affect podocyte F-actin fluorescence or cell area. Podocytes treated with 0.125 μg/ml ADR showed a 35% decrease in F-actin fluorescence ($P<0.01$) and 25% decrease in cell area ($P<0.05$), which exogenous TB4 was unable to prevent (**Figure 2.11d, e**).

Taken together, these results demonstrate that exogenous TB4 prevented ADR induced podocyte cytoskeletal rearrangements.

2.4.3.3 *TB4 had no effect on ADR-altered gene expression*

The data presented so far suggest that doses of 100 ng/ml and 1000 ng/ml exogenous TB4 exhibited similar effects in ADR injury, specifically, the level of cytoskeletal preservation was comparable. The lowest possible beneficial dose of exogenous TB4 was desired, therefore, 100 ng/ml of exogenous TB4 was selected to assess the effect of TB4 on ADR-injured podocytes.

Gene levels are analysed by qPCR 24 hours after treatment. Firstly, the effect of ADR and exogenous TB4 were examined on the β-thymosin family of actin sequestering genes. *Tmsb4x* encodes TB4 and *Tmsb10* encodes thymosin β-10, a homologue of TB4 with identical actin sequestering properties, but with a 5 fold higher affinity for G-actin (F.-X. Yu et al. 1993; Yu et al. 1994). Thymosin β-15 has three isoforms; thymosin β-15a (*Tmsb15a*), thymosin β-15b (*Tmsb15b*) and thymosin β-15-like (*Tmsb15l*) peptide which bind to G-actin with a 2.4x higher stability than TB4 (Eadie et al. 2000).

Cells treated with 0.0125 μg/ml ADR showed no statistical difference in expression of *Tmsb4x* and *Tmsb10* compared with media treated cells. The higher dose of 0.125 μg/ml led to a 61 ± 5% reduction in *Tmsb4x* and a 52 ± 13% reduction in *Tmsb10* expression compared to media treated cells. Exogenous TB4 was unable to prevent the reduction in either transcript (**Figure 2.12a, b**). While 0.0125 μg/ml ADR had no effect on podocyte *Tmsb15a*, 0.125 μg/ml ADR caused 3.3-fold (± 0.4)

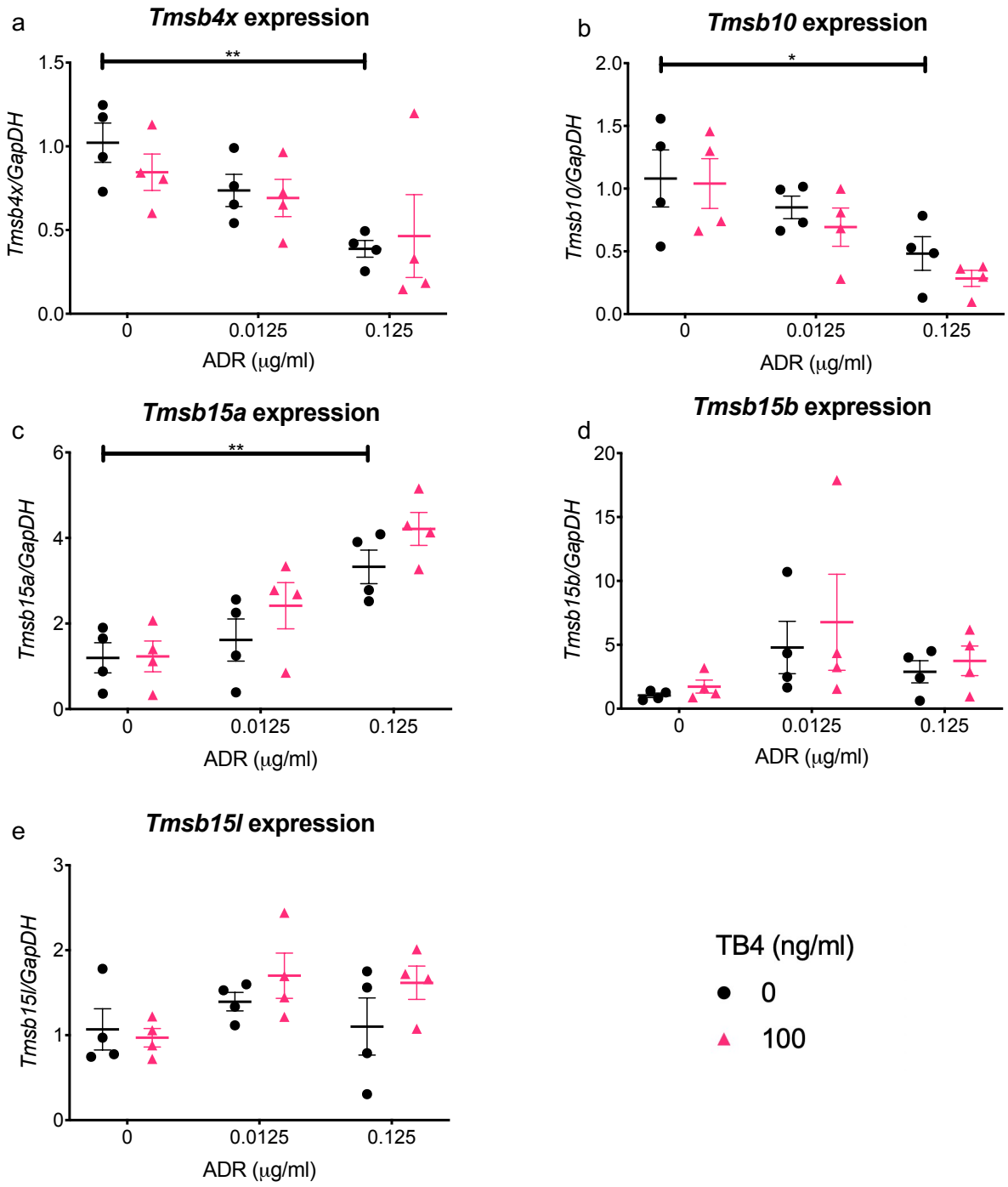

Figure 2.12 – Exogenous TB4 does not prevent ADR-induced β-thymosin mRNA level alterations. *Differentiated immortalised mouse podocytes were treated with 0, 0.0125 and 0.125 μg/ml of ADR with 0-1000 ng/ml of TB4 and mRNA was extracted after 24 hours. Expression of* ***(a)*** *Tmsbx4,* ***(b)*** *Tmsb10,* ***(c)*** *Tmsb15a* ***(d)*** *Tmsb15b and* ***(e)*** *Tmsb15l was quantified by real time PCR and Gapdh was used as a housekeeping gene. Each data point represents the average of replicates of a single experiment. All data are shown as the mean ±SEM of 4 individual experiments. *P≤0.05, **P≤0.01. Tmsb4x, TB4; Tmsb10, Thymosin β-10; Tmsb15a, Thymosin β15a; Tmsb15b, Thymosin β-15b; Tmsb15l, Thymosin β-15-like.*

upregulation in *Tmsb15a* compared to media treated cells (P<0.01) which exogenous TB4 did not prevent (**Figure 2.12c**). There were no alterations to *Tmsb15b* or *Tmsb15l* in any treatment group compared to media treated cells (**Figure 2.12d, e**).

Collectively, these results demonstrate that ADR alters the mRNA level of some of the β-thymosin family, suggesting there could be changes to the balance of the actin-regulating molecules within the cell.

Consistent with 2.4, 0.0125 μg/ml ADR did not alter *Schip1* or *Cfl1* expression but 0.125 μg/ml ADR lead to a 50 ±0.4% reduction in both genes compared to media treated cells (P<0.01). However, cells treated with 0.0125 μg/ml ADR and 1000 ng/ml exogenous TB4 showed an increase of 44 ±0.1% in *Schip1* levels compared with cells treated with 0.0125 μg/ml ADR (P<0.05). Exogenous TB4 was unable to prevent the reduction in *Cfl1* expression (**Figure 2.13a, b**).

Dstn encodes destrin/ADF, an F-actin regulating protein that promotes actin severing and depolymerisation (Vartiainen et al. 2002) and *Pfl1* and *Pfl2* encode Profilin 1 and profilin 2 respectively. Profilin has been shown to promote actin polymerisation in the presence of TB4 (Pantaloni and Carlier 1993). Profilin 1 and profilin 2 have opposing effects on the actin cytoskeleton – profilin 1 promotes actin bundling whereas profilin 2 supresses actin bundling (Ding and Roy 2013). There were no alterations to *Dstn, Pfl1* or *Pfl2* levels after exogenous TB4 administration compared to media treated cells or either dose of ADR (**Figure 2.13c, d, e**).

Synpo encodes synaptopodin, a podocyte actin regulating serine/threonine kinase (Mundel, Heid, et al. 1997). Treatment of podocytes with 0.0125 μg/ml of ADR showed no change in the level of *Synpo* compared with media treated cells. Treatment with 0.125 μg/ml of ADR showed a 4-fold (± 0.9) increase in *Synpo* expression in comparison to untreated podocytes (P<0.01). Exogenous TB4 had no effect on *Synpo* expression at any dose of ADR (**Figure 2.13f**).

Ezrin and Nherf2 link the cytoskeleton to the SD plasma membrane via interactions with podocalyxin (Takeda 2003), a SD molecule coated with sialic acid residues that

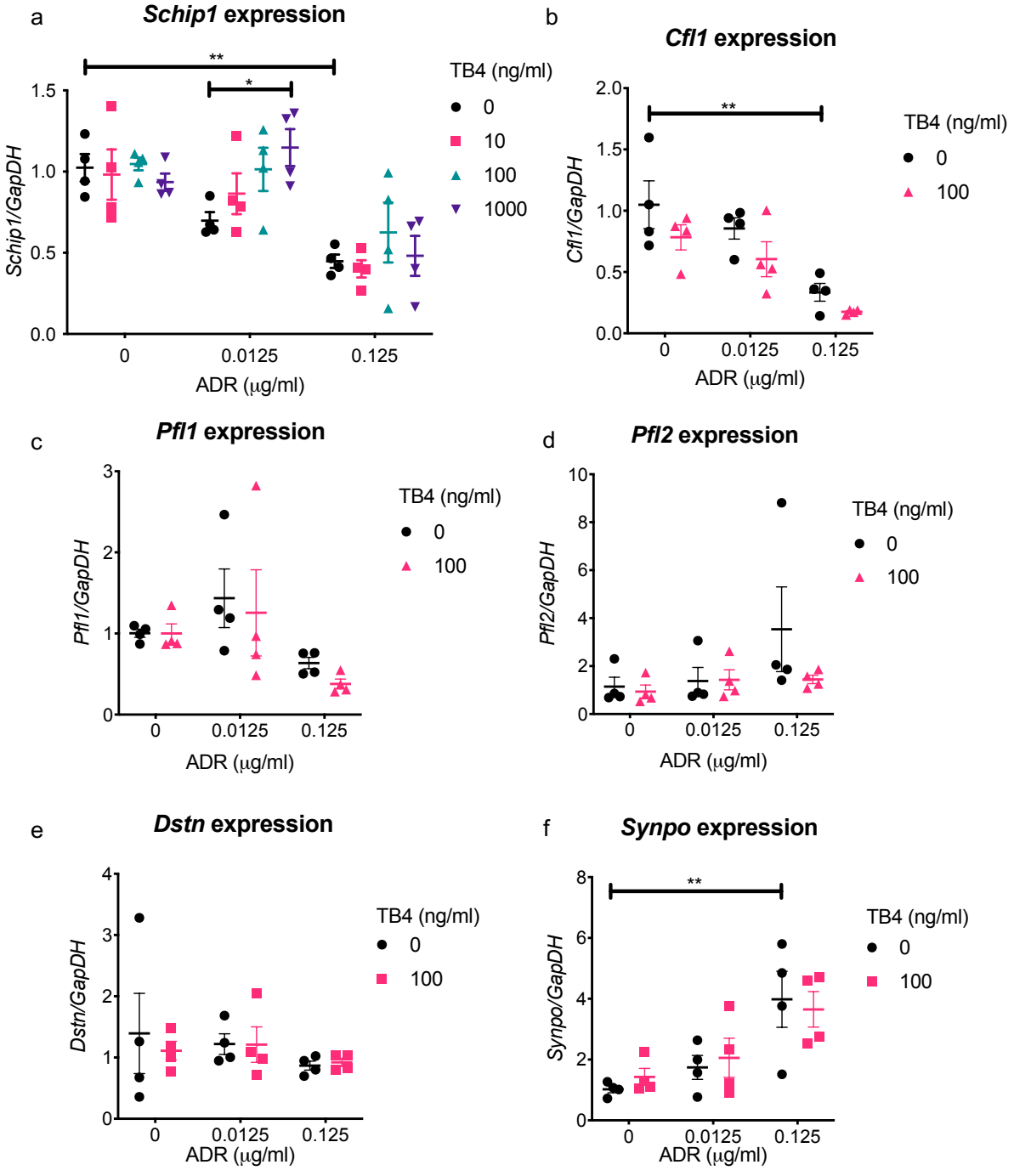

Figure 2.13 – The effect of ADR and exogenous TB4 on podocyte actin associated genes. *Differentiated immortalised mouse podocytes were treated with 0, 0.0125 and 0.125 μg/ml of ADR with 0-1000 ng/ml of TB4 and mRNA was extracted after 24 hours. Expression of* ***(a)*** *Schip1* ***(b)*** *Cfl1,* ***(c)*** *Pfl1* ***(d)*** *Pfl2,* ***(e)*** *Dstn and* ***(f)*** *Synpo was quantified by qPCR and Gapdh was used as a housekeeping gene. Each data point represents the average of replicate values of 1 individual experiment. Data are shown as the mean ±SEM of 4 independent experiments. **P≤0.01. Schip1, Schwannomin interacting protein 1; Cfl1, Cofilin-1; Pfl1, Profilin-1; Pfl2, Profilin-2; Dstn, Destrin; Synpo, synaptopodin.*

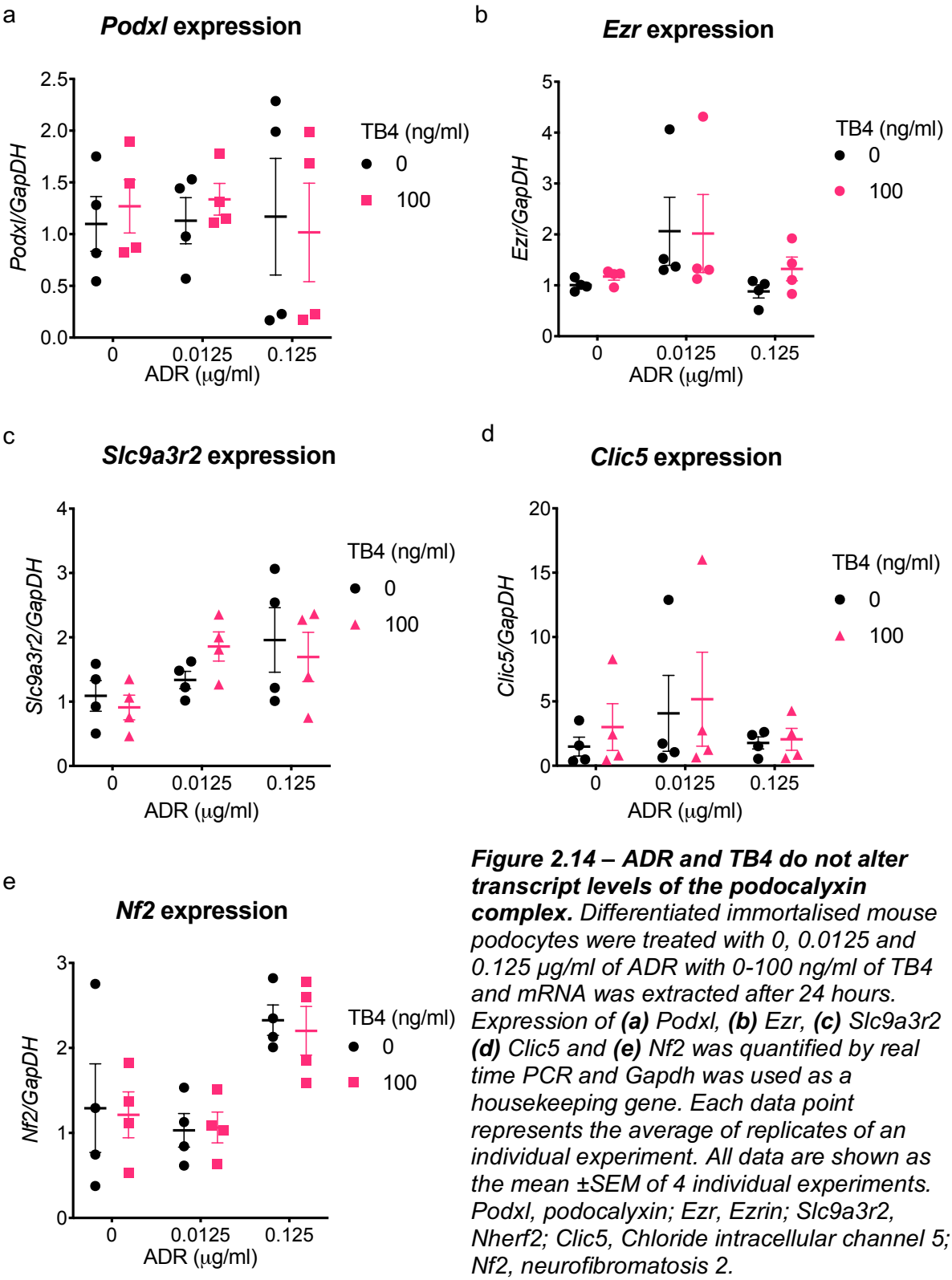

Figure 2.14 – ADR and TB4 do not alter transcript levels of the podocalyxin complex. *Differentiated immortalised mouse podocytes were treated with 0, 0.0125 and 0.125 μg/ml of ADR with 0-100 ng/ml of TB4 and mRNA was extracted after 24 hours. Expression of* ***(a)*** *Podxl,* ***(b)*** *Ezr,* ***(c)*** *Slc9a3r2* ***(d)*** *Clic5 and* ***(e)*** *Nf2 was quantified by real time PCR and Gapdh was used as a housekeeping gene. Each data point represents the average of replicates of an individual experiment. All data are shown as the mean ±SEM of 4 individual experiments. Podxl, podocalyxin; Ezr, Ezrin; Slc9a3r2, Nherf2; Clic5, Chloride intracellular channel 5; Nf2, neurofibromatosis 2.*

promotes charge exclusion of negatively charged plasma molecules from the ultrafiltrate (Nielsen and Mcnagny 2009). Adjacent to this complex is the chloride intracellular channel 5a (CLIC5a), which phosphorylates ezrin (Wegner et al. 2010), stimulating the essential process of ezrin binding to F-actin, leading to coupling of podocalyxin to the cytoskeleton (Orlando et al. 2001; Takeda et al. 2001).

Treatment with 0.0125 μg/ml or 0.125 μg/ml ADR did not alter podocyte levels of *Podxl, Ezr, Slc9a3r2* or *Clic5* compared with untreated cells. Exogenous TB4 also did not alter the levels of these transcripts in any condition compared with the media treated only cells, suggesting that this complex may not be involved in the TB4 mediated podocyte cytoskeletal protection (**Figure 2.14a, b, c, d**).

Nf2 encodes the protein neurofibromin 2, a protein that has only been shown previously to be expressed in glial cells, linking the cortical cytoskeleton to the plasma membrane (Cole et al. 2008) and interacting with Schip1 (Goutebroze et al. 2000). It was not known previously if *Nf2* was expressed by podocytes, however *Nf2* was detected at Ct values between 19-24, showing relatively high expression. Again, neither ADR nor exogenous TB4 altered the expression of *Nf2* (**Figure 2.14e**).

2.5 **Discussion**

This chapter of the thesis has demonstrated that exogenous TB4 has no effect on healthy podocyte viability, migration or the podocyte cytoskeleton. Subsequently, a strategy was employed to explore the effect of exogenous TB4 on podocytes damaged by ADR. A dose response experiment identified two appropriate concentrations of ADR to induce (i) cytoskeletal disorganisation without a significant loss of cell viability at 24 hours after ADR and (ii) cytoskeletal disorganisation accompanied by significant reduction in podocyte viability and reduced *Tmsb4x*. Importantly, this chapter has provided strong evidence that exogenous TB4 prevented ADR-induced cytoskeletal disorganisation but has no effect on ADR-altered cell viability.

2.5.1 The effect of exogenous TB4 on healthy podocytes

To date, no studies have examined exposure of healthy podocytes to exogenous TB4 *in vitro*. Therefore, this chapter has provided the first evidence that exogenous TB4 does not alter healthy podocyte viability, migration or the F-actin cytoskeleton. The only study to date examining TB4 in podocytes showed that TB4 was expressed in mouse podocytes and then subsequently investigated the effects of knocking down endogenous TB4 by siRNA (Vasilopoulou et al. 2016). Loss of endogenous TB4 did not alter podocyte viability, suggesting that endogenous TB4 is expendable for podocyte survival (Vasilopoulou et al. 2016). In accord with the findings in podocytes, exogenous TB4 does not alter cell viability in other cell types. Healthy human corneal epithelial cells cultured with 1 μg/ml of exogenous TB4 showed no change in viability after 24 hours of exposure as measured by MTT assay (Ho et al. 2007). Similarly, exogenous TB4 (100 ng/ml – 5000 ng/ml) also did not affect cell viability of adipose derived stem cells compared to untreated cells when assessed by trypan blue staining 24 hours after treatment (Jeon et al. 2013). Therefore, the data presented in this thesis have provided further evidence that exogenous TB4 has no effect on cell viability of healthy cells grown in culture.

Whilst endogenous TB4 knockdown did not affect cell viability, there was a reorganisation of cortical stress fibres to cytoplasmic stress fibres and an increase in cell migration (Vasilopoulou et al. 2016). It was subsequently postulated that since a lack of endogenous *Tmsb4x* caused an increase in podocyte migration, exogenous TB4 may reduce migration of healthy podocytes, however this proved not to be the case.

There was ~10-fold increase in migration between 6 and 24 hours in healthy untreated podocytes reported in this thesis. Other studies examining podocyte migration indicate that healthy podocytes do undergo motility in culture. One study that utilised the scratch wound method found that healthy primary podocytes from C57BL/6 mice showed 50% wound closure after 24 hours (Cechova et al. 2018). Another study using the same scratch wound assay with mouse immortalised podocytes found at least 20 cells had migrated into the wound after 72 hours, and live imaging revealed these cells travelled at 0.1 μm/min (Kruger et al. 2018).

Furthermore, human immortalised podocytes showed complete wound closure after just 17 hours (Yu et al. 2020). Therefore, there is significant evidence that healthy podocytes do display a migratory phenotype *in vitro*, but different culture conditions and cell lines influence rates of migration.

Exogenous TB4 has been shown to induce migration in healthy cultured cells. Exogenous TB4 (100 ng/ml) induced a 4-fold increase in healthy embryonic mouse myocardial cell migration (Bock-Marquette et al. 2004). HCECs exposed to 1 μg/ml exogenous TB4 showed increased scratch wound healing 24 and 48 hours after wound induction compared to untreated cells, which was dependent on the presence of MMP4 (Qiu, Kurpakus-Wheater, and Sosne 2007). Additionally, 100 ng/ml of exogenous TB4 stimulated HUVEC migration as shown by a Boyden chamber assay after 4 hours (Philp et al. 2003). The results presented in this thesis chapter provide contrasting results to these other cell types, as no alterations to motility compared to untreated cells were present. There could be multiple explanations as to why the effects on podocytes differ from other cell types. It would not be due to the dose of TB4, as the previous doses used were the same as in this thesis. The culture conditions and type of assay used may have caused the variations. Myocardial cells were exposed to TB4 for 24 hours longer than in this thesis, which allowed more time for migration to occur. The HUVEC cells were examined by Boyden chamber assay, which may facilitate migration more than scratch wound assay. In fact, the cells on the wound line in the scratch wound assay may have been damaged by the wound induction, which could have affected their health and motility. Boyden chamber assay does not inflict a wound on the cell; therefore, the cells have less chance to be damaged. The natural migratory behaviour of each cell type may have influenced the variations; podocytes may not be as naturally motile as HUVEC or myocardial cell types.

Endogenous TB4 is responsible for cytoskeletal stability in healthy podocytes *in vitro*, as loss of TB4 resulted in a reorganisation from cortical actin fibres to cytoplasmic stress fibres (Vasilopoulou et al. 2016). However, the effect of exogenous TB4 on podocyte F-actin has not been examined, and this chapter has provided evidence that the amount and organisation F-actin is unaffected by exogenous TB4 in healthy

podocytes *in vitro*. The actin regulating properties have influenced actin dynamics in other healthy cell types. Increasing concentrations (10 ng/ml – 500 ng/ml) of exogenous TB4 reduced the F-actin to G-actin ratio in HUVECs, indicating that a higher degree of G-actin was sequestered in these cells (Kim and Kwon 2015). A reduction in the F-actin to G-actin ratio was also identified in human cerebral endothelial cells exposed to 10 ng/ml – 500 ng/ml of TB4. However, the representative images of the cells stained with phalloidin to visualise F-actin seem identical to untreated cells, and quantification was not undertaken indicating no change to overall F-actin organisation (Song et al. 2020). Changes to F-actin organisation could be expected if there were reductions to the F-actin to G-actin ratio, as there could be less F-actin fibres in certain cellular compartments such as the cortex or centre of the cell. Further studies could examine the F-actin to G-actin ratio in healthy podocytes to determine if exogenous TB4 is indeed causing further G-actin sequestration as seen in other cell types.

There could be due to a number of reasons why exogenous TB4 does not alter the F-actin cytoskeleton in podocytes. Healthy podocytes have an innate level of endogenous TB4 peptide that is already sequestering the majority of G-actin, therefore saturating the cells with exogenous TB4 and causing further G-actin sequestering would be unlikely to alter F-actin organisation stability. Cell motility is dependent on actin polymerisation (Mogilner and Oster 1996), which could explain why *Tmsb4x* knockdown in podocytes displayed increased migration (loss of G-actin sequestering leading to actin polymerisation) (Vasilopoulou et al. 2016), but not in podocytes with increased levels of TB4. Furthermore, treatment with exogenous TB4 did not alter the mRNA transcript levels of some members of the β-thymosin family or other known actin regulating proteins, such as cofilin-1, profilin and destrin. The lack of alterations to other actin sequestering and regulating molecules induced by exogenous TB4 suggests that intracellular actin regulation is unaffected and TB4 is the only molecule that is present in excess.

A potential caveat of our experiment using exogenous TB4 is that the internalisation of TB4 into the cells has not been examined. Internalisation of exogenous TB4 has been proven in HUVECs by an increase in intracellular TB4 immunostaining (Grant

et al. 1999). The effects of exogenous TB4 treatment and transfection of *Tmsb4x* to cardiac endothelial cells were comparable, suggesting that exogenous TB4 was also internalised in this cell type (Bock-Marquette et al. 2004). Furthermore, internalisation of TB4 was confirmed in human corneal endothelial cells by utilising a His-tagged TB4 peptide, as the intracellular immunofluorescent staining of Histidine dramatically increased 2 hours after treatment (Ho et al. 2007). The exact mechanisms of TB4 internalisation are not well understood, however, due to the small size (4.9 kilodaltons) it is likely that TB4 enters cells via active or passive transport. Other mechanisms of internalisation have not been explored, but TB4 has been shown to bind to two extracellular purinergic receptor classes, P2X and P2Y classes (Freeman, Bowman, and Zetter 2011), which are expressed on podocytes (Forst et al. 2016; Szrejder et al. 2020). TB4 induced purinergic signalling has been associated with corneal epithelial cell migration (H. M. Yang et al. 2020), demonstrating that this TB4-induced stimulation of this pathway does have intracellular effects, even though there was no alterations to motility in healthy podocytes in this thesis. To confirm internalisation of exogenous TB4 to podocytes, future studies could utilise previously reported methods, such as using His-tagged TB4, to quantify an increase in intracellular TB4 amount by immunofluorescence. Additionally, co-immunoprecipitation assays to detect TB4/purinergic receptor binding could be utilised to identify if there is an increase in binding after treatment with exogenous TB4. Finally, podocyte transfection to overexpress *Tmsb4x* mRNA could also be undertaken to see if similar effects are observed.

2.5.2 Optimising an *in vitro* model of ADR-induced podocyte injury

ADR is a widely used podocyte injury model, that leads to decreased podocyte viability and cytoskeletal rearrangements (Marshall *et al.*, 2010; Liu *et al.*, 2012). Previously, a wide range of concentrations between 0.125 μg/ml, to 20 μg/ml ADR have been used to induce loss of cell viability and cytoskeletal disorganisation *in vitro* (Chen et al. 2017; Liu et al. 2012; X. Liu et al. 2018; Maimaitiyiming, Zhou, and Wang 2016; Marshall et al. 2010). It was therefore important to identify the optimum dose to induce podocyte damage in the available laboratory conditions.

Doses of 0.0125 μg/ml and 0.125 μg/ml ADR were selected for subsequent experiments utilising exogenous TB4, as 0.0125 μg/ml did not reduce cell viability at 24 hours, but 0.125 μg/ml did. The doses above 0.125 μg/ml all induced the same extent of cell viability reduction and cytoskeletal reorganisation. In fact, doses above 0.125 μg/ml caused such an extreme loss of cell viability (>90%) that there were few cells left to analyse in subsequent assays. Other studies have examined cell viability following ADR exposure in podocytes. Human immortalised podocytes treated with 20 μg/ml of ADR (160-fold higher concentration than 0.125 μg/ml) showed 15% prevalence of apoptotic cells, one cause of reduced cell viability, and a loss of F-actin cortical fibres to unorganised F-actin after 24 hours (Maimaitiyiming et al. 2016). In contrast to this, immortalised mouse podocytes (the same cell line used in this study), exposed to 0.2 μg/ml, 0.3 μg/ml and 0.4 μg/ml ADR led to 15 – 20% prevalence of apoptotic cells (Xie et al. 2017; Yi et al. 2017). It is clear from previous studies that external factors influence the extent by which ADR induces podocyte damage. These factors may include culture conditions, the matrix the cells are grown on, the source of the cell line used, and the batch of ADR used. This has been confirmed in a study using different lines of human, mouse and rat immortalised podocytes exposed to ADR. The mouse and human cells displayed similar reductions in cell viability when exposed to 0.05 μg/ml, 0.2 μg/ml, 0.5 μg/ml, 1 μg/ml and 2.5 μg/ml ADR, whilst the rat immortalised podocytes did not experience a loss in cell viability at any concentration (Chittiprol et al. 2011). Therefore, it is important for researchers to identify appropriate doses to induce desired outcomes when performing experiments with podocytes exposed to ADR.

The doses of 0.0125 μg/ml and 0.125 μg/ml ADR (and also higher concentrations) led to F-actin disorganisation. The podocyte cytoskeleton is critical for maintaining the glomerular filtration barrier *in vivo* (Welsh and Saleem 2012) with the majority of podocyte F-actin *in vivo* is located in the foot processes (Shirato *et al.*, 1996). Therefore, molecules that induce changes in podocyte F-actin *in vitro* are likely to alter F-actin *in vivo*. F-actin disorganisation which presents as a “mat” of disorganised actin parallel to the GBM has been associated with ADR-induced foot process effacement *in vivo* (Kriz et al. 2013; Suleiman et al. 2017), therefore, highly regulated cytoskeletal organisation and structure is critical for maintaining the unique

architecture of podocytes. Alterations to F-actin *in vitro* and *in vivo* have been demonstrated in Ste20-like kinase (SLK) knockout mice exposed to ADR, where glomerular phalloidin mean fluorescence increased and there was an increased prevalence of an F-actin mat juxtaposed to the GBM, rather than F-actin bundles lining capillary walls. SLK knockdown podocytes with ADR *in vitro* conversely showed a decrease in phalloidin staining and loss of F-actin cytoplasmic fibres (Woychyshyn et al. 2020). Even though the effects on F-actin fluorescence were contrasting, alterations did indeed occur *in vitro* and *in vivo*, therefore, the changes to F-actin reported in this thesis chapter are likely to translate to podocytes *in vivo*.

One of the most interesting results of the ADR dose response study is the loss of podocyte *Tmsb4x* after 24 hours of 0.125 μg/ml ADR exposure. To date, there have been no studies associating a lack of *Tmsb4x* with glomerular disease. An increase in interstitial TB4 prevalence was reported in the UUO model of kidney injury, but it was confirmed that the increased TB4 was from macrophages (F4/80 co-labelling) and myofibroblasts (αSMA co-labelling) (Zuo et al. 2013). Since lack of *Tmsb4x* accelerates glomerular injury *in vivo* and leads to podocyte cytoskeletal reorganisation *in vitro* (Vasilopoulou et al. 2016), this finding provides rationale that restoring the level of TB4 in podocytes with exogenous TB4 may prevent the cytoskeletal disorganisation that is observed in ADR-injury *in vitro* (Marshall *et al.*, 2010; Liu *et al.*, 2012, 2018; Chen *et al.*, 2017) and prevent albuminuria *in vivo*.

Due to the significant reduction in podocyte viability after ADR-treatment, assessing migration in this model is a challenge. There is a limited amount of research into ADR-induced motility *in vitro*, however some authors have succeeded. Mouse immortalised podocytes treated with 0.27 μg/ml ADR for 18 hours showed a 50% increase in wound closure compared to untreated cells when measured by scratch wound assay (Gao et al. 2010). The short ADR exposure time used in this experiment may have contributed to the fact that the researchers were able to assess migration before cell detachment. Another study utilised the scratch wound assay with mouse immortalised podocytes exposed to 0.25 μg/ml ADR for 24 hours and saw a 25% increase in wound closure compared to untreated cells, accompanied by an increased assembly and disassembly of podocyte focal

adhesions (Xu et al. 2014). Podocyte viability was not examined in this study, so it is unclear how ADR-induced loss of viability was accounted for. It is possible that in the laboratory conditions the cells were assessed in, ADR did not reduce cell viability at this dose, due to variable factors mentioned previously. Future studies employing ADR as an injury model could therefore identify a suitable end point where podocyte loss does not occur to enable the assessment of migration. Alternatively, live cell imaging is another assay that could be utilised to track the distance that individual cells travel before detaching.

These dose response assays in this thesis provided valuable information for subsequent assays in this study. The two doses of 0.0125 μg/ml and 0.125 μg/ml of ADR were deemed appropriate to analyse the therapeutic potential of TB4 in co-treatment experiments. The dose of 0.0125 μg/ml caused a high degree of cytoskeletal disorganisation without a loss of *Tmsb4x* or cell viability at 24 hours, allowing the effect of exogenous TB4 to be studied at a level of moderate podocyte injury. The higher dose of 0.125 μg/ml of ADR allowed the effect of exogenous TB4 to be studied in podocytes which express lower levels of endogenous *Tmsb4x*, have a greater extent of cytoskeletal disorganisation, a significant decrease in cell viability at 24, 48 and 72 hours and thus more severe podocyte injury.

2.5.3 Assessing the effect of exogenous TB4 on ADR-injured podocytes

A key finding of this chapter is that exogenous TB4 prevented ADR-induced disorganisation of the podocyte F-actin cytoskeleton. Specifically, TB4 prevented the loss of cortical actin stress fibres and the increase in the prevalence of unorganised actin fibres that was caused by ADR. TB4 is protective of cytoskeletal disorganisation in other cell types. Exogenous TB4 was shown to prevent uncontrolled F-actin polymerisation and loss of cell viability in HUVECs challenged with AGE *in vitro* (Kim and Kwon 2015). Uncontrolled F-actin polymerisation was also reported in human cerebral cells injured with scrapie prion protein, which exogenous TB4 completely prevented (Song et al. 2020). The findings presented in this chapter provide further evidence of the cytoskeletal stabilising effect of exogenous TB4. Since exogenous TB4 can prevent ADR-induced cytoskeletal disorganisation *in vitro*, it is postulated that TB4 may also be able to prevent the

cytoskeletal disorganisation seen *in vivo*. Cytoskeletal reorganisation is a common factor in many podocyte injury models in rodents and cultured cells, including PAN, ADR and diabetic nephropathy (Marshall *et al.*, 2010; Liu *et al.*, 2012; Wang *et al.*, 2016; Ling *et al.*, 2018). There have been no reported studies specifically examining the F-actin cytoskeleton in healthy human samples, or FSGS patients, potentially due to difficulty obtaining cryo-samples of human kidney tissue. Phalloidin staining, the gold-standard for labelling F-actin, only works on cryo-sections, therefore FFPE sections are unsuitable.

The protection of F-actin by exogenous TB4 may be mediated by other podocyte actin-associated proteins, such as α-actinin-4 and integrins. Mouse immortalised podocytes transfected to overexpress the actin-focal adhesion cross linking protein plectin showed almost complete prevention of ADR-induced reduction of podocyte F-actin fluorescence (Ni et al. 2018). The cytoskeletal protection was mediated by suppression of a6β4 integrin and maintenance of a3β1 integrin, focal adhesion kinase and p38 activation (Ni et al. 2018). Exogenous TB4 has been shown to increase α1, α2 and α3 integrin mRNA levels in human dental pulp cells (Lee et al. 2013). A3 integrins are the dominant type in healthy podocytes (Shirato 2002), and changes in integrin balance can alter cytoskeletal organisation (Defilippi et al. 1999). The shift of ADR-induced integrin expression may warrant further investigation to determine if changes in integrin subunit expression are occurring in this injury model which TB4 could be preventing. Increased α-actinin-4, an actin bundling protein found in podocytes (Asanuma et al. 2005), was shown to be involved in the formation of unorganised actin in mouse immortalised podocytes exposed to 0.27 μg/ml ADR (Liu et al. 2012), the same phenotype observed in this study. Dexamethasone, a glucocorticoid, was able to fully prevent the ADR-induced actin disorganisation via modulation of α-actinin-4 (Liu et al. 2012). Dexamethasone has been shown to preserve the F-actin to G-actin ratio in injured mouse hippocampi (N. Yang et al. 2020), suggesting that *de novo* formation of F-actin from G-actin could be associated with the actin bunding properties of α-actinin-4. Since TB4 is a G-actin sequestering peptide (Safer et al. 1991) future studies could examine the effect of exogenous TB4 on α-actinin-4 levels to determine if this could be a potential mechanism of protection of F-actin organisation. The F-actin to G-actin ratio could

also be examined to determine if the protective effects induced by exogenous TB4 were via G-actin sequestering.

It was hypothesised that due to its anti-apoptotic properties, such as the inhibition of caspase-3 activation (Moon, Song, and Yang 2007), and prevention of oxidative stress (Ho et al. 2008; Kumar and Gupta 2011), exogenous TB4 would be able to prevent ADR-induced loss of cell viability, however this was not the case. ADR has been shown to induce apoptosis by activation of NFκB pathway (Karger et al. 2016). TB4 prevented activation of the NFκB pathway in HCECs treated with TNF-α, therefore preventing apoptosis (Sosne, Qiu, Christopherson, et al. 2007). ADR also leads to detachment of podocytes from the matrix via integrin loss facilitated by activation of ILK (Dai et al. 2019; Wang et al. 2018). Studies in other cells types have shown that TB4 binds to and activates the ILK pathway (Bock-Marquette et al. 2004), which may contribute to reduction in cell viability. However, the decrease in podocyte viability following ADR injury was not affected by exogenous TB4 treatment, so this was unlikely to be the case in the context of podocyte injury mediated by ADR.

Exogenous TB4 has previously been shown to improve cell viability in other damaged cell types. *Tmsb4x* knockdown in human cerebral endothelial cells and then subsequently treated with 500 ng/ml exogenous TB4 were injured with damaged with prion protein (106-126). Cell viability was improved compared to non-exogenous TB4 treated cells, as assessed by MTT assay 24 hours after treatment (Song et al. 2020). This data showed that exogenous TB4 was protective of the human cerebral cells, even in TB4 knockdown cells. In endothelial progenitor cells challenged with AGE to induce oxidative stress, 0.5 μg/ml of exogenous TB4 fully prevented a reduction in cell viability as measured by MTT assay 24 hours after treatment (Q. Chen et al. 2019). Exogenous TB4 (2,500 ng/ml and 5,000 ng/ml) also prevented H_2O_2-induced reduction in neural stem/progenitor cell viability *in vitro.* This was associated with prevention of reactive oxygen species and inflammatory cytokine (interleukin -1β and -6, and toll like receptor 4) production (Li *et al.*, 2019). There are significant differences between these studies and the experimental set up of this thesis chapter; the first is the cell type used. Different cell types have varying intracellular signalling patterns and proteins, which may have worked in parallel with

TB4 to prevent the loss of cell viability. The previous studies also used a higher dosage of TB4 than this thesis chapter: 500 ng/ml, 2,500 ng/ml and 5,000 ng/ml compared to 1000 ng/ml in this thesis. It is possible that the higher dosage of TB4 provided further protection than the doses used in this thesis and follow up studies could attempt to prevent ADR-induced cell viability in podocytes with increased concentrations of TB4.

Thymosin β10 and thymosin β15 are TB4 homologues which also bind to and sequester G-actin (Yu *et al.*, 1993; Yu *et al.*, 1994; Eadie *et al.*, 2000). This thesis has provided the first evidence that *Tmsb10* and *Tmsb15a, Tmsb15b* and *Tmsb15l* transcripts are localised to podocytes. *Tmsb10* mRNA levels were reduced and *Tmsb15a* transcript levels were upregulated in response to ADR-injury. There is relatively little known about thymosin β10 and thymosin β15 in the kidney compared to TB4. Thymosin β10 is expressed in the human kidney in development, and localised to the proximal and distal tubules (Gerosa et al. 2010), suggesting that it has a role in nephrogenesis. *Tmsb10* transcripts have been detected in human adult kidneys by Southern blot analysis (Hall 1994) and adult C57BL/6 mice by qPCR (Vasilopoulou et al. 2016). The human protein atlas (www.proteinatlas.org) identifies *Tmsb10* transcripts in human kidneys, but only localised to proximal tubular cells, distal tubular cells, collecting duct cells and immune cells, with no mention of any glomerular specific cell. The protein atlas also states the three isoforms of *Tmsb15* are present in very low levels in the kidney compared to *Tmsb10*, with some expression only seen in collecting duct cells, T cells and some proximal tubular cells. However, it seems from the website that glomerular cell types have not been examined in any context, so it is possible that the mRNA transcripts are present in human glomeruli. Further studies using *in situ* hybridisation of FFPE kidney sections or single cell RNA sequencing (scRNAseq) could confirm this. Thymosin β15 is expressed in the mouse adult kidney, but it hasn't been localised to specific cells. Future studies could explore the effects of knocking down *Tmsb10* or *Tmsb15a* in podocytes *in vitro* to see if similar cytoskeletal disorganisation occurs. The loss of both *Tmsb4x* and *Tmsb10* mRNA in ADR injury is interesting and warrants further exploration. Future studies could perhaps treat ADR-injured podocytes with a combination of exogenous TB4 and thymosin β10 to examine if this synergistic

approach is able to maintain cell viability and further prevent cytoskeletal disorganisation.

To date, there have been no reports on the effect of ADR on cofilin-1, profilin-1 or -2, therefore this thesis has provided the first evidence that the transcripts of these actin-regulating proteins are unchanged in ADR nephropathy. Collectively, the effects of ADR on actin modulating genes were not altered by TB4, except for *Schip1*. Previous studies have shown that in whole kidney homogenates, lack of *Tmsb4x* upregulates *Cfl1* levels (Vasilopoulou et al. 2016). It has been suggested that TB4 promotes cofilin-1 activity, by disassociating G-actin:cofilin-1 complexes, therefore allowing cofilin-1 to sever F-actin (Al Haj et al. 2014). The steady mRNA expression of *Pfl1* and *Pfl2,* proteins that promote actin polymerisation (Mouneimne et al. 2012), coupled with the loss of *Tmsb4x, Tmsb10* and *Cfl1* in ADR-injury may provide an explanation of the ADR-induced F-actin disorganisation, as collectively there is significantly reduced expression of factors that negatively regulate F-actin polymerisation.

Synaptopodin is a mature podocyte actin-associated protein (Mundel, Reiser, et al. 1997) that has previously been shown to orchestrate cytoskeletal organisation through RhoA signalling (Asanuma et al. 2006) and regulating the actin-bundling activity of α-actinin (Asanuma et al. 2005). The results presented in this study show that *Synpo* was upregulated 4-fold in response to ADR-injury. This data is in contrast to previously reported *Synpo* levels in ADR injury. Mouse immortalised podocytes treated with 0.25 μg/ml ADR showed a 50% reduction in *Synpo* mRNA expression and synaptopodin protein expression as measured by qPCR and Western blot respectively (Wang et al. 2018). It is possible that the higher concentration of ADR induced a different effect on *Synpo* levels in podocytes in this study. This would have to be confirmed by repeating the experiment in the same laboratory conditions as this thesis and treating with an increased dose of ADR. Previous studies have shown that when *Tmsb4x* is downregulated, the expression of *Synpo* remains constant (Vasilopoulou et al. 2016). ADR induced a reduction of *Tmsb4x* in this thesis, so the upregulation of *Synpo* is unlikely to be directly due to the reduction of *Tmsb4x,* but other intracellular effects of ADR. Endogenous *Synpo* expression has been recently

shown to decelerate ADR nephropathy *in vivo* through suppression of Rac1 activity and activation of RhoA (Ning et al. 2020). Although this study did not quantify *Synpo* mRNA expression after ADR exposure, perhaps podocytes upregulate *Synpo* as a protective mechanism in ADR injury.

One gene of interest that exogenous TB4 affected the levels of was *Schip1*. *Schip1* is a member of the complex linking the cytoskeleton to podocalyxin (Perisic *et al.*, 2015), a protein that is essential for charge based filtration of the blood (Kerjaschki et al. 1984). *Schip1* overexpression was shown to prevent the loss of the podocyte cortical actin cytoskeleton and formation of cytoplasmic stress fibres in response to PDGF-BB (Perisic *et al.*, 2015) and TB4 is predicted to bind to the human homologue of Schip1 (Miyamoto-Sato *et al.*, 2010). The other members of the podocalyxin-cytoskeleton complex were unaltered, except *Schip1*, meaning that if this complex breaks down in ADR injury, the loss of *Schip1* is likely to be the cause. Neurofibromin 2 has mostly been characterised in glial cells, linking the cortical cytoskeleton to the membrane (Cole et al. 2008) and Schip1 has been shown to bind to Neurofibromin 2 (Goutebroze et al. 2000), however the significance of this binding is not yet clear. The presence of Neurofibromin 2, a member of the ERM family of proteins that organise membrane-cytoskeletal interactions (Fehon, McClatchey, and Bretscher 2010; McClatchey and Fehon 2009) in podocyte cells, may be significant in the future of understanding cytoskeletal-membrane interactions and receptor organisation in podocytes.

2.6 **Conclusions**

The results demonstrated in this thesis chapter show that in ADR-injury there is a clear downregulation of endogenous *Tmsb4x* expression. ADR causes a disruption of the F-actin cytoskeleton, unravelling the highly organised cortical actin stress fibres to unorganised F-actin. Exogenous TB4 has a protective role of the podocyte cytoskeleton in response to ADR-induced cytoskeletal rearrangements (**Figure 2.15**).

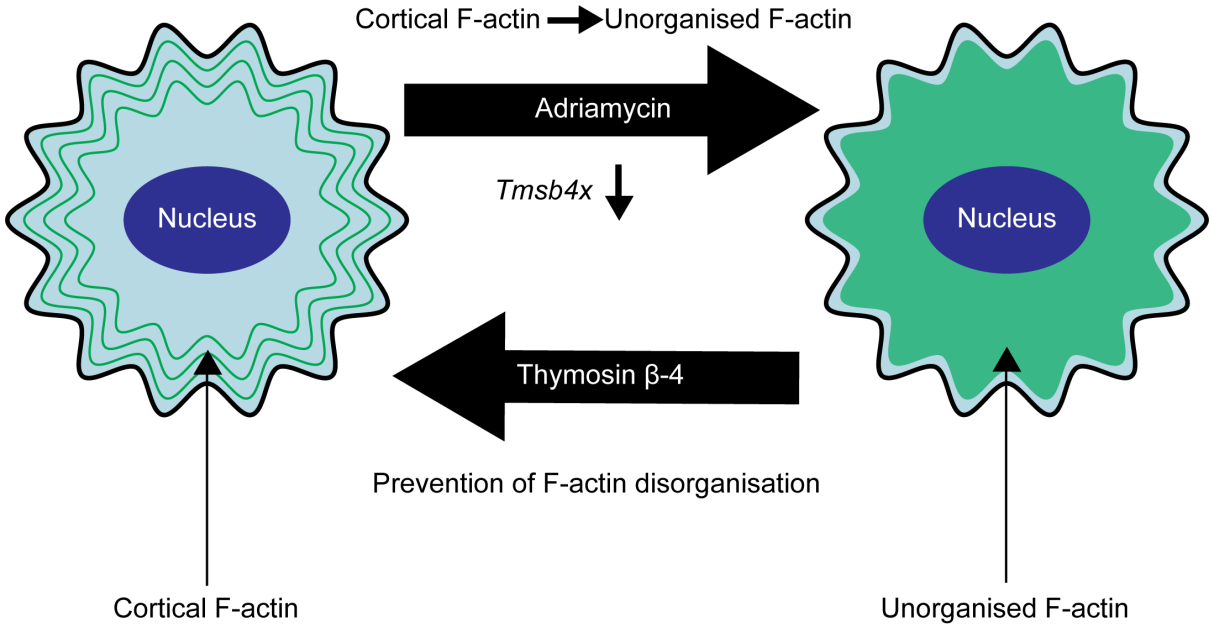

Figure 2.15 - Diagram depicting the function of TB4 in ADR injury. *ADR causes a reduction in podocyte Tmsb4x expression and actin cytoskeletal disorganisation. Treatment with exogenous TB4 prevented ADR-induced disorganisation of the actin cytoskeleton. Original diagram.*

Chapter 3: Systemic thymosin β4 delivery alleviates Adriamycin-induced glomerular injury

3.1 Introduction

The results presented in the previous chapter of this thesis demonstrate that exogenous TB4 prevents ADR-induced F-actin disorganisation in cultured podocytes. However, it is imperative to explore the role of exogenous TB4 *in vivo*. The *in vitro* model allows exploration into cell specific mechanisms, however, using *in vivo* models of glomerular injury provides insight into the therapeutic potential of molecules in a living system, which encompasses blood flow, a key component missing from culture systems.

So far, there have been a limited number of studies that have used exogenous TB4 as a therapeutic agent in kidney injury. In the UUO model, a model of renal fibrosis, C57BL/6 mice were treated with 150 μg/day of TB4, resulting in a 33% reduction of interstitial fibrosis compared to sham mice. Administration of either 1 mg/kg or 5 mg/kg of synthetic TB4 to UUO injured Sprague-Dawley rats reduced 24h proteinuria and histopathological changes (Yuan et al. 2017). Daily injection of synthetic TB4 (100 ng/g/day) to C57BL6 mice attenuated albuminuria and histopathological changes in the diabetic nephropathy model (Zhu et al. 2015). Furthermore, Sprague-Dawley rats injured with the acute ischaemia reperfusion kidney model and injected intravenously with 10 mg/kg synthetic TB4 showed reduced inflammatory and apoptotic markers and improved kidney function (Aksu et al. 2019). These studies show that exogenous TB4 may have a protective role in acute and CKD models, however, the effect of exogenous TB4 in glomerular injury is unknown.

It is estimated that in the U.K., around 0.8 in 100,000 individuals are diagnosed with FSGS but many cases do not respond to the current treatment of steroids to slow the progression to ESKD (Hogg, Middleton, and Vehaskari 2007), highlighting the urgent need for novel therapies that can circumvent steroid resistance. ADR mimics some of the characteristics of human FSGS when administered to rodents (Bertani et al. 1986; Lee and Harris 2011; Wang et al. 2015), including albuminuria, foot process effacement, glomerulosclerosis, podocyte detachment and cytoskeletal disorganisation (Guo *et al.*, 2008; Heikkilä *et al.*, 2010; Zou *et al.*, 2010; Lee and

Harris, 2011; Suleiman *et al.*, 2017). The previous chapter showed that exogenous TB4 is able to prevent ADR-induced cytoskeletal reorganisation *in vitro*, suggesting that exogenous TB4 may have beneficial effects in ADR injury *in vivo*.

To examine this, a systemic gene therapy strategy was undertaken. TB4 is metabolised relatively quickly when the recombinant peptide is administered *in vivo*, and the concentration of circulating TB4 returns to basal levels within 6 hours (Mora et al. 1997). Therefore, an AAV construct encoding *Tmsb4x* was used (Bongiovanni *et al.*, 2015) to achieve systemic, long-term upregulation of TB4. AAV 2/7 has the capsule of AAV 7, which displays strong tissue tropism for the liver and brain (Van Der Perren et al. 2011). AAV infects liver cells before inducing transgene expression via transcription and translation (Schultz and Chamberlain 2008). Specific targeting of the kidney is a challenge that renal scientists employing AAV therapy face, due to low tissue tropism of known serotypes (Zincarelli et al. 2008). Therefore, this thesis chapter employed a systemic upregulation of TB4 with AAV.*Tmsb4x* (the mRNA precursor of TB4), as it has been proven that TB4 is a secreted peptide (Mora et al. 1997). AAV infection is also slow and can take over 1 week for full infection and replication to occur (Davidoff et al. 2005), so AAV.2/7 was used as a preventative therapy, rather than an intervention after disease had been induced.

3.2 **Aims and hypothesis**

It was hypothesised that exogenous TB4 would prevent ADR-induced glomerular injury by protection of the podocyte cytoskeleton. The first aim of this chapter is to examine if endogenous TB4 is downregulated in glomeruli and podocytes in ADR injury *in vivo.* The second aim of this chapter is to confirm that AAV.*Tmsb4x* can infect liver cells and induce systemic upregulation of TB4. The final aim of this chapter will aim to investigate if exogenous TB4 can prevent ADR-induced glomerular injury and to determine if ADR or TB4 affect the podocyte cytoskeleton *in vivo*.

3.3 **Materials and methods**

3.3.1 Analysis of single cell RNA sequencing data

Analysis of scRNAseq data from a recently published study (Chung et al. 2020) was performed in collaboration with Mr Daniyal J. Jafree and Mr Gideon Pomeranz, from University College London Great Ormand Street Hospital Institute of Child Health. scRNAseq analysis was performed using RStudio for Macintosh (RStudio Inc., v1.2.5042) using R (v4.0.2).

3.3.1.1 *Data acquisition*

The raw scRNAseq dataset used in this analysis was acquired from a study characterising the single-cell transcriptome of murine ADR nephropathy using the 10X Genomics platform (Chung et al. 2020). Matrices of gene counts per droplet, generated after alignment of reads to genes, were acquired from the National Center for Biotechnology Information Gene Expression Omnibus (GSE146912) and are available at https://www.ncbi.nlm.nih.gov/geo/query/acc.cgi?acc=GSE146912.

3.3.1.2 *Quality control, data processing and integration*

All of the following analyses were performed using the Seurat toolkit (Butler et al. 2018). The count matrices from n = 2 control samples (8,412 cells) and n = 2 samples with ADR nephropathy (8,296 cells) were merged into a single object. Genes expressed in two or fewer droplets were excluded and droplets with < 200 and > 4000 detected genes and > 10% of features mapping to the mitochondrial genome were excluded. The data were then normalized using the NormalizeData function and the data scaled by all detected genes using the ScaleData function before principal component analysis (PCA), using the top nine components for downstream analyses. Integration and matching of cell types between experimental conditions was performed using the Harmony package for R (Korsunsky et al. 2019).

3.3.1.3 *Clustering, cell type identification and counting*

Shared nearest neighbour graphing was performed using the FindNeighbors function. Unsupervised clustering was performed with the FindClusters function using the Louvain algorithm and a resolution of 0.4, generating 14 transcriptionally distinct clusters of cells, before dimension reduction using Uniform Manifold

Approximation and Projection (UMAP). Cell type identification was performed by assessing the top ten differentially expressed genes per cluster calculated using the FindAllMarkers function and canonical markers for glomerular cell types were compared from previous scRNAseq studies (Chung et al. 2020; Fu et al. 2019; Karaiskos et al. 2018). Ten glomerular cell types were subsequently identified and assigned. The number of cell types by experimental condition was exported and graphed in Prism (GraphPad, v9.0.0)

3.3.1.4 *Comparison of Tmsb4x expression*

The FindAllMarkers function was used to compare the scaled expression of *Tmsb4x* between ADR nephropathy and control datasets. The average log fold change was calculated for podocytes or all glomerular cell types (glomerular endothelial cells, mesangial cells, and podocytes) between experimental conditions. Wilcoxon Rank Sum tests was used to assess statistical significance.

3.3.2 Experimental animals and procedures

ADR nephropathy was induced in BALB/c mice, as they harbour low levels of PRKDC, rendering them sensitive to ADR-induced glomerular injury (Papeta et al. 2010). All procedures described were approved by the Home Office. All materials listed below were obtained from Merck U.K unless stated otherwise. All incubations were at room temperature unless stated otherwise.

Male BALB/c mice aged between 7 – 10 weeks were housed in cages of three, exposed to constant temperature (22 °C) and light cycle (12 hours light, 12 hours dark), and provided with standard laboratory chow and tap water *ad libitum*. Blood and urine were collected prior to the mice being injected with $5x10^{12}$ viral particles of either AAV.*LacZ* serotype 2/7 or AAV.*Tmsb4x* serotype 2/7 via the tail vein. The AAV constructs were a kind gift from the lab group of Professor Christian Kupatt (Bongiovanni *et al.*, 2015). Three weeks later (day 0 in **Figure 3.1**), mice were weighed and then injected with 10 mg/kg of ADR or vehicle (0.9% saline) via the tail vein and culled 14 days later. The final treatment groups to be compared were administered (i) AAV.*LacZ* and vehicle (control group) (*LacZ*/saline), (ii) AAV.*LacZ*

and 10 mg/kg ADR (glomerular injury group) (*LacZ*/ADR) and (iii) AAV.*Tmsb4x* and ADR (glomerular injury and treatment group) (*Tmsb4x*/ADR).

Mice were weighed at day 0, 2, 7 and 14 after ADR/vehicle administration. Blood (collected in MicroVette EDTA coated capillary action tube, SARSTEDT, Nümbrecht, Germany) and urine were collected at day 2 and mice were culled by CO_2 asphyxiation at day 14 after ADR administration for kidney and liver collection, following overnight urine collection in metabolic cages. Death was confirmed by exsanguination. A 25G needle was used for blood collection via the lateral saphenous vein while the mice were alive and via cardiac puncture post-mortem. The collected blood was centrifuged for 15 minutes at 3000 rpm. The separated plasma was extracted and stored at -80 °C until further use. Urine was centrifuged at 10,000 rpm for 5 minutes and the supernatant was stored at -80 °C until further use. An overview of the experimental set up can be found (**Figure 3.1**).

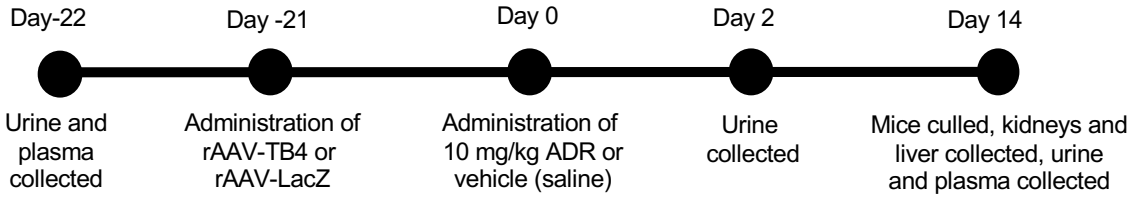

Figure 3.1 – Experimental design for in vivo ADR experiment. *A graphic displaying the chronological experimental design for the in vivo experiment. Day 0 was designated as the day of ADR/vehicle administration.*

3.3.3 Tissue processing

Left kidneys and part of the liver were immediately snap frozen on dry ice after extraction from the mice. Right kidneys were weighed to obtain kidney weight to body weight ratio and then cut in half with a scalpel medially along the basal side. The kidney halves along with the liver were fixed in 4% PFA in dH_2O overnight at 4 °C while rotating. After fixation, one half of the kidney was cryo-preserved and the other half, along with the liver and heart, was embedded in paraffin wax.

For cryo-preservation, the tissue was incubated in 30% sucrose in dH_2O overnight following fixation at 4 °C while rotating. The kidney was then rinsed in OCT medium (Agar Scientific, Stansted, U.K.) before cryo-preservation in OCT medium on dry ice,

with the cut side of the kidney face down, and stored at -80 °C until further use. Cryo-sections were cut on a cryostat (Clinicut 60, Bright Instruments, Huntingdon, U.K.) to 8 μm, adhered to SuperFrost Plus microscope slides (VWR International, PA, U.S.A) and stored at –20 °C until further use. For paraffin wax embedding, the tissue was prepared by a series of dehydration and washing steps. The tissues were dehydrated by 1-hour subsequent incubations in 70%, 80%, 90% and 100% ethanol. The tissues were then cleared by 2 one-hour incubations in Histoclear II (National Diagnostics, GA, USA). The Histoclear II was drawn out from the tissues by incubation in a 1:1 solution of Histoclear II and paraffin wax at 80 °C for 1 hour. Finally, the tissues were washed in paraffin wax for 2 one-hour incubations at 80 °C. Tissues were then embedded in fresh wax with cut side face down until solidified. The wax blocks were then sectioned to 5 μm on a microtome (RM2255, Leica Biosystems, Milton Keynes, U.K.) and adhered to SuperFrost Plus microscope slides.

3.3.4 Antibodies used

Table 3.1 – List of primary antibodies used in in vivo experiments

Antibody	Dilution (application)	Antigen retrieval method	Reference
Polyclonal sheep IgG α-human TB4	1:200 (IHC, IF) 1:4000 (ELISA)	Proteinase K	R&D Systems, MN, USA, AF6796
Goat α-mouse albumin (capture)	1:100 (ELISA)	N/A	Bethyl Laboratories, TX, USA, A90-134A
Polyclonal guinea pig α–mouse synaptopodin	1:200 (IF)	N/A	2B Scientific, Oxfordshire, U.K., 163-004-SY
Monoclonal rabbit α-mouse WT-1	1:200 (IHC)	Tris-EDTA	Abcam, Cambridge, U.K., AB89901
Monoclonal rat α-mouse F4/80	1:1000 (IHC)	Trypsin	Bio-Rad, CA, USA, MCA497R
Polyclonal rabbit α–mouse Ki67	1:400 (IF)	N/A	Abcam, Cambridge, U.K., AB15580

Table 3.1 – List of primary antibodies used. *α, anti; IgG, immunoglobulin G; WT-1, Wilms tumour 1; F4/80, EGF-like module containing mucin-like hormone receptor-like 1; Ki67, antigen Ki67; IHC, immunohistochemistry; IF, immunofluorescence; ELISA, enzyme linked immunosorbent assay; N/A, not applicable; EDTA, ethylenediaminetetraacetic acid. acid.*

Table 3.3.2 – List of secondary antibodies used in in vivo experiments

Antibody	Dilution (application)	Reference
Goat α–mouse albumin HRP conjugate (detection)	1:40,000 (ELISA)	Bethyl Laboratories, TX, USA, A90-134P-7
Goat α-sheep HRP conjugate	1:2000 (ELISA)	Dako, Ely, U.K., P0450
Goat α–guinea pig Alexa Fluor 488 conjugate	1:200 (IF)	ThermoFisher Scientific, MA, USA, A11073
Goat α-guinea pig Alexa Fluor 594 conjugate	1:200 (IF)	ThermoFisher Scientific, MA, USA, A11076
Donkey α-sheep Alexa Fluor 594 conjugate	1:200 (IF)	ThermoFisher Scientific, MA, USA, A11016
Rabbit α-rat IgG HRP conjugate	1:200 (IHC)	Agilent, CA, USA P0450
Rabbit α-sheep IgG HRP conjugate	1:200 (IHC)	ThermoFisher Scientific, MA, USA, 61-8620
Donkey α-rabbit IgG Alexa Fluor 594 conjugate	1:200 (IF)	Abcam, Cambridge, U.K., AB89901

Table 3.2 – List of secondary antibodies used. *α, anti; IgG, immunoglobulin G; IHC, immunohistochemistry; IF, immunofluorescence; ELISA, enzyme linked immunosorbent assay.*

3.3.5 TB4 ELISA

To determine if TB4 was upregulated in the mice treated with AAV.*Tmsb4x* compared with AAV.*LacZ* treated mice, plasma concentration of TB4 was measured by a customised ELISA, which was refined based on a previously used protocol (Mora et al. 1997). Standards using synthetic TB4 (ReGeneRx Biopharmaceuticals Inc), diluted in incubation buffer (pH 7.4, Na_2HPO_4 (0.01M), NaCl (0.15M), Tween-20 (0.055 % v/v), BSA (1 % v/v)), were prepared by serial dilutions to obtain the following concentrations: 10,000 ng/ml, 5,000 ng/ml, 2,500 ng/ml, 1,250 ng/ml, 625 ng/ml, 312.5 ng/ml, 156 ng/ml, 78 ng/ml, 39 ng/ml, 0 ng/ml. A 1:1 homogenous ratio of standards/samples and incubation buffer was added to a sterile borosilicate tube (Scientific Laboratory Supplies, Nottingham, U.K.). Sheep anti-serum to TB4 (**Table 3.1**) was diluted 1/4000 in incubation buffer and 100 µl was added to each tube of standard/sample. The tubes were sealed, vortexed and incubated at 4 °C overnight. The ELISA plate (Greiner Bio-One, 96 well, flat transparent) was coated with 100 µl of 50 ng/ml synthetic TB4 in coating buffer (carbonate/bicarbonate capsule in 100 ml

H_2O). Negative control wells with coating buffer only were also prepared and the ELISA plate was incubated at 4 °C overnight.

The plate was washed 5 times with washing buffer (pH 7.4, Na_2HPO_4 (0.01M), NaCl (0.15M), $CaCl_2$ (1 mM), $MgCl_2$ (0.5 mM), Tween-20 (0.55% v/v)) (all subsequent washes were 5x with washing buffer) and blocked with 200 μl of blocking buffer (5 % dry fat milk in incubation buffer) for 1 hour. After washing, 100 μl of the standards/samples were added to the ELISA plate wells and left to incubate for 2 hours. The plate was then washed and 100 μl of goat anti-sheep HRP-conjugated (**Table 3.2**) secondary antibody, diluted 1/2000 in incubation buffer was added to each well. The plate was left for 1 hour to incubate and then washed again. Substrate solution (containing equal parts stabilised H_2O_2 and stabilised tetramethylbenzidine) was prepared (R&D Systems, Stansted, U.K.) and 100 μl was added to each well of the plate, which was left to incubate for 15 minutes in the dark. The reaction was stopped with the addition of 50 μl of 2M sulphuric acid per well and absorbance (Abs) was read at 450 nm using a plate reader.

A blank value (incubation buffer only) was subtracted from each Abs_{450} value before a standard curve of the log_{10} values vs Abs_{450} was generated on Graph Pad Prism 9.0 (**Figure 3.2**). Sample log_{10} transformed values were compared to the standard curves to determine sample TB4 concentration.

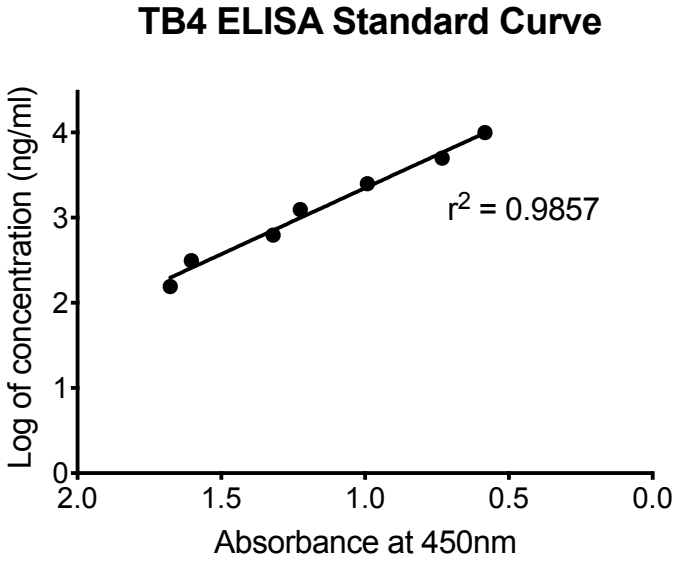

Figure 3.2 - TB4 ELISA standard curve. *Example of a standard curve used to calculate plasma TB4 concentration. r^2 value indicates how well points align to line of best fit (0.9999 = perfect fit).*

3.3.6 Albumin ELISA

To measure albuminuria, a commercially available ELISA kit was used (Bethyl Laboratories, TX, USA). Tris Buffered Saline (TBS) (5 x 50 mM), pH 8.0 in H_2O was prepared; using Tris Base (44.37 mM), Tris HCl (0.21 M), NaCl (0.69 M) and KCl (13.42 mM). The wash solution (pH 8.0, 1 x TBS in H_2O and 0.05 % (v/v) Tween-20), postcoat solution (pH 8.0, 1 x TBS in H_2O and 0.1 % BSA (v/v) and sample diluent (postcoat solution and 0.05 Tween-20 (v/v)) were also prepared prior to the start of the experiment.

Goat α-mouse albumin antibody (**Table 3.1**) was diluted 1/100 in coating buffer, added to each well of the ELISA plate and left to incubate for 1 hour. After incubation, the ELISA plate was washed 3x with wash buffer (all subsequent washes were 3x in wash buffer) and blocked by adding 200 μl of PostCoat solution to each well for 30 minutes. Standards of mouse albumin were prepared by serial dilutions to obtain concentrations of: 500 ng/ml, 250 ng/ml, 125 ng/ml, 62.5 ng/ml, 31.25 ng/ml, 15.625 ng/ml and 7.8 ng/ml in sample diluent. Urine samples were either diluted 1/1,000 or 1/10,000 in incubation buffer depending on the amount of urinary albumin present. The plate was then washed before the standards/samples were added to the appropriate wells and left to incubate for 1 hour. The plate was washed and 100 μl of the goat α-mouse albumin antibody conjugated to HRP (**Table 3.2**) diluted in sample diluent for a final dilution of 1:100 was added to each well. After washing again, 100 μl of substrate solution (containing equal parts H_2O_2 and tetramethylbenzidine) (R&D Systems) was added to each well for 15 minutes in the dark. The reaction was halted with 50 μl of 2M sulphuric acid and the Abs was read at 405 nm. All standards and samples were assessed in duplicate.

The average Abs_{405} – blank (sample diluent only) values, were transferred to Graph Pad Prism 8.0 where a standard curve of Abs_{405} vs $\log_{10}$ was plotted. The sample albumin concentrations (ng/ml) were determined based on comparison of their Abs_{450} values with the standard curve (**Figure 3.3**). The concentration was then multiplied by the volume of urine produced by the mouse at each time point to give the amount of albumin in the urine (ng). The final value of μg of albumin over a 24-

hour period was calculated by the following formula: amount of albumin (ng)/time in metabolic cage (hours) X 24 (hours)/1000.

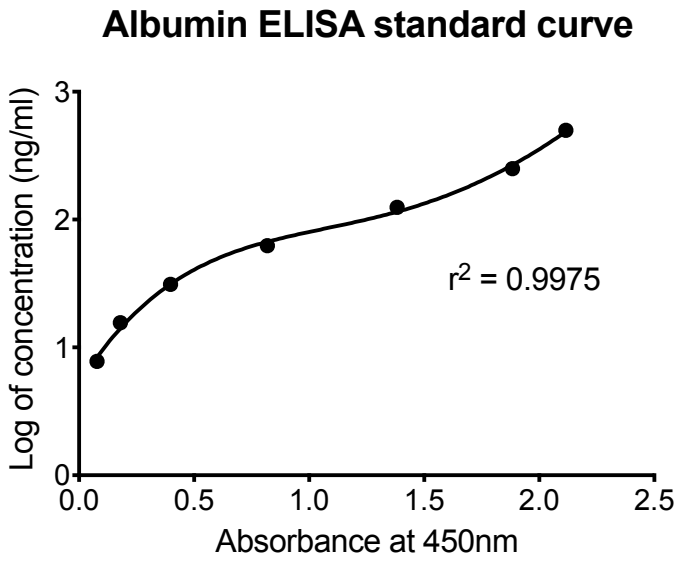

Figure 3.3 – Albumin ELISA standard curve. *Example of a standard curve used to calculate urinary albumin amount.*

3.3.7 Creatinine assay

Creatinine is a muscle metabolite that freely filtered through the glomerular filtration barrier and used to adjust urinary albumin amount for body weight (Wyss et al. 2000), so urinary creatinine levels were quantified using a commercially available kit (Cayman Chemicals, MI, USA). Creatinine standards were serially diluted in distilled H_2O: 0 mg/dl, 2 mg/dl, 4 mg/dl, 6 mg/dl, 8 mg/dl, 10 mg/dl, 12 mg/dl, 15 mg/dl, and the urine samples were diluted 1/10 in distilled H_2O. Next, 15 μl of the diluted sample was added to the assay plate in duplicate. The reaction was started by the addition of 150 μl of alkaline picrate solution, the plate was sealed and incubated on a shaker for 10 minutes. The Abs was then read at 495 nm, designated initial Abs (I_{abs}), and 5 μl of acid solution was added to each well and left to incubate for 20 minutes on a shaker. The Abs_{495} was once again read, designated final Abs (F_{abs}).

The average I_{abs} and F_{abs} of duplicate values were calculated and the corrected Abs was calculated by subtracting F_{abs} from I_{abs}. The change in Abs of the standard 0 mg/dl was subtracted from itself and all other standards and the standard curve was generated from these values. The concentration of creatinine in mg/dl was calculated by the formula - ((Sample absorbance – standard curve y intercept)/slope of standard curve) X sample dilution. Sample creatinine concentration was converted

from mg/dl to μmol/l by multiplying by 88.4 (creatinine molecular weight is 113.12) and then to μmol/μl by division by 1,000,000. This value was then converted to μmol by multiplication with the urine volume of each sample. Conversion to mg was achieved by multiplying the μmol value by 113.12 (creatinine molecular weight) and dividing by 1000. Albumin to creatinine ratio was determined by dividing this value by the amount of albumin (μg) in the urine as calculated in 3.3.6.

3.3.8 BUN assay

BUN assay was used as a measure of plasma urea concentration and was assessed using a commercially available kit (BioAssay Systems, CA, USA). Blood was collected and plasma was prepared as described in 3.3.2. Standards were prepared of 50 mg/dl, 10 mg/dl, 5 mg/dl, 2.5 mg/dl, 1 mg/dl, 0.5 mg/dl and 0 mg/dl of urea in distilled H_2O. The 96 well plate wells were filled with 5 μl of water (blank), standards or plasma samples in duplicate and 200 μl of the working reagent was added before tapping to mix. Abs was read at 520 nm after 20 minutes of incubation. A standard curve was generated of Abs_{520} against concentration of urea standard (mg/dl). Sample urea concentration was calculated with the following formula: [urea (mg/dl)] = (Abs_{520} of sample – Abs_{520} of blank)/ (Abs_{520} of standard – Abs_{520} of blank) x concentration of standard. Urea concentration was then converted to BUN by division by 2.14. BUN reflects only the nitrogen content of urea (molecular weight 28), but urea measurement reflects the whole molecule (molecular weight 60). Hence, urea is 2.14 x (60/28 =2.14) that of BUN.

3.3.9 Glomerular extraction

Glomerular extraction was undertaken by Dr Eugenia Papakrivopoulou of the Clinique Saint Jean, Brussels (Eugenia Papakrivopoulou et al. 2018) in male BALB/c mice administered 10 mg/kg ADR intravenously. The mice were anesthetised and perfused with $1x10^8$ Dynabeads (Invitrogen, Paisley, U.K.) through the left ventricle of the heart. The kidneys were removed, decapsulated, minced and digested. The glomeruli containing Dynabeads were extracted by a magnetic particle concentrator before mRNA was extracted for qPCR analysis (Long et al. 2013).

3.3.10 qPCR

Snap frozen tissues were thawed and mechanically homogenised (PRO Scientific Inc, PRO 200, Oxford, U.K.) in 700 μl of buffer RLT (RNEasy Mini kit, Qaigen, USA). One volume of 70% ethanol in dH_2O was added to the lysate and mRNA extraction was undertaken as described in 2.3.7. cDNA synthesis was performed as described in 2.3.8 and qPCR was performed as described in 2.3.10 using primers previously listed to examine *Tmsb4x*, *Tmsb10, Tmsb15a, Tmsb15b,* and *Tmsb15l* (**Table 2.1**).

3.3.11 IHC

IHC was performed on FFPE sections, prepared as described in 3.3.3. Sections were dewaxed twice for 5 minutes in Histoclear II (National Diagnostics) and rehydrated by sequential incubations in 100% ethanol (twice for 5 minutes), 70% ethanol (5 minutes) and distilled H_2O (5 minutes). For immunoreactivity to occur, antigen retrieval must take place. The antigen retrieval methods used in this thesis are listed below:

- Proteinase K – slides were incubated in 20 μg/ml Proteinase K diluted in distilled H_2O for 20 minutes at 37 °C.
- Trypsin – 1 mg tablet was dissolved in 1 ml distilled H_2O. Slides were incubated in trypsin for 15 minutes at 37 °C.
- Tris-EDTA (pH 9.0) – 10 mM Tris-buffer (Fisher Scientific) 1 mM EDTA, 0.05% Tween-20 dissolved in distilled H_2O was prepared. The buffer was heated in a microwavable container for 10 minutes on high power. Slides were placed in the heated buffer and then heated for another 25 minutes on medium power. Slides were allowed to cool before proceeding.

After antigen retrieval, the slides were washed in dH_2O before incubation in 1.6% hydrogen peroxide diluted in 1xPBS, to quench any endogenous peroxidase on the tissue. The sections were washed in dH_2O and a hydrophobic ring was drawn around the tissues using a PAP pen (Vector Laboratories, Inc, Peterborough, U.K.). The slides were rinsed in 0.1% PBS-Tween 20 and then incubated in block solution (10% FCS, 1% BSA in 0.1% PBS-Tween 20 in dH_2O) for 1 hour in a humidified

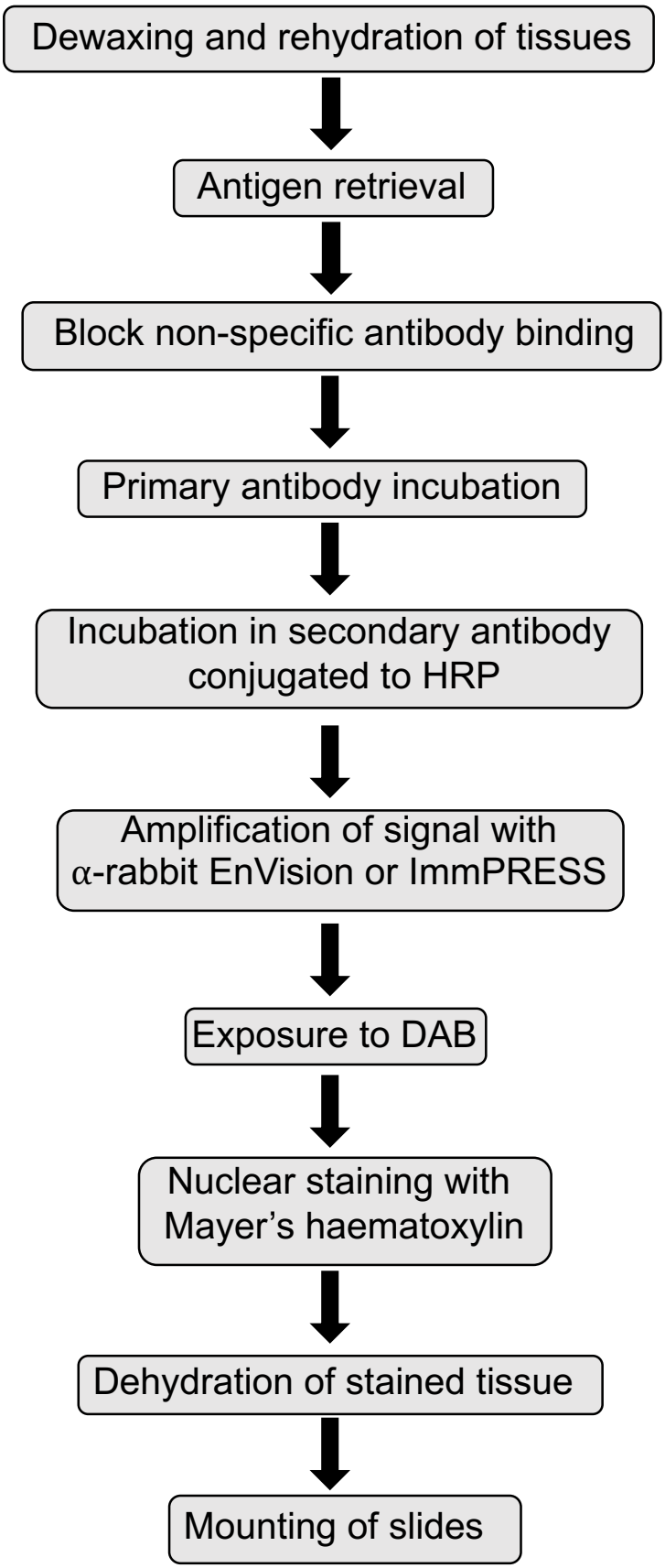

Figure 3.4 – Flow diagram of IHC protocol. *Simplified protocol of IHC experiments to aid in the explanation of the procedure. HRP, horse radish peroxidase; DAB, 3,3'-Diaminobenzidine.*

chamber. Immediately after blocking, the primary antibody (**Table 3.1**), diluted in block solution was applied to the sections before overnight incubation at 4 °C in the humidified chamber.

The primary antibody was then washed off in 0.1% PBS-Tween 20 in dH_2O. In cases where the primary antibodies were not raised in rabbit, an additional HRP-conjugated secondary antibody (raised in rabbit) step (**Table 3.2**), diluted in block solution, was undertaken for 1 hour to display a rabbit epitope. The sections were washed in 0.1% PBS-Tween 20 for three times for 5 minutes and incubated in either α-rabbit EnVision (Dako, Ely, U.K.) or α-rabbit ImmPRESS (Vector Laboratories) for 40 minutes in the humidified chamber to amplify positive staining. The slides were then washed in PBS and incubated in 3,3'-Diaminobenzidine (DAB) for up to 5 minutes to reveal positive staining. After another washing stage of 5 minutes in tap water, counterstaining with Mayer's haematoxylin for 30 seconds to 1 minute to visualise nuclei took place. Subsequently, the sections were thoroughly washed in running tap water for 10 minutes. The slides were then rehydrated in 70% ethanol (5 minutes), 100% ethanol (twice for 5 minutes) before washing in Histoclear II (National Diagnostics) (twice for 5 minutes). Finally, the sections were mounted with Histomount (National Diagnostics) and stored at room temperature. A flow diagram simplifying this protocol can be found in **Figure 3.4**. Negative controls were also generated by omitting the primary antibody to confirm antibody specificity. Immunohistochemically stained sections were imaged on a Leica DM5500 B histological microscope (Leica Biosystems) with either the 20x or 40x objective.

3.3.12 Immunofluorescence

All washing steps were three times for 5 minutes unless stated otherwise. To fluorescently label proteins, cryo-sections were prepared as described in 3.3.3 and the slides were defrosted in PBS before a hydrophobic ring was drawn around the tissue with a PAP pen. The sections were then permeabilised for 10 minutes in 0.3% PBS-Triton X-100 before incubation in block solution (10% FCS, 1% BSA, 0.3% PBS-Triton X-100) for 1 hour in a humidified chamber. The primary antibody (**Table 3.1**) was diluted in block solution and applied to the section, which was then incubated overnight at 4 °C in a humidified chamber.

The primary antibody was then washed off with 0.3% PBS-Triton X-100 before incubation with the appropriate fluorophore conjugated secondary antibody (**Table 3.2**) diluted in block for 1 hour in the humidified chamber. The antibody was then washed off in 0.3% PBS-Triton X-100, and the slides incubated in 0.1% Sudan black (in 70% ethanol) for 20 minutes to suppress tissue autofluorescence and then washed again in PBS. The tissues were then incubated in 10 μg/ml Hoechst 33342 diluted in PBS for 10 minutes to stain nuclei and washed in PBS. The slides were then dabbed dry, mounted with SlowFade then a coverslip was placed over the tissue and sealed with nail varnish. The slides were kept at 4 °C until further use. Negative control sections were also generated that omitted the primary antibody to confirm antibody specificity.

3.3.13 Confocal microscopy

Fluorescent images were obtained using a Laser Scanning 880 confocal microscope (Zeiss, Oberkochen, Germany) with the 63x 1.4 objective lens with immersion oil (Zeiss). ZEN Black software (Zeiss) was used for image acquisition set up. The images were captured with a diode (405 nm), an Argon (488 nm) and a Helium-Neon laser (594 nm). A negative control slide was prepared as described in 3.3.12, omitting either the 488 nm fluorophore or the 594 nm fluorophore so that channel bleed through and exposure could be assessed. The glomerulus with the brightest fluorescence was located on a control section and the gain was adjusted to maximise the fluorescence visualisation without inducing saturation (**Figure 3.5a, b, c**). The selected gain for each channel was adjusted so that any bleed through in the 488 nm channel (**Figure 3.5d, e, f**) and the 594 nm channel (**Figure 3.5g, h, i**) was minimised. The “best signal” mode of image acquisition was selected, and the emission spectra (**Figure 3.6**) generated by ZEN black software indicated approximately 3% bleed through from the 405 nm channel into the 488 nm channel, however it was clear from the control images (**Figure 3.5**) that this did not affect the image acquisition.

The image was acquired unidirectionally to reduce the number of scan lines the laser undertook, therefore reducing the time taken for image capture. The frame size was

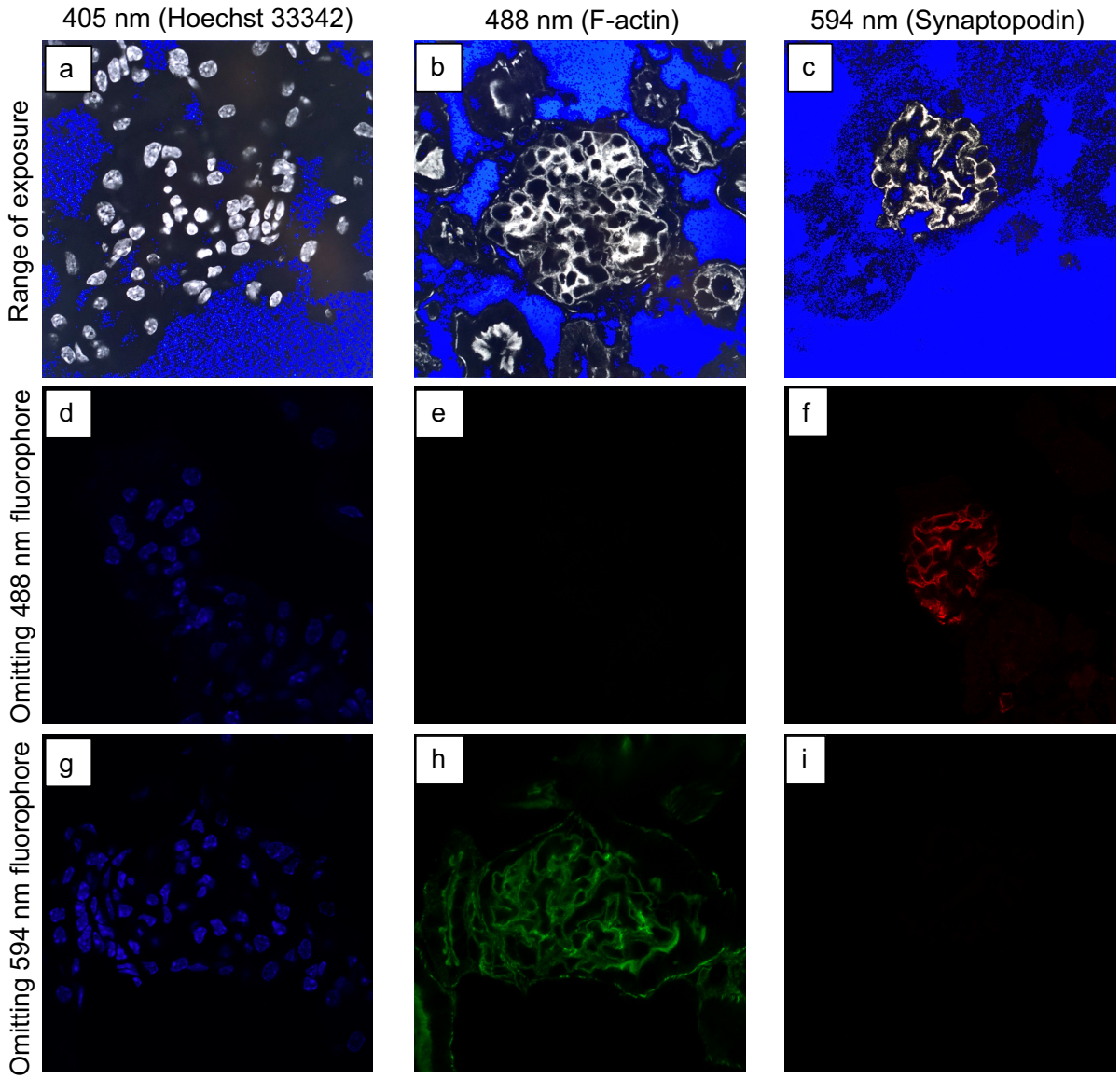

Figure 3.5 - Confocal microscopy experimental set up. *Single stain sections were prepared using either Acti-Stain 488 Phalloidin or Alexa Fluor 594 nm conjugated secondary antibodies. The gain was adjusted for the* ***(a)*** *405 nm,* ***(b)*** *488 nm and* ***(c)*** *594 nm laser to the maximum gain that would not saturate the images. Representative images of the first section, omitting Acti Stain 488 nm Phalloidin, was imaged with the* ***(d)*** *405 nm,* ***(e)*** *488 nm and* ***(f)*** *594 nm lasers. Representative images of the second section, omitting the Alexa Fluor 594 nm conjugated secondary antibody was imaged with the* ***(g)*** *405 nm,* ***(h)*** *488 nm and* ***(i)*** *594 nm lasers.*

set to the optimal setting, which was 1304x1304 pixels for 63x magnified images. The scan speed was set to 4 (out of 10), which increased pixel dwell time to reduce noise compared to the fastest scan speed (10) but did not cause bleaching of the pixels compared to the slowest scan speed (1). The line average time was set to 4, which caused the laser to scan each line 4 times and the pixel values were averaged. The images were saved as 16-bit images, which contained higher grey levels (bit depth) in comparison to 8-bit images. Finally, the pinhole was set to 1 Airy unit, which allowed the optimal ratio of light to resolution.

3.3.14 Image analysis

All image analyses were conducted on Fiji ImageJ software (Schindelin et al. 2012). Fifty glomeruli per sample were analysed unless stated otherwise. WT-1 is specific to podocyte nuclei in the glomerular tuft (Wagner et al. 2004), therefore to assess podocyte loss, WT-1 immunostained tissue images were acquired. For each glomerulus, the area was measured and the number of WT-1 positive nuclei in the tuft were assessed. This number was normalised to the tuft area. For each group, an average of 50 glomeruli was calculated for each sample. Additionally to the number in each glomerulus, the number of WT-1 positive nuclei in the parietal epithelium were counted.

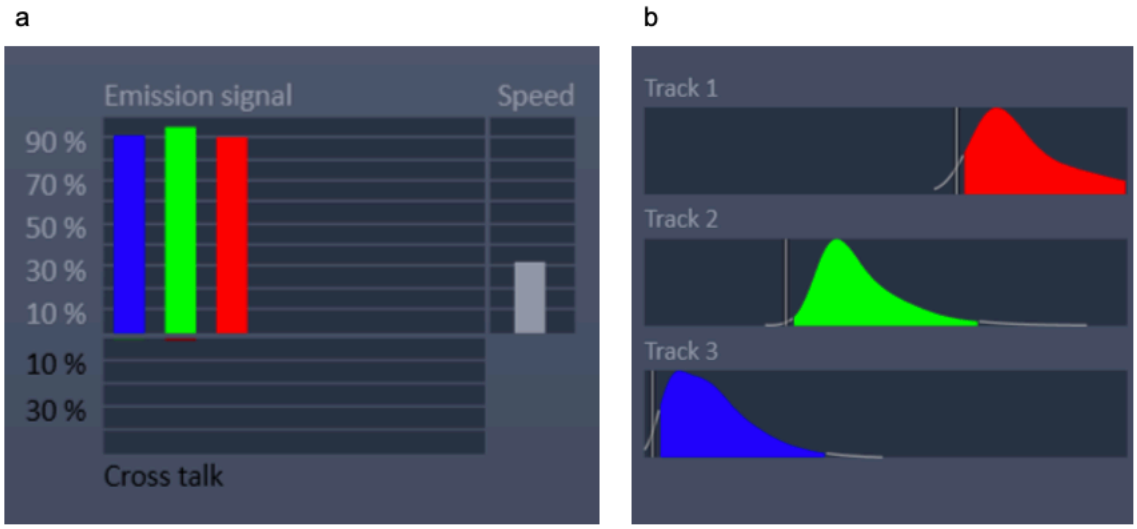

Figure 3.6 – Emission spectra of the wavelengths used in confocal microscopy studies. (a) *The cross talk between each laser used in image acquisition.* ***(b)*** *Individual wavelengths of each track used. Track 1, red, 594 nm, synaptopodin; track 2, blue, 405 nm, nuclei; Track 3, green, 488 nm, F-actin.*

Previous studies have identified through intravital multiphoton imaging that in disease, podocytes will cluster together before migration away from the glomerular tuft towards the Bowman's capsule (Burford et al. 2014; Hackl et al. 2013). To assess podocyte clustering, a minimum of 30 glomeruli stained for WT-1 were used per mouse. The vascular pole of the glomeruli was designated the "lower" pole and the tubular pole was designated the "upper" pole. The glomerulus was divided into quarters and the number of WT-1 positive glomeruli in each quarter of the glomerulus was counted.

To quantify renal inflammation, IHC sections were immunostained with F4/80 antiserum which visualised macrophages. Images were captured on a Leica DM5500 B histological microscope with the 40x objective. The number of $F4/80^{+}$ cells inside and out of the glomerular tuft in a constant region of interest were counted in each glomerulus.

To assess glomerular F-actin alterations *in vivo,* cryosections were stained with phalloidin and images captured on a confocal microscope. The mean grey value of the background was subtracted from the images to remove background staining. The circumference of the glomerulus was traced, and the mean glomerular fluorescence was measured. The images were then thresholded to a value that caused the software to detect the lowest fluorescence but would not oversaturate the brightest fluorescence. The total area (μm^2) and percentage area of the glomerulus covered by the F-actin was calculated using Fiji ImageJ. This experiment was repeated on sections immunostained to visualise synaptopodin.

To determine alterations to podocyte F-actin *in vivo*, cryosections were immunostained with synaptopodin antiserum and phalloidin. A macro, that was designed by Dr Dale Moulding of GOSHICH, was used to automate image analysis. The circumference of the glomerulus was traced and measured, and the area outside of the glomerular tuft was cleared. A Gaussian blur with a Sigma (radius) value of 2.0 was applied to each channel to create a solid mask that defined the area of each individual protein (synaptopodin or F-actin) before each channel was thresholded. The mean fluorescence of F-actin within the synaptopodin positive area

was measured. The total area (μm^2) of F-actin in the synaptopodin positive regions was also measured before normalising to the area of synaptopodin (percentage area of podocytes covered of F-actin).

3.3.15 Statistical analysis

All statistical analyses were performed using GraphPad Prism 9.00 for Mac, GraphPad Software, La Jolla California USA, www.graphpad.com. Normal distribution was assessed by Shapiro-Wilk test. Where data was not normally distributed, values were $\log_{10}$ transformed, and parametric statistical analysis was undertaken on the transformed values. For experiments where two groups were compared, an unpaired t-test was performed. Where 3 treatment groups were assessed, one-way ANOVA with Tukey's multiple comparison tests were used to compare statistical significance between all three groups. For experiments with two variables, two-way ANOVA with Tukey's multiple comparison test was used to compare statistical difference between all values. For data that analysed individual glomeruli (at least 250 glomeruli per group), normal distribution of the data could not be achieved through any transformation. In this case, a Kruskal-Wallis test, the non-parametric equivalent of one-way ANOVA, was performed with Dunn's multiple comparison test to compare statistical significance between all three groups.

3.4 **Results**

3.4.1 Glomerular and podocyte *Tmsb4x* levels in ADR injury

Firstly, the levels of *Tmsb4x* were examined in Dynabead extracted glomeruli from mice injected with ADR by qPCR. There was a tendency for a reduction in glomerular endogenous *Tmsb4x* mRNA after 7 days of 10 mg/kg ADR injection, compared with saline injected mice, however, this was not statistically significant (P=0.072). By 14 days, the level of *Tmsb4x* mRNA had increased compared with 7 days (P=0.104) (**Figure 3.7**).

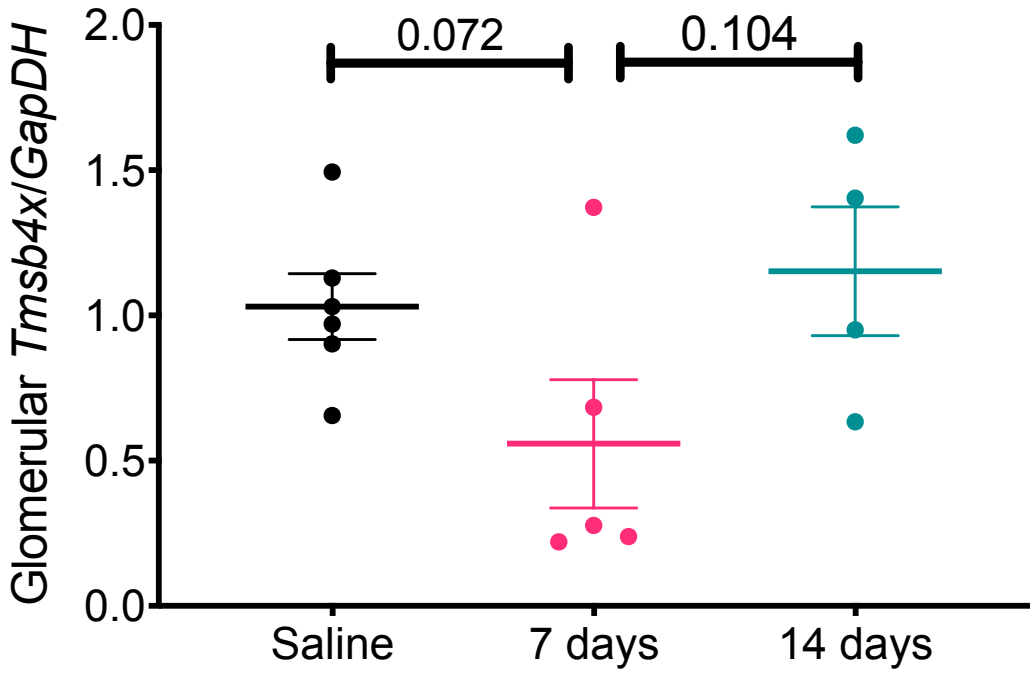

Figure 3.7 – The effect of ADR on glomerular Tmsb4x levels. *Glomeruli were extracted by Dynabead perfusion and cDNA was synthesised from the extracted mRNA. mRNA level examination revealed the expression of glomerular Tmsb4x was altered at 7 days in ADR nephropathy. Gapdh was used as a housekeeping gene. Each data point represents the average of duplicates from the same individual experiment. Data are shown as the mean ±SEM of at least 4 mice in each group. N=5 for saline group, N=5 for 7 days group and N=4 for 14 days group.*

To investigate the expression of *Tmsb4x* in specific glomerular cells following ADR injury, a recently published scRNAseq dataset obtained from glomeruli isolated by Dynabeads of healthy or ADR-injured C57BL/6J mice 14 days after ADR or vehicle administration was analysed (Chung et al. 2020). Using unsupervised clustering analysis, ten transcriptionally distinct cell types were found (**Figure 3.8**) which were identified using established markers of differentiated kidney cell types (Karaiskos et al. 2018) (**Figure 3.9**). All cell types of the glomerulus were present in control and ADR-injured glomeruli (**Figure 3.10a**). This strategy detected a podocyte cluster which expressed both *Nphs1* and *Nphs2*, components of the podocyte SD (**Figure 3.10b**). As previously described (Chung et al. 2020), there was a reduction in the proportion of podocyte cells in the ADR injured glomeruli compared with controls (**Figure 3.11a**). ADR injury was associated with significant downregulation of *Tmsb4x* in the glomerular tuft, assessed by grouped analysis of glomerular endothelial, mesangial and podocyte cells (**Figure 3.11b**; 0.14 log fold change;

P<0.05). When podocyte cells were analysed individually, a larger 0.37 log fold reduction in *Tmsb4x* was observed in those obtained from ADR-injured compared with healthy glomeruli (**Figure 3.11c**; P<0.05).

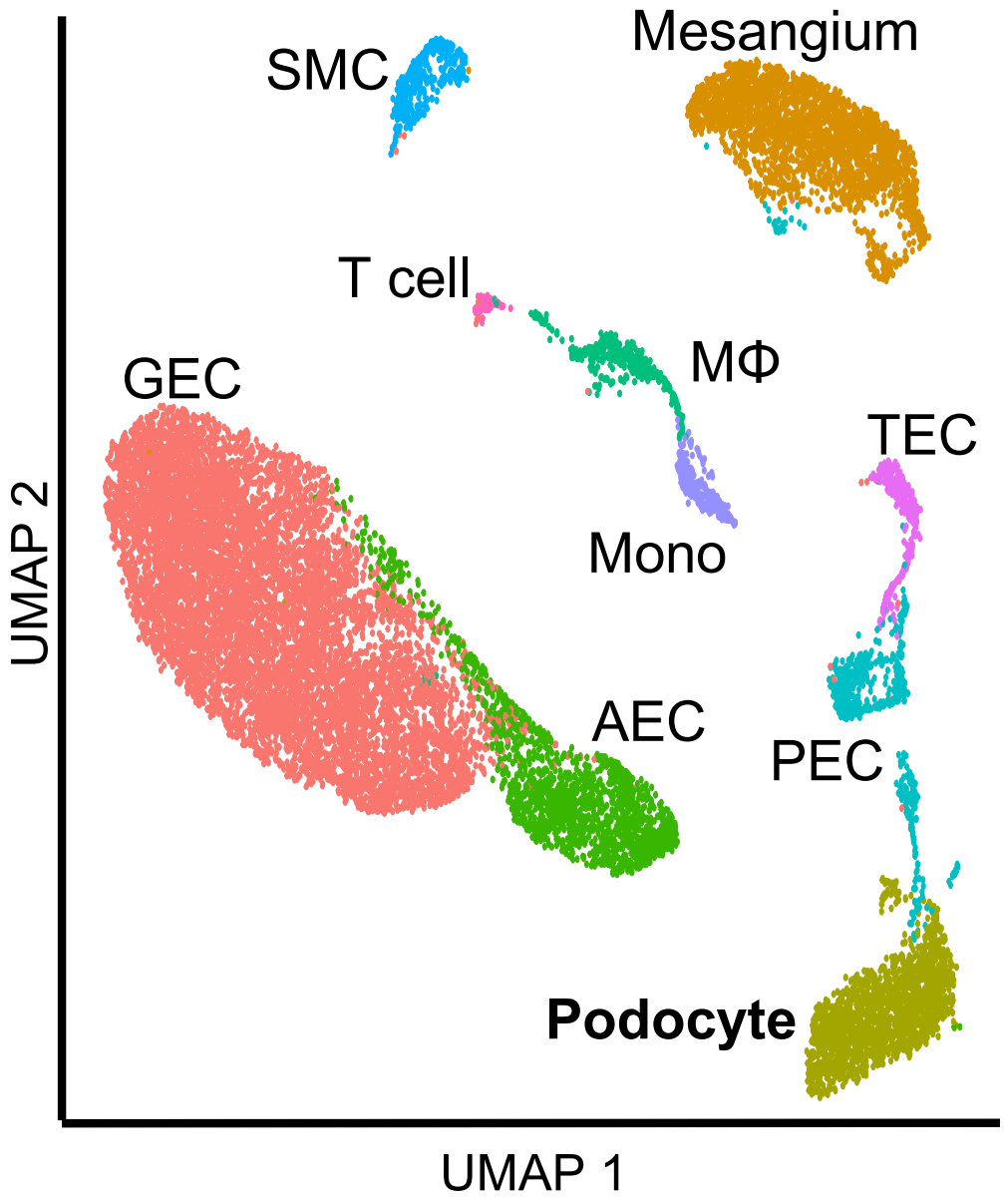

Figure 3.8 - Identification of transcriptionally different cell clusters. (a) *Uniform manifold approximation and projection (UMAP) from single cell RNA sequencing data of 8,412 glomerular cells from two wildtype (control) mice and 8,296 glomerular cells from mice with ADR nephropathy. After analysis and cell type assignment, ten transcriptionally distinct cell populations were discriminated including arterial endothelial cells (AEC), glomerular endothelial cells (GEC), macrophages (MΦ), mesangial cells, monocytes (Mono), parietal epithelial cells (PEC), podocytes, smooth muscle cells (SMC), T cells, tubular epithelial cells (TEC).*

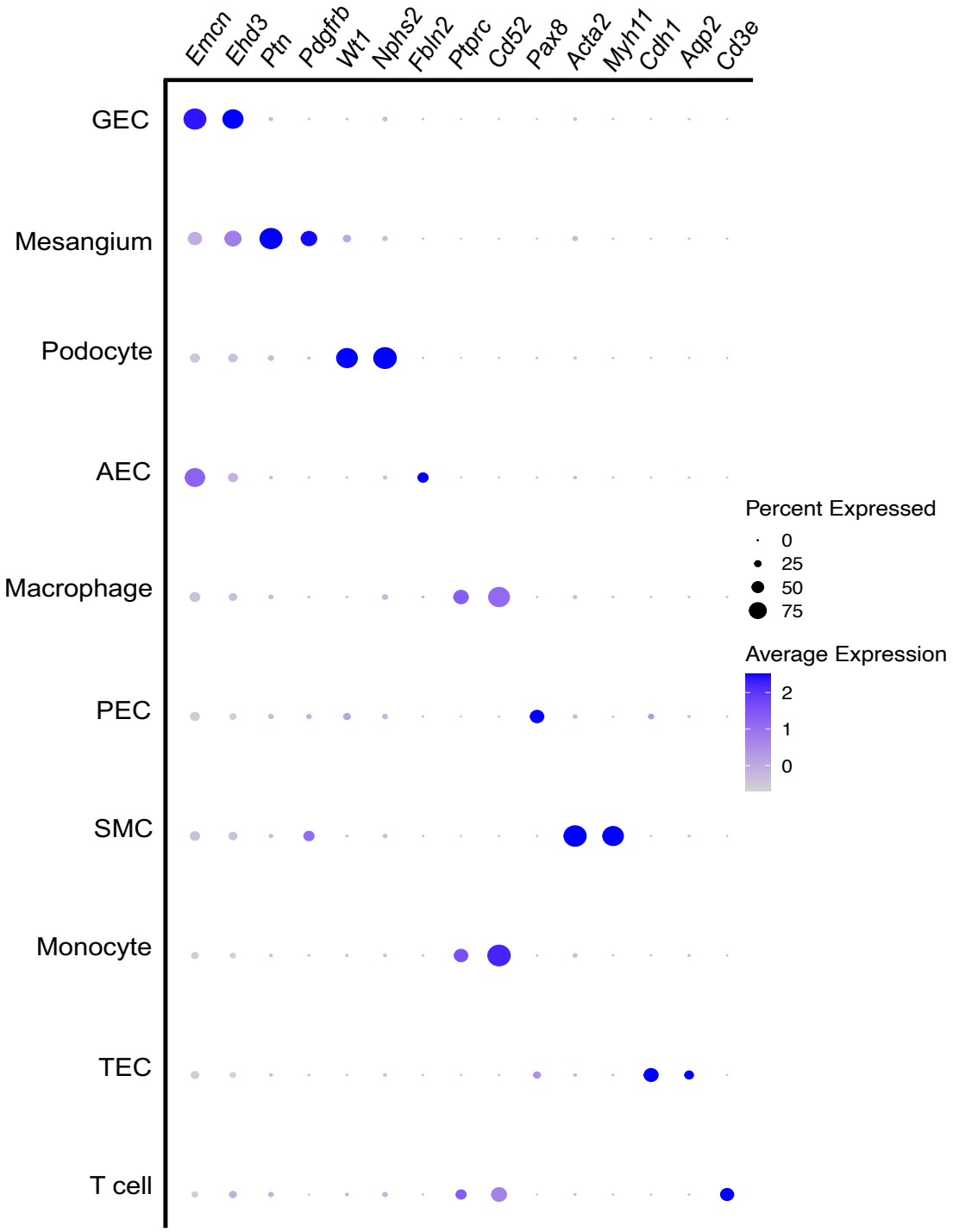

Figure 3.9 – Canonical markers between cell types. *Dotplot showing enrichment of canonical markers between cell types within the single cell RNA sequencing dataset. The markers include endomucin (Emcn) and Eps15 homology domain-containing protein 3 (Edh3) for glomerular endothelial cells (GEC), pleiotrophin (Ptn) and platelet-derived growth factor receptor beta (Pdgfrb) for mesangial cells, Wilms' tumour 1 (Wt1) and podocin (Nphs2) for podocytes, Emcn and fibulin 2 (Fbln2) for arterial endothelial cells (AEC), protein tyrosine phosphatase receptor type C (Ptprc) and campath 1 antigen (Cd52) for monocytes and macrophages, paired box gene 8 (Pax8) for parietal epithelial cells (PEC), actin alpha 2 (Acta2) and myosin heavy chain 11 (Myh11) for smooth muscle cells (SMC), E-cadherin (Cdh1) and aquaporin 2 (Aqp2) for tubular epithelial cells (TEC) and T cell surface glycoprotein CD3 epsilon chain (Cd3e) for T cells.*

Collectively, these findings demonstrate that ADR injury is associated with reduced *Tmsb4x* expression in the glomerulus and specifically in podocytes.

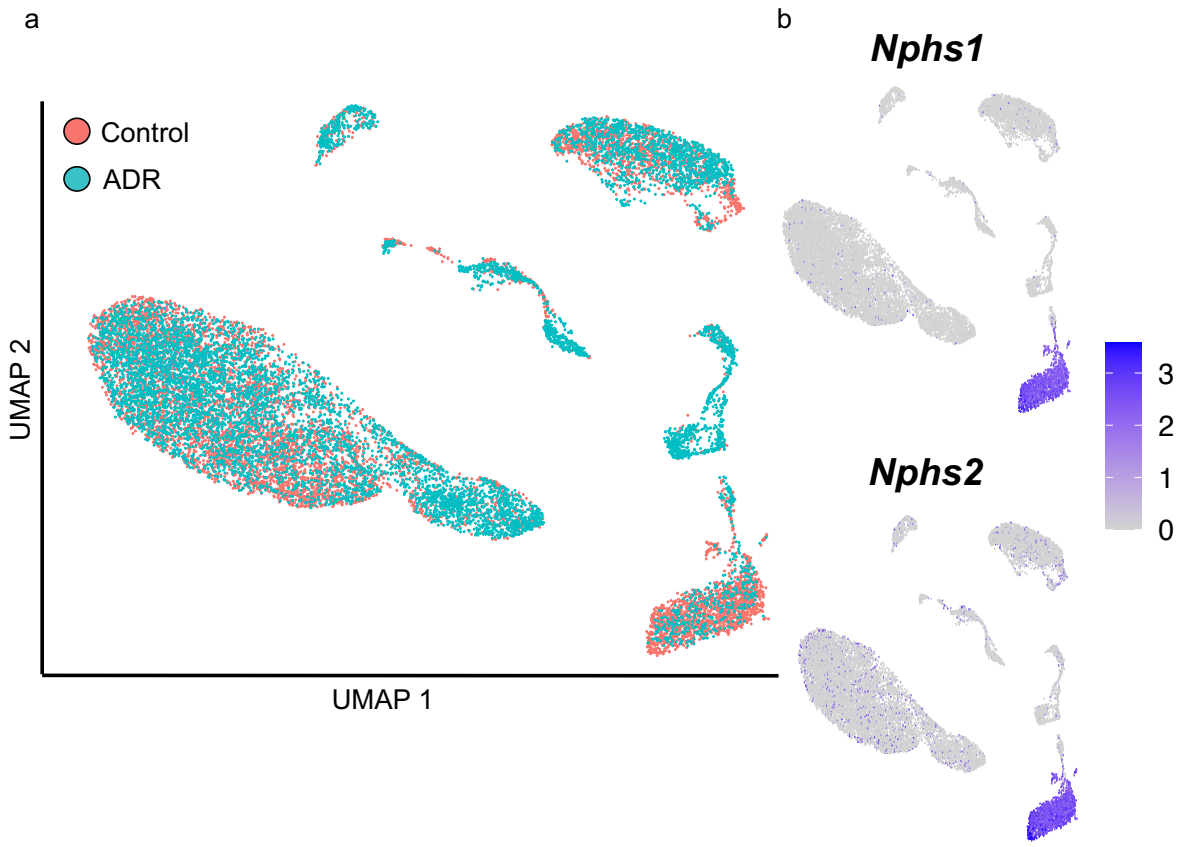

Figure 3.10 – Comparison of cells in healthy glomeruli and in ADR nephropathy and identification of podocytes from Chung et al., 2020. (a) *Uniform manifold approximation and projection (UMAP) grouped by experimental condition in the scRNAseq dataset. The UMAP corresponds to Figure 1A, showing concordance of cell types between ADR and control.* ***(b)*** *Bar graphs comparing the proportions of cell types between ADR and control. In the control dataset, n = 4,402 GECs, n = 1,302 mesangial cells, n = 1,486 podocytes, n = 477 AECs, n = 218 macrophages, n = 143 PECs, n = 118 SMCs, n = 34 monocytes, n = 47 TECs and n = 69 T cells were detected. In the ADR dataset n = 3,895 GECs, n = 1,239 mesangial cells, n = 378 podocytes, n = 1,207 AECs, n = 245 macrophages, n = 505 PECs, n = 290 SMCs, n = 271 monocytes, n = 256 TECs and n = 36 T cells were detected.* ***(b)*** *Feature plots showing expression of nephrin (Nphs1) and podocin (Nphs2), canonical markers of podocytes, across the data set.*

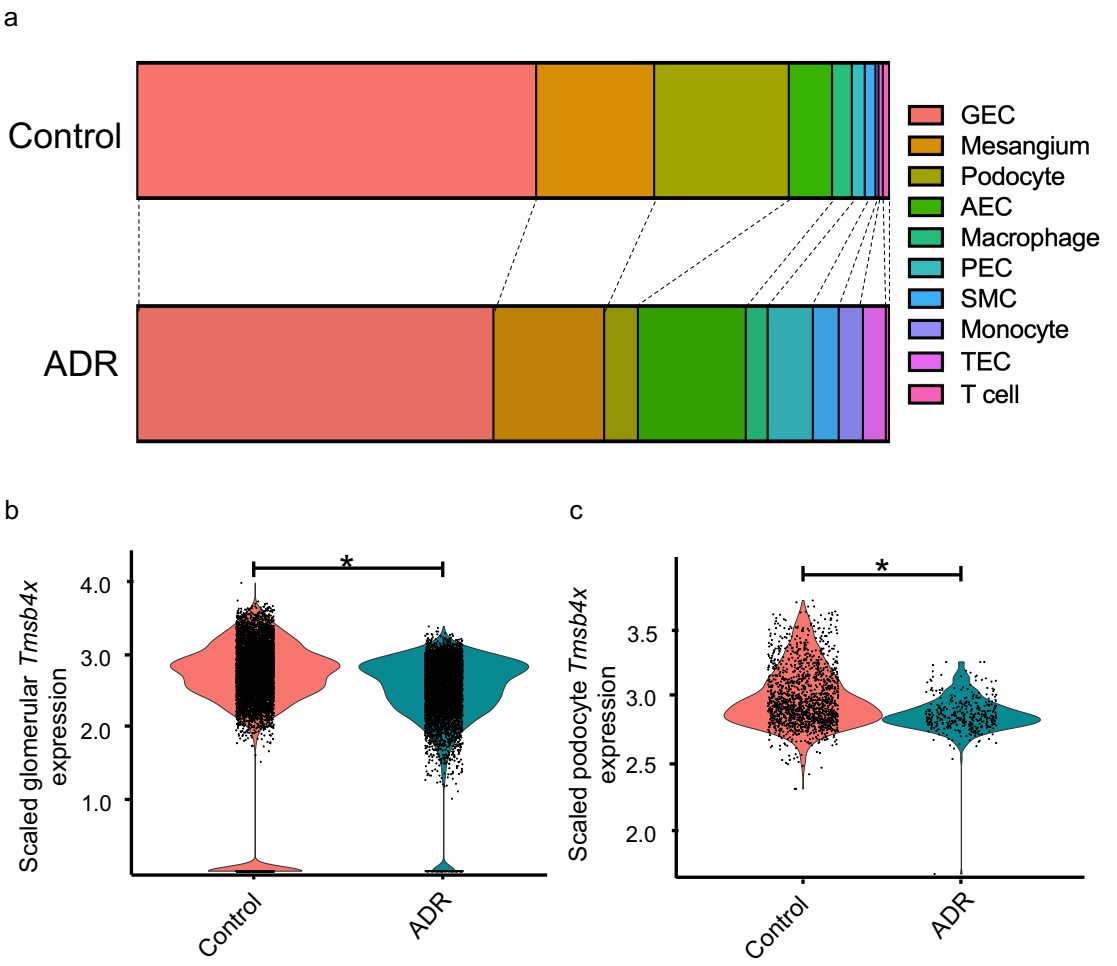

Figure 3.11 – ADR reduced glomerular and podocyte levels of Tmsb4x. ***(a)*** *Bar graphs comparing the proportions of cell types between ADR and control. In the control dataset, n = 4,402 GECs, n = 1,302 mesangial cells, n = 1,486 podocytes, n = 477 AECs, n = 218 macrophages, n = 143 PECs, n = 118 SMCs, n = 34 monocytes, n = 47 TECs and n = 69 T cells were detected. In the ADR dataset n = 3,895 GECs, n = 1,239 mesangial cells, n = 378 podocytes, n = 1,207 AECs, n = 245 macrophages, n = 505 PECs, n = 290 SMCs, n = 271 monocytes, n = 256 TECs and n = 36 T cells were detected.* ***(b)*** *Violin plot comparing the scaled expression of Tmsb4x of all glomerular cells (podocytes, GECs, mesangium) between ADR (n = 5,602 cells) and control (n = 7,190 cells) An average log fold decrease of 0.13 was detected in ADR compared to control (*: adjusted p value < 0.0001).* ***(c)*** *Violin plot comparing the scaled expression of Tmsb4x of podocytes between ADR (n = 378 cells) and control (n = 1,486 cells). An average log fold decrease of 0.36 was detected in ADR compared to control (*: adjusted p value < 0.0001). Each data point represents 1 cell. Data are shown as mean ±SEM.*

3.4.2 AAV.2/7 upregulated TB4 in the circulation in mice with ADR nephropathy

Since the levels of glomerular *Tmsb4x* were decreased in the early stages of ADR nephropathy, it was hypothesised that replenishing the supply of TB4 peptide may alleviate some of the phenotypes of ADR injury. TB4 has a relatively short half-life and plasma concentration returns to basal levels just 6 hours after injection of synthetic TB4 (Mora et al. 1997). Therefore, to induce a persistent upregulation of TB4, mice were treated with AAV.2/7 with a *Tmsb4x* (TB4) transgene, or *LacZ* (β-galactosidase) transgene as a control.

Firstly, to confirm that intravenous AAV.2/7 infected the liver of ADR injured mice, one of the organs that AAV.2/7 displays tissue tropism for (Zincarelli et al. 2008), liver mRNA levels of *Tmsb4x* were assessed by qPCR. There was a 10-fold increase in liver *Tmsb4x* levels in *Tmsb4x*/ADR mice compared to *LacZ*/ADR treated mice 5 weeks after injection of AAV to healthy mice ($P<0.001$) (**Figure 3.12a**), demonstrating efficient transduction of *Tmsb4x* by AAV.2/7. To determine if the system was efficient in producing TB4 peptide, liver FFPE sections were immunostained to visualise TB4 expression. The livers of AAV.*LacZ* treated mice showed low expression of TB4 peptide (**Figure 3.12c, d**) compared to high expression of TB4 peptide in AAV.*Tmsb4x* treated mice livers (**Figure 3.12e**). The antibody was specific for TB4, as determined by the negative control omitting the primary antibody (**Figure 3.12f**).

TB4 is a secreted peptide (Wise et al. 1992), therefore, it was hypothesised that the circulating plasma concentration of TB4 would be increased in AAV.*Tmsb4x* treated mice compared to *LacZ* treated mice. A custom ELISA protocol was designed based on a previously used method (Mora et al. 1997) to determine the concentration of TB4 in the plasma 14 days after ADR/vehicle injection. ADR had no effect on the plasma concentration of TB4, with levels in *LacZ*/saline and *LacZ*/ADR treated mice of 1.2 ± 0.3 ng/ml and 1.9 ± 0.3 ng/ml respectively. *Tmsb4x*/ADR treated mice had a plasma TB4 concentration of 3.4 ± 0.5 ng/ml, which was significantly increased compared with both *LacZ*/saline ($P<0.01$) and *LacZ*/ADR ($P<0.05$) treated mice (**Figure 3.12b**).

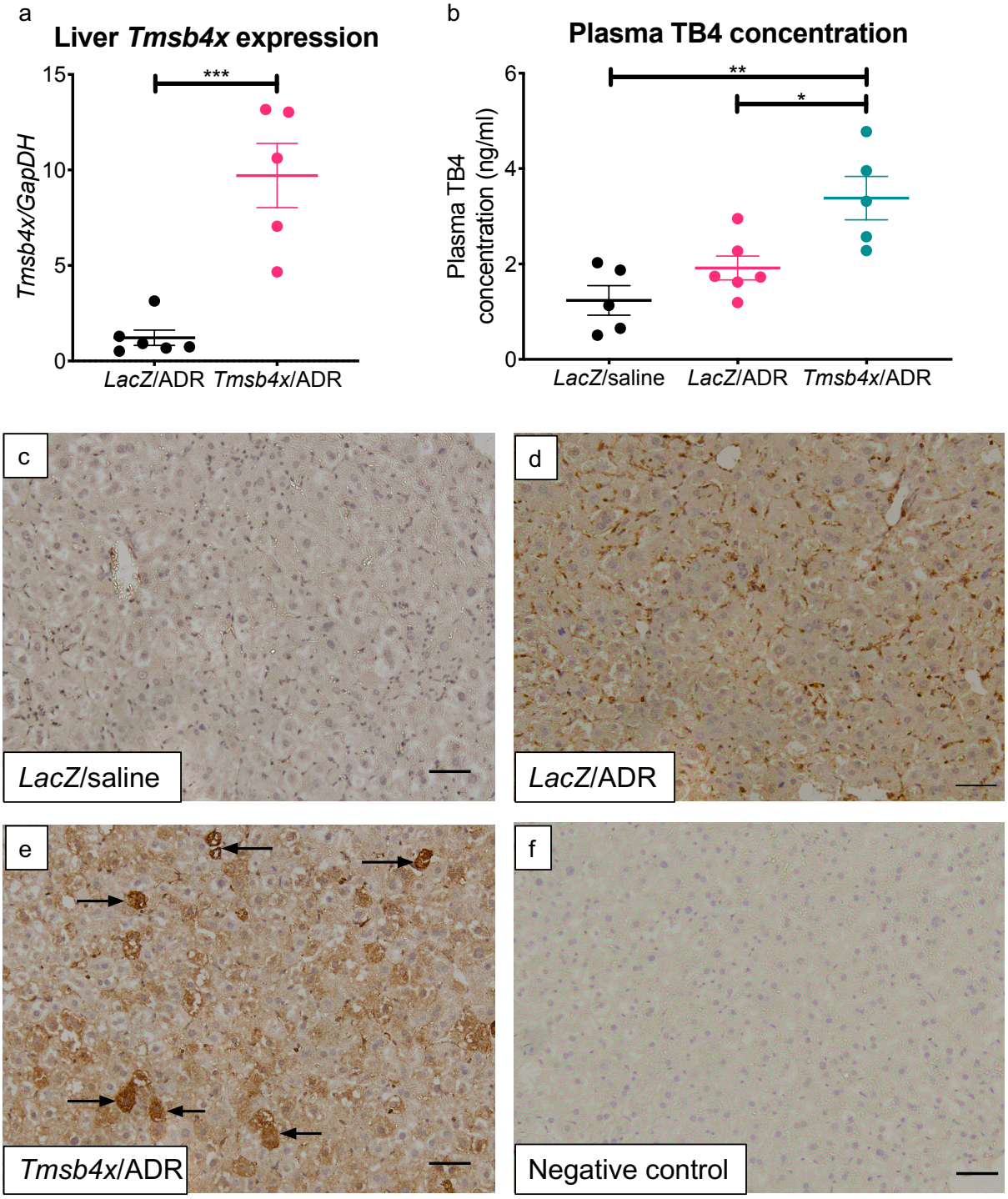

Figure 3.12 – AAV.2/7 upregulated TB4 in circulation of mice with ADR nephropathy. *Mice were injected with AAV.2/7 and 5 weeks later when the mice were culled, the livers were snap frozen on dry ice.* ***(a)*** *mRNA was extracted from the livers and cDNA synthesised before analysis for Tmsb4x by qPCR. Gapdh was used as a housekeeping gene. Each data point represents the average of replicates from individual mouse livers.* ***(b)*** *Blood was harvested by cardiac puncture 5 weeks after AAV injection and plasma TB4 concentration was determined by ELISA. Each data point represents a single experiment with plasma from individual mice. Representative images of FFPE livers immunostained to visualise TB4 from* ***(c)*** *LacZ/saline,* ***(d)*** *LacZ/ADR and* ***(e)*** *Tmsb4x/ADR treated mice.* ***(f)*** *Negative control omitting the primary antibody. Data are shown as the mean ±SEM of at least 5 mice. N=9 in LacZ/saline group, N=6 in LacZ/ADR and N=5 in Tmsb4x/ADR. *P≤0.05, **P≤0.01, ***P≤0.001 between groups.*

3.4.3 ADR altered the kidney mRNA levels of some members of the β-thymosin family

qPCR was performed to determine if ADR with or without TB4 gene therapy affected kidney levels of TB4 and other members of the β-thymosin family transcripts. ADR with or without TB4 gene therapy did not alter the levels of *Tmsb4x* (**Figure 3.13a**), *Tmsb15a* (**Figure 3.13c**) or *Tmsb15l* (**Figure 3.13e**) compared with healthy mice.

ADR induced a 3.5-fold increase in kidney *Tmsb10* expression compared to *LacZ*/saline treated mice ($P<0.001$). The added TB4 suppressed the ADR-induced increase in *Tmsb10* expression ($P<0.05$), however, *Tmsb4x*/ADR mice still showed a significant 2.27-fold increase in kidney *Tmsb10* levels compared with *LacZ*/saline mice ($P<0.01$) (**Figure 3.13b**).

Conversely, ADR caused a tendency for kidney expression of *Tmsb15b* levels to be reduced compared to *LacZ*/saline mice ($P=0.078$, *LacZ*/saline vs *LacZ*/ADR), and *Tmsb4x*/ADR mice showed a 44 ± 5% reduction of *Tmsb15b* compared with *LacZ/*saline treated mice ($P<0.05$) (**Figure 3.13d**).

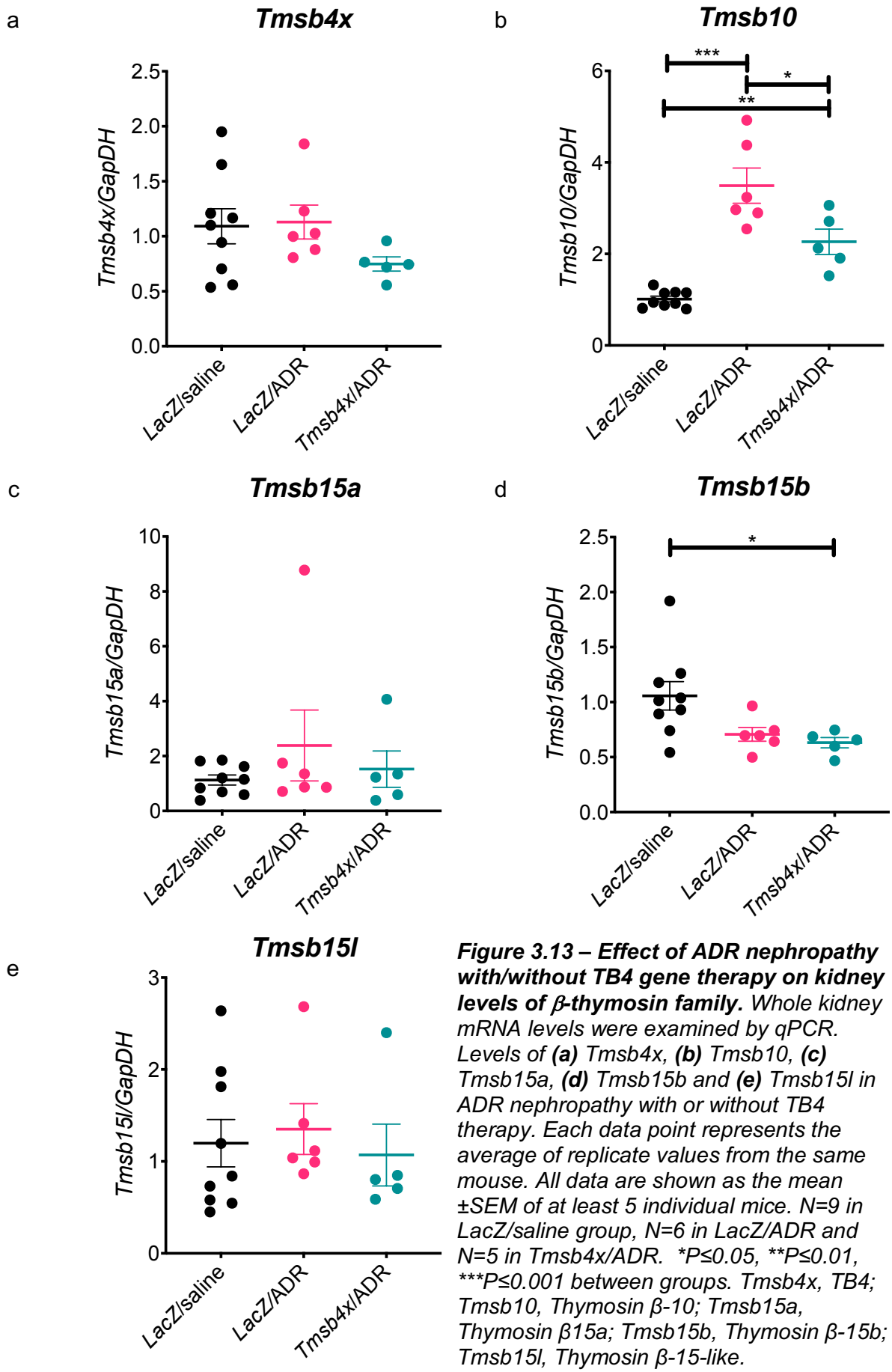

Figure 3.13 – Effect of ADR nephropathy with/without TB4 gene therapy on kidney levels of β-thymosin family. *Whole kidney mRNA levels were examined by qPCR. Levels of* ***(a)*** *Tmsb4x,* ***(b)*** *Tmsb10,* ***(c)*** *Tmsb15a,* ***(d)*** *Tmsb15b and* ***(e)*** *Tmsb15l in ADR nephropathy with or without TB4 therapy. Each data point represents the average of replicate values from the same mouse. All data are shown as the mean ±SEM of at least 5 individual mice. N=9 in LacZ/saline group, N=6 in LacZ/ADR and N=5 in Tmsb4x/ADR. *P≤0.05, **P≤0.01, ***P≤0.001 between groups. Tmsb4x, TB4; Tmsb10, Thymosin β-10; Tmsb15a, Thymosin β15a; Tmsb15b, Thymosin β-15b; Tmsb15l, Thymosin β-15-like.*

3.4.4 TB4 was expressed in glomeruli and podocytes in all three mouse groups

To assess the expression of TB4 in healthy BALB/c mice and ADR injured BALB/c mice with or without TB4 gene therapy, 8 μm cryosections were prepared and immunostained with α-TB4 antibody (**Table 3.1**) and fluorescent secondary antibody (**Table 3.2**). Co-localisation with synaptopodin was used to evaluate podocyte TB4 expression.

The expression of synaptopodin was consistent between healthy mice and mice with ADR nephropathy with and without TB4 gene therapy. Synaptopodin covered large proportions of the glomeruli in patterns which were consistent with podocyte cell bodies and processes. This stable synaptopodin expression between the groups allowed TB4 expressed to be examined in podocytes and non-podocyte areas of the glomeruli (**Figure 3.14a, b, c**).

TB4 was expressed in the podocyte cell bodies (white arrows) and podocyte processes (white arrowheads) of the glomeruli in healthy mice. TB4 was also expressed in non-podocyte areas, which could either be mesangial cells or glomerular capillary endothelial cells (black and white arrowheads) in healthy mice. TB4 was also expressed in podocytes and glomeruli in ADR-injured mice with and without TB4 gene therapy (**Figure 3.14a, b, c**). Antibody specificity was confirmed by the negative controls omitting the primary antibodies (**Figure 3.14d**).

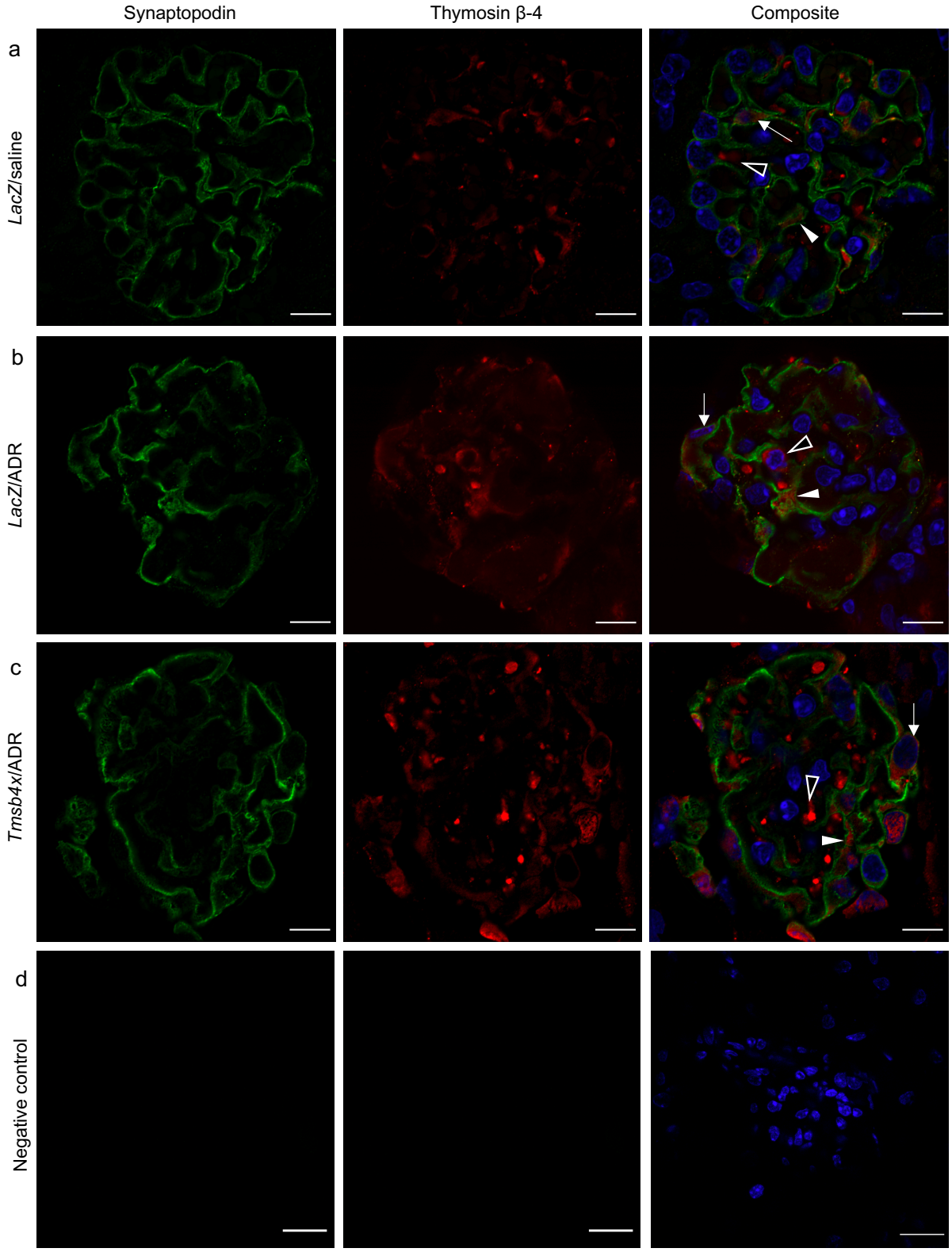

Figure 3.14 - Kidney TB4 expression in ADR nephropathy with or without TB4 gene therapy. *Cryosections were stained with antibodies to label synaptopodin and TB4. TB4 was expressed in glomeruli and podocytes of mice in the* ***(a)*** *LacZ/saline,* ***(b)*** *LacZ/ADR and* ***(c)*** *Tmsb4x/ADR groups.* ***(d)*** *Negative control omitting primary antibody. Scale bar = 20 µm.*

3.4.5 Mouse body and kidney weights were reduced after ADR and TB4 treatment

Body weight is an indicator of general well-being and a decrease in body weight is indicative of poor health (Ullman-Culleré and Foltz 1999). Healthy mice and mice exposed to ADR with and without TB4 gene therapy were weighed on the day of ADR/vehicle injection, 2, 7 and 14 days later. There was no statistical difference between body weights on the day of ADR/vehicle administration (**Figure 3.15b**).

LacZ/saline treated mice lost 1.4 ± 0.4% of body weight after 2 days compared with day 0 of vehicle administration. However, this steadily increased back to baseline 7 days after ADR/vehicle injection and further increased by another 2.7 ± 0.7% at 14 days. In mice with ADR nephropathy without TB4 gene therapy, the weight loss at 2 days was exacerbated, and mice lost 4.5 ± 0.3% of body weight compared to the day of ADR administration, which was significantly lower compared with *LacZ*/saline mice ($P<0.001$). This weight loss was sustained at 3.7 ± 0.5% and 3.2 ± 0.7% below their weight at day 0 at both 7 days ($P<0.01$ vs *LacZ*/saline) and 14 days after ADR injection respectively ($P<0.001$ vs *LacZ*/saline). ADR treated mice with TB4 therapy experienced a similar pattern of weight loss to ADR-only mice, as there was no significant difference between these two groups at any time point. The *Tmsb4x*/ADR group lost 4.9 ± 0.6% of body weight 2 days after ADR injection ($P<0.01$ vs *LacZ*/saline). The weight loss persisted, and mice weighed 2.5 ± 0.4% less and 1.8 ± 1.1% less at 7 and 14 days respectively ($P<0.05$ in both cases vs *LacZ*/saline) compared with their weights on the day of ADR administration (**Figure 3.15a**).

The left kidneys were weighed and normalised to body weight 14 days after ADR/vehicle administration. Mice treated with *LacZ*/saline had a kidney weight of 0.306 ±0.02g, which was 0.011 ±0.001 grams per gram of body weight. Administration of ADR without TB4 gene therapy slightly, but not significantly reduced these values, as their kidney weight was 0.25 ±0.01 g and 0.01 grams per gram of body weight. ADR administration with TB4 gene therapy significantly reduced both kidney weight (0.23 ±0.02 g) and kidney weight to body weight ratio (0.009 ±0.001 g/g) compared with *LacZ*/saline treated mice ($P<0.05$ in both cases) (**Figure 3.15c, d**).

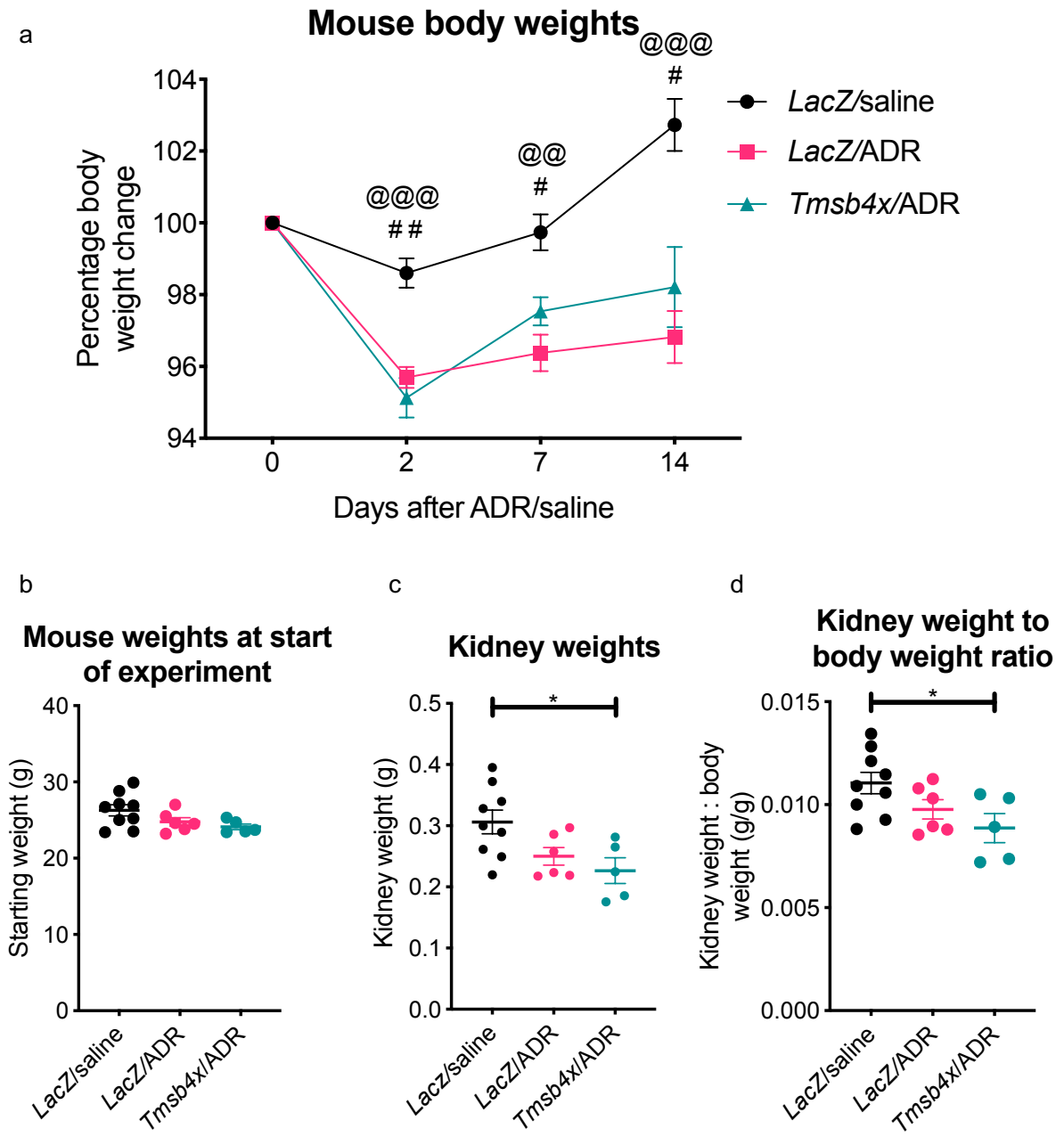

Figure 3.15 – Body weights of ADR-injured mice with or without TB4 gene therapy at day 0, 2, 7 and 14 days after ADR/vehicle injection and kidney weights at 14 days after ADR/vehicle administration. (a) *Mice were weighed at day 0, 2, 7 and 14 after ADR/vehicle administration. Statistical annotations using @ refer to comparison between LacZ/saline and LacZ/ADR. Statistical annotations using # refer to comparison between LacZ/saline and Tmsb4x/ADR* ***(b)*** *Mouse weights at day 0.* ***(c)*** *Left kidney weight and* ***(d)*** *kidney weight to body weight ratio 14 days after ADR/vehicle administration. Each data point represents 1 mouse. All data are shown as the mean ±SEM of at least 5 individual mice. N=9 in LacZ/saline group, N=6 in LacZ/ADR and N=5 in Tmsb4x/ADR. *P≤0.05, **P≤0.01, ***P≤0.001 between groups.*

3.4.6 Urine excretion 2 and 14 days after administration of ADR

To determine if any changes to urine excretion were occurring following ADR administration with or without TB4 gene therapy, the urine volumes were measured at day 0, 2 and 14 by using metabolic cages. *LacZ*/saline treated mice excreted 500 ± 126 μl of urine/24 hours on the day of vehicle administration. Addition of ADR caused mice to urinate 255 ± 90 μl/24 hours without TB4 gene therapy, and 324 ± 85 μl/24 hours with TB4 gene therapy on the day of ADR administration. At day 2 of vehicle exposure, mice treated with saline urinated 687 ± 96 μl/24 hours. Mice treated injected with ADR without TB4 gene therapy urinated 637 ± 101 μl/24 hours of urine 2 days after ADR exposure, which was unchanged after addition of TB4 (872 ± 107 μl of urine/24 hours). At 14 days, mice injected with *LacZ*/saline excreted 657 ± 93 μl of urine/24 hours. Addition of ADR with or without TB4 gene therapy did not change urine excretion, as each group urinated 756 ± 87 μl/24 hours and 804 ± 105 μl/24 hours. There were no significant differences between any groups at any time point measured (**Figure 3.16**).

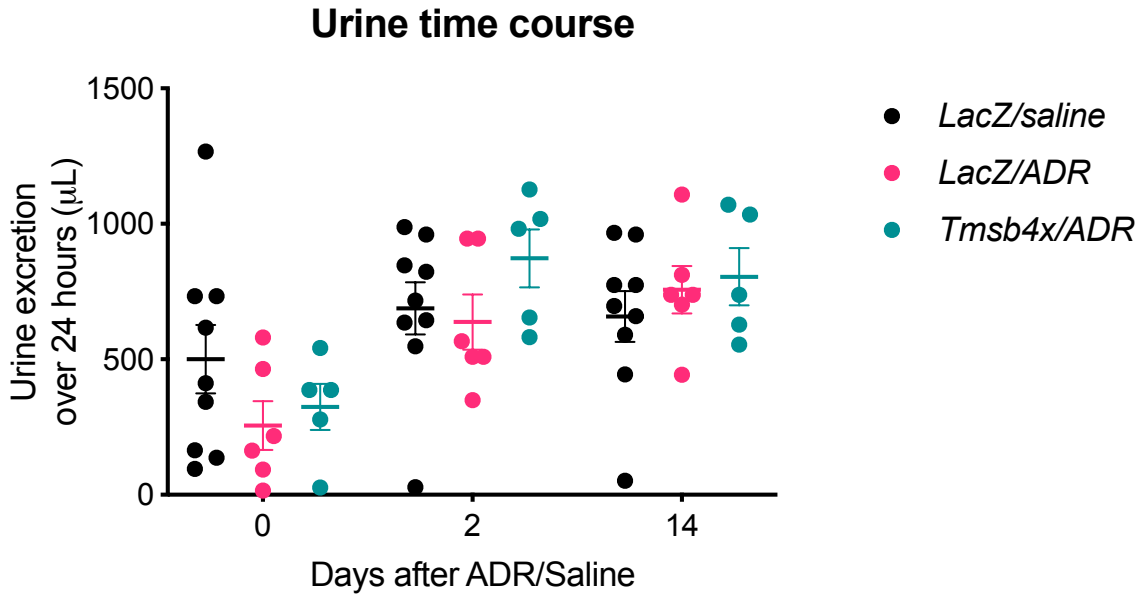

Figure 3.16 – Urine excretion at 2- and 14-days post-ADR injection. *Urine was collected overnight in metabolic cages at day 0, 2 and 14 after ADR/vehicle injection and values were extrapolated to 24 hours. Each data point represents 1 mouse. Data are shown as mean ±SEM of at least 5 individual mice. N=9 in LacZ/saline group, N=6 in LacZ/ADR and N=5 in Tmsb4x/ADR.*

3.4.7 Exogenous TB4 prevented ADR-induced albuminuria, but there were no alterations to BUN

Albumin cannot pass through the glomerular filtration barrier in the healthy kidney. Therefore, an increase in the amount of urinary albumin is a hallmark of damage to the glomerular filtration barrier (Suh and Miner 2013). ELISA was undertaken to examine albuminuria after ADR with and without TB4 gene therapy (3.3.6).

Prior to either ADR or vehicle injection, *LacZ*/saline mice excreted 94.7 ± 16 μg of albumin/24 hours, *LacZ*/ADR mice excreted 41 ±16 μg/24 hours and *Tmsb4x*/ADR treated mice 60 ± 31 μg/24 hours. There was no significant difference between the groups. Two days following the injection of ADR or vehicle, there were no significant differences in urinary albumin concentration between any group. *LacZ*/saline mice excreted 103 μg/ml ± 20 μg/24 hours, *LacZ*/ADR mice 65 ± 10 μg/24 hours and *Tmsb4x*/ADR treated mice 73 ± 7 μg/24 hours. Fourteen days after either ADR or vehicle injection the *LacZ*/saline mice urinary albumin value was 107 ± 21 μg/24 hours. The albuminuria values of the *LacZ*/ADR treated mice were to 1448 ± 115 μg/24 hours, which was significantly more than *LacZ*/ADR treated mice ($P<0.001$). TB4 gene therapy prevented the increase in urinary albumin excretion, with an albuminuria value of 214 ± 43 μg/24 hours ($P<0.01$ vs *LacZ*/ADR), providing evidence that TB4 prevented albumin excretion (**Figure 3.17a**).

The albumin to creatinine ratio (ACR) was examined 14 days after ADR or vehicle injection to normalise albuminuria to mouse body weight. *LacZ*/saline treated mice had an ACR of 153 ± 18.2 μg/mg. ADR administration without TB4 gene therapy caused an ACR of 2473 ± 229 μg/mg, which was significantly more than *LacZ*/saline treated mice ($P<0.001$). TB4 gene therapy prevented the ADR induced increase in ACR, as mice had an ACR of 249 ± 37 μg/mg ($P<0.001$) (**Figure 3.17b**).

BUN is a measure of circulating plasma urea concentration and was measured by colourimetric assay 14 days after ADR or vehicle injection. *LacZ*/saline treated mice had a BUN concentration of 32.1 ± 6.8 mg/DL. Mice treated with ADR

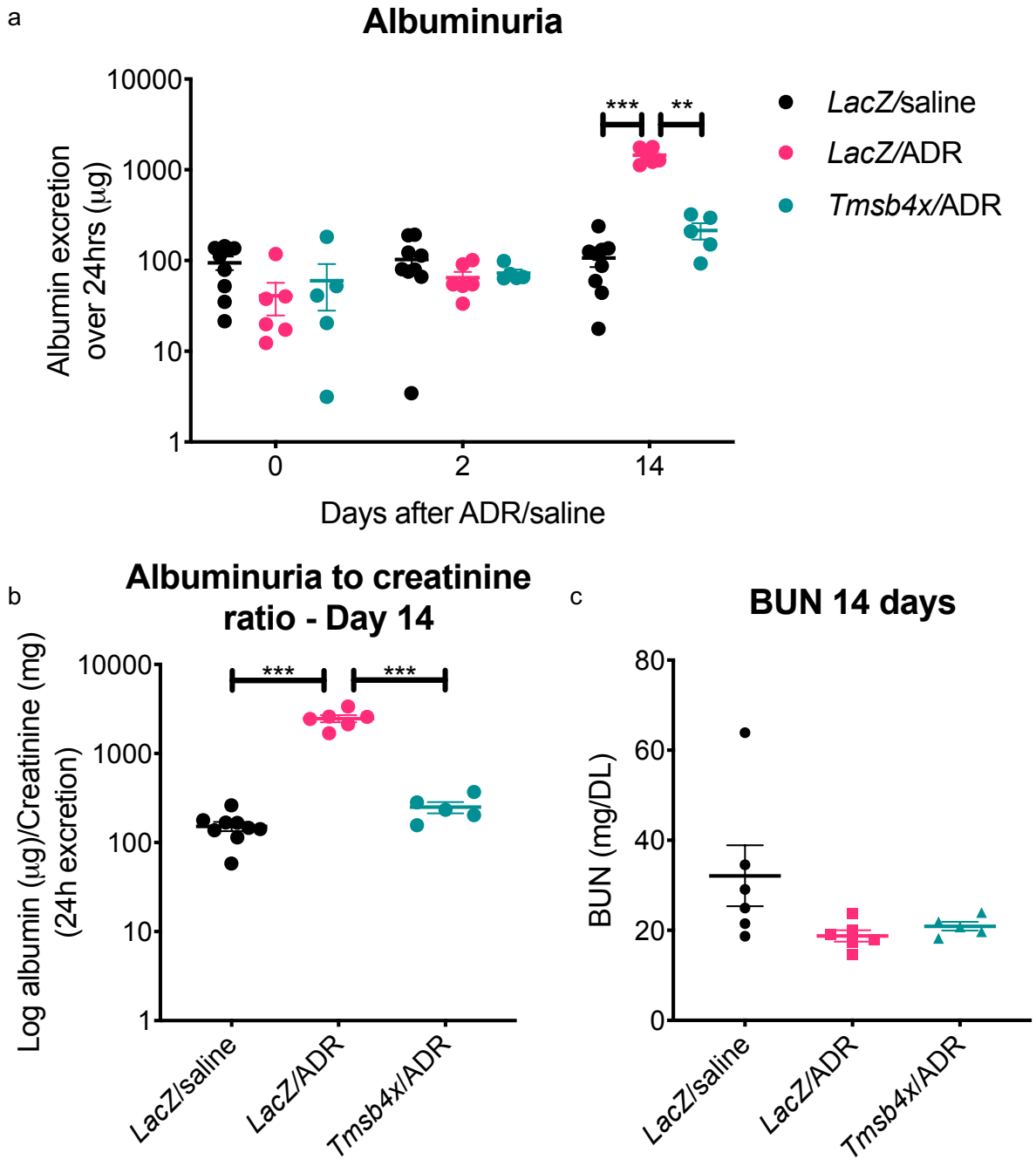

Figure 3.17 – TB4 prevents ADR-induced albuminuria, but there were no changes to BUN. *Urine was collected overnight in metabolic cages and urinary albumin concentration was determined at baseline, 48 hours and 14 days post saline/ADR injection by ELISA.* ***(a)*** *Quantification of urinary albumin concentration. Urine creatinine concentration was determined by colourimetric assay and then the* ***(b)*** *urinary albumin (µg) to urinary creatinine (mg) ratio was determined at 14 days. BUN was assessed by colourimetric assay of the plasma at 14 days and* ***(c)*** *quantified. Each data point represents the average of replicate values from a single mouse. Data are shown as the mean ±SEM of at least 5 mice. N=9 in LacZ/saline group, N=6 in LacZ/ADR group and N=5 in Tmsb4x/ADR group. **P≤0.01, ***P≤0.001 between groups.*

without TB4 gene therapy had a BUN concentration of 18.8 ± 1.2 mg/DL and addition of TB4 gene therapy did not change BUN concentration (20.9 ± 1 mg/DL). There were no significant differences between any groups (**Figure 3.17c**).

3.4.8 ADR did not cause glomerular inflammation

One of the major properties of TB4 is its anti-inflammatory action (Vasilopoulou et al. 2016, 2018). Therefore, it was postulated that if inflammation was occurring in this model of ADR injury that contributed to glomerular injury, the mechanism by which TB4 may protect the glomerulus could be due to suppression of inflammation. To examine this, kidney FFPE sections were stained with α-mouse F4/80 antibody.

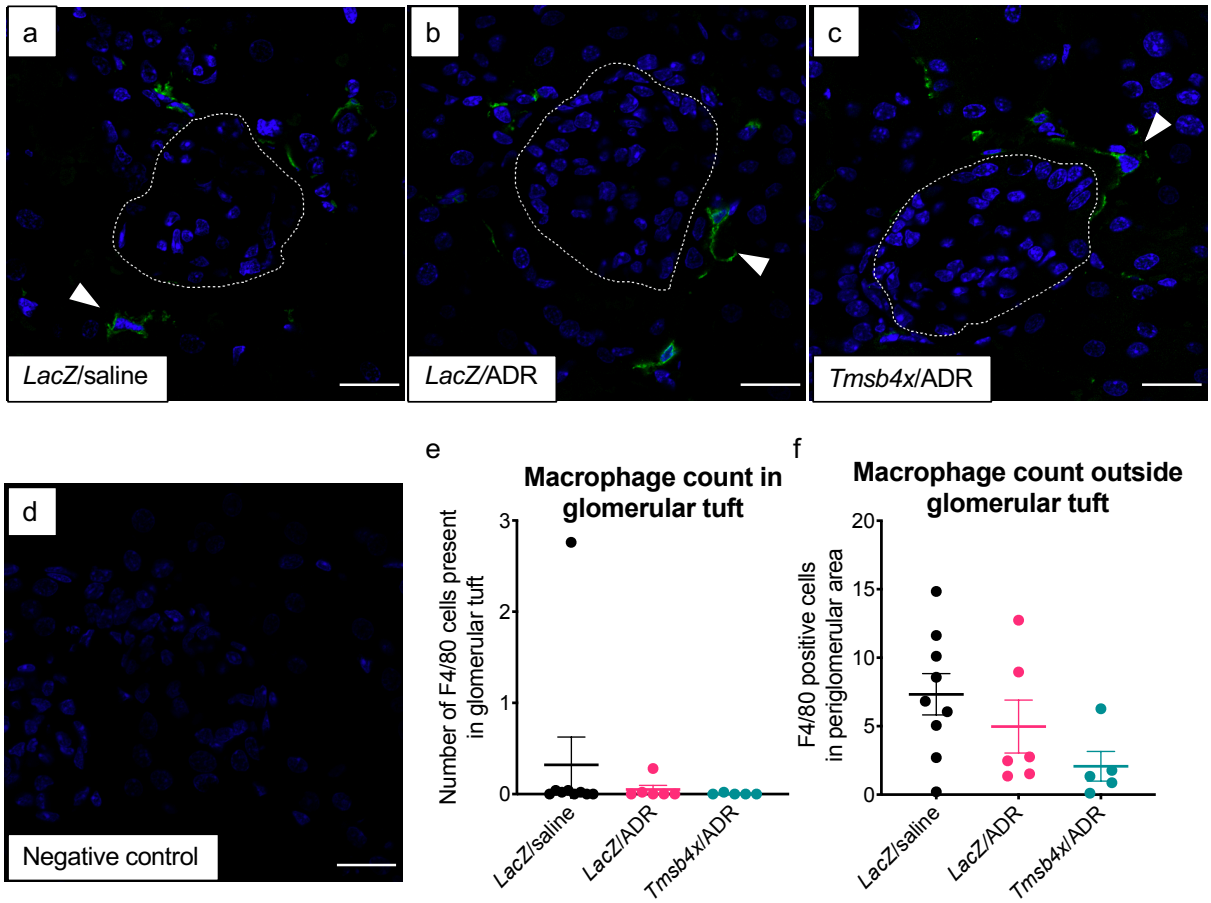

Figure 3.18 – ADR did not induce an immune response at 14 days. *FFPE kidneys were cut into 5 µm sections and incubated with a rat anti-mouse F4/80 primary antibody followed by a goat anti-rat secondary antibody conjugated to 488 nm fluorophore. Representative images of* ***(a)*** *LacZ/saline,* ***(b)*** *LacZ/ADR and* ***(c)*** *Tmsb4x/ADR treated glomeruli.* ***(d)*** *Negative control omitting the primary antibody. Arrowheads indicate positive F4/80 staining. White dashed line indicates glomerular tuft. Scale bar = 20 µm. F4/80 positive cells were counted* ***(e)*** *in the glomerular tuft and* ***(f)*** *outside the glomerular tuft. Each data point represents the average of 50 glomeruli from each mouse. Data are shown as the mean ±SEM of at least 5 mice. N=9 in LacZ/saline group, N=6 in LacZ/ADR group and N=5 in Tmsb4x/ADR group.*

Representative images are presented in **Figure 3.18a, b, c,** with antibody specificity confirmed by omitting the primary antibody (**Figure 3.18d**). ADR administration with and without TB4 gene therapy did not induce a glomerular immune response, as there were no significant alterations to macrophage numbers inside or outside the glomerular tuft compared with *LacZ*/saline treated mice. (**Figure 3.18e, f**). Therefore, it can be concluded that inflammation was unlikely to be contributing to glomerular damage in this mouse model.

3.4.9 TB4 prevented ADR-induced podocyte loss

To count the number of podocytes per glomerulus, mouse kidney sections were immunostained using α-WT-1 antibody, which is specifically expressed in podocyte nuclei in the adult glomerulus (Lefebvre et al. 2015). Representative images of WT-1 immunostaining from all three treatment groups can be found in **Figure 3.19a, b, c**, and antibody specificity was confirmed by omitting the primary antibody (**Figure 3.19d**).

Firstly, the area of each glomerular cross section was measured. The average area of *LacZ*/saline treated glomerular cross sections was 2658 ± 54 μm^2. Administration of ADR lead to an increase of glomerular cross section area to 3846 ± 92 μm^2, which was significantly larger than *LacZ*/saline treated mice ($P<0.001$). Treatment with exogenous TB4 dampened the ADR-induced increased in glomerular cross section, as the average glomerular cross section was 3278 ± 95 μm^2. This value was significantly smaller than the *LacZ*/ADR treated mice ($P<0.001$), but significantly larger than the *LacZ*/saline treated mice glomeruli ($P<0.001$), showing that exogenous TB4 dampened the ADR-induced increase in glomerular cross section (**Figure 3.19j**).

Next, the number of WT-1 positive cells were counted per glomerulus. Fourteen days after injection of either ADR or vehicle, *LacZ*/saline treated mice had 10.9 ± 1 podocytes per glomerular cross section. There was a reduction with ADR treatment, where each mouse showed on average 8.9 ± 1.6 podocytes per glomerular cross section, but this reduction was not significant compared to *LacZ*/saline treated mice. *Tmsb4x*/ADR treated mice had an average of 10.4 ± 1.4 podocytes on each

glomerular cross section (**Figure 3.19e**). Since ADR with and without TB4 gene therapy altered the glomerular cross-sectional area, the number of WT-1 positive cells were normalised to glomerular area (podocyte density). *LacZ*/saline treated mice had a podocyte density of 6.6 $x10^{-3}$ ± 0.3 $x10^{-3}$ podocytes/μm^2. Again, the average podocyte density of *LacZ*/ADR treated mice was reduced to 5.3 $x10^{-3}$ ± 1 $x10^{-3}$ podocytes/μm^2, however not statistically significant compared to *LacZ*/saline treated mice. Mice treated with *Tmsb4x*/ADR showed an average podocyte density of 6.6 $x10^{-3}$ ± 0.8 $x10^{-3}$ podocytes/μm^2 (**Figure 3.19f**), but this was not significantly different to *LacZ*/saline or *LacZ*/ADR treated mice.

ADR is a rodent model of FSGS (Chen et al. 1998), which is defined as scarring to a part of (segmental) some, but not all (focal) glomeruli in the kidney, meaning that some glomeruli will be more damaged than others within the same individual mouse (Jefferson and Shankland 2014). It was postulated that the healthier glomeruli may be "masking" the more damaged glomeruli when the average of 50 glomeruli was calculated in each mouse, therefore, individual glomeruli from each group were examined. A separate analysis using each individual glomerulus from each group was performed.

When glomeruli were analysed as individual values 14 days after ADR or vehicle injection, ADR nephropathy without TB4 gene therapy reduced the average number of WT-1 positive cells in the glomerular tuft and podocyte density count compared with *LacZ*/saline treated mice ($P<0.001$ in both data sets). Mice treated with ADR and TB4 gene therapy prevented the reduction in podocyte number and density compared with ADR without TB4 gene therapy ($P<0.001$ in both data sets) (**Figure 3.19g, h**).

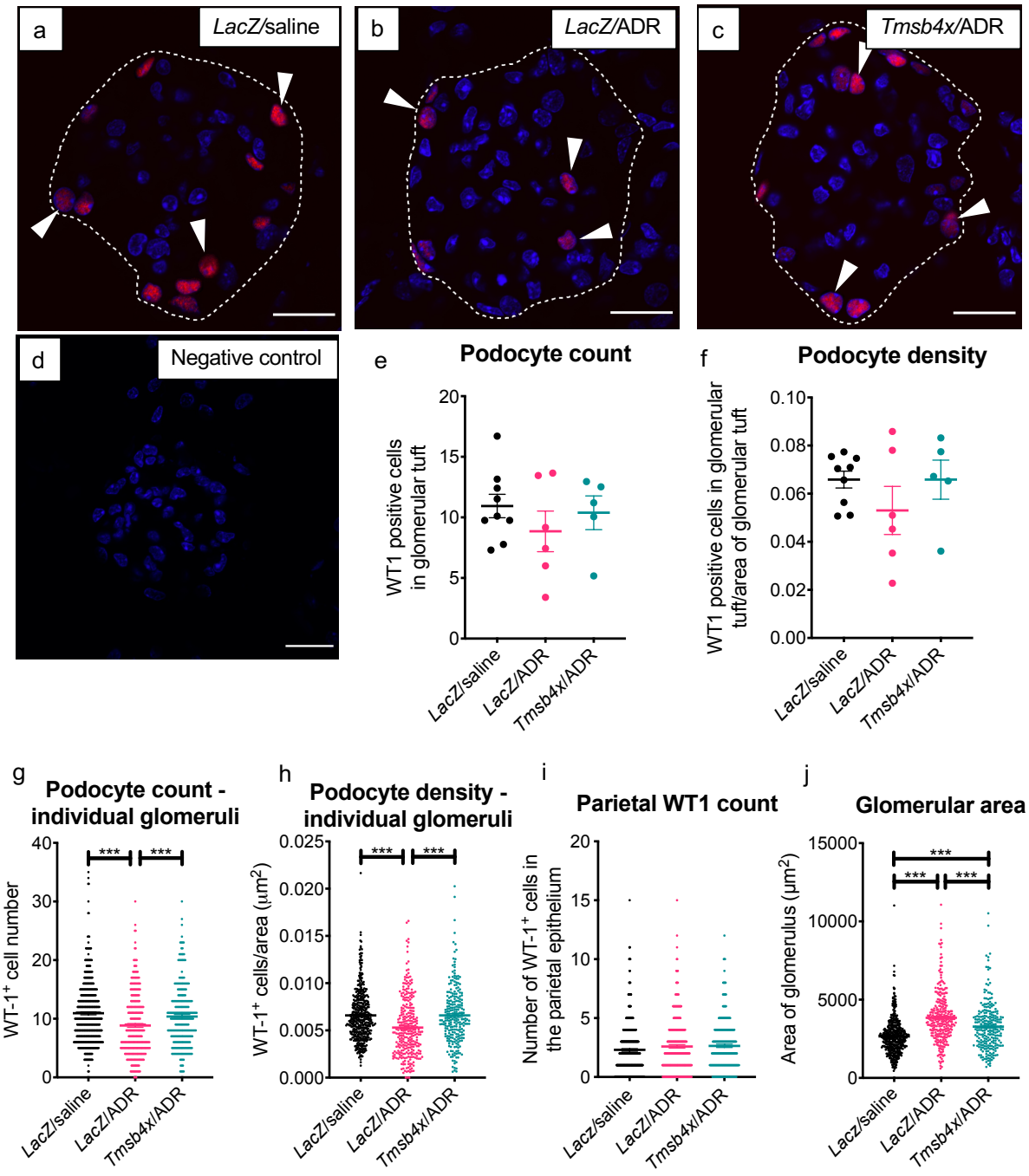

Figure 3.19 – Exogenous TB4 prevents ADR-induced podocyte loss. *FFPE kidneys were incubated with a rabbit anti-mouse WT-1 primary antibody followed by donkey anti-rabbit conjugated to 594 nm fluorophore (ThermoFisher). Representative images of* ***(a)*** *LacZ/saline,* ***(b)*** *LacZ/ADR and* ***(c)*** *Tmsb4x/ADR glomeruli. Arrowheads indicate positive WT-1 staining. White dashed line indicates glomerular tuft boundary.* ***(d)*** *Negative control omitting primary antibody. Scale bar = 20 µm. WT-1 positive cells were* ***(e)*** *counted inside the glomerular tuft and* ***(f)*** *normalised to the glomerular tuft area (podocyte density). Each data point represents the average of 50 glomeruli from each individual mouse. Data are presented as the mean ±SEM of 5 individual mice. N=9 for LacZ/saline group, N=6 for LacZ/ADR group, N=5 for Tmsb4x/ADR group.* ***(g)*** *Podocyte count and* ***(h)*** *and podocyte density,* ***(i)*** *WT-1 positive nuclei outside the glomerular tuft and* ***(j)*** *glomerular cross-sectional area were plotted as individual data points. Data are presented as the mean ±SEM of at least 250 individual glomeruli. N=450 for LacZ/saline group, N=300 for LacZ/ADR group, N=250 for Tmsb4x/ADR group. *P≤0.05, ***P≤0.001 between groups.*

The number of WT-1 positive cells were counted in the parietal epithelium and analysed per individual glomerulus. There were 2.3 ± 0.1 WT-1 positive cells in the parietal epithelium in *LacZ*/saline treated mice. Treatment of mice with ADR without TB4 gene therapy did not alter parietal WT-1 count compared to *LacZ*/saline treated mice, as each glomerulus had on average 2.6 ± 0.3 WT-1 positive cells outside glomerular tuft. Treatment with ADR and TB4 gene therapy did not alter parietal WT-1 count compared to *LacZ*/saline treated mice, as each glomerulus had on average 2.6 ± 0.2 WT-1 positive cells outside glomerular tuft (**Figure 3.19i**).

3.4.10 ADR or TB4 did not alter podocyte distribution

Podocyte clustering has been observed in animal models of kidney injury, where podocytes appeared to cluster together prior to migration towards the parietal epithelium in response to stress (Burford et al. 2014; Hackl et al. 2013). Therefore, the WT-1 immunostained images were used to investigate if podocytes were clustering in the ADR model of glomerular injury (3.3.14). Only images where visible vascular and tubular poles of the glomeruli were used. It was hypothesised that podocytes in a healthy glomerulus would be evenly distributed throughout the glomerulus, with approximately 25% of the total podocyte number located in each quadrant of the glomerulus and that alterations to their distribution could suggest further podocyte injury.

Podocyte clustering was defined as more than 50% of all podocytes occupying 25% of total glomerular space, as it was thought that this would be a sufficient threshold to define podocyte clustering. A representative image of a glomerulus displaying podocyte clustering is provided in **Figure 3.20a**. *LacZ*/saline treated mice had on average 12.1 ± 3% of glomeruli displaying podocyte clustering. Treatment with ADR without TB4 gene therapy slightly increased this value to 21.2 ± 5.1%, but this

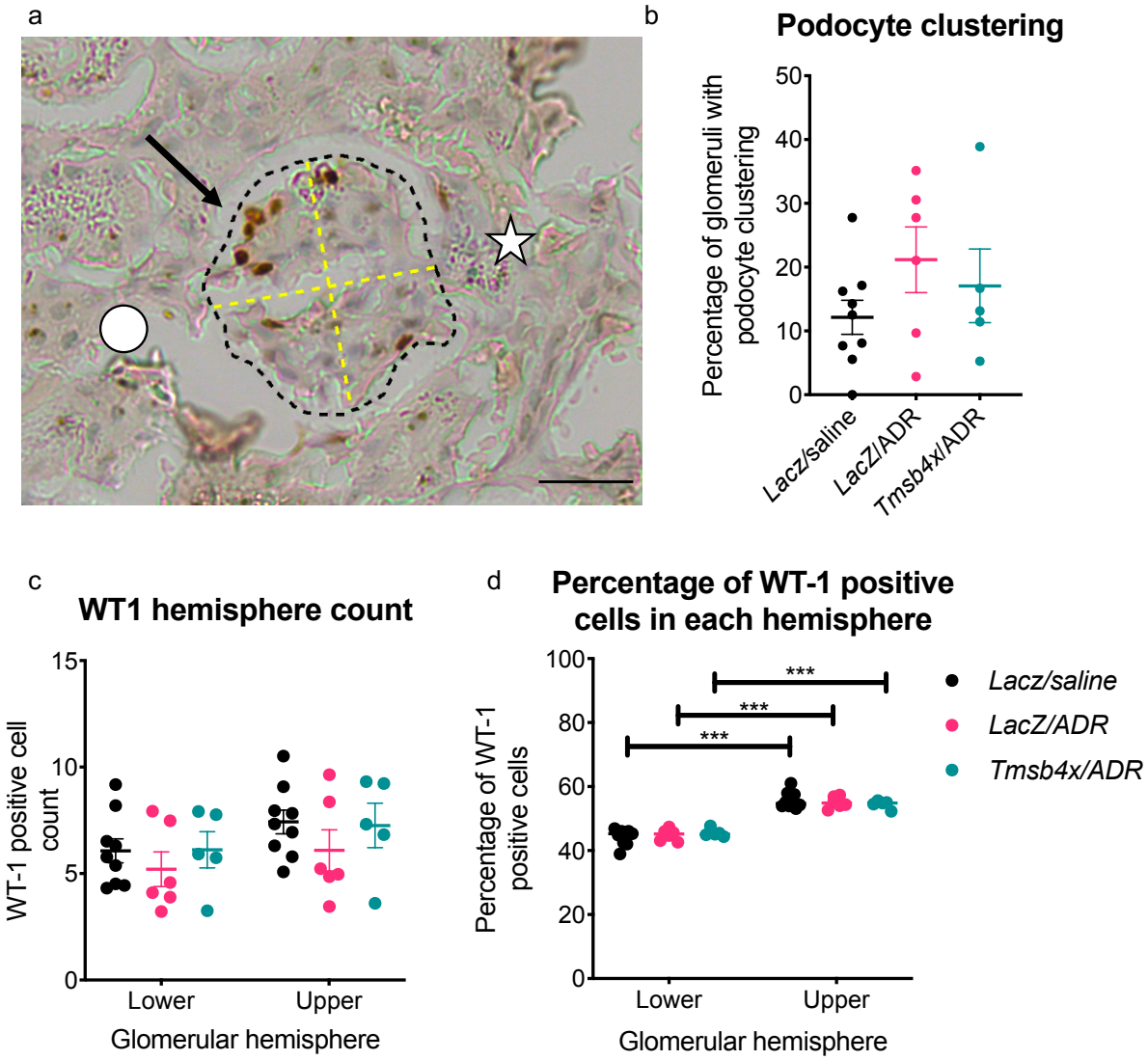

Figure 3.20 – ADR or TB4 did not alter podocyte distribution. *FFPE kidneys were incubated with a rabbit anti-mouse WT-1 primary antibody followed by anti-rabbit EnVision conjugated to HRP and then positive staining was visualised by 3,3'-Diaminobenzidine incubation. Mayer's haematoxylin was used to stain nuclei.* ***(a)*** *Representative image of a LacZ/ADR treated glomerulus displaying podocyte clustering (>50% of podocytes in 1 quadrant of the glomerulus). Black dashed line indicates glomerular tuft circumference, yellow dashed line indicates glomerular quartiles. White star indicates the lower hemisphere (vascular pole), and white circle indicates upper hemisphere (tubular pole). Black arrow indicates quadrant of glomerulus with clustering. Quantification of* ***(b)*** *the percentage of glomeruli displaying podocyte clustering,* ***(c)*** *the number of podocytes in each hemisphere of the glomerulus and* ***(d)*** *the number of cells in each glomerular hemisphere as a percentage of total podocyte number. Scale bar = 20 µm. Each data point represents the average of at least 30 glomeruli. n=33 for LacZ/saline, n=31 for LacZ/ADR and n=30 for Tmsb4x/ADR. Data are shown as the mean ±SEM of at least 5 mice. ***P≤0.001 between groups.*

was not significantly different than *LacZ*/saline treated mice. Mice treated with ADR with TB4 gene therapy displayed on average 17.1 ± 5.8% of glomeruli with podocyte clustering. There were no significant differences between any group (**Figure 3.20b**). Since the glomerulus is spherical, it was not possible to definitively determine which was the "left" and "right" side of the glomerulus on a 5 μm cross section. The one parameter that could be determined was the upper and lower hemispheres of the glomeruli. The upper hemisphere was designated as the pole closest to the proximal tubule and the lower hemisphere was designated the as the vascular pole. *LacZ*/saline treated mice had on average 6.1 ± 0.6 podocytes in the lower hemisphere and 7.4 ± 0.6 podocytes in the lower hemisphere of their glomeruli. Mice treated with ADR without TB4 gene therapy had an average of 5.2 ± 0.8 podocytes in the lower hemisphere and 6.1 ± 1 podocytes in the upper hemisphere of the glomeruli. ADR treated mice with TB4 gene therapy had an average of 6.1 ± 0.9 podocytes in the lower hemisphere and 7.3 ± 1 podocytes in the upper hemisphere of the glomeruli. There were no differences between any groups (**Figure 3.20c**).

The number of podocytes in each hemisphere of the glomeruli were then calculated as a percentage of the total number of podocytes in the glomeruli. *LacZ*/saline treated mice had an average of 44.2 ± 0.9% of podocytes in the lower hemisphere and 55.8 ± 0.9% of podocytes in the upper hemisphere of the glomeruli. In ADR treated mice without gene therapy, this value was unchanged. The mice had an average of 44.9 ± 0.7% of podocytes in the lower hemisphere, and 55.1 ± 0.7% of podocytes in the upper hemisphere. Mice treated with ADR with TB4 gene therapy had an average of 45.5 ± 0.6% of podocytes in the lower hemisphere and 54.5 ± 0.6% of podocytes in the upper hemisphere. There were no significant differences between the treatment groups, however, in all three groups it was found that there was a significant difference in the number of podocytes in each hemisphere of the glomeruli ($P<0.001$ in all treatment groups) (**Figure 3.20d**).

3.4.11 TB4 prevented ADR-induced reduction of glomerular F-actin

Next, the F-actin content of the glomeruli was examined, as F-actin alterations to the podocytes is a feature of ADR nephropathy and has been associated with podocyte

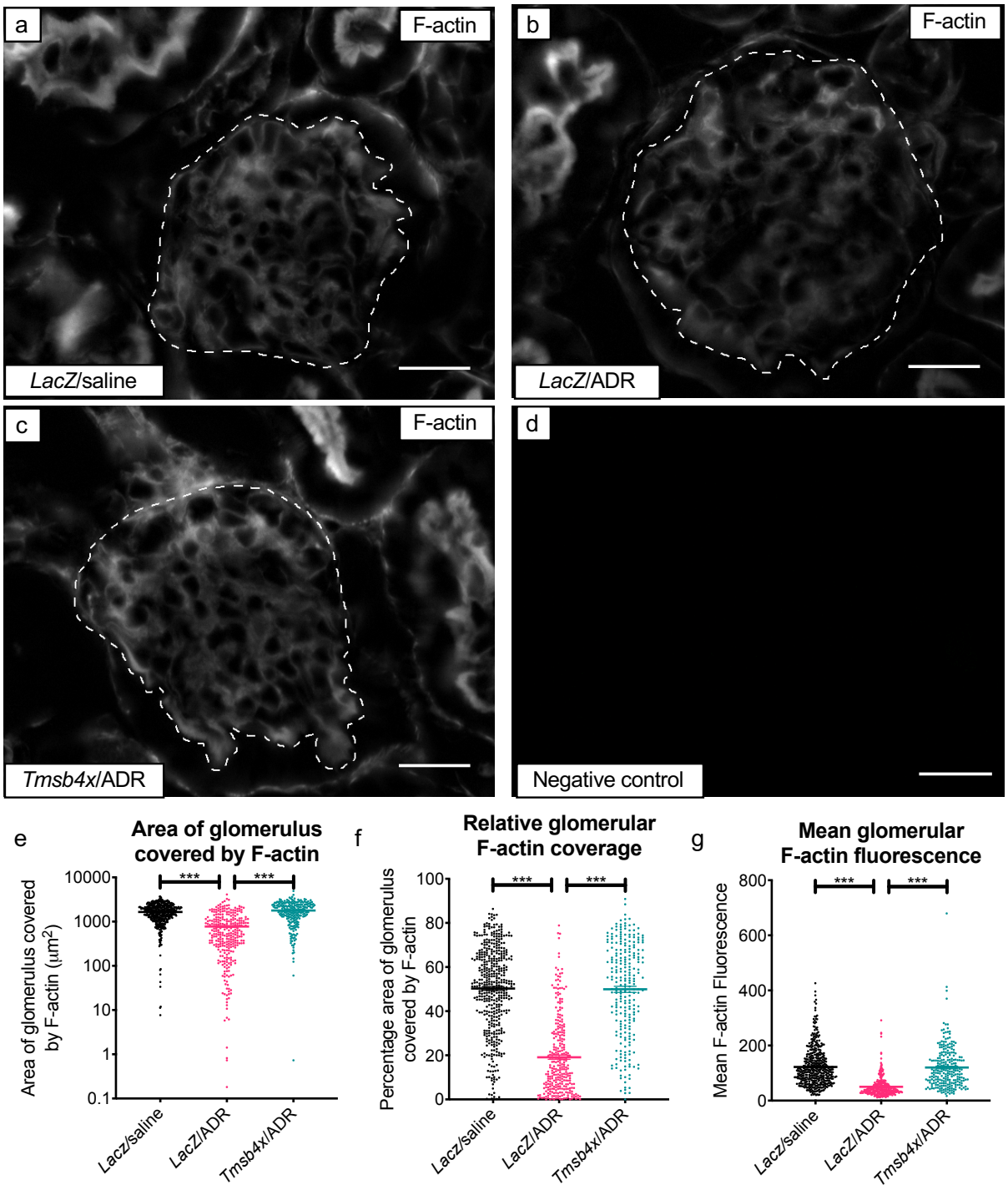

Figure 3.21 – TB4 prevents ADR-induced alterations to glomerular F-actin. *Kidney cryosections were stained with phalloidin to visualise glomerular F-actin. Representative images of* ***(a)*** *LacZ/saline,* ***(b)*** *LacZ/ADR and* ***(c)*** *Tmsb4x/ADR treated glomeruli. White dashed line indicates glomerular tuft. Scale bar = 20 μm.* ***(d)*** *Negative control omitting phalloidin. Quantification of* ***(e)*** *area of glomerulus covered by F-actin (μm²),* ***(f)*** *percentage area of glomerulus covered by F-actin and* ***(g)*** *glomerular mean F-actin fluorescence. Each group contained at least 50 glomeruli per mouse. Data are shown as the mean ±SEM of at least 250 glomeruli from at least 5 mice. N=450 for LacZ/saline group, N=300 for LacZ/ADR group, N=250 for Tmsb4x/ADR group. ***P≤0.001 between groups.*

foot process effacement and albuminuria (Oh, Reiser, and Mundel 2004; Suleiman et al. 2017; Yu et al. 2013). Glomerular F-actin content was examined by phalloidin staining of cryosections. Representative images of glomeruli from all three treatment groups stained with phalloidin are provided in **Figure 3.21a, b, c** and specificity was confirmed by omitting phalloidin **Figure 3.21d**. Individual glomeruli were quantified from all three treatment groups, 14 days after ADR or vehicle administration.

In *LacZ*/saline treated mice, F-actin covered on average 1660 ± 33 μm^2 of the glomerular cross section, which equated to 50 ± 0.9% of the total glomerular cross section. Administration of ADR with TB4 gene therapy caused a loss of glomerular F-actin coverage to 776 ± 40 μm^2 (P<0.001 vs *LacZ*/saline), equivalent to 31 ± 0.1% of the total glomerular cross section (P<0.001 vs *LacZ*/saline). Treatment with TB4 gene therapy prevented this loss of F-actin, and *Tmsb4x*/ADR treated mice showed a glomerular F-actin coverage of 1781 ± 54 μm^2 (P<0.001 vs *LacZ*/ADR), which equated to 49 ± 1.3% of glomerular cross-sectional area (P<0.001 vs *LacZ*/ADR) (**Figure 3.21e, f**). ADR also caused a reduction in mean glomerular F-actin fluorescence (P<0.001 vs *LacZ*/saline) which TB4 prevented (P<0.001 vs *LacZ*/ADR) (**Figure 3.21g**). Collectively, these results suggest that TB4 protects glomerular F-actin in ADR nephropathy.

3.4.12 Examination of podocyte synaptopodin content

Following analysis of glomerular F-actin content, the amount of the podocyte cytoskeletal protein synaptopodin was quantified in individual glomeruli by immunofluorescence 14 days after ADR or vehicle injection. Representative images of glomeruli immunostained for synaptopodin from all three treatment groups are provided in **Figure 3.22a, b, c**. The specificity of the staining was confirmed by omitting the primary antibody (**Figure 3.22d**).

Synaptopodin covered 336.1 ±15.7 μm^2 of *LacZ*/saline treated glomeruli, and treatment with ADR without TB4 gene therapy significantly increased this amount to 514.7 ±27.6 μm^2 (P<0.001 vs *LacZ*/saline). Treatment with TB4 gene therapy prevented the ADR induced increase in synaptopodin, as synaptopodin covered on

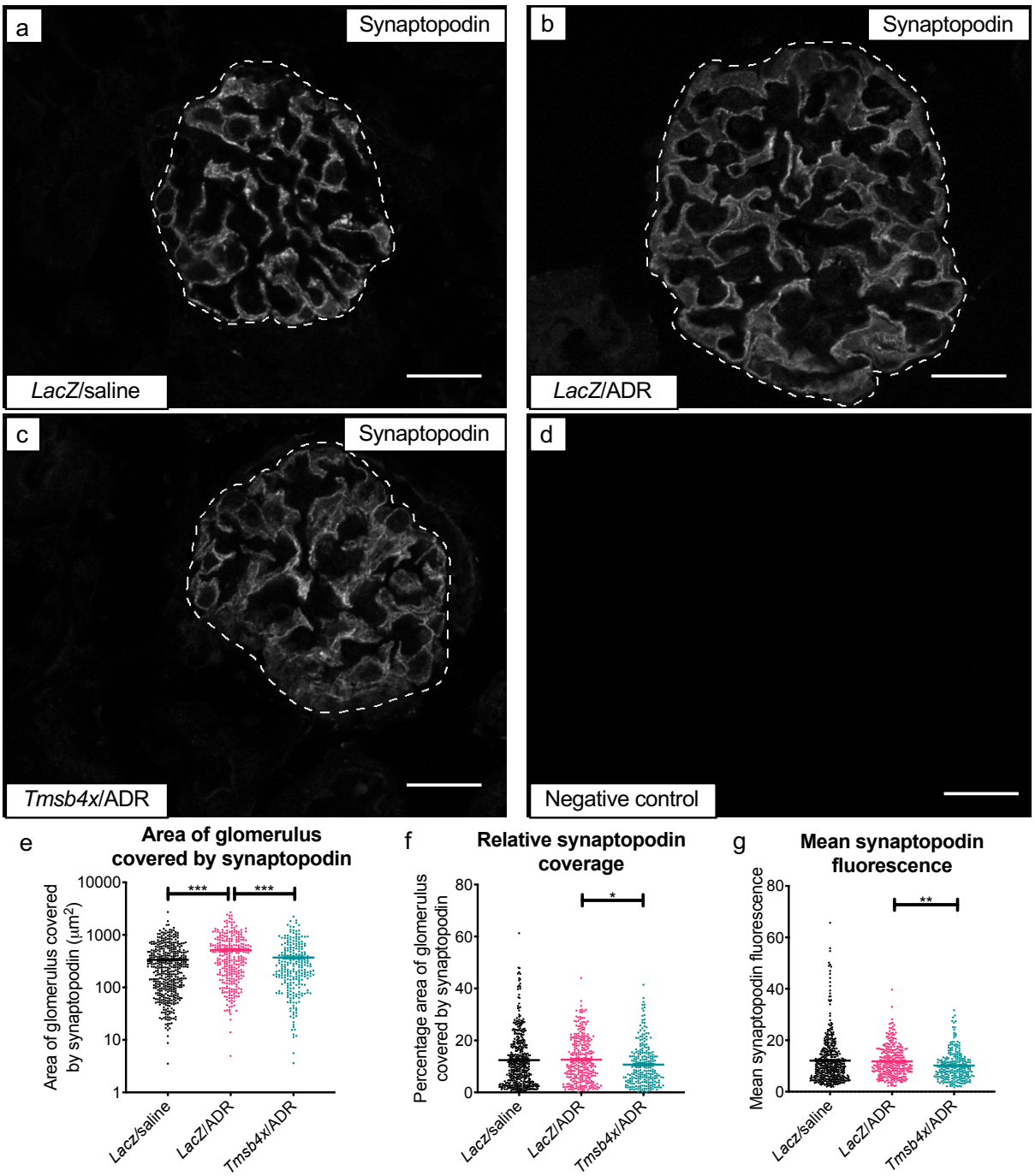

Figure 3.22 – The effect of ADR and TB4 on synaptopodin. *Kidneys cryosections were immunostained with guinea-pig anti-mouse synaptopodin followed by goat anti-guinea pig secondary antibody conjugated to 488 nm fluorophore. Representative images of **(a)** LacZ/saline, **(b)** LacZ/ADR and **(c)** Tmsb4x/ADR treated glomeruli. White dotted line refers to the boundaries of the glomerular tuft. **(d)** Negative control omitting the primary antibody. Quantification of the **(e)** total area covered by synaptopodin of glomeruli (µm²), **(f)** the percentage area of glomeruli covered by synaptopodin and **(g)** mean glomerular synaptopodin fluorescence. Scale bar = 20 µm. Each group contained at least 50 glomeruli per mouse. Data are shown as the mean ±SEM of at least 250 glomeruli from at least 5 mice. N=450 for LacZ/saline group, N=300 for LacZ/ADR group, N=250 for Tmsb4x/ADR group. *P≤0.05, **P≤0.01, ***P≤0.001 between groups.*

average 371.5 ±23.8 μm^2 of the glomerular cross section (P<0.001 vs *LacZ*/ADR) (**Figure 3.22e**).

The total area of synaptopodin was then normalised to glomerular cross-sectional area. Synaptopodin covered on average 12.5 ± 0.5% of glomeruli when treated with *LacZ*/saline, and an average of 12.6 ± 0.5% of glomeruli treated with ADR with TB4 gene therapy. There was no significant difference between these two groups. Treatment with ADR with TB4 gene therapy reduced synaptopodin coverage to 10.7 ± 0.5% compared with the ADR without TB4 gene therapy group (P<0.05), but this value was not significantly different to *LacZ*/saline group (**Figure 3.22f**). The mean fluorescence of synaptopodin in the glomeruli was also measured as an alternative measure of synaptopodin content. *LacZ*/saline treated mice had an average glomerular synaptopodin fluorescence of 12.1 ± 0.4 arbitrary units (AU). Mice treated with ADR without TB4 gene therapy had an average glomerular synaptopodin fluorescence of 11.8 ± 0.6 AU. ADR treated mice with TB4 gene therapy had an average glomerular synaptopodin fluorescence of 10.1 ± 0.4, which was significantly less than ADR treated mice without TB4 gene therapy (P<0.01) (**Figure 3.22g**).

3.4.13 Analysis of podocyte F-actin

It was postulated that the alterations observed to glomerular F-actin content could be localised to the podocytes. Therefore, kidney cryosections were immunostained to visualise F-actin and synaptopodin, as a marker for podocytes. Representative images of glomeruli from all three treatment groups can be found in **Figure 3.23a, b, c**. The staining was specific for synaptopodin and F-actin, as seen in the negative controls omitting the primary antibody or phalloidin (**Figure 3.23d**).

In *LacZ*/saline treated mice, there was on average 356 ± 21 μm^2 F-actin in synaptopodin positive areas. Treatment with ADR reduced the area of F-actin to 280 ± 19 μm^2 in synaptopodin positive regions, but this was not significantly different to *LacZ*/saline. *Tmsb4x*/ADR treated mice showed an average 318 ± 30 μm^2 of F-actin in synaptopodin positive regions, which was not significantly different to either of the other groups (**Figure 3.24a**). It was shown previously in this thesis chapter that synaptopodin

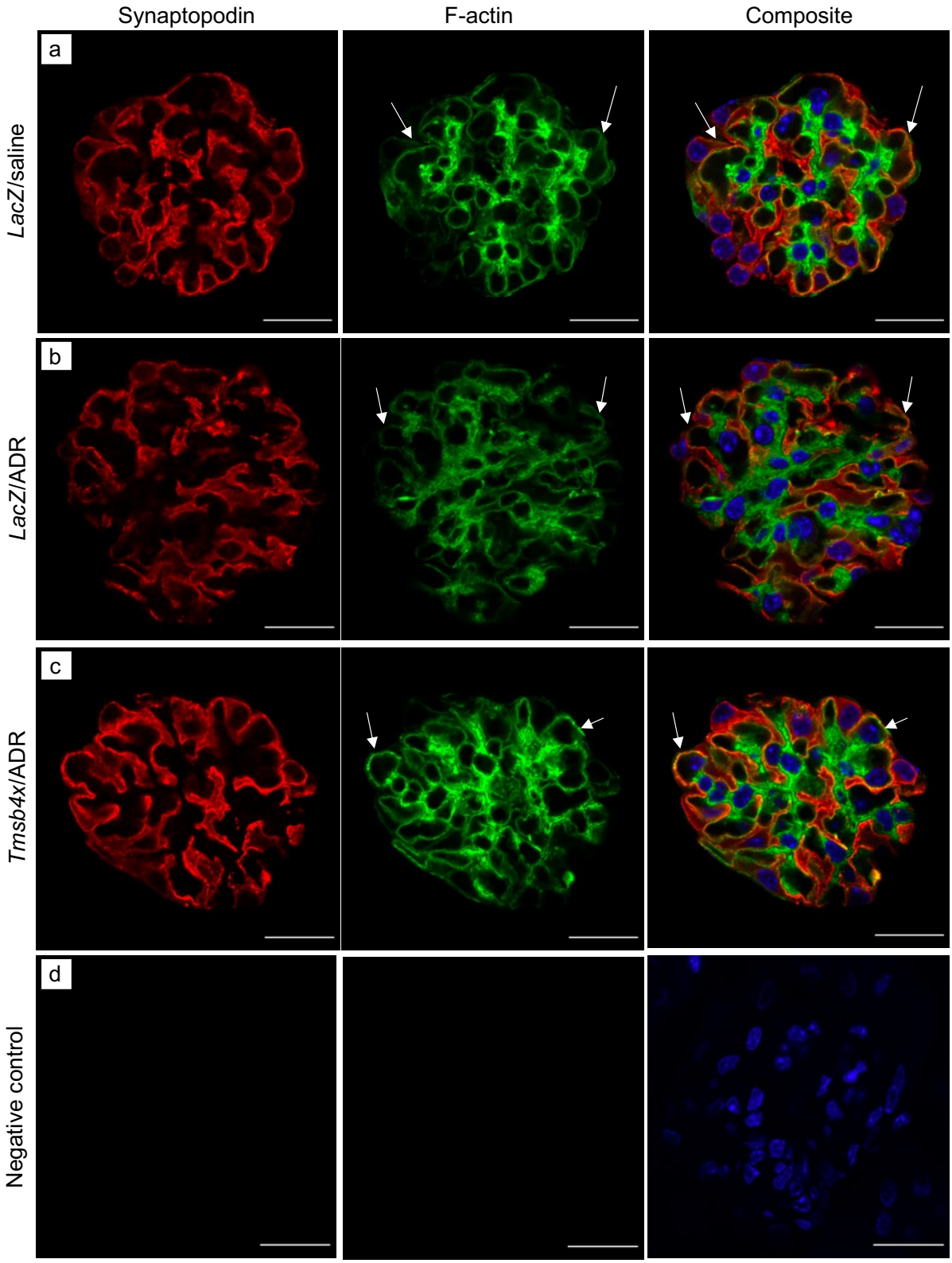

Figure 3.23 – Visualisation of podocyte F-actin. *Kidney cryosections were immunostained with α-synaptopodin antibody to visualise synaptopodin and phalloidin to visualise F-actin. Nuclei were immunostained with Hoechst 33332. Representative images of* ***(a)*** *LacZ/saline,* ***(b)*** *LacZ/ADR and* ***(c)*** *Tmsb4x/ADR treated glomeruli.* ***(d)*** *Negative control omitting primary antibody and phalloidin. White arrows indicate F-actin in synaptopodin positive areas. Scale bar = 20 μm. Images have been altered to exclude positive phalloidin staining outside the glomerular tuft to ensure accuracy of macro used for quantification.*

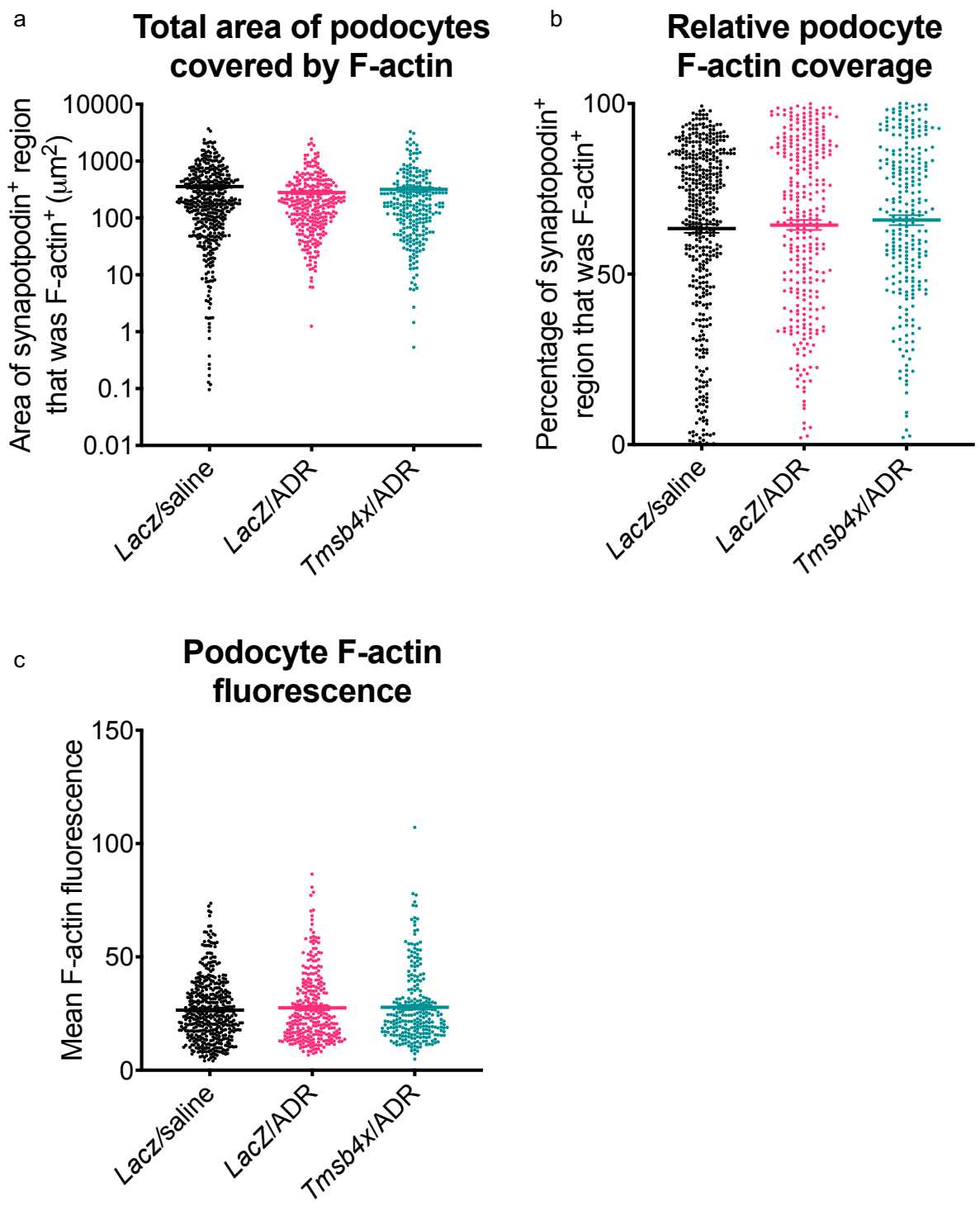

Figure 3.24 – ADR or TB4 do not alter amount of podocyte F-actin. *Quantification of* ***(a)*** *total area of F-actin in synaptopodin positive area (μm^2),* ***(b)*** *the percentage of synaptopodin positive area covered by F-actin and* ***(c)*** *mean F-actin fluorescence in synaptopodin positive areas. Each group contained at least 50 glomeruli per mouse. Data are shown as the mean ±SEM of at least 250 glomeruli from at least 5 mice. N=450 for LacZ/saline group, N=300 for LacZ/ADR group, N=250 for Tmsb4x/ADR group.*

content was altered in ADR treatment with and without TB4 gene therapy, therefore to account for this, F-actin area was normalised to synaptopodin area. F-actin covered 63.4 ±1.2% of the synaptopodin positive area in *LacZ*/saline treated mice, which was unchanged with administration of ADR (64.4 ±1.4%) or TB4 (65.8 ±1.5%) (**Figure 3.24b**). The mean fluorescence of F-actin in synaptopodin positive regions was also examined as a surrogate for the amount of F-actin. *LacZ*/saline treated mice F-actin had a mean fluorescence of 26.6 ±0.65 in synaptopodin positive regions. Again, this result was unchanged after treatment with ADR with TB4 gene therapy (27.5 ±0.9) or with TB4 gene therapy (27.8 ±1.1) (**Figure 3.24c**). Taken together, these results suggest that there was no change to the amount of F-actin in podocytes after ADR/TB4 treatment.

3.4.14 TB4 prevented formation of vesicles induced by ADR

Recently, a mechanism of albuminuria has been shown using a combined use of focused-ion beam/scanning electron microscopy (FIB/SEM) in PAN nephrosis. Vesicles (approximately 500 nm to 1 μm in diameter) form at the basal side of the foot processes, travel through the cytoplasm and then open at the apical membrane as a vector for albumin to travel from the bloodstream to urinary space in nephrotic podocytes (Burford et al. 2017; Ichimura et al. 2019; Schießl et al. 2016). While examining the F-actin and synaptopodin images used in 3.4.13, small structures in the F-actin regions were observed that resembled the shape of vesicles identified previously (Ichimura et al. 2019). These vesicles were F-actin positive, but not all seemed to be encapsulated by synaptopodin, suggesting that they were formed of F-actin (**Figure 3.25a, b, c**).

The diameter of the vesicle labelled in **Figure 3.25b** were between 1 and 1.3 μm, suggesting that these structures could be the vesicles described by Ichimura *et al.*, as they were described as up to approximately 1 μm in diameter (Ichimura et al. 2019). Therefore, the identity of each mouse was blinded to the observer, and the number of vesicles were counted on each glomerulus to determine if this could be contributing to the increase in albuminuria.

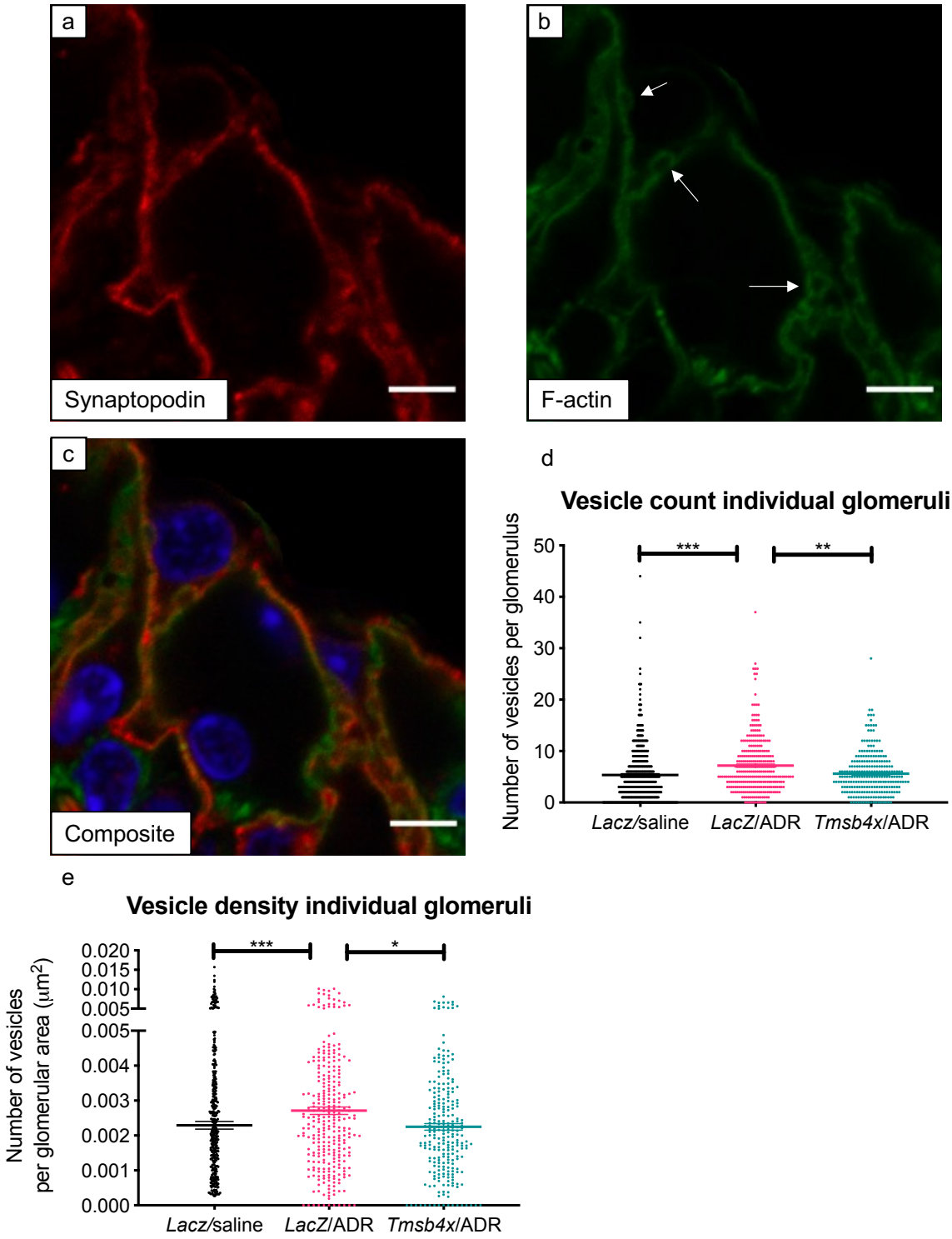

Figure 3.25 – TB4 prevents ADR-induced podocyte suspected vesicle formation. *Kidney cryosections were immunostained with α-mouse synaptopodin and phalloidin to visualise synaptopodin and F-actin. Nuclei were stained with Hoechst 33342. Representative images of* ***(a)*** *synaptopodin,* ***(b)*** *F-actin and* ***(c)*** *the composite including nuclei from a LacZ/ADR treated glomerulus. White arrows indicate vesicles. Quantification of* ***(d)*** *the number of vesicles per glomerulus and* ***(e)*** *the vesicle density of each glomerulus. Each group contained at least 50 glomeruli per mouse, with at least 250 glomeruli in each group. n=450 for LacZ/saline group, n=300 for LacZ/ADR group, n=250 for Tmsb4x/ADR group. Data are shown as the mean ±SEM of at least 250 glomeruli from at least 5 different mice. *P≤0.05, **P≤0.01, ***P≤0.001.*

When counting the number of vesicles per glomerulus, *LacZ*/saline treated mice had an average of 5.3 ± 0.3 vesicles per glomerulus. This number rose to 7.2 ± 0.3 vesicles per glomerulus after treatment with ADR without TB4 gene therapy, which was significantly more than *LacZ*/saline treated mice (P<0.001). Treatment with exogenous TB4 prevented this increase, as each glomerulus displayed an average of 5.6 ± 0.3 vesicles per glomerulus, which was significantly lower than the *LacZ*/ADR treated group (P<0.01) (**Figure 3.25d**). Since glomerular area was altered in ADR nephropathy (3.4.9), the number of vesicles were normalised to glomerular area (vesicle density). *LacZ*/saline glomeruli had an average vesicle density of 2.3 $x10^{-3}$ ± 0.1 $x10^{-3}$ vesicles per μm^2. Again, this value increased to 2.7 $x10^{-3}$ ± 0.1 vesicles per μm^2 after ADR treatment without TB4 gene therapy, which was significantly greater than *LacZ*/saline glomeruli (P<0.001). *Tmsb4x*/ADR treated glomeruli had 2.2 $x10^{-3}$ ± 0.1 $x10^{-3}$ vesicles per μm^2, which was significantly less that *LacZ*/ADR treated mice (P<0.05) (**Figure 3.25e**). These results suggest that vesicle formation may be contributing to ADR-induced albuminuria, which TB4 gene therapy prevented.

3.5 **Discussion**

This chapter of the thesis has shown that ADR administration to mice results in a reduction in the levels of glomerular and podocyte *Tmsb4x* mRNA. To restore the levels of TB4 in ADR-induced glomerular injury, the novel strategy of AAV gene therapy was utilised. AAV.*Tmsb4x* infected and transduced cells in the liver. This transduction caused a significant increase in systemic TB4 compared to AAV.*LacZ* treated mice, which persisted throughout the experiment. Systemic upregulation of exogenous TB4 in ADR treated mice prevented albuminuria and podocyte loss compared to mice treated with ADR without TB4 gene therapy. Collectively, this thesis chapter has provided the first evidence that exogenous TB4 prevents ADR-induced glomerular injury via protection of podocytes.

This thesis chapter used novel analyses of published scRNAseq data (Chung et al. 2020), and also qPCR, to show that glomerular and podocyte levels of *Tmsb4x* were downregulated in ADR nephropathy. The reduction in podocyte *Tmsb4x* levels in ADR nephropathy provided rationale to administer mice with TB4 as a therapeutic

agent. Global loss of endogenous *Tmsb4x* in C57BL/6 mice resulted in exacerbated proteinuria, podocyte loss and inflammation in NTS nephritis (Vasilopoulou et al. 2016). Furthermore, healthy podocyte specific knockdown of *Tmsb4x* caused an increase in podocyte migration and F-actin reorganisation, demonstrating that loss of endogenous *Tmsb4x* has detrimental effects to podocytes (Vasilopoulou et al. 2016). Therefore, one of the main hypotheses of this thesis chapter, after the reduction in podocyte *Tmsb4x* was confirmed, was that restoring the levels of TB4 would alleviate the phenotypes of ADR nephropathy and damage to podocytes.

Analysis of scRNAseq data is a novel method of analysis that an increasing number of researchers are utilising to identify potential targets in pathological settings. scRNAseq can also reveal hidden differences in gene expression. For example, in this thesis, it was shown from the scRNAseq data that podocyte *Tmsb4x* was downregulated 14 days after ADR injection. qPCR examination of mRNA from glomerular extracts showed no difference between saline treated mice and 14-day ADR treated mice, only at 7 days. It is possible that another cell type in the glomerulus was masking the reduction of *Tmsb4x* levels in podocytes by showing increased levels of *Tmsb4x*. To confirm if this was the case, the same pipeline could be used to analyse the scRNAseq data from Chung et al., but instead of examining the podocyte cluster, the endothelial cell cluster would be analysed. However, the scRNAseq data analysed from Chung et al., does have limitations. Firstly, the mouse strain used was C57BL/6, which is thought to be resistant to ADR nephropathy, due to the presence of the mitochondrial genome protector PRKDC (Papeta et al. 2010). The scRNAseq study attempted to circumvent this issue by administering the mice with 20 mg/kg ADR (Chung et al. 2020), double the dose used in this thesis. While the study did not provide albuminuria data, interrogation of the data in this thesis showed that there was a lower proportion of podocytes in ADR treated mice compared with the vehicle treated mice, suggesting damage to the glomeruli occurred. This also means that the most damaged podocytes might have been lost in the urine, and unusable for analysis. Another limitation is the sample size of the scRNAseq data. The authors only included 2 mice in each treatment group, however the general protocol undertaken in many scRNAseq experiments has a low sample number (Fu et al. 2019; Lu et al. 2017; Ransick et al. 2019), due to the high cost of scRNAseq experiments. On the other hand, the argument could be made that the

cell numbers examined was very high, as there were at least 8296 cells in each group of the scRNAseq data analysed in this experiment. Undoubtedly, as the technology advances, the experiments will become cheaper, allowing a higher number of mice to be analysed. The data does provide valuable insight of cellular genetics at *in situ* single cell resolution, which is normally unattainable with conventional qPCR.

After the downregulation of *Tmsb4x* in glomeruli and podocytes was confirmed, this thesis chapter provided further evidence that AAV therapy is a suitable method of systemically upregulating secreted proteins to deliver therapies for kidney disease. This study to utilised AAV.*Tmsb4x* gene therapy in a rodent model of kidney injury, and it was demonstrated that AAV2/7 induces a systemic upregulation of TB4. AAV vectors have been previously used to deliver molecules to alleviate podocyte and glomerular injury. Treatment of C57BL/6 mice with AAV to systemically upregulate myeloid-derived growth factor (MYDGF) suppressed increased albuminuria, podocyte foot process effacement, nephrin loss and glomerular hypertrophy in a model of diabetic nephropathy (He et al. 2020). Glomerular transduction by AAV and overexpression of Protein S via AAV injection into the renal vein prevented increased albuminuria, podocyte loss and mesangial matrix expansion in the OVE26 transgenic mouse model of type 2 diabetes (Zhong et al. 2018). Delivery of human tissue kallikrein, a serine proteinase that converts kininogen to kinin (Yousef and Diamandis 2001), by AAV2 reduced increased albuminuria, glomerulosclerosis and reduced creatinine clearance in the surgical 5/6 nephrectomy model of kidney injury in rats (Tu et al. 2008). Although glomerular targeted therapy has been demonstrated in other models, AAV therapy has not been utilised in ADR nephropathy until now.

AAV therapy is an attractive method of inducing long term transgene upregulation (Zincarelli et al. 2008) and previous studies have shown high tissue tropism for the liver using AAV2/7 (Van Der Perren et al. 2011). AAV infection of highly proliferative cells leads to rapid diminishment of viral episomal DNA (Cunningham et al. 2008; Halbert et al. 1997). Liver parenchymal cells are mostly senescent (Berasain and Avila 2015; Macdonald 1961), meaning that there is a lower chance of viral episomal DNA to degrade compared to if AAV infected an organ with a high population of

proliferative cells. Furthermore, the liver has a rich blood supply with many blood vessels (Mitra and Metcalf 2009). This means that TB4, or other secreted therapeutic proteins produced by the cells after AAV transduction, has a high chance of being introduced into the bloodstream, leading to systemic upregulation (**Figure 3.26**).

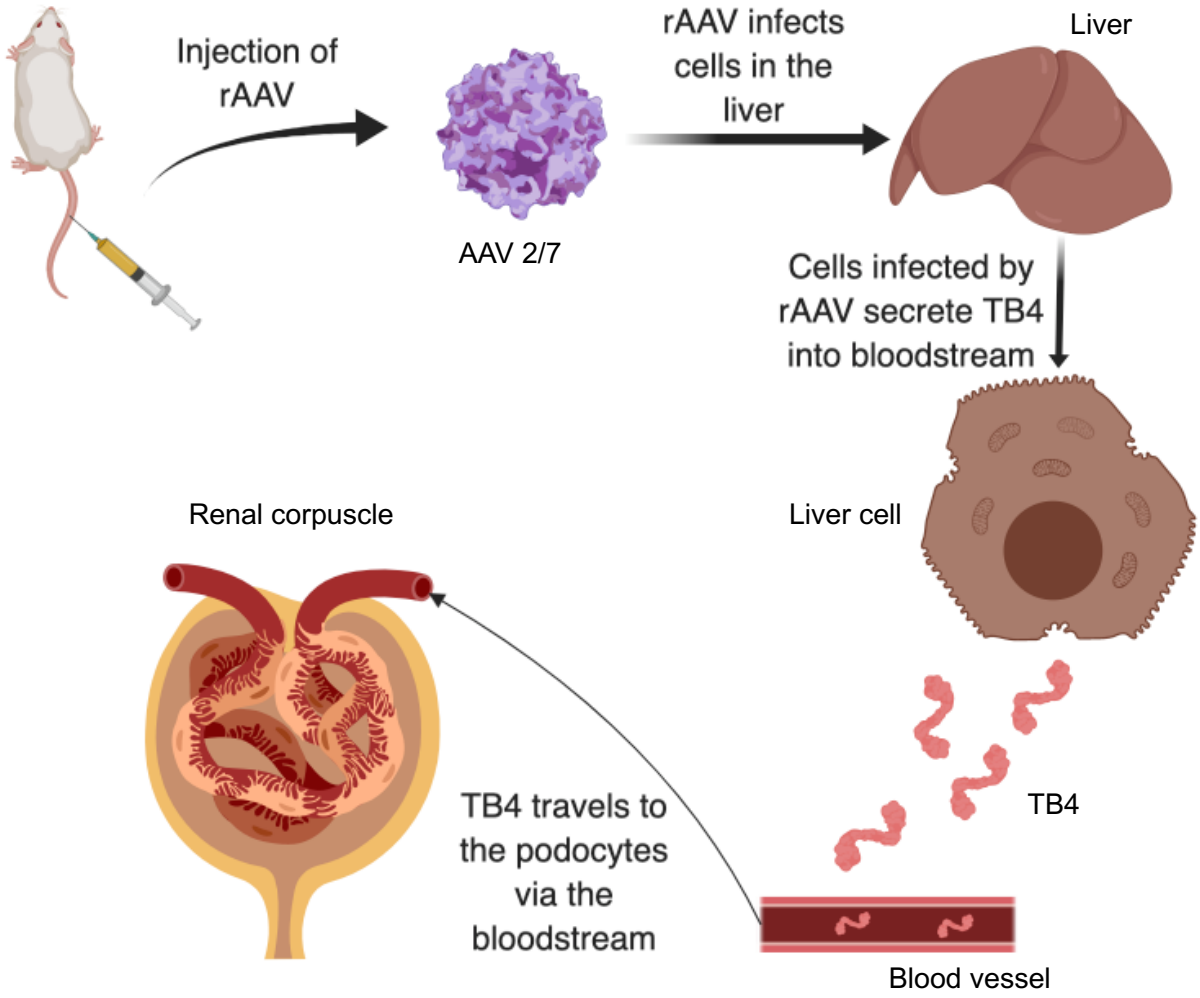

Figure 3.26 – Proposed route of TB4 delivery to glomeruli. *Diagram depicting the proposed mechanism of how exogenous TB4 reached the glomeruli. rAAV, recombinant adeno associated virus; TB4, thymosin β4. Original diagram.*

No other study has used AAV therapy to treat mice with TB4 in models of kidney disease, but AAV.*Tmsb4x* has been used in other pathological settings. AAV encoding *Tmsb4x* has been used previously as a therapeutic strategy in animal models of experimental injury. Intracolonic injection of $4x10^4$ AAV serotype 2

particles encoding *Tmsb4x* to mice has been shown to transduce colonic cells, significantly increasing TB4 expression (Zheng et al. 2017). The increased TB4 expression ameliorated some of the phenotypes of experimental colitis in these mice compared with AAV.*LacZ* injected mice, by attenuating inflammation, apoptosis and oxidative damage (Zheng et al. 2017). Tail vein injection of $5x10^{12}$ AAV serotype 2/9 particles encoding *Tmsb4x* to mice was shown to cause AAV transduction of cells in the heart and peripheral muscle, improving some of the phenotypes of LPS induced sepsis (Bongiovanni *et al.*, 2015). AAV.*Tmsb4x* was shown to prevent pericyte loss, perivascular leakage, and improved haemodynamics and survival compared to AAV.*LacZ* treated mice (Bongiovanni *et al.*, 2015). Intramuscular injection of $5x10^{12}$ AAV serotype 2/9 particles encoding *Tmsb4x* to the hindlimb of pigs prevented some of the effects of ischaemia. AAV.*Tmsb4x* increased vessel endothelial cell density, pericyte coverage and cardiac function compared with AAV.*LacZ* treated pigs (Ziegler et al. 2018). There are similarities between this thesis chapter and these three previous studies. Firstly, AAV.*Tmsb4x* in this thesis prevented glomerular inflammation, and it was shown that AAV.*Tmsb4x* prevented inflammation in the study by Zheng et al., highlighting the anti-inflammatory properties of TB4 (Sosne, Qiu, Christopherson, et al. 2007). The anti-inflammatory effects seen by Zheng et al., were suppression of TNF-α, IL-1β and IL-10 protein levels, and this thesis chapter did not present data to show that TB4 had any effect on these cytokines. Macrophage levels were not examined in the study by Zheng et al.. LPS induced sepsis is also an experimental model that induces a systemic inflammatory response (Schouten et al. 2008), however, Bongiovanni et al., focussed on the haemodynamic changes induced by LPS and AAV.*Tmsb4x*, and inflammation was not measured. This thesis chapter used a lower viral dose than the studies by Bongiovanni et al., and Ziegler et al., however, all three studies saw a beneficial effect induced by AAV.*Tmsb4x* compared with AAV.*LacZ*. This suggests that the therapeutic dose range of AAV.*Tmsb4x* can be tailored to the experimental requirements. The main difference between this thesis chapter and the three previous studies using AAV.*Tmsb4x* was the tissue that each study was targeting. The previous studies targeted the colon, muscle, vasculature, whereas this thesis chapter used AAV.*Tmsb4x* in a model of experimental kidney injury. Therefore, this thesis chapter has provided further evidence that AAV.*Tmsb4x* can be used to target pathologies in

multiple tissues. AAV.*Tmsb4x* circumvents the issue of rapid metabolism of TB4 after injection of the recombinant peptide, a method which has been used to explore the beneficial effects of TB4 in other kidney injury models. TB4 has been administered intraperitoneally daily in the UUO model of kidney injury and a model of type 2 diabetes in mice (Zhu et al. 2015; Zuo et al. 2013). Exogenous TB4 has been administered intravenously in the IRI model of kidney injury (Aksu et al. 2019). Intragastric lavage has also been used to administer rats daily with TB4 in the UUO model of kidney injury (Yuan et al. 2017). The reason that these studies injected the rodents with TB4 daily is because of the short half-life of TB4, as plasma levels of TB4 return to basal levels 6 hours after injection (Mora et al. 1997). However, daily injection can cause undue stress to rodents, as it has been shown that blood levels of corticosterone increase after injection of saline, which could alter the outcomes of experimental models of injury (Drude et al. 2011). While the experiments performed with daily injections did show positive outcomes, the experiment performed in this thesis chapter has an advantage over the studies that injected daily with TB4. Only one injection was needed for AAV administration and one was needed for either ADR or vehicle administration, which would have reduced the stress caused to the mice.

Currently, renal targeted AAV transduction is a challenge. The mean diameter of AAV particles is smaller (~22 nm) (Chen 2007) than the glomerular filtration barrier pores (~40 nm) (Rodewald and Karnovsky 1974), therefore a large number of circulating AAV particles will be lost in the urine. Screening of AAV serotypes 1-9 by luciferase assay revealed that even though the viral genome could be detected in the kidney, no luciferase protein was detected from any serotype 100 days post injection (Zincarelli et al. 2008). Novel administration routes have had some success in circumventing this issue. AAV8 induced transgene expression in the kidneys when administered by retrograde ureteral and subcapsular injections, with some recombinant protein localised to glomerular cells and tubular cells (Rubin et al. 2019). AAV9 expressing the green fluorescent protein (GFP) transgene injected into the renal vein showed a ~12.5-fold increase in glomerular GFP mRNA expression and 2-fold increase in glomerular GFP immunostaining compared to non-injected kidneys (Zhong et al. 2018). While these routes of administration show promise, they are more invasive and stressful than intravenous tail vein injection, hence systemic

upregulation of TB4 via a single intravenous injection was chosen in this thesis chapter.

Using AAV mediated systemic delivery of TB4, this thesis chapter has shown that exogenous TB4 prevents ADR-induced albuminuria 14 days after ADR administration. Since the glomerular filtration barrier becomes highly permeable to albumin in pathological conditions (Butt et al. 2020), it is likely that exogenous TB4 prevented ADR-induced damage to the glomerular filtration barrier. The severity of ADR-induced albuminuria (1448 μg/24h) was different compared to previous studies. BALB/c mice injected with 10 mg/kg ADR excreted approximately 20,000 μg/24 hours after 14 days in two previous studies (Teramoto et al. 2020; Wang et al. 2000). On the other hand, BALB/c mice injected with 10 mg/kg ADR in another study only excreted 800 μg/24 hours after 14 days of ADR treatment (X. Liu et al. 2018), half of what was observed in this thesis chapter. It is likely that many factors affect observed albuminuria levels in the previous studies, as well as this thesis chapter, including age of the mice, or the ELISA kit used to measure albuminuria, which could explain the discrepancies between these studies and the data presented in this thesis chapter. The mice were the same age (all between 7 and 10 weeks) in all three previous studies, along with this thesis chapter making the age unlikely to be the cause of difference. However, all three studies used different ways to analyse albuminuria concentration. The study from Wang et al., Liu et al., and this thesis chapter all used ELISA kits from different companies, but Teramoto et al., quantified albumin concentration by SDS-PAGE and Coomassie Brilliant Blue staining, making the method of quantification a potential source of the discrepancies.

This is the first study to focus on the effect of exogenous TB4 in a specific model of glomerular injury. The role of endogenous TB4 has been investigated in glomerular injury previously, where it was shown that a loss of endogenous *Tmsb4x* exacerbated an increase in albuminuria in NTS nephritis compared with wild type mice injected with NTS (Vasilopoulou et al. 2016). One of the key differences between this thesis chapter and the previous study by Vasilopoulou et al*.,* was the mechanism of glomerular damage. ADR induces a cytotoxic effect to the podocytes (Papeta et al. 2010), whereas NTS causes an autoimmune response against the

whole glomerulus (Khan et al. 2005). Wild-type mice treated with NTS excreted approximately 20,000 μg/24 hours of albumin after 21 days, but *Tmsb4x* knockout mice injected with NTS excreted 5 to 7-fold more albumin. This was a significantly increased amount, highlighting the importance of endogenous TB4 in slowing the progression of glomerular injury. Loss of endogenous *Tmsb4x* was also shown to exacerbate albuminuria compared to wild type mice in the angiotensin-II model of hypertension (Kumar *et al.*, 2018). One key difference between the injury model employed in this study and ADR, is that hypertension affected the whole of the kidney and the cardiovascular system, not just the kidney glomeruli, so the increase in albuminuria could have been a secondary effect to other alterations induced by angiotensin-II. Exogenous TB4 has been shown to prevent secondary-caused albuminuria in other models. In a model of diabetic kidney disease in *KK Cg-Ay* mice, exogenous TB4 prevented microalbuminuria compared to vehicle treated mice (Zhu et al. 2015). Proteinuria was also prevented by exogenous TB4 in the UUO model of kidney injury (Yuan et al. 2017). But these two models are multi-organ pathologies, and it is possible that albuminuria occurred as a secondary pathology, due to medullary fibrosis. ADR is an injury model that targets primarily the podocytes and glomeruli (Lee and Harris 2011). This thesis has provided evidence that exogenous TB4 prevents primary glomerular injury, specifically a rodent model of primary FSGS.

This thesis has shown that TB4 gene therapy prevented ADR-induced podocyte loss, a potential mechanism by which TB4 prevented albuminuria. Podocyte loss would have resulted in less coverage of the GBM by podocyte foot processes, resulting in naked areas of the GBM, allowing albumin to leak into the urine from the blood stream. Endogenous TB4 has been shown to prevent podocyte loss in NTS nephritis, as loss of *Tmsb4x* in mice resulted in a lower number of WT-1 positive cells in the glomerular tuft compared with wild type mice treated with NTS (Vasilopoulou et al. 2016). Both this thesis chapter and the study by Vasilopoulou et al., is that both have shown that TB4 prevents podocyte loss, and this is a mechanism that is very likely to have contributed to the prevention of albuminuria in both cases. This study also used the same method of quantification as this thesis, counting of WT-1 positive cells, making the data more likely to be comparable. There

were differences between the *Tmsb4x* knockout study and this thesis chapter, such as WT-1 loss in the glomerular tuft was accompanied by an increase in parietal WT-1 positive cells. The authors suggested that this could be indicative of podocyte migration towards the parietal epithelium in response to injury. There was a slight increase in parietal WT-1 expression in ADR treated mice with TB4 gene therapy compared to ADR mice without TB4 gene therapy. Parietal cells have been shown to express podocyte-like proteins, such as WT-1 (Kaverina et al. 2017; Zhang et al. 2012), when the glomerulus becomes injured, a potential explanation for the increase in WT-1 positive cells induced by ADR with TB4 gene therapy. Exogenous TB4 has also been shown to prevent cell loss in other organs. In rats subjected to traumatic brain injury, exogenous TB4 prevented hippocampal cell loss compared with sham rats (Xiong et al. 2011). The prevention of myocyte loss following ischaemic myocardial injury has also been attributed to exogenous TB4 administration to rats (Bao et al. 2013). In the study by Bao et al., the authors found that exogenous TB4 increased Akt phosphorylation in ischaemic tissue compared with non-treated ischaemic tissue. Activation of the Akt pathway has been shown to increase cell adhesion in cancer cells (Kraus et al. 2002) and human embryonic stem cells (Godoy-Parejo et al. 2019) which may provide an explanation for the effect of TB4 on podocyte loss in this study. Collectively, this thesis has provided the first evidence that exogenous TB4 prevents podocyte loss in glomerular disease.

This thesis chapter has shown that exogenous TB4 prevented the ADR-induced loss of glomerular F-actin, a potential mechanism by which TB4 prevented ADR-induced albuminuria. This is important, because the podocyte foot processes are enriched in F-actin compared with the cell body (Cortes et al. 2000), and disorganisation of foot process F-actin has been associated with foot process effacement and albuminuria (Shirato *et al.*, 1996; Yu *et al.*, 2013; Suleiman *et al.*, 2017). Although the glomerular amount of F-actin was protected by TB4, there were no differences between ADR with and without TB4 gene therapy when podocyte specific F-actin was examined using synaptopodin as a marker for podocytes. The representative images of glomeruli visualising F-actin and synaptopodin provided in this thesis chapter showed that a large proportion of the glomerular F-actin was located in synaptopodin negative areas. This suggests that much of the F-actin located in glomeruli was not localised to podocytes, and that alterations to the amount of F-actin were localised to

other glomerular cell types, such as the mesangium or endothelium. To prove this, the analysis could be repeated with markers to identify the mesangial cells (Ng2) or endothelial cells (endomucin). However, this does not mean that alterations to podocyte F-actin were not occurring. Alterations could have occurred to the organisation of podocyte F-actin in foot processes without changing the amount, as described previously (Shirato *et al.*, 1996). To examine this, access to super resolution microscopes would be required, as the resolving power of the confocal microscope that the images were taken on was not high enough to see individual F-actin fibres.

Alterations to glomerular F-actin in ADR nephropathy have been previously described using super resolution microscopy. The authors employed stochastic optical reconstruction microscopy (STORM) and Airyscan imaging of BALB/c mice injected with 14 mg/kg of ADR, and suggested that the actin cytoskeleton in the foot processes of podocytes becomes disorganised leading to a mat of contractile F-actin filaments in effaced foot processes (Suleiman et al. 2017). The study used synaptopodin as a marker of the podocyte cytoskeleton and myosin IIa as a marker of contractile actin fibres and found that there was a shift of myosin IIa expression from the cell body and primary processes to the foot processes in ADR injury. The authors confirmed synaptopodin or myosin IIa and F-actin colocalization in healthy podocytes. A higher dose of ADR could have induced more severe F-actin disorganisation compared with the data in this thesis chapter, which is why F-actin disorganisation could be detected at the podocyte level. The use of myosin IIa as a method of quantifying contractile F-actin fibres is an advantage that this study has over the quantification performed in this thesis. Future studies could perform this type of analysis to investigate if TB4 prevents the ADR induced reorganisation of contractile F-actin fibres, as a mechanism of the prevention of albuminuria. Another study used C57BL/6 mice injected with 12 mg/kg ADR, and glomerular F-actin content was assessed by phalloidin staining to show that ADR induced an increase in F-actin fluorescence after 4 weeks (Woychyshyn et al. 2020), which is in contrast to the results presented in this thesis chapter. There were differences between this study and this thesis chapter, for example the mouse strain (C57BL/6 mice are resistant to ADR nephropathy (Papeta et al. 2010)), the dose of ADR used and the time of exposure, which could all account for the differences in results. The authors

speculated that the increase in F-actin intensity around the capillary loops could be due to podocyte foot process F-actin reorganisation to a mat of unorganised actin adjacent to the GBM. The analysis performed in this thesis has the advantage over this study because synaptopodin was used to segment out podocytes. If Woychyshyn et al., had used this method of quantification, they could have determined if the increase in F-actin fluorescence around the capillary loops was localised to podocytes, and not the endothelium or mesangium.

Although no previous studies have examined F-actin content in the kidney after exogenous TB4 treatment, modulation of the F-actin cytoskeleton by TB4 has been reported in other pathologies. One study induced burns on the hindlimbs of C57BL/6 mice and found that 30 mg/kg of exogenous TB4 intravenously accelerated dermal wound healing by prevention of uncontrolled F-actin polymerisation up to 7 days after burn induction, as shown by quantifying the F-actin to G-actin ratio (Kim and Kwon 2017). An *ex vivo* experiment using embryonic chick hearts found that the actin-binding domain on TB4 promoted vessel sprouting and angiogenesis (Philp et al. 2003), suggesting that exogenous TB4 mediated angiogenesis after myocardial infarction seen previously (Chiu et al. 2012; Poh et al. 2020) is actin-mediated. In contrast to this thesis chapter, these two studies did not perform phalloidin staining to examine the amount of F-actin, however, the analyses they performed does provide information into the mechanism by which TB4 modulated F-actin in the respective cell types. Analysing the F-actin to G-actin ratio in podocytes after ADR treatment with and without TB4 gene therapy would identify if the main property of TB4, G-actin sequestering, was a mechanism by which TB4 prevented ADR-induced glomerular and podocyte damage.

While examining the images immunostained to visualise synaptopodin and F-actin, structures resembling vesicles were identified, and quantification revealed that TB4 gene therapy prevented the ADR-induced formation of F-actin buds. The buds were F-actin positive, but synaptopodin did not cover all of the buds, suggesting they were not dependent on synaptopodin. The size (~1 μm) and location (processes, close to the capillaries) of the F-actin is in agreement with previous studies demonstrating vesicular transcytosis of albumin with electron microscopy (Ichimura et al. 2019).

Vesicular transport of albumin from the basal side of the foot processes through to the urinary space is a mechanism that has been proposed and described by a mix of electron microscopy (Ichimura et al. 2019) and multiphoton microscopy live imaging (Schießl et al. 2016), where fluorescently tagged albumin has been recorded passing from the blood stream to the urinary space. It is proposed that the F-actin buds observed in this study contained albumin, however, immunofluorescent studies to visualise albumin and F-actin are required to confirm this hypothesis. It has been shown that F-actin dynamics are required for vesicle formation and transport, as HeLa cells treated with Latrunculin A and B (molecules that sequester G-actin) and Cytochalasin D (caps F-actin) ceased vesicular formation and intracellular transport (Boucrot et al. 2006). Furthermore, vesicles harbouring an F-actin coat have been identified *in vitro* in primary alveolar type II cells from rats (Miklavc et al. 2012), and actin coating was inhibited by the actin sequestering molecule Latrunculin B (Miklavc et al. 2009). This suggests that vesicular actin coating formation occurs *de novo* from G-actin monomers. It is possible that in this study, exogenous TB4s sequestering of G-actin, in the same way as Latrunculin B, prevented podocyte transcytosis of albumin via G-actin sequestering.

The podocyte SD, the space between adjacent podocyte foot processes, is the gateway in which the ultrafiltrate can escape the blood, but also the barrier which prevents loss of proteins, such as albumin (Jarad and Miner 2009; Pavenstädt et al. 2003). The SD is thought of as a modified adherens junction, and its structure is regulated by a complex network of intercellular and extracellular proteins, such as nephrin, podocin and cadherins (Patrakka and Tryggvason 2010; Tabatabaeifar et al. 2017; Wartiovaara et al. 2004). ADR is known to cause podocyte foot process effacement in mice as soon as 1 week after administration (Wang et al. 2000; Zhou et al. 2011). Furthermore, ADR caused a reduction in the SD proteins nephrin and podocin and increase in P-cadherin compared with vehicle treated rodents (Li, Yuan, and Zhang 2003; Wu et al. 2014). These previous studies show that ADR significantly disrupts the balance of SD proteins, which likely contributes to foot process effacement and albuminuria. Recently, it has been shown that endogenous TB4 stabilises adherens junctions, as in *Tmsb4x* knockdown embryonic mice, the pattern of E-cadherin (a major adherens junction protein) was disrupted in basal and suprabasal cells in the epidermis, accompanied by alterations to the actin

cytoskeleton (Padmanabhan et al. 2020). It is possible that administration of exogenous TB4 provided further stability of the SD in podocytes through its adherens junction stabilising properties. To confirm this, future studies could examine the expression of P-cadherin and other SD proteins in ADR nephropathy with and without TB4 gene therapy to determine if TB4 protects the integrity of the SD.

3.6 **Conclusions**

The results presented in this thesis chapter demonstrated that AAV.2/7 was effective in causing transgene upregulation in liver cells and persistent secretion of TB4 into the blood stream. Exogenous TB4 prevented ADR-induced damage to the glomerular filtration barrier by preventing podocyte loss. Exogenous TB4 also prevented alterations to the actin cytoskeleton, by preventing a reduction in the amount of glomerular F-actin and inhibiting suspected vesicle formation instigated by ADR (**Figure 3.27**) Collectively, it is proposed that actin modulation is a mechanism that underlies the protective action of TB4 in the glomerular filtration barrier, which may have implications for understanding the therapeutic benefits of TB4 in other pathological contexts.

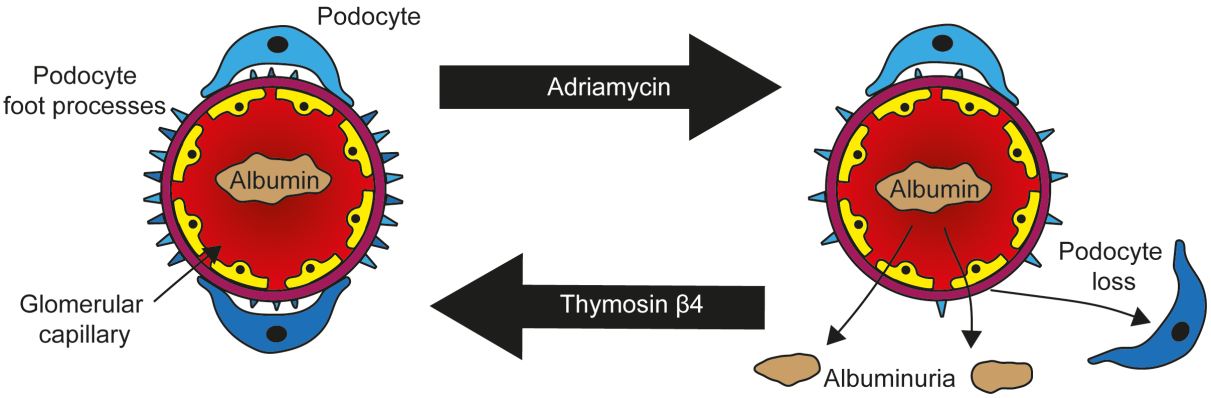

Figure 3.27 – Exogenous TB4 prevents ADR-induced glomerular filtration barrier damage. *Diagram illustrating the critical results presented in this chapter of the thesis. Original diagram.*

Chapter 4: Exogenous thymosin β4 suppresses glomerular damage in NTS nephritis

4.1 Introduction

The previous chapters of this thesis have shown that exogenous TB4 protects podocytes from ADR injury *in vitro* (Chapter 2) and *in vivo* (Chapter 3). One of the major beneficial properties of TB4 is its ability to suppress inflammation (Sosne et al. 2001; Sosne, Qiu, Christopherson, et al. 2007; Vasilopoulou et al. 2016), but the model of ADR nephropathy induced in Chapter 3 did not involve an inflammatory response. Therefore, to investigate if exogenous TB4 could protect glomeruli in immune mediated glomerular injury, NTS nephritis was utilised in this thesis chapter.

NTS nephritis is an inducible rodent model of autoimmune mediated glomerular injury that replicates some of the effects of human glomerulonephritis (Pippin et al. 2009). NTS is generated by injecting glomerular extracts from the experimental species (in this case mouse) into a host organism (in this case sheep) (Hoppe and Vielhauer 2014). The sheep generates polyclonal antibodies against the epitopes of mouse glomerular structures, such as the GBM, endothelial cells and podocytes, which are then extracted and purified. The mice are immunised with sheep IgG prior to NTS injection to prime the immune system before injection of NTS (Hoppe and Vielhauer 2014). When administered, the sheep polyclonal anti-glomerular antibodies bind to their respective epitopes on the mouse glomeruli. The mouse then creates an autoimmune response against the sheep polyclonal antibodies, mediated by complement activation, neutrophil inflammation, T cell activation and macrophage accumulation (Assmann et al. 1985; Hébert et al. 1998; Tipping and Holdsworth 2006). The T cells induce B cell activation, causing glomerular deposition of autologous antibodies against the sheep-anti-glomerular antibodies. Large immune complexes of IgG are then generated which exacerbate glomerular injury (Hoppe and Vielhauer 2014). The chronic immune response occurs typically 1 week after NTS injection and can injure glomerular cells causing albuminuria, glomerulosclerosis, increased BUN, decreased creatinine clearance and death in mice (Chen et al. 2002).

Exogenous TB4 has beneficial effects in ADR nephropathy (Chapter 3), diabetic nephropathy (Zhu et al. 2015), acute UUO injury (Yuan et al. 2017; Zuo et al. 2013) and kidney IRI (Aksu et al. 2019). The beneficial effects of TB4 in the study by Aksu et al., was associated with the anti-inflammatory action of TB4. A previous study assessed the role of endogenous TB4 in NTS nephritis and found that endogenous TB4 slowed the progression of albuminuria, prevented decreased creatinine clearance and podocyte loss and inhibited an increase in BUN (Vasilopoulou et al. 2016). Endogenous TB4 also suppressed glomerular macrophage and T cell accumulation, as well as collagen IV and αSMA deposition, demonstrating its anti-inflammatory and anti-fibrotic properties (Vasilopoulou et al. 2016). It is not yet known if exogenous TB4 can alleviate NTS nephritis, therefore, to explore if this is the case, AAV.*Tmsb4x* was administered in this form of glomerular injury.

4.2 **Aims and hypothesis**

It was hypothesised that exogenous TB4 would alleviate the phenotypes of NTS nephritis through suppression of inflammation. The first aim of this thesis chapter is to confirm systemic TB4 upregulation following gene therapy. Secondly, this thesis chapter will explore the beneficial potential of exogenous TB4 in NTS nephritis to determine if exogenous TB4 prevents NTS induced albuminuria and loss of kidney function. The final aim of this thesis chapter is to elucidate potential mechanisms of the beneficial effect of TB4 in NTS nephritis.

4.3 **Materials and methods**

This laboratory work for this thesis was undertaken during the COVID-19 pandemic, which enforced the closure of the laboratory for an extended period. Therefore, some of the laboratory work undertaken for this thesis chapter was completed by Dr Elisavet Vasilopoulou, who has allowed the data to be used in this thesis chapter. The following data was collected by the author of this thesis: assessment of podocyte number by WT-1 IHC; quantification of podocyte clustering by WT-1 IHC; analysis of glomerular proliferation by Ki67 and synaptopodin staining and quantification of glomerular inflammation by F4/80 IHC. All materials used in this thesis chapter were obtained from Merck U.K., Dorset, U.K. unless stated otherwise.

4.3.1 Experimental animals

In this experimental procedure, all animals were subjected to NTS-induced glomerular injury and all experimental procedures were approved by the Home Office. Male C57BL/6 mice aged between 7-10 weeks were housed in cages of three, kept at a constant temperature (22 °C) and light cycle (12 hours light, 12 hours dark), and provided with standard laboratory chow and tap water *ad libitum*. The mice were injected with $2x10^{12}$ viral particles of AAV serotype 2/7 encoding *Tmsb4x* (TB4) or *LacZ* (β-galactosidase) via the tail vein. Sterile PBS was used as an additional control. There was a 4-week transcriptional activation window, before NTS injection. The final treatment groups were treated with NTS to induce glomerular injury and (i) PBS (PBS/NTS), (ii) AAV.*LacZ* (*LacZ*/NTS) or (iii) AAV.*Tmsb4x* (*Tmsb4x*/NTS).

Urine was collected overnight in metabolic cages and plasma was collected via the lateral saphenous vein, which was stored in MicroVette EDTA-coated capillary action tubes. To prime the mouse immune system to target the sheep anti-mouse glomeruli polyclonal antibodies, mice were then pre-immunised sub-cutaneously with 250 μg of sheep IgG diluted in complete Freund's adjuvant. Five days later (day 0), mice were injected with 250 μl of NTS intravenously to induce kidney disease. Urine and plasma were collected 7 days later. At day 21 after NTS injection, the mice were culled by CO_2 asphyxiation and death was confirmed by exsanguination after

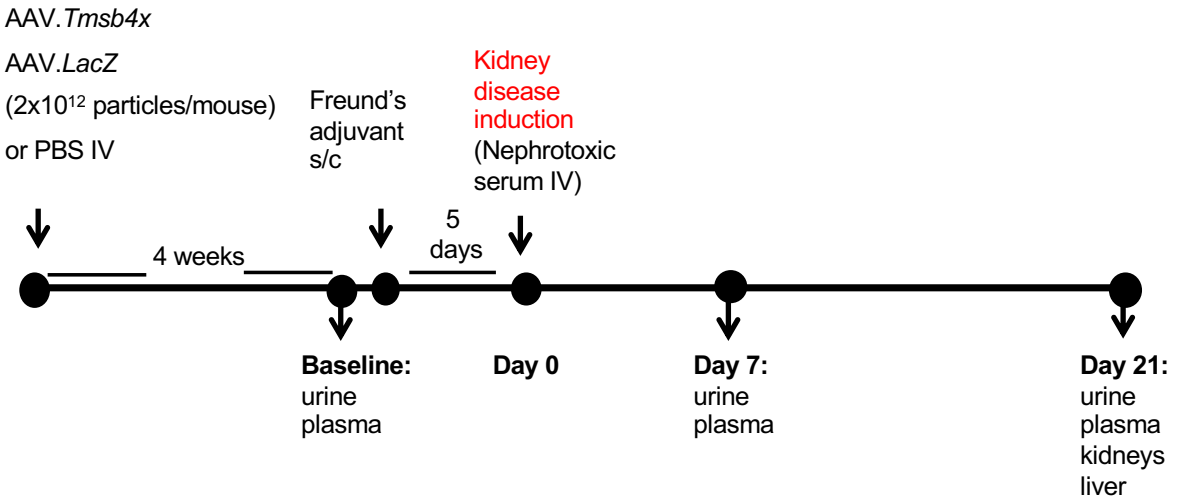

Figure 4.1 – Experimental design. *Graphic displaying the experimental design for the NTS nephritis study undertaken. Adeno associated virus, AAV; Thymosin β4, Tmsb4x; β-galactosidase, LacZ; phosphate buffered saline, PBS; Intravenous, IV; Sub cutaneously, S/C.*

overnight urine collection in metabolic cages. Blood was collected via cardiac puncture and the right kidney and part of the liver were snap frozen on dry ice. The left kidney and a separate part of the liver were placed in 4% PFA in dH_2O (**Figure 4.1**). Blood and plasma were processed as described in 3.3.2 and tissues were processed as described in 3.3.3.

4.3.2 qPCR

mRNA was extracted from kidneys and livers snap frozen in liquid nitrogen 21 days after kidney disease induction and qPCR was performed on subsequently generated cDNA as described in 3.3.10. The primers used in this chapter can be found in (**Table 4.1**).

Table 4.1 – List of primers

Target gene/translated protein (annealing temp, °C)	Primer sequence (5' to 3')	Location on mRNA (amplicon size, base pairs)
Tmsb4x/TB4 (60)	Fwd: ATGTCTGACAAACCCGATATGGC	Bp 76 - 200. Exon 1 – 2 (125)
	Rvs: CCAGCTTGCTTCTCTTGTTCA	
Cd68/CD68 (60)	Fwd: GGGGCTCTTGGGAACTACAC	Bp 481 - 647. Exon 2 - 3 (167)
	Rvs: GTACCGTCACAACCTCCCTG	
Ccl2/Monocyte chemoattractant protein-1 (60)	Fwd: CCCCAAGAAGGAATGGGTCC	Bp 316 - 497. Exon 2 - 3 (182)
	Rvs: TGCTTGAGGTGGTTGTGGAA	
Tnfa/Tumour necrosis factor α (60)	Fwd: AGCCGATGGGTTGTACCTTG	Bp 509 - 607. Exon 2 - 3 (99)
	Rvs: ATAGCAAATCGGCTGACGGT	
Acta2/α-smooth muscle actin (60)	Fwd: GCCATCTTTCATTGGGATGGA	Bp 902 - 1017. Exon 7 - 8 (116)
	Rvs: CCCCTGACAGGACGTTGTTA	
Col4a1/Collagen IV (58)	Fwd: TTCCTTCGTGATGCACACCA	Bp 4970 - 5080. Exon 50-51 (111)
	Rvs: CCGTGGCACTCGATGAATG	
Hprt/Hypoxanthine-guanine phosphoribosyltransferase (same as gene of interest)	Fwd: AAGCTTGCTGGTGAAAAGGA	Bp 629 - 982. Exon 7 - 9 (354)
	Rvs: GCAAATCAAAAGTCTGGGGA	

Table 4.1 – Primer details. *Details of all primers used for NTS experiments, including target gene and its translated protein; the nucleotide sequences; the size of the amplicons; the location of the amplicon on the target gene and the annealing temperature used in quantitative PCR experiments. Tmsb4x, Thymosin β4, TB4; Cd68, cluster of differentiation 68; Ccl2, chemokine ligand 2; fwd, forward; rvs, Reverse; temp, temperature. Bp, base pairs.*

4.3.3 TB4 ELISA

To determine if TB4 was systemically upregulated, the TB4 ELISA described in 3.3.5 was performed on plasma extracted 21 days after NTS induction.

4.3.4 Kidney function

Albuminuria was measured at day 0, 7 days and 21 days after NTS injection by ELISA as described in 3.3.6, however samples were diluted 1/100,000 as the level of albuminuria was much greater than following ADR injury. BUN was analysed at 21 days after NTS nephritis induction by colourimetric assay as described in 3.3.8.

4.3.5 IHC and immunofluorescence

Tissues were fixed in 4% PFA in dH_2O before FFPE and cryo-sections were generated. For FFPE sections, samples were dehydrated in increasing concentrations of ethanol, cleared in Histoclear II and embedded in wax and then sectioned to 5 μm on a microtome as described in 3.3.3. For cryo-sections, tissues were incubated in 30% sucrose overnight, embedded in OCT medium and sectioned to 8 μm on a cryostat as described in 3.3.3. Immunohistochemical and immunofluorescent experiments of NTS mice kidney sections were undertaken as described in 3.3.11 and 3.3.12 respectively. WT-1 positive and F4/80 positive cells were revealed by using previously referenced antibodies (**Table 3.1**). Proliferating nuclei were revealed by immunostaining with anti-Ki67 primary antibody (**Table 3.1**) and then incubation with donkey anti-rabbit secondary antibody conjugated to a 594 nm fluorophore (**Table 3.2**). Sections were co-stained with α-mouse synaptopodin antibody (**Table 3.1**) and anti-guinea pig antibody conjugated to 594 nm fluorophore (**Table 3.2**) to identify podocytes.

4.3.6 Image and statistical analysis

All image analysis was performed on Fiji ImageJ software (Schindelin et al. 2012). Quantification of the number and distribution of WT-1 positive cells and F4/80 positive cells was performed as described in 3.3.14. Proliferating cells were quantified by counting the number of Ki67 positive nuclei inside the whole glomerular tuft and in synaptopodin positive areas. Statistical analyses were performed as described in 3.3.15.

4.4 **Results**

4.4.1 AAV 2/7 induced systemic upregulation of TB4

To induce a sustained systemic upregulation of TB4, C57BL/6 mice were treated with AAV serotype 2/7 encoding the *Tmsb4x* transgene. To determine if AAV was successfully transducing liver cells, levels of *Tmsb4x* mRNA in the liver were examined by qPCR. Mice injected with AAV.*Tmsb4x* showed a 2.7 ± 0.3-fold increase in *Tmsb4x* mRNA in the livers, which was significantly higher than PBS ($P<0.01$) and AAV.*LacZ* ($P<0.05$) treated mice (**Figure 4.2a**).

To confirm that the increase in liver *Tmsb4x* levels caused systemic upregulation of TB4, the plasma concentration of TB4, was quantified by ELISA 3 weeks after NTS injection. The TB4 plasma concentration in PBS and AAV.*LacZ* treated mice was 3.4 ± 2.2 μg/ml and 1 ± 0.4 μg/ml respectively. Mice injected with NTS with TB4 gene therapy had a plasma TB4 concentration of 11.9 ± 2 μg/ml, which was significantly more than both PBS ($P<0.05$) and *LacZ* ($P<0.05$) treated mice, confirming the systemic upregulation of TB4 (**Figure 4.2b**). TB4 gene therapy did not change whole kidney levels of *Tmsb4x* mRNA compared with PBS and AAV.*LacZ* injected mice with NTS (**Figure 4.2c**).

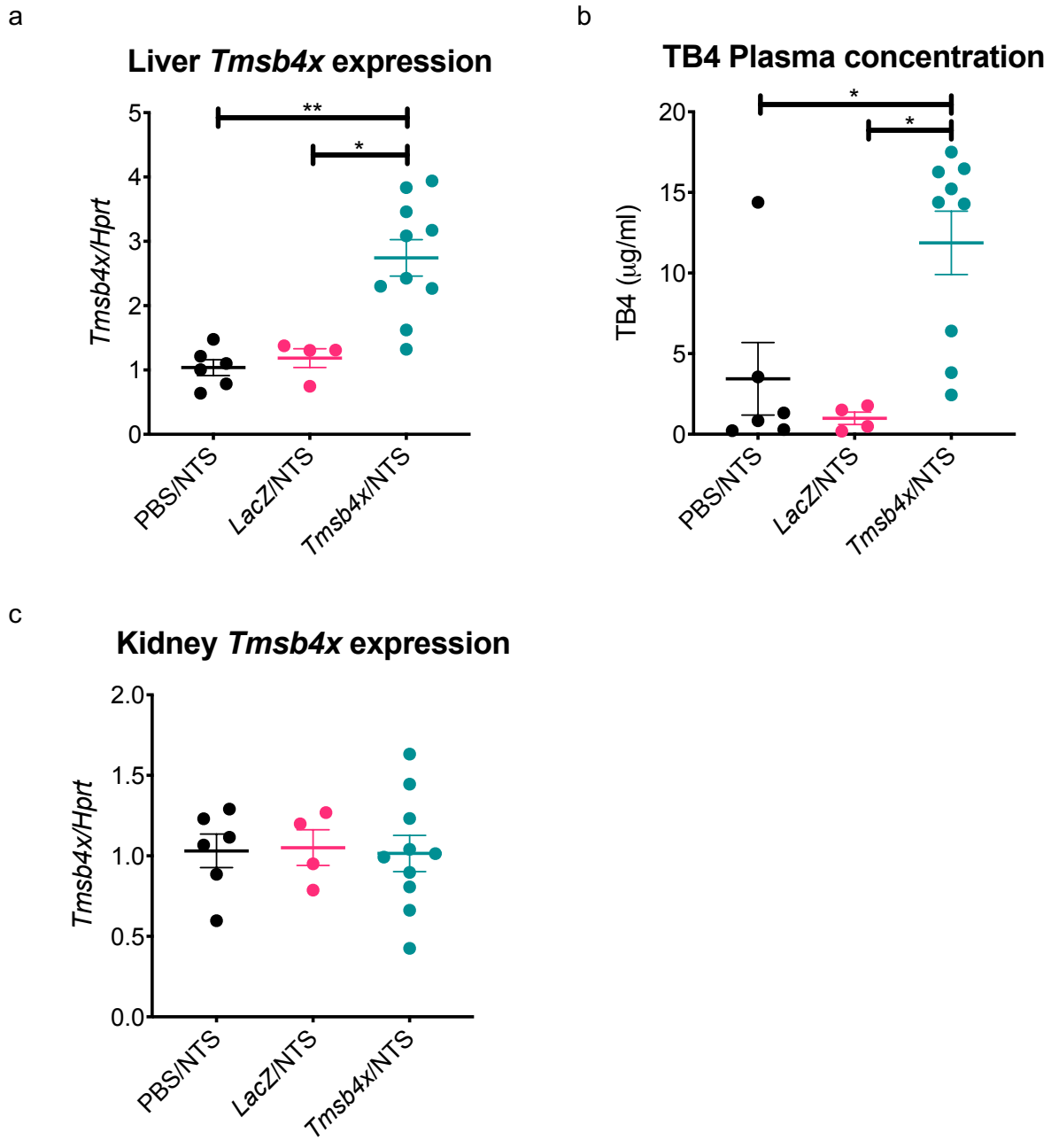

Figure 4.2 – AAV 2/7 systemically upregulated TB4. *7-10-week-old mice were injected with PBS, AAV.LacZ or AAV.Tmsb4x 4 weeks before injection of NTS. Blood was taken by cardiac puncture 21 days after NTS injection and assessment of circulating TB4 concentration was quantified by ELISA. qPCR was performed to assess levels of Tmsb4x in livers and kidneys 21 days after NTS injection.* ***(a)*** *Tmsb4x mRNA levels in the liver.* ***(b)*** *Quantification of circulating TB4 concentration in the plasma.* ***(c)*** *Expression of Tmsb4x in the kidney. Hprt was used as a housekeeping gene for qPCR. Each data point represents the mean of duplicate values from 1 individual mouse. Data are shown as the mean ±SEM of at least 4 individual mice. N=6 for PBS/NTS, N=4 for LacZ/NTS group and N=10 for Tmsb4x/NTS group. *P≤0.05, **P≤0.01 between treatment groups. Tmsb4x, TB4; LacZ, β-galactosidase; PBS, Phosphate buffered saline; Hprt, Hypoxanthine-guanine phosphoribosyltransferase.*

4.4.2 NTS reduced mouse body weight

To examine the effect of NTS and TB4 on the body weight of mice, mice from all three groups were weighed at day 0, day 7 and day 21 after NTS induction. There was no significant difference between the body weights of the mice before NTS injection (day 0) (**Figure 4.3b**).

After 7 days, NTS injured mice injected with PBS mice weighed 0.9 ± 1.3% less than the day of NTS injection, which was not significantly different, however, the mice weighed 6.3 ± 1.2% less 21 days after NTS injection, which was significantly lower than the same group at day 0 ($P<0.05$). Mice treated with *LacZ*/NTS weighed 4.1 ± 1.8% less after 7 days, but this was not significant compared to day 0. At day 21 of NTS treatment, *LacZ*/NTS mice weighed 5.3 ± 1.6% less than the day of NTS injection, but once again this was not significantly lower than day 0. After 7 days of NTS treatment, NTS treated mice with TB4 gene therapy lost 1.2 ± 2.8% of their body weight compared to day 0, which was not significant. At day 21, the weight loss was increased to 3.7 ± 2.5% but was not significantly lower than day 0 or day 7. There were no significant differences between the treatment groups at any time point (**Figure 4.3a**).

To examine if TB4 had any effect of the kidney weights in NTS nephritis, the right kidneys were weighed 21 days after NTS injection, and kidney weights were also normalised to body weight (g/g). Kidneys from mice treated with PBS and NTS weighed on average 0.25 ± 0.01 g, which equated to a kidney weight to body weight ratio of $8.6 \times 10^{-3} \pm 0.3 \times 10^{-3}$ g/g. Kidneys from mice injected with AAV.*LacZ* and NTS weighed on average 0.24 ± 0.01 g, which was equal to $8.2 \times 10^{-3} \pm 0.3 \times 10^{-3}$ g/g. TB4 gene therapy did not alter kidney weights after NTS injection, as kidneys weighed on average 0.22 ± 0.01 g, which equated to $7.9 \times 10^{-3} \pm 0.2 \times 10^{-3}$ g/g. There were no significant differences between groups in either set of data (**Figure 4.3c, d**).

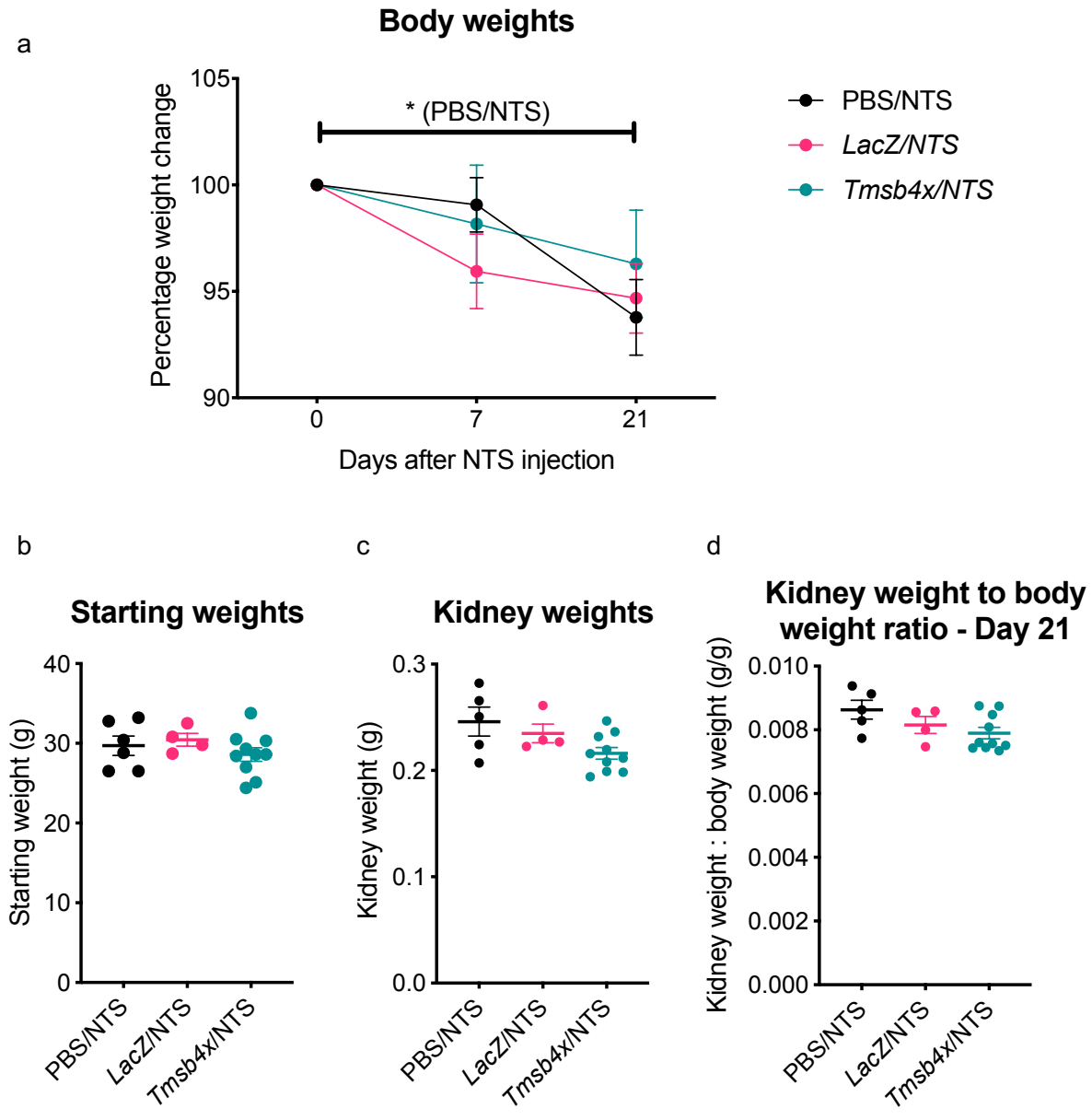

Figure 4.3 - TB4 did not affect body or kidney weight. ***(a)*** *Mouse body weights were recorded at day 0, 7 and 21 after NTS induction.* ***(b)*** *Mice from all three groups weighed the same on day 0.* ***(c)*** *There was no difference in the kidney or* ***(d)*** *kidney weight to body weight to body weight ratio 21 days after NTS induction. Each data point represents 1 mouse. All data are shown as the mean ±SEM of at least 4 individual mice. N=6 for PBS/NTS, N=4 for LacZ/NTS group and N=10 for Tmsb4x/NTS group. *P≤0.05 between time points.*

4.4.3 NTS or TB4 did not alter urine volume

Next, to examine how much urine the mice were excreting throughout the experiment, the urine volumes were recorded on day 0, 7 and 21 after NTS injection. On day 0, PBS treated mice excreted 778 ± 112 μl/24 hours, which rose to 830 ± 240 μl/24 hours 7 days later. After 21 days of NTS treatment, PBS treated mice excreted 1691 ± 296 μl/24 hours. Mice treated with AAV.*LacZ* urinated 612 ± 88 μl/24 hours prior to NTS injection, which rose slightly to 630 ± 293 μl over 24 hours on day 7 and 1237 ± 314 μl/24 hours on day 21 after NTS injection. Before NTS injection, mice treated with TB4 gene therapy urinated 547 ± 161 μl/24 hours, and 483 ± 176 μl/24 hours on day 7. After 21 days of NTS nephritis, *Tmsb4x*/NTS mice urinated 1483 ± 333 μl/24 hours. There were no significant differences between any groups at any time point or within each group (**Figure 4.4**).

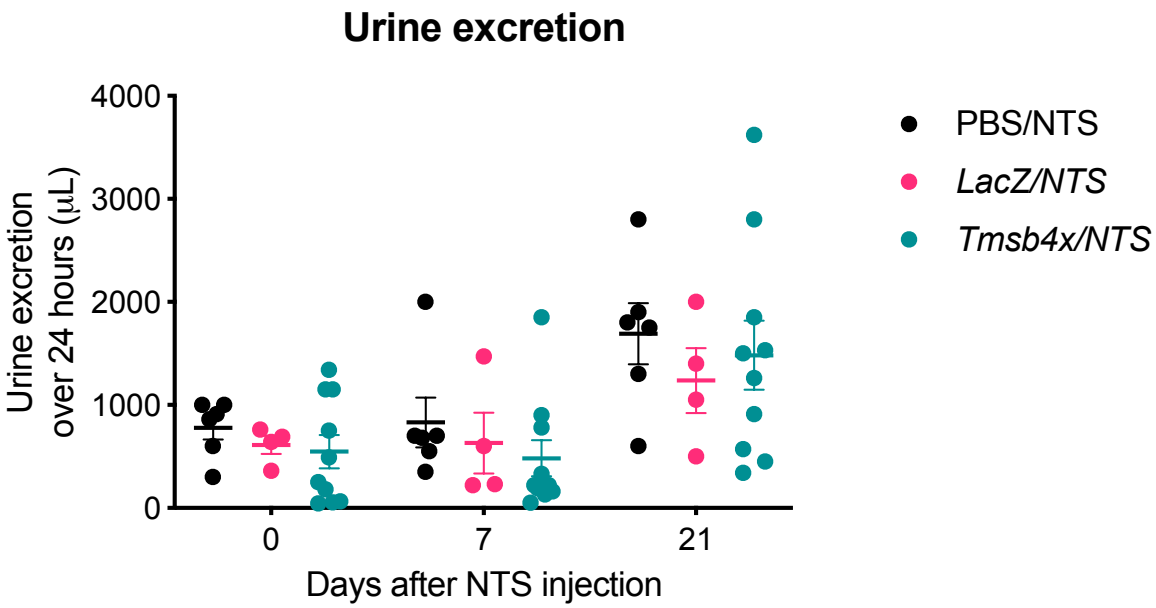

Figure 4.4 – Urine excretion in NTS experiment. *Urine volumes were recorded at day 0, 7 and 21 after NTS injection, and adjusted for 24-hour volume. Each data point represents the 24-hour urine volume of 1 mouse. All data are shown as the mean ±SEM of at least 4 individual mice. N=6 for PBS/NTS, N=4 for LacZ/NTS group and N=10 for Tmsb4x/NTS group.*

4.4.4 Exogenous TB4 prevented NTS-induced early albuminuria but there were no alterations to BUN

One of the features of NTS nephritis in C57BL/6 mice is an increase in albuminuria (Vasilopoulou et al. 2016), therefore the amount of albumin in the urine was assessed by ELISA. Before NTS injection (day 0), PBS treated mice excreted on

average 13 ± 2 μg of albumin in 24 hours, AAV.*LacZ* treated mice 14 ± 3 μg/24 hours and mice treated with TB4 gene therapy 10 ± 2 μg/24 hours of albumin with no significant differences between the groups. After 7 days of NTS nephritis, PBS and AAV.*LacZ* treated mice urinated on average 8635 ± 3781 μg and 10956 ± 4472 μg/24 hours respectively, each significantly more than their respective day 0 values ($P<0.05$ vs day 0 in both groups). Mice treated with TB4 gene therapy urinated on average 2144 ±1193 μg/24 hours, which was significantly less than both PBS ($P<0.05$) and AAV.*LacZ* ($P<0.05$) treated mice. On day 21 after NTS injection, PBS treated mice albumin excretion was on average 33494 ± 7151 μg/24, which was significantly more than the same group at day 7 ($P<0.05$). AAV.*LacZ* treated mice urinated 32757 ± 9012 μg albumin per 24 hours, which was significantly more than the same group at day 7 ($P<0.05$). NTS injected mice with TB4 gene therapy excreted 33015 ± 6811 μg/24 hours, which was significantly more compared with the same mice 7 days post NTS induction ($P<0.01$). There were no significant differences between the mouse groups 21 days after NTS injection (**Figure 4.5a**).

NTS nephritis has been associated with an increase in BUN (Kvirkvelia et al. 2013), therefore BUN was assessed 21 days after NTS injection. PBS and AAV.*LacZ* treated mice had a BUN concentration of 50.8 ± 6.8 mg/DL and 42.3 ± 4.6 mg/DL respectively, and there were no significant differences between these two groups. Mice treated with TB4 gene therapy had a plasma BUN concentration on 50.7 ± 5.3 mg/DL, which was not significantly different to either group (**Figure 4.5b**).

Collectively, these results show that TB4 gene therapy dampened the NTS induced increase in albuminuria at day 7 of NTS nephritis, but not at day 21. This thesis chapter then proceeded to examine the glomeruli to investigate any potential mechanisms of TB4 mediated protection.

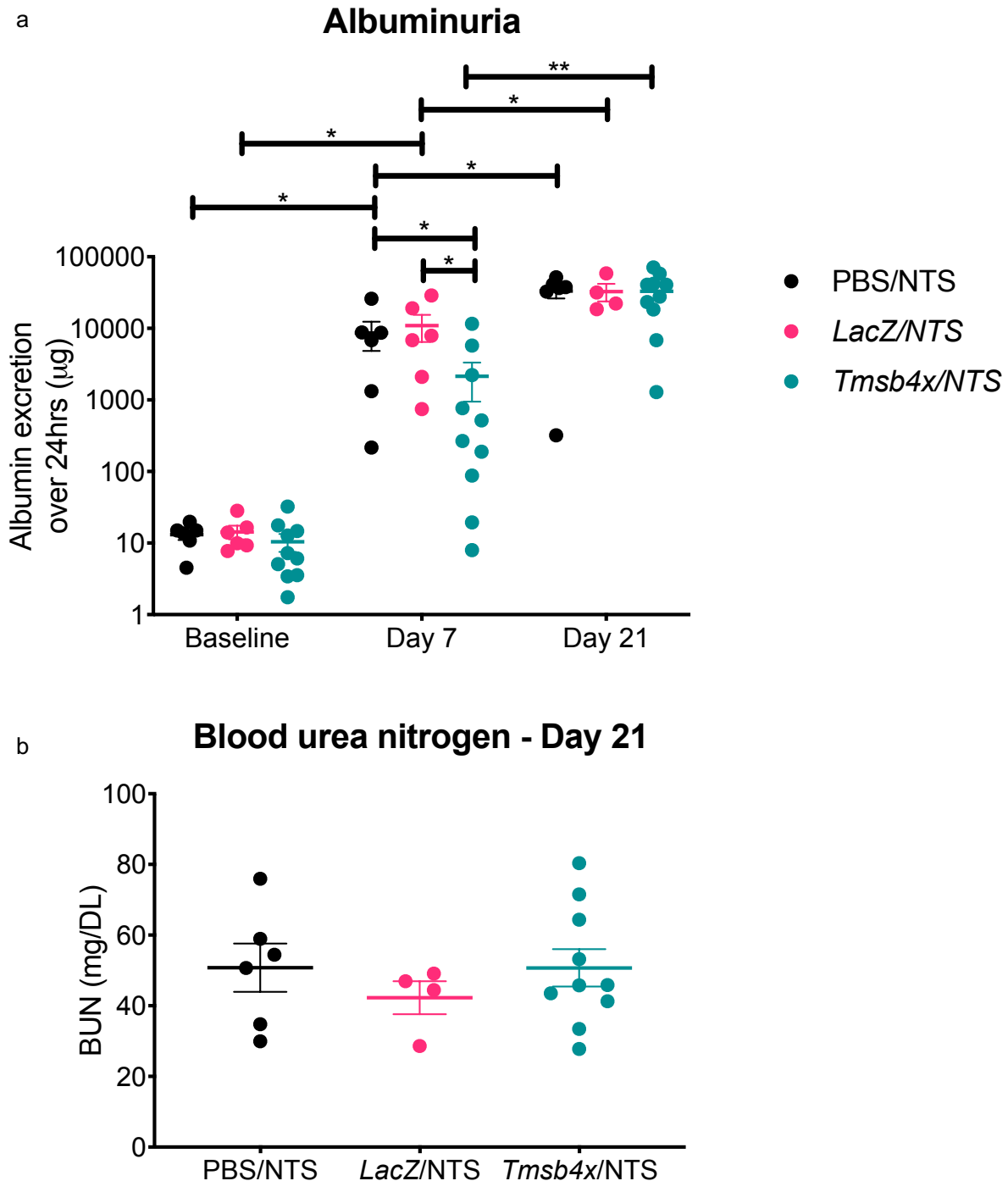

Figure 4.5 – Exogenous TB4 suppressed albuminuria but not BUN in NTS nephritis. *Urinary albumin concentration was determined at day 0, 7 days, and 21 days after NTS injection.* ***(a)*** *Amount of urinary albumin excreted over 24 hours by mice on day 0, 7 and 21 after NTS injection.* ***(b)*** *BUN concentration 21 days after NTS injection. Each data point represents the mean of replicate values from 1 individual mouse. All data are shown as the mean ±SEM of at least 4 mice. N=6 for PBS/NTS, N=4 for LacZ/NTS group and N=10 for Tmsb4x/NTS group. *P≤0.05, **P≤0.01 between groups.*

4.4.5 Exogenous TB4 increased podocyte number 21 days after NTS induction

Podocyte loss has been reported as early as day 1 in NTS nephritis (Shirato *et al.*, 1996; Puelles *et al.*, 2019). Therefore, to determine if exogenous TB4 could prevent podocyte loss in NTS nephritis, FFPE sections obtained 21 days after NTS injection were stained with α-mouse WT-1 antiserum followed by a HRP conjugated secondary antibody. Representative images of glomeruli from all three treatment groups immunostained for WT-1, a nuclear marker specific to podocytes in the glomerular tuft (Lefebvre et al. 2015) are provided in **Figure 4.6a, b, c**. Antibody specificity was confirmed by omitting the primary antibody (**Figure 4.6d**).

Firstly, the area of individual glomerular cross sections was measured. PBS treated mice had an average glomerular cross section of 3849 ± 194 μm^2. AAV.*LacZ* treated mice average glomerular cross-sectional area was 3606 ± 121 μm^2. TB4 gene therapy did not alter glomerular cross-sectional area, as the average area was 3696 ± 83 μm^2. There were no significant differences between the groups (**Figure 4.6e**).

The number of WT-1 positive cells were then counted in the glomerular tuft and measured as an average of 50 glomeruli per mouse and as individual glomeruli. When the average of 50 glomeruli per mouse were analysed, PBS treated mice had an average of 14.3 ± 1.2 WT-1 positive cells per glomerulus. AAV.*LacZ* treated mice had an average of 15.3 ± 1.1 WT-1 positive cells per glomerulus, and there was no significant difference between these groups. Mice treated with NTS and TB4 gene therapy had an average of 18.3 ± 0.7 WT-1 positive cells per glomerulus, which was significantly more than PBS treated mice ($P<0.05$) (**Figure 4.6f**). The number of WT-1 cells were then normalised to glomerular area (podocyte density). Mice treated with PBS and NTS had an average podocyte density of 4.5 $x10^{-3}$ ± 0.5 $x10^{-3}$ podocytes /μm^2, and mice treated with AAV.*LacZ* and NTS had an average podocyte density of 4.8 $x10^{-3}$ ± 0.3 $x10^{-3}$ podocytes /μm^2. There was no significant difference between the groups. Treatment of NTS injected mice with TB4 gene therapy caused no significant differences to podocyte density compared to both other groups, and the mice had an average of 5.6 $x10^{-3}$ ± 0.2 $x10^{-3}$ podocytes/μm^2 ($P=0.067$) (**Figure 4.6g**).

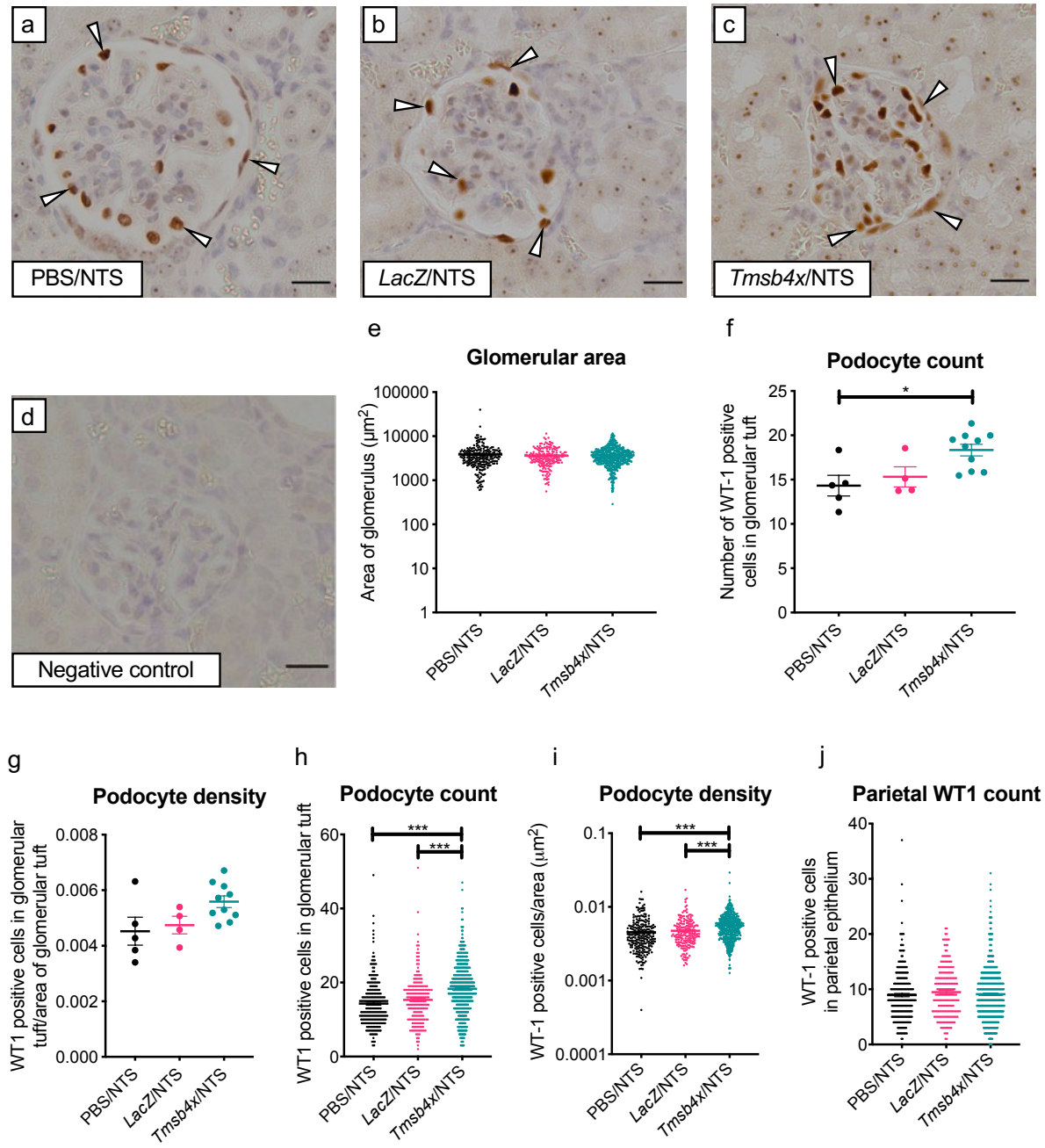

Figure 4.6 – Exogenous TB4 increased podocyte number in NTS nephritis. *Representative images of* ***(a)*** *PBS/NTS,* ***(b)*** *LacZ/NTS and* ***(c)*** *Tmsb4x/NTS glomeruli immunostained with α-WT-1 antiserum. Mayer's haematoxylin was used to stain nuclei. Arrowheads indicate positive WT-1 staining.* ***(d)*** *Negative control omitting primary antibody. Scale bar = 20 μm.* ***(e)*** *Comparison of glomerular cross-sectional area, as assessed by individual glomeruli. WT-1 positive cells were counted and analysed as the average of 50 glomeruli per mouse* ***(f)*** *inside the glomerular tuft and* ***(g)*** *normalised to the glomerular tuft area. Each data point represents the average of 50 glomeruli from 1 mouse. Data are shown as the mean ±SEM of at least 4 mice. N=6 for PBS/NTS, N=4 for LacZ/NTS group and N=10 for Tmsb4x/NTS group. Analysis of* ***(h)*** *WT-1 positive cell count,* ***(i)*** *podocyte density, and* ***(j)*** *the number of WT-1 cells in the parietal epithelium when analysed as individual glomeruli. Each data point represents 1 glomerulus. Data are shown as the mean ±SEM of at least 200 glomeruli from at least 4 individual mice. N=300 for PBS/NTS, N=200 for LacZ/NTS group and N=500 for Tmsb4x/NTS group. *P≤0.05, ***P≤0.001 between groups.*

When individual glomeruli were analysed, there was no significant difference in podocyte number or density between PBS and AAV.*LacZ* treated mice. Mice treated with NTS and TB4 gene therapy had significantly increased podocyte number and density than both PBS and AAV.*LacZ* treated mice ($P<0.001$ vs both groups in both data sets) (**Figure 4.6h, i**). Collectively, these results suggest that exogenous TB4 prevented podocyte loss in NTS nephritis.

NTS has been associated with an increase in the number of WT-1 positive PECs (Le Hir et al. 2001; Vasilopoulou et al. 2016), therefore to determine if exogenous TB4 could affect parietal WT-1 expression, the number of WT-1 positive cells in the parietal epithelium were counted. After 21 days of NTS nephritis, PBS treated mice had an average parietal epithelial WT-1 cell count of 8.9 ± 0.3. Mice treated with AAV.*LacZ* had an average of 9.5 ± 0.3 WT-1 positive cells in the parietal epithelium. TB4 gene therapy treated mice had average of 9.1 ± 0.2 WT-1 positive cells in the parietal epithelium, which was not significantly different to either group (**Figure 4.6j**).

4.4.6 NTS did not induce podocyte clustering

WT-1 immunostained images were used to quantify if podocyte clustering was occurring. Clustering was defined as >50% of total podocyte number occupying 25% of the glomerular cross section. However, in this model of NTS nephritis and NTS with exogenous TB4 treatment, podocyte clustering was not observed 21 days after NTS injection. Mice treated with PBS and AAV.*LacZ* showed on average 5.3 ± 3.1% and 6.7 ± 2.8% of glomeruli with podocyte clustering respectively. Treatment with TB4 gene therapy did not alter this number, as mice showed an average of 4.7 ± 1.2% of glomeruli with podocyte clustering. There were no significant differences between the groups (**Figure 4.7a**).

The distribution of podocytes in the upper (tubular pole) and lower (vascular pole) hemispheres of each glomeruli was also examined 21 days after NTS injection. Mice treated with PBS had an average of 52.2 ± 0.4% podocytes in the upper hemisphere and 47.8 ± 0.4% of podocytes in the lower hemisphere. AAV.*LacZ* treated mice had an average of 53.5 ± 0.8% podocytes in the upper hemisphere and 46.5 ± 0.8%

podocytes in the lower hemisphere. TB4 gene therapy did not alter podocyte distribution compared with the two other groups, as mice had an average of 53.5 ± 0.7% of podocytes in the upper hemisphere and 46.5 ± 0.7% podocytes in the lower hemisphere. While there were no significant differences in the distribution of podocytes between the groups, each groups upper and lower hemisphere values were significantly different (P<0.001 within all groups) (**Figure 4.7b**).

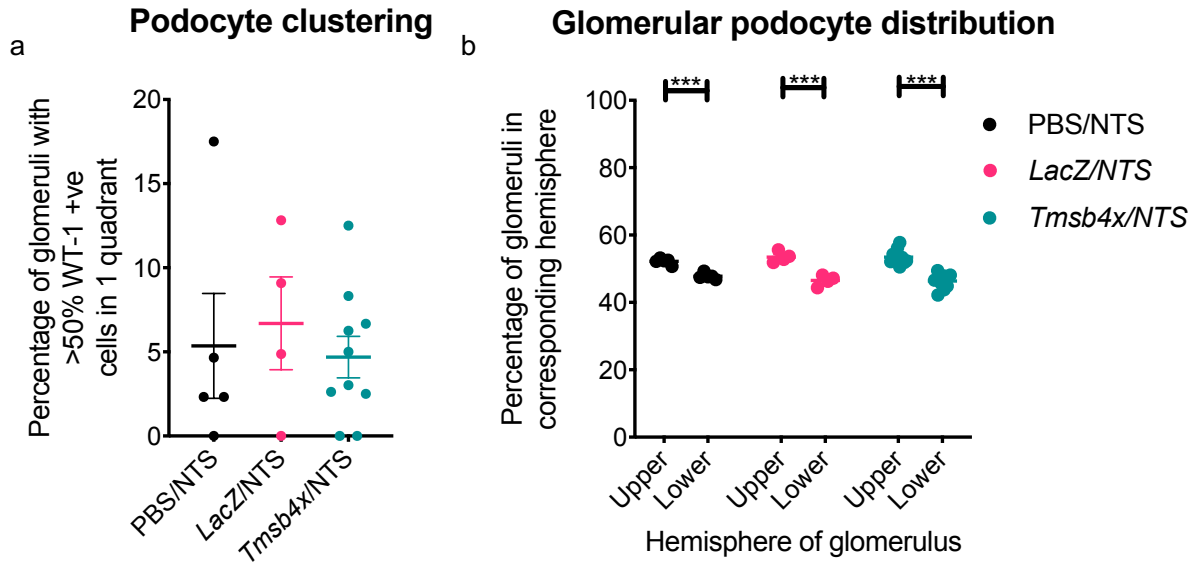

Figure 4.7 – Podocyte distribution in NTS nephritis and exogenous TB4 treatment. *Quantification of **(a)** the number of glomeruli displaying podocyte clustering (>50% of podocytes in 1 quadrant of the glomerulus) and **(b)** the number of cells in each glomerular hemisphere as a percentage of total podocyte number. Each data point represents the mean value of at least 30 glomeruli from 1 mouse. n = 30 for PBS/NTS group, n = 32 for LacZ/NTS group and n = 31 for Tmsb4x/NTS group. All data are shown as the mean ±SEM of at least 4 mice. N=6 for PBS/NTS, N=4 for LacZ/NTS group and N=10 for Tmsb4x/NTS group. ***P≤0.001 between groups.*

4.4.7 NTS induced glomerular proliferation

Next, it was determined if the higher number of WT-1 positive cells caused by TB4 gene therapy was because of podocyte proliferation, which has been observed in NTS nephritis (Bruggeman et al. 2011; Henique et al. 2017). Kidney cryosections were immunostained with α-Ki67 antiserum, a marker of nuclei undergoing proliferation (Polley et al. 2013). Podocytes were identified by co-immunostaining with α-synaptopodin antiserum, and the number of Ki67 positive nuclei in synaptopodin positive regions were counted per glomerulus. Representative images from all three groups are provided in **Figure 4.8a, b, c**. Antibody specificity was confirmed by omitting the primary antibodies (**Figure 4.8d, e, f**). Proliferating

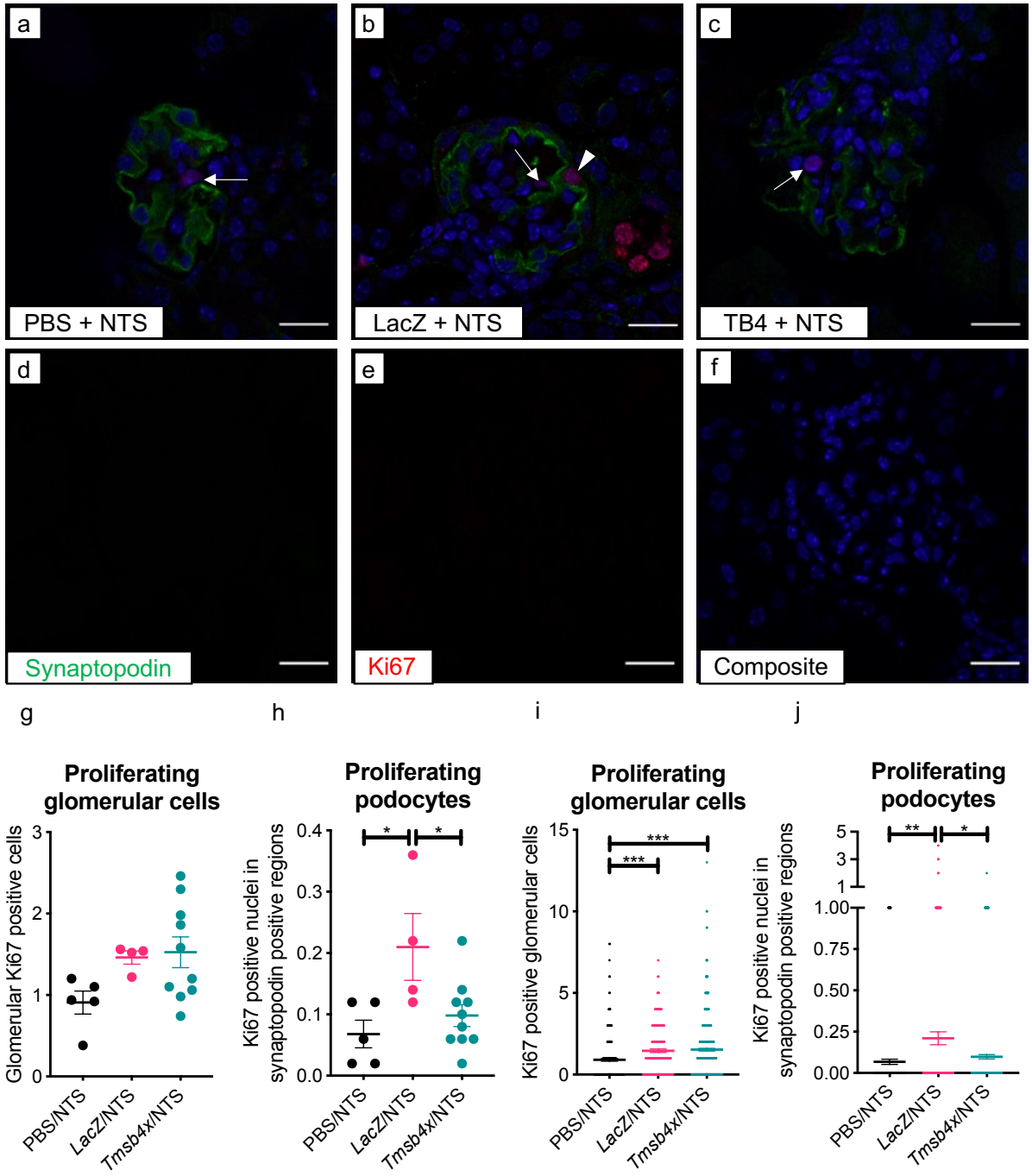

Figure 4.8 – Glomerular proliferation. *Kidney cryo-sections were incubated with rabbit anti-mouse Ki67 primary antibody, guinea pig anti-mouse synaptopodin primary antibody, donkey anti-rabbit secondary antibody conjugated to 594 nm fluorophore and fluorophore conjugated secondary antibodies. Nuclei were stained with Hoechst 33342. Representative images of* ***(a)*** *PBS/NTS,* ***(b)*** *LacZ/NTS and* ***(c)*** *Tmsb4x/NTS glomeruli. Arrows indicate glomerular Ki67 positive nuclei. Arrowhead indicates Ki67 positive podocyte. Negative control of* ***(d)*** *488 nm channel,* ***(e)*** *594 nm channel and* ***(f)*** *composite of all three channels. Scale bar = 20 µm. Ki67 positive cells were counted* ***(g)*** *in the glomerular tuft and* ***(h)*** *in synaptopodin positive regions. Each data point represents the average of 50 glomeruli. Data are shown as the mean ±SEM from at least 4 mice. N=6 for PBS/NTS, N=4 for LacZ/NTS group and N=10 for Tmsb4x/NTS group. Quantification of* ***(i)*** *proliferating glomerular cells and* ***(j)*** *proliferating podocytes when analysed as individual glomeruli. Each data point represents 1 glomerulus. Data are shown as the mean ±SEM from at least 200 glomeruli from at least 4 mice. N=300 for PBS/NTS, N=200 for LacZ/NTS group and N=500 for Tmsb4x/NTS group. *P ≤0.05, **P ≤0.01, ***P ≤0.001 between groups.*

glomerular cells were analysed as an average of 50 glomeruli per mouse and as individual glomeruli.

Firstly, glomerular and podocyte proliferation was examined as an average of 50 glomeruli per mouse 21 days after NTS injection. Mice treated with PBS had an average of 0.9 ± 0.1 Ki67 positive nuclei per glomerulus. AAV.*LacZ* treated mice had an average of 1.5 ± 0.1 Ki67 positive nuclei per glomerulus. TB4 gene therapy treated mice had an average of 1.5 ± 0.2 Ki67 positive nuclei per glomerulus. There were no significant differences between the groups (**Figure 4.8g**). The number of Ki67 positive nuclei in synaptopodin positive regions was then examined. Mice treated with PBS had an average of 0.07 ± 0.02 Ki67 nuclei in synaptopodin positive regions. AAV.*LacZ* treated mice had an average of 0.2 ± 0.05 Ki67 positive nuclei in synaptopodin positive regions, which was significantly more than PBS treated mice ($P<0.05$). Treatment with TB4 gene therapy caused 0.01 ± 0.02 Ki67 positive nuclei in synaptopodin positive regions, which was significantly lower than AAV.*LacZ* treated mice ($P<0.05$), but not significantly different to PBS treated mice (**Figure 4.8h**).

Next, the glomerular and podocyte Ki67 positive cells were analysed as individual glomeruli. *LacZ*/NTS glomeruli showed an increased number of proliferating glomerular cells compared with PBS treated mice ($P<0.001$ vs PBS/NTS). *Tmsb4x*/NTS treated glomeruli showed a similar number to AAV.*LacZ* treated mice, as the number of proliferating glomerular cells was significantly more than PBS treated mice ($P<0.001$ v PBS/NTS) (**Figure 4.8i**). The number of Ki67 positive nuclei in synaptopodin positive regions were also counted, as a measure of proliferating podocytes. Mice treated with AAV.*LacZ* had significantly more proliferating podocytes than PBS/NTS treated mice ($P<0.01$). *Tmsb4x*/NTS treated mice had significantly fewer proliferating podocytes than *LacZ*/NTS treated mice ($P<0.05$) (**Figure 4.8j**). These results suggest that podocyte proliferation was not the cause of the increased podocyte number observed in 4.4.5, as there was only a small number of proliferating podocytes observed.

4.4.8 Whole kidney Inflammatory and fibrotic mRNA levels in NTS nephritis were not altered by TB4

NTS nephritis induces glomerular inflammation, fibrosis and collagen deposition (Le Hir et al. 2001; Vasilopoulou et al. 2016). Therefore, the levels of some fibrotic and inflammatory mRNA transcripts in whole kidneys were examined by qPCR 21 days after NTS injection.

Cluster of differentiation 68 (CD68) is expressed in monocytes and tissue macrophages (Holness and Simmons 1993), therefore alterations to *Cd68* mRNA in whole kidneys could suggest changes in inflammation. Exogenous TB4 did not alter *Cd68* mRNA expression compared to PBS/NTS and *LacZ*/NTS treated mice (**Figure 4.9a**). MCP-1, also known as C-C motif chemokine 2 precursor (CCL2) is a chemokine produced in the inflammatory response (Deshmane et al. 2009), that recruits macrophages (Cranford et al. 2016). Macrophages, among other immune cells, then produce and secrete TNF-α in the acute inflammatory reaction to promote apoptosis and necrosis (Idriss and Naismith 2000).

The mRNA levels of *Ccl2* and *Tnf-*α were examined, however, exogenous TB4 had no effect on the levels of either mRNA transcript compared with PBS/NTS and *LacZ*/NTS treated mice (**Figure 4.9b, c**). α-SMA and collagen IV are markers of interstitial fibrosis and mesangial expansion and increased expression of these proteins is associated with glomerular injury, including NTS nephritis (Boukhalfa et al. 1996; Johnson et al. 1991; Khan et al. 2005). After 21 days of NTS nephritis, exogenous TB4 did not alter the mRNA levels of *Acta2* or *Col4a1* compared with both PBS/NTS and *LacZ*/NTS treated mice (**Figure 4.9d, e**).

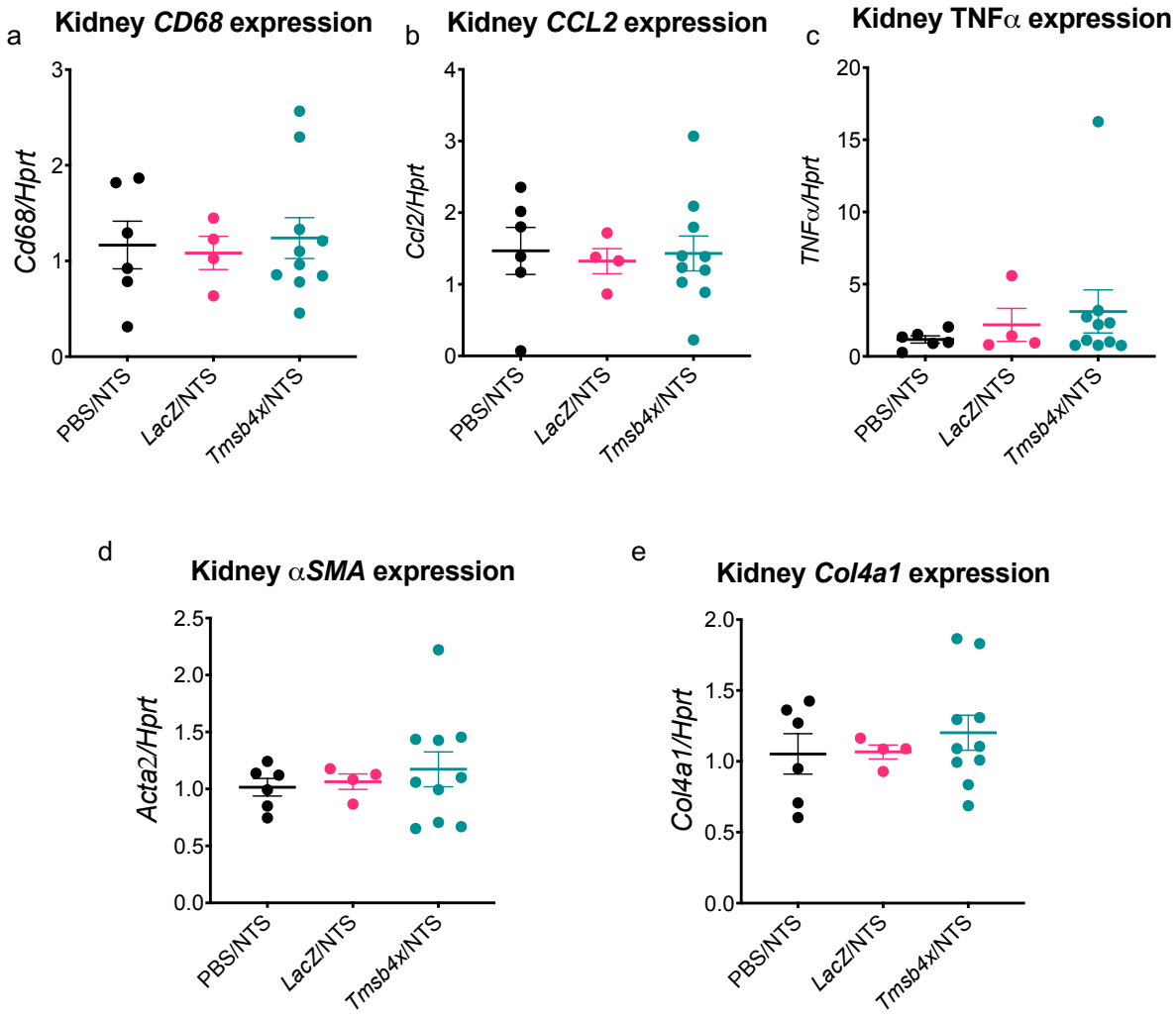

Figure 4.9 – mRNA levels of inflammatory and fibrotic markers in whole kidney lysates. *Kidneys were harvested 21 days after kidney disease induction and mRNA was extracted. Gene expression was assessed by real time PCR. Expression of* ***(a)*** *Cd68* ***(b)*** *Ccl2,* ***(c)*** *Tnf-α,* ***(d)*** *αSMA and* ***(e)*** *Col4a1 21 days after kidney disease induction. Hprt was used as a housekeeping gene. Each data point represents the mean of replicate values from 1 mouse kidney. All data are shown as the mean ±SEM of at least 4 individual mice. N=6 for PBS/NTS, N=4 for LacZ/NTS group and N=10 for Tmsb4x/NTS group. CD68, cluster of differentiation 68; αSMA, α smooth muscle actin; Col4a1, Collagen IV; CCL2, monocyte chemoattractant protein 1; TNF-α, tumour necrosis factor α.*

4.4.9 Effect of TB4 gene therapy on glomerular inflammation in NTS nephritis

The previous section of this thesis chapter suggested that exogenous TB4 did not alter the mRNA levels of inflammation and fibrosis markers. Although screening of whole kidney mRNA levels is informative, it does not always translate to protein expression and does not provide information about localised changes in the glomerulus. Glomerular inflammation and macrophage accumulation are associated with increased albuminuria in NTS nephritis (Chalmers et al. 2015; Kaneko et al. 2018). Therefore, glomerular inflammation was assessed by IHC for F4/80, a marker for macrophages (Austyn and Gordon 1981). Representative images of glomeruli from all three groups are presented in **Figure 4.10a, b, c**. Antibody specificity was confirmed by omitting the primary antibody (**Figure 4.10d**). Data was analysed as an average of 50 glomeruli per mouse and as individual glomeruli 21 days after NTS injection.

Firstly, the number of F4/80 positive cells were quantified inside and outside the glomerular tuft and analysed as an average of 50 glomeruli per mouse. PBS and NTS treated mice had an average of 0.1 ± 0.04 F4/80 positive cells in the glomerular tuft. AAV.*LacZ* treated mice had an average of 0.07 ± 0.05 F4/80 positive cells inside the glomerular tuft. Mice treated with NTS and TB4 gene therapy had an average of 0.05 ± 0.02 F4/80 positive cells inside the glomerular tuft. There were no significant differences between any groups (**Figure 4.10e**). The number of F4/80 positive cells were then counted outside the glomerular tuft. PBS treated mice had an average of 27.1 ± 2.5 F4/80 cells outside the glomerular tuft. AAV.*LacZ* treated mice had an average of 13.1 ± 1.9 F4/80 positive cells outside the glomerular tuft, which was significantly less than PBS treated mice ($P<0.05$). Mice treated with TB4 gene therapy had an average of 19 ± 2.5 F4/80 positive cells outside the glomerular tuft, and this value was not significantly different to either group (**Figure 4.10f**).

The number of F4/80 positive cells was then analysed as individual glomeruli. AAV.*LacZ* treated mice had significantly less F4/80 positive cells inside the glomerular tuft than PBS/NTS treated mice ($P<0.05$). Mice treated with TB4 gene therapy did not have significantly altered F4/80 positive cells in the glomerular tuft compared with either PBS/NTS or *LacZ*/NTS mice (**Figure 4.10g**). The number of

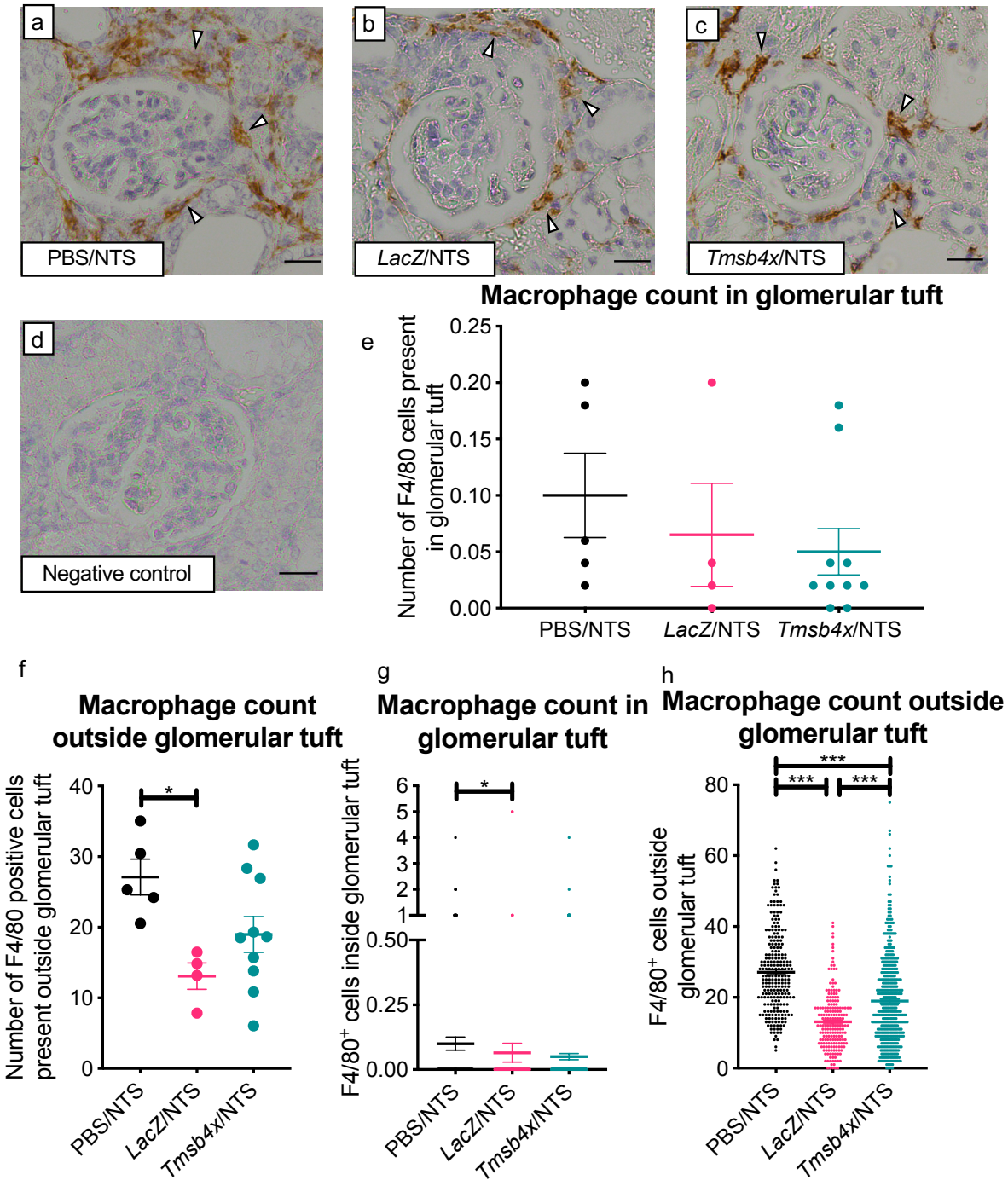

Figure 4.10 – Effect of TB4 gene therapy on glomerular inflammation. *FFPE kidneys sections were incubated with a rat anti-mouse F4/80 primary antibody, rabbit anti-rat secondary antibody conjugated to HRP and anti-rabbit EnVision conjugated to HRP and then positive staining was revealed by 3,3'-Diaminobenzidine incubation. Nuclei were stained with Mayer's haematoxylin. Representative images of **(a)** PBS/NTS, **(b)** LacZ/NTS and **(c)** Tmsb4x/NTS glomeruli. Arrow heads indicate positive F4/80 staining. **(d)** Negative control omitting the primary antibody. Scale bar = 20 µm. F4/80 positive cells were counted **(e)** in the glomerular tuft and **(f)** outside the glomerular tuft. Each data point represents the average of 50 glomeruli. Data are shown as the mean ±SEM of at least 4 mice. N=6 for PBS/NTS, N=4 for LacZ/NTS group and N=10 for Tmsb4x/NTS group. Quantification of the number of F4/80 positive cells **(g)** inside and **(h)** outside the glomerular tuft. Each data point represents 1 glomerulus. Data are shown as the mean ±SEM from at least 200 glomeruli from at least 4 mice. N=300 for PBS/NTS, N=200 for LacZ/NTS group and N=500 for Tmsb4x/NTS group. *P ≤0.05, ***P ≤0.001 between groups.*

F4/80 positive cells was then analysed outside the glomerular tuft. AAV.*LacZ* treated mice significantly less F4/80 positive cells outside the tuft compared with PBS treated mice (P<0.001). Treatment with exogenous TB4 caused significantly more F4/80 positive cells outside the glomerular than AAV.*LacZ* treated mice (P<0.001), but significantly less than PBS treated mice (P<0.001) (**Figure 4.10h**).

4.5 **Discussion**

This thesis chapter has provided evidence that exogenous TB4 suppresses the onset of NTS nephritis a form of severe, autoimmune glomerular injury (Pippin et al. 2009). AAV gene therapy successfully upregulated the circulating TB4 concentration in C57BL/6 mice. Exogenous TB4 suppressed albuminuria after 7 days of NTS nephritis compared with PBS and AAV.*LacZ* treated mice, but not at 21 days after NTS injection. Interrogation of the glomeruli through IHC and immunofluorescence at 21 days of NTS nephritis revealed that exogenous TB4 prevented podocyte loss. This was likely to be independent of TB4s anti-inflammatory properties, as TB4 had no effect on glomerular macrophage accumulation in this model. Collectively, the results presented in this thesis chapter provide some evidence that exogenous TB4 has a beneficial role in the progression of NTS nephritis.

This chapter of the thesis demonstrated that AAV.2/7 successfully transduced the liver, as shown by the increase in *Tmsb4x* transcript levels in the liver by qPCR. ELISAs showed that AAV.*Tmsb4x* treated mice had a higher plasma concentration of TB4 than PBS or AAV.*LacZ* injected mice, providing strong evidence that AAV.*Tmsb4x* caused systemic upregulation of TB4. AAV.2/7 did not transduce kidney cells, as there was no increase in kidney *Tmsb4x* mRNA levels. Therefore, a single injection of AAV induced a long-term increase in plasma TB4 concentration, as the ELISA to measure plasma TB4 concentration was undertaken on plasma taken from the mice 7 weeks after injection. Different doses of intravenous AAV.*Tmsb4x* injection than this thesis have previously been used. The previous chapter of this thesis used $5x10^{12}$ viral particles in comparison to $2x10^{12}$ viral particles in this chapter. Intravenous injection of $5x10^{12}$ viral particles of AAV.*Tmsb4x* has also been used to treat mice with LPS induced sepsis (Bongiovanni *et al.*, 2015). These two higher doses may have induced a higher

upregulation of TB4 than in this thesis chapter, providing a higher degree of protection. Indeed, the previous chapter of this thesis reported a 10-fold upregulation of liver *Tmsb4x* levels compared with AAV.*LacZ* treated mice. However, the plasma circulating concentration was not as high as this thesis chapter, perhaps due to the way the TB4 ELISAs were performed. Collectively, this thesis chapter has provided further evidence that AAV.*Tmsb4x* is an effective method of treating mice with kidney injury.

This thesis chapter showed that exogenous TB4 delays the onset of severe albuminuria in NTS nephritis, an experimental form of severe autoimmune glomerulonephritis (Pippin et al. 2009). An increase in albuminuria is a hallmark of glomerular injury (Gorriz and Martinez-Castelao 2012). Therefore, the prevention of albuminuria by exogenous TB4 provides evidence that exogenous TB4 is protective of the glomerular filtration barrier in NTS nephritis. The levels of albuminuria reflected the severity of glomerular injury. The urinary albumin concentration rose 1000-fold after 7 days compared to the day of NTS injection, and then a further 3.3-fold 21 days after NTS injection in AAV.*LacZ* and PBS treated mice. It is feasible that exogenous TB4 could not prevent the NTS-induced increase in albuminuria 21 days after NTS injection due to the severity of the injury making it possible that exogenous TB4 can prevent albuminuria up to a certain threshold of damage. The role of TB4 in NTS-induced albuminuria has been investigated before. Global knockout of *Tmsb4x* in C57BL/6 mice with NTS nephritis led to a ~5-fold increase in albuminuria after 21 days of NTS nephritis compared with wild type littermates injected with NTS (Vasilopoulou et al. 2016). This study provided evidence that endogenous TB4 acts as a brake to slow the progression of glomerular injury in NTS nephritis. This thesis chapter provides evidence that boosting TB4 levels, at least transiently, therefore, slowing the progression of glomerular injury. The viral titre administered to mice in this thesis chapter was lower than administered to animals in other experimental pathological models (Bongiovanni *et al.*, 2015; Ziegler *et al.*, 2018), therefore future studies could investigate whether a higher dose of AAV may provide increased prevention of albuminuria in NTS nephritis.

In the model of NTS nephritis employed in this thesis chapter, there was a higher number of WT-1 positive nuclei in the TB4 gene therapy treated group compared

with both PBS and AAV.*LacZ* treated mice, and it was shown that this was not due to podocyte proliferation. Therefore, the conclusion can be drawn that exogenous TB4 prevents podocyte loss, which is likely to be a mechanism by which exogenous TB4 prevented albuminuria. Podocyte loss causes areas of the GBM denuded of podocytes, the final component of the glomerular filtration barrier, allowing albumin to enter the urine (Shirato *et al.*, 1996). Podocyte loss has previously been associated with an increase in albuminuria in glomerulonephritis. Mice injected intraperitoneally with 5 mg/kg NTS had podocyte loss after 14 days of NTS nephritis (Puelles et al. 2019). Interestingly, this study used 3D optical clearing techniques to visualise the whole glomerulus, instead of a cross section. Therefore, the number of podocytes reported in healthy glomeruli was ~80 on average, which was reduced to ~30 in NTS nephritis (Puelles et al. 2019). Another study reported progressive loss of podocytes and podocyte density in rats after 7, 14 and 28 days of NTS nephritis, and viable podocytes were detected in the urine at each time point, suggesting that these podocytes had not undergone apoptosis or necrosis (Fukuda et al. 2017). The only previous study that examined TB4 in podocyte loss found that global loss of endogenous TB4 resulted in a lower number of WT-1 positive cells in the glomerular tuft 21 days after injection of NTS, suggesting that endogenous TB4 also prevents podocyte loss in NTS nephritis (Vasilopoulou et al. 2016). Overall, there is significant evidence that TB4 prevents podocyte loss in NTS nephritis, a form of severe glomerular injury, which is likely to be a contributing mechanism by which TB4 protects glomerular function.

This thesis chapter has shown that the protective effects of TB4 in NTS nephritis are likely independent of inflammation. One of the key mechanisms of glomerular damage in NTS nephritis is the inflammatory response (Khan et al. 2005; Moschovaki Filippidou et al. 2020). Macrophages are antigen presenting cells (Martinez-Pomares and Gordon 2007), and can be stimulated by either IFN-γ, LPS or interleukin secretion in inflamed tissues (Fairweather and Cihakova 2009). Macrophages and neutrophils are the major infiltrating cells in autoimmune diseases, and cause damage to inflamed tissues by phagocytosis of healthy cells, release of proteases and oxidants to cause further damage to the tissue (Fairweather and Cihakova 2009). Macrophage depletion in NTS nephritis has been shown to prevent

increased proteinuria, BUN and decreased creatinine clearance (Chalmers et al. 2015; Duffield et al. 2005). This provides strong evidence that macrophages play a key role in the pathogenesis of NTS nephritis and significantly contribute to albuminuria. Therefore, it is a surprise that TB4 was not likely to be modulating inflammation in this model of glomerular injury. The anti-inflammatory properties of TB4 in other tissues, such as the eye (Sosne 2018; Sosne et al. 2002; Sosne, Qiu, Christopherson, et al. 2007), are well established, but TB4 has also previously been shown to prevent inflammation in experimental models of kidney injury. Firstly, endogenous TB4 has been shown to suppress glomerular T cell infiltration and macrophage accumulation after 21 days in NTS nephritis (Vasilopoulou et al. 2016). Endogenous TB4 has also been shown to prevent kidney macrophage infiltration and expression of ICAM-1 in the angiotensin-II model of systemic and kidney hypertension (Kumar *et al.*, 2018). In the IRI model of kidney injury, exogenous TB4 suppressed levels of the pro-inflammatory cytokines NFκB, TNF-α, IL-1β and IL-6 (Aksu et al. 2019). There are similarities and differences between this thesis chapter and the previous studies examining TB4 in the kidney. Firstly, the studies by Vasilopoulou et al., and Kumar et al., both investigated the role of endogenous TB4 in kidney injury, in contrast to the analysis of exogenous TB4 in this thesis chapter. Also, the studies undertaken by Aksu et al., and Kumar et al., were in different forms of kidney injury (IRI and angiotensin-II induced hypertension) that do not specifically target the glomeruli. Like the study by Aksu et al., this thesis chapter did assess the levels of some inflammatory cytokines, such as TNF-α, but in this thesis chapter, the levels were unchanged in mice treated with TB4 gene therapy compared with PBS and AAV.*LacZ* treated mice. The differences between the data are likely because two different injury models were employed, that may induce the inflammatory response in different ways. Also, the study by Aksu et al., examined the protein concentration of these cytokines by Western Blot, whereas this thesis chapter assessed mRNA levels by qPCR, which could account for differences in the data. Taken together, there is significant data available that TB4 is effective in suppressing inflammation in different kidney pathologies, but potentially not NTS nephritis.

One of the limitations of this thesis chapter was that there were some discrepancies between the control groups (PBS and AAV.*LacZ*) in the examination of macrophage

accumulation and in the number of proliferating podocytes and glomerular cells. To date, there has not been any data published examining anti-inflammatory properties of *LacZ* or its translated protein β-galactosidase, only that *LacZ* is expressed in macrophages (Hall et al. 2016). Furthermore, there have been no studies reporting the effects of β-galactosidase in cellular proliferation. The PBS and AAV.*LacZ* treated mouse groups had a lower sample size compared with the TB4 gene therapy treated mouse group. It is likely that the lower sample size in each group contributed to the discrepancies seen. To circumvent this issue, the experiment could be repeated with a higher number of mice in each group. The nephrotoxic phenotypes of NTS are well documented, such as severe albuminuria, podocyte loss and inflammation (Chen et al. 2002; Hoppe and Vielhauer 2014; Vasilopoulou et al. 2016). Therefore, the main aim of this thesis chapter was to determine if TB4 gene therapy can alleviate some of the phenotypes of NTS nephritis. To make the data easier to interpret, an additional mouse group injected with only vehicle, and no NTS, could be included in future studies. One important aspect of this study is that the effect of TB4 on podocyte loss and inflammation was confirmed 21 days after NTS injection. TB4 gene therapy prevented albuminuria at 7 days, but not day 21. It is possible that at 21 days, the damage to the glomeruli that contributed to albuminuria was independent of both podocyte loss and inflammation. One important factor that has not been assessed in this thesis chapter was foot process effacement. This could be examined by electron microscopy, to determine if the interdigitating pattern of podocyte foot processes is still present at 21 days in AAV.*Tmsb4x* compared with PBS and AAV.*LacZ* treated mice. Alternatively, another experiment could be undertaken which culls mice at 7 days of NTS nephritis to examine histology, podocyte number and inflammation to see if the effects of TB4 are seen at this time point.

The main function of TB4 is to regulate the F-actin cytoskeleton (Sanders et al. 1992), therefore the therapeutic effect at 7 days, as seen by decreased albuminuria, could be due to preservation of the cytoskeleton. So far, there has been a limited amount of research into modulating actin-regulating molecules in NTS nephritis. Endogenous sirtuin 1, a NAD^+-dependent deacetylase, is crucial for slowing the progression of NTS nephritis, as *Sirt1* mRNA knockout mice experienced increases

albuminuria, BUN, glomerulosclerosis and tubular cast formation after 7 days (Motonishi et al. 2015). The authors then examined the effect of inhibiting sirtuin 1 in podocytes *in vitro*, and found that the podocytes experienced actin reorganisation, which was induced by sirtuin 1 being unable to deacetylate cortactin, an actin-binding protein that stabilises F-actin (Motonishi et al. 2015; Weaver et al. 2001). This study suggests that protection of the podocyte cytoskeleton by overexpressing sirtuin 1 could prevent NTS nephritis in rodents. Another study examined the effect of knocking out roundabout guidance receptor 2 (Robo2), a cell surface receptor that inhibits myosin IIa activity and podocyte actin polymerisation induced by nephrin (Fan et al. 2012, 2016). Podocyte specific Robo2 inhibition by Cre recombinase alleviated NTS induced albuminuria, foot process effacement and preserved SDs in mice of a C57BL/6 background (Pisarek-Horowitz et al. 2020). Furthermore, Robo2 overexpression in mouse podocytes *in vitro* significantly reduced podocyte F-actin fluorescence intensity, as determined by phalloidin staining, accompanied by podocyte detachment (Pisarek-Horowitz et al. 2020), suggesting that the podocyte protective effects of Robo2 knockout in podocytes could be mediated by the podocyte actin cytoskeleton. There has also been little research into how NTS affects the glomerular cytoskeleton *in vivo,* however, it has been shown that glomerular F-actin alterations occur 6 and 7 days after induction of NTS injury. This is presented as a decrease in mean glomerular F-actin fluorescence and a shift from regular F-actin expression along the capillary loops to irregular expression along the GBM, with some areas showing high accumulation of F-actin, and a build-up in the podocyte cell body in C57BL/6 mice (Besse-Eschmann et al. 2004; Kvirkvelia et al. 2013). Future studies could investigate the effect of exogenous TB4 on the glomerular cytoskeleton at 7 and 21 days by phalloidin staining, to determine if the effect seen on albuminuria is associated with protection of the F-actin cytoskeleton.

4.6 **Conclusions**

The results in this thesis chapter have provided evidence that exogenous TB4 decelerates the onset of NTS nephritis. Systemic gene therapy for TB4 suppressed albuminuria 7 days after NTS injection, which was likely mediated by protection of podocyte loss. Collectively, it is proposed that TB4 is an important component in the

progression of NTS nephritis, and that modulation of TB4 alleviates the phenotypes experienced in glomerulonephritis via podocyte protection.

Chapter 5: General discussion

5.1 The beneficial effect of exogenous TB4 in glomerular and podocyte pathology

This thesis utilised a combination of *in vitro* and *in vivo* experiments to investigate the beneficial potential of exogenous TB4 in podocyte and glomerular injury. Using a novel strategy of gene therapy to systemically upregulate TB4 *in vivo,* it was demonstrated that exogenous TB4 prevented ADR-induced albuminuria by preventing podocyte loss. *In vitro* assessment of the podocyte F-actin cytoskeleton revealed that exogenous TB4 prevented ADR-induced F-actin disorganisation. Furthermore, exogenous TB4 decelerated the early stages of NTS nephritis by preventing podocyte loss, which was likely independent of TB4s anti-inflammatory properties.

Glomerular injury is seen in a large proportion of patients with renal pathologies and is a leading cause of ESKD worldwide (Bikbov et al. 2020). Podocytes are a key component of the glomerular filtration barrier, the component responsible for the ultrafiltration of the blood (Brinkkoetter, Ising, and Benzing 2013). Podocyte foot process effacement and podocyte loss are hallmarks of glomerular injury (Menzel and Moeller 2011). Podocyte actin disorganisation is a significant contributing factor to podocyte foot process effacement and glomerular injury (Shirato *et al.*, 1996; Welsh and Saleem, 2012; Tian and Ishibe, 2016). There are currently therapies available to patients that alleviate proteinuria, that have been proven to protect the podocyte cytoskeleton in experimental models of rodent glomerular injury and podocyte damage in culture. Cyclosporine A is used as a therapy for CKD patients and has been shown to prevent LPS induced proteinuria in severe combined immunodeficient (SCID) mice. This was attributed to blocking the calcineurin-mediated dephosphorylation of the actin regulating protein synaptopodin as demonstrated in cultured podocytes *in vitro* (Faul et al. 2008). The chemotherapeutic drug Vincristine has been used to rescue albuminuria, foot process effacement and glomerulosclerosis in Sprague Dawley rats injured with ADR (Yin et al. 2017). This was associated with the F-actin cytoskeleton, as cultured podocytes exposed to ADR and Vincristine showed stabilised podocyte cell area and loss of actin stress fibres after phalloidin staining, in a similar method to this thesis (Yin et al. 2017).

Fluvastatin is another molecule that modulates the podocyte F-actin cytoskeleton. PAN injured Sprague-Dawley rats treated with Fluvastatin showed reduced proteinuria, improved creatinine clearance, and preserved glomerular expression of the SD proteins nephrin and podocin compared to PAN rats. Podocyte culture *in vitro* showed that Fluvastatin prevented PAN-induced actin reorganisation by suppression of RhoA upregulation (Shibata, Nagase, and Fujita 2006). These studies examining existing therapies demonstrate that targeting the podocyte cytoskeleton is an effective strategy to supress nephrotic syndrome. However, many glomerular pathologies remain resistant to pharmacological intervention (Hejazian et al. 2020). Identification of molecules, such as TB4, that decelerate and prevent the onset of glomerular injury in rodents will facilitate the development of novel therapies that can translate to therapeutic options for CKD patients.

It was shown in this thesis by the novel analysis of single cell RNA sequencing data that podocyte *Tmsb4x* transcripts are reduced in ADR nephropathy *in vivo*. This was *in vitro*, where *Tmsb4x* levels were reduced by ADR in podocytes. By restoring levels of TB4 in ADR nephropathy *in vivo*, increased albuminuria was prevented, and podocyte loss was attenuated. Furthermore, restoring podocyte TB4 levels *in vitro* resulted in prevention of F-actin disorganisation from cortical F-actin fibres to unorganised F-actin. Podocyte specific loss of *Tmsb4x* mRNA in NTS nephritis could be confirmed by undertaking single cell analysis of the published data by (Chung et al. 2020). Loss of endogenous *Tmsb4x* has been previously shown to exacerbate the effects of NTS nephritis *in vivo,* and induce F-actin reorganisation and migration in healthy podocytes *in vitro* (Vasilopoulou et al. 2016). The reduced *Tmsb4x* mRNA levels caused by ADR exposure in this thesis could have contributed to albuminuria and podocyte loss *in vivo* and F-actin disorganisation *in vitro*. Collectively, stabilising the levels of TB4 in injured podocytes and glomeruli is critical for maintaining glomerular function, preventing podocyte loss *in vivo* and preventing podocyte F-actin disorganisation *in vitro*.

Altered levels of endogenous TB4 have recently been implicated in the progression of CKD in human patients. The amniotic fluid concentration of TB4 was 2-fold higher in compromised renal outcome foetal patients compared to healthy patients (Klein et al. 2020). This study also performed IHC of foetal kidneys with congenital

abnormalities, where it was shown that although the expression of TB4 was localised to the tubules in both healthy and compromised renal outcome patients, the renal parenchyma was disorganised in compromised renal outcome patients compared to healthy patients. The study did not quantify the amount of TB4 peptide in diseased kidneys compared to healthy kidneys, which would have provided stronger evidence that the increased levels of amniotic fluid TB4 are linked to the compromised renal outcome. Positive TB4 immunostaining was also absent from both the glomeruli in healthy and compromised renal outcome patients, suggesting that the increased TB4 presence in the amniotic fluid was not derived from podocytes or the glomeruli (Klein et al. 2020). This is a difference to the results presented in this thesis, where it was shown that in adult healthy and ADR-injured mice, TB4 was expressed in the glomeruli and podocytes, which is likely due to the stage of kidney development. In another study examining adult human CKD patients, mass spectrometry identified that patients with ESKD had a 44-fold increased urinary secretion of TB4 compared with healthy patients (Kim et al. 2021). However, patients with primarily glomerular damage, primarily tubular damage and unknown causes of CKD were grouped in the analysis of urinary TB4 quantification, making it impossible to determine if glomerular injury specifically caused increased urinary TB4 concentration. Lysis of cells from different components of the kidney, such as tubular cells, podocytes, or immune cells, such as macrophages that express high levels of TB4 (Vasilopoulou et al. 2016) could have contributed to the increased urinary TB4 concentration, depending on the specific pathology. Taken together, these two studies suggest that kidney disease is associated with increased urinary secretion of TB4. This could a result of TB4 upregulation as a compensatory mechanism to attempt to protect the kidney from further damage. It could also be because there may be a loss of TB4 protein by cellular lysis in the kidney in CKD, causing increased TB4 secretion to the urine. To explore these hypotheses, Western blot protein analysis of homogenised kidney biopsies from CKD patients could confirm if there was an upregulation or downregulation in the amount of TB4 peptide. However, it is a challenge to perform quantification analyses in human tissues, due to difficulty obtaining sufficient amounts of tissue. Therefore, studies in experimental models of rodent glomerular injury allow deeper examination of mechanisms that can cause, or alleviate, pathology.

This thesis employed cytotoxic (ADR) and immune mediated (NTS) forms of glomerular injury models in rodents to investigate the potential of TB4 to improve glomerular disease. Until now, the effect of exogenous TB4 in glomerular injury models was unknown, and this thesis has provided the first evidence that exogenous TB4 is effective in slowing the progression of glomerular injury and development of albuminuria in ADR nephropathy and NTS nephritis. Since the glomerular filtration barrier becomes permeable to albumin in pathology (Savin et al. 1996), it is likely that TB4 prevented glomerular filtration barrier damage in the ADR and NTS nephritis models used in this thesis. This could be proven by electron microscopy studies to examine the podocyte foot processes in high resolution. The preventative effects of TB4 to slow an increase in albuminuria are in agreement with previously published data. Loss of endogenous TB4 exacerbated an increase in albuminuria in NTS nephritis (Vasilopoulou et al. 2016). *Tmsb4x* knockout has also been shown to exacerbate albuminuria compared to wild-type littermates in the non-glomerular specific injury model of angiotensin-II induced hypertension (Kumar *et al.*, 2018). Taken together, TB4 prevents an increase in albuminuria in a diverse range of pathological conditions, providing strong evidence that TB4 is protective of the glomerular filtration barrier.

This thesis is the first study to examine the effect of exogenous TB4 specifically on injured podocytes *in vitro* and *in vivo* and it was shown that exogenous TB4 prevents podocyte loss in ADR nephropathy and NTS nephritis *in vivo*. However, exogenous TB4 was not able to prevent ADR-induced loss of podocyte viability *in vitro*. Differences in the culture conditions *in vitro* and the glomerular microenvironment *in vivo* could account for the variations in the data between the *in vitro* and *in vivo* studies. One major difference between the *in vivo* and *in vitro* conditions is the presence of blood flow *in vivo*, which circulating factors, such as nitric oxide that TB4 has been induce production of (Ryu, Lee, and Moon 2015), that could have contributed synergistically with TB4 to the prevention of podocyte loss *in vivo*. Furthermore, the GBM *in vivo* is perfectly tailored for podocyte adhesion. Differences in the substrate stiffness between the GBM and Matrigel, the basement matrix that was used to culture the podocytes *in vitro* could have also contributed to discrepancies between the data *in vivo* and *in vitro*. The only previous study examining TB4 in podocytes *in vivo* focused on endogenous TB4 and quantified the

number of WT-1 positive cells in the glomerular tuft in NTS nephritis in *Tmsb4x* knockout and wild-type mice. Loss of endogenous TB4 exacerbated podocyte loss in NTS nephritis compared to wild-type mice with NTS nephritis (Vasilopoulou et al. 2016). One potential mechanism for the TB4 induced protection of podocyte loss *in vivo* is by prevention of podocyte detachment. The F-actin cytoskeleton is linked to the podocyte adhesion molecules integrin and dystroglycan (Lennon, Randles, and Humphries 2014). Exogenous TB4 prevented ADR-induced podocyte F-actin disorganisation *in vitro*, it is therefore possible that exogenous TB4 may also protect the podocyte F-actin cytoskeleton *in vivo*, thus preventing disruption to podocyte adhesion molecules and podocyte detachment from the GBM. Detachment from the GBM could be proved by culturing the urine collected from the mice. If there were viable cells in the urine, that expressed podocyte markers such as nephrin or podocin, it could be concluded that the mechanism of podocyte loss in ADR nephropathy was by podocyte detachment. Another possible mechanism for the prevention of podocyte loss by exogenous TB4 in ADR and NTS glomerular injury *in vivo* is by prevention of apoptosis, as ADR been shown to induce podocyte apoptosis (Zou *et al.*, 2010). Yuan *et al*. demonstrated that exogenous TB4 reduced the number of TUNEL positive tubular cells in response to TGF-β exposure *in vitro*, showing that TB4 can prevent apoptosis in kidney derived cells (Yuan et al. 2017). Exogenous TB4 has also been shown to prevent apoptosis by suppression of increase in the pro-apoptotic transcripts caspase-3 and Bax in cardiomyocytes (Wei et al. 2012). TUNEL staining could be undertaken on kidney sections to prove if this was the mechanism of podocyte loss in this thesis.

This is the first study to quantify the amount of F-actin in injuryed podocytes *in vivo*. One of the major mechanisms proposed in this study is that exogenous TB4 does not alter the amount of podocyte F-actin but prevents disorganisation of the podocyte F-actin cytoskeleton, therefore preventing damage to the glomerular filtration barrier. Previously, loss of endogenous *Tmsb4x* was shown to cause increased RhoA activity, which was linked with increased podocyte cytoplasmic stress fibres *in vitro* (Vasilopoulou et al. 2016). There are differences in the actin arrangements observed following loss of TB4 or ADR injury, however, collectively these results demonstrate that TB4 can maintain F-actin organisation in podocytes. Overall, the results

presented in this thesis, along with previous literature, re-enforce the evidence that exogenous TB4 is protective of F-actin in pathological conditions. Future studies could examine Rho GTPase activation levels or the F-actin to G-actin ratio to elucidate the mechanisms that underlie the protective effects of TB4 on the podocyte cytoskeleton.

An alternative mechanism that contributes to albuminuria is the vesicular transcytosis of albumin in podocytes from the bloodstream to the urinary space. This has been demonstrated in rodents as assessed by electron, confocal and intravital microscopy in experimental models of glomerular injury (Burford et al. 2017; Ichimura et al. 2019; Schießl et al. 2016). Increased prevalence of vesicles was observed in ADR nephropathy, which TB4 prevented. F-actin encapsulated vesicles were not observed in ADR-injury *in vitro*, likely due to the absence of a blood supple, therefore, an absence of albumin to trigger vesicle formation. Polymerisation of F-actin is critical for the formation of endocytic vesicles (Hinze and Boucrot 2018), and since the major property of TB4 is to sequester G-actin, it is possible that G-actin sequestering prevented vesicle formation in ADR nephropathy. TB4 has been shown to reduce endocytic vesicle formation *in vitro* (Lamaze et al. 1997). TB4 has also been recently shown to bind to the endocytic receptor low density lipoprotein receptor related protein 1 (LRP1) (Munshaw et al. 2021). It has not yet been investigated whether TB4 interacts with receptors that facilitate albumin endocytosis and downstream processing in the kidney. Modulation of vesicle formation and transcytosis of albumin by exogenous TB4 may provide a novel strategy to prevent albuminuria in glomerular disease. Future studies could also perform immunofluorescent staining on kidneys with NTS nephritis, to investigate if vesicle formation was occurring in this immune mediated glomerular injury model.

This thesis used two different glomerular injury models, ADR, which did not involve an inflammatory response, and NTS, which has a significant inflammatory component. Suppression of inflammation is a key characteristic of TB4 (Sosne, Qiu, and Kurpakus-Wheater 2007), and its anti-inflammatory properties have previously been showcased in kidney injury. *Tmsb4x* knockout in C57BL/6 mice exacerbated glomerular inflammation in both the NTS nephritis and angiotensin II hypertensive kidney injury models (Vasilopoulou *et al.*, 2016; Kumar *et al.*, 2018). Exogenous TB4

was also shown to suppress inflammatory cytokine levels such as NFκB, TNFα, IL-1β and IL-6, in the IRI model of kidney injury compared to vehicle treated rats as shown by Western blot of whole kidney lysates (Aksu et al. 2019). Interestingly, TB4 did not affect inflammation in the UUO model in C57BL/6 mice, as determined by F4/80 immunostaining, however, its metabolite AcSDKP significantly reduced glomerular macrophage accumulation compared to vehicle treated mice (Zuo et al. 2013). It is possible that any anti-inflammatory effects that occurred in the NTS nephritis model, but not observed in this thesis such as T or B cell suppression, were due to AcSDKP, as TB4 is metabolised within 6 hours of generation (Mora et al. 1997). To confirm if this is the case, the study could be repeated with the addition of a POP inhibitor, to prevent AcSDKP formation from TB4.

Fibrosis is caused by prolonged injury, and the inflammatory response has been associated with increased fibrosis in the kidney (Lee and Kalluri 2010). Prevention of fibrosis is a major mechanism in which TB4 has been implicated as a beneficial agent in kidney injury. In the UUO model of kidney injury, daily injection of 150 μg of TB4 intraperitoneally prevented interstitial fibrosis as quantified by Sirius red staining (Zuo et al. 2013). This was mediated by suppressing PAI-1 and TGF-β signalling, as determined by Western blot experiments of whole kidney lysates (Zuo et al. 2013). Intragastric lavage administration of 1 mg/kg/day and 5 mg/kg/day of exogenous TB4 reduced the protein levels of TGF-β, α-SMA and increased P-cadherin in the UUO model in Sprague-Dawley rats, as determined by Western blot (Yuan et al. 2017). In this thesis, it was shown that exogenous TB4 did not alter mRNA transcript levels of α-SMA and collagen IV in NTS nephritis. Future studies could determine if TB4 is alleviating fibrosis in the NTS and ADR models of glomerular injury by periodic acid Schiff or Sirius red staining, or quantifying the protein levels of fibrotic markers, such as TGF-β and α-SMA by Western blot.

5.2 **Limitations and future perspectives**

The data presented in this thesis has demonstrated that exogenous TB4 is a beneficial molecule in the context of early glomerular injury by modulation of the podocyte cytoskeleton and inflammation. This thesis has provided groundwork for follow up studies examining TB4 in kidney disease. Pharmacological interventions to

treat CKD are often prescribed when the progression of CKD is too advanced, as a large proportion of patients are asymptomatic until kidney function is depleted (Hirst et al. 2020). The experimental models used in this thesis pre-treated mice with AAV encoding *Tmsb4x* prior to the induction of glomerular injury as a preventative strategy. This is a limitation, because if the use of AAV.*Tmsb4x* was to be translated to human glomerular injury, it would be a challenge to treat the population with AAV.*Tmsb4x* in the chance that they may develop ESKD. The preventative therapy strategy was used because the transcriptional activation window is variable when using AAV gene therapy (Lackner and Muzyczka 2002), making it difficult to induce systemic TB4 upregulation that coincides with the onset of glomerular injury. To circumvent this issue, future studies could perform a time course experiment to identify when circulating TB4 concentration peaks. Mice would be injected with $5x10^{12}$ viral particles, the highest dose used in this thesis, and plasma extracted at day 0, 4, 7, 10, 14 and 21 after injection of AAV to determine when TB4 concentration peaks. Using this data, the ADR and NTS experiments could be repeated to induce systemic upregulation of TB4 after the onset of glomerular injury, to examine whether TB4 can reverse glomerular pathologies, as well as preventing them in these experimental models.

There were some differences in the efficacy of TB4 gene therapy suppressing increased albuminuria in ADR nephropathy and NTS nephritis in this thesis. Exogenous TB4 completely prevented the ADR-induced increase in albuminuria at 14 days, but only suppressed the increase transiently at 7 days in NTS nephritis. There were variable factors between the experiments which could explain these differences, such as the severity of injury. The maximum average albuminuria value induced by ADR was 1,448 μg/24 hours at 14 days, whereas the NTS-induced albuminuria values reached ~10,000 μg/24 hours at 7 days and ~33,000 μg/24 hours at 21 days. It is possible that NTS induced too severe glomerular injury at 21 days and the systemic upregulation of TB4 was not enough to alleviate this. Another difference was the mechanism of damage. ADR induces a cytotoxic effect to podocytes (Papeta et al. 2010), whereas NTS nephritis induces an autoimmune response against the whole glomerulus (Khan et al. 2005). To determine if the cause of the variance in albuminuria was the experimental model used, the ADR

nephropathy experiment could be repeated, but instead of a 14-day end point, a longer exposure to ADR could be utilised. Prolonged ADR exposure would result in more severe damage to the podocytes, causing higher albuminuria values. If TB4 was still able to fully prevent albuminuria, it could be postulated that exogenous TB4 has a higher efficacy to prevent albuminuria in an injury model that specifically targets the podocytes. Taking this further, the experiment could also be repeated in other kidney injury models such as diabetic nephropathy. Diabetes is a disease that affects many other organs in the body, and glomerular filtration barrier damage is a co-morbidity of hyperglycaemia (Dronavalli et al. 2008). Exogenous TB4 has been shown to suppress microalbuminuria in a model of type 2 diabetic nephropathy, however, TB4 was administered by daily intraperitoneal injection, and the effects of exogenous TB4 on the glomeruli were not examined in great detail (Zhu et al. 2015). TB4 gene therapy could therefore be explored in other forms of glomerular and kidney injury to determine if the effect seen in ADR nephropathy and NTS nephritis is translatable.

Another limitation of this thesis is the differences in the dosing of AAV between the two injury models, which could have contributed to differences in the ability of TB4 to prevent albuminuria. ADR treated mice were pre-treated with $5x10^{12}$ viral particles (Chapter 3) versus a lower dose of $2x10^{12}$ viral particles in the NTS experiment (Chapter 4). The liver mRNA levels of *Tmsb4x* were telling of this, as $5x10^{12}$ viral particles caused a 10-fold increase in *Tmsb4x* and $2x10^{12}$ viral particles only caused a 2.5-fold increase. Conversely, the TB4 ELISA of mouse plasmas indicated that $5x10^{12}$ viral particles caused a 3.5-fold increase in plasma TB4 concentration, whereas $2x10^{12}$ viral particles increased plasma TB4 concentration by 10-fold. This difference could be due to a number of factors, such as the mouse strain (BALB/c vs C57BL/6), the quality of plasma extraction and handling of plasma, or the laboratory conditions in which the ELISA was undertaken. Future studies utilising AAV therapy should undertake dose response experiments, in order to identify the AAV titre that is most effective at combating glomerular injury. For example, mice could be injected with 2 $x10^{12}$, 5 $x10^{12}$, 8 $x10^{12}$ and 1 $x10^{13}$ viral particles alongside NTS to examine if a higher viral load could further prevent increased albuminuria.

Delivery of TB4 to the podocytes via AAV injection has not been proven. It was shown that there was no upregulation of *Tmsb4x* mRNA in the kidneys, suggested that viral transduction did not occur in the kidneys. The glomeruli and podocytes both expressed TB4 at high levels in this thesis. There is an abundance of TB4 in healthy and diseased kidneys, making it difficult to distinguish between endogenous and exogenous TB4. In addition, due to its small molecular weight (~4kDa) (Safer et al. 1991), quantification of TB4 by Western blot is challenging. Future studies could use *Tmsb4x* knockout mice (Vasilopoulou et al. 2016), administer AAV.*Tmsb4x* and then perform IHC experiments on kidney sections to identify and localise viral TB4 peptide. An additional control group injecting mice with only PBS (the vehicle that the viral particles were diluted in) could have been included in order to rule out any effects caused by hepatic viral transduction.

The reduction in albuminuria in ADR nephropathy and NTS nephritis provides strong evidence that TB4 gene therapy is protective of the final component of the glomerular filtration barrier. The definitive way to prove that the glomerular filtration barrier is protected by TB4 would be electron microscopy. Electron microscopy offers high resolving power compared with fluorescence and light microscopy, meaning that individual podocyte foot processes can be clearly imaged. Foot process effacement is a defining characteristic of glomerular filtration barrier break down (Deegens et al. 2008). Use of electron microscopy to image the podocyte foot processes in ADR nephropathy and NTS nephritis with and without TB4 gene therapy would conclusively prove if TB4 was protective of the final component glomerular filtration barrier; the podocyte foot processes, as they could be clearly visualised. Furthermore, the use of gold-conjugated antibodies with electron microscopy allows protein expression to be identified and localised to subcellular compartments (Peters, Bos, and Griekspoor 2006). Immunogold labelling has previously been used to identify foot process F-actin reorganisation in NTS nephritis (Shirato *et al.*, 1996), therefore, future studies could quantify podocyte F-actin disorganisation in ADR and NTS nephropathy *in vivo* using this method of imaging.

The glomerular filtration barrier is composed of three components; the podocytes, GBM and capillary endothelial cells (Patrakka and Tryggvason 2010). Mesangial cells also constitute a significant proportion of the glomerular tuft (Shoskes and

McMahon 2012). TB4 was identified to be a therapeutic molecule in the context of podocyte injury in this thesis, however, as the *in vivo* experiments induced a systemic upregulation of TB4, the GBM, mesangium and endothelium would have also been exposed to exogenous TB4. Damage to the endothelium has been associated with increased albuminuria in diabetic nephropathy (Weil et al. 2012), ADR nephropathy (Sun et al. 2013) and NTS nephritis (Kirsch et al. 2012). Alterations to the glomerular mesangial matrix have also been implicated in the progression of diabetic nephropathy (Tung et al. 2018) and nephrotoxic serum nephritis (Toda et al. 2017). The data from the ADR *in vivo* chapter (0) showed that ADR injury reduced the amount of total glomerular F-actin compared to saline treated mice. TB4 gene therapy prevented this change and preserved the amount of glomerular F-actin following ADR injury. Further investigation showed that the amount of F-actin in podocytes was unchanged in response to ADR injury with and without TB4 gene therapy. It is therefore possible that alterations to the amount of glomerular F-actin were localised to either the mesangium or capillary endothelium, as both cell types contain F-actin (Cortes et al. 2000). Therefore, follow up studies could quantify F-actin in those cells *in vivo* and culture glomerular mesangial cells or endothelial cells *in vitro*, to determine if ADR or NTS induces cytoskeletal changes in each respective cell type, and examine if TB4 prevents these potential changes.

To fully elucidate the role of endogenous TB4 in podocyte health and disease, a mouse line with podocyte-specific knockout of TB4 could be generated. This would involve generating a mouse line with the Cre-recombinase gene tagged to *Nphs2* so that Cre-recombinase is specifically expressed in the podocytes (Papakrivopoulou *et al.*, 2018). These mice would then be crossed with mice expressing TB4-LoxP (although this mouse line has not been generated yet), which would insert two LoxP sites into intron regions that flank one exon of the *Tmsb4x* gene. Cre-mediated excision of the LoxP flanked regions would result in *in vivo* deletion of *Tmsb4x* gene, and therefore deletion of TB4 peptide in podocytes (Friedel et al. 2011). These mice without podocyte expression of TB4 would then be treated with ADR and NTS to determine if the effects of each experimental model are exacerbated. To take this further, these mice could be exposed to ADR or NTS after pre-treatment with AAV.*Tmsb4x*, which could determine if exogenous TB4 in the absence of endogenous TB4 is sufficient to prevent glomerular damage.

The sample sizes in the NTS nephritis chapter were another limitation of this thesis. Although the *Tmsb4x*/NTS group had an adequate sample size of 10, the PBS and *LacZ* treated mice only had 5 and 4 mice in them respectively. This could account for discrepancies seen within the chapter, such as the glomerular macrophage accumulation, where PBS/NTS mice displayed more macrophages than *Tmsb4x*/NTS, but *LacZ*/NTS treated mice showed less than *Tmsb4x*/NTS mice. There were also differences between the number of proliferating glomerular cells and podocytes between the PBS/NTS and *LacZ*/NTS groups, which could have been due to low samples sizes. In order to eliminate this limitation, the experiment could be repeated with more mice in each group, which would give each statistical calculation more power, increasing the reliability of the results.

Long term, the data presented in this thesis and previously published research suggest that exogenous TB4 may be a therapeutic option that could translate to human glomerular injury. Exogenous TB4 is already used clinically to treat eye disorders and is in clinical trials for a range of other pathologies, with little unexpected adverse events (Sosne, 2018, 1.6.6). Further pre-clinical trials for use in kidney disease are necessary. Models of glomerular injury with TB4 gene therapy could be induced in greater mammals, such as non-human primates to determine if the effects seen in mice can translate to species more closely related to humans.

5.3 **General conclusion**

In conclusion, the data presented in this thesis provides strong experimental evidence that sustained upregulation of exogenous TB4 prevents early glomerular filtration barrier damage in two models of glomerular disease, ADR nephropathy and NTS nephritis. The proposed mechanism of action is that TB4 protects podocyte F-actin distribution and prevents podocyte loss, independent of inflammation suppression, therefore preserving the final component of the glomerular filtration barrier. Taken together, these results provide strong evidence that exogenous TB4 alleviates the phenotypes of glomerular injury in rodents and future studies further investigating the underlying mechanisms of its protective effects are justified. Identification of novel therapeutic molecules to alleviate glomerular injury are crucial to develop therapeutic strategies to combat CKD in humans.

Chapter 6: Bibliography

Aksu, Ugur, Onur M. Yaman, Ibrahim Guner, Gulcan Guntas, Fuat Sonmez, Gamze Tanriverdi, Mediha Eser, Aris Cakiris, Sibel Akyol, İsmail Seçkin, Hafize Uzun, Nermin Yelmen, and Gulderen Sahin. 2019. “The Protective Effects of Thymosin-β-4 in a Rat Model of Ischemic Acute Kidney Injury.” *Journal of Investigative Surgery* 8:1–9.

Almaani, Salem, Alexa Meara, and Brad H. Rovin. 2017. “Update on Lupus Nephritis.” *Clinical Journal of the American Society of Nephrology* 12(5):825–35.

Amr, Khalda, Hala T. El-Bassyouni, Eman Rabie, Abeer Selim, Moushira E. Zaki, Eman Abobakr Abd Alazem, Shereen El-Shaer, Sahar Rady, and Doaa M. Salah. 2020. “A Descriptive Study of NPHS1 and NPHS2 Mutations in Children with Congenital Nephrotic Syndrome.” *Gene Reports* 20:100722.

Amura, Claudia R., R. Silverstein, and D. C. Morrison. 1998. “Mechanisms Involved in the Pathogenesis of Sepsis Are Not Necessarily Reflected by in Vitro Cell Activation Studies.” *Infection and Immunity* 66(11):5372–78.

Andrews, Peter M. 1977. “The Effect of Vinblastine-Induced Microtubule Loss on Kidney Podocyte Morphology.” *American Journal of Anatomy* 150(1):53–61.

Andrianantoandro, Ernesto and Thomas D. Pollard. 2006. “Mechanism of Actin Filament Turnover by Severing and Nucleation at Different Concentrations of ADF/Cofilin.” *Molecular Cell* 24(1):13–23.

Anon. 2021. “RegeneRx Biopharmaceuticals, Inc.” Retrieved January 20, 2021 (http://www.regenerx.com/home).

Applewhite, Derek A., Melanie Barzik, Shin Ichiro Kojima, Tatyana M. Svitkina, Frank B. Gertler, and Gary G. Borisy. 2007. “Ena/VASP Proteins Have an Anti-Capping Independent Function in Filopodia Formation.” *Molecular Biology of the Cell* 18(7):2579–91.

Arends, Jon, Jean Wu, Jason Borillo, Luan Troung, Cindy Zhou, Nadarajah Vigneswaran, and Ya-Huan Lou. 2006. “T Cell Epitope Mimicry in Antiglomerular Basement Membrane Disease.” *The Journal of Immunology* 176(2):1252–58.

Arkill, Kenton P., Klaus Qvortrup, Tobias Starborg, Judith M. Mantell, Carlo Knupp, C. Charles Michel, Steve J. Harper, Andy H. Salmon, John M. Squire, Dave O. Bates, and Chris R. Neal. 2014. “Resolution of the Three Dimensional Structure

of Components of the Glomerular Filtration Barrier." *BMC Nephrology* 15(1):1–13.

Aronson, Doron, Murray A. Mittleman, and Andrew J. Burger. 2004. "Elevated Blood Urea Nitrogen Level as a Predictor of Mortality in Patients Admitted for Decompensated Heart Failure." *The American Journal of Medicine* 116(7):466–73.

Asanuma, Katsuhiko, Kwanghee Kim, Jun Oh, Laura Giardino, Sophie Chabanis, Christian Faul, Jochen Reiser, and Peter Mundel. 2005. "Synaptopodin Regulates the Actin-Bundling Activity of α-Actinin in an Isoform-Specific Manner." *Journal of Clinical Investigation* 115(5):1188–98.

Asanuma, Katsuhiko, Etsuko Yanagida-Asanuma, Christian Faul, Yasuhiko Tomino, Kwanghee Kim, and Peter Mundel. 2006. "Synaptopodin Orchestrates Actin Organization and Cell Motility via Regulation of RhoA Signalling." *Nature Cell Biology* 8(5):485–91.

Assmann, Karel J. M., Martina M. Tangelder, Will P. J. Lange, Gideon Schrijver, and Robert AP Koene. 1985. "Anti-GBM Nephritis in the Mouse: Severe Proteinuria in the Heterologous Phase." *Virchows Archiv A Pathological Anatomy and Histopathology* 406(3):285–99.

Atkinson, Simon J., Melanie A. Hosford, and Bruce A. Molitoris. 2004. "Mechanism of Actin Polymerization in Cellular ATP Depletion." *Journal of Biological Chemistry* 279(7):5194–99.

Austyn, Jonathan M. and Siamon Gordon. 1981. "F4/80, a Monoclonal Antibody Directed Specifically against the Mouse Macrophage." *European Journal of Immunology* 11(10):805–15.

Azizi, Michel, Eric Ezan, Jean Luc Reny, Joanna Wdzieczak-Bakala, Vincent Gerineau, and Joël Ménard. 1999. "Renal and Metabolic Clearance of N-Acetyl-Seryl-Aspartyl-Lysyl-Proline (AcSDKP) during Angiotensin-Converting Enzyme Inhibition in Humans." *Hypertension* 33(3):879–86.

Bachmann, Christiane, Lieselore Fischer, Ulrich Walter, and Matthias Reinhard. 1999. "The EVH2 Domain of the Vasodilator-Stimulated Phosphoprotein Mediates Tetramerization, F-Actin Binding, and Actin Bundle Formation." *Journal of Biological Chemistry* 274(33):23549–57.

Badamchian, Mahnaz, Mirela O. Fagarasan, Robert L. Danner, Anthony F. Suffredini, Hadi Damavandy, and Allan L. Goldstein. 2003. "Thymosin B4

Reduces Lethality and Down-Regulates Inflammatory Mediators in Endotoxin-Induced Septic Shock." *International Immunopharmacology* 3(8):1225–33.

Bakris, George L., Rajiv Agarwal, Juliana C. Chan, Mark E. Cooper, Ron T. Gansevoort, Hermann Haller, Giuseppe Remuzzi, Peter Rossing, Roland E. Schmieder, Christina Nowack, Peter Kolkhof, Amer Joseph, Alexander Pieper, Nina Kimmeskamp-Kirschbaum, and Luis M. Ruilope. 2015. "Effect of Finerenone on Albuminuria in Patients with Diabetic Nephropathy a Randomized Clinical Trial." *Journal of the American Medical Association* 314(9):884–94.

Ball, Linda J., Thomas Jarchau, Hartmut Oschkinat, and Ulrich Walter. 2002. "EVH1 Domains: Structure, Function and Interactions." *FEBS Letters* 513(1):45–52.

Bao, Weike, Victoria L. Ballard, Saul Needle, Bao Hoang, Stephen C. Lenhard, James R. Tunstead, Beat M. Jucker, Robert N. Willette, and G. Teg Pipes. 2013. "Cardioprotection by Systemic Dosing of Thymosin Beta Four Following Ischemic Myocardial Injury." *Frontiers in Pharmacology* 4:149.

Barletta, Gina-Marie, Iulia A. Kovari, Rakesh K. Verma, Dontscho Kerjaschki, and Lawrence B. Holzman. 2003. "Nephrin and Neph1 Co-Localize at the Podocyte Foot Process Intercellular Junction and Form *Cis* Hetero-Oligomers." *Journal of Biological Chemistry* 278(21):19266–71.

Beijing Northland Biotech. Co. Ltd. 2021. "NL005." Retrieved (http://www.northland-bio.com/onepage9.html).

Beijing Northland Biotech. Co. Ltd. - NCT04555850. 2020. "A Phase 1b Study of Thymosin Beta 4 in Healthy Volunteers - Full Text View - ClinicalTrials.Gov." *ClinicalTrials.Gov*. Retrieved January 21, 2021 (https://clinicaltrials.gov/ct2/show/NCT04555850?term=thymosin+beta+4&draw=2&rank=9).

Beijing Northland Biotech. Co. Ltd - NCT04555824. 2020. "A Phase 1a Study of Thymosin Beta 4 in Healthy Volunteers - Full Text View - ClinicalTrials.Gov." *ClinicalTrials.Gov*. Retrieved January 21, 2021 (https://clinicaltrials.gov/ct2/show/NCT04555824?term=thymosin+beta+4&draw=2&rank=10).

Berasain, Carmen and Matías A. Avila. 2015. "Regulation of Hepatocyte Identity and Quiescence." *Cellular and Molecular Life Sciences* 72(20):3831–51.

Berg, Anna-Lena and Peter Nilsson-Ehle. 1996. "ACTH Lowers Serum Lipids in

Steroid-Treated Hyperlipemic Patients with Kidney Disease." *Kidney International* 50:538–42.

Berger, James M., Steven J. Gamblin, Stephen C. Harrison, and James C. Wang. 1996. "Structure and Mechanism of DNA Topoisomerase II." *Nature* 379(6562):225–32.

Bernstein, Barbara W. and James R. Bamburg. 2010. "ADF/Cofilin: A Functional Node in Cell Biology." *Trends in Cell Biology* 20(4):187–95.

Bertani, T., A. Poggi, R. Pozzoni, F. Delaini, G. Sacchi, Y. Thoua, G. Mecca, G. Remuzzi, and M. B. Donati. 1982. "Adriamycin-Induced Nephrotic Syndrome in Rats. Sequence of Pathologic Events." *Laboratory Investigation* 46(1):16–23.

Bertani, Tullio, Giovanna Rocchi, Giuseppe Sacchi, Giuliano Mecca, and Giuseppe Remuzzi. 1986. "Adriamycin-Induced Glomerulosclerosis in the Rat." *American Journal of Kidney Diseases* 7(1):12–19.

Bertram, John F., Rebecca N. Douglas-Denton, Boucar Diouf, Michael D. Hughson, and Wendy E. Hoy. 2011. "Human Nephron Number: Implications for Health and Disease." Pp. 1529–33 in *Pediatric Nephrology*. Vol. 26. Springer.

Besse-Eschmann, Valérie, Michel Le Hir, Nicole Endlich, and Karlhans Endlich. 2004. "Alterations of Podocytes in a Murine Model of Crescentic Glomerulonephritis." *Histochemistry and Cell Biology* 122(2):139–49.

Bharakhada, Nilesh, Thomas Yates, Melanie J. Davies, Emma G. Wilmot, Charlotte Edwardson, Joe Henson, David Webb, and Kamlesh Khunti. 2012. "Association of Sitting Time and Physical Activity with CKD: A Cross-Sectional Study in Family Practices." *American Journal of Kidney Diseases* 60(4):583–90.

Bierzynska, Agnieszka, Katrina Soderquest, and Ania Koziell. 2014. "Genes and Podocytes - New Insights into Mechanisms of Podocytopathy." *Frontiers in Endocrinology* 5:23.

Bikbov, Boris, Caroline A. Purcell, Andrew S. Levey, Mari Smith, Amir Abdoli, Molla Abebe, Oladimeji M. Adebayo, Mohsen Afarideh, Sanjay Kumar Agarwal, Marcela Agudelo-Botero, Elham Ahmadian, Ziyad Al-Aly, Vahid Alipour, Amir Almasi-Hashiani, Rajaa M. Al-Raddadi, Nelson Alvis-Guzman, Saeed Amini, Tudorel Andrei, Catalina Liliana Andrei, Zewudu Andualem, Mina Anjomshoa, Jalal Arabloo, Alebachew Fasil Ashagre, Daniel Asmelash, Zerihun Ataro, Maha Moh d. Wahb. Atout, Martin Amogre Ayanore, Alaa Badawi, Ahad Bakhtiari, Shoshana H. Ballew, Abbas Balouchi, Maciej Banach, Simon Barquera, Sanjay

Basu, Mulat Tirfie Bayih, Neeraj Bedi, Aminu K. Bello, Isabela M. Bensenor, Ali Bijani, Archith Boloor, Antonio M. Borzì, Luis Alberto Cámera, Juan J. Carrero, Félix Carvalho, Franz Castro, Ferrán Catalá-López, Alex R. Chang, Ken Lee Chin, Sheng Chia Chung, Massimo Cirillo, Ewerton Cousin, Lalit Dandona, Rakhi Dandona, Ahmad Daryani, Rajat Das Gupta, Feleke Mekonnen Demeke, Gebre Teklemariam Demoz, Desilu Mahari Desta, Huyen Phuc Do, Bruce B. Duncan, Aziz Eftekhari, Alireza Esteghamati, Syeda Sadia Fatima, João C. Fernandes, Eduarda Fernandes, Florian Fischer, Marisa Freitas, Mohamed M. Gad, Gebreamlak Gebremedhn Gebremeskel, Begashaw Melaku Gebresillassie, Birhanu Geta, Mansour Ghafourifard, Alireza Ghajar, Nermin Ghith, Paramjit Singh Gill, Ibrahim Abdelmageed Ginawi, Rajeev Gupta, Nima Hafezi-Nejad, Arvin Haj-Mirzaian, Arya Haj-Mirzaian, Ninuk Hariyani, Mehedi Hasan, Milad Hasankhani, Amir Hasanzadeh, Hamid Yimam Hassen, Simon I. Hay, Behnam Heidari, Claudiu Herteliu, Chi Linh Hoang, Mostafa Hosseini, Mihaela Hostiuc, Seyed Sina Naghibi Irvani, Sheikh Mohammed Shariful Islam, Nader Jafari Balalami, Spencer L. James, Simerjot K. Jassal, Vivekanand Jha, Jost B. Jonas, Farahnaz Joukar, Jacek Jerzy Jozwiak, Ali Kabir, Amaha Kahsay, Amir Kasaeian, Tesfaye Dessale Kassa, Hagazi Gebremedhin Kassaye, Yousef Saleh Khader, Rovshan Khalilov, Ejaz Ahmad Khan, Mohammad Saud Khan, Young Ho Khang, Adnan Kisa, Csaba P. Kovesdy, Barthelemy Kuate Defo, G. Anil Kumar, Anders O. Larsson, Lee Ling Lim, Alan D. Lopez, Paulo A. Lotufo, Azeem Majeed, Reza Malekzadeh, Winfried März, Anthony Masaka, Hailemariam Abiy Alemu Meheretu, Tomasz Miazgowski, Andreea Mirica, Erkin M. Mirrakhimov, Prasanna Mithra, Babak Moazen, Dara K. Mohammad, Reza Mohammadpourhodki, Shafiu Mohammed, Ali H. Mokdad, Linda Morales, Ilais Moreno Velasquez, Seyyed Meysam Mousavi, Satinath Mukhopadhyay, Jean B. Nachega, Girish N. Nadkarni, Jobert Richie Nansseu, Gopalakrishnan Natarajan, Javad Nazari, Bruce Neal, Ruxandra Irina Negoi, Cuong Tat Nguyen, Rajan Nikbakhsh, Jean Jacques Noubiap, Christoph Nowak, Andrew T. Olagunju, Alberto Ortiz, Mayowa Ojo Owolabi, Raffaele Palladino, Mona Pathak, Hossein Poustchi, Swayam Prakash, Narayan Prasad, Alireza Rafiei, Sree Bhushan Raju, Kiana Ramezanzadeh, Salman Rawaf, David Laith Rawaf, Lal Rawal, Robert C. Reiner, Aziz Rezapour, Daniel Cury Ribeiro, Leonardo Roever, Dietrich Rothenbacher, Godfrey M. Rwegerera,

Seyedmohammad Saadatagah, Saeed Safari, Berhe Weldearegawi Sahle, Hosni Salem, Juan Sanabria, Itamar S. Santos, Arash Sarveazad, Monika Sawhney, Elke Schaeffner, Maria Inês Schmidt, Aletta Elisabeth Schutte, Sadaf G. Sepanlou, Masood Ali Shaikh, Zeinab Sharafi, Mehdi Sharif, Amrollah Sharifi, Diego Augusto Santos Silva, Jasvinder A. Singh, Narinder Pal Singh, Malede Mequanent M. Sisay, Amin Soheili, Ipsita Sutradhar, Berhane Fseha Teklehaimanot, Berhe etsay Tesfay, Getnet Fetene Teshome, Jarnail Singh Thakur, Marcello Tonelli, Khanh Bao Tran, Bach Xuan Tran, Candide Tran Ngoc, Irfan Ullah, Pascual R. Valdez, Santosh Varughese, Theo Vos, Linh Gia Vu, Yasir Waheed, Andrea Werdecker, Haileab Fekadu Wolde, Adam Belay Wondmieneh, Sarah Wulf Hanson, Tomohide Yamada, Yigizie Yeshaw, Naohiro Yonemoto, Hasan Yusefzadeh, Zoubida Zaidi, Leila Zaki, Sojib Bin Zaman, Nelson Zamora, Afshin Zarghi, Kaleab Alemayehu Zewdie, Johan Ärnlöv, Josef Coresh, Norberto Perico, Giuseppe Remuzzi, and Chris J. L. Murray. 2020. “Global, Regional, and National Burden of Chronic Kidney Disease, 1990–2017: A Systematic Analysis for the Global Burden of Disease Study 2017.” *The Lancet* 395(10225):709–33.

Bilancia, Colleen G., Jonathan D. Winkelman, Denis Tsygankov, Stephanie H. Nowotarski, Jennifer A. Sees, Kate Comber, Iwan Evans, Vinal Lakhani, Will Wood, Timothy C. Elston, David R. Kovar, and Mark Peifer. 2014. “Enabled Negatively Regulates Diaphanous-Driven Actin Dynamics in Vitro and in Vivo.” *Developmental Cell* 28(4):394–408.

Birmingham, Daniel J. and Lee A. Hebert. 2015. “The Complement System in Lupus Nephritis.” *Seminars in Nephrology* 35(5):444–54.

Blaine, Judith and James Dylewski. 2020. “Regulation of the Actin Cytoskeleton in Podocytes.” *Cells* 9(7):1700.

Bock-Marquette, I., A. Saxena, M. White, J. DiMaio, and D. Srivastava. 2004. “Thymosin Beta4 Activates Integrin-Linked Kinase and Promotes Cardiac Cell Migration, Survival and Cardiac Repair.” *Nature* 432:466–72.

Bongiovanni, D, T. Ziegler, S. D’Almeida, T. Zhang, J. K. Ng, S. Dietzel, R. Hinkel, and C. Kupatt. 2015. “Thymosin Beta4 Attenuates Microcirculatory and Hemodynamic Destabilization in Sepsis.” *Expert Opin Biol Ther* 15 Suppl 1:S203-10.

Bongiovanni, Dario, Tilman Ziegler, Sascha D’almeida, Tianqiong Zhang, Judy Km

Ng, Steffen Dietzel, Rabea Hinkel, and Christian Kupatt. 2015. “Thymosin B4 Attenuates Microcirculatory and Hemodynamic Destabilization in Sepsis.” *Expert Opinion on Biological Therapy* 15(Sup1):203–10.

Boucrot, Emmanuel, Saveez Saffarian, Ramiro Massol, Tomas Kirchhausen, and Marcelo Ehrlich. 2006. “Role of Lipids and Actin in the Formation of Clathrin-Coated Pits.” *Experimental Cell Research* 312(20):4036–48.

Boukhalfa, G., A. Desmoulière, E. Rondeau, G. Gabbiani, and J. .. Sraer. 1996. “Relationship between Alpha-Smooth Muscle Actin Expression and Fibrotic Changes in Human Kidney - PubMed.” *Experimental Nephrology* 4(4):241–47.

Boute, Nicolas, Olivier Gribouval, Séverine Roselli, France Benessy, Hyunjoo Lee, Arno Fuchshuber, Karin Dahan, Marie Claire Gubler, Patrick Niaudet, and Corinne Antignac. 2000. “NPHS2, Encoding the Glomerular Protein Podocin, Is Mutated in Autosomal Recessive Steroid-Resistant Nephrotic Syndrome.” *Nature Genetics* 24(4):349–54.

Braam, Branko, Kenneth D. Mitchell, John Fox, L. Gabriel Navar, and L. Gabriel Navar Proximal. 1993. “Proximal Tubular Secretion of Angiotensin II in Rats.” *American Phsiological Society* 264(33):F891–98.

Brähler, Sebastian, Haiyang Yu, Hani Suleiman, Gokul M. Krishnan, Brian T. Saunders, Jeffrey B. Kopp, Jeffrey H. Miner, Bernd H. Zinselmeyer, and Andrey S. Shaw. 2016. “Intravital and Kidney Slice Imaging of Podocyte Membrane Dynamics.” *Journal of the American Society of Nephrology* 27:3285–90.

Breitsprecher, Dennis, Antje K. Kiesewetter, Joern Linkner, Marlene Vinzenz, Theresia E. B. Stradal, John Victor Small, Ute Curth, Richard B. Dickinson, and Jan Faix. 2011. “Molecular Mechanism of Ena/VASP-Mediated Actin-Filament Elongation.” *The EMBO Journal* 30(3):456–67.

Brieher, William. 2013. “Mechanisms of Actin Disassembly.” *Molecular Biology of the Cell* 24(15):2299–2302.

Brinkkoetter, Paul Thomas, Christina Ising, and Thomas Benzing. 2013. “The Role of the Podocyte in Albumin Filtration.” *Nature Reviews Nephrology* 9(6):328–36.

Brown, Matthew D. and David B. Sacks. 2006. “IQGAP1 in Cellular Signaling: Bridging the GAP.” *Trends in Cell Biology* 16(5):242–49.

Bruggeman, Leslie A., Paul E. Drawz, Nicole Kahoud, Ke Lin, Laura Barisoni, and Peter J. Nelson. 2011. “TNFR2 Interposes the Proliferative and NF-B-Mediated Inflammatory Response by Podocytes to TNF-α.” *Laboratory Investigation*

91(3):413–25.

Brunskill, Eric W., Joo-Seop Park, Eunah Chung, Feng Chen, Bliss Magella, and Steven S. Potter. 2014. “Single Cell Dissection of Early Kidney Development: Multilineage Priming.” *Development* 141:3093–3101.

Bubb, Michael R., Elena G. Yarmola, Bruce G. Gibson, and Frederick S. Southwick. 2003. “Depolymerization of Actin Filaments by Profilin: Effects of Profilin on Capping Protein Function.” *Journal of Biological Chemistry* 278(27):24629–35.

Bundy, Joshua D., Lydia A. Bazzano, Dawei Xie, Janet Cohan, Jacqueline Dolata, Jeffrey C. Fink, Chi Yuan Hsu, Kenneth Jamerson, James Lash, Gail Makos, Susan Steigerwalt, Xue Wang, Katherine T. Mills, Jing Chen, Jiang He, Lawrence J. Appel, Harold I. Feldman, Alan S. Go, John W. Kusek, Akinlolu Ojo, Mahboob Rahman, and Raymond R. Townsend. 2018. “Self-Reported Tobacco, Alcohol, and Illicit Drug Use and Progression of Chronic Kidney Disease.” *Clinical Journal of the American Society of Nephrology* 13(7):993–1001.

Burford, James L., Georgina Gyarmati, Isao Shirato, Wilhelm Kriz, Kevin V. Lemley, and János Peti-Peterdi. 2017. “Combined Use of Electron Microscopy and Intravital Imaging Captures Morphological and Functional Features of Podocyte Detachment.” *Pflugers Archiv - European Journal of Physiology* 469:965–74.

Burford, James L., Karie Villanueva, Lisa Lam, Anne Riquier-Brison, Matthias J. Hackl, Jeffrey Pippin, Stuart J. Shankland, and János Peti-Peterdi. 2014. “Intravital Imaging of Podocyte Calcium in Glomerular Injury and Disease.” *Journal of Clinical Investigation* 124(5):2050–58.

Burke, James F., J. Frederick Laucius, Harvey S. Brodovsky, and Raymond Z. Soriano. 1977. “Doxorubicin Hydrochloride-Associated Renal Failure.” *Archives of Internal Medicine* 137(3):385–88.

Butler, Andrew, Paul Hoffman, Peter Smibert, Efthymia Papalexi, and Rahul Satija. 2018. “Integrating Single-Cell Transcriptomic Data across Different Conditions, Technologies, and Species.” *Nature Biotechnology* 36(5):411–20.

Butt, Linus, David Unnersjö-Jess, Martin Höhne, Aurelie Edwards, Julia Binz-Lotter, Dervla Reilly, Robert Hahnfeldt, Vera Ziegler, Katharina Fremter, Markus M. Rinschen, Martin Helmstädter, Lena K. Ebert, Hayo Castrop, Matthias J. Hackl, Gerd Walz, Paul T. Brinkkoetter, Max C. Liebau, Kálmán Tory, Peter F. Hoyer, Bodo B. Beck, Hjalmar Brismar, Hans Blom, Bernhard Schermer, and Thomas Benzing. 2020. “A Molecular Mechanism Explaining Albuminuria in Kidney

Disease.” *Nature Metabolism* 1–14.

Buvall, Lisa, Priyanka Rashmi, Esther Lopez-Rivera, Svetlana Andreeva, Astrid Weins, Hanna Wallentin, Anna Greka, and Peter Mundel. 2013. “Proteasomal Degradation of Nck1 but Not Nck2 Regulates RhoA Activation and Actin Dynamics.” *Nature Communications* 4:2863.

Buvall, Lisa, Hanna Wallentin, Jonas Sieber, Svetlana Andreeva, Hoon Young Choi, Peter Mundel, and Anna Greka. 2017. “Synaptopodin Is a Coincidence Detector of Tyrosine versus Serine/Threonine Phosphorylation for the Modulation of Rho Protein Crosstalk in Podocytes.” *Journal of the American Society of Nephrology* 28(3):837–51.

Call, Matthew E., Jason Pyrdol, Martin Wiedmann, and Kai W. Wucherpfennig. 2002. “The Organizing Principle in the Formation of the T Cell Receptor-CD3 Complex.” *Cell* 111(7):967–79.

Carlier, Marie-France, Catherine Jean, Klaus J. Riegert, Maryse Lenfantt, and Dominique Pantaloni. 1993. “Modulation of the Interaction between G-Actin and Thymosin I4 by the ATP/ADP Ratio: Possible Implication in the Regulation of Actin Dynamics.” *Biochemistry* 90:5034–38.

Carliers, Marie-France, Dominique Pantalonis, and Edward D. Korns. 1987. “The Mechanisms of ATP Hydrolysis Accompanying the Polymerization of Mg-Actin and Ca-Actin.” *The Journal of Biological Chemistry* 262(7):3052–59.

Carroll, Thomas J., Joo Seop Park, Shigemi Hayashi, Arindam Majumdar, and Andrew P. McMahon. 2005. “Wnt9b Plays a Central Role in the Regulation of Mesenchymal to Epithelial Transitions Underlying Organogenesis of the Mammalian Urogenital System.” *Developmental Cell* 9(2):283–92.

Cassimeris, Lynne, Daniel Safer, Vivianne T. Nachmias, and S. H. Zigmond. 1992. “Thymosin B4 Sequesters the Majority of G-Actin in Resting Human Polymorphonuclear Leukocytes.” *Journal of Cell Biology* 119(5):1261–70.

Castoldi, G., C. R. T. Di Gioia, C. Bombardi, C. Preziuso, M. Leopizzi, S. Maestroni, B. Corradi, G. Zerbini, and A. Stella. 2013. “Renal Antifibrotic Effect of N-Acetyl-Seryl-Aspartyl-Lysyl-Proline in Diabetic Rats.” *American Journal of Nephrology* 37(1):65–73.

Castrop, Hayo, Klaus Höcherl, Armin Kurtz, Frank Schweda, Vladimir Todorov, and Charlotte Wagner. 2010. “Physiology of Kidney Renin.” *Physiological Reviews* 90(2):607–73.

Cattran, Daniel C., Rosanna Coppo, H. Terence Cook, John Feehally, Ian S. D. Roberts, Stéphan Troyanov, Charles E. Alpers, Alessandro Amore, Jonathan Barratt, Francois Berthoux, Stephen Bonsib, Jan A. Bruijn, Vivette D'Agati, Giuseppe D'Amico, Steven Emancipator, Francesco Emma, Franco Ferrario, Fernando C. Fervenza, Sandrine Florquin, Agnes Fogo, Colin C. Geddes, Hermann Josef Groene, Mark Haas, Andrew M. Herzenberg, Prue A. Hill, Ronald J. Hogg, Stephen I. Hsu, J. Charles Jennette, Kensuke Joh, Bruce A. Julian, Tetsuya Kawamura, Fernand M. Lai, Chi Bon Leung, Lei Shi Li, Philip K. T. Li, Zhi Hong Liu, Bruce MacKinnon, Sergio Mezzano, F. Paolo Schena, Yasuhiko Tomino, Patrick D. Walker, Haiyan Wang, Jan J. Weening, Nori Yoshikawa, and Hong Zhang. 2009. "The Oxford Classification of IgA Nephropathy: Rationale, Clinicopathological Correlations, and Classification." *Kidney International* 76(5):534–45.

Cavasin, Maria A., Tang Dong Liao, Xiao Ping Yang, James J. Yang, and Oscar A. Carretero. 2007. "Decreased Endogenous Levels of Ac-SDKP Promote Organ Fibrosis." *Hypertension* 50(1):130–36.

Cechova, Sylvia, Fan Dong, Fang Chan, Michael J. Kelley, Phillip Ruiz, and Thu H. Le. 2018. "MYH9 E1841K Mutation Augments Proteinuria and Podocyte Injury and Migration." *Journal of the American Society of Nephrology* 29:155–67.

Chalmers, Samantha A., Violeta Chitu, Leal C. Herlitz, Ranjit Sahu, E. Richard Stanley, and Chaim Putterman. 2015. "Macrophage Depletion Ameliorates Nephritis Induced by Pathogenic Antibodies." *Journal of Autoimmunity* 57:42–52.

Chan, Gary C. W., Wai Han Yiu, Hao Jia Wu, Dickson W. L. Wong, Miao Lin, Xiao Ru Huang, Hui Yao Lan, and Sydney C. W. Tang. 2015. "N-Acetyl-Seryl-Aspartyl-Lysyl-Proline Alleviates Renal Fibrosis Induced by Unilateral Ureteric Obstruction in BALB/C Mice." *Mediators of Inflammation* 2015.

Chang, Jei Wen, Victoriano Pardo, Junichiro Sageshima, Linda Chen, Hsin Lin Tsai, Jochen Reiser, Changli Wei, Gaetano Ciancio, George W. Burke, and Alessia Fornoni. 2012. "Podocyte Foot Process Effacement in Postreperfusion Allograft Biopsies Correlates with Early Recurrence of Proteinuria in Focal Segmental Glomerulosclerosis." *Transplantation* 93(12):1238–44.

Chen, A., L. F. Sheu, Y. S. Ho, Y. F. Lin, W. Y. Chou, T. C. Chou, and W. H. Lee. 1998. "Experimental Focal Segmental Glomerulosclerosis in Mice." *Nephron*

78(4):440–52.

Chen, Heng. 2007. “Comparative Observation of the Recombinant Adeno-Associated Virus 2 Using Transmission Electron Microscopy and Atomic Force Microscopy.” *Microscopy and Microanalysis* 13:384–89.

Chen, Qi, Zhida Shen, Yanjun Mao, Qinfeng Li, Yu Liu, Menghan Mei, Fuyu Qiu, and Meihui Wang. 2019. “Inhibition of MicroRNA-34a Mediates Protection of Thymosin Beta 4 in Endothelial Progenitor Cells against Advanced Glycation Endproducts by Targeting B-Cell Lymphoma 2.” *Canadian Journal of Physiology and Pharmacology* 97(10):945–51.

Chen, Shih-Ming, Takuya Mukoyama, Noriko Sato, Shin-Ichi Yamagata, Yuichiro Arai, Nobunori Satoh, and Shiro Ueda. 2002. “Induction of Nephrotoxic Serum Nephritis in Inbred Mice and Suppressive Effect of Colchicine on the Development of This Nephritis.” *Pharmacological Research* 45(4):319–24.

Chen, Teresa K., Daphne H. Knicely, and Morgan E. Grams. 2019. “Chronic Kidney Disease Diagnosis and Management: A Review.” *JAMA - Journal of the American Medical Association* 322(13):1294–1304.

Chen, Zhuyun, Xiaofei An, Xi Liu, Jia Qi, Dafa Ding, Min Zhao, Suyan Duan, Zhimin Huang, Chengning Zhang, Lin Wu, Bo Zhang, Aihua Zhang, Yanggang Yuan, and Changying Xing. 2017. “Hyperoside Alleviates Adriamycin-Induced Podocyte Injury via Inhibiting Mitochondrial Fission.” *Oncotarget* 8(51):88792–803.

Chesarone, Melissa A. and Bruce L. Goode. 2009. “Actin Nucleation and Elongation Factors: Mechanisms and Interplay.” *Current Opinion in Cell Biology* 21(1):28–37.

Chiorini, J. A., L. Yang, Y. Liu, B. Safer, and R. M. Kotin. 1997. “Cloning of Adeno-Associated Virus Type 4 (AAV4) and Generation of Recombinant AAV4 Particles.” *Journal of Virology* 71(9):6823–33.

Chiorini, John A., Frank Kim, Linda Yang, and Robert M. Kotin. 1999. “Cloning and Characterization of Adeno-Associated Virus Type 5.” *Journal of Virology* 73(2):1309–19.

Chittiprol, Seetharamaiah, Phylip Chen, Danica Petrovic-Djergovic, Tad Eichler, and Richard F. Ransom. 2011. “Marker Expression, Behaviors, and Responses Vary in Different Lines of Conditionally Immortalized Cultured Podocytes.” *American Journal of Physiology-Renal Physiology* 301(3):F660–71.

Chiu, Loraine LY, Lewis A. Reis, Abdul Momen, and Milica Radisic. 2012. "Controlled Release of Thymosin B4 from Injected Collagen–Chitosan Hydrogels Promotes Angiogenesis and Prevents Tissue Loss after Myocardial Infarction." *Regenerative Medicine* 7(4):523–33.

Chiurchiu, Carlos, Giuseppe Remuzzi, and Piero Ruggenenti. 2005. "Angiotensin-Converting Enzyme Inhibition and Renal Protection in Nondiabetic Patients: The Data of the Meta-Analyses." *Journal of the American Society of Nephrology* 16(SUPPL. 1):S58–63.

Choi, Jae Won, Bala Murali Krishna Vasamsetti, Jaebum Choo, and Hak Yong Kim. 2020. "Analysis of Deoxyribonuclease Activity by Conjugation-Free Fluorescence Polarisation in Sub-Nanolitre Droplets." *Analyst* 145(9):3222–28.

Chrysohoou, C., D. B. Panagiotakos, C. Pitsavos, J. Skoumas, M. Toutouza, I. Papaioannou, and C. Stefanadis. 2010. "Renal Function, Cardiovascular Disease Risk Factors' Prevalence and 5-Year Disease Incidence; the Role of Diet, Exercise, Lipids and Inflammation Markers: The ATTICA Study." *QJM* 103(6):413–22.

Chung, Jun Jae, Leonard Goldstein, Ying Jiun J. Chen, Jiyeon Lee, Joshua D. Webster, Merone Roose-Girma, Sharad C. Paudyal, Zora Modrusan, Anwesha Dey, and Andrey S. Shaw. 2020. "Single-Cell Transcriptome Profiling of the Kidney Glomerulus Identifies Key Cell Types and Reactions to Injury." *Journal of the American Society of Nephrology* 31(10):2341–54.

Ciani, Lorenza, Anjla Patel, Nicholas D. Allen, and Charles ffrench-Constant. 2003. "Mice Lacking the Giant Protocadherin MFAT1 Exhibit Renal Slit Junction Abnormalities and a Partially Penetrant Cyclopia and Anophthalmia Phenotype." *Molecular and Cellular Biology* 23(10):3575–82.

Clarke, Margaret and James A. Spudich. 1977. "NONMUSCLE CONTRACTILE PROTEINS: The Role of Actin and Myosin in Cell Motility and Shape Determination." *Annual Review of Biochemistry* 46:797–822.

Cole, Banumathi K., Marcello Curto, Annie W. Chan, and Andrea I. Mcclatchey. 2008. "Localization to the Cortical Cytoskeleton Is Necessary for Nf2/Merlin-Dependent Epidermal Growth Factor Receptor Silencing †." *MOLECULAR AND CELLULAR BIOLOGY* 28(4):1274–84.

Conte, Enrico, Tiziana Genovese, Elisa Gili, Emanuela Esposito, Maria Iemmolo, Mary Fruciano, Evelina Fagone, Maria P. Pistorio, Nunzio Crimi, Salvatore

Cuzzocrea, and Carlo Vancheri. 2013. “Thymosin B4 Protects C57BL/6 Mice from Bleomycin-Induced Damage in the Lung.” *European Journal of Clinical Investigation* 43(3):309–15.

Cormack-Aboud, F. C., P. T. Brinkkoetter, J. W. Pippin, S. J. Shankland, and R. V. Durvasula. 2008. “Rosuvastatin Protects against Podocyte Apoptosis in Vitro.” *Nephrology Dialysis Transplantation* 24(2):404–12.

Cortes, P., M. Mendez, B. L. Riser, C. J. Guerin, A. Rodriguez-Barbero, C. Hassett, and J. Yee. 2000. “F-Actin Fiber Distribution in Glomerular Cells: Structural and Functional Implications.” *Kidney International* 58(6):2452–61.

Costantini, Frank and Raphael Kopan. 2010. “Patterning a Complex Organ: Branching Morphogenesis and Nephron Segmentation in Kidney Development.” *Developmental Cell* 18(5):698–712.

Courtemanche, Naomi and Thomas D. Pollard. 2013. “Interaction of Profilin with the Barbed End of Actin Filaments.” *Biochemistry* 52(37):6456–66.

Couser, William G. 2012. “Basic and Translational Concepts of Immune-Mediated Glomerular Diseases.” *Journal of the American Society of Nephrology* 23(3):381–99.

Couser, William G. 2016. “Pathogenesis and Treatment of Glomerulonephritis-an Update.” *Brazilian Journal of Nephrology* 38(1):107–22.

Cranford, T. L., R. T. Enos, K. T. Velázquez, J. L. McClellan, J. M. Davis, U. P. Singh, M. Nagarkatti, P. S. Nagarkatti, C. M. Robinson, and E. A. Murphy. 2016. “Role of MCP-1 on Inflammatory Processes and Metabolic Dysfunction Following High-Fat Feedings in the FVB/N Strain.” *International Journal of Obesity* 40(5):844–51.

Crews, Deidra C., Marie Fanelli Kuczmarski, Vanessa Grubbs, Elizabeth Hedgeman, Vahakn B. Shahinian, Michele K. Evans, Alan B. Zonderman, Nilka Rios Burrows, Desmond E. Williams, Rajiv Saran, and Neil R. Powe. 2014. “Effect of Food Insecurity on Chronic Kidney Disease in Lower-Income Americans.” *American Journal of Nephrology* 39(1):27–35.

Crowther, S. M., L. A. Reynolds, and E. M. Tansey. 2010. *History of Dialysis in the UK: C.1950-1980*. Vol. 37. 1st ed. edited by S. M. Crowther, L. A. Reynolds, and E. M. Tansey. London: Wellcome Trust Centre for the History of Medicine at UCL.

Cunningham, Sharon C., Allison P. Dane, Afroditi Spinoulas, and Ian E. Alexander.

2008. “Gene Delivery to the Juvenile Mouse Liver Using AAV2/8 Vectors.” *Molecular Therapy* 16(6):1081–88.

Curthoys, Norman P. and Orson W. Moe. 2014. “Proximal Tubule Function and Response to Acidosis.” *Clinical Journal of the American Society of Nephrology* 9:1627–38.

Curtin, John A., Elizabeth Quint, Vicky Tsipouri, Ruth M. Arkell, Bruce Cattanach, Andrew J. Copp, Deborah J. Henderson, Nigel Spurr, Philip Stanier, Elizabeth M. Fisher, Patrick M. Nolan, Karen P. Steel, Steve D. M. Brown, Ian C. Gray, and Jennifer N. Murdoch. 2003. “Mutation of Celsr1 Disrupts Planar Polarity of Inner Ear Hair Cells and Causes Severe Neural Tube Defects in the Mouse.” *Current Biology* 13(13):1129–33.

Cutts, Suzanne M., Peter G. Parsons, Richard A. Sturm, and Don R. Phillips. 1996. “Adriamycin-Induced DNA Adducts Inhibit the DNA Interactions of Transcription Factors and RNA Polymerase.” *Journal of Biological Chemistry* 271(10):5422–29.

Daha, Mohamed R. and Cees van Kooten. 2016. “Role of Complement in IgA Nephropathy.” *Journal of Nephrology* 29(1):1–4.

Dai, Chunsun, Moin A. Saleem, Lawrence B. Holzman, Peter Mathieson, and Youhua Liu. 2010. “Hepatocyte Growth Factor Signaling Ameliorates Podocyte Injury and Proteinuria.” *Kidney International* 77(11):962–73.

Dai, Rufeng, Haimei Liu, Xinli Han, Junchao Liu, Yihui Zhai, Jia Rao, Qian Shen, and Hong Xu. 2019. “Angiopoietin-like-3 Knockout Protects against Glomerulosclerosis in Murine Adriamycin-Induced Nephropathy by Attenuating Podocyte Loss.” *BMC Nephrology* 20(1):185.

Dai, Yan, Anqun Chen, Ruijie Liu, Leyi Gu, Shuchita Sharma, Weijing Cai, Fadi Salem, David J. Salant, Jeffrey W. Pippin, Stuart J. Shankland, Marcus J. Moeller, Norbert B. Ghyselinck, Xiaoqiang Ding, Peter Y. Chuang, Kyung Lee, and John Cijiang He. 2017. “Retinoic Acid Improves Nephrotoxic Serum–Induced Glomerulonephritis through Activation of Podocyte Retinoic Acid Receptor α.” *Kidney International* 92(6):1444–57.

Daugirdas, John T., Peter Gerard Blake, and Todd S. Ing. 2007. *Handbook of Dialysis*. Lippincott Williams & Wilkins.

Davidoff, Andrew M., John T. Gray, Catherine Y. C. Ng, Youbin Zhang, Junfang Zhou, Yunyu Spence, Yusura Bakar, and Amit C. Nathwani. 2005. “Comparison

of the Ability of Adeno-Associated Viral Vectors Pseudotyped with Serotype 2, 5, and 8 Capsid Proteins to Mediate Efficient Transduction of the Liver in Murine and Nonhuman Primate Models." *Molecular Therapy* 11(6):875–88.

Deegens, Jeroen K. J., Henry B. P. M. Dijkman, George F. Borm, Eric J. Steenbergen, José G. van den Berg, Jan J. Weening, and Jack F. M. Wetzels. 2008. "Podocyte Foot Process Effacement as a Diagnostic Tool in Focal Segmental Glomerulosclerosis." *Kidney International* 74(12):1568–76.

Deen, Peter M. T., Bas W. M. Van Balkom, and Erik Jan Kamsteeg. 2000. "Routing of the Aquaporin-2 Water Channel in Health and Disease." *European Journal of Cell Biology* 79(8):523–30.

Deen, W. M., C. R. Robertson, B. M. Brenner, and B. M. A. Brenner. 1972. "A Model of Glomerular Ultrafiltration in the Rat." *American Journal of Physiology* 223(5):1178–83.

Deffie, Abdul M., Janendra K. Batra, and Gerald J. Goldenberg. 1989. "Direct Correlation between DNA Topoisomerase II Activity and Cytotoxicity in Adriamycin-Sensitive and -Resistant P388 Leukemia Cell Lines." *Cancer Research* 49(1):58–62.

Defilippi, Paola, Cristina Olivo, Mascia Venturino, Laura Dolce, Lorenzo Silengo, and Guido Tarone. 1999. "Actin Cytoskeleton Organization in Response to Integrin-Mediated Adhesion." *Microscopy Research and Technique* 47(1):67–78.

Deshmane, Satish L., Sergey Kremlev, Shohreh Amini, and Bassel E. Sawaya. 2009. "Monocyte Chemoattractant Protein-1 (MCP-1): An Overview." *Journal of Interferon and Cytokine Research* 29(6):313–25.

Ding, G., Z. Zhang, M. Chopp, L. Li, L. Zhang, Q. Li, M. Wei, and Q. Jiang. 2014. "MRI Evaluation of BBB Disruption after Adjuvant AcSDKP Treatment of Stroke with TPA in Rat." *Neuroscience* 271:1–8.

Ding, Zhijie and Partha Roy. 2013. "Profilin-1 versus Profilin-2: Two Faces of the Same Coin?" *Breast Cancer Research* 15(3):1–2.

Ditrich, Hans. 2007. "The Origin of Vertebrates: A Hypothesis Based on Kidney Development." *Zoological Journal of the Linnean Society* 150(2):435–41.

Donoviel, Dorit B., Deon D. Freed, Hannes Vogel, David G. Potter, Edith Hawkins, James P. Barrish, Brian N. Mathur, C. Alexander Turner, Robert Geske, Charles A. Montgomery, Michael Starbuck, Mary Brandt, Anupma Gupta, Ramiro Ramirez-Solis, Brian P. Zambrowicz, and David R. Powell. 2001. "Proteinuria

and Perinatal Lethality in Mice Lacking NEPH1, a Novel Protein with Homology to NEPHRIN." *Molecular and Cellular Biology* 21(14):4829–36.

Drenckhahn, D. and R. P. Franke. 1988. "Ultrastructural Organization of Contractile and Cytoskeletal Proteins in Glomerular Podocytes of Chicken, Rat, and Man." *Laboratory Investigation* 59(5):673–82.

Dronavalli, Suma, Irena Duka, and George L. Bakris. 2008. "The Pathogenesis of Diabetic Nephropathy." *Nature Clinical Practice Endocrinology and Metabolism* 4(8):444–52.

Drude, Solveig, Annett Geißler, Jakob Olfe, Astrid Starke, Grazyna Domanska, Christine Schuett, and Cornelia Kiank-Nussbaum. 2011. "Side Effects of Control Treatment Can Conceal Experimental Data When Studying Stress Responses to Injection and Psychological Stress in Mice." *Lab Animal* 40(4):119–28.

Duan, Dongsheng, Prerna Sharma, Jusan Yang, Yongping Yue, Lorita Dudus, Yulong Zhang, Krishna J. Fisher, and John F. Engelhardt. 1998. "Circular Intermediates of Recombinant Adeno-Associated Virus Have Defined Structural Characteristics Responsible for Long-Term Episomal Persistence in Muscle Tissue." *Journal of Virology* 72(11):8568–77.

Dudek, Amanda M., Sirika Pillay, Andreas S. Puschnik, Claude M. Nagamine, Fang Cheng, Jianming Qiu, Jan E. Carette, and Luk H. Vandenberghe. 2018. "An Alternate Route for Adeno-Associated Virus (AAV) Entry Independent of AAV Receptor." *Journal of Virology* 92(7):2213–30.

Duffield, Jeremy S., Peter G. Tipping, Tiina Kipari, Jean François Cailhier, Spike Clay, Richard Lang, Joseph V. Bonventre, and Jeremy Hughes. 2005. "Conditional Ablation of Macrophages Halts Progression of Crescentic Glomerulonephritis." *American Journal of Pathology* 167(5):1207–19.

Dunn, Steven P., David G. Heidemann, Christopher Y. C. Chow, David Crockford, Nabila Turjman, Janet Angel, Christian B. Allan, and Gabriel Sosne. 2010. "Treatment of Chronic Nonhealing Neurotrophic Corneal Epithelial Defects with Thymosin B4." *Annals of the New York Academy of Sciences* 1194(1):199–206.

Eadie, James S., Sonia W. Kim, Philip G. Allen, Lloyd M. Hutchinson, Jason D. Kantor, and Bruce R. Zetter. 2000. "C-Terminal Variations in β-Thymosin Family Members Specify Functional Differences in Actin-Binding Properties." *Journal of Cellular Biochemistry* 77(2):277–87.

Eckardt, Kai Uwe, Josef Coresh, Olivier Devuyst, Richard J. Johnson, Anna Köttgen,

Andrew S. Levey, and Adeera Levin. 2013. “Evolving Importance of Kidney Disease: From Subspecialty to Global Health Burden.” *The Lancet* 382(9887):158–69.

Edwards, Marc, Adam Zwolak, Dorothy A. Schafer, David Sept, Roberto Dominguez, and John A. Cooper. 2014. “Capping Protein Regulators Fine-Tune Actin Assembly Dynamics.” *Nature Reviews Molecular Cell Biology* 15(10):677–89.

Eknoyan, Garabed. 2009. “The Wonderful Apparatus of John Jacob Abel Called the ‘Artificial Kidney.’” *Seminars in Dialysis* 22(3):287–96.

Elalouf, J. M., N. Roinel, and C. de Rouffignac. 1984. “Effects of Antidiuretic Hormone on Electrolyte Reabsorption and Secretion in Distal Tubules of Rat Kidney.” *Pflügers Archiv European Journal of Physiology* 401(2):167–73.

Endlich, Karlhans, Felix Kliewe, and Nicole Endlich. 2017. “Stressed Podocytes-Mechanical Forces, Sensors, Signaling and Response.” *European Journal of Physiology* 469:937–49.

Endlich, Nicole, Florian Siegerist, and Karlhans Endlich. 2017. “Are Podocytes Motile?” *Pflugers Archiv European Journal of Physiology* 469(7–8):951–57.

Endlich, Nicole, Ole Simon, Achim Göpferich, Henny Wegner, Marcus J. Moeller, Elisabeth Rumpel, Ahmed M. Kotb, and Karlhans Endlich. 2014. “Two-Photon Microscopy Reveals Stationary Podocytes in Living Zebrafish Larvae.” *J Am Soc Nephrol* 25:681–86.

Etienne-Manneville, Sandrine. 2018. “Cytoplasmic Intermediate Filaments in Cell Biology.” *Annual Review of Cell and Developmental Biology* 34:1–28.

Etienne-Manneville, Sandrine and Alan Hall. 2002. “Rho GTPases in Cell Biology.” *Nature* 420(6916):629–35.

Eulitz, Dirk and Hans Georg Mannherz. 2007. “Inhibition of Deoxyribonuclease I by Actin Is to Protect Cells from Premature Cell Death.” *Apoptosis* 12(8):1511–21.

Evans, Mark A., Nicola Smart, Karina N. Dubé, Sveva Bollini, James E. Clark, Hayley G. Evans, Leonie S. Taams, Rebecca Richardson, Mathieu Lévesque, Paul Martin, Kevin Mills, Johannes Riegler, Anthony N. Price, Mark F. Lythgoe, and Paul R. Riley. 2013. “Thymosin B4-Sulfoxide Attenuates Inflammatory Cell Infiltration and Promotes Cardiac Wound Healing.” *Nature Communications* 4:2081.

Fairweather, De Lisa and Daniela Cihakova. 2009. “Alternatively Activated Macrophages in Infection and Autoimmunity.” *Journal of Autoimmunity* 33(3–

4):222–30.

Fan, Jun, Marissa G. Saunders, Esmael J. Haddadian, Karl F. Freed, Enrique M. De La Cruz, and Gregory A. Voth. 2013. “Molecular Origins of Cofilin-Linked Changes in Actin Filament Mechanics.” *Journal of Molecular Biology* 425(7):1225–40.

Fan, Xueping, Qinggang Li, Anna Pisarek-Horowitz, Hila Milo Rasouly, Xiangling Wang, Ramon G. Bonegio, Hang Wang, Margaret McLaughlin, Steve Mangos, Raghu Kalluri, Lawrence B. Holzman, Iain A. Drummond, Dennis Brown, David J. Salant, and Weining Lu. 2012. “Inhibitory Effects of Robo2 on Nephrin: A Crosstalk between Positive and Negative Signals Regulating Podocyte Structure.” *Cell Reports* 2(1):52–61.

Fan, Xueping, Hongying Yang, Sudhir Kumar, Kathleen E. Tumelty, Anna Pisarek-Horowitz, Hila Milo Rasouly, Richa Sharma, Stefanie Chan, Edyta Tyminski, Michael Shamashkin, Mostafa Belghasem, Joel M. Henderson, Anthony J. Coyle, David J. Salant, Stephen P. Berasi, and Weining Lu. 2016. “SLIT2/ROBO2 Signaling Pathway Inhibits Nonmuscle Myosin IIA Activity and Destabilizes Kidney Podocyte Adhesion.” *JCI Insight* 1(19):e86934.

Fan, Yi, Yanqing Gong, Prabar K. Ghosh, Linda M. Graham, and Paul L. Fox. 2009. “Spatial Coordination of Actin Polymerization and ILK–Akt2 Activity during Endothelial Cell Migration.” *Developmental Cell* 16(5):661–74.

Farber, Gregory, Romulo Hurtado, Sarah Loh, Sébastien Monette, James Mtui, Raphael Kopan, Susan Quaggin, Catherine Meyer-Schwesinger, Doris Herzlinger, Rizaldy P. Scott, and Carl P. Blobel. 2018. “Glomerular Endothelial Cell Maturation Depends on ADAM10, a Key Regulator of Notch Signaling.” *Angiogenesis* 21(2):335–47.

Faul, Christian, Katsuhiko Asanuma, Etsuko Yanagida-Asanuma, Kwanghee Kim, and Peter Mundel. 2007. “Actin up: Regulation of Podocyte Structure and Function by Components of the Actin Cytoskeleton.” *Trends in Cell Biology* 17(9):428–37.

Faul, Christian, Mary Donnelly, Sandra Merscher-Gomez, Yoon Hee Chang, Stefan Franz, Jacqueline Delfgaauw, Jer-Ming Chang, Hoon Young Choi, Kirk N. Campbell, Kwanghee Kim, Jochen Reiser, and Peter Mundel. 2008. “The Actin Cytoskeleton of Kidney Podocytes Is a Direct Target of the Antiproteinuric Effect of Cyclosporine A.” *Nature Medicine* 14(9):931–38.

Fehon, Richard G., Andrea I. McClatchey, and Anthony Bretscher. 2010. “Organizing the Cell Cortex: The Role of ERM Proteins.” *Nature Reviews Molecular Cell Biology* 11(4):276–87.

Feldt, Jessica, Martin Schicht, Fabian Garreis, Jessica Welss, Ulrich W. Schneider, and Friedrich Paulsen. 2019. “Structure, Regulation and Related Diseases of the Actin-Binding Protein Gelsolin.” *Expert Reviews in Molecular Medicine* 20(e7):1–10.

Feng, Di, Jacob Notbohm, Ava Benjamin, Shijie He, Minxian Wang, Lay Hong Ang, Minaspi Bantawa, Mehdi Bouzid, Emanuela Del Gado, Ramaswamy Krishnan, and Martin R. Pollak. 2018. “Disease-Causing Mutation in α-Actinin-4 Promotes Podocyte Detachment through Maladaptation to Periodic Stretch.” *Proceedings of the National Academy of Sciences of the United States of America* 115(7):1517–22.

Feng, Lei, Meijin Guo, Shuxiang Zhang, Ju Chu, Yingping Zhuang, and Siliang Zhang. 2007. “Optimization of Transfection Mediated by Calcium Phosphate for Plasmid RAAV-LacZ (Recombinant Adeno-Associated Virus–β-Galactosidase Reporter Gene) Production in Suspension-Cultured HEK-293 (Human Embryonic Kidney 293) Cells.” *Biotechnology and Applied Biochemistry* 46(2):135.

Feng, Lili, Gabriela E. Garcia, Young Yang, Yiyang Xia, Francis B. Gabbai, Orjan W. Peterson, Judith A. Abraham, Roland C. Blantz, and Curtis B. Wilson. 2000. “Heparin-Binding EGF-like Growth Factor Contributes to Reduced Glomerular Filtration Rate during Glomerulonephritis in Rats.” *Journal of Clinical Investigation* 105(3):341–50.

Ferrari, F. K., T. Samulski, T. Shenk, and R. J. Samulski. 1996. “Second-Strand Synthesis Is a Rate-Limiting Step for Efficient Transduction by Recombinant Adeno-Associated Virus Vectors.” *Journal of Virology* 70(5):3227–34.

Ferron, François, Grzegorz Rebowski, Sung Haeng Lee, and Roberto Dominguez. 2007. “Structural Basis for the Recruitment of Profilin–Actin Complexes during Filament Elongation by Ena/VASP.” *The EMBO Journal* 26(21):4597–4606.

Filipowicz, A. W. and B. L. Horecker. 1983. “In Vitro Synthesis of Thymosin B4 Encoded by Rat Spleen MRNA.” *Proceedings of the National Academy of Sciences of the United States of America* 80(7 I):1811–15.

Filippatos, Gerasimos, Stefan D. Anker, Michael Böhm, Mihai Gheorghiade, Lars

Køber, Henry Krum, Aldo P. Maggioni, Piotr Ponikowski, Adriaan A. Voors, Faiez Zannad, So-Young Kim, Christina Nowack, Giovanni Palombo, Peter Kolkhof, Nina Kimmeskamp-Kirschbaum, Alexander Pieper, and Bertram Pitt. 2016. “A Randomized Controlled Study of Finerenone vs. Eplerenone in Patients with Worsening Chronic Heart Failure and Diabetes Mellitus and/or Chronic Kidney Disease.” *European Heart Journal* 37(27):2105–14.

Fisher, K. J., G. P. Gao, M. D. Weitzman, R. DeMatteo, J. F. Burda, and J. M. Wilson. 1996. “Transduction with Recombinant Adeno-Associated Virus for Gene Therapy Is Limited by Leading-Strand Synthesis.” *Journal of Virology* 70(1):520–32.

Foreman, Kyle J., Neal Marquez, Andrew Dolgert, Kai Fukutaki, Nancy Fullman, Madeline McGaughey, Martin A. Pletcher, Amanda E. Smith, Kendrick Tang, Chun Wei Yuan, Jonathan C. Brown, Joseph Friedman, Jiawei He, Kyle R. Heuton, Mollie Holmberg, Disha J. Patel, Patrick Reidy, Austin Carter, Kelly Cercy, Abigail Chapin, Dirk Douwes-Schultz, Tahvi Frank, Falko Goettsch, Patrick Y. Liu, Vishnu Nandakumar, Marissa B. Reitsma, Vince Reuter, Nafis Sadat, Reed J. D. Sorensen, Vinay Srinivasan, Rachel L. Updike, Hunter York, Alan D. Lopez, Rafael Lozano, Stephen S. Lim, Ali H. Mokdad, Stein Emil Vollset, and Christopher J. L. Murray. 2018. “Forecasting Life Expectancy, Years of Life Lost, and All-Cause and Cause-Specific Mortality for 250 Causes of Death: Reference and Alternative Scenarios for 2016–40 for 195 Countries and Territories.” *The Lancet* 392(10159):2052–90.

Forst, Anna Lena, Vlad Sorin Olteanu, Géraldine Mollet, Tanja Wlodkowski, Franz Schaefer, Alexander DIetrich, Jochen Reiser, Thomas Gudermann, Michael Mederos Schnitzler, and Ursula Storch. 2016. “Podocyte Purinergic P2X4 Channels Are Mechanotransducers That Mediate Cytoskeletal Disorganization.” *Journal of the American Society of Nephrology* 27(3):848–62.

Franke, W. W., C. Grund, and A. Fink. 1978. “Location of Actin in the Microfilament Bundles Associated with the Junctional Specialisations between Sertoli Cells and Spermatids.” *Biologie Cellulaire* 31(1):7–13.

Freeman, Kevin W., Brian R. Bowman, and Bruce R. Zetter. 2011. “Regenerative Protein Thymosin Beta-4 Is a Novel Regulator of Purinergic Signaling.” *The FASEB Journal* 25:907–15.

Friedel, Roland H., Wolfgang Wurst, Benedikt Wefers, and Ralf Kühn. 2011.

"Generating Conditional Knockout Mice." *Methods in Molecular Biology (Clifton, N.J.)* 693:205–31.

Friedland, Julie C., Mark H. Lee, and David Boettiger. 2009. "Mechanically Activated Integrin Switch Controls A5β1 Function." *Science* 323(5914):642–44.

Fu, Jia, Kemal M. Akat, Zeguo Sun, Weijia Zhang, Detlef Schlondorff, Zhihong Liu, Thomas Tuschl, Kyung Lee, and John Cijiang He. 2019. "Single-Cell RNA Profiling of Glomerular Cells Shows Dynamic Changes in Experimental Diabetic Kidney Disease." *Journal of the American Society of Nephrology* 30(4):533–45.

Fukuda, Akihiro, Akihiro Minakawa, Yuji Sato, Takashi Iwakiri, Shuji Iwatsubo, Hiroyuki Komatsu, Masao Kikuchi, Kazuo Kitamura, Roger C. Wiggins, and Shouichi Fujimoto. 2017. "Urinary Podocyte and TGF-B1 MRNA as Markers for Disease Activity and Progression in Anti-Glomerular Basement Membrane Nephritis." *Nephrology Dialysis Transplantation* 32(11):1818–30.

Gallagher, J. C., Prema Rapuri, and Lynette Smith. 2007. "Falls Are Associated with Decreased Renal Function and Insufficient Calcitriol Production by the Kidney." *Journal of Steroid Biochemistry and Molecular Biology* 103(3–5):610–13.

Gao, Guang Ping, Mauricio R. Alvira, Lili Wang, Roberto Calcedo, Jule Johnston, and James M. Wilson. 2002. "Novel Adeno-Associated Viruses from Rhesus Monkeys as Vectors for Human Gene Therapy." *Proceedings of the National Academy of Sciences of the United States of America* 99(18):11854–59.

Gao, Guangping, Luk H. Vandenberghe, Mauricio R. Alvira, You Lu, Roberto Calcedo, Xiangyang Zhou, and James M. Wilson. 2004. "Clades of Adeno-Associated Viruses Are Widely Disseminated in Human Tissues." *Journal of Virology* 78(12):6381–88.

Gao, Xia, Hong Xu, Haimei Liu, Jia Rao, Yunling Li, and Xiliang Zha. 2010. "Angiopoietin-like Protein 3 Regulates the Motility and Permeability of Podocytes by Altering Nephrin Expression in Vitro." *Biochemical and Biophysical Research Communications* 399(1):31–36.

Garg, Puneet. 2018. "A Review of Podocyte Biology." *American Journal of Nephrology* 47(Suppl. 1):3–13.

Garg, Puneet, Rakesh Verma, Leslie Cook, Abdul Soofi, Madhusudan Venkatareddy, Britta George, Kensaku Mizuno, Christine Gurniak, Walter Witke, and Lawrence B. Holzman. 2010. "Actin-Depolymerizing Factor Cofilin-1 Is Necessary in Maintaining Mature Podocyte Architecture." *The Journal of*

Biological Chemistry 285(29):22676–88.

Gatto, Mariele, Margherita Zen, Anna Ghirardello, Silvano Bettio, Nicola Bassi, Luca Iaccarino, Leonardo Punzi, and Andrea Doria. 2013. “Emerging and Critical Issues in the Pathogenesis of Lupus.” *Autoimmunity Reviews* 12(4):523–36.

Gavin, R. H. 1997. “Microtubule-Microfilament Synergy in the Cytoskeleton.” *International Review of Cytology* 173:207–42.

George, Britta, Rakesh Verma, Abdulsalam A. Soofi, Puneet Garg, Jidong Zhang, Tae Ju Park, Laura Giardino, Larisa Ryzhova, Duncan B. Johnstone, Hetty Wong, Deepak Nihalani, David J. Salant, Steven K. Hanks, Tom Curran, Maria Pia Rastaldi, and Lawrence B. Holzman. 2012. “Crk1/2-Dependent Signaling Is Necessary for Podocyte Foot Process Spreading in Mouse Models of Glomerular Disease.” *Journal of Clinical Investigation* 122(2):674–92.

George, Lindsey A., Spencer K. Sullivan, Adam Giermasz, John E. J. Rasko, Benjamin J. Samelson-Jones, Jonathan Ducore, Adam Cuker, Lisa M. Sullivan, Suvankar Majumdar, Jerome Teitel, Catherine E. McGuinn, Margaret V. Ragni, Alvin Y. Luk, Daniel Hui, J. Fraser Wright, Yifeng Chen, Yun Liu, Katie Wachtel, Angela Winters, Stefan Tiefenbacher, Valder R. Arruda, Johannes C. M. van der Loo, Olga Zelenaia, Daniel Takefman, Marcus E. Carr, Linda B. Couto, Xavier M. Anguela, and Katherine A. High. 2017. “Hemophilia B Gene Therapy with a High-Specific-Activity Factor IX Variant.” *New England Journal of Medicine* 377(23):2215–27.

Gerke, Peter, Tobias B. Huber, Lorenz Sellin, Thomas Benzing, and Gerd Walz. 2003. “Homodimerization and Heterodimerization of the Glomerular Podocyte Proteins Nephrin and NEPH1.” *Journal of the American Society of Nephrology : JASN* 14(4):918–26.

Gerke, Peter, Lorenz Sellin, Oliver Kretz, Daniel Petraschka, Hanswalter Zentgraf, Thomas Benzing, and Gerd Walz. 2005. “NEPH2 Is Located at the Glomerular Slit Diaphragm, Interacts with Nephrin and Is Cleaved from Podocytes by Metalloproteinases.” *J Am Soc Nephrol* 16:1693–1702.

Gerosa, Clara, Daniela Fanni, Sonia Nemolato, Annalisa Locci, Viviana Marinelli, Tiziana Cabras, Irene Messana, Massimo Castagnola, and Guido Monga. 2010. “Thymosin Beta-10 Expression in Developing Human Kidney.” *The Journal of Maternal-Fetal & Neonatal Medicine* 23(S3):125–28.

Gertler, Frank B., Kirsten Niebuhr, Matthias Reinhard, Jürgen Wehland, and Philippe

Soriano. 1996. “Mena, a Relative of VASP and Drosophila Enabled, Is Implicated in the Control of Microfilament Dynamics.” *Cell* 87(2):227–39.

Gigante, Maddalena, Paola Pontrelli, Eustacchio Montemurno, Leonarda Roca, Filippo Aucella, Rosa Penza, Gianluca Caridi, Elena Ranieri, Gian Marco Ghiggeri, and Loreto Gesualdo. 2009. “CD2AP Mutations Are Associated with Sporadic Nephrotic Syndrome and Focal Segmental Glomerulosclerosis (FSGS).” *Nephrology Dialysis Transplantation* 24(6):1858–64.

Godoy-Parejo, Carlos, Chunhao Deng, Weiwei Liu, and Guokai Chen. 2019. “Insulin Stimulates PI3K/AKT and Cell Adhesion to Promote the Survival of Individualized Human Embryonic Stem Cells.” *Stem Cells* 37(8):1030–41.

Gokal, R. and N. P. Mallick. 1999. “Peritoneal Dialysis.” *Lancet* 353(9155):823–28.

Goldman, Robert D., Satya Khuon, Ying Hao Chou, Puneet Opal, and Peter M. Steinert. 1996. “The Function of Intermediate Filaments in Cell Shape and Cytoskeletal Integrity.” *The Journal of Cell Biology* 134(4):971–83.

Goldschmidt-Clermont, P. J., M. I. Furman, D. Wachsstock, D. Safer, V. T. Nachmias, and T. D. Pollard. 1992. “The Control of Actin Nucleotide Exchange by Thymosin Beta 4 and Profilin. A Potential Regulatory Mechanism for Actin Polymerization in Cells.” *Molecular Biology of the Cell* 3(9):1015–24.

Gooch, Katherine, Bruce F. Culleton, Braden J. Manns, Jianguo Zhang, Helman Alfonso, Marcello Tonelli, Cy Frank, Scott Klarenbach, and Brenda R. Hemmelgarn. 2007. “NSAID Use and Progression of Chronic Kidney Disease.” *American Journal of Medicine* 120(3):280.e1-280.e7.

Goodall, G. J., J. L. Hempstead, and J. I. Morgan. 1983. “Production and Characterization of Antibodies to Thymosin Beta 4.” *The Journal of Immunology* 131(2):821–25.

Goodson, Holly V and Erin M. Jonasson. 2018. “Microtubules and Microtubule-Associated Proteins.” *Cold Spring Harb Perspect Biol* 10:a022608.

Gorman, C. M., D. Gies, G. McCray, and M. Huang. 1989. “The Human Cytomegalovirus Major Immediate Early Promoter Can Be Trans-Activated by Adenovirus Early Proteins.” *Virology* 171(2):377–85.

Gorriz, Jose Luis and Alberto Martinez-Castelao. 2012. “Proteinuria: Detection and Role in Native Renal Disease Progression.” *Transplantation Reviews* 26(1):3–13.

Goutebroze, Laurence, Estelle Brault, Christian Muchardt, Jacques Camonis, and

Gilles Thomas. 2000. *Cloning and Characterization of SCHIP-1, a Novel Protein Interacting Specifically with Spliced Isoforms and Naturally Occurring Mutant NF2 Proteins*. Vol. 20.

Grahammer, Florian, Christoph Schell, and Tobias B. Huber. 2013. "The Podocyte Slit Diaphragm—from a Thin Grey Line to a Complex Signalling Hub." *Nature Publishing Group* 9:587–98.

Grant, D. S., W. Rose, C. Yaen, A. Goldstein, J. Martinez, and H. Kleinman. 1999. "Thymosin Beta4 Enhances Endothelial Cell Differentiation and Angiogenesis." *Angiogenesis* 3(2):125–35.

Gross, Oliver, Bogdan Beirowski, Scott J. Harvey, Catherine Mcfadden, Dilys Chen, Stephanie Tam, Paul S. Thorner, Neil Smyth, Klaus Addicks, Wilhelm Bloch, Yoshifumi Ninomiya, Yoshikazu Sado, Manfred Weber, and Wolfgang F. Vogel. 2004. "DDR1-Deficient Mice Show Localized Subepithelial GBM Thickening with Focal Loss of Slit Diaphragms and Proteinuria." *Kidney International* 66(1):102–11.

Guarnera, G., A. DeRosa, and R. Camerini. 2010. "The Effect of Thymosin Treatment of Venous Ulcers." *Annals of the New York Academy of Sciences* 1194(1):207–12.

Guilbaud, Mickaë L., Marie Devaux, Celia Couzinié, Johanne Le Duff, Alice Toromanoff, Cé Line Vandamme, Nicolas Jaulin, Gwladys Gernoux, Thibaut Larcher, Philippe Moullier, Caroline Le Guiner, and Oumeya Adjali. 2019. "Five Years of Successful Inducible Transgene Expression Following Locoregional Adeno-Associated Virus Delivery in Nonhuman Primates with No Detectable Immunity." *Human Gene Therapy* 30(7):802–13.

Guinobert, Isabelle, Melanie Viltard, David Piquemal, Jean-Marc Elalouf, Jacques Marti, and Martine Lelievre-Pegorier. 2005. "Identification of Differentially Expressed Genes between Fetal and Adult Mouse Kidney: Candidate Gene in Kidney Development." *Nephron Physiology* 102:81–91.

Gunning, P. W., U. Ghoshdastider, S. Whitaker, D. Popp, and R. C. Robinson. 2015. "The Evolution of Compositionally and Functionally Distinct Actin Filaments." *Journal of Cell Science* 128(11):2009–19.

Guo, Jian-Kan, Aswin L. Menke, Marie-Claire Gubler, Alan R. Clarke, David Harrison, Annette Hammes, Nicholas D. Hastie, and Andreas Schedl. 2002. "WT1 Is a Key Regulator of Podocyte Function: Reduced Expression Levels

Cause Crescentic Glomerulonephritis and Mesangial Sclerosis." *Human Molecular Genetics* 11(6):651–59.

Guo, Jiancheng, Radha Ananthakrishnan, Wu Qu, Yan Lu, Nina Reiniger, Shan Zeng, Wanchao Ma, Rosa Rosario, Shi Fang Yan, Ravichandran Ramasamy, Vivette D'agati, and Ann Marie Schmidt. 2008. "RAGE Mediates Podocyte Injury in Adriamycin-Induced Glomerulosclerosis The Interaction of Receptor for Advanced Glyca-Tion End Products (RAGE) with Its Ligands." *J Am Soc Nephrol* 19:961–72.

Guo, Na, Jin Guo, and Dongfang Su. 2016. "MicroRNA-206 and Its down-Regulation of Wilms'Tumor-1 Dictate Podocyte Health in Adriamycin-Induced Nephropathy." *Renal Failure* 38(6):989–95.

Gutiérrez, Orlando M. 2015. "Contextual Poverty, Nutrition, and Chronic Kidney Disease." *Advances in Chronic Kidney Disease* 22(1):31–38.

Hackl, Matthias J., James L. Burford, Karie Villanueva, Lisa Lam, Katalin Suszták, Bernhard Schermer, Thomas Benzing, and János Peti-Peterdi. 2013. "Tracking the Fate of Glomerular Epithelial Cells in Vivo Using Serial Multiphoton Imaging in New Mouse Models with Fluorescent Lineage Tags." *Nature Medicine* 19(12):1661–66.

Hadjiyanni, I., K. A. Siminovitch, J. S. Danska, and D. J. Drucker. 2010. "Glucagon-like Peptide-1 Receptor Signalling Selectively Regulates Murine Lymphocyte Proliferation and Maintenance of Peripheral Regulatory T Cells." *Diabetologia* 53(4):730–40.

Haemmerli, Gisela, Beatrice Arnold, and Peter Sträuli. 1983. "Cellular Motility on Glass and in Tissues: Similarities and Dissimilarities." *Cell Biology International Reports* 7(9):709–25.

Al Haj, Abdulatif, Antonina Joanna Mazur, Sabine Buchmeier, Christine App, Carsten Theiss, Unai Silvan, Cora-Ann Schoenenberger, Brigitte M. Jockusch, Ewald Hannappel, Alan G. Weeds, and Hans Georg Mannherz. 2014. "Thymosin Beta4 Inhibits ADF/Cofilin Stimulated F-Actin Cycling and Hela Cell Migration: Reversal by Active Arp2/3 Complex." *Cytoskeleton* 71(2):95–107.

Halbert, C. L., T. A. Standaert, M. L. Aitken, I. E. Alexander, D. W. Russell, and A. D. Miller. 1997. "Transduction by Adeno-Associated Virus Vectors in the Rabbit Airway: Efficiency, Persistence, and Readministration." *Journal of Virology* 71(8):5932–41.

Hall, Alan. 1998. “Rho GTPases and the Actin Cytoskeleton.” *Science* 279(509):509–14.

Hall, Alan K. 1994. “Amplification-Independent Overexpression of Thymosin Beta-10 MRNA in Human Renal Cell Carcinoma.” *Renal Failure* 16(2):243–54.

Hall, Brandon M., Vitaly Balan, Anatoli S. Gleiberman, Evguenia Strom, Peter Krasnov, Lauren P. Virtuoso, Elena Rydkina, Slavoljub Vujcic, Karina Balan, Ilya Gitlin, Katerina Leonova, Alexander Polinsky, Olga B. Chernova, and Andrei V. Gudkov. 2016. “Aging of Mice Is Associated with P16(Ink4a)- and β-Galactosidasepositive Macrophage Accumulation That Can Be Induced in Young Mice by Senescent Cells.” *Aging* 8(7):1294–1315.

Hanamura, Kikuno, Akihiro Tojo, Satoshi Kinugasa, Kensuke Asaba, and Toshiro Fujita. 2012. “The Resistive Index Is a Marker of Renal Function, Pathology, Prognosis, and Responsiveness to Steroid Therapy in Chronic Kidney Disease Patients.” *International Journal of Nephrology* 2012(Article ID 139565):1–9.

Hanna, Mary, Haibo Liu, Jawaria Amir, Yi Sun, Stephan W. Morris, M. A. Q. Siddiqui, Lester F. Lau, and Brahim Chaqour. 2009. “Mechanical Regulation of the Proangiogenic Factor CCN1/CYR61 Gene Requires the Combined Activities of MRTF-A and CREB-Binding Protein Histone Acetyltransferase.” *Journal of Biological Chemistry* 284(34):23125–36.

Hanna, Samer and Mirvat El-Sibai. 2013. “Signaling Networks of Rho GTPases in Cell Motility.” *Cellular Signalling* 25(10):1955–61.

Hannappel, E., G. J. Xu, J. Morgan, J. Hempstead, and B. L. Horecker. 1982. “Thymosin B4: A Ubiquitous Peptide in Rat and Mouse Tissues.” *Proceedings of the National Academy of Sciences of the United States of America* 79(7 I):2172–75.

Hansen, Scott D. and R. Dyche Mullins. 2010. “VASP Is a Processive Actin Polymerase That Requires Monomeric Actin for Barbed End Association.” *Journal of Cell Biology* 191(3):571–84.

Harker, Alyssa J., Harshwardhan H. Katkar, Tamara C. Bidone, Fikret Aydin, Gregory A. Voth, Derek A. Applewhite, and David R. Kovar. 2019. “Ena/VASP Processive Elongation Is Modulated by Avidity on Actin Filaments Bundled by the Filopodia Cross-Linker Fascin” edited by M. Théry. *Molecular Biology of the Cell* 30(7):851–62.

Harris, Jessica J., Hugh J. McCarthy, Lan Ni, Matthew Wherlock, Heegyung Kang,

Jack F. Wetzels, Gavin I. Welsh, and Moin A. Saleem. 2013. “Active Proteases in Nephrotic Plasma Lead to a Podocin-Dependent Phosphorylation of VASP in Podocytes via Protease Activated Receptor-1.” *Journal of Pathology* 229(5):660–71.

Haupt, Ygal, Ruth Maya, Anat Kazaz, and Moshe Oren. 1997. “Mdm2 Promotes the Rapid Degradation of P53.” *Nature* 387(6630):296–99.

He, Mingjuan, Yixiang Li, Li Wang, Bei Guo, Wen Mei, Biao Zhu, Jiajia Zhang, Yan Ding, Biying Meng, Liming Zhang, Lin Xiang, Jing Dong, Min Liu, Lingwei Xiang, and Guangda Xiang. 2020. “MYDGF Attenuates Podocyte Injury and Proteinuria by Activating Akt/BAD Signal Pathway in Mice with Diabetic Kidney Disease.” *Diabetologia* 63(9):1916–31.

Hébert, Marie Josée, Tomoko Takano, Aikaterina Papayianni, Helmut G. Rennke, Andrew Minto, David J. Salant, Michael C. Carroll, and Hugh R. Brady. 1998. “Acute Nephrotoxic Serum Nephritis in Complement Knockout Mice: Relative Roles of the Classical and Alternate Pathways in Neutrophil Recruitment and Proteinuria.” *Nephrology Dialysis Transplantation* 13(11):2799–2803.

Heerspink, Hiddo J. L., Avraham Karasik, Marcus Thuresson, Cheli Melzer-Cohen, Gabriel Chodick, Kamlesh Khunti, John P. H. Wilding, Luis Alberto Garcia Rodriguez, Lucia Cea-Soriano, Shun Kohsaka, Antonio Nicolucci, Giuseppe Lucisano, Fang Ju Lin, Chih Yuan Wang, Eric Wittbrodt, Peter Fenici, and Mikhail Kosiborod. 2020. “Kidney Outcomes Associated with Use of SGLT2 Inhibitors in Real-World Clinical Practice (CVD-REAL 3): A Multinational Observational Cohort Study.” *The Lancet Diabetes and Endocrinology* 8(1):27–35.

Heikkilä, Eija, Juuso Juhila, Markus Lassila, Marcel Messing, Nina Perälä, Eero Lehtonen, Sanna Lehtonen, Joseph Sjef Verbeek, and Harry Holthofer. 2010. “β-Catenin Mediates Adriamycin-Induced Albuminuria and Podocyte Injury in Adult Mouse Kidneys.” *Nephrology Dialysis Transplantation* 25(8):2437–46.

Hejazian, Seyede Mina, Sepideh Zununi Vahed, Hakimeh Moghaddas Sani, Ziba Nariman-Saleh-Fam, Milad Bastami, Seyed Mahdi Hosseiniyan Khatibi, Mohammadreza Ardalan, and Nasser Samadi. 2020. “Steroid-Resistant Nephrotic Syndrome: Pharmacogenetics and Epigenetic Points and Views.” *Expert Review of Clinical Pharmacology* 13(2):147–56.

Heng, Yi Wen and Cheng Gee Koh. 2010. “Actin Cytoskeleton Dynamics and the

Cell Division Cycle." *International Journal of Biochemistry and Cell Biology* 42(10):1622–33.

Henique, Carole, Guillaume Bollée, Xavier Loyer, Florian Grahammer, Neeraj Dhaun, Marine Camus, Julien Vernerey, Léa Guyonnet, François Gaillard, Hélène Lazareth, Charlotte Meyer, Imane Bensaada, Luc Legrès, Takashi Satoh, Shizuo Akira, Patrick Bruneval, Stefanie Dimmeler, Alain Tedgui, Alexandre Karras, Eric Thervet, Dominique Nochy, Tobias B. Huber, Laurent Mesnard, Olivia Lenoir, and Pierre Louis Tharaux. 2017. "Genetic and Pharmacological Inhibition of MicroRNA-92a Maintains Podocyte Cell Cycle Quiescence and Limits Crescentic Glomerulonephritis." *Nature Communications* 8(1).

Hermonat, P. L. and N. Muzyczka. 1984. "Use of Adeno-Associated Virus as a Mammalian DNA Cloning Vector: Transduction of Neomycin Resistance into Mammalian Tissue Culture Cells." *Proceedings of the National Academy of Sciences of the United States of America* 81(20 I):6466–70.

Hildinger, Markus, Alberto Auricchio, Guangping Gao, Lili Wang, Narendra Chirmule, and James M. Wilson. 2001. "Hybrid Vectors Based on Adeno-Associated Virus Serotypes 2 and 5 for Muscle-Directed Gene Transfer." *Journal of Virology* 75(13):6199–6203.

Hinkel, Rabea, Teresa Trenkwalder, Björn Petersen, Wira Husada, Florian Gesenhues, Seungmin Lee, Ewald Hannappel, Ildiko Bock-Marquette, Daniel Theisen, Laura Leitner, Peter Boekstegers, Czeslaw Cierniewski, Oliver J. Müller, Ferdinand le Noble, Ralf H. Adams, Christine Weinl, Alfred Nordheim, Bruno Reichart, Christian Weber, Eric Olson, Guido Posern, Elisabeth Deindl, Heiner Niemann, and Christian Kupatt. 2014. "MRTF-A Controls Vessel Growth and Maturation by Increasing the Expression of CCN1 and CCN2." *Nature Communications* 5:3970.

Hinze, Claudia and Emmanuel Boucrot. 2018. "Local Actin Polymerization during Endocytic Carrier Formation." *Biochemical Society Transactions* 46(3):565–76.

Le Hir, Michel, Cornelia Keller, Valérie Eschmann, Brunhilde Hähnel, Hiltraude Hosser, and Wilhelm Kriz. 2001. "Podocyte Bridges between the Tuft and Bowman's Capsule: An Early Event in Experimental Crescentic Glomerulonephritis | American Society of Nephrology." *Journal of the American Society of Nephrology* 12(10):2060–71.

Hirst, Jennifer A., José M. Ordóñez Mena, Clare J. Taylor, Yaling Yang, F. D. Richard Hobbs, Chris A. O'Callaghan, Richard J. McManus, Emma Ogburn, Maria D. L. A. Vazquez-Montes, Nathan Hill, Daniel Lasserson, and Brian Shine. 2020. "Prevalence of Chronic Kidney Disease in the Community Using Data from OxRen: A UK Population-Based Cohort Study." *British Journal of General Practice* 70(693):E285–93.

Ho, J. H. C., K. C. Tseng, W. H. Ma, K. H. Chen, O. K. S. Lee, and Y. Su. 2008. "Thymosin Beta-4 Upregulates Anti-Oxidative Enzymes and Protects Human Cornea Epithelial Cells against Oxidative Damage." *British Journal of Ophthalmology* 92(7):992–97.

Ho, Jennifer Hui Chun, Chiao Hui Chuang, Chih Yuan Ho, Yu Ru Vernon Shih, Oscar Kuang Sheng Lee, and Yeu Su. 2007. "Internalization Is Essential for the Antiapoptotic Effects of Exogenous Thymosin β-4 on Human Corneal Epithelial Cells." *Investigative Ophthalmology and Visual Science* 48(1):27–33.

Hogg, Ronald, John Middleton, and V. Matti Vehaskari. 2007. "Focal Segmental Glomerulosclerosis - Epidemiology Aspects in Children and Adults." *Pediatric Nephrology* 22(2):183–86.

Holland, Steven M. 2010. "Chronic Granulomatous Disease." *Clinical Reviews in Allergy and Immunology* 38(1):3–10.

Hollenbeck, Peter. 2001. "Cytoskeleton: Microtubules Get the Signal." *Current Biology* 11(20):R820–23.

Holness, C. .. and D. .. Simmons. 1993. "Molecular Cloning of CD68, a Human Macrophage Marker Related to Lysosomal Glycoproteins - PubMed." *Blood* 81(6):1607–13.

Honda, Kazufumi, Tesshi Yamada, Ritsuko Endo, Yoshinori Ino, Masahiro Gotoh, Hitoshi Tsuda, Yozo Yamada, Hiroshige Chiba, and Setsuo Hirohashi. 1998. "Actinin-4, a Novel Actin-Bundling Protein Associated with Cell Motility and Cancer Invasion." *Journal of Cell Biology* 140(6):1383–93.

Hoppe, John M. and Volker Vielhauer. 2014. "Induction and Analysis of Nephrotoxic Serum Nephritis in Mice." Pp. 159–74 in *Methods in Molecular Biology*. Vol. 1169, edited by H. Anders and A. Migliorini. New York, NY: Humana Press Inc.

Hosoe-Nagai, Yoshiko, Teruo Hidaka, Ayano Sonoda, Yu Sasaki, Kanae Yamamoto-Nonaka, Takuto Seki, Rin Asao, Eriko Tanaka, Juan Alejandro Oliva Trejo, Fumiko Kodama, Miyuki Takagi, Nobuhiro Tada, Takashi Ueno, Ryuichi

Nishinakamura, Yasuhiko Tomino, and Katsuhiko Asanuma. 2017. “Re-Expression of Sall1 in Podocytes Protects against Adriamycin-Induced Nephrosis.” *Laboratory Investigation* 97(11):1306–20.

Hotulainen, Pirta, Eija Paunola, Maria K. Vartiainen, and Pekka Lappalainen. 2005. “Actin-Depolymerizing Factor and Cofilin-1 Play Overlapping Roles in Promoting Rapid F-Actin Depolymerization in Mammalian Nonmuscle Cells □ D □ V.” *Molecular Biology of the Cell* 16:649–64.

Hu, Jianwen, Jizhong Han, Haoran Li, Xian Zhang, Lan lan Liu, Fei Chen, and Bin Zeng. 2018. “Human Embryonic Kidney 293 Cells: A Vehicle for Biopharmaceutical Manufacturing, Structural Biology, and Electrophysiology.” *Cells Tissues Organs* 205(1):1–8.

Huang, Z., L. Zhang, Y. Chen, H. Zhang, Q. Zhang, R. Li, J. Ma, Z. Li, C. Yu, Y. Lai, T. Lin, X. Zhao, B. Zhang, Z. Ye, S. Liu, W. Wang, X. Liang, R. Liao, and W. Shi. 2016. “Cdc42 Deficiency Induces Podocyte Apoptosis by Inhibiting the Nwasp/Stress Fibers/YAP Pathway.” *Cell Death and Disease* 7(3):e2142–e2142.

Huber, Tobias B., Miriam Schmidts, Peter Gerke, Bernhard Schermer, Anne Zahn, Björn Hartleben, Lorenz Sellin, Gerd Walz, and Thomas Benzing. 2003. “The Carboxyl Terminus of Neph Family Members Binds to the PDZ Domain Protein Zonula Occludens-1.” *Journal of Biological Chemistry* 278(15):13417–21.

Huehn, Andrew, Wenxiang Cao, W. Austin Elam, Xueqi Liu, Enrique M. De La Cruz, and Charles V. Sindelar. 2018. “The Actin Filament Twist Changes Abruptly at Boundaries between Bare and Cofilin-Decorated Segments.” *Journal of Biological Chemistry* 293(15):5377–83.

Hueschen, Christina L., Samuel J. Kenny, Ke Xu, and Sophie Dumont. 2017. “NuMA Recruits Dynein Activity to Microtubule Minus-Ends at Mitosis.” *ELife* 6:e29328.

Husson, Clotilde, François-Xavier Cantrelle, Pierre Roblin, Dominique Didry, Kim Ho, Diep Le, Javier Perez, Eric Guittet, Carine Van Heijenoort, Louis Renault, and Marie-France Carlier. 2010. “Multifunctionality of the β-Thymosin/WH2 Module: G-Actin Sequestration, Actin Filament Growth, Nucleation, and Severing.” *Annals of the New York Academy of Sciences* 1194:44–52.

Ichimura, Koichiro, Hidetake Kurihara, and Tatsuo Sakai. 2003. “Actin Filament Organization of Foot Processes in Rat Podocytes.” *Journal of Histochemistry & Cytochemistry* 51(12):1589–1600.

Ichimura, Koichiro, Hidetake Kurihara, and Tatsuo Sakai. 2007. “Actin Filament Organization of Foot Processes in Vertebrate Glomerular Podocytes.” *Cell and Tissue Research* 329(3):541–57.

Ichimura, Koichiro, Takayuki Miyaki, Yuto Kawasaki, Mui Kinoshita, Soichiro Kakuta, and Tatsuo Sakai. 2019. “Morphological Processes of Foot Process Effacement in Puromycin Aminonucleoside Nephrosis Revealed by FIB/SEM Tomography.” *Journal of the American Society of Nephrology* 30(1):96–108.

Idriss, Haitham T. and James H. Naismith. 2000. “TNFα and the TNF Receptor Superfamily: Structure-Function Relationship(S).” *Microscopy Research and Technique* 50(3):184–95.

Ikeda, Yoichiro, Zhao Sun, Xiao Ru, Luk H. Vandenberghe, and Benjamin D. Humphreys. 2018. “Efficient Gene Transfer to Kidney Mesenchymal Cells Using a Synthetic Adeno-Associated Viral Vector.” *Journal of the American Society of Nephrology* 29(9):2287–97.

Ikezumi, Yohei, Toshiaki Suzuki, Tamaki Karasawa, Hiroshi Kawachi, David J. Nikolic-Paterson, and Makoto Uchiyama. 2008. “Activated Macrophages Down-Regulate Podocyte Nephrin and Podocin Expression via Stress-Activated Protein Kinases.” *Biochemical and Biophysical Research Communications* 376(4):706–11.

Isambert, H., P. Venier, A. C. Maggs, A. Fattoum, R. Kassab, D. Pantaloni, and M. F. Carlier. 1995. “Flexibility of Actin Filaments Derived from Thermal Fluctuations. Effect of Bound Nucleotide, Phalloidin, and Muscle Regulatory Proteins.” *Journal of Biological Chemistry* 270(19):11437–44.

Jacobson, Samuel G., Artur V. Cideciyan, Alejandro J. Roman, Alexander Sumaroka, Sharon B. Schwartz, Elise Heon, and William W. Hauswirth. 2015. “Improvement and Decline in Vision with Gene Therapy in Childhood Blindness.” *New England Journal of Medicine* 372(20):1920–26.

Jarad, George and Jeffrey H. Miner. 2009. “Update on the Glomerular Filtration Barrier.” *Current Opinion in Nephrology and Hypertension* 18(3):226–32.

Jat, Parmjit S., Mark D. Noble, Paris Ataliotis, Yujiro Tanaka, Nikos Yannoutsos, Lena Larsen, and Dimitris Kioussis. 1991. “Direct Derivation of Conditionally Immortal Cell Lines from an H-2Kb-TsA58 Transgenic Mouse.” *Proceedings of the National Academy of Sciences of the United States of America* 88(12):5096–5100.

Jefferson, J. Ashley and Stuart J. Shankland. 2014. “The Pathogenesis of Focal Segmental Glomerulosclerosis.” *Advances in Chronic Kidney Disease* 21(5):408–16.

Jennette, J. Charles and Ronald J. Falk. 1997. “Small-Vessel Vasculitis.” *New England Journal of Medicine* 337(21):1512–23.

Jeon, Byung Joon, Yoolhee Yang, Su Kyung Shim, Heung Mo Yang, Daeho Cho, and Sa Ik Bang. 2013. “Thymosin Beta-4 Promotes Mesenchymal Stem Cell Proliferation via an Interleukin-8-Dependent Mechanism.” *Experimental Cell Research* 319(17):2526–34.

Johnson, R. J., C. E. Alpers, A. Yoshimura, D. Lombardi, P. Pritzl, J. Floege, and S. M. Schwartz. 1992. “Renal Injury from Angiotensin II-Mediated Hypertension.” *Hypertension* 19(5):464–74.

Johnson, Richard J., Hiroyuki Lida, Charles E. Alpers, Mark W. Majesky, Stephen M. Schwartz, Pam Pritzl, Kathy Gordon, and Allen M. Gownt. 1991. “Expression of Smooth Muscle Cell Phenotype by Rat Mesangial Cells in Immune Complex Nephritis.” *Journal of Clinical Investigation* 87:847–58.

Jones, Nina, Ivan M. Blasutig, Vera Eremina, Julie M. Ruston, Friedhelm Bladt, Hongping Li, Maiming Huang, Louise Larose, Shawn S. C. Li, Tomoko Takano, Susan E. Quaggin, and Tony Pawson. 2006. “Nck Adaptor Proteins Link Nephrin to the Actin Cytoskeleton of Kidney Podocytes.” *Nature* 440(7085):818–23.

Junot, Christophe, Laurence Nicolet, Eric Ezan, Marie-Francoise Gonzales, Joel Menard, and Michel Azizi. 1999. “Effect of Angiotensin-Converting Enzyme Inhibition on Plasma, Urine, and Tissue Concentrations of Hemoregulatory Peptide Acetyl-Ser-Asp-Lys-Pro in Rats.” *The Journal of Pharmacology and Experimental Therapeutics* 291(3):982–87.

Kandel, Mikhail E., Kai Wen Teng, Paul R. Selvin, and Gabriel Popescu. 2017. “Label-Free Imaging of Single Microtubule Dynamics Using Spatial Light Interference Microscopy.” *ACS Nano* 11(1):647–55.

Kaneko, Yoshikatsu, Takamasa Cho, Yuya Sato, Kei Goto, Suguru Yamamoto, Shin Goto, Michael P. Madaio, and Ichiei Narita. 2018. “Attenuated Macrophage Infiltration in Glomeruli of Aged Mice Resulting in Ameliorated Kidney Injury in Nephrotoxic Serum Nephritis.” *The Journals of Gerontology: Series A* 73(9):1178–86.

Kaplan, Joshua M., Sung Han Kim, Kathryn N. North, Helmut Rennke, Lori Ann Correia, Hui Qi Tong, Beverly J. Mathis, José Carlos Rodríguez-Pérez, Philip G. Allen, Alan H. Beggs, and Martin R. Pollak. 2000. “Mutations in ACTN4, Encoding α-Actinin-4, Cause Familial Focal Segmental Glomerulosclerosis.” *Nature Genetics* 24(3):251–56.

Karaiskos, Nikos, Mahdieh Rahmatollahi, Anastasiya Boltengagen, Haiyue Liu, Martin Hoehne, Markus Rinschen, Bernhard Schermer, Thomas Benzing, Nikolaus Rajewsky, Christine Kocks, Martin Kann, and Roman Ulrich Müller. 2018. “A Single-Cell Transcriptome Atlas of the Mouse Glomerulus.” *Journal of the American Society of Nephrology* 29(8):2060–68.

Kardos, Roland, Andrea Vig, József Orbán, Gábor Hild, Miklós Nyitrai, and Dénes Lorinczy. 2007. “The Effect of Jasplakinolide on the Thermodynamic Properties of ADP.BeFx Bound Actin Filaments.” *Thermochimica Acta* 463(1–2):77–80.

Karger, S., Li-Hong Ren, Hai-Tao Zhang, Wei-Wei Wang, Xia-Xia Zhao, Zhi-Hui Wang, De-Li Zhuang, and Yun-Nuo Bai. 2016. “The MTORC2/Akt/NFκB Pathway-Mediated Activation of TRPC6 Participates in Adriamycin-Induced Podocyte Apoptosis.” *Cell Physiol Biochem* 40:1079–93.

Karnovsky, M. J. and S. K. Ainsworth. 1972. “The Structural Basis of Glomerular Filtration.” *Advances in Nephrology from the Necker Hospital* 2:35–60.

Kaverina, Natalya V., Diana G. Eng, Andrea D. Largent, Ilse Daehn, Anthony Chang, Kenneth W. Gross, Jeffrey W. Pippin, Peter Hohenstein, and Stuart J. Shankland. 2017. “WT1 Is Necessary for the Proliferation and Migration of Cells of Renin Lineage Following Kidney Podocyte Depletion.” *Stem Cell Reports* 9(4):1152–66.

Keith, Allison R., Kirk Twaroski, Christen L. Ebens, and Jakub Tolar. 2020. “Leading Edge: Emerging Drug, Cell, and Gene Therapies for Junctional Epidermolysis Bullosa.” *Expert Opinion on Biological Therapy* 20(8):911–23.

Kelich, Joseph M., Jiong Ma, Biao Dong, Qizhao Wang, Mario Chin, Connor M. Magura, Weidong Xiao, and Weidong Yang. 2015. “Super-Resolution Imaging of Nuclear Import of Adeno-Associated Virus in Live Cells.” *Molecular Therapy - Methods and Clinical Development* 2:15047.

Kerjaschki, Dontscho, David J. Sharkey, and Marilyn Gist Farquhar. 1984. “Identification and Characterization of Podocalyxin-the Major Sialoprotein of the Renal Glomerular Epithelial Cell.” *The Journal of Cell Biology* 98:1591–96.

Kerr, Marion, Benjamin Bray, James Medcalf, Donal J. O'Donoghue, and Beverley Matthews. 2012. "Estimating the Financial Cost of Chronic Kidney Disease to the NHS in England." *Nephrology Dialysis Transplantation* 27(SUPPL. 3):iii73-80.

Kestilä, Marjo, Ulla Lenkkeri, Minna Männikkö, Jane Lamerdin, Paula McCready, Heli Putaala, Vesa Ruotsalainen, Takako Morita, Marja Nissinen, Riitta Herva, Clifford E. Kashtan, Leena Peltonen, Christer Holmberg, Anne Olsen, and Karl Tryggvason. 1998. "Positionally Cloned Gene for a Novel Glomerular Protein—Nephrin—Is Mutated in Congenital Nephrotic Syndrome." *Molecular Cell* 1(4):575–82.

Kevany, Brian M., Scott Kerns, Linas Padegimas, and Timothy J. Miller. 2019. "AAV Gene Therapy for the Treatment of Fabry Disease: A Novel Capsid with Improved Tropism to Heart, Kidney and CNS and Improved GLA Expression." *Molecular Genetics and Metabolism* 126(2):S83.

Khan, Sarah B., H. Terence Cook, Gurjeet Bhangal, Jennifer Smith, Frederick W. K. Tam, and Charles D. Pusey. 2005. "Antibody Blockade of TNF-α Reduces Inflammation and Scarring in Experimental Crescentic Glomerulonephritis." *Kidney International* 67(5):1812–20.

Khoshnoodi, Jamshid, Kristmundur Sigmundsson, Lars Göran Öfverstedt, Ulf Skoglund, Björn Obrink, Jorma Wartiovaara, and Karl Tryggvason. 2003. "Nephrin Promotes Cell-Cell Adhesion through Homophilic Interactions." *American Journal of Pathology* 163(6):2337–46.

Kim, Jae-Gyu, Rokibul Islam, Jung Y. Cho, Hwalrim Jeong, Kim-Cuong Cap, Yohan Park, Abu J. Hossain, and Jae-Bong Park. 2018. "Regulation of RhoA GTPase and Various Transcription Factors in the RhoA Pathway." *Journal of Cellular Physiology* 233(9):6381–92.

Kim, Jane H., Martha Konieczkowski, Amitava Mukherjee, Sam Schechtman, Shenaz Khan, Jeffrey R. Schelling, Michael D. Ross, Leslie A. Bruggeman, and John R. Sedor. 2010. "Podocyte Injury Induces Nuclear Translocation of WTIP via Microtubule-Dependent Transport." *The Journal of Biological Chemistry* 285(13):9995–10004.

Kim, Ji Eun, Dohyun Han, Jin Seon Jeong, Jong Joo Moon, Hyun Kyung Moon, Sunhwa Lee, Yong Chul Kim, Kyung Don Yoo, Jae Wook Lee, Dong Ki Kim, Young Joo Kwon, Yon Su Kim, and Seung Hee Yang. 2021. "Multi-Sample

Mass Spectrometry-Based Approach for Discovering Injury Markers in Chronic Kidney Disease." *Molecular & Cellular Proteomics*.

Kim, S. H. and J. H. Kim. 1972. *Lethal Effect of Adriamycin on the Division Cycle of HeLa Cells1*. Vol. 32.

Kim, Seyun and Pierre A. Coulombe. 2007. "Intermediate Filament Scaffolds Fulfill Mechanical, Organizational, and Signaling Functions in the Cytoplasm." *Genes and Development* 21:1581–97.

Kim, Sokho and Jungkee Kwon. 2015. "Actin Cytoskeletal Rearrangement and Dysfunction Due to Activation of the Receptor for Advanced Glycation End Products Is Inhibited by Thymosin Beta 4." *The Journal of Physiology* 593(8):1873–86.

Kim, Sokho and Jungkee Kwon. 2017. "Thymosin *β* 4 Has a Major Role in Dermal Burn Wound Healing That Involves Actin Cytoskeletal Remodelling via Heat-Shock Protein 70." *Journal of Tissue Engineering and Regenerative Medicine* 11(4):1262–73.

Kirsch, A. H., V. Riegelbauer, A. Tagwerker, M. Rudnicki, A. R. Rosenkranz, and K. Eller. 2012. "The MTOR-Inhibitor Rapamycin Mediates Proteinuria in Nephrotoxic Serum Nephritis by Activating the Innate Immune Response." *American Journal of Physiology-Renal Physiology* 303(4):F569–75.

Kitada, Munehiro, Yoshio Ogura, and Daisuke Koya. 2016. "Rodent Models of Diabetic Nephropathy: Their Utility and Limitations." *International Journal of Nephrology and Renovascular Disease* 9:279–90.

Klastersky, J., J. P. Sculier, J. P. Dumont, D. Becquart, G. Vandermoten, P. Rocmans, J. Michel, E. Longeval, and O. Dalesio. 1985. "Combination Chemotherapy with Adriamycin, Etoposide, and Cyclophosphamide for Small Cell Carcinoma of the Lung. A Study by the EORTC Lung Cancer Working Party (Belgium)." *Cancer* 56(1):71–75.

Klein, Julie, Bénédicte Buffin-Meyer, Franck Boizard, Nabila Moussaoui, Ophélie Lescat, Benjamin Breuil, Camille Fedou, Guylène Feuillet, Audrey Casemayou, Eric Neau, An Hindryckx, Luc Decatte, Elena Levtchenko, Anke Raaijmakers, Christophe Vayssière, Valérie Goua, Charlotte Lucas, Franck Perrotin, Sylvie Cloarec, Alexandra Benachi, Marie-Christine Manca-Pellissier, Hélène Laurichesse Delmas, Lucie Bessenay, Claudine Le Vaillant, Emma Allain-Launay, Jean Gondry, Bernard Boudailliez, Elisabeth Simon, Fabienne Prieur,

Marie-Pierre Lavocat, Anne-Hélène Saliou, Loic De Parscau, Laurent Bidat, Catherine Noel, Corinne Floch, Guylène Bourdat-Michel, Romain Favre, Anne-Sophie Weingertner, Jean-François Oury, Véronique Baudouin, Jean-Paul Bory, Christine Pietrement, Maryse Fiorenza, Jérôme Massardier, Sylvie Kessler, Nadia Lounis, Françoise Conte Auriol, Pascale Marcorelles, Sophie Collardeau-Frachon, Petra Zürbig, Harald Mischak, Pedro Magalhães, Julie Batut, Patrick Blader, Jean-Sebastien Saulnier Blache, Jean-Loup Bascands, Franz Schaefer, Stéphane Decramer, Joost P. Schanstra, Karel Allegaert, Yves Aubard, Odile Basmaison, Jean-Baptiste Benevent, Florence Biquard, Gérard Champion, Jean-Marie Delbosc, Philippe Eckart, Marie-Françoise Froute, Pascal Gaucherand, Marion Groussolles, Vincent Guigonis, Blandine Hougas, Gwenaelle Le Bouar, Alain Martin, Sophie Martin, Mariannick Maupin-Hyvonnet, Marina Merveille, Eve Mousty, François Nobili, Amelie Ryckewaert, Agnes Sartor, Sophie Taque, and Norbert Winer. 2020. “Amniotic Fluid Peptides Predict Postnatal Kidney Survival in Developmental Kidney Disease.” *Kidney International* S0085-2538(20):30894–2.

Kobayashi, Akio, M. Todd Valerius, Joshua W. Mugford, Thomas J. Carroll, Michelle Self, Guillermo Oliver, and Andrew P. McMahon. 2008. “Six2 Defines and Regulates a Multipotent Self-Renewing Nephron Progenitor Population throughout Mammalian Kidney Development.” *Cell Stem Cell* 3(2):169–81.

Kobayashi, Naoto, Jochen Reiser, Wilhelm Kriz, Ryoko Kuriyama, and Peter Mundel. 1998. “Nonuniform Microtubular Polarity Established by CHO1/MKLP1 Motor Protein Is Necessary for Process Formation of Podocytes.” *Journal of Cell Biology* 143(7):1961–70.

Kobayashi, Naoto, Jochen Reiser, Karin Schwarz, Tatsuo Sakai, Wilhelm Kriz, and Peter Mundel. 2001. “Process Formation of Podocytes: Morphogenetic Activity of Microtubules and Regulation by Protein Serine/Threonine Phosphatase PP2A.” *Histochemistry and Cell Biology* 115(3):255–66.

Kokko, Juha P. 1970. “Sodium Chloride and Water Transport in the Descending Limb of Henle.” *The Journal of Clinical Investigation* 49:1838–46.

Kolkhof, Peter, Martina Delbeck, Axel Kretschmer, Wolfram Steinke, Elke Hartmann, Lars Bärfacker, Frank Eitner, Barbara Albrecht-Küpper, and Stefan Schäfer. 2014. “Finerenone, a Novel Selective Nonsteroidal Mineralocorticoid Receptor Antagonist Protects From Rat Cardiorenal Injury.” *Journal of Cardiovascular*

Pharmacology 64(1):69–78.

Koning, Sarah H., Ron T. Gansevoort, Kenneth J. Mukamal, Eric B. Rimm, Stephan J. L. Bakker, and Michel M. Joosten. 2015. “Alcohol Consumption Is Inversely Associated with the Risk of Developing Chronic Kidney Disease.” *Kidney International* 87(5):1009–16.

Korhonen, M., J. Ylänne, L. Laitinen, and I. Virtanen. 1990. “Distribution of Beta 1 and Beta 3 Integrins in Human Fetal and Adult Kidney - PubMed.” *Lab Invest.* 62(5):616–25.

Korsunsky, Ilya, Nghia Millard, Jean Fan, Kamil Slowikowski, Fan Zhang, Kevin Wei, Yuriy Baglaenko, Michael Brenner, Po ru Loh, and Soumya Raychaudhuri. 2019. “Fast, Sensitive and Accurate Integration of Single-Cell Data with Harmony.” *Nature Methods* 16(12):1289–96.

Kovar, David R., Elizabeth S. Harris, Rachel Mahaffy, Henry N. Higgs, and Thomas D. Pollard. 2006. “Control of the Assembly of ATP- and ADP-Actin by Formins and Profilin.” *Cell* 124(2):423–35.

Kraus, Alison C., Ines Ferber, Sven Oliver Bachmann, Hannah Specht, Anja Wimmel, Markus W. Gross, Juergen Schlegel, Guntram Suske, and Marcus Schuermann. 2002. “In Vitro Chemo- and Radio-Resistance in Small Cell Lung Cancer Correlates with Cell Adhesion and Constitutive Activation of AKT and MAP Kinase Pathways.” *Oncogene* 21(57):8683–95.

Kretzler, Matthias, Vicente P. C. Teixeira, Paul G. Unschuld, Clemens D. Cohen, Rüdiger Wanke, Ilka Edenhofer, Peter Mundel, Detlef Schlöndorff, and Harry Holthöfer. 2001. “Integrin Linked Kinase as a Candidate Downstream Effector in Proteinuria.” *The FASEB Journal* 15(10):1843–45.

Kriz, W., N. Gretz, and K. V. Lemley. 1998. “Progression of Glomerular Diseases: Is the Podocyte the Culprit?” *Kidney International* 54(3):687–97.

Kriz, Wilhelm, Eberhard Hackenthal, Rainer Nobiling, Tatsuo Sakai, and Marlies Elger. 1994. “A Role for Podocytes to Counteract Capillary Wall Distension.” *Kidney International* 45:369–76.

Kriz, Wilhelm, Isao Shirato, Michio Nagata, Michel LeHir, and Kevin V. Lemley. 2013. “The Podocyte’s Response to Stress: The Enigma of Foot Process Effacement.” *American Journal of Physiology - Renal Physiology* 304(4).

Kruger, Claudia, Susan J. Burke, J. Jason Collier, Trang Tiffany Nguyen, J. Michael Salbaum, and Krisztian Stadler. 2018. “Lipid Peroxidation Regulates Podocyte

Migration and Cytoskeletal Structure through Redox Sensitive RhoA Signaling." *Redox Biology* 16:248–54.

Kubo, Ayano, Teruo Hidaka, Maiko Nakayama, Yu Sasaki, Miyuki Takagi, Hitoshi Suzuki, and Yusuke Suzuki. 2020. "Protective Effects of DPP-4 Inhibitor on Podocyte Injury in Glomerular Diseases." *BMC Nephrology* 21(1):402.

Kumar, Nitin, Tang-Dong Liao, Cesar A. Romero, Mani Maheshwari, Edward L. Peterson, and Oscar A. Carretero. 2018. "Thymosin Beta4 Deficiency Exacerbates Renal and Cardiac Injury in Angiotensin-II-Induced Hypertension." *Hypertension* (71):1133–42.

Kumar, Nitin, Tang Dong Liao, Cesar A. Romero, Mani Maheshwari, Edward L. Peterson, and Oscar A. Carretero. 2018. "Thymosin B4 Deficiency Exacerbates Renal and Cardiac Injury in Angiotensin-II-Induced Hypertension." *Hypertension* 71(6):1133–42.

Kumar, Nitin, Pablo Nakagawa, Branislava Janic, Cesar A. Romero, Morel E. Worou, Sumit R. Monu, Edward L. Peterson, Jiajiu Shaw, Frederick Valeriote, Elimelda M. Ongeri, Jean-Marie V. Niyitegeka, Nour-Eddine Rhaleb, and Oscar A. Carretero. 2016. "The Anti-Inflammatory Peptide Ac-SDKP Is Released from Thymosin-B4 by Renal Meprin-α and Prolyl Oligopeptidase." *American Journal of Physiology-Renal Physiology* 310(10):F1026–34.

Kumar, Nitin and Congcong Yin. 2018. "The Anti-Inflammatory Peptide Ac-SDKP: Synthesis, Role in ACE Inhibition, and Its Therapeutic Potential in Hypertension and Cardiovascular Diseases." *Pharmacological Research* 134:268–79.

Kumar, S. and S. Gupta. 2011. "Thymosin Beta 4 Prevents Oxidative Stress by Targeting Antioxidant and Anti-Apoptotic Genes in Cardiac Fibroblasts." *PLoS ONE* 6(10):26912.

Kurimasa, Akihiro, Honghai Ouyang, Li Jin Dong, Sa Wang, Xiaoling Li, Carlos Cordon-Cardo, David J. Chen, and Gloria C. Li. 1999. "Catalytic Subunit of DNA-Dependent Protein Kinase: Impact on Lymphocyte Development and Tumorigenesis." *Proceedings of the National Academy of Sciences of the United States of America* 96(4):1403–8.

Kursula, Petri, Inari Kursula, Marzia Massimi, Young Hwa Song, Joshua Downer, Will A. Stanley, Walter Witke, and Matthias Wilmanns. 2008. "High-Resolution Structural Analysis of Mammalian Profilin 2a Complex Formation with Two Physiological Ligands: The Formin Homology 1 Domain of MDia1 and the

Proline-Rich Domain of VASP." *Journal of Molecular Biology* 375(1):270–90.

Kvirkvelia, Nino, Malgorzata McMenamin, Kapil Chaudhary, Manuela Bartoli, and Michael P. Madaio. 2013. "Prostaglandin E $_2$ Promotes Cellular Recovery from Established Nephrotoxic Serum Nephritis in Mice, Prosurvival, and Regenerative Effects on Glomerular Cells." *American Journal of Physiology-Renal Physiology* 304(5):F463–70.

Kwiatkowski, Adam V., Frank B. Gertler, and Joseph J. Loureiro. 2003. "Function and Regulation of Ena/VASP Proteins." *Trends in Cell Biology* 13(7):386–92.

De La Cruz, E M, E. Michael Ostap, Rodney A. Brundage, K. S. Reddy, H. Lee Sweeney, and Daniel Safer. 2000. "Thymosin-ℕ 4 Changes the Conformation and Dynamics of Actin Monomers." *Biophysical Journal* 78:2516–27.

De La Cruz, Enrique M. 2009. "How Cofilin Severs an Actin Filament." *Biophysical Reviews* 1(2):51–59.

De La Cruz, Enrique M., E. Michael Ostap, Rodney A. Brundage, K. S. Reddy, H. Lee Sweeney, and Daniel Safer. 2000. "Thymosin-B4 Changes the Conformation and Dynamics of Actin Monomers." *Biophysical Journal* 78(5):2516–27.

Lackner, Daniel F. and Nicholas Muzyczka. 2002. "Studies of the Mechanism of Transactivation of the Adeno-Associated Virus P19 Promoter by Rep Protein." *Journal of Virology* 76(16):8225–35.

Lamaze, C., L. M. Fujimoto, H. L. Yin, and S. L. Schmid. 1997. "The Actin Cytoskeleton Is Required for Receptor-Mediated Endocytosis in Mammalian Cells." *The Journal of Biological Chemistry* 272(33):20332–35.

Lankelma, Jan, Henk Dekker, Rafael Fernández Luque, Sylvia Luykx, Klaas Hoekman, Paul Van Der Valk, Paul J. Van Diest, and Herbert M. Pinedo. 1999. "Doxorubicin Gradients in Human Breast Cancer." *Clinical Cancer Research* 5:1703–7.

Larson, Adam M. 2011. "Multiphoton Microscopy." *Nature Photonics* 5(1):1–1.

Lazarides, E. and U. Lindberg. 1974. "Actin Is the Naturally Occurring Inhibitor of Deoxyribonuclease I." *Proceedings of the National Academy of Sciences of the United States of America* 71(12):4742–46.

Le, Shimin, Miao Yu, Alexander Bershadsky, and Jie Yan. 2020. "Mechanical Regulation of Formin-Dependent Actin Polymerization." *Seminars in Cell and*

Developmental Biology 102:73–80.

Lee, Sang-Im, Duck-Su Kim, Hwa-Jeong Lee, Hee-Jae Cha, and Eun-Cheol Kim. 2013. “The Role of Thymosin Beta 4 on Odontogenic Differentiation in Human Dental Pulp Cells” edited by I. Kerkis. *PLoS ONE* 8(4):e61960.

Lee, Soo Bong and Raghu Kalluri. 2010. “Mechanistic Connection between Inflammation and Fibrosis.” *Kidney International* 78(SUPPL. 119):S22–26.

Lee, Vincent WS and David CH Harris. 2011. “Adriamycin Nephropathy: A Model of Focal Segmental Glomerulosclerosis.” *Nephrology* 16(1):30–38.

Lefebvre, Jonathan, Michael Clarkson, Filippo Massa, Stephen T. Bradford, Aurelie Charlet, Fabian Buske, Sandra Lacas-Gervais, Herbert Schulz, Charlotte Gimpel, Yutaka Hata, Franz Schaefer, and Andreas Schedl. 2015. “Alternatively Spliced Isoforms of WT1 Control Podocyte-Specific Gene Expression.” *Kidney International* 88(2):321–31.

Lenkkeri, Ulla, Minna Männikkö, Paula McCready, Jane Lamerdin, Olivier Gribouval, Patrick Niaudet, Corinne Antignac, Clifford E. Kashtan, Christer Holmberg, Anne Olsen, Marjo Kestilä, and Karl Tryggvason. 1999. “Structure of the Gene for Congenital Nephrotic Syndrome of the Finnish Type (NPHS1) and Characterization of Mutations.” *The American Journal of Human Genetics* 64(1):51–61.

Lennon, Rachel, Michael J. Randles, and Martin J. Humphries. 2014. “The Importance of Podocyte Adhesion for a Healthy Glomerulus.” *Frontiers in Endocrinology* 5(OCT):160.

Leube, Rudolf E., Marcin Moch, and Reinhard Windoffer. 2015. “Intermediate Filaments and the Regulation of Focal Adhesion.” *Current Opinion in Cell Biology* 32:13–20.

Levey, Andrew S. and Josef Coresh. 2012. “Chronic Kidney Disease.” *The Lancet* 379(9811):165–80.

Li, Chao, Li Zhang, Chunyang Wang, Hua Teng, Baoyan Fan, Michael Chopp, and Zheng Gang Zhang. 2019. “N-Acetyl-Seryl-Aspartyl-Lysyl-Proline Augments Thrombolysis of TPA (Tissue-Type Plasminogen Activator) in Aged Rats After Stroke.” *Stroke* 50(9):2547–54.

Li, Chengwen and R. Jude Samulski. 2020. “Engineering Adeno-Associated Virus Vectors for Gene Therapy.” *Nature Reviews Genetics* 21(4):255–72.

Li, Hongwei, Yonggang Wang, Xuchang Hu, Bing Ma, and Haihong Zhang. 2019.

"Thymosin Beta 4 Attenuates Oxidative Stress-Induced Injury of Spinal Cord-Derived Neural Stem/Progenitor Cells through the TLR4/MyD88 Pathway." *Gene* 707:136–42.

Li, Jinhua, Xinli Qu, and John F. Bertram. 2009. "Endothelial-Myofibroblast Transition Contributes to the Early Development of Diabetic Renal Interstitial Fibrosis in Streptozotocin-Induced Diabetic Mice." *American Journal of Pathology* 175(4):1380–88.

Li, Xiaozhong, Haitao Yuan, and Xueguang Zhang. 2003. "Adriamycin Increases Podocyte Permeability: Evidence and Molecular Mechanism." *Chinese Medical Journal* 116(12):1831–35.

Liao, Tang-Dong, Pablo Nakagawa, Branislava Janic, Martin D'Ambrosio, Morel E. Worou, Edward L. Peterson, Nour-Eddine Rhaleb, Xiao-Ping Yang, and Oscar A. Carretero. 2015. "N-Acetyl-Seryl-Aspartyl-Lysyl-Proline: Mechanisms of Renal Protection in Mouse Model of Systemic Lupus Erythematosus." *American Journal of Physiology - Renal Physiology* 308(10):F1146–54.

Liapis, Helen, Paola Romagnani, and Hans Joachim Anders. 2013. "New Insights into the Pathology of Podocyte Loss: Mitotic Catastrophe." *American Journal of Pathology* 183(5):1364–74.

Licette, C. Y., Elise Liu, and Ron Schutte. 2015. "Finerenone: Third-Generation Mineralocorticoid Receptor Antagonist for the Treatment of Heart Failure and Diabetic Kidney Disease." *Expert Opinion on Investigational Drugs* 24(8):1123–35.

Lim, Beom Jin, Jae Won Yang, Woo Sung Do, and Agnes B. Fogo. 2016. "Pathogenesis of Focal Segmental Glomerulosclerosis." *Journal of Pathology and Translational Medicine* 50(6):405–10.

Lin, Fu Jun, Lei Yao, Xue Qing Hu, Fan Bian, Gang Ji, Geng Ru Jiang, Daniel P. Gale, and Hong Qi Ren. 2019. "First Identification of PODXL Nonsense Mutations in Autosomal Dominant Focal Segmental Glomerulosclerosis." *Clinical Science* 133(1):9–21.

Lindström, Nils O., Melanie L. Lawrence, Sally F. Burn, Jeanette A. Johansson, Elvira R. M. Bakker, Rachel A. Ridgway, C. Hong Chang, Michele J. Karolak, Leif Oxburgh, Denis J. Headon, Owen J. Sansom, Ron Smits, Jamie A. Davies, and Peter Hohenstein. 2014. "Integrated β-Catenin, BMP, PTEN, and Notch Signalling Patterns the Nephron." *ELife* 3:e04000.

Ling, Li, Libo Chen, Changning Zhang, Shuyan Gui, Haiyan Zhao, and Zhengzhang Li. 2018. “High Glucose Induces Podocyte Epithelial-to-Mesenchymal Transition by Demethylation-Mediated Enhancement of MMP9 Expression.” *Molecular Medicine Reports* 17(4):5642–51.

Lipshultz, Steven E., Rebecca E. Scully, Stuart R. Lipsitz, Stephen E. Sallan, Lewis B. Silverman, Tracie L. Miller, Elly V. Barry, Barbara L. Asselin, Uma Athale, Luis A. Clavell, Eric Larsen, Albert Moghrabi, Yvan Samson, Bruno Michon, Marshall A. Schorin, Harvey J. Cohen, Donna S. Neuberg, E. John Orav, and Steven D. Colan. 2010. “Assessment of Dexrazoxane as a Cardioprotectant in Doxorubicin-Treated Children with High-Risk Acute Lymphoblastic Leukaemia: Long-Term Follow-up of a Prospective, Randomised, Multicentre Trial.” *The Lancet Oncology* 11(10):950–61.

Liu, Gary W., Alexander N. Prossnitz, Diana G. Eng, Yilong Cheng, Nithya Subrahmanyam, Jeffrey W. Pippin, Robert J. Lamm, Chayanon Ngambenjawong, Hamidreza Ghandehari, Stuart J. Shankland, and Suzie H. Pun. 2018. “Glomerular Disease Augments Kidney Accumulation of Synthetic Anionic Polymers.” *Biomaterials* 178:317–25.

Liu, Haimei, Xia Gao, Hong Xu, Chun Feng, Xinyu Kuang, Zengxia Li, and Xiliang Zha. 2012. “A-Actinin-4 Is Involved in the Process by Which Dexamethasone Protects Actin Cytoskeleton Stabilization from Adriamycin-Induced Podocyte Injury.” *Nephrology* 17:669–75.

Liu, Xi, Wei Cao, Jia Qi, Qing Li, Min Zhao, Zhuyun Chen, Jingfeng Zhu, Zhimin Huang, Lin Wu, Bo Zhang, Yanggang Yuan, and Changying Xing. 2018. “Leonurine Ameliorates Adriamycin-Induced Podocyte Injury via Suppression of Oxidative Stress.” *Free Radical Research* 52(9):952–60.

Liu, Yujuan and Hans-Joachim Anders. 2014. “Lupus Nephritis: From Pathogenesis to Targets for Biologic Treatment.” *Nephron Clinical Practice* 128(3–4):224–31.

Lo, Eng H., Turgay Dalkara, and Michael A. Moskowitz. 2003. “Neurological Diseases: Mechanisms, Challenges and Opportunities in Stroke.” *Nature Reviews Neuroscience* 4(5):399–414.

Long, David A., Maria Kolatsi-Joannou, Karen L. Price, Cecile Dessapt-Baradez, Jennifer L. Huang, Eugenia Papakrivopoulou, Mike Hubank, Ron Korstanje, Luigi Gnudi, and Adrian S. Woolf. 2013. “Albuminuria Is Associated with Too Few Glomeruli and Too Much Testosterone.” *Kidney International* 83(6):1118–

29.

Low, T. L. and A. L. Goldstein. 1982. “Chemical Characterization of Thymosin Beta 4.” *Journal of Biological Chemistry* 257(2):1000–1006.

Low, T. L., S. K. Hu, and A. L. Goldstein. 1981. “Complete Amino Acid Sequence of Bovine Thymosin Beta 4: A Thymic Hormone That Induces Terminal Deoxynucleotidyl Transferase Activity in Thymocyte Populations.” *Proceedings of the National Academy of Sciences of the United States of America* 78(2):1162–66.

Lu, Huan, Qun Zhao, Hao Jiang, Tongge Zhu, Peng Xia, William Seffens, Felix Aikhionbare, Dongmei Wang, Zhen Dou, and Xuebiao Yao. 2014. “Characterization of Ring-like F-Actin Structure as a Mechanical Partner for Spindle Positioning in Mitosis.” *PLoS ONE* 9(10):e102547.

Lu, Yuqiu, Yuting Ye, Qianqian Yang, and Shaolin Shi. 2017. “Single-Cell RNA-Sequence Analysis of Mouse Glomerular Mesangial Cells Uncovers Mesangial Cell Essential Genes.” *Kidney International* 92(2):504–13.

Lv, Shumin, Hongwen Cai, Yifei Xu, Jin Dai, Xiqing Rong, and Lanzhi Zheng. 2020. “Thymosin-β 4 Induces Angiogenesis in Critical Limb Ischemia Mice via Regulating Notch/NF-KB Pathway.” *International Journal of Molecular Medicine* 46(4):1347–58.

Von Der Maase, Hans, Lisa Sengelov, James T. Roberts, Sergio Ricci, Luigi Dogliotti, T. Oliver, Malcolm J. Moore, Annamaria Zimmermann, and Michael Arning. 2005. “Long-Term Survival Results of a Randomized Trial Comparing Gemcitabine Plus Cisplatin, With Methotrexate, Vinblastine, Doxorubicin, Plus Cisplatin in Patients With Bladder Cancer.” *Journal of Clinical Oncology* 23(21):4602–8.

Macdonald, Richard A. 1961. “‘Lifespan’ of Liver Cells: Autoradiographic Study Using Tritiated Thymidine in Normal, Cirrhotic, and Partially Hepatectomized Rats.” *Archives of Internal Medicine* 107(3):335–43.

Magistroni, Riccardo, Vivette D. D’Agati, Gerald B. Appel, and Krzysztof Kiryluk. 2015. “New Developments in the Genetics, Pathogenesis, and Therapy of IgA Nephropathy.” *Kidney International* 88(5):974–89.

Maheshwari, Mani, Cesar A. Romero, Sumit R. Monu, Nitin Kumar, Tang Dong Liao, Edward L. Peterson, and Oscar A. Carretero. 2018. “Renal Protective Effects of N -Acetyl-Seryl-Aspartyl-Lysyl-Proline (Ac-SDKP) in Obese Rats on a High-Salt

Diet.” *American Journal of Hypertension* 31(8):902–9.

Maimaitiyiming, Hasiyeti, Qi Zhou, and Shuxia Wang. 2016. “Thrombospondin 1 Deficiency Ameliorates the Development of Adriamycin-Induced Proteinuric Kidney Disease” edited by Z. Jia. *PLOS ONE* 11(5):e0156144.

Mallick, N. P. and R. Gokal. 1999. “Haemodialysis.” *Lancet* 353(9154):737–42.

Marshall, Caroline B., Ron D. Krofft, Jeffrey W. Pippin, and Stuart J. Shankland. 2010. “CDK Inhibitor P21 Is Prosurvival in Adriamycin-Induced Podocyte Injury, in Vitro and in Vivo.” *American Journal of Physiology-Renal Physiology* 298(5):F1140–51.

Martin, Claire E. and Nina Jones. 2018. “Nephrin Signaling in the Podocyte: An Updated View of Signal Regulation at the Slit Diaphragm and Beyond.” *Frontiers in Endocrinology* 9(302).

Martinez-Pomares, Luisa and Siamon Gordon. 2007. “Antigen Presentation the Macrophage Way.” *Cell* 131(4):641–43.

McCarty, D. M., H. Fu, P. E. Monahan, C. E. Toulson, P. Naik, and R. J. Samulski. 2003. “Adeno-Associated Virus Terminal Repeat (TR) Mutant Generates Self-Complementary Vectors to Overcome the Rate-Limiting Step to Transduction in Vivo.” *Gene Therapy* 10(26):2112–18.

McClatchey, Andrea I. and Richard G. Fehon. 2009. “Merlin and the ERM Proteins - Regulators of Receptor Distribution and Signaling at the Cell Cortex.” *Trends in Cell Biology* 19(5):198–206.

McCullagh, Martin, Marissa G. Saunders, and Gregory A. Voth. 2014. “Unraveling the Mystery of ATP Hydrolysis in Actin Filaments.” *Journal of the American Chemical Society* 136(37):13053–58.

McMahon, Andrew P. 2016. “Development of the Mammalian Kidney.” *Current Topics in Developmental Biology* 117:31–64.

Melak, Michael, Matthias Plessner, and Robert Grosse. 2017. “Actin Visualization at a Glance.” *Journal of Cell Science* 130(3):525–30.

Menzel, Sylvia and Marcus J. Moeller. 2011. “Role of the Podocyte in Proteinuria.” *Pediatric Nephrology* 26(10):1775–80.

Merino, Felipe, Sabrina Pospich, Johanna Funk, Thorsten Wagner, Florian Küllmer, Hans Dieter Arndt, Peter Bieling, and Stefan Raunser. 2018. “Structural Transitions of F-Actin upon ATP Hydrolysis at near-Atomic Resolution Revealed by Cryo-EM.” *Nature Structural and Molecular Biology* 25(6):528–37.

Le Meur, Yannick, Valerie Lorgeot, Lydie Comte, Jean Christophe Szelag, Jean Claude Aldigier, Claude Leroux-Robert, and Vincent Praloran. 2001. “Plasma Levels and Metabolism of AcSDKP in Patients with Chronic Renal Failure: Relationship with Erythropoietin Requirements.” *American Journal of Kidney Diseases* 38(3):510–17.

Miao, Yansong, Catherine C. L. Wong, Vito Mennella, Alphee Michelot, David A. Agard, Liam J. Holt, John R. Yates, and David G. Drubin. 2013. “Cell-Cycle Regulation of Formin-Mediated Actin Cable Assembly.” *Proceedings of the National Academy of Sciences of the United States of America* 110(47):E4446–55.

Miklavc, Pika, Elena Hecht, Nina Hobi, Oliver H. Wittekindt, Paul Dietl, Christine Kranz, and Manfred Frick. 2012. “Actin Coating and Compression of Fused Secretory Vesicles Are Essential for Surfactant Secretion - a Role for Rho, Formins and Myosin II.” *Journal of Cell Science* 125(11):2765–74.

Miklavc, Pika, Oliver H. Wittekindt, Edward Felder, and Paul Dietl. 2009. “Ca $^{2+}$ - Dependent Actin Coating of Lamellar Bodies after Exocytotic Fusion: A Prerequisite for Content Release or Kiss-and-Run.” *Annals of the New York Academy of Sciences* 1152(1):43–52.

Miner, Jeffrey H. 2008. “Glomerular Filtration: The Charge Debate Charges Ahead.” *Kidney International* 74(3):259–61.

Mirski, Shelagh E. L., James H. Gerlach, and Susan P. C. Cole2. 1987. *Multidrug Resistance in a Human Small Cell Lung Cancer Cell Line Selected in Adriamycin*. Vol. 47.

Mitchison, T. J. and L. P. Cramer. 1996. “Actin-Based Cell Motility and Cell Locomotion.” *Cell* 84(3):371–79.

Mitra, Vikramjit and Jane Metcalf. 2009. “Functional Anatomy and Blood Supply of the Liver.” *Anaesthesia and Intensive Care Medicine* 10(7):332–33.

Miyamoto-Sato, Etsuko, Shigeo Fujimori, Masamichi Ishizaka, Naoya Hirai, Kazuyo Masuoka, Rintaro Saito, Yosuke Ozawa, Katsuya Hino, Takanori Washio, Masaru Tomita, Tatsuhiro Yamashita, Tomohiro Oshikubo, Hidetoshi Akasaka, Jun Sugiyama, Yasuo Matsumoto, and Hiroshi Yanagawa. 2010. “A Comprehensive Resource of Interacting Protein Regions for Refining Human Transcription Factor Networks.” *PloS One* 5(2):e9289.

Miyata, Kohei, Fusanori Yotsumoto, Sung Ouk Nam, Masahide Kuroki, and Shingo

Miyamoto. 2012. “Regulatory Mechanisms of the HB-EGF Autocrine Loop in Inflammation, Homeostasis, Development and Cancer.” *Anticancer Research* 32(6):2347–52.

Moëll, Hans. 1956. “Size of Normal Kidneys.” *Acta Radiologica* 46(5):640–45.

Mogilner, Alexander and George Oster. 1996. “Cell Motility Driven by Actin Polymerization.” *Biophysical Journal* 71(6):3030–45.

Molina, D. Kimberley and Vincent J. M. DiMaio. 2012. “Normal Organ Weights in Men.” *The American Journal of Forensic Medicine and Pathology* 33(4):368–72.

Momparler, R. L., M. Karon, S. E. Siegel, and F. Avila. 1976. “Effect of Adriamycin on DNA, RNA, and Protein Synthesis in Cell-Free Systems and Intact Cells.” *Cancer Research* 36(8):2891–95.

Mon La, The, Hiromi Tachibana, Shun-Ai Li, Tadashi Abe, Sayaka Seiriki, Hikaru Nagaoka, Eizo Takashima, Tetsuya Takeda, Daisuke Ogawa, Shin-ichi Makino, Katsuhiko Asanuma, Masami Watanabe, Xuefei Tian, Ayuko Sakane, Takuya Sasaki, Jun Wada, Kohji Takei, and Hiroshi Yamada. 2020. “Dynamin 1 Is Important for Microtubule Organization and Stabilization in Glomerular Podocytes.” *The FASEB Journal* 34:16449–63.

Moon, Eun-Yi, Ji-Hee Song, and Kyu-Hwan Yang. 2007. “Actin-Sequestering Protein, Thymosin-Beta-4 (TB4), Inhibits Caspase-3 Activation in Paclitaxel-Induced Tumor Cell Death.” *Oncology Research Featuring Preclinical and Clinical Cancer Therapeutics* 16(11):507–16.

Moore, Nicholas A., Nuria Morral, Thomas A. Ciulla, and Peter Bracha. 2018. “Gene Therapy for Inherited Retinal and Optic Nerve Degenerations.” *Expert Opinion on Biological Therapy* 18(1):37–49.

Mora, Carlos A., Christian A. Baumann, Javier E. Paino, Allan L. Goldstein, and Mahnaz Badamchian. 1997. “Biodistribution of Synthetic Thymosin Beta 4 in the Serum, Urine and Major Organs of Mice.” *Int. J. Immunopharmac* 19(1):1–8.

Mori, Seiichiro, Lina Wang, Takamasa Takeuchi, and Tadahito Kanda. 2004. “Two Novel Adeno-Associated Viruses from Cynomolgus Monkey: Pseudotyping Characterization of Capsid Protein.” *Virology* 330(2):375–83.

Moriguchi, Takashi, Michito Hamada, Naoki Morito, Tsumoru Terunuma, Kazuteru Hasegawa, Chuan Zhang, Tomomasa Yokomizo, Ritsuko Esaki, Etsushi Kuroda, Keigyou Yoh, Takashi Kudo, Michio Nagata, David R. Greaves, James Douglas Engel, Masayuki Yamamoto, and Satoru Takahashi. 2006. “MafB Is

Essential for Renal Development and F4/80 Expression in Macrophages." *Molecular and Cellular Biology* 26(15):5715–27.

Morita, Tsuyoshi and Ken'ichiro Hayashi. 2013. "G-Actin Sequestering Protein Thymosin-B4 Regulates the Activity of Myocardin-Related Transcription Factor." *Biochemical and Biophysical Research Communications* 437(3):331–35.

Morris, D. C., Y. Cui, W. L. Cheung, M. Lu, L. Zhang, Z. G. Zhang, and M. Chopp. 2014. "A Dose–Response Study of Thymosin B4 for the Treatment of Acute Stroke." *Journal of the Neurological Sciences* 345(1–2):61–67.

Morris, Daniel C., Wing Lee Cheung, Richard Loi, Talan Zhang, Mei Lu, Zheng G. Zhang, and Michael Chopp. 2017. "Thymosin B4 for the Treatment of Acute Stroke in Aged Rats." *Neuroscience Letters* 659:7–13.

Morris, Daniel C., Zheng G. Zhang, and Michael Chopp. 2018. "Thymosin B4 for the Treatment of Acute Stroke: Neurorestorative or Neuroprotective?" *Expert Opinion on Biological Therapy* 18(SUP1):149–58.

Morrison, Avril A., Rebecca L. Viney, Moin A. Saleem, and Michael R. Ladomery. 2008. "New Insights into the Function of the Wilms Tumor Suppressor Gene WT1 in Podocytes." *Am J Physiol Renal Physiol* 295:12–17.

Moschovaki Filippidou, Foteini, Alexander H. Kirsch, Matthias Thelen, Máté Kétszeri, Katharina Artinger, Ida Aringer, Corinna Schabhüttl, Agnes A. Mooslechner, Bianca Frauscher, Marion Pollheimer, Tobias Niedrist, Andreas Meinitzer, Daniel J. Drucker, Thomas R. Pieber, Philipp Eller, Alexander R. Rosenkranz, Akos Heinemann, and Kathrin Eller. 2020. "Glucagon-Like Peptide-1 Receptor Agonism Improves Nephrotoxic Serum Nephritis by Inhibiting T-Cell Proliferation." *American Journal of Pathology* 190(2):400–411.

Motonishi, Shuta, Masaomi Nangaku, Takehiko Wada, Yu Ishimoto, Takamoto Ohse, Taiji Matsusaka, Naoto Kubota, Akira Shimizu, Takashi Kadowaki, Kazuyuki Tobe, and Reiko Inagi. 2015. "Sirtuin1 Maintains Actin Cytoskeleton by Deacetylation of Cortactin in Injured Podocytes." *J Am Soc Nephrol* 26:1939–59.

Mouneimne, Ghassan, Scott D. Hansen, Laura M. Selfors, Lara Petrak, Michele M. Hickey, Lisa L. Gallegos, Kaylene J. Simpson, James Lim, Frank B. Gertler, John H. Hartwig, R. Dyche Mullins, and Joan S. Brugge. 2012. "Differential Remodeling of Actin Cytoskeleton Architecture by Profilin Isoforms Leads to Distinct Effects on Cell Migration and Invasion." *Cancer Cell* 22(5):615–30.

Mount, David B. 2014. “Thick Ascending Limb of the Loop of Henle.” *Clinical Journal of the American Society of Nephrology* 9:1974–86.

Mueller, C. Barber, A. D. Mason, and D. G. Stout. 1955. “Anatomy of the Glomerulus.” *The American Journal of Medicine* 18(2):267–76.

Mulay, Shrikant R., Dana Thomasova, Mi Ryu, Onkar P. Kulkarni, Adriana Migliorini, Hauke Bruns, Regina Gröbmayr, Elena Lazzeri, Laura Lasagni, Helen Liapis, Paola Romagnani, and Hans-Joachim Anders. 2013. “Podocyte Loss Involves MDM2-Driven Mitotic Catastrophe.” *The Journal of Pathology* 230(3):322–35.

Mundel, P., H. W. Heid, T. M. Mundel, M. Krüger, J. Reiser, and W. Kriz. 1997. “Synaptopodin: An Actin-Associated Protein in Telencephalic Dendrites and Renal Podocytes.” *The Journal of Cell Biology* 139(1):193–204.

Mundel, P., J. Reiser, A. Zúñiga Mejía Borja, H. Pavenstädt, G. R. Davidson, W. Kriz, and R. Zeller. 1997. “Rearrangements of the Cytoskeleton and Cell Contacts Induce Process Formation during Differentiation of Conditionally Immortalized Mouse Podocyte Cell Lines.” *Experimental Cell Research* 236(1):248–58.

Mundlos, S., J. Pelletier, A. Darveau, M. Bachmann, A. Winterpacht, and B. Zabel. 1993. “Nuclear Localization of the Protein Encoded by the Wilms’ Tumor Gene WT1 in Embryonic and Adult Tissues | Development.” *Development* 119:1329–41.

Munshaw, Sonali, Susann Bruche, Andia N. Redpath, Alisha Jones, Jyoti Patel, Karina N. Dubé, Regent Lee, Svenja S. Hester, Rachel Davies, Giles Neal, Ashok Handa, Michael Sattler, Roman Fischer, Keith M. Channon, and Nicola Smart. 2021. “Thymosin B4 Protects against Aortic Aneurysm via Endocytic Regulation of Growth Factor Signaling.” *The Journal of Clinical Investigation*.

Muramatsu, Shin Ichi, Hiroaki Mizukami, Neal S. Young, and Kevin E. Brown. 1996. “Nucleotide Sequencing and Generation of an Infectious Clone of Adeno-Associated Virus 3.” *Virology* 221(1):208–17.

Mutchnick, Milton G., Horchang H. Lee, David I. Hollander, Gregory D. Haynes, and David C. Chua. 1988. “Defective in Vitro Gamma Interferon Production and Elevated Serum Immunoreactive Thymosin B4 Levels in Patients with Inflammatory Bowel Disease.” *Clinical Immunology and Immunopathology* 47(1):84–92.

Muzyczka, N. 1992. “Use of Adeno-Associated Virus as a General Transduction

Vector for Mammalian Cells." *Current Topics in Microbiology and Immunology* 158:97–129.

Myrehaug, Sten, Melania Pintilie, Richard Tsang, Robert Mackenzie, Michael Crump, Zhongliang Chen, Alexander Sun, and David C. Hodgson. 2008. "Cardiac Morbidity Following Modern Treatment for Hodgkin Lymphoma: Supra-Additive Cardiotoxicity of Doxorubicin and Radiation Therapy." *Leukemia & Lymphoma* 49(8):1486–93.

Nachmias, Vivianne T. 1993. "Small Actin-Binding Proteins: The β-Thymosin Family." *Current Opinion in Cell Biology* 5(1):56–62.

Nag, Shalini, Mårten Larsson, Robert C. Robinson, and Leslie D. Burtnick. 2013. "Gelsolin: The Tail of a Molecular Gymnast." *Cytoskeleton* 70(7):360–84.

Nagai, Takako, Megumi Kanasaki, Swayam Prakash Srivastava, Yuka Nakamura, Yasuhito Ishigaki, Munehiro Kitada, Sen Shi, Keizo Kanasaki, and Daisuke Koya. 2014. "N-Acetyl-Seryl-Aspartyl-Lysyl-Proline Inhibits Diabetes-Associated Kidney Fibrosis and Endothelial-Mesenchymal Transition." *BioMed Research International* 2014.

Nagai, Takako, Kyoko Nitta, Megumi Kanasaki, Daisuke Koya, and Keizo Kanasaki. 2015. "The Biological Significance of Angiotensin-Converting Enzyme Inhibition to Combat Kidney Fibrosis." *Clinical and Experimental Nephrology* 19(1):65–74.

Nagao, Tomokazu, Mimiko Matsumura, Ayako Mabuchi, Akiko Ishida-Okawara, Osamu Koshio, Toshinori Nakayama, Haruyuki Minamitani, and Kazuo Suzuki. 2007. "Up-Regulation of Adhesion Molecule Expression in Glomerular Endothelial Cells by Anti-Myeloperoxidase Antibody." *Nephrology Dialysis Transplantation* 22(1):77–87.

Nakagawa, Takahiko, Yoneko Hayase, Masakiyo Sasahara, Masakazu Haneda, Ryuichi Kikkawa, Shigeki Higashiyama, Naoyuki Taniguchi, and Fumitada Hazama. 1997. "Distribution of Heparin-Binding EGF-like Growth Factor Protein and MRNA in the Normal Rat Kidneys." *Kidney International* 51(6):1774–79.

Nakai, Hiroyuki, Theresa A. Storm, and Mark A. Kay. 2000. "Recruitment of Single-Stranded Recombinant Adeno-Associated Virus Vector Genomes and Intermolecular Recombination Are Responsible for Stable Transduction of Liver In Vivo." *Journal of Virology* 74(20):9451–63.

Nakazawa, Daigo, Sakiko Masuda, Utano Tomaru, and Akihiro Ishizu. 2019. "Pathogenesis and Therapeutic Interventions for ANCA-Associated Vasculitis."

Nature Reviews Rheumatology 15(2):91–101.

Nasr, Samih H. and Vivette D. D'Agati. 2011. "IgA-Dominant Postinfectious Glomerulonephritis: A New Twist on an Old Disease." *Nephron Clinical Practice* 119(1):c18–26.

Nasrallah, Rania, Susan J. Robertson, Jacob Karsh, and Richard L. Hébert. 2013. "Celecoxib Modifies Glomerular Basement Membrane, Mesangium and Podocytes in OVE26 Mice, but Ibuprofen Is More Detrimental." *Clinical Science* 124(11):685–94.

Nass, Shelley A., Maryellen A. Mattingly, Denise A. Woodcock, Brenda L. Burnham, Jeffrey A. Ardinger, Shayla E. Osmond, Amy M. Frederick, Abraham Scaria, Seng H. Cheng, and Catherine R. O'Riordan. 2018. "Universal Method for the Purification of Recombinant AAV Vectors of Differing Serotypes." *Molecular Therapy - Methods and Clinical Development* 9:33–46.

Nathwani, Amit C., Ulreke M. Reiss, Edward G. D. Tuddenham, Cecilia Rosales, Pratima Chowdary, Jenny McIntosh, Marco Della Peruta, Elsa Lheriteau, Nishal Patel, Deepak Raj, Anne Riddell, Jun Pie, Savita Rangarajan, David Bevan, Michael Recht, Yu-Min Shen, Kathleen G. Halka, Etiena Basner-Tschakarjan, Federico Mingozzi, Katherine A. High, James Allay, Mark A. Kay, Catherine Y. C. Ng, Junfang Zhou, Maria Cancio, Christopher L. Morton, John T. Gray, Deokumar Srivastava, Arthur W. Nienhuis, and Andrew M. Davidoff. 2014. "Long-Term Safety and Efficacy of Factor IX Gene Therapy in Hemophilia B." *New England Journal of Medicine* 371(21):1994–2004.

Nathwani, Amit C., Edward G. D. Tuddenham, Savita Rangarajan, Cecilia Rosales, Jenny McIntosh, David C. Linch, Pratima Chowdary, Anne Riddell, Arnulfo Jaquilmac Pie, Chris Harrington, James O'Beirne, Keith Smith, John Pasi, Bertil Glader, Pradip Rustagi, Catherine Y. C. Ng, Mark A. Kay, Junfang Zhou, Yunyu Spence, Christopher L. Morton, James Allay, John Coleman, Susan Sleep, John M. Cunningham, Deokumar Srivastava, Etiena Basner-Tschakarjan, Federico Mingozzi, Katherine A. High, John T. Gray, Ulrike M. Reiss, Arthur W. Nienhuis, and Andrew M. Davidoff. 2011. "Adenovirus-Associated Virus Vector–Mediated Gene Transfer in Hemophilia B." *New England Journal of Medicine* 365(25):2357–65.

Neal, Christopher R., Hayley Crook, Edward Bell, Steven J. Harper, and David O. Bates. 2005. "Three-Dimensional Reconstruction of Glomeruli by Electron

Microscopy Reveals a Distinct Restrictive Urinary Subpodocyte Space." *Journal of the American Society of Nephrology* 16(5):1223–35.

Neidt, Erin M., Bonnie J. Scott, and David R. Kovar. 2009. "Formin Differentially Utilizes Profilin Isoforms to Rapidly Assemble Actin Filaments." *Journal of Biological Chemistry* 284(1):673–84.

Nemolato, S., T. Cabras, M. U. Fanari, F. Cau, D. Fanni, C. Gerosa, B. Manconi, I. Messana, M. Castagnola, and G. Faa. 2010. "Immunoreactivity of Thymosin Beta 4 in Human Foetal and Adult Genitourinary Tract." *European Journal of Histochemistry* 54(4):193–96.

Neuen, Brendon L., Tamara Young, Hiddo J. L. Heerspink, Bruce Neal, Vlado Perkovic, Laurent Billot, Kenneth W. Mahaffey, David M. Charytan, David C. Wheeler, Clare Arnott, Severine Bompoint, Adeera Levin, and Meg J. Jardine. 2019. "SGLT2 Inhibitors for the Prevention of Kidney Failure in Patients with Type 2 Diabetes: A Systematic Review and Meta-Analysis." *The Lancet Diabetes and Endocrinology* 7(11):845–54.

Neuhaus, Jean-Marc, Michael Wanger, Thomas Keiser, and Albrecht Wegner. 1983. "Treadmilling of Actin." *Journal of Muscle Research and Cell Motility* 4:507–27.

Ngo, Kien Xuan, Noriyuki Kodera, Eisaku Katayama, Toshio Ando, and Taro Qp Uyeda. 2015. "Cofilin-Induced Unidirectional Cooperative Conformational Changes in Actin Filaments Revealed by High-Speed Atomic Force Microscopy." *ELife* 4(e04806):1–22.

Nguyen, Nga T. Q., Paul Cockwell, Alexander P. Maxwell, Matthew Griffin, Timothy O'Brien, and Ciaran O'Neill. 2018. "Chronic Kidney Disease, Health-Related Quality of Life and Their Associated Economic Burden among a Nationally Representative Sample of Community Dwelling Adults in England" edited by D. Bolignano. *PLOS ONE* 13(11):e0207960.

Ni, Yongliang, Xin Wang, Xiaoxuan Yin, Yan Li, Xigao Liu, Haixin Wang, Xiangjv Liu, Jun Zhang, Haiqing Gao, Benkang Shi, and Shaohua Zhao. 2018. "Plectin Protects Podocytes from Adriamycin-Induced Apoptosis and F-Actin Cytoskeletal Disruption through the Integrin A6β4/FAK/P38 MAPK Pathway." *Journal of Cellular and Molecular Medicine* 22(11):5450–67.

Nichols, Kelly K., David G. Evans, and Paul M. Karpecki. 2020. "A Comprehensive Review of the Clinical Trials Conducted for Dry Eye Disease and the Impact of the Vehicle Comparators in These Trials." *Current Eye Research* 1–6.

Nielsen, Julie S. and Kelly M. Mcnagny. 2009. “The Role of Podocalyxin in Health and Disease.” *Journal of the American Society of Nephrology* 20:1669–76.

Nijenhuis, Tom, Alexis J. Sloan, Joost G. J. Hoenderop, Jan Flesche, Harry van Goor, Andreas D. Kistler, Marinka Bakker, Rene J. M. Bindels, Rudolf A. de Boer, Clemens C. Möller, Inge Hamming, Gerjan Navis, Jack F. M. Wetzels, Jo H. M. Berden, Jochen Reiser, Christian Faul, and Johan van der Vlag. 2011. “Angiotensin II Contributes to Podocyte Injury by Increasing TRPC6 Expression via an NFAT-Mediated Positive Feedback Signaling Pathway.” *The American Journal of Pathology* 179(4):1719–32.

Ning, Liang, Hani Y. Suleiman, and Jeffrey H. Miner. 2020. “Synaptopodin Is Dispensable for Normal Podocyte Homeostasis but Is Protective in the Context of Acute Podocyte Injury.” *Journal of the American Society of Nephrology* 31:ASN.2020050572.

Nitta, Kyoko, Takako Nagai, Yuiko Mizunuma, Munehiro Kitada, Atsushi Nakagawa, Masaru Sakurai, Masao Toyoda, Masakazu Haneda, Keizo Kanasaki, and Daisuke Koya. 2019. “N-Acetyl-Seryl-Aspartyl-Lysyl-Proline Is a Potential Biomarker of Renal Function in Normoalbuminuric Diabetic Patients with EGFR ≥ 30 Ml/Min/1.73 M2.” *Clinical and Experimental Nephrology* 23(8):1004–12.

Novick, Tessa, Yang Liu, Anika Alvanzo, Alan B. Zonderman, Michele K. Evans, and Deidra C. Crews. 2016. “Lifetime Cocaine and Opiate Use and Chronic Kidney Disease.” *American Journal of Nephrology* 44:447–53.

O’Brien, Stephen P., Mandy Smith, Hong Ling, Lucy Phillips, William Weber, John Lydon, Colleen Maloney, Steven Ledbetter, Cynthia Arbeeny, and Stefan Wawersik. 2013. “Glomerulopathy in the KK.Cg- Ay/J Mouse Reflects the Pathology of Diabetic Nephropathy.” *Journal of Diabetes Research* 2013:Article ID 498925.

Oh, Jun, Jochen Reiser, and Peter Mundel. 2004. “Dynamic (Re)Organization of the Podocyte Actin Cytoskeleton in the Nephrotic Syndrome.” *Pediatric Nephrology* 19(2):130–37.

Okuda, Seiya, Yukinori Oh, Hiroshi Tsuruda, Kaoru Onoyama, Satoru Fujimi, and Masatoshi Fujishima. 1986. “Adriamycin-Induced Nephropathy as a Model of Chronic Progressive Glomerular Disease.” *Kidney International* 29:502–10.

Olin, Jeffrey W., Kathleen M. Beusterien, Mary Beth Childs, Caroline Seavey, Linda McHugh, and Robert I. Griffiths. 1999. “Medical Costs of Treating Venous Stasis

Ulcers: Evidence from a Retrospective Cohort Study." *Vascular Medicine* 4(1):1–7.

Omata, Mitsugu, Hajime Taniguchi, Daisuke Koya, Keizo Kanasaki, Rumiko Sho, Yoshimi Kato, Ryoji Kojima, Masakazu Haneda, and Norio Inomata. 2006. "N-Acetyl-Seryl-Asparlyl-Lysyl-Proline Ameliorates the Progression of Renal Dysfunction and Fibrosis in WKY Rats with Established Anti-Glomerular Basement Membrane Nephritis." *Journal of the American Society of Nephrology* 17(3):674–85.

Oosawa, Fumio, Sho Asakura, Ken Hotta, Nobuhisa Imai, and Tatsuo Ooi. 1959. "G-F Transformation of Actin as a Fibrous Condensation." *Journal of Polymer Science* 37(132):323–36.

Orlando, Robert A., Tetsuro Takeda, Beverly Zak, Sandra Schmieder, Vivian M. Benoit, Tammie Mcquistan, Heinz Furthmayr, and Marilyn G. Farquhar. 2001. "The Glomerular Epithelial Cell Anti-Adhesin Podocalyxin Associates with the Actin Cytoskeleton through Interactions with Ezrin." *Journal of the American Society of Nephrology* 12:1589–98.

Orlowski, Robert Z., Arnon Nagler, Pieter Sonneveld, Joan Bladé, Roman Hajek, Andrew Spencer, San Miguel, Tadeusz Robak, Anna Dmoszynska, Noemi Horvath, Ivan Spicka, Heather J. Sutherland, Alexander N. Suvorov, Sen H. Zhuang, Trilok Parekh, Liang Xiu, Zhilong Yuan, Wayne Rackoff, and Jean-Luc Harousseau. 2007. "Randomized Phase III Study of Pegylated Liposomal Doxorubicin Plus Bortezomib Compared With Bortezomib Alone in Relapsed or Refractory Multiple Myeloma: Combination Therapy Improves Time to Progression." *Journal of Clinical Oncology* 25(25):3892–3901.

Otey, C. A., G. B. Vasquez, K. Burridge, and B. W. Erickson. 1993. "Mapping of the Alpha-Actinin Binding Site Within the Beta 1 Integrin Cytoplasmic Domain." *J Biol Chem.* 268(28):21193–97.

Ougaard, M. K. E., P. H. Kvist, H. E. Jensen, C. Hess, I. Rune, and H. Søndergaard. 2018. "Murine Nephrotoxic Nephritis as a Model of Chronic Kidney Disease." *International Journal of Nephrology* 2018(Article ID 8424502):1–12.

Paavilainen, Ville O., Enni Bertling, Sandra Falck, and Pekka Lappalainen. 2004. "Regulation of Cytoskeletal Dynamics by Actin-Monomer-Binding Proteins." *Trends in Cell Biology* 14(7):386–94.

Padmanabhan, Krishnanand, Hanna Grobe, Jonathan Cohen, Arad Soffer, Adnan

Mahly, Orit Adir, Ronen Zaidel-Bar, and Chen Luxenburg. 2020. “Thymosin B4 Is Essential for Adherens Junction Stability and Epidermal Planar Cell Polarity.” *Development (Cambridge, England)* 147(23):1–15.

Pai, Shan and M. Peter Marinkovich. 2002. “Epidermolysis Bullosa: New and Emerging Trends.” *American Journal of Clinical Dermatology* 3(6):371–80.

Pan, Chi-syuan, Teressa Reanne Ju, Chi Chan Lee, Yu-Pei Chen, Chung-Y. Hsu, Dong-Zong Hung, Wei-Kung Chen, and I. Kuan Wang. 2018. “Alcohol Use Disorder Tied to Development of Chronic Kidney Disease: A Nationwide Database Analysis” edited by W. Cheungpasitporn. *PLOS ONE* 13(9):e0203410.

Pantaloni, Dominique and Marie-France Carlier. 1993. “How Profilin Promotes Actin Filament Assembly in the Presence of Thymosin P4.” *Cell* 75:1007–14.

Papakrivopoulou, E, E. Vasilopoulou, M. T. Lindenmeyer, S. Pacheco, H. Ł. Brzóska, K. L. Price, M. Kolatsi-Joannou, K. E. White, D. J. Henderson, C. H. Dean, C. D. Cohen, A. D. Salama, A. S. Woolf, and D. A. Long. 2018. “Vangl2, a Planar Cell Polarity Molecule, Is Implicated in Irreversible and Reversible Kidney Glomerular Injury.” *Journal of Pathology* 246(4).

Papakrivopoulou, Eugenia, Daniyal J. Jafree, Charlotte H. Dean, and David A. Long. 2021. “The Biological Significance and Implications of Planar Cell Polarity for Nephrology.” *Frontiers in Physiology* 12:599529.

Papakrivopoulou, Eugenia, Elisavet Vasilopoulou, Maja T. Lindenmeyer, Sabrina Pacheco, Hortensja Ł. Brzóska, Karen L. Price, Maria Kolatsi-Joannou, Kathryn E. White, Deborah J. Henderson, Charlotte H. Dean, Clemens D. Cohen, Alan D. Salama, Adrian S. Woolf, and David A. Long. 2018. “Vangl2, a Planar Cell Polarity Molecule, Is Implicated in Irreversible and Reversible Kidney Glomerular Injury.” *The Journal of Pathology* 246(4):485–96.

Papeta, Natalia, Zongyu Zheng, Eric A. Schon, Sonja Brosel, Mehmet M. Altintas, Samih H. Nasr, Jochen Reiser, Vivette D. D’Agati, and Ali G. Gharavi. 2010. “Prkdc Participates in Mitochondrial Genome Maintenance and Prevents Adriamycin-Induced Nephropathy in Mice.” *The Journal of Clinical Investigation* 120(11):4055–64.

Parsons, J. Thomas, Alan Rick Horwitz, and Martin A. Schwartz. 2010. “Cell Adhesion: Integrating Cytoskeletal Dynamics and Cellular Tension.” *Nature Reviews Molecular Cell Biology* 11(9):633–43.

Patrakka, Jaakko and Karl Tryggvason. 2010. “Molecular Make-up of the Glomerular Filtration Barrier.” *Biochemical and Biophysical Research Communications* 396(1):164–69.

Paul, Aditya S. and Thomas D. Pollard. 2009. “Review of the Mechanism of Processive Actin Filament Elongation by Formins.” *Cell Motility and the Cytoskeleton* 66(8):606–17.

De Paulo Castro Teixeira, Vicente, Simone Monika Blattner, Min Li, Hans Joachim Anders, Clemens David Cohen, Ilka Edenhofer, Novella Calvaresi, Monika Merkle, Maria Pia Rastaldi, and Matthias Kretzler. 2005. “Functional Consequences of Integrin-Linked Kinase Activation in Podocyte Damage.” *Kidney International* 67(2):514–23.

Paulussen, Melissa, Bart Landuyt, Liliane Schoofs, Walter Luyten, and Lut Arckens. 2009. “Thymosin Beta 4 MRNA and Peptide Expression in Phagocytic Cells of Different Mouse Tissues.” *Peptides* 30(10):1822–32.

Pavenstädt, Hermann, Wilhelm Kriz, and Matthias Kretzler. 2003. “Cell Biology of the Glomerular Podocyte.” *Physiological Reviews* 83(1):253–307.

Pedchenko, Vadim, Olga Bondar, Agnes B. Fogo, Roberto Vanacore, Paul Voziyan, A. Richard Kitching, Jörgen Wieslander, Clifford Kashtan, Dorin-Bogdan Borza, Eric G. Neilson, Curtis B. Wilson, and Billy G. Hudson. 2010. “Molecular Architecture of the Goodpasture Autoantigen in Anti-GBM Nephritis.” *New England Journal of Medicine* 363(4):343–54.

Peng, Hongmei, Jiang Xu, Xiao Ping Yang, Xiangguo Dai, Edward L. Peterson, Oscar A. Carretero, and Nour Eddine Rhaleb. 2014. “Thymosin-B4 Prevents Cardiac Rupture and Improves Cardiac Function in Mice with Myocardial Infarction.” *American Journal of Physiology - Heart and Circulatory Physiology* 307(5):H751.

Pereira, Wagner de Fátima, Gustavo Eustáquio A. Brito-Melo, Cayo Antônio Soares de Almeida, Lázaro Lopes Moreira, Cleiton Willian Cordeiro, Thiago Guimarães Rosa Carvalho, Elvis Cueva Mateo, and Ana Cristina Simões e Silva. 2015. “The Experimental Model of Nephrotic Syndrome Induced by Doxorubicin in Rodents: An Update.” *Inflammation Research* 64(5):287–301.

Perico, Luca, Sara Conti, Ariela Benigni, and Giuseppe Remuzzi. 2016. “Podocyte-Actin Dynamics in Health and Disease.” *Nature Reviews Nephrology* 12(11):692–710.

Perisic, Ljubica, Patricia Q. Rodriguez, Kjell Hultenby, Ying Sun, Mark Lal, Christer Betsholtz, Mathias Uhlén, Annika Wernerson, Ulf Hedin, Timo Pikkarainen, Karl Tryggvason, and Jaakko Patrakka. 2015. “Schip1 Is a Novel Podocyte Foot Process Protein That Mediates Actin Cytoskeleton Rearrangements and Forms a Complex with Nherf2 and Ezrin” edited by M. P. Rastaldi. *PLOS ONE* 10(3):e0122067.

Van Der Perren, A., J. Toelen, M. Carlon, C. Van Den Haute, F. Coun, B. Heeman, V. Reumers, L. H. Vandenberghe, J. M. Wilson, Z. Debyser, and V. Baekelandt. 2011. “Efficient and Stable Transduction of Dopaminergic Neurons in Rat Substantia Nigra by RAAV 2/1, 2/2, 2/5, 2/6.2, 2/7, 2/8 and 2/9.” *Gene Therapy* 18(5):517–27.

Peters, Peter J., Erik Bos, and Alexander Griekspoor. 2006. “Cryo-Immunogold Electron Microscopy.” *Current Protocols in Cell Biology* 30(1):4.7.1-4.7.19.

Peti-Peterdi, János and Arnold Sipos. 2010. “A High-Powered View of the Filtration Barrier.” *Journal of the American Society of Nephrology* 21(11):1835–41.

Philp, D., T. Huff, Y. S. Gho, E. Hannappel, and H. K. Kleinman. 2003. “The Actin Binding Site on Thymosin β 4 Promotes Angiogenesis.” *The FASEB Journal* 17(14):1–13.

Pillay, S., N. L. Meyer, A. S. Puschnik, O. Davulcu, J. Diep, Y. Ishikawa, L. T. Jae, J. E. Wosen, C. M. Nagamine, M. S. Chapman, and J. E. Carette. 2016. “An Essential Receptor for Adeno-Associated Virus Infection.” *Nature* 530(7588):108–12.

Pinto, Nicole, Fei Chi Yang, Atsuko Negishi, Maikel C. Rheinstädter, Todd E. Gillis, and Douglas S. Fudge. 2014. “Self-Assembly Enhances the Strength of Fibers Made from Vimentin Intermediate Filament Proteins.” *Biomacromolecules* 15(2):574–81.

Pippin, Jeffrey W., Paul T. Brinkkoetter, Fionnualla C. Cormack-Aboud, Raghu V. Durvasula, Peter V. Hauser, Jolanta Kowalewska, Ronald D. Krofft, Christine M. Logar, Caroline B. Marshall, Takamoto Ohse, and Stuart J. Shankland. 2009. “Inducible Rodent Models of Acquired Podocyte Diseases.” *American Journal of Physiology - Renal Physiology* 296(2):213–29.

Pisarek-Horowitz, Anna, Xueping Fan, Sudhir Kumar, Hila M. Rasouly, Richa Sharma, Hui Chen, Kathryn Coser, Crystal T. Bluette, Dinesh Hirenallur-Shanthappa, Sarah R. Anderson, Hongying Yang, Laurence H. Beck, Ramon G.

Bonegio, Joel M. Henderson, Stephen P. Berasi, David J. Salant, and Weining Lu. 2020. “Loss of Roundabout Guidance Receptor 2 (Robo2) in Podocytes Protects Adult Mice from Glomerular Injury by Maintaining Podocyte Foot Process Structure.” *American Journal of Pathology* 190(4):799–816.

Piscitelli, Stephen C., Keith A. Rodvold, Daniel A. Rushing, and Duane A. Tewksbury. 1993. “Pharmacokinetics and Pharmacodynamics of Doxorubicin in Patients with Small Cell Lung Cancer.” *Clinical Pharmacology and Therapeutics* 53(5):555–61.

Pocock, Gillian and Christopher D. Richards. 2009. *The Human Body - An Introduction for the Biomedical and Health Sciences*. Oxford: Oxford University Press.

Poh, Kian Keong, Poay Sian Sabrina Lee, Andie Hartanto Djohan, Mary Joyce Galupo, Geronica Gorospe Songco, Tiong Cheng Yeo, Huay Cheem Tan, Arthur Mark Richards, and Lei Ye. 2020. “Transplantation of Endothelial Progenitor Cells in Obese Diabetic Rats Following Myocardial Infarction: Role of Thymosin Beta-4.” *Cells* 9(4):949.

Polley, Mei-Yin C., Samuel C. Y. Leung, Lisa M. McShane, Dongxia Gao, Judith C. Hugh, Mauro G. Mastropasqua, Giuseppe Viale, Lila A. Zabaglo, Frédérique Penault-Llorca, John M. S. Bartlett, Allen M. Gown, W. Fraser Symmans, Tammy Piper, Erika Mehl, Rebecca A. Enos, Daniel F. Hayes, Mitch Dowsett, and Torsten O. Nielsen. 2013. “An International Ki67 Reproducibility Study.” *Journal of the National Cancer Institute* 105(24):1897–1906.

Pollitt, Alice Y. and Robert H. Insall. 2009. “WASP and SCAR/WAVE Proteins: The Drivers of Actin Assembly.” *Journal of Cell Science* 122(15):2575–78.

Pozzi, Ambra, George Jarad, Gilbert W. Moeckel, Sergio Coffa, Xi Zhang, Leslie Gewin, Vera Eremina, Billy G. Hudson, Dorin Bogdan Borza, Raymond C. Harris, Lawrence B. Holzman, Carrie L. Phillips, Reinhard Fassler, Susan E. Quaggin, Jeffrey H. Miner, and Roy Zent. 2008. “B1 Integrin Expression by Podocytes Is Required to Maintain Glomerular Structural Integrity.” *Developmental Biology* 316(2):288–301.

Pradelles, Philippe, Yveline Frobert, Christophe Créminon, Hélène Ivonine, and Emilia Frindel. 1991. “Distribution of a Negative Regulator of Haematopoietic Stem Cell Proliferation (AcSDKP) and Thymosin, B4 in Mouse Tissues.” *FEBS Letters* 289(2):171–75.

Prochniewicz, Ewa, Neal Janson, David D. Thomas, and Enrique M. De La Cruz. 2005. “Cofilin Increases the Torsional Flexibility and Dynamics of Actin Filaments.” *Journal of Molecular Biology* 353(5):990–1000.

Puelles, Victor G., D. Fleck, Lena Ortz, Stella Papadouri, Thiago Strieder, Alexander M. C. Böhner, James W. van der Wolde, Michael Vogt, Turgay Saritas, Christoph Kuppe, Astrid Fuss, Sylvia Menzel, Barbara M. Klinkhammer, Gerhard Müller-Newen, F. Heymann, Leon Decker, Fabian Braun, Oliver Kretz, Tobias B. Huber, Etsuo A. Susaki, Hiroki R. Ueda, P. Boor, Jürgen Floege, Rafael Kramann, Christian Kurts, John F. Bertram, Marc Spehr, David J. Nikolic-Paterson, and Marcus J. Moeller. 2019. “Novel 3D Analysis Using Optical Tissue Clearing Documents the Evolution of Murine Rapidly Progressive Glomerulonephritis.” *Kidney International* 96(2):505–16.

Qiao, Xi, Rong-Shan Li, Hong Li, Guo-Zhen Zhu, Xiao-Guang Huang, Shan Shao, and Bo Bai. 2013. “Intermedin Protects against Renal Ischemia-Reperfusion Injury by Inhibition of Oxidative Stress.” *American Journal of Physiology-Renal Physiology* 304(1):F112–19.

Qin, D. D., D. Song, J. Huang, Feng Yu, and M. H. Zhao. 2015. “Plasma-Soluble Urokinase-Type Plasminogen Activator Receptor Levels Are Associated with Clinical and Pathological Activities in Lupus Nephritis: A Large Cohort Study from China.” *Lupus* 24(6):546–57.

Qiu, Ping, Michelle Kurpakus-Wheater, and Gabriel Sosne. 2007. “Matrix Metalloproteinase Activity Is Necessary for Thymosin Beta 4 Promotion of Epithelial Cell Migration.” *Journal of Cellular Physiology* 212(1):165–73.

Raats, C. J. Ils., Jacob van den Born, Marinka A. H. Bakker, Birgitte Oppers-Walgreen, Brenda J. M. Pisa, Henry B. P. M. Dijkman, Karel J. M. Assmann, and Jo H. M. Berden. 2000. “Expression of Agrin, Dystroglycan, and Utrophin in Normal Renal Tissue and in Experimental Glomerulopathies.” *American Journal of Pathology* 156(5):1749–65.

Radford, David J., Caroline O. S. Savage, and Gerard B. Nash. 2000. “Treatment of Rolling Neutrophils with Antineutrophil Cytoplasmic Antibodies Causes Conversion to Firm Integrin-Mediated Adhesion.” *Arthritis and Rheumatism* 43(6):1337–45.

Radice, G. L., M. C. Ferreira-Cornwell, S. D. Robinson, H. Rayburn, L. A. Chodosh, M. Takeichi, and R. O. Hynes. 1997. “Precocious Mammary Gland Development

in P-Cadherin-Deficient Mice." *The Journal of Cell Biology* 139(4):1025–32.

Raje, Shailja, Kumud Pandav, and Ritu Barthwal. 2020. "Binding of Anticancer Drug Adriamycin to Parallel G-quadruplex DNA [D-(TTAGGGT)] $_4$ Comprising Human Telomeric DNA Leads to Thermal Stabilization: A Multiple Spectroscopy Study." *Journal of Molecular Recognition* 33(2).

Ransick, Andrew, Nils O. Lindström, Jing Liu, Qin Zhu, Jin Jin Guo, Gregory F. Alvarado, Albert D. Kim, Hannah G. Black, Junhyong Kim, and Andrew P. McMahon. 2019. "Single-Cell Profiling Reveals Sex, Lineage, and Regional Diversity in the Mouse Kidney." *Developmental Cell* 51(3):399-413.e7.

Regele, H. M., E. Fillipovic, B. Langer, H. Poczewki, I. Kraxberger, R. E. Bittner, and D. Kerjaschki. 2000. "Glomerular Expression of Dystroglycans Is Reduced in Minimal Change Nephrosis but Not in Focal Segmental Glomerulosclerosis." *Journal of the American Society of Nephrology* 11(3):403–12.

RegeneRx - NCT00311766. 2012. "A Phase 2 Study on Effect of Thymosin Beta 4 on Wound Healing in Patients With Epidermolysis Bullosa - Full Text View - ClinicalTrials.Gov." *ClinicalTrials.Gov*. Retrieved January 20, 2021 (https://www.clinicaltrials.gov/ct2/show/NCT00311766?term=thymosin+beta+4&draw=2&rank=6).

RegeneRx - NCT00598871. 2010. "A Phase 2 Study of the Safety and Efficacy of Thymosin Beta 4 for Treating Corneal Wounds - Study Results - ClinicalTrials.Gov." *ClinicalTrials.Gov*. Retrieved January 20, 2021 (https://www.clinicaltrials.gov/ct2/show/results/NCT00598871?term=thymosin+beta+4&draw=2&rank=3).

RegeneRx - NCT00832091. 2010. "Study of Thymosin Beta 4 in Patients With Venous Stasis Ulcers - Study Results - ClinicalTrials.Gov." *ClinicalTrials.Gov*. Retrieved January 20, 2021 (https://www.clinicaltrials.gov/ct2/show/results/NCT00832091?term=thymosin+beta+4&draw=2&rank=1).

RegeneRx - NCT01311518. 2015. "A Study of the Safety and Efficacy of Injectable Thymosin Beta 4 for Treating Acute Myocardial Infarction - Full Text View - ClinicalTrials.Gov." *ClinicalTrials.Gov*. Retrieved January 20, 2021 (https://www.clinicaltrials.gov/ct2/show/NCT01311518?term=thymosin+beta+4&draw=1&rank=4).

RegeneRx - NCT01393132. 2015. "Comparative Study of Thymosin Beta 4 Eye

Drops vs. Vehicle in the Treatment of Severe Dry Eye - Study Results - ClinicalTrials.Gov." *ClinicalTrials.Gov*. Retrieved January 20, 2021 (https://www.clinicaltrials.gov/ct2/show/results/NCT01393132?term=thymosin+beta+4&draw=2&rank=5).

RegeneRx - NCT03578029. 2019. "Evaluation of the Safety and Efficacy Study of RGN-137 Topical Gel for Junctional and Dystrophic Epidermolysis Bullosa - Full Text View - ClinicalTrials.Gov." *ClinicalTrials.Gov*. Retrieved January 20, 2021 (https://clinicaltrials.gov/ct2/show/NCT03578029?term=NCT03578029&draw=2&rank=1).

RegeneRx - NCT03937882. 2020. "Assessment of the Safety and Efficacy of RGN-259 Ophthalmic Solutions for Dry Eye Syndrome: ARISE-3 - Full Text View - ClinicalTrials.Gov." *ClinicalTrials.Gov*. Retrieved January 20, 2021 (https://www.clinicaltrials.gov/ct2/show/NCT03937882?term=thymosin+beta+4&draw=2&rank=11).

Reidy, Kimberly and Frederick J. Kaskel. 2007. "Pathophysiology of Focal Segmental Glomerulosclerosis." *Pediatric Nephrology* 22(3):350–54.

Reiser, J., W. Kriz, M. Kretzler, and P. Mundel. 2000. "The Glomerular Slit Diaphragm Is a Modified Adherens Junction." *Journal of the American Society of Nephrology : JASN* 11(1):1–8.

Reiser, Jochen and Mehmet M. Altintas. 2016. "Podocytes." *F1000Research* 5.

Reiser, Jochen, Jun Oh, Isao Shirato, Katsuhiko Asanuma, Andreas Hug, Thomas M. Mundel, Karen Honey, Kazumi Ishidoh, Eiki Kominami, Jordan A. Kreidberg, Yasuhiko Tomino, and Peter Mundel. 2004. "Podocyte Migration during Nephrotic Syndrome Requires a Coordinated Interplay between Cathepsin L and Alpha3 Integrin." *The Journal of Biological Chemistry* 279(33):34827–32.

Renga, Giorgia, Vasilis Oikonomou, Silvia Moretti, Claudia Stincardini, Marina M. Bellet, Marilena Pariano, Andrea Bartoli, Stefano Brancorsini, Paolo Mosci, Andrea Finocchi, Paolo Rossi, Claudio Costantini, Enrico Garaci, Allan L. Goldstein, and Luigina Romani. 2019. "Thymosin B4 Promotes Autophagy and Repair via HIF-1α Stabilization in Chronic Granulomatous Disease." *Life Science Alliance* 2(6):e201900432.

Rhaleb, Nour Eddine, Saraswati Pokharel, Umesh Sharma, and Oscar A. Carretero. 2011. "Renal Protective Effects of N-Acetyl-Ser-Asp-Lys-Pro in Deoxycorticosterone Acetate-Salt Hypertensive Mice." *Journal of Hypertension*

29(2):330–38.

Robinson, R. C., K. Turbedsky, D. A. Kaiser, J. B. Marchand, H. N. Higgs, S. Choe, and T. D. Pollard. 2001. “Crystal Structure of Arp2/3 Complex.” *Science* 294(5547):1679–84.

Rodewald, R. and M. J. Karnovsky. 1974. “Porous Substructure of the Glomerular Slit Diaphragm in the Rat and Mouse.” *The Journal of Cell Biology* 60(2):423–33.

Romero, Stéphane, Christophe Le Clainche, Dominique Didry, Coumaran Egile, Dominique Pantaloni, and Marie France Carlier. 2004. “Formin Is a Processive Motor That Requires Profilin to Accelerate Actin Assembly and Associated ATP Hydrolysis.” *Cell* 119(3):419–29.

Roselli, Séverine, Olivier Gribouval, Nicolas Boute, Mireille Sich, France Benessy, Tania Attié, Marie Claire Gubler, and Corinne Antignac. 2002. “Podocin Localizes in the Kidney to the Slit Diaphragm Area.” *American Journal of Pathology* 160(1):131–39.

Rosenberg, Avi Z. and Jeffrey B. Kopp. 2017. “Focal Segmental Glomerulosclerosis.” *Clinical Journal of the American Society of Nephrology* 12(3):502–17.

Rouiller, Isabelle, Xiao Ping Xu, Kurt J. Amann, Coumaran Egile, Stephan Nickell, Daniela Nicastro, Rong Li, Thomas D. Pollard, Niels Volkmann, and Dorit Hanein. 2008. “The Structural Basis of Actin Filament Branching by the Arp2/3 Complex.” *Journal of Cell Biology* 180(5):887–95.

Rould, Mark A., Qun Wan, Peteranne B. Joel, Susan Lowey, and Kathleen M. Trybus. 2006. “Crystal Structures of Expressed Non-Polymerizable Monomeric Actin in the ADP and ATP States.” *Journal of Biological Chemistry* 281(42):31909–19.

Rubin, Jeffrey D., Tien V. Nguyen, Kari L. Allen, Katayoun Ayasoufi, and Michael A. Barry. 2019. “Comparison of Gene Delivery to the Kidney by Adenovirus, Adeno-Associated Virus, and Lentiviral Vectors after Intravenous and Direct Kidney Injections.” *Human Gene Therapy* 30(12):1559–71.

Ruff, Dennis, David Crockford, Gino Girardi, and Yuxin Zhang. 2010. “A Randomized, Placebo-Controlled, Single and Multiple Dose Study of Intravenous Thymosin B4 in Healthy Volunteers.” *Annals of the New York Academy of Sciences* 1194:223–29.

Rutledge, Elizabeth A., Christine L. Halbert, and David W. Russell. 1998. “Infectious Clones and Vectors Derived from Adeno-Associated Virus (AAV) Serotypes Other Than AAV Type 2.” *Journal of Virology* 72(1):309–19.

Ryu, Yun Kyoung, Jae Wook Lee, and Eun Yi Moon. 2015. “Thymosin Beta-4, Actin-Sequestering Protein Regulates Vascular Endothelial Growth Factor Expression via Hypoxia-Inducible Nitric Oxide Production in Hela Cervical Cancer Cells.” *Biomolecules and Therapeutics* 23(1):19–25.

Sacchetti, Marta and Alessandro Lambiase. 2014. “Diagnosis and Management of Neurotrophic Keratitis.” *Clinical Ophthalmology* 8:571–79.

Safer, Daniel, Marshall Elzinga, and Vivianne T. Nachmias. 1991. “Thymosin B4 and Fx, an Actin- Sequestering Peptide, Are Indistinguishable.” *The Journal of Biological Chemistry* 266(7):4029–32.

Safer, Daniel, Rajasree Golla, and Vivianne T. Nachmias. 1990. “Isolation of a 5-Kilodalton Actin-Sequestering Peptide from Human Blood Platelets.” *Cell Biology* 87:2536–40.

Samnegård, Bjoörn, Stefan H. Jacobson, Georg Jaremko, Bo Lennart Johansson, Karin Ekberg, Britta Isaksson, Linda Eriksson, John Wahren, and Mats Sjöquist. 2005. “C-Peptide Prevents Glomerular Hypertrophy and Mesangial Matrix Expansion in Diabetic Rats.” *Nephrology Dialysis Transplantation* 20(3):532–38.

Sanders, Mitchell C., Allan L. Goldstein, and Yu-Li Wang. 1992. “Thymosin B4 (Fx Peptide) Is a Potent Regulator of Actin Polymerization in Living Cells.” *Cell Biology* 89:4678–82.

Savin, Virginia J., Ram Sharma, Mukut Sharma, Ellen T. McCarthy, Suzanne K. Swan, Eileen Ellis, Helen Lovell, Bradley Warady, Sripad Gunwar, Arnold M. Chonko, Mary Artero, and Flavio Vincenti. 1996. “Circulating Factor Associated with Increased Glomerular Permeability to Albumin in Recurrent Focal Segmental Glomerulosclerosis.” *New England Journal of Medicine* 334(14):878–83.

Scheen, André J. 2015. “Pharmacokinetics, Pharmacodynamics and Clinical Use of SGLT2 Inhibitors in Patients with Type 2 Diabetes Mellitus and Chronic Kidney Disease.” *Clinical Pharmacokinetics* 54(7):691–708.

Schell, Christoph and Tobias B. Huber. 2017. “The Evolving Complexity of the Podocyte Cytoskeleton.” *Journal of the American Society of Nephrology* 28:3166–74.

Schießl, Ina Maria, Anna Hammer, Veronika Kattler, Bernhard Gess, Franziska Theilig, Ralph Witzgall, and Hayo Castrop. 2016. “Intravital Imaging Reveals Angiotensin II-Induced Transcytosis of Albumin by Podocytes.” *Journal of the American Society of Nephrology* 27(3):731–44.

Schievenbusch, Stephanie, Ingo Strack, Melanie Scheffler, Roswitha Nischt, Oliver Coutelle, Marianna Hösel, Michael Hallek, Jochen Wu Fries, Hans Peter Dienes, Margarete Odenthal, and Hildegard Büning. 2010. “Combined Paracrine and Endocrine AAV9 Mediated Expression of Hepatocyte Growth Factor for the Treatment of Renal Fibrosis.” *Molecular Therapy* 18(7):1302–9.

Schindelin, Johannes, Ignacio Arganda-Carreras, Erwin Frise, Verena Kaynig, Mark Longair, Tobias Pietzsch, Stephan Preibisch, Curtis Rueden, Stephan Saalfeld, Benjamin Schmid, Jean-Yves Tinevez, Daniel James White, Volker Hartenstein, Kevin Eliceiri, Pavel Tomancak, and Albert Cardona. 2012. “Fiji: An Open-Source Platform for Biological-Image Analysis.” *Nature Methods* 9(7):676–82.

Schneider, Remington R. S., Diana G. Eng, J. Nathan Kutz, Mariya T. Sweetwyne, Jeffrey W. Pippin, and Stuart J. Shankland. 2017. “Compound Effects of Aging and Experimental FSGS on Glomerular Epithelial Cells.” *Aging* 9(2):524–46.

Schouten, Marcel, Willem Joost Wiersinga, Marcel Levi, and Tom van der Poll. 2008. “Inflammation, Endothelium, and Coagulation in Sepsis.” *Journal of Leukocyte Biology* 83(3):536–45.

Schuh, Melina. 2011. “An Actin-Dependent Mechanism for Long-Range Vesicle Transport.” *Nature Cell Biology* 13(12):1431–36.

Schultz, Brian R. and Jeffrey S. Chamberlain. 2008. “Recombinant Adeno-Associated Virus Transduction and Integration.” *Molecular Therapy* 16(7):1189–99.

Schwarz, Karin, Matias Simons, Jochen Reiser, Moin A. Saleem, Christian Faul, Wihelm Kriz, Andrey S. Shaw, Lawrence B. Holzman, and Peter Mundel. 2001. “Podocin, a Raft-Associated Component of the Glomerular Slit Diaphragm, Interacts with CD2AP and Nephrin.” *Journal of Clinical Investigation* 108(11):1621–29.

Seldin, Donald W. and Gerhard Giebisch. 2008. *The Kidney: Physiology & Pathophysiology 1-2*. Vol. 1. 4th ed. edited by R. J. Alpern and S. C. Hebert. New Haven, Connecticut, USA: Elsevier.

Senís, Elena, Chronis Fatouros, Stefanie Große, Ellen Wiedtke, Dominik Niopek,

Ann-Kristin Mueller, Kathleen Börner, and Dirk Grimm. 2014. “CRISPR/Cas9-Mediated Genome Engineering: An Adeno-Associated Viral (AAV) Vector Toolbox.” *Biotechnology Journal* 9(11):1402–12.

Sethi, Sanjeev. 2018. “The Changing Spectrum of Heroin-Associated Kidney Disease.” *Clinical Journal of the American Society of Nephrology* 13(7):975–76.

Sethi, Sanjeev, Fernando C. Fervenza, Yuzhou Zhang, Ladan Zand, Nicole C. Meyer, Nicolò Borsa, Samih H. Nasr, and Richard J. H. Smith. 2013. “Atypical Postinfectious Glomerulonephritis Is Associated with Abnormalities in the Alternative Pathway of Complement.” *Kidney International* 83(2):293–99.

Shankar, Anoop, Ronald Klein, and Barbara E. K. Klein. 2006. “The Association among Smoking, Heavy Drinking, and Chronic Kidney Disease.” *American Journal of Epidemiology* 164(3):263–71.

Shibata, Shigeru, Miki Nagase, and Toshiro Fujita. 2006. “Fluvastatin Ameliorates Podocyte Injury in Proteinuric Rats via Modulation of Excessive Rho Signaling.” *J Am Soc Nephrol* 17:754–64.

Shibuya, Kazuyuki, Keizo Kanasaki, Motohide Isono, Haruhisa Sato, Mitsugu Omata, Toshiro Sugimoto, Shin Ichi Araki, Keiji Isshiki, Atsunori Kashiwagi, Masakazu Haneda, and Daisuke Koya. 2005. “N-Acetyl-Seryl-Aspartyl-Lysyl-Proline Prevents Renal Insufficiency and Mesangial Matrix Expansion in Diabetic Db/Db Mice.” *Diabetes* 54(3):838–45.

Shirato, I, T. Sakai, K. Kimura, Y. Tomino, and W. Kriz. 1996. “Cytoskeletal Changes in Podocytes Associated with Foot Process Effacement in Masugi Nephritis.” *The American Journal of Pathology* 148(4):1283–96.

Shirato, Isao. 2002. “Podocyte Process Effacement in Vivo.” *Microscopy Research and Technique* 57(4):241–46.

Shirato, Isao, Hiltraud Hosser, Kenjiro Kimura, Tatsuo Sakai, Yasuhiko Tomino, and Wilhelm Kriz. 1996. “The Development of Focal Segmental Glomerulosclerosis in Masugi Nephritis Is Based on Progressive Podocyte Damage.” *Virchows Archiv* 429(4–5):255–73.

Shoskes, Daniel A. and Alan W. McMahon. 2012. *Urology - Volume 2*. 10th ed. edited by L. R. Kavouissi, A. W. Partin, A. C. Novick, and C. A. Peters. Philadelphia: Elsevier Saunders.

Sidorenkov, Grigory and Gerjan Navis. 2014. “Safety of ACE Inhibitor Therapies in Patients with Chronic Kidney Disease.” *Expert Opinion on Drug Safety*

13(10):1383–95.

Silacci, P., L. Mazzolai, C. Gauci, N. Stergiopulos, H. L. Yin, and D. Hayoz. 2004. “Gelsolin Superfamily Proteins: Key Regulators of Cellular Functions.” *Cellular and Molecular Life Sciences* 61(19–20):2614–23.

Sit, Soon-Tuck and Ed Manser. 2011. “Rho GTPases and Their Role in Organizing the Actin Cytoskeleton.” *Journal of Cell Science* 124:679–83.

Siton, Orit and Anne Bernheim-Groswasser. 2014. “Reconstitution of Actin-Based Motility by Vasodilator-Stimulated Phosphoprotein (VASP) Depends on the Recruitment of F-Actin Seeds from the Solution Produced by Cofilin.” *Journal of Biological Chemistry* 289(45):31274–86.

Smadel, Joseph E. 1937. “Experimental Nephritis in Rats Induced by Injection of Anti-Kidney Serum: III. Pathological Studies of the Acute and Chronic Disease.” *Journal of Experimental Medicine* 65(4):541–56.

Smart, N., C. A. Risebro, A. A. D. Melville, K. Moses, R. J. Schwartz, K. R. Chien, and P. R. Riley. 2007. “Thymosin Beta-4 Is Essential for Coronary Vessel Development and Promotes Neovascularization via Adult Epicardium.” *Annals of the New York Academy of Sciences* 1112(1):171–88.

Smart, Nicola, Sveva Bollini, Karina N. Dubé, Joaquim M. Vieira, Bin Zhou, Sean Davidson, Derek Yellon, Johannes Riegler, Anthony N. Price, Mark F. Lythgoe, William T. Pu, and Paul R. Riley. 2011. “De Novo Cardiomyocytes from within the Activated Adult Heart after Injury.” *Nature* 474(7353):640–44.

Smart, Nicola, Alison A. Hill, James C. Cross, and Paul R. Riley. 2002. “A Differential Screen for Putative Targets of the BHLH Transcription Factor Hand1 in Cardiac Morphogenesis.” *Mechanisms of Development* 119(SUPPL. 1):S65–71.

Smith, Benjamin A., Karen Daugherty-Clarke, Bruce L. Goode, and Jeff Gelles. 2013. “Pathway of Actin Filament Branch Formation by Arp2/3 Complex Revealed by Single-Molecule Imaging.” *Proceedings of the National Academy of Sciences of the United States of America* 110(4):1285–90.

Song, Kibbeum, Hye Ju Han, Sokho Kim, and Jungkee Kwon. 2020. “Thymosin Beta 4 Attenuates PrP(106-126)-Induced Human Brain Endothelial Cells Dysfunction.” *European Journal of Pharmacology* 869:172891.

Sonntag, F., K. Kother, K. Schmidt, M. Weghofer, C. Raupp, K. Nieto, A. Kuck, B. Gerlach, B. Bottcher, O. J. Muller, K. Lux, M. Horer, and J. A. Kleinschmidt. 2011. “The Assembly-Activating Protein Promotes Capsid Assembly of Different

Adeno-Associated Virus Serotypes." *Journal of Virology* 85(23):12686–97.

Sonntag, Florian, Svenja Bleker, Barbara Leuchs, Roger Fischer, and Jürgen A. Kleinschmidt. 2006. "Adeno-Associated Virus Type 2 Capsids with Externalized VP1/VP2 Trafficking Domains Are Generated Prior to Passage through the Cytoplasm and Are Maintained until Uncoating Occurs in the Nucleus." *Journal of Virology* 80(22):11040–54.

Sosne, Gabriel. 2018. "Thymosin Beta 4 and the Eye: The Journey from Bench to Bedside." *Expert Opinion on Biological Therapy* 18(sup1):99–104.

Sosne, Gabriel, Chi Chao Chan, Khoan Thai, Michael Kennedy, Elizabeth A. Szliter, Linda D. Hazlett, Hynda K. Kleinman, Gabriel Sosne, Chi Chao Chan, Khoan Thai, Michael Kennedy, Elizabeth A. Szliter, Linda D. Hazlett, Hynda K. Kleinman, Gabriel Sosne, Chi Chao Chan, Khoan Thai, Michael Kennedy, Elizabeth A. Szliter, Linda D. Hazlett, Hynda K. Kleinman, Gabriel Sosne, Chi Chao Chan, Khoan Thai, Michael Kennedy, Elizabeth A. Szliter, Linda D. Hazlett, Hynda K. Kleinman, Gabriel Sosne, Chi Chao Chan, Khoan Thai, Michael Kennedy, Elizabeth A. Szliter, Linda D. Hazlett, and Hynda K. Kleinman. 2001. "Thymosin Beta 4 Promotes Corneal Wound Healing and Modulates Inflammatory Mediators in Vivo." *Experimental Eye Research* 72(5):605–8.

Sosne, Gabriel, Patricia L. Christopherson, Ronald P. Barrett, and Rafael Fridman. 2005. "Thymosin-B4 Modulates Corneal Matrix Metalloproteinase Levels and Polymorphonuclear Cell Infiltration after Alkali Injury." *Investigative Ophthalmology and Visual Science* 46(7):2388–95.

Sosne, Gabriel, Steven Dunn, David Crockford, Chaesik Kim, and Elizabeth Dixon. 2013. "Thymosin Beta 4 Eye Drops Significantly Improve Signs and Symptoms of Severe Dry Eye in a Physician-Sponsored Phase 2 Clinical Trial | IOVS | ARVO Journals." *Investigative Ophthalmology & Visual Science* 54:6033.

Sosne, Gabriel and George W. Ousler. 2015. "Thymosin Beta 4 Ophthalmic Solution for Dry Eye: A Randomized, Placebo-Controlled, Phase II Clinical Trial Conducted Using the Controlled Adverse Environment (CAE™) Model." *Clinical Ophthalmology (Auckland, N.Z.)* 9:877–84.

Sosne, Gabriel, Ping Qiu, Patricia L. Christopherson, and Michelle Kurpakus Wheater. 2007. "Thymosin Beta 4 Suppression of Corneal NFκB: A Potential Anti-Inflammatory Pathway." *Experimental Eye Research* 84(4):663–69.

Sosne, Gabriel, Ping Qiu, and Michelle Kurpakus-Wheater. 2007. “Thymosin Beta 4: A Novel Corneal Wound Healing and Anti-Inflammatory Agent.” *Clinical Ophthalmology* 1(3):201–7.

Sosne, Gabriel, Elizabeth A. Szliter, Ronald Barrett, Karen A. Kernacki, Hynda Kleinman, and Linda D. Hazlett. 2002. “Thymosin Beta 4 Promotes Corneal Wound Healing and Decreases Inflammation in Vivo Following Alkali Injury.” *Experimental Eye Research* 74(2):293–99.

Sosne, Gabriel, Lihua Xu, Lisa Prach, Linda K. Mrock, Hynda K. Kleinman, John J. Letterio, Linda D. Hazlett, and Michelle Kurpakus-Wheater. 2004. “Thymosin Beta 4 Stimulates Laminin-5 Production Independent of TGF-Beta.” *Experimental Cell Research* 293(1):175–83.

Srivastava, A., E. W. Lusby, and K. I. Berns. 1983. “Nucleotide Sequence and Organization of the Adeno-Associated Virus 2 Genome.” *Journal of Virology* 45(2):555–64.

Srivastava, D., A. Saxena, J. M. Dimaio, and I. Bock-Marquette. 2007. “Thymosin Beta4 Is Cardioprotective after Myocardial Infarction.” *Annals of the New York Academy of Sciences* 1112(1):161–70.

Srivastava, Swayam Prakash, Julie E. Goodwin, Keizo Kanasaki, and Daisuke Koya. 2020. “Metabolic Reprogramming by *N* -acetyl-seryl-aspartyl-lysyl-proline Protects against Diabetic Kidney Disease.” *British Journal of Pharmacology* 177(16):3691–3711.

Stark, Kevin, Seppo Vainio, Galya Vassileva, and Andrew P. McMahon. 1994. “Epithelial Transformation of Metanephric Mesenchyme in the Developing Kidney Regulated by Wnt-4.” *Nature* 372(6507):679–83.

Steinert, Peter M., Jonathan C. R. Jones, and Robert D. Goldman. 1984. “Intermediate Filaments.” *The Journal of Cell Biology* 99(1):22–27.

Steinmetz, Michel O., Kenneth N. Goldie, and Ueli Aebi. 1997. “A Correlative Analysis of Actin Filament Assembly, Structure, and Dynamics.” *Journal of Cell Biology* 138(3):559–74.

Stengel, Bénédicte, Michelle E. Tarver–Carr, Neil R. Powe, Mark S. Eberhardt, and Frederick L. Brancati. 2003. “Lifestyle Factors, Obesity and the Risk of Chronic Kidney Disease.” *Epidemiology* 14(4):479–87.

Streck, Christian J., Paxton V. Dickson, Catherine Y. C. Ng, Junfang Zhou, John T. Gray, Amit C. Nathwani, and Andrew M. Davidoff. 2005. “Adeno-Associated

Virus Vector-Mediated Systemic Delivery of IFN-β Combined with Low-Dose Cyclophosphamide Affects Tumor Regression in Murine Neuroblastoma Models." *Clinical Cancer Research* 11(16):6020–29.

Stump, Craig S. 2011. "Physical Activity in the Prevention of Chronic Kidney Disease." *Cardiorenal Medicine* 1(3):164–73.

Stumvoll, Michael, Christian Meyer, Gabriele Perriello, Maryl Kreider, Stephen Welle, and John Gerich. 1998. "Human Kidney and Liver Gluconeogenesis: Evidence for Organ Substrate Selectivity." *American Journal of Physiology - Endocrinology and Metabolism* 274(5):E817–26.

Suarez, Cristian, Jérémy Roland, Rajaa Boujemaa-Paterski, Hyeran Kang, Brannon R. McCullough, Anne Cécile Reymann, Christophe Guérin, Jean Louis Martiel, Enrique M. De La Cruz, and Laurent Blanchoin. 2011. "Cofilin Tunes the Nucleotide State of Actin Filaments and Severs at Bare and Decorated Segment Boundaries." *Current Biology* 21(10):862–68.

Subbarayan, Meena S., Charles Hudson, Lauren D. Moss, Kevin R. Nash, and Paula C. Bickford. 2020. "T Cell Infiltration and Upregulation of MHCII in Microglia Leads to Accelerated Neuronal Loss in an α-Synuclein Rat Model of Parkinson's Disease." *Journal of Neuroinflammation* 17(1):1–16.

Succar, Lena, Ross A. Boadle, David C. Harris, and Gopala K. Rangan. 2016. "Formation of Tight Junctions between Neighboring Podocytes Is an Early Ultrastructural Feature in Experimental Crescentic Glomerulonephritis." *International Journal of Nephrology and Renovascular Disease* 9:297–312.

Succar, Lena, Julia Lai-Kwon, David J. Nikolic-Paterson, and Gopala K. Rangan. 2014. "Induction Monotherapy with Sirolimus Has Selected Beneficial Effects on Glomerular and Tubulointersititial Injury in Nephrotoxic Serum Nephritis." *International Journal of Nephrology and Renovascular Disease* 7:303–13.

Sugiyama, Seigo, Hideaki Jinnouchi, Akira Yoshida, Kunio Hieshima, Noboru Kurinami, Katsunori Jinnouchi, Motoko Tanaka, Tomoko Suzuki, Fumio Miyamoto, Keizo Kajiwara, and Tomio Jinnouchi. 2019. "Renoprotective Effects of Additional SGLT2 Inhibitor Therapy in Patients With Type 2 Diabetes Mellitus and Chronic Kidney Disease Stages 3b-4: A Real World Report From A Japanese Specialized Diabetes Care Center." *Journal of Clinical Medicine Research* 11(4):267–74.

Suh, J. H. and J. H. Miner. 2013. "The Glomerular Basement Membrane as a Barrier

to Albumin.” *Nature Reviews Nephrology* 9:470–77.

Suleiman, Hani Y., Robyn Roth, Sanjay Jain, John E. Heuser, Andrey S. Shaw, and Jeffrey H. Miner. 2017. “Injury-Induced Actin Cytoskeleton Reorganization in Podocytes Revealed by Super-Resolution Microscopy.” *JCI Insight* 2(16).

Suliman, Hagir B., Martha Sue Carraway, Abdelwahid S. Ali, Chrystal M. Reynolds, Karen E. Welty-Wolf, and Claude A. Piantadosi. 2007. “The CO/HO System Reverses Inhibition of Mitochondrial Biogenesis and Prevents Murine Doxorubicin Cardiomyopathy.” *Journal of Clinical Investigation* 117(12):3730–41.

Sun, Yu Bo Yang, Xinli Qu, Xueming Zhang, Georgina Caruana, John F. Bertram, and Jinhua Li. 2013. “Glomerular Endothelial Cell Injury and Damage Precedes That of Podocytes in Adriamycin-Induced Nephropathy” edited by M. P. Rastaldi. *PLoS ONE* 8(1):e55027.

Suraneni, Praveen, Boris Rubinstein, Jay R. Unruh, Michael Durnin, Dorit Hanein, and Rong Li. 2012. “The Arp2/3 Complex Is Required for Lamellipodia Extension and Directional Fibroblast Cell Migration.” *Journal of Cell Biology* 197(2):239–51.

Svitkina, Tatyana. 2018. “The Actin Cytoskeleton and Actin-Based Motility.” *Cold Spring Harbor Perspectives in Biology* 10(1):a018267.

Szrejder, Maria, Patrycja Rachubik, Dorota Rogacka, Irena Audzeyenka, Michał Rychłowski, Stefan Angielski, and Agnieszka Piwkowska. 2020. “Extracellular ATP Modulates Podocyte Function through P2Y Purinergic Receptors and Pleiotropic Effects on AMPK and CAMP/PKA Signaling Pathways.” *Archives of Biochemistry and Biophysics* 695:108649.

Tabatabaeifar, Mansoureh, Tanja Wlodkowski, Ivana Simic, Helga Denc, Geraldine Mollet, Stefanie Weber, John Julius Moyers, Barbara Brühl, Michael Joseph Randles, Rachel Lennon, Corinne Antignac, and Franz Schaefer. 2017. “An Inducible Mouse Model of Podocin-Mutation-Related Nephrotic Syndrome” edited by S. E. Dryer. *PLOS ONE* 12(10):e0186574.

Takeda, Tetsuro. 2003. “Podocyte Cytoskeleton Is Connected to the Integral Membrane Protein Podocalyxin through Na+/H+-Exchanger Regulatory Factor 2 and Ezrin.” *Clinical and Experimental Nephrology* 7(4):260–69.

Takeda, Tetsuro, Tammie McQuistan, Robert A. Orlando, and Marilyn G. Farquhar. 2001. “Loss of Glomerular Foot Processes Is Associated with Uncoupling of

Podocalyxin from the Actin Cytoskeleton." *Journal of Clinical Investigation* 108(2):289–301.

Takeya, Ryu, Kenichiro Taniguchi, Shuh Narumiya, and Hideki Sumimoto. 2008. "The Mammalian Formin FHOD1 Is Activated through Phosphorylation by ROCK and Mediates Thrombin-Induced Stress Fibre Formation in Endothelial Cells." *The EMBO Journal* 27(4):618–28.

Tang, Mei-Chuan, Li-Chuan Chan, Yi-Chen Yeh, Cheng-Yu Chen, Teh-Ying Chou, Wei-Shu Wang, and Yeu Su. 2011. "Thymosin Beta 4 Induces Colon Cancer Cell Migration and Clinical Metastasis via Enhancing ILK/IQGAP1/Rac1 Signal Transduction Pathway." *Cancer Letters* 308(2):162–71.

Tarantal, Alice F., C. Chang I. Lee, Michele L. Martinez, Aravind Asokan, and R. Jude Samulski. 2017. "Systemic and Persistent Muscle Gene Expression in Rhesus Monkeys with a Liver De-Targeted Adeno-Associated Virus Vector." *Human Gene Therapy* 28(5):385–91.

Teramoto, Keisuke, Yu Tsurekawa, Mary Ann Suico, Shota Kaseda, Kohei Omachi, Tsubasa Yokota, Misato Kamura, Mariam Piruzyan, Tatsuya Kondo, Tsuyoshi Shuto, Eiichi Araki, and Hirofumi Kai. 2020. "Mild Electrical Stimulation with Heat Shock Attenuates Renal Pathology in Adriamycin-Induced Nephrotic Syndrome Mouse Model." *Scientific Reports* 10(1):1–12.

Tham, El Li, Simon J. Freeley, Siobhan Bearder, Fernanda Florez Barros, Mark S. Cragg, Attila Mócsai, and Michael G. Robson. 2020. "VISTA Deficiency Protects from Immune Complex-Mediated Glomerulonephritis by Inhibiting Neutrophil Activation." *Journal of Autoimmunity* 113:102501.

Thomas, Clare E., Theresa A. Storm, Zan Huang, and Mark A. Kay. 2004. "Rapid Uncoating of Vector Genomes Is the Key to Efficient Liver Transduction with Pseudotyped Adeno-Associated Virus Vectors." *Journal Of Virology* 78(6):3110–22.

Tian, Xuefei and Shuta Ishibe. 2016. "Targeting the Podocyte Cytoskeleton: From Pathogenesis to Therapy in Proteinuric Kidney Disease." *Nephrology Dialysis Transplantation* 31(10):1577–83.

Tipping, Peter G. and Stephen R. Holdsworth. 2006. "T Cells in Crescentic Glomerulonephritis." *Journal of the American Society of Nephrology* 17(5):1253–63.

Toda, Naohiro, Kiyoshi Mori, Masato Kasahara, Akira Ishii, Kenichi Koga, Shoko

Ohno, Keita P. Mori, Yukiko Kato, Keisuke Osaki, Takashige Kuwabara, Katsutoshi Kojima, Daisuke Taura, Masakatsu Sone, Taiji Matsusaka, Kazuwa Nakao, Masashi Mukoyama, Motoko Yanagita, and Hideki Yokoi. 2017. “Crucial Role of Mesangial Cell-Derived Connective Tissue Growth Factor in a Mouse Model of Anti-Glomerular Basement Membrane Glomerulonephritis.” *Scientific Reports* 7(1):1–16.

Tolliday, Nicola, Lynn VerPlank, and Rong Li. 2002. “Rho1 Directs Formin-Mediated Actin Ring Assembly during Budding Yeast Cytokinesis.” *Current Biology* 12(21):1864–70.

Tompa, Peter. 2005. “The Interplay between Structure and Function in Intrinsically Unstructured Proteins.” *FEBS Letters* 579(15):3346–54.

Torres, Vicente E., Arlene B. Chapman, Olivier Devuyst, Ron T. Gansevoort, Jared J. Grantham, Eiji Higashihara, Ronald D. Perrone, Holly B. Krasa, John Ouyang, and Frank S. Czerwiec. 2012. “Tolvaptan in Patients with Autosomal Dominant Polycystic Kidney Disease.” *New England Journal of Medicine* 367(25):2407–18.

Tratschin, J. D., M. H. West, T. Sandbank, and B. J. Carter. 1984. “A Human Parvovirus, Adeno-Associated Virus, as a Eucaryotic Vector: Transient Expression and Encapsidation of the Procaryotic Gene for Chloramphenicol Acetyltransferase.” *Molecular and Cellular Biology* 4(10):2072–81.

Tryggvason, Karl, Timo Pikkarainen, and Jaakko Patrakka. 2006. “Nck Links Nephrin to Actin in Kidney Podocytes.” *Cell* 125(2):221–24.

Tu, Ling, Xizhen Xu, Huaibing Wan, Changqing Zhou, Juanjuan Deng, Gang Xu, Xiao Xiao, Yipu Chen, Matthew L. Edin, James W. Voltz, Darryl C. Zeldin, and Dao Wen Wang. 2008. “Delivery of Recombinant Adeno-Associated Virus-Mediated Human Tissue Kallikrein for Therapy of Chronic Renal Failure in Rats.” *Human Gene Therapy* 19(4):318–30.

Tung, Chun-Wu, Yung-Chien Hsu, Ya-Hsueh Shih, Pey-Jium Chang, and Chun-Liang Lin. 2018. “Glomerular Mesangial Cell and Podocyte Injuries in Diabetic Nephropathy.” *Nephrology* 23:32–37.

Turner, Jeffrey M., Carolyn Bauer, Matthew K. Abramowitz, Michal L. Melamed, and Thomas H. Hostetter. 2012. “Treatment of Chronic Kidney Disease.” *Kidney International* 81(4):351–62.

Ullman-Culleré, Mollie H. and Charmaine J. Foltz. 1999. “Body Condition Scoring: A

Rapid and Accurate Method for Assessing Health Status in Mice." *Laboratory Animal Science* 49(3):319–23.

Vallon, Volker, Kenneth A. Platt, Robyn Cunard, Jana Schroth, Jean Whaley, Scott C. Thomson, Hermann Koepsell, and Timo Rieg. 2011. "SGLT2 Mediates Glucose Reabsorption in the Early Proximal Tubule." *J Am Soc Nephrol* 22:104–12.

Vartiainen, Maria K., Tuija Mustonen, Pieta K. Mattila, Pauli J. Ojala, Irma Thesleff, Juha Partanen, and Pekka Lappalainen. 2002. "The Three Mouse Actin-Depolymerizing Factor/Cofilins Evolved to Fulfill Cell-Type-Specific Requirements for Actin Dynamics." *Molecular Biology of the Cell* 13(1):183–94.

Vasilopoulou, Elisavet, Maria Kolatsi-Joannou, Maja T. Lindenmeyer, Kathryn E. White, Michael G. Robson, Clemens D. Cohen, Neil J. Sebire, Paul R. Riley, Paul J. Winyard, and David A. Long. 2016. "Loss of Endogenous Thymosin B4 Accelerates Glomerular Disease." *Kidney International* 90(5):1056–70.

Vasilopoulou, Elisavet, Paul R. Riley, and David A. Long. 2018. "Thymosin-B4: A Key Modifier of Renal Disease." *Expert Opinion of Biological Therapy* 18(Sup1):185–92.

Vavylonis, Dimitrios, David R. Kovar, Ben O'Shaughnessy, and Thomas D. Pollard. 2006. "Model of Formin-Associated Actin Filament Elongation." *Molecular Cell* 21(4):455–66.

Vincent, K. A., S. T. Piraino, and S. C. Wadsworth. 1997. "Analysis of Recombinant Adeno-Associated Virus Packaging and Requirements for Rep and Cap Gene Products." *Journal of Virology* 71(3):1897–1905.

Vladar, Eszter K., Roy D. Bayly, Ashvin M. Sangoram, Matthew P. Scott, and Jeffrey D. Axelrod. 2012. "Microtubules Enable the Planar Cell Polarity of Airway Cilia." *Current Biology* 22(23):2203–12.

Vogelmann, Stefanie U., W. James Nelson, Bryan D. Myers, and Kevin V. Lemley. 2003. "Urinary Excretion of Viable Podocytes in Health and Renal Disease." *American Journal of Physiology - Renal Physiology* 285(1 54-1):F40.

Vogtländer, Nils P. J., Henk Jan Visch, Marinka A. H. Bakker, Jo H. M. Berden, and Johan van der Vlag. 2009. "Ligation of α-Dystroglycan on Podocytes Induces Intracellular Signaling: A New Mechanism for Podocyte Effacement?" edited by J. Z. Rappoport. *PLoS ONE* 4(6):e5979.

Wagner, Mark C., George Rhodes, Exing Wang, Vikas Pruthi, Ehtesham Arif, Moin

A. Saleem, Sarah E. Wean, Puneet Garg, Rakesh Verma, Lawrence B. Holzman, Vince Gattone, Bruce A. Molitoris, and Deepak Nihalani. 2008. “Ischemic Injury to Kidney Induces Glomerular Podocyte Effacement and Dissociation of Slit Diaphragm Proteins Neph1 and ZO-1.” *Journal of Biological Chemistry* 283(51):35579–89.

Wagner, Nicole, Kay Dietrich Wagner, Yiming Xing, Holger Scholz, and Andreas Schedl. 2004. “The Major Podocyte Protein Nephrin Is Transcriptionally Activated by the Wilms’ Tumor Suppressor WT1.” *Journal of the American Society of Nephrology* 15(12):3044–51.

Walker, P. Roy, Catherine Smith, Tony Youdale, Julie Leblanc, James F. Whitfield, and Marianna Sikorska. 1991. “Topoisomerase II-Reactive Chemotherapeutic Drugs Induce Apoptosis in Thymocytes.” *Cancer Research* 51(4):1078–85.

Wang, Dan, Phillip W. L. Tai, and Guangping Gao. 2019. “Adeno-Associated Virus Vector as a Platform for Gene Therapy Delivery.” *Nature Reviews Drug Discovery* 18(5):358–78.

Wang, Juan, Teruo Hidaka, Yu Sasaki, Eriko Tanaka, Miyuki Takagi, Terumi Shibata, Ayano Kubo, Juan Alejandro Oliva Trejo, Lining Wang, Katsuhiko Asanuma, and Yasuhiko Tomino. 2018. “Neurofilament Heavy Polypeptide Protects against Reduction in Synaptopodin Expression and Prevents Podocyte Detachment.” *Scientific Reports* 8(1):1–14.

Wang, Mingao, Ruichan Liu, Xibei Jia, Suhong Mu, and Rujuan Xie. 2010. “N-Acetyl-Seryl-Aspartyl-Lysyl-Proline Attenuates Renal Inflammation and Tubulointerstitial Fibrosis in Rats.” *International Journal of Molecular Medicine* 26(6):795–801.

Wang, Siyuan, Cheng Chen, Ke Su, Dongqing Zha, Wei Liang, JL Hillebrands, Harry van Goor, and Guohua Ding. 2016. “Angiotensin II Induces Reorganization of the Actin Cytoskeleton and Myosin Light-Chain Phosphorylation in Podocytes through Rho/ROCK-Signaling Pathway*.” *Renal Failure* 38(2):268–75.

Wang, Yang, Yi Ping Wang, Yuet-Ching Tay, and David C. H. Harris. 2000. “Progressive Adriamycin Nephropathy in Mice: Sequence of Histologic and Immunohistochemical Events.” *Kidney International* 58(4):1797–1804.

Wang, Yanshu and Jeremy Nathans. 2007. “Tissue/Planar Cell Polarity in Vertebrates: New Insights and New Questions.” *Development* 134(4):647–58.

Wang, Yuan Min, Yiping Wang, David C. H. Harris, Stephen I. Alexander, and

Vincent W. S. Lee. 2015. “Adriamycin Nephropathy in BALB/c Mice.” Pp. 15.28.1-15.28.6 in *Current Protocols in Immunology*. Vol. 108. Hoboken, NJ, USA: John Wiley & Sons, Inc.

Wartiovaara, Jorma, Lars Göran Öfverstedt, Jamshid Khoshnoodi, Jingjing Zhang, Eetu Mäkelä, Sara Sandin, Vesa Ruotsalainen, R. Holland Cheng, Hannu Jalanko, Ulf Skoglund, and Karl Tryggvason. 2004. “Nephrin Strands Contribute to a Porous Slit Diaphragm Scaffold as Revealed by Electron Tomography.” *Journal of Clinical Investigation* 114(10):1475–83.

Weaver, Alissa M., Andrei V. Karginov, Andrew W. Kinley, Scott A. Weed, Yan Li, J. Thomas Parsons, and John A. Cooper. 2001. “Cortactin Promotes and Stabilizes Arp2/3-Induced Actin Filament Network Formation.” *Current Biology* 11(5):370–74.

Weber, A, V. T. Nachmias, C. R. Pennise, M. Pring, and D. Safer. 1992. “Interaction of Thymosin SS4 with Muscle and Platelet Actin: Implications for Actin Sequestration in Resting Platelets.” *Biochemistry* 31:6179–85.

Weber, A., C. R. Pennise, V. T. Nachmias, D. Safer, and M. Pring. 1992. “Interaction of Thymosin B4 with Muscle and Platelet Actin : Implications for Actin Sequestration in Resting Platelets.” *Biochemistry* 31(27):6179–85.

Wegner, A., T. P. Walsh, K. Ruhnau, Y. Yamashiro-Matsumura, F. Matsumura, E. Yokota, and K. Maruyama. 1989. “Effects of CapZ, an Actin Capping Protein of Muscle, on the Polymerization of Actin.” *Biochemistry* 28(21):8506–14.

Wegner, Binytha, Abass Al-Momany, Stephen C. Kulak, Kathy Kozlowski, Marya Obeidat, Nadia Jahroudi, John Paes, Mark Berryman, and Barbara J. Ballermann. 2010. “CLIC5A, a Component of the Ezrin-Podocalyxin Complex in Glomeruli, Is a Determinant of Podocyte Integrity.” *American Journal of Physiology - Renal Physiology* 298(6):F1492-503.

Wei, Changli, Shafic El Hindi, Jing Li, Alessia Fornoni, Nelson Goes, Junichiro Sageshima, Dony Maiguel, S. Ananth Karumanchi, Hui Kim Yap, Moin Saleem, Qingyin Zhang, Boris Nikolic, Abanti Chaudhuri, Pirouz Daftarian, Eduardo Salido, Armando Torres, Moro Salifu, Minnie M. Sarwal, Franz Schaefer, Christian Morath, Vedat Schwenger, Martin Zeier, Vineet Gupta, David Roth, Maria Pia Rastaldi, George Burke, Phillip Ruiz, and Jochen Reiser. 2011. “Circulating Urokinase Receptor as a Cause of Focal Segmental Glomerulosclerosis.” *Nature Medicine* 17(8):952–60.

Wei, Chuanyu, Sandeep Kumar, Il-Kwon Kim, and Sudhiranjan Gupta. 2012. "Thymosin Beta 4 Protects Cardiomyocytes from Oxidative Stress by Targeting Anti-Oxidative Enzymes and Anti-Apoptotic Genes" edited by R. Mohanraj. *PLoS ONE* 7(8):e42586.

Weil, E. Jennifer, Kevin V. Lemley, Clinton C. Mason, Berne Yee, Lois I. Jones, Kristina Blouch, Tracy Lovato, Meghan Richardson, Bryan D. Myers, and Robert G. Nelson. 2012. "Podocyte Detachment and Reduced Glomerular Capillary Endothelial Fenestration Promote Kidney Disease in Type 2 Diabetic Nephropathy." *Kidney International* 82(9):1010–17.

Welsh, Gavin I. and Moin A. Saleem. 2012. "The Podocyte Cytoskeleton-Key to a Functioning Glomerulus in Health and Disease." *Nat. Rev. Nephrol* 8:14–21.

Welte, Michael A. 2004. "Bidirectional Transport along Microtubules." *Current Biology* 14(13):R525–37.

Westhaus, Adrian, Marti Cabanes-Creus, Arkadiusz Rybicki, Grober Baltazar, Renina Gale Navarro, Erhua Zhu, Matthieu Drouyer, Maddison Knight, Razvan F. Albu, Boaz H. Ng, Predrag Kalajdzic, Magdalena Kwiatek, Kenneth Hsu, Giorgia Santilli, Wendy Gold, Belinda Kramer, Anai Gonzalez-Cordero, Adrian J. Thrasher, Ian E. Alexander, and Leszek Lisowski. 2020. "High-Throughput in Vitro, Ex Vivo, and in Vivo Screen of Adeno-Associated Virus Vectors Based on Physical and Functional Transduction." *Human Gene Therapy* 31(9–10):575–89.

Wharram, Bryan L., Meera Goyal, Patrick J. Gillespie, Jocelyn E. Wiggins, David B. Kershaw, Lawrence B. Holzman, Robert C. Dysko, Thomas L. Saunders, Linda C. Samuelson, and Roger C. Wiggins. 2000. "Altered Podocyte Structure in GLEPP1 (Ptpro)-Deficient Mice Associated with Hypertension and Low Glomerular Filtration Rate." *Journal of Clinical Investigation* 106(10):1281–90.

Wioland, Hugo, Berengere Guichard, Yosuke Senju, Sarah Myram, Pekka Lappalainen, Antoine Jégou, and Guillaume Romet-Lemonne. 2017. "ADF/Cofilin Accelerates Actin Dynamics by Severing Filaments and Promoting Their Depolymerization at Both Ends." *Current Biology* 27(13):1956-1967.e7.

Wise, T., G. J. MacDonald, J. Klindt, and J. J. Ford. 1992. "Characterization of Thymic Weight and Thymic Peptide Thymosin-Beta 4: Effects of Hypophysectomy, Sex, and Neonatal Sexual Differentiation." *Thymus* 19(4):235–44.

Wolfe, Robert A., Valarie B. Ashby, Edgar L. Milford, Akinlolu O. Ojo, Robert E.

Ettenger, Lawrence Y. C. Agodoa, Philip J. Held, and Friedrich K. Port. 1999. “Comparison of Mortality in All Patients on Dialysis, Patients on Dialysis Awaiting Transplantation, and Recipients of a First Cadaveric Transplant.” *New England Journal of Medicine* 341(23):1725–30.

Wollina, Uwe, Tim Graefe, and Kerstin Karte. 2000. “Treatment of Relapsing or Recalcitrant Cutaneous T-Cell Lymphoma with Pegylated Liposomal Doxorubicin.” *Journal of the American Academy of Dermatology* 42(1 I):40–46.

Wong, Jenny S., Elizabeth Iorns, Michelle N. Rheault, Toby M. Ward, Priyanka Rashmi, Ursula Weber, Marc E. Lippman, Christian Faul, Marek Mlodzik, and Peter Mundel. 2012. “Rescue of Tropomyosin Deficiency in *Drosophila* and Human Cancer Cells by Synaptopodin Reveals a Role of Tropomyosin α in RhoA Stabilization.” *The EMBO Journal* 31(4):1028–40.

Woodrum, Diane T., Steven A. Rich, and Thomas D. Pollard. 1975. “Evidence for Biased Bidirectional Polymerization of Actin Filaments Using Heavy Meromyosin Prepared by an Improved Method.” *Journal of Cell Biology* 67(1):231–37.

Worawichawong, Suchin, Louis Girard, Kiril Trpkov, James C. Gough, Daniel B. Gregson, and Hallgrimur Benediktsson. 2011. “Immunoglobulin A-Dominant Postinfectious Glomerulonephritis: Frequent Occurrence in Nondiabetic Patients with Staphylococcus Aureus Infection.” *Human Pathology* 42(2):279–84.

World Health Organisation. 2018. “International Nonproprietary Names for Pharmaceutical Substances (INN) RECOMMENDED International Nonproprietary Names: List 80.” *WHO Drug Information* 32(3):425–508.

Woychyshyn, Boyan, Joan Papillon, Julie Guillemette, Jose R. Navarro-Betancourt, and Andrey V Cybulsky. 2020. “Genetic Ablation of SLK Exacerbates Glomerular Injury in Adriamycin Nephrosis in Mice.” *American Journal of Physiology-Renal Physiology* 318(6):F1377–90.

Wu, Haijing, Yi Lo, Albert Chan, Ka Sin Law, and Mo Yin Mok. 2016. “Rel B-modified Dendritic Cells Possess Tolerogenic Phenotype and Functions on Lupus Splenic Lymphocytes *in Vitro*.” *Immunology* 149(1):48–61.

Wu, Jinzi and Liang Jun Yan. 2015. “Streptozotocin-Induced Type 1 Diabetes in Rodents as a Model for Studying Mitochondrial Mechanisms of Diabetic β Cell Glucotoxicity.” *Diabetes, Metabolic Syndrome and Obesity: Targets and Therapy* 8:181–88.

Wu, Xili, Peng An, Bingyu Ye, Xingmin Shi, Huimin Dang, Rongguo Fu, and

Chenglin Qiao. 2014. “Artemisinin Ameliorated Proteinuria in Rats with Adriamycin-Induced Nephropathy through Regulating Nephrin and Podocin Expressions.” *Journal of Traditional Chinese Medicine* 34(1):63–68.

Wyss, Markus, Rima Kaddurah-Daouk, F. Hoffmann-, and La Roche. 2000. “Creatine and Creatinine Metabolism.” *Physiological Reviews* 80(3):1107–1213.

Xiao, P. J. and R. J. Samulski. 2012. “Cytoplasmic Trafficking, Endosomal Escape, and Perinuclear Accumulation of Adeno-Associated Virus Type 2 Particles Are Facilitated by Microtubule Network.” *Journal of Virology* 86(19):10462–73.

Xiao, W., N. Chirmule, S. C. Berta, B. McCullough, G. Gao, and J. M. Wilson. 1993. “Gene Therapy Vectors Based on Adeno-Associated Virus Type 1.” *Journal of Virology* 73(5):3994–4003.

Xiao, Wu, Kenneth H. Warrington, Patrick Hearing, Jeffrey Hughes, and Nicholas Muzyczka. 2002. “Adenovirus-Facilitated Nuclear Translocation of Adeno-Associated Virus Type 2.” *Journal of Virology* 76(22):11505–17.

Xiao, X., J. Li, and R. J. Samulski. 1996. “Efficient Long-Term Gene Transfer into Muscle Tissue of Immunocompetent Mice by Adeno-Associated Virus Vector.” *Journal of Virology* 70(11):8098–8108.

Xie, Kewei, Chenqi Xu, Minfang Zhang, Minzhou Wang, Lulin Min, Cheng Qian, Qin Wang, Zhaohui Ni, Shan Mou, Huili Dai, Huihua Pang, and Leyi Gu. 2019. “Yes-Associated Protein Regulates Podocyte Cell Cycle Re-Entry and Dedifferentiation in Adriamycin-Induced Nephropathy.” *Cell Death and Disease* 10(12):1–15.

Xie, Kewei, Mingli Zhu, Peng Xiang, Xiaohuan Chen, Ayijiaken Kasimumali, Renhua Lu, Qin Wang, Shan Mou, Zhaohui Ni, Leyi Gu, and Huihua Pang. 2017. “Protein Kinase A/CREB Signaling Prevents Adriamycin-Induced Podocyte Apoptosis via Upregulation of Mitochondrial Respiratory Chain Complexes.” *Molecular and Cellular Biology* 38(1):e00181-17.

Xie, Qing, Weishu Bu, Smita Bhatia, Joan Hare, Thayumanasamy Somasundaram, Arezki Azzi, and Michael S. Chapman. 2002. “The Atomic Structure of Adeno-Associated Virus (AAV-2), a Vector for Human Gene Therapy.” *Proceedings of the National Academy of Sciences of the United States of America* 99(16):10405–10.

Xiong, Ye, Asim Mahmood, Yuling Meng, Yanlu Zhang, Zheng Gang Zhang, Daniel C. Morris, and Michael Chopp. 2011. “Treatment of Traumatic Brain Injury with

Thymosin B4in Rats: Laboratory Investigation." *Journal of Neurosurgery* 114(1):102–15.

Xu, Baogang J., Yu Shyr, Xiubin Liang, Li Jun Ma, Ellen M. Donnert, Jeremy D. Roberts, Xueqiong Zhang, Valentina Kon, Nancy J. Brown, Richard M. Caprioli, and Agnes B. Fogo. 2005. "Proteomic Patterns and Prediction of Glomerulosclerosis and Its Mechanisms." *Journal of the American Society of Nephrology* 16(10):2967–75.

Xu, Han, Na Guan, Ya Li Ren, Qi Jiao Wei, Ying Hong Tao, Guo Sheng Yang, Xiao Ya Liu, Ding Fang Bu, Ying Zhang, and Sai Nan Zhu. 2018. "IP3R-Grp75-VDAC1-MCU Calcium Regulation Axis Antagonists Protect Podocytes from Apoptosis and Decrease Proteinuria in an Adriamycin Nephropathy Rat Model." *BMC Nephrology* 19(1):140.

Xu, Weiwei, Yan Ge, Zhihong Liu, and Rujun Gong. 2014. "Glycogen Synthase Kinase 3β Dictates Podocyte Motility and Focal Adhesion Turnover by Modulating Paxillin Activity: Implications for the Protective Effect of Low-Dose Lithium in Podocytopathy." *The American Journal of Pathology* 184(10):2742–56.

Xue, B. and R. C. Robinson. 2016. "Actin-Induced Structure in the Beta-Thymosin Family of Intrinsically Disordered Proteins." Pp. 55–71 in *Vitamins and Hormones*. Vol. 102. Academic Press Inc.

Xue, Bo, Cedric Leyrat, Jonathan M. Grimes, and Robert C. Robinson. 2014. "Structural Basis of Thymosin-B4/Profilin Exchange Leading to Actin Filament Polymerization." *Proceedings of the National Academy of Sciences of the United States of America* 111(43):E4596-605.

Yacoub, Rabi, Habib Habib, Ayham Lahdo, Radwan Al Ali, Leon Varjabedian, George Atalla, Nader Kassis Akl, Saleem Aldakheel, Saeed Alahdab, and Sami Albitar. 2010. "Association between Smoking and Chronic Kidney Disease: A Case Control Study." *BMC Public Health* 10(1):731.

Yamada, Hiroyuki, Naritoshi Shirata, Shinichi Makino, Takafumi Miyake, Juan Alejandro Oliva Trejo, Kanae Yamamoto-Nonaka, Mitsuhiro Kikyo, Maulana A. Empitu, Ika N. Kadariswantiningsih, Maiko Kimura, Koichiro Ichimura, Hideki Yokoi, Masashi Mukoyama, Akitsu Hotta, Katsuhiko Nishimori, Motoko Yanagita, and Katsuhiko Asanuma. 2020. "MAGI-2 Orchestrates the Localization of Backbone Proteins in the Slit Diaphragm of Podocytes." *Kidney*

International.

Yamaji, Satoshi, Atsushi Suzuki, Heiwa Kanamori, Wataru Mishima, Ryusuke Yoshimi, Hirotaka Takasaki, Maki Takabayashi, Katsumichi Fujimaki, Shin Fujisawa, Shigeo Ohno, and Yoshiaki Ishigatsubo. 2004. “Affixin Interacts with α-Actinin and Mediates Integrin Signaling for Reorganization of F-Actin Induced by Initial Cell-Substrate Interaction.” *Journal of Cell Biology* 165(4):539–51.

Yamashita, Atsuko, Kayo Maeda, and Yuichiro Maéda. 2003. “Crystal Structure of CapZ: Structural Basis for Actin Filament Barbed End Capping.” *EMBO Journal* 22(7):1529–38.

Yang, Chun, Wenhong Tian, Sisi Ma, Mengmeng Guo, Xiao Lin, Fengying Gao, Xiaoyan Dong, Mingming Gao, Yuhui Wang, George Liu, and Xunde Xian. 2020. “AAV-Mediated ApoC2 Gene Therapy: Reversal of Severe Hypertriglyceridemia and Rescue of Neonatal Death in ApoC2-Deficient Hamsters.” *Molecular Therapy - Methods and Clinical Development* 18:692–701.

Yang, Fang, Xiao Ping Yang, Yun He Liu, Jiang Xu, Oscar Cingolani, Nour Eddine Rhaleb, and Oscar A. Carretero. 2004. “Ac-SDKP Reverses Inflammation and Fibrosis in Rats with Heart Failure after Myocardial Infarction.” *Hypertension* 43(2 I):229–36.

Yang, Heung Mo, Shin Wook Kang, Jihye Sung, Kyeongsoon Kim, and Hynda Kleinman. 2020. “Purinergic Signaling Involvement in Thymosin B4-Mediated Corneal Epithelial Cell Migration.” *Current Eye Research* 45(11):1352–58.

Yang, J. and Y. Liu. 2001. “Dissection of Key Events in Tubular Epithelial to Myofibroblast Transition and Its Implications in Renal Interstitial Fibrosis.” *American Journal of Pathology* 159(4):1465–75.

Yang, Jae Won, Anne Katrin Dettmar, Andreas Kronbichler, Heon Yung Gee, Moin Saleem, Seong Heon Kim, and Jae Il Shin. 2018. “Recent Advances of Animal Model of Focal Segmental Glomerulosclerosis.” *Clinical and Experimental Nephrology* 22(4):752–63.

Yang, Nuo, Yan Zhang, Jiang Tao Wang, Chen Chen, Yan Song, Jian Min Liang, Di Hui Ma, and Yan Feng Zhang. 2020. “Effects of Dexamethasone on Remodeling of the Hippocampal Synaptic Filamentous Actin Cytoskeleton in a Model of Pilocarpine-Induced Status Epilepticus.” *International Journal of Medical Sciences* 17(12):1683–91.

Yaoita, Eishin, Hidetake Kurihara, Yutaka Yoshida, Tsutomu Inoue, Asako Matsuki,

Tatsuo Sakai, and Tadashi Yamamoto. 2005. “Role of Fat1 in Cell-Cell Contact Formation of Podocytes in Puromycin Aminonucleoside Nephrosis and Neonatal Kidney.” *Kidney International* 68(2):542–51.

Yi, Mixuan, Lei Zhang, Yu Liu, Man J. Livingston, Jian-Kang Chen, N. Stanley Nahman, Fuyou Liu, and Zheng Dong. 2017. “Autophagy Is Activated to Protect against Podocyte Injury in Adriamycin-Induced Nephropathy.” *American Journal of Physiology-Renal Physiology* 313(1):F74–84.

Yin, Lei, Youying Mao, Hejie Song, Ye Wang, Wei Zhou, and Zhen Zhang. 2017. “Vincristine Alleviates Adriamycin-Induced Nephropathy through Stabilizing Actin Cytoskeleton.” *Cell and Bioscience* 7(1):10.

Ylä-Herttuala, Seppo. 2012. “Endgame: Glybera Finally Recommended for Approval as the First Gene Therapy Drug in the European Union.” *Molecular Therapy* 20(10):1831–32.

Yoshimi, Michihiro, Takashige Maeyama, Mizuho Yamada, Naoki Hamada, Jyutaro Fukomoto, Tomonobu Kawaguchi, Kazuyoshi Kuwano, and Yoichi Nakanishi. 2008. “Recombinant Human Erythropoietin Reduces Epithelial Cell Apoptosis and Attenuates Bleomycin-Induced Pneumonitis in Mice.” *Respirology* 13(5):639–45.

Yoshimura, Yasuhiro and Ryuichi Nishinakamura. 2019. “Podocyte Development, Disease, and Stem Cell Research.” *Kidney International* 96(5):1077–82.

Yoshioka, T., T. Okada, Y. Maeda, U. Ikeda, M. Shimpo, T. Nomoto, K. Takeuchi, M. Nonaka-Sarukawa, T. Ito, M. Takahashi, T. Matsushita, H. Mizukami, Y. Hanazono, A. Kume, S. Ookawara, M. Kawano, S. Ishibashi, K. Shimada, and K. Ozawa. 2004. “Adeno-Associated Virus Vector-Mediated Interleukin-10 Gene Transfer Inhibits Atherosclerosis in Apolipoprotein E-Deficient Mice.” *Gene Therapy* 11(24):1772–79.

Young, J. D., A. J. Lawrence, A. G. Maclean, B. P. Leung, I. B. Mcinnes, B. Canas, D. J. C. Pappin, and R. D. Stevenson. 1999. “Thymosin B4 Sulfoxide Is an Anti-Inflammatory Agent Generated by Monocytes in the Presence of Glucocorticoids.” *Nature Medicine* 5(12):1424–27.

Yousef, George M. and Eleftherios P. Diamandis. 2001. “The New Human Tissue Kallikrein Gene Family: Structure, Function, and Association to Disease.” *Endocrine Reviews* 22(2):184–204.

Yu, F. X., S. C. Lin, M. Morrison-Bogorad, M. A. Atkinson, and H. L. Lin. 1993.

"Thymosin Beta 10 and Thymosin Beta 4 Are Both Actin Monomer Sequestering Proteins." *Journal of Biological Chemistry* 268:502–9.

Yu, Fu-Xin, Sheng-Cai Lin, Marcelle Morrison-Bogorad, Mark A. L. Atkinson, and Helen L. Yin. 1993. "Thymosin B10 and Thymosin B4 Are Both Actin Monomer Sequestering Proteins." *The Journal of Biological Chemistry* 268(1):502–9.

Yu, Fu-Xin -X, Helen L. Yin, Marcelle Morrison-Bogorad, and Sheng-Cai -C Lin. 1994. "Effects of Thymosin B4 and Thymosin B10 on Actin Structures in Living Cells." *Cell Motility and the Cytoskeleton* 27(1):13–25.

Yu, Haiyang, Hani Suleiman, Alfred H. J. Kim, Jeffrey H. Miner, Adish Dani, Andrey S. Shaw, and Shreeram Akilesh. 2013. "Rac1 Activation in Podocytes Induces Rapid Foot Process Effacement and Proteinuria." *Molecular and Cellular Biology* 33(23):4755–64.

Yu, Miao, Shimin Le, Artem K. Efremov, Xiangjun Zeng, Alexander Bershadsky, and Jie Yan. 2018. "Effects of Mechanical Stimuli on Profilin- and Formin-Mediated Actin Polymerization." *Nano Letters* 18(8):5239–47.

Yu, Seyoung, Won Il Choi, Yo Jun Choi, Hye Youn Kim, Friedhelm Hildebrandt, and Heon Yung Gee. 2020. "PLCE1 Regulates the Migration, Proliferation, and Differentiation of Podocytes." *Experimental and Molecular Medicine* 52(4):594–603.

Yuan, Huaiping, Emiko Takeuchi, and David J. Salant. 2002. "Podocyte Slit-Diaphragm Protein Nephrin Is Linked to the Actin Cytoskeleton." *American Journal of Physiology-Renal Physiology* 282(4):F585–91.

Yuan, Jing, Yan Shen, Xia Yang, Ying Xie, Xin Lin, Wen Zeng, Yingting Zhao, Maolu Tian, and Yan Zha. 2017. "Thymosin B4 Alleviates Renal Fibrosis and Tubular Cell Apoptosis through TGF-β Pathway Inhibition in UUO Rat Models." *BMC Nephrology* 18(1):314.

Zhang, Jiong, Kim M. Hansen, Jeffrey W. Pippin, Alice M. Chang, Yoshinori Taniguchi, Ronald D. Krofft, Scott G. Pickering, Zhi-Hong Liu, Christine K. Abrass, and Stuart J. Shankland. 2012. "De Novo Expression of Podocyte Proteins in Parietal Epithelial Cells in Experimental Aging Nephropathy." *American Journal of Physiology-Renal Physiology* 302(5):F571–80.

Zhang, Yanshu, Aiko Yoshida, Nobuaki Sakai, Yoshitsugu Uekusa, Masahiro Kumeta, and Shige H. Yoshimura. 2017. "In Vivo Dynamics of the Cortical Actin Network Revealed by Fast-Scanning Atomic Force Microscopy." *Microscopy*

66(4):272–82.

Zhang, Yuqing, Louis W. Feurino, Qihui Zhai, Hao Wang, William E. Fisher, Changyi Chen, Qizhi Yao, and Min Li. 2008. “Thymosin Beta 4 Is Overexpressed in Human Pancreatic Cancer Cells and Stimulates Proinflammatory Cytokine Secretion and JNK Activation.” *Cancer Biology & Therapy* 7(3):1–5.

Zheng, Xiao Yan, Yi Fei Lv, Shuang Li, Qian Li, Qian Nan Zhang, Xue Ting Zhang, and Zhi Ming Hao. 2017. “Recombinant Adeno-Associated Virus Carrying Thymosin B4 Suppresses Experimental Colitis in Mice.” *World Journal of Gastroenterology* 23(2):242–55.

Zheng, Zongyu, Kai M. Schmidt-Ott, Streamson Chua, Kirk A. Foster, Rachelle Z. Frankel, Paul Pavlidis, Jonathan Barasch, Vivette D. D’Agati, and Ali G. Gharavi. 2005. “A Mendelian Locus on Chromosome 16 Determines Susceptibility to Doxorubicin Nephropathy in the Mouse.” *Proceedings of the National Academy of Sciences of the United States of America* 102(7):2502–7.

Zhong, Fang, Haibing Chen, Yifan Xie, Evren U. Azeloglu, Chengguo Wei, Weijia Zhang, Zhengzhe Li, Peter Y. Chuang, Belinda Jim, Hong Li, Firas Elmastour, Jalish M. Riyad, Thomas Weber, Hongyu Chen, Yongjun Wang, Aihua Zhang, Weiping Jia, Kyung Lee, and John C. He. 2018. “Protein S Protects against Podocyte Injury in Diabetic Nephropathy.” *Journal of the American Society of Nephrology* 29(5):1397–1410.

Zhong, Li, Baozheng Li, Cathryn S. Mah, Lakshmanan Govindasamy, Mavis Agbandje-McKenna, Mario Cooper, Roland W. Herzog, Irene Zolotukhin, Kenneth H. Warrington, Kirsten A. Weigel-Van Aken, Jacqueline A. Hobbs, Sergei Zolotukhin, Nicholas Muzyczka, and Arun Srivastava. 2008. “Next Generation of Adeno-Associated Virus 2 Vectors: Point Mutations in Tyrosines Lead to High-Efficiency Transduction at Lower Doses.” *Proceedings of the National Academy of Sciences of the United States of America* 105(22):7827–32.

Zhong, Li, Xiaohuai Zhou, Yanjun Li, Keyun Qing, Xiao Xiao, Richard Jude Samulski, and Arun Srivastava. 2008. “Single-Polarity Recombinant Adeno-Associated Virus 2 Vector-Mediated Transgene Expression In Vitro and In Vivo: Mechanism of Transduction.” *Molecular Therapy* 16(2):290–95.

Zhou, Qingzhang, Wenhong Tian, Chunguo Liu, Zhonghui Lian, Xiaoyan Dong, and Xiaobing Wu. 2017. “Deletion of the B-B’ and C-C’ Regions of Inverted Terminal

Repeats Reduces RAAV Productivity but Increases Transgene Expression." *Scientific Reports* 7(1):1–13.

Zhou, Wuding and Steven H. Sacks. 2001. "Why Is Erythropoietin Made in the Kidney? The Kidney Functions as a Critmeter." *American Journal of Kidney Diseases* 38(2):415–25.

Zhou, Xiaohuai, Xinghua Zeng, Zhenghong Fan, Chengwen Li, Thomas McCown, R. Jude Samulski, and Xiao Xiao. 2008. "Adeno-Associated Virus of a Single-Polarity DNA Genome Is Capable of Transduction in Vivo." *Molecular Therapy* 16(3):494–99.

Zhou, Yunfeng, Xiaomu Kong, Pan Zhao, Hang Yang, Lihong Chen, Jing Miao, Xiaoyan Zhang, Jichun Yang, Jie Ding, and Youfei Guan. 2011. "Peroxisome Proliferator-Activated Receptor-α Is Renoprotective in Doxorubicin-Induced Glomerular Injury." *Kidney International* 79(12):1302–11.

Zhu, Jian, Li-Ping Su, Yue Zhou, Lei Ye, Kok-Onn Lee, and Jian-Hua Ma. 2015. "Thymosin B4 Attenuates Early Diabetic Nephropathy in a Mouse Model of Type 2 Diabetes Mellitus." *American Journal of Therapeutics* 22(2):141–46.

Ziegler, Tilman, Markus Kraus, Wira Husada, Florian Gesenhues, Qui Jiang, Olaf Pinkenburg, Teresa Trenkwalder, Karl Ludwig Laugwitz, Ferdinand Le Noble, Christian Weber, Christian Kupatt, and Rabea Hinkel. 2018. "Steerable Induction of the Thymosin B4/MRTF-A Pathway via AAV-Based Overexpression Induces Therapeutic Neovascularization." *Human Gene Therapy* 29(12):1407–15.

Zincarelli, Carmela, Stephen Soltys, Giuseppe Rengo, and Joseph E. Rabinowitz. 2008. "Analysis of AAV Serotypes 1-9 Mediated Gene Expression and Tropism in Mice after Systemic Injection." *Molecular Therapy* 16(6):1073–80.

Ziyadeh, Fuad N. 2004. "Mediators of Diabetic Renal Disease: The Case for TGF-β as the Major Mediator." *Journal of the American Society of Nephrology* 15(1 SUPPL.):S55–57.

Zou, Jun, Eishin Yaoita, Yusuke Watanabe, Yutaka Yoshida, Masaaki Nameta, Huiping Li, Zhenyun Qu, and Tadashi Yamamoto. 2006. "Upregulation of Nestin, Vimentin, and Desmin in Rat Podocytes in Response to Injury." *Virchows Archiv* 448(4):485–92.

Zou, Min-Shu, Jian Yu, Jian-Hua Zhou, Guo-Ming Nie, Dong-Sheng Ding, Li-Man Luo, Hong-Tao Xu, and Wei-Sun He. 2010. "1,25-Dihydroxyvitamin D3

Ameliorates Podocytopenia in Rats with Adriamycin-Induced Nephropathy." *International Medicine* 49:2677–86.

Zou, Min Shu, Jian Yu, Guo Ming Nie, Wei Sun He, Li Man Luo, and Hong Tao Xu. 2010. "1, 25-Dihydroxyvitamin D3 Decreases Adriamycin-Induced Podocyte Apoptosis and Loss." *International Journal of Medical Sciences* 7(5):290–99.

Zou, Yizhou, Peter Stastny, Caner Süsal, Bernd Döhler, and Gerhard Opelz. 2007. "Antibodies against MICA Antigens and Kidney-Transplant Rejection." *New England Journal of Medicine* 357(13):1293–1300.

Zuo, Yiqin, Bongkwon Chun, Sebastian A. Potthoff, Naj Kazi, Tyler J. Brolin, Diclehan Orhan, Hai-Chun Yang, Li-Jun Ma, Valentina Kon, Timo Myöhänen, Nour-Eddine Rhaleb, Oscar A. Carretero, and Agnes B. Fogo. 2013. "Thymosin B4 and Its Degradation Product, Ac-SDKP, Are Novel Reparative Factors in Renal Fibrosis." *Kidney International* 84(6):1166–75.